Advanced Polymer Coatings for Aerospace Industry by Nitroxide Mediated Polymerization in Organic Solvents and Miniemulsion

Saeid Tajbakhsh

Department of Chemical Engineering

McGill University

Montreal, Canada

May 2021

A thesis submitted to McGill University in partial fulfillment of the requirements of the degree of Doctor of Philosophy.

DEDICATION

To my wife, Faezeh

my parents, Shirin & Hamid

and my siblings, Adel & Elahe

Preface

In accordance with the "McGill Guidelines for Thesis Preparation", this thesis is presented in a manuscript-based format. An introduction to the subject-matter of this thesis and literature review are presented in Chapters 1 and 2. Chapters 3-9 present seven original research manuscripts. Lastly, the thesis conclusions and suggestions for future works are presented in Chapter 10.

Acknowledgements

First, I would like to express my gratitude to my research supervisor, Prof. Milan Marić for his persistent support, invaluable guidance and encouragement during my PhD study. I am extremely grateful for his understanding, patience, wisdom and his help to foster my professional development. I am thankful to all members of Prof. Milan Marić's laboratory for providing a pleasant research atmosphere and their help during my research. I would like to thank "polymer coating" group: Kieran, Farhad and Masa for their friendship and fruitful talks. Special thanks go to Dr. Adrien Métafiot, Dr. Hatem Titi, Dr. Robin Stein and Mr. Petr Fiurasek for trainings and valuable discussions.

Finally, my sincerest thanks to my beautiful wife, Faezeh, for her unwavering love, support, and patience throughout all my academic years. Her intelligence, kindness and perseverance always inspires me and I am truly grateful for having her in my life. I would like to thank my parents, my siblings, and my in-laws for their unconditional love and support. I also thank my friends for their emotional supports during these years.

Abstract

This study investigated the preparation of polymers for wood coating applications. To produce such materials, reversible deactivation radical polymerization (RDRP) was used to prepare polymers with a low dispersity (Đ, narrow molecular weight distribution), controlled polymer microstructure and low solution viscosity. In addition, RDRP enables a facile polymerization process in dispersed aqueous media. The polymers synthesized in this study were mainly made of methacrylic monomers with high bio-content. Here, nitroxide mediated polymerization (NMP) was used as a simple RDRP technique. NMP only requires heat and alkoxyamine to initiate and control the polymerization (control means a linear increase of number-average molecular weight (M_n) with conversion and a low dispersity). First, the statistical copolymers of isobornyl methacrylate (IBOMA, from pine sap) and C13 alkyl methacrylate (C13MA, from natural oils) were synthesized by nitroxide mediated polymerization in miniemulsion to minimize the volatile organic compounds (VOCs) in coatings. Two different techniques were studied for the NMP of IBOMA/C13MA in miniemulsion. The first method involved using an SG1-based amphiphilic macroinitiator to initiate and control the polymerization. SG1 (*N-tert*-butyl-*N*-[1-diethylphosphono-(2,2-dimethylpropyl)]) is a nitroxide that has been commonly used for the NMP of a wide range of monomers. The macroinitiator also helped with the stabilization of monomer droplets in the latex. Second, the miniemulsion polymerization was initiated by Dispolreg 007 alkoxyamine and the particles were stabilized by surfactant and co-stabilizer. The resulted polymers had M_n up to 68000 g mol^{-1} and Đ as low as 1.62. Using this method, IBOMA/C13MA statistical copolymers with various glass transition temperature (T$_g$) (-52 °C < T$_g$ < 123 °C) were prepared in miniemulsion. Next, the addition of methacryloisobutyl POSS (POSSMA) to the IBOMA/C13MA polymer chains was studied. To check the possibility of POSSMA polymerization in miniemulsion, firstly, homopolymers and copolymers of POSSMA with C13MA were produced by NMP. This was followed by polymerization of POSSMA/IBOMA/C13MA to improve the thermal properties and hardness of polymer resins. The preparation of the self-healing polymers for coating applications was investigated in the second part of this thesis. The aim of this study was to develop a polymer formulation with self-healing properties that can be eventually used as a wood coating. Then, this formulation was applied for NMP in miniemulsion to prepare water-borne self-healable coatings without VOCs. The self-healing polymers were first prepared by incorporation of a low concentration (2 to 15 mol% in the initial monomer mixture) of 4-vinylphenylboronic acid (VPBA) and glycerol monomethacrylate (GMMA) into IBOMA/C13MA polymers via NMP in 1,4-dioxane. The VPBA-containing and GMMA-containing polymers were mixed to prepare polymer blends with boronic ester dynamic covalent bonds. The dynamic covalent cross-linking bonds can heal the cuts and scratches at ambient conditions in a relatively short time (healed scratches in 12 days and cuts in 10 days). The transition of self-healing formulation to a water-

borne system was enabled by synthesis of (VPBA+GMMA) dimer before the miniemulsion polymerization to increase the availability of the functional groups in monomer droplets. The resulting polymers had a high recyclability via a simple process by hot pressing at 80 °C for 45 minutes. The hardness and flexibility of self-healing polymers were tunable and could be modified by changing the ratio of IBOMA and C13MA monomers in the copolymer feed. Finally, epoxy-based polymers were developed as an alternative approach for preparation of polymer wood coatings. The NMP of glycidyl methacrylate (GMA)/C13MA compositions was done using Dispolreg 007 alkoxyamine in 50 wt% 1,4-dioxane. Consequently, various statistical, deblock, triblock and gradient copolymers with different ratios of GMA/C13MA were synthesized. The polymerization kinetics, thermal and rheological properties of copolymers were investigated thoroughly. The high ash content (13 wt%) of GMA/C13MA statistical copolymers suggests the possibility of high flame retardancy for polymers.

Résumé

Cette étude a examiné la préparation de polymères pour les applications de revêtement de bois. La polymérisation radicalaire par désactivation réversible (RDRP) a été utilisée à préparer des polymères avec une faible dispersité (*Đ*, distribution étroite des poids moléculaires), une microstructure de polymère contrôlée et une faible viscosité en solution. De plus, le RDRP permet le processus de polymérisation facile dans des milieux aqueux dispersés. Les polymères synthétisés étaient principalement constitués de monomères méthacryliques à haute teneur en bio composant. La polymérisation radicalaire contrôlée par des radicaux nitroxyde (NMP) a été utilisée comme technique RDRP simple pour produire les polymères. La technique NMP a besoin de la chaleur et une alcoxyamine permettant d'amorcer et de contrôler la polymérisation. Premièrement, les copolymères statistiques ont été synthétisés par NMP de méthacrylate d'isobornyle (IBOMA, dérivé de la sève de pin) et du méthacrylate C13 (C13MA, dérivé d'huiles végétales) en miniémulsion pour minimiser les composés organiques volatils (COV) dans les revêtements. Deux techniques différentes ont été étudiées pour la NMP d'IBOMA / C13MA en miniémulsion. La première méthode utilisait un macro-initiateur amphiphile à base de SG1 pour initier et contrôler la polymérisation. Le SG1 (N-tert-butyl-N- [1-diéthylphosphono- (2,2-diméthylpropyl)]) est un nitroxyde couramment utilisé à la NMP d'une large gamme de monomères. Le macro-initiateur a également contribué à la stabilisation des gouttelettes de monomère dans le latex. Deuxièmement, la polymérisation en mini-émulsion a été initiée par l'alcoxyamine Dispolreg 007 et les particules ont été stabilisées par un tensioactif et un co-stabilisant. Les polymères résultants avaient M_n jusqu'à 68 000 g mol^{-1} et *Đ* aussi bas que 1.62. En utilisant cette méthode, des copolymères statistiques IBOMA/C13MA avec diverses températures de transition vitreuse (T_g) (-52 °C < T_g < 123 °C) préparés en miniémulsion. Ensuite, l'addition de méthacryloisobutyl POSS (POSSMA) aux chaînes polymères IBOMA/C13MA a été étudiée. Pour vérifier la possibilité de polymérisation POSSMA en miniémulsion, dans un premier temps, des homopolymères et copolymères de POSSMA avec C13MA ont été produits par NMP. Ceci a été suivi par la polymérisation de POSSMA/IBOMA/C13MA pour améliorer les propriétés thermiques et la dureté des résines polymères. La préparation des polymères auto-cicatrisants pour les applications de revêtement a été étudiée dans la deuxième partie de cette thèse. Le but de cette étude était de développer une formulation de polymère aux propriétés auto-cicatrisantes pouvant être éventuellement utilisée comme revêtement de bois. Ensuite, cette formulation a été appliquée pour la NMP en miniémulsion à préparer des revêtements auto-cicatrisables à l'eau sans COV. Les polymères auto-cicatrisants ont d'abord été préparés par incorporation d'une faible concentration (2 à 15 mol% dans le mélange initial de monomères) d'acide 4-vinylphénylboronique (VPBA) et de monométhacrylate de glycérol (GMMA) dans des polymères IBOMA/C13MA via NMP en 1,4-dioxane. Les polymères contenant VPBA et GMMA ont été mélangés pour préparer des mélanges de

polymères avec la dynamique des liaisons covalentes réversibles d'ester boronique. Les liaisons de réticulation covalentes dynamiques peuvent cicatriser les coupures et rayures à conditions ambiantes en un temps relativement court (rayures cicatrisées en 12 jours et coupures en 10 jours). La transition de la formulation auto-cicatrisante à un système aqueux a été permise par la synthèse de dimère (VPBA+GMMA) avant la polymérisation en miniémulsion pour augmenter la disponibilité des groupes fonctionnels dans les gouttelettes de monomère. Les polymères résultants avaient une recyclabilité élevée avec un processus de recyclage simple dans une presse à chaud à 80 ° C pendant 45 minutes. La dureté et la flexibilité des polymères auto-cicatrisants étaient réglables et pouvaient être modifiées en changeant le rapport des monomères IBOMA et C13MA. Enfin, des polymères à base d'époxy ont été développés comme une approche alternative pour la préparation de revêtements de bois polymère. La NMP du méthacrylate de glycidyle (GMA) et du C13MA a été effectuée en utilisant Dispolreg 007 alcoxyamine dans 50% en poids de 1,4-dioxane. Par conséquent, divers copolymères statistiques, débloquants, triblocs et gradient avec différents rapports de GMA / C13MA ont été synthétisés. La cinétique de polymérisation, les propriétés thermiques et rhéologiques des copolymères ont été étudiées de manière approfondie. La teneur élevée en cendres (13% en poids) des copolymères statistiques GMA/C13MA suggère la possibilité d'une ignifugation élevée pour les polymères.

Table of Contents

xi

List of Figures

Figure 4.3. NMP to produce poly(IBOMA-*stat*-C13MA) copolymers using Dispolreg 007 initiator in toluene (50 wt%) at 100 °C and $M_{n,target}$ = 25 kg mol^{-1}. (a) Semi-logarithmic kinetic plots of ln[(1-X)$^{-1}$] (X= monomer conversion) versus reaction time (b) The evolution of M_n and $Đ$ with conversion (X). IBOMA100-S-100C (filled circles, ●); IBOMA80/C13MA20-S (filled triangles, ▲); IBOMA60/C13MA40-S (filled diamonds, ◆); IBOMA50/C13MA50-S (gray circles, ●); IBOMA40/C13MA60-S (gray triangles, ▲); IBOMA30/C13MA70-S (gray diamonds, ◆); IBOMA20/C13MA80-S (open circles, ○); IBOMA10/C13MA90-S (open triangles, Δ); C13MA100-S-100C (open diamonds, ◊).

Figure 4.4. Mayo-Lewis plot of copolymer composition with respect to IBOMA molar fraction at low conversion or instantaneous composition ($F_{IBOMA,i}$) versus initial IBOMA feed composition (f_{IBOMA} ≈ $f_{IBOMA,0}$). The open circles represent the experimental data and the dashed line shows the trend line. The straight line is associated with the azeotropic composition ($F_{IBOMA} = f_{IBOMA}$). The copolymerization was performed at 100 °C using Dispolreg 007 initiator in 50 wt% toluene. $F_{IBOMA,i}$ of copolymers is available in Table 4.S1 in Supplementary Information.

Figure 4.5. GPC traces for chain-extension of poly(IBOMA) macroinitiator (M_n = 13.6 kg mol^{-1} and $Đ$ = 1.47) with C13MA. Chain-extension was done in 50 wt% toluene at 100 °C. The gray solid line is the macro initiator while the black solid line is the chain-extended product with M_n = 40.7 kg mol^{-1} and $Đ$ = 1.93 (Dispersity is reported for the overall peak, containing the active and dead polymers). Full characterization data for the samples shown is provided in Table 4.4.

Figure 4.6. The schematic of nitroxide-mediated miniemulsion polymerization using oil-soluble Dispolreg 007 initiator.

Figure 4.7. The miniemulsion polymerization of different ratios of IBOMA/C13MA using Dispolreg 007 initiator (a) Semi-logarithmic kinetic plots of ln[(1-X)$^{-1}$] (X= monomer conversion) versus reaction time (b) Number average molecular weight M_n and dispersity $Đ$ versus conversion (X). IBOMA100 (filled circles, ●); IBOMA90/C13MA10 (filled triangles, ▲); IBOMA80/C13MA20 (filled diamonds, ◆); IBOMA70/C13MA30 (filled squares, ■); IBOMA60/C13MA40 (gray circles, ●); IBOMA50/C13MA50 (gray triangles, ▲); IBOMA40/C13MA60 (gray diamonds, ◆); IBOMA30/C13MA70 (gray squares, ■); IBOMA20/C13MA80 (open circles, ○); IBOMA10/C13MA90 (open triangles, Δ); C13MA100 (open diamonds, ◊).

Figure 4.8. Molecular weight distribution of polymer particles in chain extension polymerization. Seed latex of poly(C13MA) (dashed black line) and poly(C13MA-*grad*-IBOMA) after the chain extension (solid black line). Characterization data for these two samples is provided in Table 4.6.

shows the theoretical azeotropic composition ($F_{GMA} = f_{GMA,0}$) for statistical copolymerization of GMA/C13MA. b) The drift in GMA molar feed (f_{GMA}) with monomer conversion for copolymerization with different ratios of GMA/C13MA. The fitted curves were determined with $r_{GMA} = 1.17 \pm 0.09$ and $r_{C13MA} = 0.65 \pm 0.09$ from the Meyer Lowry method.

Figure 9.5. Nitroxide mediated gradient copolymerization of GMA/C13MA for preparation of GMA-*grad*-C13MA (black circles ●, $M_n = 35.7$ kg mol^{-1}, Đ = 1.79) and C13MA-*grad*-GMA (red triangles ▲, $M_n = 27.6$ kg mol^{-1}, Đ = 1.60) in 1,4-dioxane at 90 °C. Full characterization results for gradient copolymerization of GMA/C13MA are available in Table 9.2. The results were shown before and after addition of the second monomer to reaction. a) semi-logarithmic kinetic plots of $\ln[(1-X)^{-1}]$ ($X=$ total monomer conversion) versus reaction time b) the evolution of M_n with total monomer conversion (X) c) the evolution of Đ with conversion (X). d and e) The shift in GPC peaks for gradient copolymerization of GMA/C13MA.

Figure 9.6. Kinetic results for preparation of GMA-*b*-C13MA (a, b and e) and C13MA-*b*-GMA (c, d and f) block copolymers (red triangles ▲) by chain extension of GMA-MI and C13MA-MI macroinitiators (black circles ●) in dioxane at 90 °C. The experimental conditions and polymers' characteristics were listed on Table 9.3. a) and c) semi-logarithmic kinetic plots of $\ln[(1-X)^{-1}]$ ($X=$ monomer conversion) versus reaction time b) and d) the evolution of M_n and Đ with monomer conversion (X) e) and f) The shift in GPC peaks after the chain extension of macroinitiators.

Figure 9.7. Preparation of triblock copolymer of GMA/C13MA (Bi-GMA-*tri*-C13MA, red triangles ▲, $M_n = 43.0$ kg mol^{-1}, Đ = 1.85) by chain extension of bifunctional GMA-based macroinitiator (Bi-GMA-MI, black circles ●, $M_n = 19.9$ kg mol^{-1}, Đ = 1.58) for 2h in dioxane at 90 °C. a) semi-logarithmic kinetic plots of $\ln[(1-X)^{-1}]$ ($X=$ monomer conversion) versus reaction time b) the evolution of M_n with conversion (X) c) GPC peaks for macroinitiator and triblock copolymers d) the evolution of Đ with conversion (X).

Figure 9.8. Preparation of triblock copolymer of GMA/C13MA (Bi-C13MA-*tri*-GMA, red triangles ▲, $M_n = 45.5$ kg mol^{-1}, Đ = 1.70) by chain extension of C13MA-based bifunctional macroinitiator (Bi-C13MA-MI, black circles ●, $M_n = 24.1$ kg mol^{-1}, Đ = 1.46) for 2h in dioxane at 90 °C. a) semi-logarithmic kinetic plots of $\ln[(1-X)^{-1}]$ ($X=$ monomer conversion) versus reaction time b) the evolution of M_n with conversion (X) c) GPC peaks for macroinitiator and triblock copolymers d) the evolution of Đ with conversion (X).

Figure 9.9. DSC curves a) statistical copolymers b) gradient polymers c) block copolymers and d) triblock copolymers of GMA/C13MA in temperature range of -80 to 130 °C. T_gs and T_ms of polymers are presented in Table 9.5.

Figure 9.10. TGA curves a) statistical copolymers b) gradient polymers c) block copolymers and d) triblock copolymers of GMA/C13MA with heating rate of 15 °C min^{-1} in temperature range of 25-600 °C. The decomposition temperatures (T_{dec}s) are listed in Table 9.5.

Figure 9.11. Storage modulus (G′), loss modulus (G″) and complex viscosity versus angular frequency (1% strain) for a) GMA/C13MA gradient, b) block and c) triblock copolymers at 30 °C.

List of Tables

Chapter 1: Introduction

Background

Wood is a remarkable material used extensively for decorative purposes in the aerospace industry, particularly for interior components. Wood can be considered as a complex of various biopolymers including cellulose, hemicelluloses, and lignin[1]. This structure can be vulnerable to the effects of stress factors such as heat, sunlight, pressure or scratches. For instance, sunlight causes photooxidation and photodegradation of the wood surface[2]. To ensure the long life of the wood-based objects, protective polymer coatings are one way of extending the product's lifetime. Coatings are designed to be transparent or semitransparent in order to exhibit the aesthetic texture of the wood support. The coatings should also have high durability and performance to protect the wood against environmental stress factors such as humidity, light and heat along with pressure, cracking and solvents. The main purpose of using wood coatings is to maintain the natural beauty of wood and enhance the physical and chemical properties of the wood support for indoor and outdoor applications[3]. In addition, environmental legislation and economic factors should be considered in order to produce wood coatings based on the market demands in different countries[4].

For ecological and health-related reasons, there is a high demand for coatings which are waterborne (to avoid using organic solvents or volatile organic compounds (VOCs) and sustainable (eg. made from natural or renewable resources). Therefore, dispersed systems such as suspension, emulsion or miniemulsion can be used to produce the coatings[5]. Nowadays, emulsion polymers are widely used for preparation of paints, adhesives and coatings.

For aerospace applications, coatings are also required to serve multiple functions based on their specific applications. High mechanical and thermal strength, chemical and solvent resistance, anti-flammability and self-healing properties are just some of the interesting properties that can be incorporated in polymer coatings for airplane interiors. Therefore, it is important to carefully design the polymer microstructure to achieve these goals in the final material. One of the approaches for production of controlled structures in polymers for coatings and other applications is the use of reversible deactivation radical polymerization (RDRP, also known as controlled radical polymerization) processes such as nitroxide mediated polymerization (NMP),[6, 7] reversible addition-fragmentation chain transfer (RAFT) polymerization[8, 9] and atom transfer radical polymerization (ATRP)[10-12]. RDRP, more commonly known by its non-IUPAC term controlled radical polymerization (CRP), offers many advantages over conventional radical polymerization and truly living polymerizations[13]. Controlled radical polymerization permits attainment of narrow

molecular weight distribution and active chain ends that are useful for preparation and exploitation of block copolymers and other complex polymeric structures. CRP does not require any reagents nor high reaction temperature and can be done in dispersed aqueous media. A wide range of monomers can be polymerized by CRP that are otherwise impossible by ionic polymerization[14-16]. In this study we used NMP to produce polymeric coatings (mainly waterborne coatings) with desired properties such as good adhesion, high flame and heat resistance, repellency of solvents and resistance to cracks for protection of the wood surface. We also developed self-healable polymer coatings with high recyclability to reduce the environmental impacts from plastic waste and to reduce repair and damage costs.

Research Objectives

The main purpose of this thesis was to prepare polymer coatings with different properties by nitroxide mediated polymerization of methacrylic monomers in miniemulsion or organic solvents.

The objectives of this thesis can be divided to the following sections:

1. Development of water-borne polymer coating formulations using different types and ratios of monomers by nitroxide mediated miniemulsion polymerization.
2. Improve the thermal stability and anti-flammability of polymers by incorporating hybrid organic-inorganic monomers.
3. Investigate polymer networks with dynamic cross-linking bonds to prepare polymer structures with self-healing properties and high recyclability.
4. Studying alternative polymer coatings (epoxy-based polymers) prepared by nitroxide mediated polymerization.

Thesis Organization

- Chapter 2: Provides a brief literature review on the nitroxide mediated polymerization of the methacrylic monomers in miniemulsion and organic solvents. Furthermore, polymer networks with dynamic covalent cross-linking bonds were discussed in detail.
- Chapter 3: Investigates the preparation of the sustainably sourced methacrylic polymers by nitroxide mediated miniemulsion polymerization using amphiphilic polymeric macroinitiators. Also, the reaction temperature, required additives (surfactant and co-stabilizer) and the stability of the polymer latexes were examined.
- Chapter 4: Bio-based poly(methacrylates) were synthesized by nitroxide mediated polymerization of the monomers in miniemulsion and organic solvents (solution polymerization). Dispolreg 007

2

alkoxyamine was used in this study, which eliminated the use of controlling co-monomers for polymerization of methacrylates.

- Chapter 5: Nitroxide mediated polymerization of methacryloisobutyl POSS in miniemulsion system was studied. To improve the mechanical properties of polymers, copolymers of methacryloisobutyl POSS with alkyl methacrylates were synthesized in miniemulsion and the kinetics of polymerization and thermal properties of polymers were examined thoroughly.

- Chapter 6: Methacryloisobutyl POSS was incorporated into bio-based poly(methacrylates) using nitroxide mediated polymerization in miniemulsion and organic solvent-based solutions. Kinetics of polymerization and thermal properties of polymers were studied and the results for miniemulsion and solution-based (in organic solvents) systems were compared.

- Chapter 7: Room temperature self-healable polymers were developed from bioresources. To prepare the polymer networks with dynamic boronic-ester bonds, two polymers with different functional monomers were synthesized. We attempted to maximize the bio-content by incorporating bio-based methacrylic monomers. The results showed the self healing of polymers at ambient conditions. The mechanical and thermal properties of polymers can be adjusted by changing the ratio of monomers in polymer chains.

- Chapter 8: This study investigated the synthesis of self-healable polymers by nitroxide mediated polymerization in miniemulsion. Using this method, organic solvents were completely removed from the system. The recyclability, mechanical and thermal properties of polymers were examined.

- Chapter 9: This chapter investigated an alternative epoxy-based polymer for wood coating applications. The synthesis of gradient, diblock and triblock copolymers was enabled by nitroxide mediated polymerization of methacrylic monomers. The kinetics of polymerizations and rheological and thermal properties of polymers were discussed.

- Chapter 10: We summarized the overall results and concluded with suggestions for future work.

Contribution of the Authors

This thesis includes 7 manuscripts. The original contributions of authors are summarized below:

1. Highly reprocessable, room temperature self-healable bio-based materials with boronic-ester dynamic cross-linking, *Reactive and Functional Polymers*,158, 104794, 2021.

Authors: Saeid Tajbakhsh, Faezeh Hajiali, Kieran Guinan, Milan Marić

Saeid Tajbakhsh: Conceptualization, Investigation, Validation, Writing – original draft, review & editing. Faezeh Hajiali: Investigation, Formal Analysis, Writing – Review & editing. Kieran Guinan: Investigation,

Formal Analysis. Milan Marić: Conceptualization, Supervision, Funding acquisition, Writing – Review & editing.

2. Nitroxide-mediated emulsion polymerization of bio-based methacrylates, *Industrial & Engineering Chemistry Research*, 59 (19), 8921-8936, 2020.

Authors: Saeid Tajbakhsh, Faezeh Hajiali, Milan Marić

Contributions: S. Tajbakhsh and F. Hajiali synthesized the polymers and studied the polymerization kinetics and thermal properties of polymers. S. Tajbakhsh measured rheological and mechanical properties of polymers and wrote and edited most of the manuscript. M. Marić supervised the project, read, provided feedback and edited the manuscript.

3. Nitroxide mediated miniemulsion polymerization of methacryloisobutyl POSS: Homopolymers and copolymers with alkyl methacrylates, *Journal of Polymer Science*, 58 (19), 2741-2754, 2020.

Authors: Saeid Tajbakhsh, Milan Marić

Contributions: S. Tajbakhsh synthesized the polymers and studied the polymerization kinetics and thermal properties of polymers. S. Tajbakhsh wrote and edited most of the manuscript. M. Marić supervised the project, read, provided feedback, and edited the manuscript.

4. Incorporation of methacryloiobutyl in bio-based copolymers by nitroxide mediated polymerization in miniemulsion and solution systems, *Journal of Applied Polymer Science*,138 (13), 50095, 2021.

Authors: Saeid Tajbakhsh, Faezeh Hajiali, Milan Marić

Contributions: S. Tajbakhsh and F. Hajiali synthesized the polymers and studied the polymerization kinetics and thermal properties of polymers. S. Tajbakhsh wrote and edited most of the manuscript. M. Marić supervised the project, read, provided feedback and edited the manuscript.

5. Synthesis of bio-based poly(methacrylates) using SG1-containing amphiphilic macroinitiators by nitroxide mediated miniemulsion polymerization, *Journal of Polymer Science*, 59, 547-560, 2021,

Authors: Saeid Tajbakhsh, Milan Marić

Contributions: S. Tajbakhsh synthesized the polymers and studied the polymerization kinetics, thermal properties of polymers, particle size and latex stability. S. Tajbakhsh wrote and edited most of the manuscript. M. Marić supervised the project, read, provided feedback, and edited the manuscript.

6. Epoxy-based triblock, diblock, gradient and statistical copolymers of glycidyl methacrylate and alkyl methacrylates by nitroxide mediated polymerization, Submitted to *Reactive and Functional Polymers*, 2021.

Authors: Saeid Tajbakhsh, Faezeh Hajiali, Milan Marić

Contributions: S. Tajbakhsh and F. Hajiali synthesized the polymers and studied the polymerization kinetics and polymer characterizations. S. Tajbakhsh wrote and edited most of the manuscript. M. Marić supervised the project, read, provided feedback, and edited the manuscript.

7. Recyclable polymers with boronic-ester dynamic bonds prepared by miniemulsion polymerization, Submitted to *ACS Applied Polymer Materials,* 2021.

Authors: Saeid Tajbakhsh, Faezeh Hajiali, Milan Marić

Contributions: S. Tajbakhsh and F. Hajiali synthesized the polymers and studied the polymerization kinetics and polymer characterizations. S. Tajbakhsh wrote and edited most of the manuscript. M. Marić supervised the project, read, provided feedback, and edited the manuscript.

Preamble to Chapter 2

In this chapter, the underlying features of controlled radical polymerization are provided. The importance of using nitroxide mediated polymerization (NMP) for preparation of polymers was explained and compared with other common controlled radical polymerization techniques (RAFT or ATRP). Next, different polymerization techniques in dispersed aqueous media were discussed as most of the polymerizations in the following chapters were carried out in water as the continuous phase. This is relevant as a major component of my thesis was the development of a coating technology based on spraying a latex onto the desired substrate. Finally, we highlighted different techniques for preparation of polymers with dynamic covalent cross-linking. These polymers have high recyclability and can be reprocessed several times at moderate temperatures, mainly using boronic ester dynamic covalent bonds for preparation of room temperature self-healable polymers.

Chapter 2: Literature Review

2.3. Nitroxide mediated polymerization

The control over the polymer structure and polymerization rate has always been of interest for various applications. Ionic polymerization as a controlled polymerization traditionally has been used to synthesize polymers with narrow molecular weight distributions and controlled polymer microstructure, although the rigorous polymerization conditions (often very low reaction temperature, the need for reagents with high purity and complete removal of air and moisture) were required. The advent of reversible deactivation radical polymerization (henceforward referred as RDRP) provided an approach to efficiently control the polymerization of a wide range of monomers under relatively mild conditions. RDRP, also termed more colloquially as controlled free radical polymerization (CRP), consists of three major categories: nitroxide-mediated polymerization (NMP), reversible addition-fragmentation chain transfer (RAFT) polymerization[8, 17] and atom transfer radical polymerization (ATRP)[11, 18, 19]. The main characteristics of all CRP methods are their relatively narrow molecular weight distribution and active polymer chain ends[20], traits typically exhibited by truly living polymerizations. Unlike conventional RAFT and ATRP techniques, NMP does not need any sulfur-based chain transfer agents nor metallic ligands and as a consequence, NMP does not require exhaustive post-polymerization treatments to remove residual catalysis or other reagents[20, 21]. NMP starts a controlled polymerization in the presence of alkoxyamines. The heating causes the homolytic decomposition of the C-ON bond in the alkoxyamine and the formation of a nitroxide and initiator. An equilibrium occurs between the active NO• macro-radical and the dormant state (a reversible termination), which is favoured[22]. This consequently leads to a low concentration of macro-radicals at any given time and thus reduces probability of irreversible termination reactions, which allows a controlled growth with a linear progression of degree of polymerization with conversion, for a substantial portion of the polymerization. Figure 2.1 shows the activation-deactivation equilibrium in nitroxide mediated controlled/living free-radical polymerization.
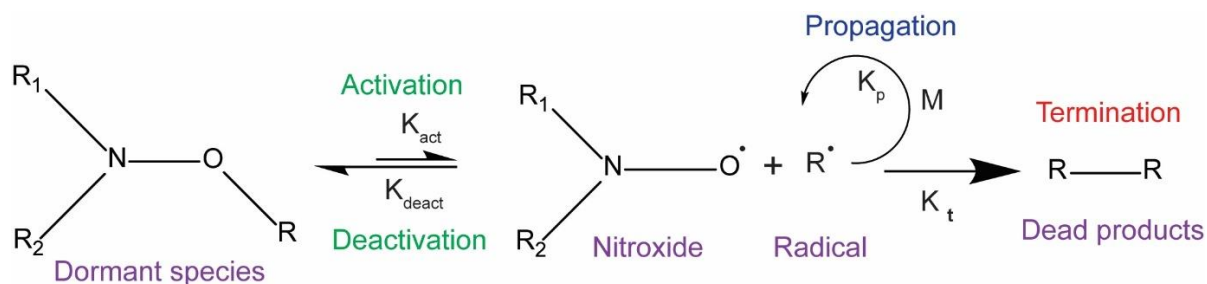
Figure 2.1. Simplified scheme for NMP. This method is based on the reversible activation–deactivation equilibrium between active and dormant species. The reaction controls the concentration of active radicals,

limits the irreversible self-termination reaction and allows the controlled growth of the macro-radicals [23, 24].

The first attempts to conduct NMP was restricted to the synthesis of styrenic-based polymers[25]. However, NMP was improved dramatically during the early 2000s due to the development of new alkoxyamines such as 2,2,5-tri-methyl-4-phenyl-3-azahexane-3-nitroxide (TIPNO) based alkoxyamines[26], N-(2-methyl propyl)-N-(1-(diethyl phosphono-2,2-dimethyl propyl)-O-(2-carboxyl prop-2-yl) hydroxyl amine) (BlocBuilder-MA)[27] and later with 3-(((2-cyanopropan-2-yl)oxy) - (cyclohexyl) amino)-2, 2-dimethyl-3-phenylpropanenitrile (Dispolreg 007)[28, 29]. Figure 2.2 presents the structures of some common alkoxyamines and nitroxides used in NMP. Today, a wide range of monomers can be successfully polymerized in a controlled manner and NMP is reported as a method to make polymers for applications such as drug delivery[30-32], batteries (block copolymer electrolytes (BCE))[33, 34], solar cells[35-37] and coatings[38-40].

a) Nitroxides:

D7   TEMPO   TIPNO   SG1   TEISO

b) Alkoxyamines:
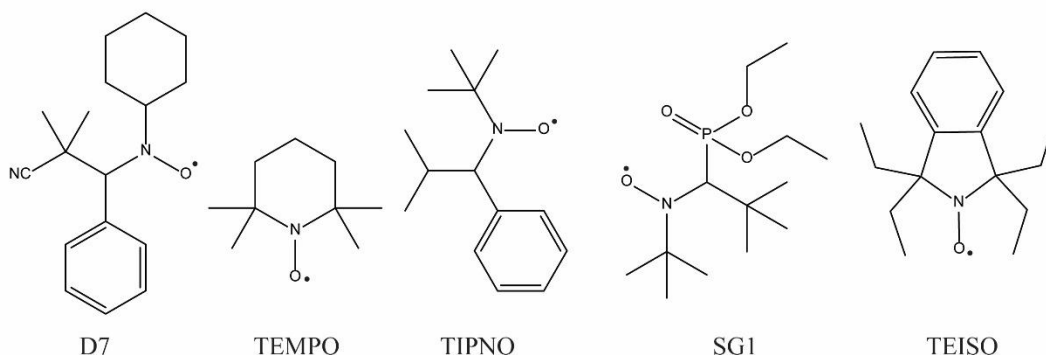
Dispolreg 007   styryl-TEMPO   styryl-TIPNO   BlocBuilder   MONAMS
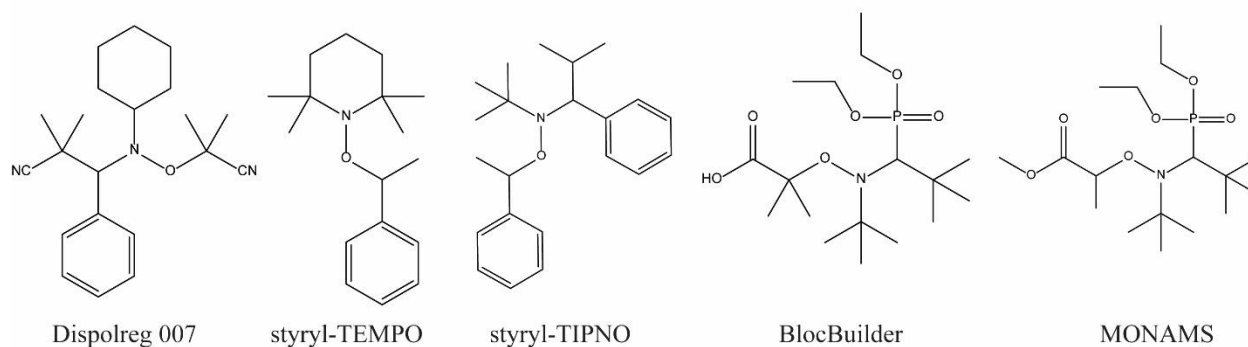
Figure 2.2. a) Structures of some common nitroxides employed in NMP [23, 24, 41, 42]. b) Structures of some common alkoxyamines employed in NMP- TEMPO (2,2,6,6-tetramethylpiperidinyl-1-oxyl)- TIPNO (N-tert-butyl-2-methyl-1-phenylpropyl nitroxide)-SG1 (N-tert-butyl-N-[1-diethylphosphono-(2,2-dimethyl-propyl)])- TEISO (1,1,3,3-tetraethylisoindoline-2-oxyl)- MONAMS (N-tert-butyl-N-1-diethylphosphono-2,2-dimenthylpropyl-0,1-methoxycarbonylet hylhydroxilamine)- Dispolreg 007 (3-(((2-cyanopropan-2-yl)oxy)(cyclohexyl)amino)-2,2-dimethyl-3-phenylpropanenitrile) [24, 28, 43].

2.4. Nitroxide Mediated Polymerization in Dispersed Media

The synthesis of polymers can be done in homogeneous media (e.g. bulk or solution) or in heterogeneous media (e.g. emulsion, miniemulsion or suspension). Bulk polymerization is attractive as solvent is avoided but the viscosity of the medium will often be high and perhaps final conversion will be limited[24]. In addition, autoacceleration phenomenon (sudden increase in polymerization rate) can occur in bulk polymerization[44, 45]. By using solution polymerization, the viscosity can be decreased but the introduction of solvents potentially poses grave environmental issues. The polymerization in aqueous dispersed media has several advantages and is highly in demand for large-scale industrial production of many polymers[46]. Some advantages towards using water are its relatively low cost, benign environmental impact in most cases while also improving heat transfer characteristics, handling and mixing[47]. As this thesis is focused mainly on utilizing polymerization in dispersed aqueous media, the variants will be introduced in detail below.

2.4.1. Emulsion polymerization

Emulsion polymerization was first reported by the Goodyear Company in the 1920s[48]. Emulsion polymerization is used to make materials used in textile treatment, construction, paper additives, paints, adhesives, drug delivery systems and diagnostic tests [49-51]. In this method, hydrophobic monomers are dispersed in the water in the form of monomer droplets having sizes on the order of hundreds of nanometers to several micrometers. The monomer droplets are stabilized by surfactants and the polymerization starts with the use of water-soluble initiator.

The mechanism of emulsion polymerization is complex [52, 53]. However, it can be generally divided into three steps. In the first step, the nucleation occurs within the first few minutes of reaction. During this step, the number of particles (i.e. polymerization loci) are set, which directly affects the dispersity and stability of the final latex. The number of particles relies on different reaction properties such as temperature, hydrophobicity of monomers, process system (batch, semi-batch or continuous), and concentration of monomers, initiator, surfactants or other additives. In the second step, the number of particles and monomer concentration inside each particle are constant. The polymerization occurs with a constant polymerization rate and the size of monomer droplets decreases. In the final step, the polymerization is completed inside the loci. The monomer droplets disappear and monomer concentration inside each particle decreases tremendously and as a result, the polymerization rate also decreases.

In order to describe the mechanism of nucleation, which occurs in the first step, two different methods are proposed. The first method is homogenous nucleation firstly suggested by Ron[54] and discussed later by Fitch and Tsai[55]. Homogenous nucleation takes place when surfactant is not available in the aqueous media and the water solubility of monomers is significant. The nucleation starts with the formation of oligoradicals

as the primary particles and the growth of polymer chains is based on monomer swelling[52]. The second method is called micellar nucleation and was introduced by Harkins[56]. This case happens when the water solubility of monomers is very low and surfactant concentration is above its critical micellar concentration (CMC)[57]. Based on this nucleation method, oligoradicals are formed in the water and start growing until they enter micelles and create new particles. In another case, the oligoradicals may enter the monomer droplets and cause destabilization and broad molecular weight distribution, which is generally not desirable in emulsion polymerization. However, by using high-shear treatments in miniemulsion systems, a high number of nano-sized droplets are achieved and the entrance of oligoradicals to monomer droplets can start a controlled polymerization with narrow molecular weight distribution, high polymerization rate and a stable final latex. Sometimes, a low fraction of nuclei is introduced to the emulsion system from the start of the polymerization. This method is called seeded polymerization in which the nucleation step is bypassed. Figure 2.3 shows the mechanism of emulsion polymerization with micellar nucleation.
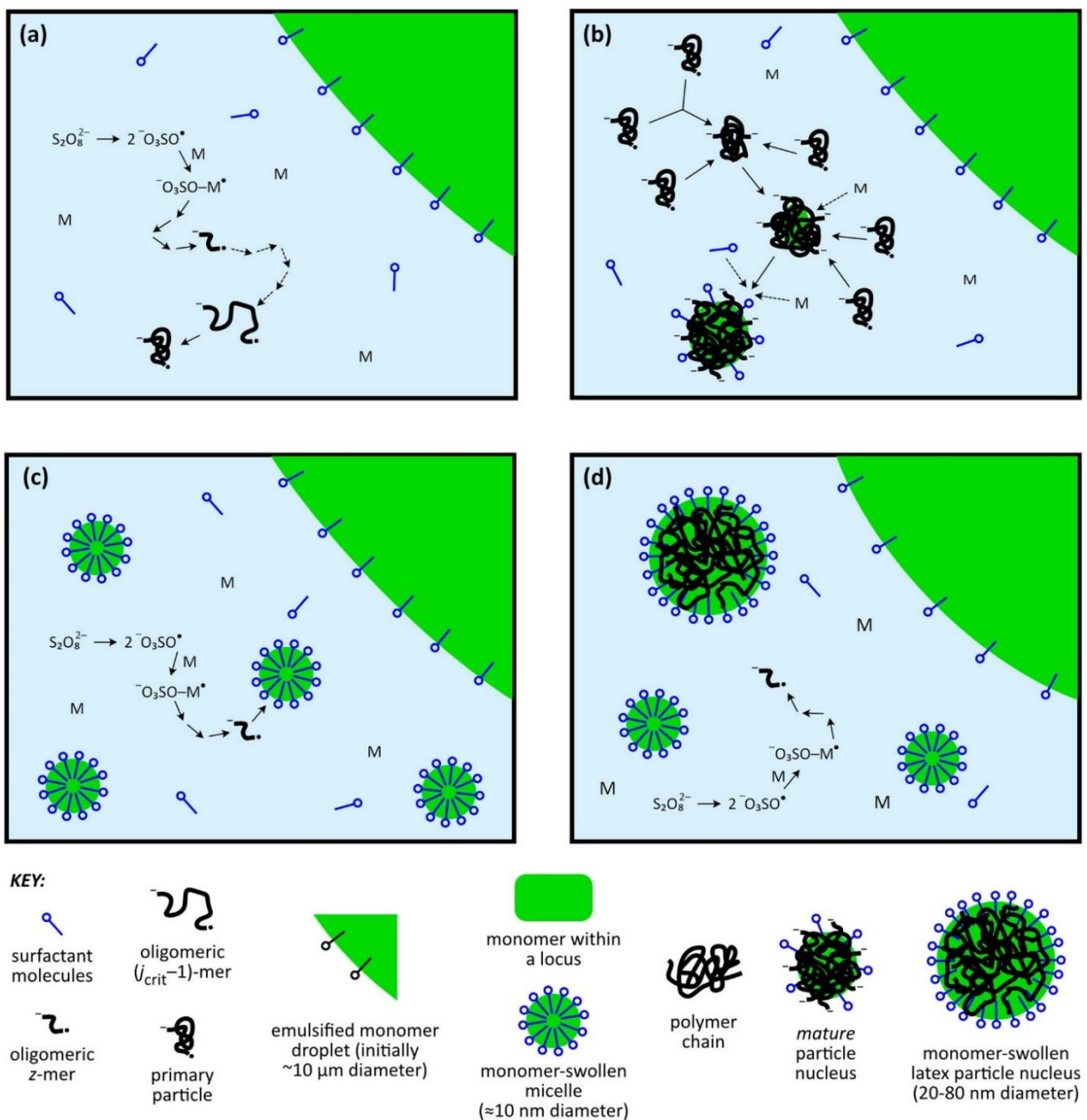
Figure 2.3. The mechanism of emulsion polymerization with micellar nucleation. a) and b) nucleation at surfactant concentration below the CMC. c) and d) nucleation at surfactant concentration higher than the CMC. Adapted with permission from American Chemical Society 2020[58].

With the emergence of RDRP techniques in the early 1990s, it did not take long for reports detailing emulsion polymerization strategies for such systems. Such studies offered the ability to produce polymers with controlled microstructure with water as the continuous phase, which is a feature not possible at the time with established controlled polymerizations like ionic polymerization.

One of the first successful attempts to perform NMP in emulsion was a study performed by Marestin et al[59] who examined the polymerization of styrene at 130 °C. Various TEMPO-based nitroxides (TEMPO, hydroxy TEMPO, tert-butoxy TEMPO, carboxy TEMPO and amino TEMPO) were tested in this study and it was shown that amino-TEMPO had the only acceptable results in terms of final conversion and dispersity. The other nitroxides showed an uncontrolled polymerization with very low conversion (below 1%). This was attributed to the better electrostatic stabilization and optimized hydrophobic and hydrophilic characteristic of amino TEMPO[59]. From that time, many successful NMP were done in emulsion systems using different alkoxyamines[47, 60-64].

2.4.2. Miniemulsion polymerization

Many NMP studies employed miniemulsion polymerization, yielding materials polymers with narrow molecular weight distributions and high latex stability [65-69]. In miniemulsion polymerization, the monomer droplets are dispersed into nm-sized droplets by a high-shear treatment (sonication, homogenization or micro-fluidization). As a result, numerous nano-sized monomer droplets are present as the fundamental particles, with the nucleation step avoided. This is in contrast to conventional emulsion polymerization were monomer droplets serve as reservoirs for monomers to enter the micellar loci. Either water-soluble or oil-soluble initiators are added in miniemulsion and the droplets are stabilized by addition of surfactants[70]. One of the biggest advantages of miniemulsion polymerization over conventional emulsion polymerization is that there are no monomer transport limitations in the aqueous phase and highly hydrophobic monomers can be easily polymerized[58]. An increase in the surfactant concentration in miniemulsion usually reduces the particle size and chain length dispersity [57, 71]. In order to improve the stability of monomer droplets and to avoid the Ostwald ripening effect (transfer of monomer molecules from small particles to larger particles through diffusion or collision), a low concentration of very hydrophobic molecules are added to the miniemulsion (such molecules are termed co-stabilizers)[72, 73]. These molecules can be non-reactive hydrophobic molecules (e.g. linear aliphatics like n-hexadecane), monomers with long alkyl side-chain which will be incorporated into polymers (eg. stearyl methacrylates) or short water-insoluble oligomers[58, 74, 75]. In miniemulsions, the polymerization takes place inside monomer droplets dispersed in aqueous media. Therefore, each droplet acts as a nano-sized reactor and the polymerization process is similar to bulk polymerization[24]. Another important factor in miniemulsion polymerization is the possibility of compartmentalization effects. The compartmentalization of propagating radicals and nitroxides in miniemulsion systems is higher than in emulsions, which decreases the termination rate and enhances the control over the polymerization[76, 77]. Figure 2.4 shows the mechanism of miniemulsion polymerization. Many studies were reported on miniemulsion NMP using different initiation systems [66, 78-82]. Most of them used either TEMPO or SG1 nitroxides along with oil-soluble or water-soluble

radical initiators [43, 66, 83-85]. The first studies by Prodpran et al[71] examined the miniemulsion NMP of styrene in the presence of benzoyl peroxide (BPO) and TEMPO at 125° C. The monomer content was 19 wt% and DOWFAX 8390 surfactant and hexadecane was used as a co-stabilizer. The final conversion of this polymerization was 90% and the molecular weight increased linearly with conversion and the dispersity was below 1.7. From that time, NMPs in miniemulsion were reported using different nitroxides such as SG1 [26, 66, 70, 86, 87], TEMPO [83, 88-90] and TIPNO [26, 91, 92]. The first example using SG1 and AIBN (oil-soluble radical initiator) used styrene as the monomer resulted in incomplete polymerization and a slow polymerization rate[93]. However, when styrene was polymerized using SG1 and a persulfate/metabisulfite initiator (water-soluble redox initiator), a fast well-controlled polymerization with 90% conversion within 8 h was observed[68, 93]. These results highlighted the importance of the high SG1 partitioning between two phases, with deactivation occurring in the aqueous phase, thereby preventing excessive termination and improving the initiator efficiency[94].

The initial molar ratio of nitroxide/initiator directly effects on latex stability and control over of miniemulsion polymerization. Miniemulsion polymerization of styrene with TEMPO as nitroxide and $K_2S_2O_8$ as the radical initiator at 135° C showed that at a ratio of $[TEMPO]/[K_2S_2O_8] = 2.9$, the polymerization was well-controlled (stable latex, no agglomeration and $Đ = 1.1$) and the final conversion was 87% within 6h. Otherwise, the control over the polymerization was not satisfying in terms of colloidal stability (bimodal particle size distributions, agglomeration in latex and reactor fouling) and high dispersity[95].
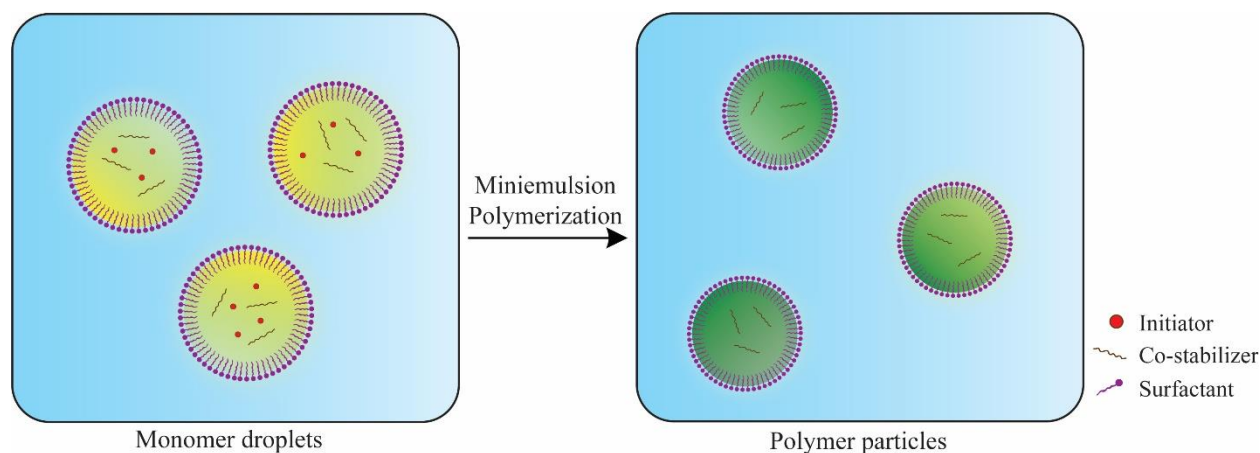
Figure 2.4. The schematic of miniemulsion/microemulsion polymerization. Surfactants and co-stabilizers provide colloidal stability for monomer droplets and polymer particles in miniemulsions.

2.4.3. Microemulsion polymerization

Microemulsions are a mixture of monomers in water with a high concentration of surfactant[96]. In addition, the monomer content is lower than in emulsion or miniemulsion systems (usually in the range of 1~10 wt%) in order to maintain the nanoparticles typically in the range of 20 to ~ 60 nm[97, 98]. The surfactant to monomer ratios (S/M) in microemulsion systems are much higher than emulsion or miniemulsions and are normally in the range of 1 : 1 to 3.3 : 1 w/w[99]. The high concentration of surfactant improves the stability of the dispersions. However, it limits the application of microemulsions in industrial applications like coatings[24, 99]. Li et al studied the NMP of n-butyl acrylate in microemulsions using BlocBuilder® and DOWFAX™ 8390 surfactant at 120° C[99]. In this study, a low S/M was used (0.2 :1 to 0.5 :1 w/w) and a high solid content of 20 wt% was achieved using microemulsion polymerization[99]. However, the dispersity was high ($Đ$ up to 2.77), and the concentration of surfactant is still much higher than in emulsion/ miniemulsion systems.

Many studies were conducted on NMP in microemulsions using different nitroxides such as SG1, TEMPO or TIPNO. By comparing the results from these various studies, it can be concluded that the hydrophobicity of nitroxides is directly related to the polymerization rate. TIPNO and TEMPO are more hydrophobic than SG1 and a stronger confined space effect on deactivation (faster reaction between nitroxide and macroradical in small particles compared to large particles and increase in deactivation rate) is expected for these nitroxides[91, 100]. Therefore, the polymerization rate decreased by adding TIPNO or TEMPO as the nitroxide. Zetterlund et al [100] studied the microemulsion NMP of styrene using 2,2′-azoisobutyronitrile (AIBN) as an initiator and tetradecyltrimethylammonium bromide (TTAB) emulsifier at 100° C to compare the effect of SG1 and TIPNO on polymerization rates and concluded that the polymerization rate using TIPNO was much lower than using SG1 due to its higher hydrophobicity.

2.4.4. Suspension polymerization

In suspension polymerization, hydrophobic droplets are dispersed in water with the help of a stabilizer such as poly(vinyl alcohol) (PVA; to avoid droplet coalescence) and the monomer droplet size is around 2-1000 µm. Although the use of surfactant is necessary to avoid aggregation, the concentration of surfactant absorbed to the polymer particle surface is negligible compared to the size of the droplet [101, 102]. Suspension polymerization does not require high-shear treatment like emulsion/ miniemulsion systems and the separation of polymer from dispersion can be done by a simple filtration[103]. Polymerization rate in suspension systems is high because of the high local monomer concentration and low viscosity of the system even with high monomer content. However, the polymerization yield may decrease due to the formation of nano-sized polymer particles. These nanoparticles are produced because of secondary nucleation during the suspension polymerization and are difficult to separate via filtration. The formation

of nanoparticles increases especially when water-soluble monomers are added to the suspensions of hydrophobic monomers[104]. The secondary nucleation can also lead to uneven nitroxide partitioning between particles and increase in dispersity. However, this drawback can be eliminated industrially by adding aqueous-based inhibitors[105]. Usually, a small amount of sodium nitrite will be added to the dispersion to hinder the polymerization and secondary nucleation in aqueous media[103].

The first suspension controlled radical polymerization was reported by Georges et al in 1993[106]. TEMPO and benzoyl peroxide (BPO) were used to initiate and control the polymerization of styrene at temperatures of 125-150° C. The final conversion was high (more than 71%) and the final dispersity was lower than 1.3. Okubo and coworkers[107] employed a suspension process for NMP of styrene and divinylbenzene (DVB) in order to make microgels. The TEMPO/BPO were used for initiation and controlling the polymerization. The monomer content was 9 wt% (1wt% of DVB) and the polymerization took place at 125° C to reach conversions of 47-72%. Ballard et al[103] polymerized butyl methacrylate and methyl methacrylate using oil-soluble Dispolreg 007 initiator at 83~87 °C to high conversion and up to 40% solids content with molecular weights up to 100,000 g mol^{-1}.

2.5. Applications of surfactants

Surfactants play a crucial role in the production of polymers in dispersed media. They provide the stability for the monomer and polymer droplets in water. However, they can adversely affect adhesion, gloss and water sensitivity of the final product [108-110]. They also can decrease the mechanical stability under high shear due to the possibility of desorption from the surface of particles in latex[49]. In order to overcome the adverse effects of conventional surfactants, polymerizable surfactants (surfmers) have been presented as an alternative. By using surfmers, decrease in water and vapor permeability and improvements in adhesion and water resistance have been observed [108, 111, 112]. One of the creative ways of using surfmers in nitroxide-mediated emulsion polymerization is making amphiphilic macroalkoxyamines to act as a dual initiator/surfactant, which is discussed in detail below.

Pan et al[113] studied the effect of surfactant concentration on particle size. Using DOWFAX™ 8390 as the surfactant, the emulsion polymerization of styrene was conducted at 125° C using TEMPO-terminated oligomers of polystyrene. It was shown that increasing the surfactant concentration from 1.25 to 15 mM resulted in a decrease in particle diameter from 150 to 60 nm and enhanced the polymerization rate. However, using surfactants causes serious drawbacks in coating applications due to reducing adhesion and gloss [108, 109, 114]. In addition, in order to achieve high solid contents with acceptable concentration of surfactant, droplet size will be in the particle size range of several microns[114, 115]. Therefore, additional steps seem necessary to achieve a higher yield.

In a related study, Cunningham et al[116] synthesized polystyrene by use of benzoylstyryl-TEMPO (BST)-initiated miniemulsion polymerization at 135 °C in presence of SDBS (sodium dodecylbenzenesulfonate) and Dowfax 8390 surfactants. It was shown that the addition of surfactants reduced the dispersity. Furthermore, by increasing the concentration of SDBS, conversion could be increased to 95%. However, changing the concentration of Dowfax 8390 did not affect the conversion.

Along with using surfactants, intensive agitation is needed to break the droplets to the size range of 60-200 nm. Several devices can be used in order to supply the high degree of agitation including high pressure homogenizers[117, 118], static mixers [117, 119] and sonicators[115]. The sonication process is hard to scale up industrially but it is very effective at lab scale[114]. However, homogenization or a combination of homogenization and static mixing are the most promising way industrially of preparing miniemulsions with high solid contents and nano-sized particles with narrow size distribution[114].

To avoid the high energy mixing necessary in miniemulsion systems, Prokopov and Gritskova[120] and Parker et al [121] proposed a technique based on *in situ* formation of surfactants. This method relies on the formation of *in situ* surfactant at the water-oil interface and is able to considerably lower the interfacial tension and reduce the dispersity of the miniemulsion systems[122, 123]. As an example, Guo et al[122] employed oleic acid/ potassium hydroxide to generate potassium oleate as the surfactant and to enhance the colloidal stability of the latexes. Although a low amount of energy is needed for a proper mixing in this miniemulsion process, this method is not practical for industrial applications. This is due to the high concentration of additives (oleic acid, hexadecane and potassium hydroxide up to 31 wt%, 7 wt%, 10 wt%, respectively, relative to the monomers) and high possibility of coagulation[122].

2.6. Macroinitiators in aqueous dispersed media

Macroinitiators can be used as stabilizers on the interface of particles or co-stabilizers inside the particles to increase the colloidal stability and simultaneously initiate and control. Using controlled free-radical polymerization methods such as NMP, ATRP and RAFT is highly attractive for the preparation of macroinitiators and polymerization of water-insoluble monomers in water. The hydrophobic macroinitiators can be synthesized by bulk or solution polymerization and added to the dispersed aqueous medium with other hydrophobic monomers. They can also be produced in mini or microemulsion and be used as the seed for the polymerization of the hydrophobic monomers in water[124, 125]. The water-insoluble macroinitiators act as a co-stabilizer within the particles and droplets and reduce Ostwald ripening[57, 126, 127].

Hydrophilic/amphiphilic macroinitiators can also be made in order to act simultaneously as initiator, stabilizer and control agent[128]. Using water-soluble macroinitiators, the amount of surfactant in the polymerization medium can be limited or the surfactant can be completely removed. The polymerization

system operates via the chain extension of the macroinitiator by addition of monomers inside the droplet. As a result of the reaction, amphiphilic block copolymer chains can be produced which in most of the cases make spherical micelles [41, 129, 130]. In a study by Stoffelbach et al[131], poly(ethylene oxide)-*b*-polystyrene block copolymer (M_n = 10 640 g mol^{-1} and $Đ$ = 1.05) was synthesized by ATRP and used as an amphiphilic macroinitiator for miniemulsion polymerization of n-butyl methacrylate (BMA), styrene (S), and butyl acrylate (BA) (M_n up to 63000 g mol^{-1} and $1.1 < Đ < 1.5$). Delaittre et al[41] used NMP (in 1,4-dioxane solution at 120 °C) to prepare SG1-based water-soluble poly(sodium acrylate) macroinitiator (M_n = 1900 g mol^{-1} and $Đ$ = 1.17). Then, the poly(sodium acrylate) macroinitiator was employed for emulsion polymerization of S and BA to produce polymers with M_n up to 100 kg mol^{-1} and $Đ < 2.8$[41]. For the use of RAFT polymerization in miniemulsion using a macroinitiator, Manguian et al[132] developed poly(2-(diethylamino)ethyl methacrylate) macroinitiator (macro-RAFT agent) (M_n = 5700 g mol^{-1} and $Đ$ = 1.31) and used it for emulsion polymerization of S at 70 °C. In a similar study, Božović-Vukić et al[133] synthesized a hydrophilic RAFT- agent functional poly(4-vinylpyridine) macroinitiator (M_n = 800 g mol^{-1} and $Đ$ = 1.04) and used it to stabilize and initiate the emulsion polymerization of an azeotropic monomer mixture of AN and S at 80 °C. The resulting block polymer (M_n = 48800 g mol^{-1} and $Đ$ = 4.0) reached a monomer conversion of 100% in 11 hours[133].

We used the miniemulsion polymerization technique for preparation of polymer resins to be used in coatings. This was done by NMP of highly hydrophobic monomers in presence of Dispolreg 007 alkoxyamine. Using miniemulsion polymerization, the nucleation step was skipped, and the monomer transportation limitations were avoided. In addition, the miniemulsion polymerization is easy to apply and the final polymer latex shows a high colloidal stability. However, additional properties are desirable and thus we studied the synthesis of self-healable polymers using NMP. To apply the polymers for coating applications, the self-healing at ambient conditions without external triggers are highly in demand in the coating industry[134-136]. In the following section, we thus provide the background concerning self-healing polymers in the context of this thesis.

Self-healing Polymers

Polymers without cross-linking bonds (i.e. thermoplastics) can be melted, recycled and reshaped by simply by applying heat. However, they are soluble in solvents (low solvent and chemical resistance) and their mechanical properties could be limited. The polymer structures with permanent cross-linking bonds, which are classically termed as thermosets, have high solvent resistance and improved mechanical properties, although they cannot be recycled or reshaped after the formation of cross-links. After the introduction of the dynamic covalent chemistry by Rowan et al[137], however, these classical definitions became blurred.. In

the past two decades, polymers with dynamic covalent bonds were introduced as an alternative for thermoplastics and thermosets[138-140]. Figure 2.5 shows the schematic of polymer structures for thermosets, thermoplastics and polymers with dynamic cross-linking and displays some of the important applications of reversible covalent bonds.
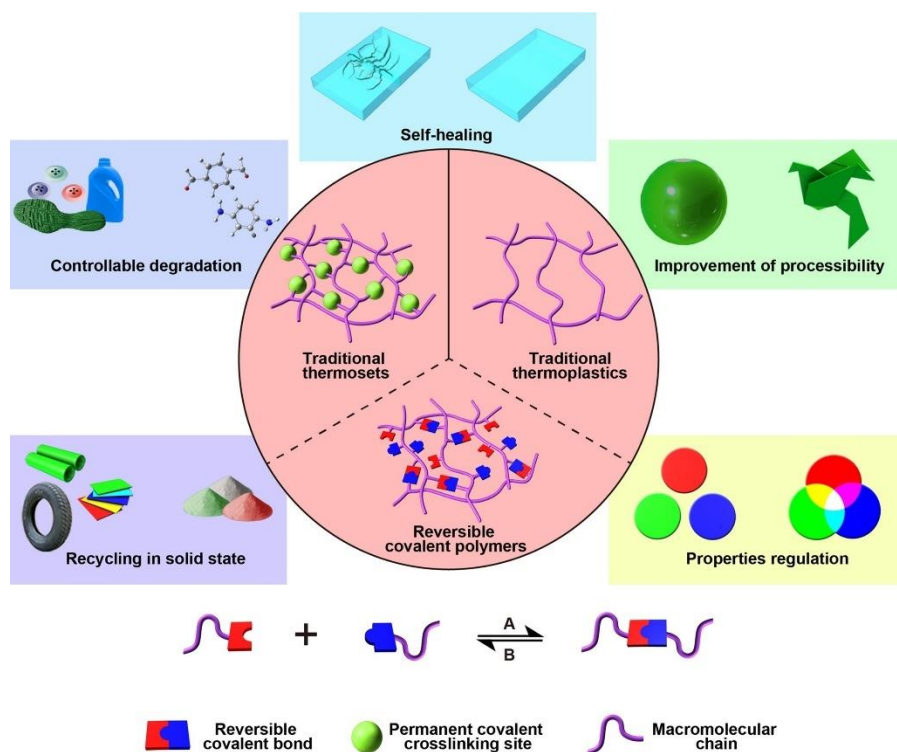
Figure 2.5. schematic representation of polymer structures for thermosets, thermoplastics and polymers with dynamic cross-linking bonds. Common applications of reversible covalent bonds in polymers have been depicted. Adapted with permission from Elsevier 2018[141].

The dynamic cross-linking bonds within the polymer structure not only result in high solvent resistance and enhanced mechanical properties but also provide high reprocessability, recyclability and self-healing[139]. Covalent adaptable networks (also known as CANs) are generally categorized into dissociative and associative cross-linking networks based on their exchange mechanisms. In dissociative CANs, the cross-linking bonds break in the presence of an external stimuli like heat and the new covalent bonds can be re-formed in another position. Reversible addition (e.g. Diels-Alder reactions) and condensation rearrangements are common examples of the dissociative CANs for polymers. It should be noted that the presence of condensate as a trigger is required for condensation reactions in polymer networks to enable the reprocessing[142]. In polymers with dissociative CANs, heating decreases the viscosity and the cross-linking density is dependent on temperature. Therefore, the stiffness and mechanical properties of polymers with dissociative CANs can vary with changes in temperature[142, 143].

The bonds in associative CANs do not break by heating and the breakage and the formation of covalent bonds occur simultaneously, with no net change in bonds at any given time. This results in polymers with similar properties of permanently cross-linked polymer networks (high stiffness, mechanical properties and solvent resistance at any temperature) but with the ability to be reprocessed[143]. However, the dynamic bond adaptability and lifetime can be limited due to termination reactions[143]. Some common dynamic associative exchange reactions are transamination of vinylogous urethanes[143, 144], carboxylate transesterification[145, 146] and disulfide exchange reactions[147, 148]. Figure 2.6 compares the dissociative and associative CANs.
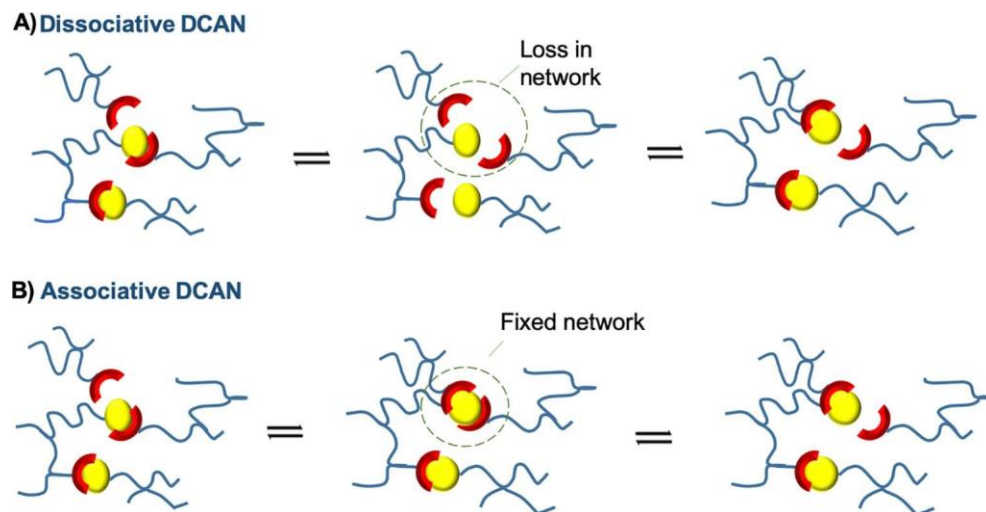
Figure 2.6. The dynamic covalent adaptive networks (DCAN) with a) dissociative b) associative bonds. Printed with permission from Elsevier 2020[149].

One of the most studied dynamic covalent cross-links for the preparation of self-healing polymers is the boronic ester cross-coupling. The boronic-based exchange reactions are either based on the boronic transesterification[150-152] or boroxine reversible bonds[153-155]. However, more attention has been paid to vitrimers based on boronic transesterification due to the kinetic tunability and strength of B-O bonds[156]. The boronate ester can be formed by the condensation reaction of a boronic acid and a diol. This reaction is reversible at room temperature in the presence of water and has been used for preparation of hydrogels [157-160]. The simple conditions for boronic ester formation (low temperature and presence of water as a trigger) enables its use for the preparation of self-healable materials for coating applications. The dynamic boronic ester covalent bonds can heal the damages and scratches on the polymer coating surface at ambient conditions without any external stimulation.

Miniemulsion permits coating materials without using any VOCs while self-healing materials have application for coatings that do not require extensive repair steps. Both of these aims were addressed in my thesis specifically targeting coatings for the aerospace industry.

In conclusion, NMP was used to prepare polymers with different mechanical and thermal properties in miniemulsions and organic solvents. Self-healable polymers were also synthesized by NMP to control the polymerization rate and to prepare polymers with well-distributed functional monomers (boronic acid and diol-functional monomers). In the following chapters, each section will be discussed thoroughly.

Preamble to Chapter 3

This chapter investigates the preparation of IBOMA/C13MA copolymers by nitroxide mediated miniemulsion polymerization using SG1-containing amphiphilic macroinitiators. The macroinitiator was synthesized by nitroxide mediated polymerization (NMP) of oligo (ethylene glycol methyl ether) methacrylate (OEGMA) and acrylonitrile in presence of BlocBuilder (BB) alkoxyamine in toluene at 90 °C. Then, after purification and isolation, the prepared macroinitiator was used to initiate the NMP of isobornyl methacrylate (IBOMA), a mixture of alkyl methacrylates with average side chain length of 13 carbons (C13MA) or a mixture of these two monomers in miniemulsion. The synthesized amphiphilic macroinitiator acts a surfactant and initiator simultaneously. However, it was shown that the best colloidal stability was provided by the addition of 2 wt% DOWFAX 8390 (surfactant) and 0.8 wt% n-hexadecane (co-stabilizer). The effect of the reaction temperature, different ratios of IBOMA/C13MA and the addition of surfactant and co-stabilizer on the kinetics of miniemulsion polymerization were studied. In general, this chapter illustrated the application of commercially available BB alkoxyamine for the polymerization of bio-based monomers in miniemulsion and ultimately for use in making polymers in such media with controlled microstructure. This study is in press to the *Journal of Polymer Science*, 1-14, 2021 (https://doi.org/10.1002/pol.20200870).

Chapter 3: Synthesis of Bio-based Poly(Methacrylates) Using SG1-containing Amphiphilic Macroinitiators by Nitroxide Mediated Miniemulsion Polymerization

ABSTRACT

SG1-based amphiphilic macroinitiators were synthesized from oligoethylene glycol methyl ether methacrylate (OEGMA) and 10 mol% acrylonitrile or styrene (as the controlling comonomer) to conduct the nitroxide mediated polymerization (NMP) of bio-based methacrylic monomers (isobornyl methacrylate (IBOMA) and C13 alkyl methacrylate (C13MA)) in mini-emulsion. The effect of the addition of surfactant (DOWFAX 8390), co-stabilizer (n-hexadecane) and different reaction temperatures (80, 90 and 100 °C) on polymerization kinetics was studied. We found that the NMP of IBOMA/C13MA using amphiphilic macroalkoxyamines were most effective during miniemulsion polymerization (linear trend of M_n versus conversion and high latex stability) in presence of 2 wt% surfactant and 0.8 wt% co-stabilizer (relative to monomer) at 90 °C. The effect of surfactant, co-stabilizer and temperature on particle size during the polymerization was studied and suggested a decrease in initial particle size with the addition of surfactant and co-stabilizer. Finally, the thermal properties of IBOMA/C13MA polymers, prepared by amphiphilic macroinitiators, were examined thoroughly, indicating a T_g in the range of -44 °C < T_g < 109 °C.

3.1. INTRODUCTION

Reversible deactivation radical polymerization (RDRP) of monomers from sustainable sources has attracted considerable attention during the last decade.[161-165] The preparation of polymers with a well-designed microstructure, the possibility of making block copolymers and narrow molecular weight distribution are some of the conventional advantages of RDRP techniques for many current technologies.[13, 23, 166] Using bio-based monomers adds potential benefits towards decreasing the carbon footprint of the process but also may provide additional benefits to the performance not necessarily originally expected.[167, 168] Nitroxide mediated polymerization (NMP) is among the simplest of RDRP techniques, only requiring a low concentration of thermally labile alkoxyamine to start the polymerization.[21, 23, 169] Upon heating, alkoxyamines decompose to form the persistent radical and initiating species to trigger the polymerization, which is governed by the reversible termination between the macroradicals and dormant, de-activated polymer. Initially, NMP was limited essentially to the polymerization of styrenic monomers and required

high reaction temperatures exceeding 120 ºC.[25] However, the advent of alkoxyamines based on 2,2,5-tri-methyl-4-phenyl-3-azahexane-3-nitroxide (TIPNO) and N-tert-butyl-N-[1-diethylphosphono-(2,2-dimethyl- propyl)] (SG1) nitroxides improved the applicability of NMP for a wider range of monomers together with comparatively lower reaction temperatures.[26, 170] One of the most studied of the SG1-based alkoxyamines is N-(2-methylpropyl)-N-(1-(diethylphosphono-2,2-dimethylpropyl)-O-(2-carboxylprop-2-yl)hydroxylamine) (BlocBuilder-MA or BB alkoxyamine, Arkema), which has been applied for the polymerization not only of styrene derivatives, but also acrylates and methacrylates, with some modification.[27, 171] With respect to the case of methacrylates, the homopolymerization of methacrylates using NMP has traditionally been difficult due to the high activation/deactivation equilibrium constant (K) of methacrylates and the cross-disproportionation effect.[172, 173] This problem can be solved by copolymerization of methacrylates with a low concentration of monomers with low K (e.g. acrylonitrile (AN) and styrene (S)) to decrease the average K.[172, 174]

In addition, the high water-solubility of BB alkoxyamine (when neutralized with base) presents interesting issues towards applications in dispersed aqueous polymerizations (e.g. emulsion, miniemulsion and suspension polymerization).[70] To use BB for NMP in dispersed aqueous systems, one common method is to prepare macroinitiators from the desired monomers and high chain-end fidelity prior to the polymerization.[41, 175-177] Depending on the monomers, the SG1-terminated macroinitiator can be either water soluble or insoluble. If hydrophobic macroinitiators are used, they can act as a co-stabilizer and also initiate the polymerization within monomer/polymer particles.[47, 113] On the contrary, water-soluble macro-alkoxyamines can be used as macromolecular surfactant and initiator simultaneously.[61, 70]

Isobornyl methacrylate (IBOMA, 71% bio carbon content, derived from pine sap) and C13-alkyl methacrylates (C13MA, 76% bio carbon content, from natural oils) can be used to synthesize copolymers with high bio-content with readily adjustable glass transition temperatures (T_gs), as IBOMA provides stiffness while C13MA provides low temperature flexibility.[178-181] The IBOMA/C13MA copolymers can be used for coating and adhesive applications. We previously synthesized IBOMA/C13MA polymers by NMP using different initiation methods (pure BB and Dispolreg 007 alkoxyamine) in organic solvents and miniemulsions.[162, 182] Herein, we polymerized IBOMA/C13MA monomers using a water-soluble macroinitiator, attempting to avoid charged species as the macroinitiator, which could degrade the alkoxyamine. The addition of an amphiphilic macroinitiator could also limit or eliminate the use of surfactants in emulsions or miniemulsions.[175, 183] This prevents the common disadvantages associated with the presence of high concentrations of surfactants in polymer structures (such as the modification of mechano-thermal properties) after drying.[184, 185] The block copolymers of oligoethylene glycol methyl ether methacrylate (OEGMA) and S were previously used as the surfactants for emulsion polymerization of S, indicating the applicability of OEGMA monomers for preparation of polymeric surfactants.[186] The

incorporation of OEGMA can also introduce self-assembly properties[187-189] and decrease cell adhesion and protein adsorption to the polymer structure in bio-applications[190, 191]. Qiao et al[192] developed SG1-based macroinitiators using OEGMA ($M_{n,Average}$ = 950 and 300 g mol^{-1}) for NMP of n-butyl methacrylate. In this study, the SG1-based amphiphilic macroinitiators were synthesized from OEGMA ($M_{n,Average}$ = 500 g mol^{-1}) and 10 mol% controlling comonomers (AN or S) to use for the emulsion polymerization of bio-based methacrylates. We adopted a similar approach to use a non-ionic poly(OEGMA)-rich macroinitiator for the polymerization of IBOMA and C13MA, hopefully leading to water-based coating/adhesive materials, where we characterized the macroinitiator, studied the kinetics of miniemulsion polymerization and assessed the colloidal and thermal stability of polymers derived from the NMP process using BlocBuilder type initiators.

3.2. EXPERIMENTAL

3.2.1. Materials

Isobornyl methacrylate (IBOMA, >99%, Evonik), C13.0 alkyl methacrylate (C13MA, methacrylic esters with an average alkyl chain length of 13 monomer units, >99%, Evonik), oligoethylene glycol methyl ether methacrylate (OEGMA, $M_{n,Average}$ = 500 g mol^{-1}, >99%, Aldrich) and acrylonitrile (AN, >99%, Aldrich) were used to prepare the polymers. The monomers were passed through a column filled of a mixture of basic alumina (Brockmann, Sigma Aldrich) and calcium hydride (5 wt% relative to basic alumina, 90-95% reagent, Sigma Aldrich) to remove inhibitors. N-(2-methylpropyl)-N-(1-diethylphosphono-2,2-dimethylpropyl)-O-(2-carboxylprop-2-yl) hydroxylamine (BlocBuilder-MA™, BB,99%, Arkema) alkoxyamine was used to initiate the polymerizations. DOWFAX™ 8390 surfactant (35 wt% active content) and n-hexadecane (99%) were received from Dow Chemical and Sigma Aldrich, respectively. Methanol (MeOH, >99%), tetrahydrofuran (THF, 99.9%, HPLC grade) and toluene (>99%) solvents were obtained from Fisher Scientific. To prepare samples for ^{1}H NMR test, samples were dissolved in deuterated chloroform (CDCl$_3$, ≥99%, Cambridge Isotopes Laboratory). Reverse osmosis water (type 2 with the resistivity of ∼ 1.10 MOhm·cm at 25 °C) was used to prepare the latexes. All the polymerizations were conducted under nitrogen (99.99%, Praxair).

3.2.2. Methods

3.2.2.1. M_n, X and $Đ$ Measurements

Monomer conversions (X) were measured gravimetrically using the procedure mentioned in our previous study[162]. Number average molecular weight (M_n) and molecular weight distribution ($Đ$) were measured by gel permeation chromatography (GPC, Waters) relative to PMMA standards (Varian Polymer Standards;

M_n range of 875 to 1677000 g mol^{-1}) at 40 °C in THF (HPLC grade). The GPC samples were dried to remove the water. Next, the THF (HPLC grade) solvent was added to dilute the samples to the concentration of ~5 mg.ml^{-1}. Three GPC columns of HR1, HR2 and HR4 Styragel® (for THF solvent) with molecular weight measurement ranges of $10^2 – 5 \times 10^3$ g mol^{-1}, $5 \times 10^2 – 2 \times 10^4$ g mol^{-1} and $5 \times 10^3 – 6 \times 10^5$ g mol^{-1}, respectively, were used to measure M_ns and Đs. A guard column was connected to the inlet to protect the GPC columns. Polymer compositions were determined by ^{1}H NMR (Bruker Avance III HD 500 MHz, 16 scans) using deuterated CDCl$_3$.

3.2.2.2. Thermoanalytical Analyses

Latex samples were dried inside a fume hood for 48 h and then under vacuum for 24 h. Dried samples were fully dissolved in toluene to prepare them for precipitation. Then, samples were precipitated in methanol to remove solvents and unreacted monomers completely before thermoanalytical analyses. The samples were dried again inside a fume hood for 24 h and then under vacuum overnight at room temperature prior to measurement. Differential scanning calorimetry (DSC, Q2000, TA Instruments) was used to measure T_ms and T_gs of polymers. T_ms and T_gs were calculated by inflection method. For each sample, three scans per cycle (heat/cool/heat) with heating rate of 15 °C min^{-1} and cooling rate of 50 °C min^{-1} was performed under nitrogen. The calibration of DSC was carried out using indium and benzoic acid standards before the test. The thermal stability of samples was determined by thermogravimetric analysis (TGA) on a Q500 TA instruments under nitrogen. The samples were placed in aluminium pans and were heated up to 600 °C with the heating rate of 15 °C min^{-1} to measure the decomposition temperatures (T_{dec}s).

3.2.2.3. Particle Size and Zeta Potential

Particle size and zeta potential of samples were measured by a Malvern Zetasizer Nano-ZS (with a 4 mW He–Ne laser at 633 nm and an avalanche photodiode detector) at 25 °C. For the dynamic light scattering (DLS), samples were diluted with RO water to an approximate concentration of 0.01-1000 mg ml^{-1} (10^{-3} – 1 % mass). The reported particle size for each sample is the average of 5 measurements. To determine zeta potential, samples were diluted by adding 0.1 ml of final latex samples in 111 ml of RO water and the pH≈7 was set for all the samples.

3.2.3. Preparation of SG1-based Amphiphilic Macroinitiators

SG1-based macroinitiators were synthesized before the polymerizations. The polymerization setup consisted of a 50 ml three neck round bottom flask with a magnetic stir bar, connected to a reflux condenser at 3°C. The condenser was filled with a mixture of ethylene glycol and distilled water (20/80 vol%). The setup was placed inside a heating mantle on a magnetic stirrer to apply a constant stirring while heating and

controlling the reaction temperature. The heating mantle was connected to a temperature controller with a temperature sensor. The temperature sensor was placed inside the reactor from one of the side necks to measure the reaction temperature and control the heating rate. To the reactor was added a mixture of 90 mol % OEGMA and (10 mol% AN or S), BB alkoxyamine and 50 wt% toluene. To achieve high chain end fidelity for macroinitiators, the reaction stopped at low conversions to prevent termination events. As an example, for preparation of p(OEGMA-*stat*-AN) macroinitiator (M_n = 7200 g mol^{-1} and $Đ$ = 1.24), theoretical molecular weight at 100% monomer conversion (target M_n) of $M_{n,target}$ = 15000 g mol^{-1} was considered for the polymerization and the reaction was stopped after 45 min (X= 33.3 %). OEGMA (91.55 g, 143.72 mmol), AN (0.85 g, 15.97 mmol), BB (2.35 g, 6.16 mmol) were dissolved in 50 wt% toluene and the solution was added to the reactor. The solution was purged with nitrogen for 30 min before heating. The solution was heated to 90 °C at a heating rate of 10 °C min^{-1}, while the nitrogen bubbling continued during the polymerization. The t=0 was considered when the temperature reached 75 °C. The samples were taken periodically for ^{1}H NMR and GPC. The final solution was dialyzed using a dialysis membrane (Spectra/Por 6; MWCO = 1 kD) in deionized water to purify the macroalkoxyamines from the unreacted monomers and toluene. Then, the final solution was dried completely to obtain the pure macroinitiator.

3.2.4. Nitroxide Mediated Miniemulsion Polymerization of IBOMA/C13MA Using SG1-based Amphiphilic Macroinitiators

Nitroxide mediated miniemulsion polymerization of IBOMA, C13MA or a mixture of both monomers in the presence of 10 mol% AN or S controlling comonomers was conducted at 90 °C. The polymerization setup was similar to the one used for the preparation of macroinitiators with some adjustment for the miniemulsion polymerization conditions. To prepare the miniemulsion, the amphiphilic macroinitiator was added to water (with or without DOWFAX™ 8390 surfactant) and mixed for 15 minutes to prepare the aqueous phase. IBOMA, C13MA and AN (with or without addition of n-hexadecane) were mixed for 15 minutes to prepare the organic phase. Next, the two solutions were mixed together in a beaker with a magnetic stirrer for another 30 minutes to make a homogeneous miniemulsion. Finally, the miniemulsion was sonicated for 10 minutes in a cold-water bath using a Hielscher sonicator UP200S (50% duty cycle and amplitude of 70%) and transferred to the reactor. The latex solid content of 21 wt% and $M_{n,target}$ of 45 kg mol^{-1} were set for all the polymerizations. The initial latex was purged with nitrogen for 30 min before the polymerization for deoxygenation of the system. The nitrogen flow was kept inside the reactor during the polymerization.

3.3. RESULTS AND DISCUSSION

3.3.1. Synthesis of Macroinitiators

The first step of miniemulsion polymerization was the preparation of SG1-based macroinitiators. The macroinitiators were synthesized from OEGMA along with 10 mol% of the controlling co-monomer, either S or AN. OEGMA is a non-ionic water-soluble monomer that was used to make amphiphilic macroinitiators and polymeric surfactants [186, 193] while BlocBuilder (BB) alkoxyamine was used as the unimolecular initiator. Consequently, OEGMA polymerized with BB served as the dual surfactant/initiator. Figure 3.S1 (Supplementary Information) displays more details about the NMP of OEGMA and preparation of macroinitiator. Figure 3.1 presents a schematic for the preparation of macroinitiators (with 10 mol% AN as the controlling comonomer).
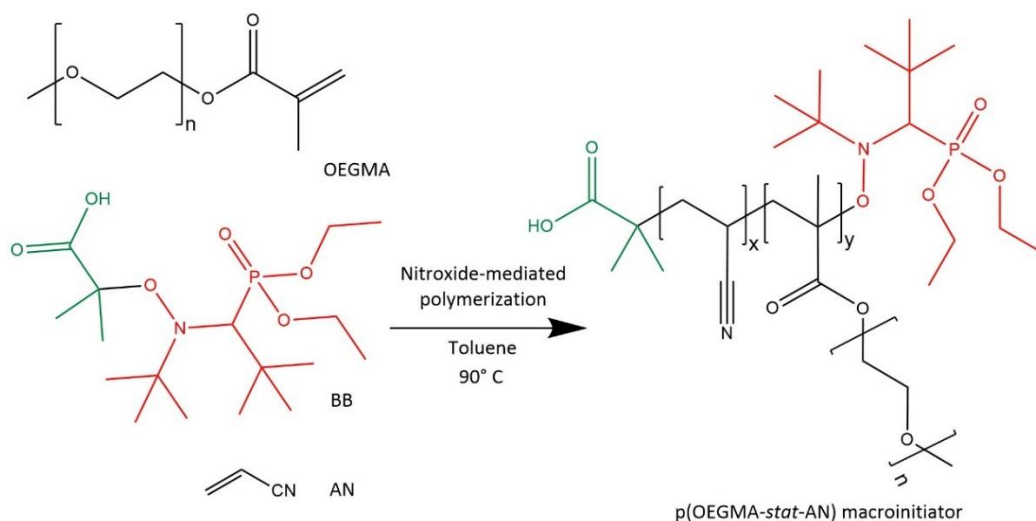
Figure 3.1. Schematic reaction for synthesis of p(OEGMA-*stat*-AN) macroinitiator. Nitroxide mediated polymerization of OEGMA monomers ($M_n \approx 500$ g mol^{-1}) with 10 mol% AN (controlling comonomer) was conducted in toluene at 90 °C using BB.

Two different macroinitiators were synthesized, employing two different controlling co-monomers; i.e. AN and S; to investigate the effect of the controlling co-monomer on the efficiency of the macroinitiator. Table 3.1 presents the characterization of macroinitiators used in this study.

Table 3.1. Molecular characteristics of the macroinitiators.

Macroinitiator	$f_{OEGMA,0}{}^{a}$	$F_{OEGMA,0}{}^{b}$	Reaction time (min)	$M_{n,target}{}^{c}$ (g mol^{-1})	$M_{n,final}{}^{d}$ (g mol^{-1})	$Đ{}^{d}$
p(OEGMA-*stat*-AN) macroinitiator ^{e}	0.90	0.91	45	15000	7200	1.24

p(OEGMA-*stat*-S) macroinitiator	0.90	0.95	10	15000	5500	1.19

[a] The molar ratio of OEGMA monomer in the initial feed for preparation of macroinitiator.

[b] Molar fraction of OEGMA in polymer composition.

[c] Target number average molecular weight (theoretical number average molecular weight at 100% monomer conversion)

[d] final number average molecular weight ($M_{n,final}$) and dispersity of polymer chains (Đ) measured by GPC with PMMA standards in THF at 40 °C.

[e] SG1-based macroinitiator prepared by the NMP of OEGMA and 10 mol% controlling comonomer (AN or S) in presence of BB alkoxyamine.

3.3.2. Nitroxide Mediated Miniemulsion Polymerization of IBOMA/C13MA Using Amphiphilic Macroalkoxyamines

The macroinitiators were subsequently used for the nitroxide mediated miniemulsion polymerization of IBOMA, C13MA or IBOMA/C13MA with the mixture of 50:50 $\frac{[IBOMA]_0}{[C13MA]_0}$. We investigated the effect of different reaction conditions, reaction temperatures and monomer compositions on polymerization kinetics and latex stability. Table 3.2 lists the experimental conditions and kinetic results of polymerizations. For all the experiments, we set the same target molecular weight ($M_{n,target}$ = 45000 g mol^{-1}) and initial macroinitiator concentration ($[MI]_0$ = 0.005 mol L^{-1}). Apparent rate constant of polymerization ($k_P[P^\bullet]$), was measured from the slope of kinetic plots ($\ln((1-X)^{-1}$) versus reaction time) in the first 60 minutes of polymerization. The results are discussed in detail in the following sections.

Table 3.2. Experimental conditions and kinetic results for nitroxide- mediated miniemulsion polymerization of IBOMA/C13MA using SG1-based amphiphilic macroinitiators.

Experiment ID	DOWFAX 8390 (wt%)[a]	N-hexadecane (wt%)[a]	$M_{n,final}$[b] (kg mol^{-1})	X^c (%)	$[MI]_0$[d] (M)	$[IBOMA]_0$ (M)	$[C13MA]_0$ (M)	$[AN]_0$ (M)	Đ[b]	T^e (°C)	$k_P[P^\bullet]^f$ (10^5 s^{-1})
IBOMA90/AN10-1[g]	0	0	37.2	31.7	0.005	0.972	0	0.108	1.83	90	9 ± 0.8
IBOMA90/AN10-2	0	0.8	35.6	49.3	0.005	0.965	0	0.107	1.84	90	23 ± 6.3
IBOMA90/AN10-3	2	0	44.2	88.9	0.005	0.956	0	0.106	1.66	90	38 ± 0.9
IBOMA90/AN10-4	2	0.8	40.8	97.7	0.005	0.948	0	0.105	1.71	90	52 ± 3.2
IBOMA90/AN10-5	2	0.8	41.7	92.8	0.005	0.948	0	0.105	2.19	80	48 ± 4.0
IBOMA90/AN10-6	2	0.8	41.4	94.3	0.005	0.948	0	0.105	1.89	100	148 ± 10.7
IBOMA90/AN10-7[h]	2	0.8	27.9	61.7	0.005	0.972	0	0.108	1.81	90	132 ± 0.1
C13MA90/AN10	2	0.8	39.5	88.3	0.005	0	0.770	0.086	2.19	90	21 ± 0.1
IBOMA45/C13MA45/AN10	2	0.8	43.9	91.4	0.005	0.425	0.425	0.094	2.16	90	33 ± 0.8

[a] wt% based on the weight of all monomers.

3.3.2.1 The Effect of Controlling Comonomers on the Efficiency of Macroinitiators

To study the effect of the comonomers (AN or S) on the ability of the macroinitiator to chain extend to form a second block, NMP was carried out in miniemulsion for IBOMA (90 mol%) /AN (10 mol%) monomer mixtures (experiment IBOMA90/AN10-4 (use of a p(OEGMA-*stat*-AN) macroinitiator) versus IBOMA90/AN10-7 (use of a p(OEGMA-*stat*-S) macroinitiator). Figure 3.2 shows a) the semi-logarithmic kinetic plots versus polymerization time and b) M_n versus conversion. Using p(OEGMA-*stat*-S) macroinitiator, the miniemulsion polymerization of IBOMA/AN stopped after 12 minutes as the latex lost its stability and the coagulation and precipitation of particles occurred in the early time. It seems that S increased the hydrophobicity of macroinitiator and reduced the efficiency of surfactant macroinitiator to stabilize the system. The lack of stability for the latex containing p(OEGMA-*stat*-S) macroinitiator is reflected in the $Đ$ of the starting point of polymerization (t=0, $Đ$ = 2.9). Therefore, p(OEGMA-*stat*-AN) macroinitiator was used for the next series of studies in miniemulsion.
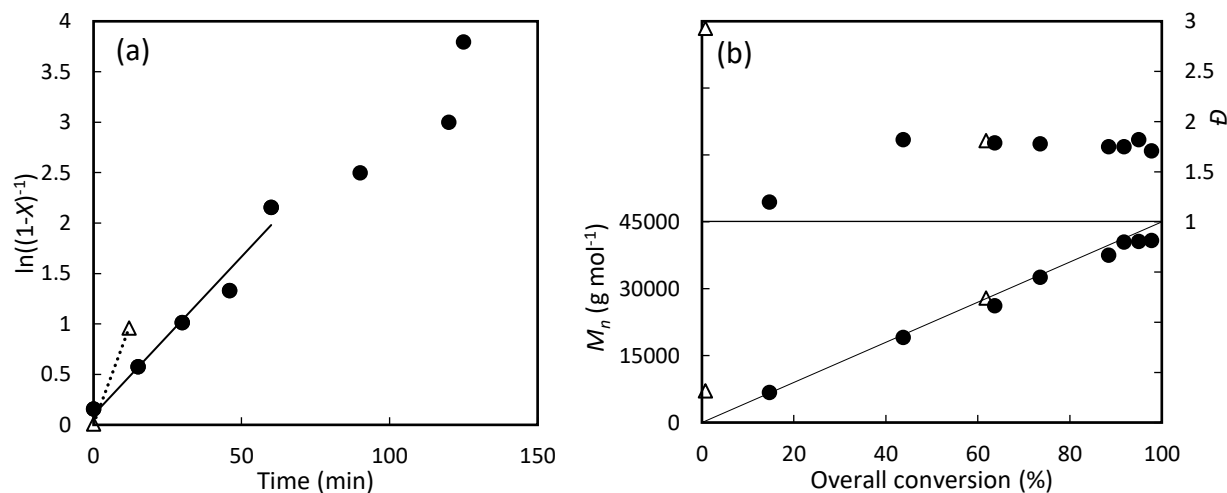
Figure 3.2. The effect of changing comonomers (AN or S) of macroinitiator on copolymerization of IBOMA/AN ($f_{AN,0}$ =0.1) (a) Kinetic plots of $\ln((1-X)^{-1})$ (X= monomer conversion) versus reaction time (b) Number average molecular weight M_n and $Đ$ versus conversion (X). IBOMA90/AN10-4 (filled circles, ●); IBOMA90/AN10-7 (open triangles, Δ).

3.3.2.2. The Effect of Surfactant and Co-stabilizer On the Stability and Kinetics of Polymerization

Having identified the p(OEGMA-*stat*-AN) as the macroinitiator that cleanly chain extended a mixture of IBOMA/AN in miniemulsion, optimization around this point ensued. This involved conducting the miniemulsion polymerizations with and without the addition of surfactant (DOWFAX 8390) and co-stabilizer (n-hexadecane). IBOMA90/AN10-1 was prepared without using any additional surfactant or co-stabilizer. IBOMA90/AN10-2 (no surfactant), IBOMA90/AN10-3 (no co-stabilizer) and IBOMA90/AN10-4 (with surfactant and co-stabilizer) were also prepared with the same experimental conditions (same initial monomer composition, $M_{n,target} = 45$ kg mol^{-1}, T = 90 °C and same preparation steps), but with different the surfactant and co-stabilizer content. Hereinto, the amount of DOWFAX 8390 surfactant and n-hexadecane co-stabilizer were considered to be 2 and 0.8 %wt based on the monomer charged. The results indicate that addition of both 2 %wbm (wt% based on monomers) of DOWFAX 8390 and 0.8 %wbm of n-hexadecane, increased the apparent rate constant ($k_P[P^•]$) from 9×10^{-5} s^{-1} to 52×10^{-5} s^{-1} (Table 3.2), while maintaining the control over the polymerization. According to Figure 3.3 (a) and (b), we conclude that the addition of 2 %wbm of surfactant is necessary to stabilize the miniemulsion and enhance the control over the polymerization. Addition of small amount of n-hexadecane (0.8 %wbm) as the stabilizer increases the polymerization rate, decreases the Đ and the M_n increases linearly with conversion. Therefore, 2 %wbm of DOWFAX and 0.8 %wbm of n-hexadecane were used for the next series of syntheses.
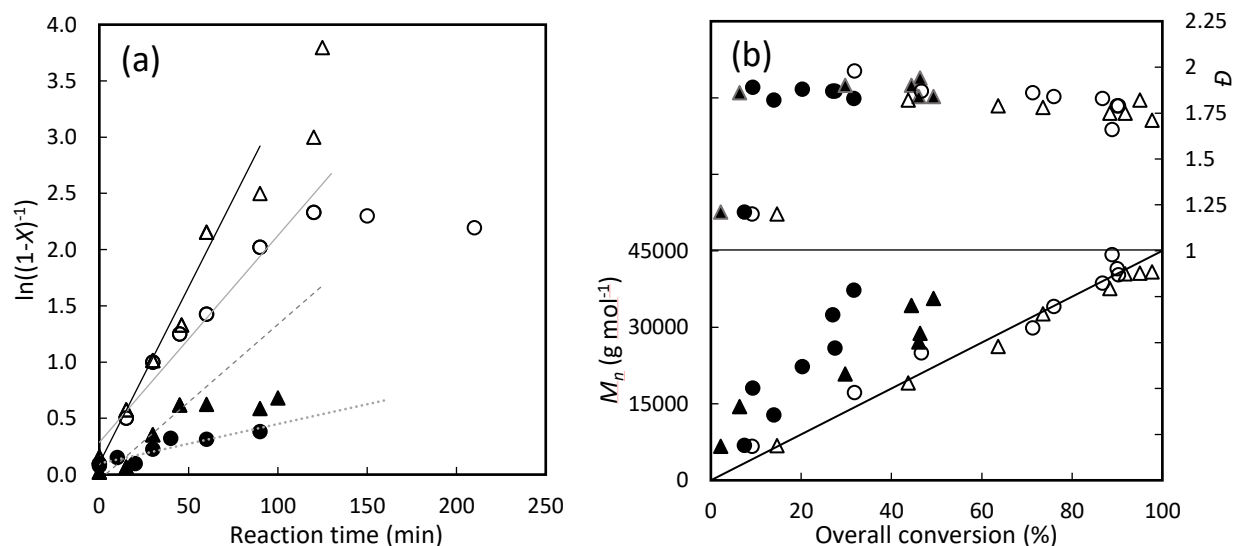
Figure 3.3. The effects of adding surfactant and stabilizer on copolymerization of IBOMA/AN ($f_{AN,0} = 0.1$) (a) Kinetic plots of $\ln((1-X)^{-1})$ ($X=$ monomer conversion) versus reaction time (b) Number average molecular weight M_n and Đ versus conversion (X). IBOMA90/AN10-1 (filled circles, ●); IBOMA90/AN10-2 (filled triangles, ▲); IBOMA90/AN10-3 (open circles, ○); IBOMA90/AN10-4 (open triangles, Δ).

3.3.2.3. The Effect of Reaction Temperature on the Kinetics of Polymerization

Next, the effect of temperature on the polymerization of IBOMA and AN was investigated for three different temperatures of 80, 90 and 100 °C (Figure 3.4). For all reaction temperatures, a linear kinetic trend was observed in semi-logarithmic kinetic plots versus reaction time in the beginning of the reaction ($t < 50$ min). However, the irreversible terminations occurred at higher rates for polymerizations at 80 or 100 °C. The un-controlled increase of M_ns with X was also observed for polymerizations at 80 and 100 °C. At 100 °C, the polymerization rate was high ($k_P[P^\bullet] = 148 \pm 11 \times 10^5$ s^{-1}) and the reaction stopped after 67 min resulted in an uncontrolled polymerization. The uncontrolled polymerization at 100 °C could also be due to the reaction temperature higher than the lower critical solution temperature (LCST) of macroinitiators. For comparison, LCST of 84-90 °C was reported for OEGMA-based homopolymers.[194, 195] The polymerization rate at 80 °C was lower than 90 °C ($k_P[P^\bullet] = 48 \pm 4 \times 10^5$ s^{-1} and $52 \pm 3 \times 10^5$ s^{-1} at 80 and 90 °C, respectively) and the reaction time was the longest (210 min). The low reaction temperature (80 °C) caused low dissociation rate of nitroxide and higher termination events.[23] However, the polymerization at 80 °C was uncontrolled with a sigmoidal trend of M_n versus X and resulted in polymers with high dispersities ($Đ$ up to 2.25). The lowest $Đ$s were at 90 °C ($Đ \approx 1.71\sim1.82$) and the M_n versus X showed a good resemblance to the theoretical line with dominance of termination events at high conversions ($X >$ 92%). Hence, the reaction temperature of 90 °C was chosen for the NMP of IBOMA/C13MA using p(OEGMA-*stat*-AN) macroinitiator.
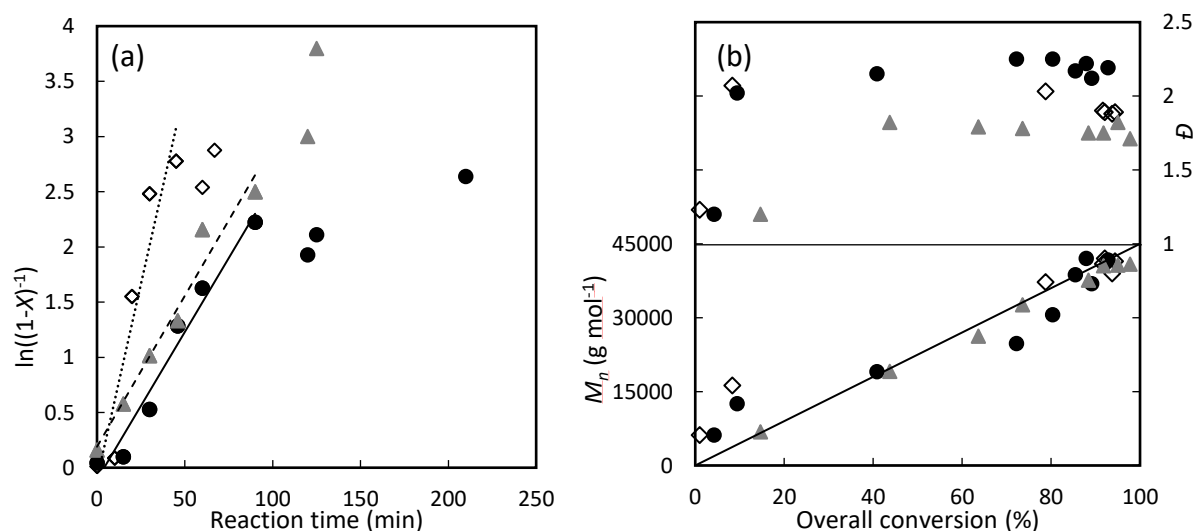
Figure 3.4. The effect of temperature on nitroxide mediated miniemulsion polymerization of IBOMA/AN ($f_{AN,0} = 0.1$) (a) Kinetic plots of $\ln((1-X)^{-1})$ ($X=$ monomer conversion) versus reaction time (b) Number average molecular weight M_n and $Đ$ versus conversion (X). IBOMA90/AN10-5 (T= 80 °C, filled circles, ●); IBOMA90/AN10-4 (T= 90 °C, gray triangles, ▲); IBOMA90/AN10-6 (T= 100 °C, open diamonds, ◊).

3.3.2.4. Nitroxide Mediated Miniemulsion Polymerization of IBOMA/C13MA Mixtures Using P(OEGMA-*stat*-AN) Macroinitiator

Nitroxide mediated miniemulsion polymerization of IBOMA/C13MA/AN mixtures (10 mol% AN as the controlling comonomer) was conducted using p(OEGMA-*stat*-AN) macroinitiator (M_n = 7200 g mol^{-1}, $Đ$ = 1.24), 2 %wbm of DOWFAX 8390 and 0.8 %wbm n-hexadecane at 90 °C. Figure 3.5 shows a schematic representation of the miniemulsion polymerization of IBOMA/C13MA/AN. The kinetic plots were linear in all cases up to ~ 100 min and slightly deviated at t > 100 min (Figure 3.6 (a)). The polymerization rate increased by increasing the ratio of $[IBOMA]_0/[C13MA]_0$ and these kinetic results are summarized in terms of the slopes of $\ln((1-X)^{-1})$ versus time ($k_P[P^\bullet]$). Figure 3.6 (b) indicates that M_n increased linearly with conversion and remained relatively close to the theoretical prediction line for all polymerizations studied. However, the final $Đ$s of samples were high (1.71 < $Đ$ < 2.19) and the $Đ$ increased by decreasing the ratio of $[IBOMA]_0/[C13MA]_0$ in the miniemulsion. This might be due to the long aliphatic chains of C13MA, which caused the formation of particles early in the nucleation stage. The high $Đ$ for polymers prepared by chain extension of amphiphilic macroinitiators was expected, probably due to chain transfer reaction and higher termination rate compare to the polymerizations with alkoxyamines such as BB. The high $Đ$ was also observed in similar studies on NMP using amphiphilic macroinitiators.[129] As an example, Delaittre et al[41] synthesized poly(S) ($Đ$ = 2, M_n = 100 kg mol^{-1}) by nitroxide mediated emulsion polymerization using SG1-terminated poly(acrylic acid) macroinitiator ($Đ$ = 1.17, M_n = 1900 g mol^{-1}) at 120 °C and 3 bar pressure, though the particle size was considerably smaller (particle size = 65 nm). Dire et al[175] also observed $Đ$ > 2 for the NMP of methyl methacrylate using SG1-based methacrylic acid macroinitiator in emulsion. Another reason could be the use of AN, which is a partially water-soluble controlling comonomer for the NMP of methacrylates using BB.[196] Consequently, some of the AN monomers may not be available inside the monomer droplets to control the polymerization rate, resulting in a relatively high $Đ$ ($Đ$ >1.7).
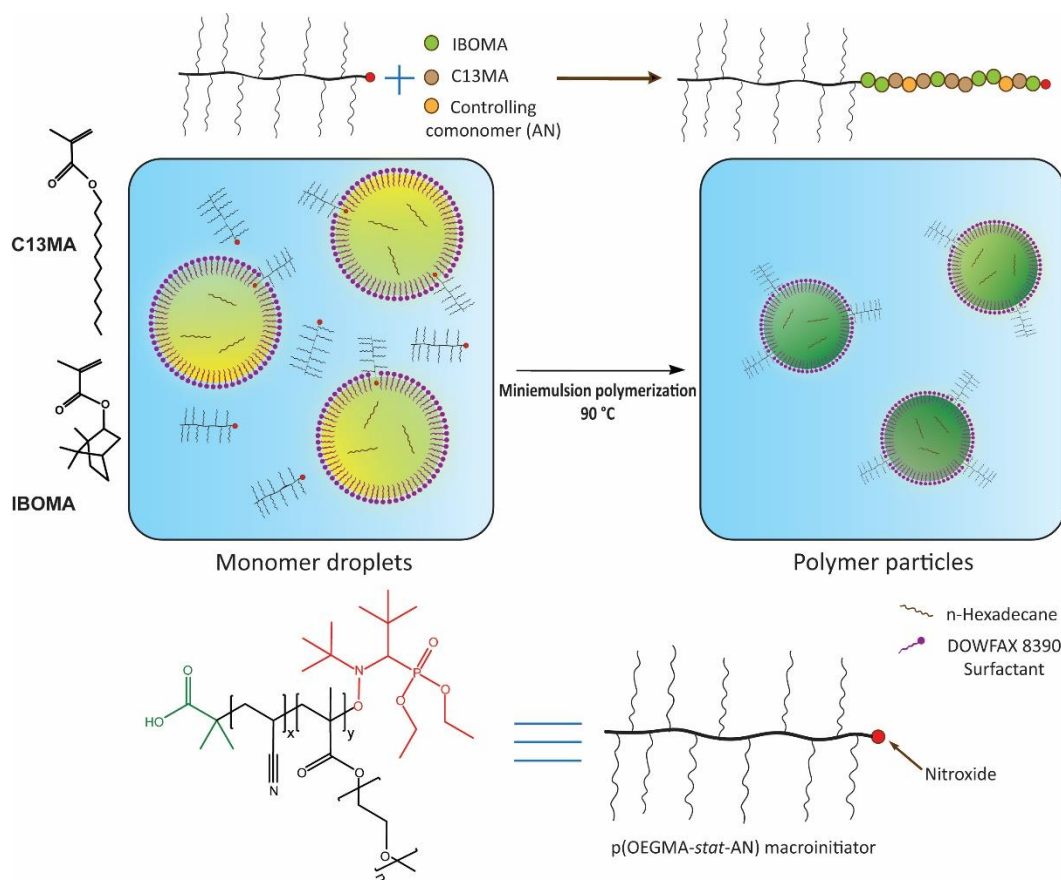
Figure 3.5. Miniemulsion polymerization of IBOMA/C13MA using p(OEGMA-*stat*-AN) macroinitiator in presence of DOWFAX 8390 and n-hexadecane at 90 °C. Amphiphilic macroinitiators were synthesized and dissolved in the aqueous phase prior to miniemulsion polymerization.
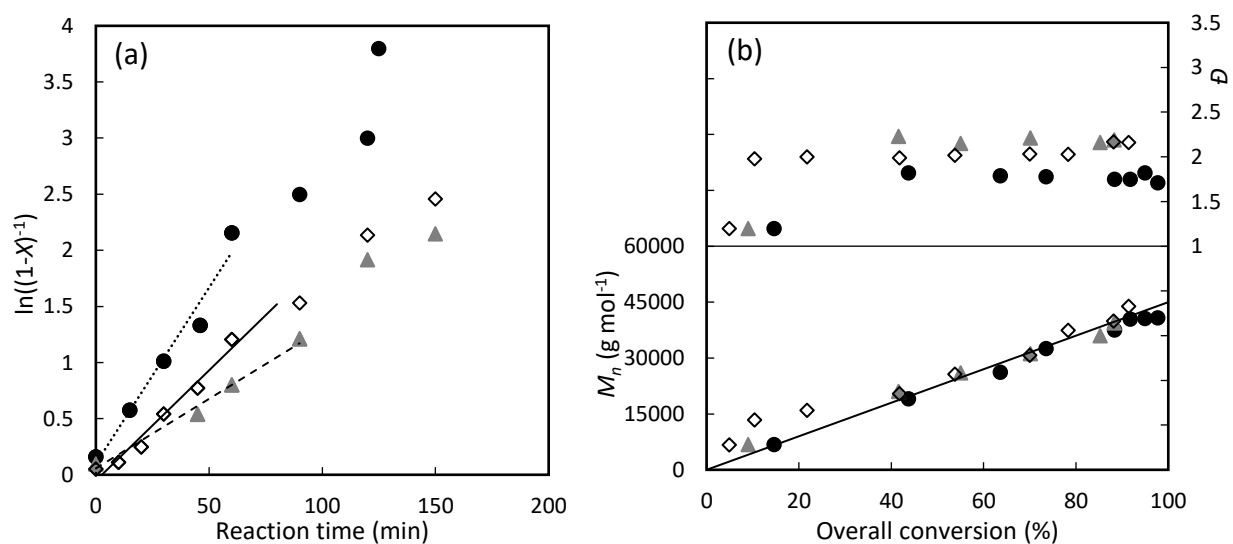
Figure 3.6. The miniemulsion polymerization of different ratios of IBOMA/C13MA/AN using p(OEGMA-*stat*-AN) macroinitiator (a) Kinetic plots of $\ln((1-X)^{-1})$ (*X*= monomer conversion) versus reaction time (b) Number average molecular weight M_n and *Đ* versus conversion (*X*). IBOMA90/AN10-4 (filled circles, ●); C13MA90/AN10 (gray triangles, ▲); C13MA/IBOMA45/AN10 (open diamonds, ◊).

Figure 3.7 demonstrates the GPC peaks shift for the chain extension of p(OEGMA-*stat*-AN) macroinitiator with IBOMA/AN ($f_{IBOMA,0}$ = 0.9) and C13MA/AN ($f_{C13MA,0}$ = 0.9) at 90 °C. The ability of the chains to re-initiate a second batch of monomer was observed by seeing the GPC peaks shift toward higher molecular weights with monomer conversion, with very little dead macroinitiator observed.
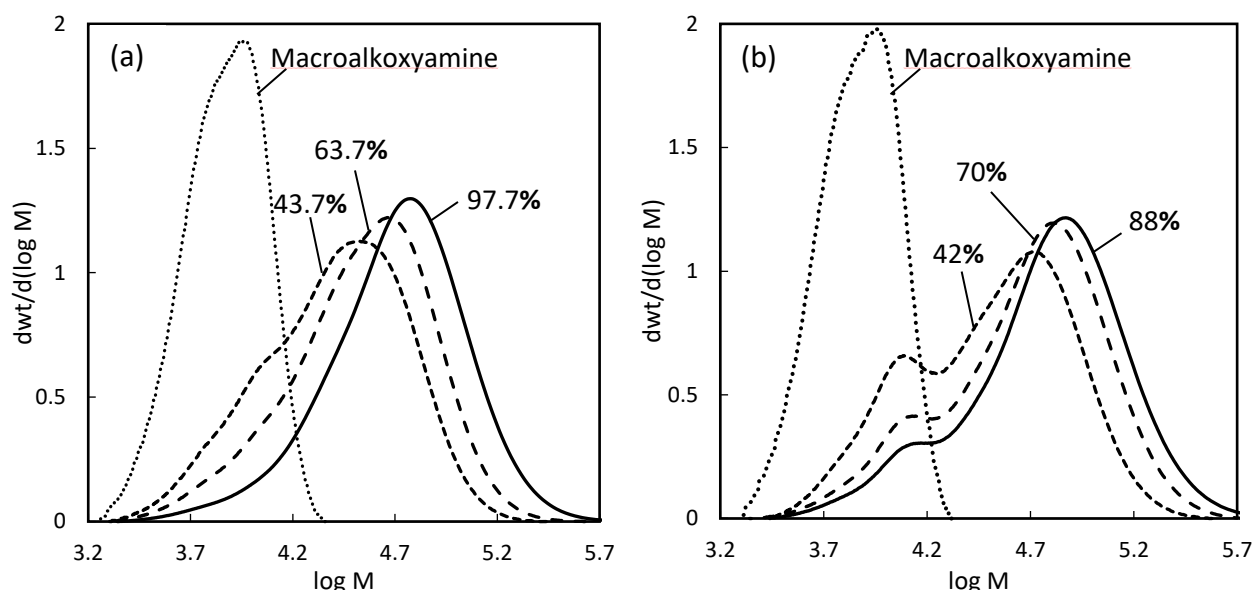
Figure 3.7. Molecular weight distribution of polymers for chain extension of p(OEGMA-*stat*-AN) macroinitiator with (a) IBOMA90/AN10-4 ($f_{\text{IBOMA},0}$ = 0.9) and (b) C13MA90/AN10 ($f_{\text{C13MA},0}$ = 0.9).

3.3.3. Particle Size and Colloidal Stability of IBOMA/C13MA Polymer Latexes

Figure 3.8 illustrates the Z-average particle size of the latex samples as measured with DLS. Initially, we studied the effect of addition of co-stabilizer (n-hexadecane) and surfactant on particle size. For the IBOMA90/AN10-1 experiment (without surfactant or co-stabilizer), the particle size varied from 0.5-2 μm. The p(OEGMA-*stat*-AN) macroinitiator acted as a dual surfactant/initiator and stabilized the miniemulsion. The particle size decreased during the polymerization, indicating the transition from monomer droplets to polymer particles. As the polymerization progressed, the nonionic macroinitiator was not able to provide as effective stabilization and the particles started to coagulate and precipitate. This resulted in an

uncontrolled polymerization for the IBOMA90/AN10-1 experiment. In the IBOMA90/AN10-2 experiment, 0.8 wt% hexadecane (relative to the monomers), was added to the organic phase to aid the stability of the colloid. Consequently, the monomer droplet size decreased significantly (from 2050 nm for IBOMA90/AN10-1 to 656 nm for IBOMA90/AN10-2). However, the macroalkoxyamines were unable to stabilize the colloids and coagulation still occurred at higher conversions. Addition of 2 wbm% DOWFAX for IBOMA90/AN10-3 experiment (without n-hexadecane) and IBOMA90/AN10-4 (with 0.8 wbm% n-hexadecane) along with the amphiphilic macroinitiator, provided much better colloidal stability for the miniemulsion polymerization, especially at higher conversions. For these two experiments, the particle size steadily decreased during the polymerization, and limiting to about 200-300 nm after 30 minutes. The particle size dispersity was high for most of the samples, which indicates the presence of particles with multiple size distributions.[197] This phenomenon can be ascribed to using two different surfactants (DOWFAX 8390 and amphiphilic macroinitiator) to stabilize the system. Further, the macroinitiator's solubility in the aqueous phase may not have been sufficiently high to avoid droplet nucleation. It was possible that macroinitiator molecules were engulfed into the bulk of the monomer droplets to initiate the polymerization and were not acting as surfactants at the interface. Similarly, Nicolas et al[60] observed broad particle size distribution for nitroxide mediated miniemulsion polymerization of n-butyl acrylate and S using an SG1-based water-soluble alkoxyamine (synthesized from BB and tri(ethylene glycol) diacrylate) and DOWFAX 8390 surfactant. The particle size versus reaction time is shown at different temperatures of 80, 90 and 100 °C (Figure 3.8 (b)) and the particle size for polymerization of IBOMA, C13MA and 10 mol% AN (controlling monomer) is depicted in Figure 3.8 (c). Using the macroinitiator, the particle size in all experiments except for IBOMA90/AN10-6, decreased drastically in the first 45 minutes of the reaction and stayed quite constant until the end of polymerization. This occurred due to the disappearance of monomer droplets and the formation of polymer particles in the latex.
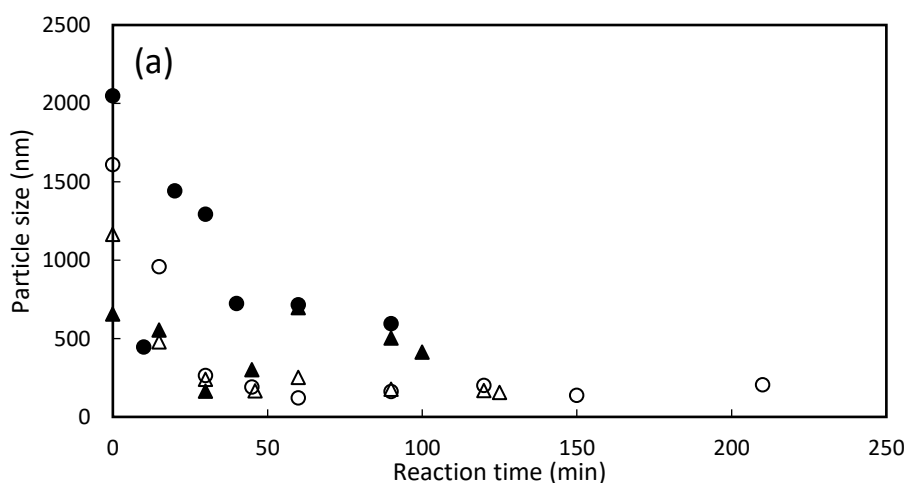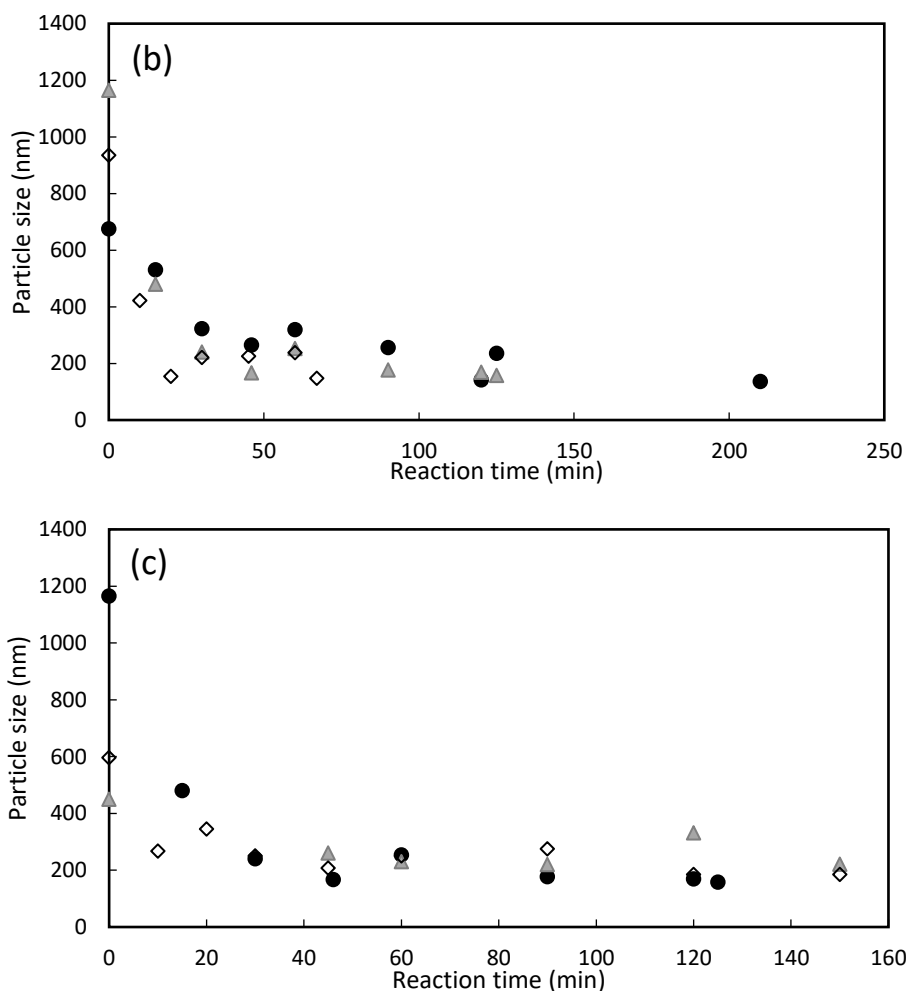
Figure 3.8. (a) Average particle size versus reaction time. IBOMA90/AN10-1 (filled circles, ●); IBOMA90/AN10-2 (filled triangles, ▲); IBOMA90/AN10-3 (open circles, ○); IBOMA90/AN10-4 (open triangles, Δ). (b) The effect of reaction temperature on particle size during the copolymerization of IBOMA/AN monomers using p(OEGMA-*stat*-AN) macroinitiator, 2 %wbm DOWFAX 8390 and 0.8 %wbm n-hexadecane. IBOMA90/AN10-5 (filled circles, ●); IBOMA90/AN10-4 (gray triangles); IBOMA90/AN10-6 (open diamonds, ◊). (c) Z-average particle size for IBOMA/C13MA/AN polymerization with time using p(OEGMA-*stat*-AN) macroinitiator, 2 %wbm DOWFAX 8390 and 0.8 %wbm n-hexadecane. IBOMA90/AN10-4 (filled circles, ●); C13MA90/AN10 (gray triangles, ▲); IBOMA45/C13MA45/AN10 (open diamonds, ◊).

The adsorption of surfactant on the surface of polymer particles directly affects the colloidal stability.[198] As the anionic surfactant (DOWFAX 8390) was used to stabilize the latex, the surface charge of polymer particles was negative. To quantify the surface charge of the particles, zeta-potentials were measured for

36

the IBOMA/C13MA experiments (Table 3.3). The zeta-potential values were between -38 to -43 mV, suggesting a high degree of stability for the particles.[199]

Table 3.3. Zeta-potential and final particle size for the polymer particles in miniemulsion.

Experiment ID	Final particle size (nm)[a]	PDI[a]	Zeta potential (mV)[b]
IBOMA90/AN10-4	157	0.345	-43.0
C13MA90/AN10	221	0.160	-39.8
IBOMA45/C13MA45/AN10	185	0.122	-38.3

[a] Z-average particle size and dispersity of the polymer particles in latex measured by DLS at room temperature. The reported results are the average of 5 measurements.
[b] Zeta potential results for polymer latexes (pH = 7).

3.3.4. Thermal properties of IBOMA/C13MA Polymers Prepared in Miniemulsion

To investigate the effect of OEGMA-based macroinitiator on thermal properties of IBOMA/C13MA/AN copolymers, TGA and DSC were performed on IBOMA90/AN10-4, C13MA90/AN10 and IBOMA45/C13MA45/AN10 samples and the results were presented in Table 3.4. Polymer compositions were listed in Table 3.4 (Figure 3.S2 in Supplementary Information, shows the polymer composition of IBOMA45/C13MA45/AN10). Theoretical glass transition temperature ($T_{g,theo}$) for the samples were estimated by the Fox equation, neglecting the effect of p(OEGMA-*stat*-AN) macroinitiator[200]:

$$\sum_i w_i \left(1 - \frac{T_{g,theo}}{T_{g,i}}\right) = 0 \tag{3.1}$$

where w_i corresponds to the mass fraction of monomers and $T_{g,i}$ is the T_g of the individual homopolymers prepared from the monomers. Herein, $T_{g,IBOMA} = 110$ °C[162, 201], $T_{g,C13MA} = -46$ °C[201, 202] and $T_{g,AN} = 95$ °C[201, 203] were taken as the literature values to calculate the $T_{g,theo}$s of polymer samples. The measured T_gs were slightly lower than $T_{g,theo}$s, suggesting a decrease in T_gs due to the existence of residual n-hexadecane in polymer samples.[204, 205] Furthermore, initiation with p(OEGMA-*stat*-AN) macroinitiators can also lower the T_gs due to the presence of OEGMA (T_g OEGMA homopolymer ($T_{g,p(OEGMA)}$) = -60 to -53 °C[206-209]) as part of the copolymer. The T_gs increased with increasing the IBOMA content in polymers. A T_m at -19 °C was detected for the C13MA-rich polymer. It should be noted that a T_m for co/terpolymers with high C13MA content was observed in previous studies.[162, 210] Table 3.4 shows the decomposition temperature for 10% weight loss ($T_{dec,1}$), decomposition temperature for maximum weight loss ($T_{dec,max}$) and decomposition temperature at the end of measurement ($T_{dec,2}$) for IBOMA90/AN10-4, C13MA90/AN10 and IBOMA45/C13MA45/AN10. Figure 3.9 presents the TGA traces for the polymers. From these results, degradation of polymers containing IBOMA occurred in two stages, due to the formation and elimination of camphene at temperatures above ~ 300 °C.[162, 211, 212]

Table 3.4. Thermal characterization of IBOMA/C13MA/AN polymers starting from p(OEGMA-stat-AN) macroinitiator prepared by NMP in miniemulsion.

Experiment ID	$T_m{}^a$ (°C)	$T_g{}^a$ (°C)	$T_{g,theo}{}^b$ (°C)	$T_{dec,1}{}^c$ (°C)	$T_{dec,max}{}^c$ (°C)	$T_{dec,2}{}^c$ (°C)	$F_{IBOMA}{}^d$	F_{C13MA}	F_{OEGMA}	$M_{n,final}{}^e$ (kg mol⁻¹)
IBOMA90/AN10-4	-	109	110	227	281	463	0.86	0	0.07	40.8
C13MA90/AN10	-19	-44	-42	225	371	470	0	0.84	0.08	39.5
IBOMA45/C13MA45/AN10	-	-3	9	229	293	479	0.41	0.45	0.10	43.9

[a] T_m (melting point) and T_g (glass transition temperature) measured by DSC under nitrogen atmosphere using (heat/cool/heat) method in the temperature range of -80 to 140 °C. The heating rate of 15 °C min⁻¹ and cooling rate of 50 °C min⁻¹ was considered for the measurement.
[b] $T_{g,theo}$ (theoretical glass transition temperature) estimated by Fox equation.[200]
[c] Decomposition temperatures (T_{dec}s) measured by TGA under nitrogen atmosphere at a heating rate of 15 °C min⁻¹. $T_{dec,1}$ (T_{dec} for 10% weight loss or onset of decomposition), $T_{dec,max}$ (T_{dec} at which highest weight loss occurs) and $T_{dec,2}$ (T_{dec} at the end of decomposition).
[d] Molar fraction of IBOMA in polymer composition, determined by ¹H NMR in CDCl₃. ¹H NMR spectra for IBOMA45/C13MA45/AN10 is available in Figure 3.S2 (Supplementary Information).
[e] Final number average molecular weight ($M_{n,final}$) and dispersity of polymer chains (Đ) measured by GPC with PMMA standards in THF at 40 °C.
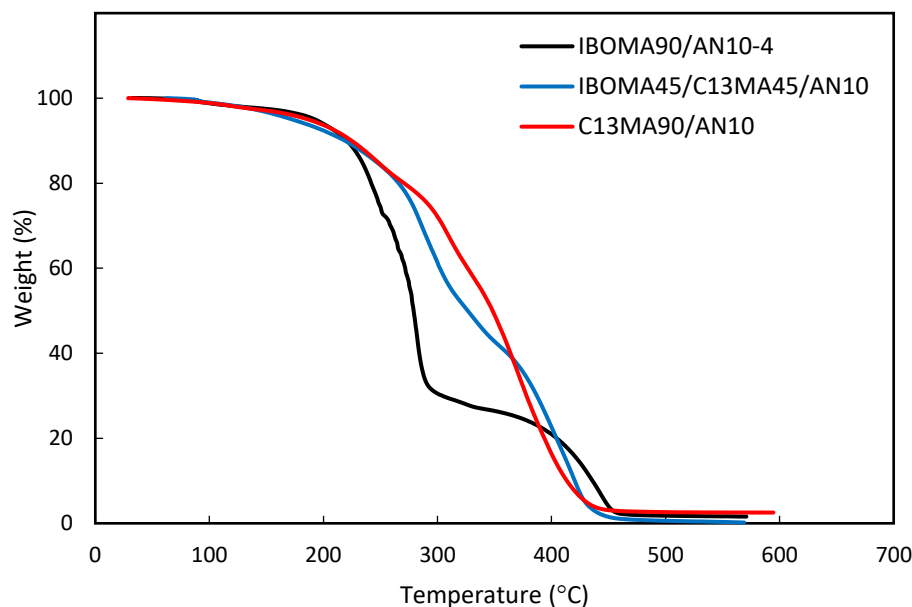
Figure 3.9. TGA thermograms for IBOMA90/AN10-4 (—, black line), IBOMA45/C13MA45/AN10 (—, blue line) and C13MA90/AN10 (—, red line) samples under nitrogen with heating rate of 15 °C min⁻¹.

3.4. CONCLUSIONS

In this study, nitroxide mediated miniemulsion polymerization of two bio-based methacrylic monomers (in presence of 10 mol% AN controlling comonomer), using SG1-terminated amphiphilic macroinitiators, was

investigated. Isobornyl methacrylate (IBOMA) and C13 alkyl methacrylate (C13MA) were the hydrobphobic monomers studied. Two different macroinitiators were synthesized from poly (ethylene glycol) methyl ether methacrylate (OEGMA, $M_{n,Average}$ = 500 g mol^{-1}) by changing the controlling comonomer (AN or S, 10 mol%) with the former being more effective in providing the control of the miniemulsion polymerization of IBOMA/C13MA in terms of linear growth of M_n with conversion and low $Đ$. The p(OEGMA-*stat*-AN) macroinitiator was used as the sole surfactant/initiator for the miniemulsion polymerization of the IBOMA or C13MA; but the best colloidal stability and control over the polymerization was accomplished in the presence of 2 wt% DOWFAX 8390 surfactant and 0.8 wt% n-hexadecane co-stabilizer (based on the weight of monomers). IBOMA/AN polymers with $Đ$ = 1.71 were successfully synthesized (X = 97.7%, M_n = 40.8 kg mol^{-1}). Subsequent temperature optimization studies revealed best polymerization control in terms of lower dispersity, occurred at 90 °C. After finding the optimal experimental conditions, the NMP of C13MA or IBOMA/C13MA with the mixture of 50:50 $\frac{[IBOMA]_0}{[C13MA]_0}$ was also conducted in presence of p(OEGMA-*stat*-AN) macroinitiator, 2 wbm% DOWFAX and 0.8 wbm% n-hexadecane in miniemulsion at 90 °C. As a result, polymers with M_ns up to 43.9 kg mol^{-1}, $Đ$ < 2.19 and 88.3% ≤ X ≤ 91.4% were produced, with good colloidal stability (-38 mV ≤ ζ potential ≤ -43 mV). Finally, the thermal properties were investigated revealing that increasing the IBOMA content increased the T_g of the polymers and was characterized by a two-stage decomposition by TGA analysis.

ACKNOWLEDGMENTS

Preamble to Chapter 4

In the previous chapter, IBOMA/C13MA copolymers were synthesized by NMP using SG1-based amphiphilic macroinitiators in miniemulsion. This method employed a two-stage process where the macroinitiators were prepared by NMP in homogeneous organic solvent (toluene) and then purified before being employed as a macroinitiator for the miniemulsion polymerization of two bio-based monomers. In this chapter, we simplified the miniemulsion polymerization process by using a more recently developed Dispolreg 007 alkoxyamine. This nitroxide is unique in that its synthesis is relatively easy to scale up but also because it does not need a controlling co-monomer to polymerize methacrylates, which has always been a prominent issue with NMP. In this chapter, the Dispolreg 007 was solubilized inside the monomer droplets, which formed a miniemulsion for the polymerization of IBOMA/C13MA monomers. However, before proceeding to the miniemulsion, the polymerization of IBOMA/C13MA was investigated in homogeneous toluene solution to understand how Dispolreg 007 controlled these specific monomers (in homogeneous or binary copolymerization). After confirming the good control of the polymerization of these methacrylic monomers in organic solvent (M_n up to 27.3 kg mol^{-1} and $1.39 < Đ < 1.66$), miniemulsion was successfully applied (M_n up to 67.9 kg mol^{-1} and $1.50 < Đ < 1.73$). By changing the ratio of IBOMA/C13MA in the initial monomer mixture, the effect of composition on thermal properties of the polymers was studied, and illustrated that IBOMA/C13MA copolymers with a wide range of glass transition temperatures can be produced. This study showed that the IBOMA/C13MA copolymers can be used as a backbone structure for preparation of more functionalized polymers in the succeeding chapters. This chapter was published in *Industrial & Engineering Chemistry Research*, 59 (19), 8921-8936, 2020.

Chapter 4: Nitroxide Mediated Miniemulsion Polymerization of Bio-based Methacrylates

ABSTRACT

Nitroxide-mediated homo and statistical copolymerization of commercially available methacrylates derived from sustainable feedstocks (isobornyl methacrylate (IBOMA) and a mixture of methacrylic esters with average alkyl side chain length = 13 units (termed C13MA)) was conducted in organic solvent (toluene) and in dispersed aqueous media using an oil-soluble unimolecular initiator (Dispolreg 007) without any controlling comonomers in a controlled manner. IBOMA homopolymerization in emulsion at 83-100 °C revealed the optimal polymerization temperature of 90 °C giving relatively narrow molecular weight distributions (1.46< dispersities ($Đ$) <1.58) and conversion up to 83% in a relatively short time (2 hours). IBOMA/C13MA statistical copolymerizations yielded copolymers with tunable glass transition temperature (T_g) prepared in emulsion (-52 °C < T_g <123 °C) and in organic solvent (-40 °C < T_g < 169 °C). Resins made in emulsion at 90 °C proceeded up to 92.7% conversion with monomodal molecular weight distributions ($\overline{M}_n$ up to 68000 g mol^{-1} and $Đ$ = 1.62 - 1.72) and were colloidally stable (24% solids and final average particle sizes = 270-481 nm). Furthermore, chain end fidelity was verified by chain extensions with IBOMA and C13MA monomers in both emulsion and organic solvent. These results constitute a readily scalable route to make polymers via nitroxide mediated polymerization with controlled architecture using bio-based feedstocks without the hazards of bulk or homogeneous organic solvent polymerization.

4.1. INTRODUCTION
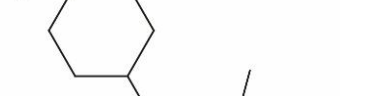
During the last couple of decades, there has been a high demand for developing industrially scalable polymerization processes to obtain materials with specific properties using controlled radical polymerization[213-215]. A controlled polymerization is considered akin to a living polymerization, which forms well-defined microstructures and produces polymers with narrow molecular weight distribution, displays a linear degree of polymerization versus conversion and active chain ends[13, 166]. To answer the demand for robust polymerization processes while controlling microstructure, reversible deactivation radical polymerization (RDRP), sometimes known as controlled radical polymerization (CRP), like nitroxide-mediated polymerization (NMP)[21, 23], reversible addition-fragmentation chain transfer (RAFT) polymerization[17, 216] and atom transfer radical polymerization (ATRP)[11, 18, 215] has been offered as one possibility. The main characteristics of all CRP methods include relatively narrow molecular weight

distribution and active polymer chain ends[20], traits typically exhibited by truly living polymerizations. Unlike living polymerizations, CRP can be readily done in dispersed aqueous media [23, 47, 64, 217]. In particular, NMP possesses some distinctive attractive features. For example, NMP often simply relies on an alkoxyamine and heat to start a polymerization. Unlike traditional RAFT and ATRP, it does not suffer from discoloration issues or unpleasant odor from any metallic ligands or sulfur-based chain transfer agents, thereby eschewing exhaustive post-polymerization treatments to remove residual catalysts or other reagents[47, 218]. It should be noted that the advent of single electron transfer-living radical polymerization (SET-LRP), activators regenerated by electron transfer (ARGET ATRP), non-metal ATRP methods and novel RAFT agents have been reported to address discoloration and odor issues [20, 21, 219-229]. At first, NMP was very limited, restricted to the synthesis of styrenic-based polymers[24]. However, NMP was improved dramatically due to the development of new alkoxyamines. Benoit *et al.*[26, 169] developed alkoxyamines based on 2,2,5-tri-methyl-4-phenyl-3-azahexane-3-nitroxide (TIPNO), which can be used for the controlled polymerization of a wide range of monomers at lower temperatures. Further improvement occurred by the introduction of N-tert-butyl-N-[1-diethylphosphono-(2,2-dimethylpropyl)] (SG1) nitroxide. A commercially available SG1-based alkoxyamine, N-(2-methylpropyl)-N-(1-(diethylphosphono-2,2-dimethylpropyl)-O-(2-carboxylprop-2 yl)hydroxylamine) BlocBuilder-MA™ (termed herein as BB, from Arkema) has enabled homopolymerization of acrylates and acrylamides and under certain conditions, methacrylates (Figure 4.1(a) shows the chemical structure of BB) [23, 230, 231]. The polymerization of methacrylates using BB is problematic because of the high activation/deactivation equilibrium constant (K) of methacrylates and the cross-disproportionation effect [172, 173, 232]. To overcome this, the copolymerization method first described by Charleux and coworkers[174] was applied, where methacrylates are copolymerized with a small amount of comonomer with a very low K such as styrene[172, 233], acrylonitrile (AN)[234, 235], 9-(4-vinylbenzyl)-9H-carbazole[236, 237] or other styrenic derivatives[130, 238, 239]. As a result, the average K, $\langle K \rangle$, of the polymerization decreases and control is enhanced, accordingly[172]. Synthesizing an alkoxyamine applicable for a wide range of monomers, with low dispersity, low reaction temperature and active chain ends has always been challenging[240-242]. Recently, Ballard *et al.*[28, 29] reported a new group of alkoxyamines such as 3-(((2-cyanopropan-2-yl) oxy) - (cyclohexyl) amino)-2, 2-dimethyl-3-phenylpropanenitrile (Dispolreg 007), that enabled homopolymerization of methacrylates without any comonomer at temperatures < 100 ºC and allowed clean cross-over from a methacrylic block to a styrenic block. These conditions also enabled clean homopolymerization of methacrylates in emulsion or suspension media[28, 243]. This initiator is used in our study to control the polymerization. Figure 4.1(b) depicts the chemical formula of the Dispolreg 007 alkoxyamine.

Polymerization in dispersed aqueous media has advantages over solution or bulk polymerization methods. Bulk polymerization often results in highly viscous mixtures with attendant autoacceleration effects [24]. Solution polymerizations decrease viscosity but introduce issues regarding the removal of solvent. Using water as the continuous phase decreases the viscosity of the solution and improves heat transfer effects [59]. Further, such emulsions do not possess volatile organic compounds (VOC) which makes them a perfect choice for many indoor applications[244, 245]. NMP of methacrylates has been done in suspension[103], emulsion[60-62], miniemulsion [43, 84, 246] and microemulsion[100, 247]. These variants all have merits and detractions. Suspension polymerization is simple to implement industrially but its possible lack of colloidal stability, high tendency for agglomeration and low compartmentalization of nitroxide and radicals may pose problems towards obtaining resins with desirable properties [76, 94, 101]. In emulsion systems, partitioning of reactants reduces the control over the polymerization. In addition, microemulsion polymerization requires high surfactant concentrations and very high shear treatments and usually low monomer content (in the range of 1~10 wt%), which directly affects the polymer structure and reduces its applicability [24, 96-98, 247]. Miniemulsion techniques have been cited with many advantages[114, 248, 249]. Reactions in miniemulsions occur inside monomer droplets (50~1000 nm) where transportation of monomers is not an issue and compartmentalization effects allow very high conversion while maintaining low dispersity, viscosity and high colloidal stability[46, 47, 57, 80, 122, 250].

Shunning organic solvent in favour of water is one example of applying the principles of green chemistry; using sustainably-sourced monomers in place of petro-based ones is another key component, which is the additional focus of this work [251-253]. In organic solvents, NMP, RAFT and ATRP methods have been used with bio-based monomers [164, 182, 254-258]. Recently, Noppalit *et al.*[163] studied the nitroxide-mediated miniemulsion polymerization of bio-based tetrahydrogeraniol methacrylate and cyclademol methacrylate using Dispolreg 007. In the present study, NMP of commercially available bio-based isobornyl methacrylate (Terra Visiomer IBOMA from Evonik) and C13 methacrylate (methacrylic ester 13.0, C13MA, from Evonik) was conducted in organic solvent and then in emulsion. IBOMA is derived from pine sap (produced by the reaction of camphene and methacrylic acid; the camphene was made by isomerization of terpenes derived from pine sap[178]) and contains a bulky bicyclic group to afford high thermal stability [259, 260] resulting in a high glass transition temperature ($T_g \approx 110~200$ °C)[201, 261-263] and can be copolymerized with other monomers to improve heat resistance [182, 264, 265]. C13MA is obtained from plant oils and provides flexibility to resins due to its long aliphatic side-chain [179]. The low T_g of poly(C13MA) (-46 °C) is attractive for copolymerization with other monomers to impart flexibility to coatings and thermoplastic elastomers, for example [201, 266-269]. RDRP in emulsion of bio-based monomers was reported via RAFT, in which Genggeng *et al.*[270] studied the RAFT emulsion polymerization of renewably-sourced

γ-methyl-α-methylene-γ-butyrolactone monomers. We also attempted to minimize or eliminate catalysts, agents, organic solvents and purification steps while maintaining the control of the polymerization and ultimately properties. In addition, moderate reaction temperature was applied for the initiation and polymerization which reduces the energy consumption. In the succeeding sections, we aim to translate the NMP of IBOMA and C13MA into a process in dispersed aqueous media with the requisite ability to make statistical and block copolymers. The reaction scheme of IBOMA and C13MA initiated by Dispolreg 007 is summarized in Figure 4.2.

Figure 4.1. Chemical structures of (a) BlocBuilder™ (b) Dispolreg 007 alkoxyamines.

Figure 4.2. NMP scheme describing the statistical copolymer of IBOMA and C13MA monomers by NMP with the Dispolreg 007 alkoxyamine initiator.

4.2. EXPERIMENTAL SECTION

4.2.1. Materials

Isobornyl methacrylate (IBOMA, >99%, Visiomer® Terra IBOMA) and C13 methacrylate (a mixture of methacrylic esters with an average chain length of 13 units, methacrylic ester 13.0, C13MA, >99%, Visiomer® Terra C13-MA) were obtained from Evonik. The monomers were purified to remove the inhibitor by passing them through a column of basic alumina (Brockmann, Type 1, 150 mesh, Sigma Aldrich) and calcium hydride (5 wt% relative to basic alumina, 90-95% reagent, Sigma Aldrich). DOWFAX™ 8390 (alkyldiphenyloxide disulfonate, 35 wt% active content, from Dow Chemical) and n-hexadecane (99%, Sigma Aldrich) were used as received. 3-(((2-Cyanopropan-2-yl) oxy) - (cyclohexyl) amino)-2, 2-dimethyl-3-phenylpropanenitrile (Dispolreg 007) was synthesized using Ballard *et al.*'s procedure[28]. Methanol (MeOH, >99%), tetrahydrofuran (THF, 99.9%, HPLC grade) and toluene (>99%) were purchased from Fisher Scientific and used as received. The deuterated chloroform (CDCl$_3$, ≥99%) was received from Cambridge Isotopes Laboratory for ^{1}H NMR tests. All the reactions were conducted under nitrogen atmosphere with high purity (99.99%, Praxair).

4.2.2. Methods

Molecular weight distribution of samples were determined by gel permeation chromatography (GPC, Waters Breeze) relative to PMMA standards without any filtration or purification at 40 °C. Three Waters HR Styragel® GPC columns (HR 1 with molecular weight measurement range of $10^2 - 5 \times 10^3$ g mol^{-1}, HR 2 with molecular weight measurement range of $5 \times 10^2 - 2 \times 10^4$ g mol^{-1} and HR 4 with molecular weight measurement range of $5 \times 10^3 - 6 \times 10^5$ g mol^{-1}, for THF solvent) and a guard column were used. Samples were diluted in THF (HPLC grade) to a concentration of approximately 5 mg ml^{-1}. To measure the Z-average particle size of samples, dynamic light scattering (DLS), was performed using a Malvern Zetasizer Nano- ZS. This instrument was equipped with a 4 mW He–Ne laser at 633 nm and an avalanche photodiode detector. The measurement angle was 173° and temperature was at 25 °C. The samples were diluted to the concentration of 0.01-1000 mg ml^{-1} ($10^{-3} - 1$ % mass) to prepare them for particle size measurement.

Conversions were determined by ^{1}H NMR (Varian NMR Mercury spectrometer, 300 MHz, 32 scans, using CDCl$_3$ deuterated solvent) for samples from solution polymerization and gravimetrically for emulsion samples. The final composition for all the polymer samples were also measured by ^{1}H NMR using the same conditions.

To measure the conversions gravimetrically, the samples were dried under ambient conditions in a fume hood for one day and then dried completely for 12 hours under vacuum at room temperature. The dried samples were dissolved in a small amount of toluene and methanol was added to the vials to precipitate the polymer. The supernatant was decanted from the vials to separate the unreacted monomers from the polymers in each sample. Finally, the samples were dried again at atmospheric pressure and room temperature for 12 hours and then dried completely for another 12 hours under vacuum. The same procedure was done for all the copolymers produced in emulsion to prepare them for further mechanical and thermal studies. The conversion was calculated from the Equation (4.1) for all the emulsion samples:

$$X = \frac{m_{precipitated}}{m_{sample}} \cdot \frac{m_{solution}}{m_{solute}} \cdot 100 \qquad (4.1)$$

where X is the monomer conversion (%); $m_{precipitated}$ is the mass of the sample after the drying and precipitation process; m_{sample} is the mass of sample before drying (the samples were directly taken from the latex); m_{solute} equals the sum of the masses of the monomers, surfactant, costabilizer and initiator in the latex; and $m_{solution}$ is the overall mass of the prepared latex. (In this study, $\frac{m_{solution}}{m_{solute}} = 4$). To determine the conversion via ^{1}H NMR results, Equation (4.2) was used:

$$X = X_{IBOMA}f_{IBOMA,0} + X_{C13MA}f_{C13MA,0} \qquad (4.2)$$

where X_{IBOMA} and X_{C13MA} are the individual conversions of IBOMA and C13MA monomers, respectively while $f_{IBOMA,0}$ and $f_{C13MA,0}$ are the initial molar fractions of IBOMA and C13MA monomers in the system (a sample ^{1}H NMR spectra for copolymerization of IBOMA and C13MA in toluene is available in Supplementary Information).

Thermogravimetric analysis (TGA) was carried out for all of the samples (previously dried as indicated above) using a TA Instruments TGA Q500TM under nitrogen flow at a ramp rate of 15 °C min^{-1} from 25 to 500 °C in aluminium pans to find the decomposition temperature (T_d). Differential scanning calorimetry (DSC, Q2000TM from TA Instruments) was performed under nitrogen to obtain the glass transition temperature (T_g) of samples. The three scans per cycle (heat/cool/heat) method was used at a heating rate of 15 °C min^{-1} and cooling rate of 50 °C min^{-1} in the temperature range of -90 to 170 °C to calculate T_gs using the inflection method.

Powder X-ray diffraction (PXRD) was carried out to assess crystallinity of the samples. A Bruker D2 Phaser diffractometer equipped with a LynxEyr linear position sensitive detector (Bruker AXS, Madison, WI, USA) and Ni-filtered CuKα radiation tube was used for this study. The voltage was 40 kV and the

current was 40 mA. The results were collected with a step of 0.02° and 0.5 seconds/step in the range of 2θ = 4-50°. The fraction of crystalline to amorphous content was calculated based on the peak area ratios.

Tensile tests were performed with an EZ-test-500N Shimadzu tensile tester. All dumbbell-shaped samples had the necks with approximately 3 mm width and 2 mm thickness and were tested based on ASTM D638 type V[271]. The samples were extended at a rate of 10 mm min^{-1} at room temperature and the reported data are the average of 5 measurements.

Rheological properties of selected samples were done using isothermal frequency sweeps on an Anton Paar MCR 302 rheometer from 1 to 1000 Hz with an amplitude of 1% under N_2 atmosphere at different temperatures (100, 140 and 150 °C). The measurements were performed in dynamic shearing mode using parallel plates (diameter = 25 mm) inside a CTD 450 convection oven. To prepare samples for different measurements, all the polymers were dried completely under vacuum overnight and precipitated in methanol to remove the unreacted monomers. After the precipitation, samples were dried again under vacuum for 24 hours at room temperature.

4.2.3. NMP of Isobornyl Methacrylate and C13 Methacrylate in Toluene Using Dispolreg 007 Initiator

To study the kinetics of polymerization and properties of copolymers with different ratios of IBOMA and C13MA, all the solution polymerizations were performed in a 15 ml, three-neck round-bottom glass flask connected to a reflux condenser which had fluid circulating at 3°C (the condenser was filled with a mixture of ethylene glycol/distilled water (20/80 vol%)). Target average molecular weight for all the studies in toluene solvent was 25 kg mol^{-1}. The bio-based monomers (IBOMA, C13MA or a mixture of them) and Dispolreg 007 alkoxyamine were dissolved in 50 wt% toluene solvent. The final solution was stirred for 10 minutes and was transferred into the reactor. A thermocouple was placed inside the reactor and connected to a temperature controller to control the reaction temperature during the polymerization. To provide a constant mixing in the reactor, a magnetic stir bar was added to the reactor and the reactor was placed inside a heating mantle on a magnetic stirrer. The reactants were deoxygenated by a purge of ultrapure nitrogen prior to polymerization for 30 minutes at room temperature. The nitrogen purging continued during the polymerization. At this point, the system was heated at a rate of about 10 °C.min^{-1} and the time when the reactor temperature reached 75 °C was taken as the commencement of the reaction. Samples were taken periodically during the reactions until a prescribed time or when the solution was too viscous to take samples using the sampling syringe. To stop the reactions, the reactor was removed from heating mantle and cooled down to room temperature.

4.2.4. Chain-Extension of Poly(IBOMA) Macroinitiator with C13MA

To check the chain end fidelity of polymer chains, chain-extension of poly(IBOMA) macroinitiators were conducted using a second batch of C13MA monomer. First, the homopolymerization of IBOMA was conducted at 100 °C with the same experimental procedure presented earlier. However, the reaction was stopped at 90 minutes to ensure polymer chains had highly active ends (X=25%, M_n = 13.6 kg mol^{-1}, $Đ$ = 1.47). The macroinitiator was then precipitated in methanol to remove the unreacted monomers. Next, 0.9259 g of poly(IBOMA) macroinitiator (0.068 mmol), C13MA (2.7777 g, 10.364 mmol) and toluene (50 wt%, 3.7036 g, 40.195 mmol) were mixed for 10 min and added to the reactor. The reactor was sealed, and the solution was purged with ultra-pure nitrogen for 30 min before the reaction was started by heating up to the desired temperature. The nitrogen purging continued during the synthesis to avoid the termination reactions. A temperature of 100 °C and $M_{n,target}$ = 40 kg mol^{-1} were used for the chain-extension reaction. The polymerization continued for 3 hours to synthesize block copolymer of IBOMA and C13MA. Finally, the reaction was stopped, and the polymer was precipitated in methanol (X=55%, M_n = 37.1 kg mol^{-1}, $Đ$ = 1.93, F_{IBOMA} = 0.22).

4.2.5. Miniemulsion Polymerization of IBOMA and C13MA Using Dispolreg 007 Initiator

Miniemulsions were prepared based on the formulation in Table 4.1 The $M_{n,target}$ for all the studies in emulsion was set to 45 kg mol^{-1}. DOWFAX™ 8390 is a biodegradable ionic surfactant with low volatility and low sorption to soils, which makes it a good candidate for a green miniemulsion polymerization [272-274]. N-hexadecane was added as the costabilizer to the miniemulsion system to inhibit Ostwald ripening and improve the colloidal stability of latex [275]. N-Hexadecane is also biodegradable and it can be extracted from sustainable bio-sources such as long pepper[276, 277]. In order to prepare the system for polymerization, monomers, n-hexadecane and Dispolreg 007 were mixed together for 10 minutes. The aqueous solution was prepared separately by dissolving DOWFAX™ 8390 as the surfactant in distilled water and stirring it for 10 minutes. Then, two solutions were mixed together for 15 minutes and the resulting emulsion was sonicated using a Hielscher sonicator (model UP200S, 50% duty cycle and amplitude 70%) for 10 minutes in a cold water bath. The final emulsion was added to a 50 ml three-neck round-bottom glass flask connected to a reflux condenser that was cooled to 3 °C. The condenser was cooled with a mixture of ethylene glycol/distilled water (20/80 vol%) from a Polyscience recirculating chiller Model MX7LR-20-A11B. A thermocouple was placed inside the reactor and connected to a temperature controller to control the reaction temperature during the polymerization. To provide mixing of the contents inside the reactor, a magnetic stir bar was added to the reactor and the reactor was placed inside a heating mantle on a magnetic stirrer. The reactants were deoxygenated by a purge of ultrapure nitrogen prior to polymerization for 30 minutes at room temperature. The nitrogen purging continued during the polymerization. At this point, the

system was heated at a rate of about 10 °C·min^{-1} and the time when the reactor temperature reached 75 °C was taken as the commencement of the reaction. Samples were taken periodically during the reaction for measurement of molecular weight, conversion and particle size.

Table 4.1. Typical recipe for the nitroxide-mediated miniemulsion polymerization of Isobornyl Methacrylate (IBOMA) and C13 Methacrylate (C13MA).

Component	Amount
Monomer (1) – IBOMA	Varies based on the experiment (0-1.082 M)
Monomer (2) – C13MA	Varies based on the experiment (0-0.872 M)
Alkoxyamine (Dispolreg 007)	0.005 M
DOWFAX™ 8390	2 wbm%
n-Hexadecane	0.8 wbm%
Water	75 wt%

4.2.6. Chain Extension of Poly(C13MA) with IBOMA Monomer in Emulsion Using Dispolreg 007 Initiator

The seed latex of poly(C13MA) was prepared in a 100 ml three-neck round-bottom glass flask connected to a reflux condenser and under nitrogen atmosphere for 150 minutes at 90° C. The recipe for preparation of poly(C13MA) seed latex is described in Table 4.2 The magnetic stirrer was added, and the temperature was controlled using a thermocouple. In the next step, IBOMA monomer (IBOMA:C13MA = 1:1 weight ratio) was bubbled with nitrogen for 30 minutes and added to the flask in a single shot. The polymerization continued for another 120 minutes under the same conditions to prepare the gradient copolymer of C13MA and IBOMA in miniemulsion system.

Table 4.2. Recipe for preparation of seed latex of poly(C13MA) at 90° C (10 wt% solid content, Dispolreg 007 initiator).

Component	Amount
C13 methacrylate (C13MA)	0.381 M
Alkoxyamine (Dispolreg 007)	0.004 M
DOWFAX™ 8390	5 wbm%

n-Hexadecane   1 wbm%

Water   89 wt%

4.3. RESULTS AND DISCUSSION

4.3.1. NMP of IBOMA and C13MA in Toluene

The NMP of IBOMA and C13MA monomers was conducted first in toluene to study the polymerization kinetics in organic solvent as a base for comparison with an emulsion-based system. The nitroxide mediated copolymerization of IBOMA and C13MA was carried out in toluene using Dispolreg 007 initiator without using any controlling comonomers. Table 4.3 represents all the studies in toluene using Dispolreg 007 initiator. First, the effect of temperature on the homopolymerization of IBOMA and C13MA was studied (please refer to Supplementary Information Section 2). Then, the effect of different ratios of IBOMA:C13MA on the kinetics of polymerization was investigated.

Table 4.3. Summary of experiments for nitroxide-mediated copolymerization of IBOMA/C13MA mixtures in toluene solvent using Dispolreg 007 initiator.

Experiment ID	Reaction time (min)	$M_{n,final}$ [c] (kg mol^{-1})	X [d] (%)	[Dispolreg 007] (M)	[IBOMA]$_0$ (M)	[C13MA]$_0$ (M)	$Đ$ [c]	T [e] (°C)
IBOMA100-S-90C [a]	90	13.6	25.0	0.018	2.054	0	1.47	90
IBOMA100-S-100C	90	16.5	69.1	0.018	2.054	0	1.54	100
IBOMA100-S-110C	60	13.9	83.6	0.018	2.054	0	1.66	110
C13MA100-S-90C	210	16.9	43.7	0.017	0	1.609	1.45	90
C13MA100-S-100C	180	24.2	82.8	0.017	0	1.609	1.39	100
C13MA100-S-110C	150	20.0	89.6	0.017	0	1.609	1.59	110
IBOMA80/C13MA20-S [b]	120	23.6	76.3	0.018	1.559	0.390	1.56	100
IBOMA60/C13MA40-S	120	25.0	78.3	0.018	1.110	0.740	1.54	100
IBOMA50/C13MA50-S	120	26.1	69.9	0.018	0.902	0.902	1.61	100
IBOMA40/C13MA60-S	120	24.1	71.2	0.018	0.704	1.057	1.52	100
IBOMA30/C13MA70-S	120	26.5	77.0	0.018	0.516	1.204	1.54	100
IBOMA20/C13MA80-S	120	27.3	70.0	0.017	0.336	1.344	1.50	100
IBOMA10/C13MA90-S	150	19.8	77.3	0.017	0.164	1.479	1.52	100

[a] Solution polymerization of 100 mol% IBOMA in the initial feed composition at 90 °C (solvent: toluene). [b] Solution polymerization of monomers with initial feed composition of 80 mol% IBOMA and 20 mol% C13MA (solvent: toluene). [c] The final number-average molecular weight (M_n) and dispersity ($Đ$) were reported from GPC relative to PMMA standards in THF at 40 °C. The target number-average molecular weight $M_{n,target}$ for all the polymerization in toluene was 25 kg mol^{-1}. [d] Overall monomer conversion measured by ^{1}H NMR. [e] T is the reaction temperature in units (°C).

4.3.1.1. Poly(IBOMA-*stat*-C13MA) Solution Copolymerization by NMP

IBOMA/C13MA mixtures, with initial IBOMA molar feed compositions f_{IBOMA} = 0.1-0.8 were copolymerized by NMP using Dispolreg 007 initiator in 50 wt% toluene at the optimal polymerization temperature of 100 ℃ (This was studied in the range of 90-110 ℃; please see the Supplementary Information Section 2). Table 4.3 presents the experimental conditions for this series of syntheses. As Figure 4.3 indicates, the semi-logarithmic kinetic plots with time were linear for all the reactions. The apparent slopes do not show a significant difference between different IBOMA/C13MA copolymerizations. This is in accordance with our previous results for NMP of IBOMA and C13MA using BB and 10 mol% AN controlling comonomer [182]. In addition, the values of the apparent rate constant $k_P[P^\bullet]$ (k_P = propagation rate constant, $[P^\bullet]$ is the concentration of polymer with radical chain ends) for the experiments at 100 ℃ using Dispolreg 007 initiator are lower than the values for BB (with 10 mol% AN as the controlling comonomer) in our previous study, indicating a slower polymerization rate when using Dispolreg 007 compared to BB[243]. It should be noted using a small amount of AN comonomer is essential to use BB initiator, however when using Dispolreg 007, no controlling comonomer is required and thus it is difficult to make a direct comparison between the two systems[182]. The Đ of samples shown in Figure 4.3(b) was in the range of $1.19 < Đ < 1.61$ which generally decreased as the molar ratio of C13MA monomer increased in the system. M_n plots versus conversion were linear at low conversion $(X \sim < 40\%)$ and all of them have an over-prediction in terms of adherence to the theoretical line due to slow initiation of the Dispolreg 007 initiator[278]. At higher conversions $(X > 40\%)$, the slope of M_n versus conversion plots slightly decreases. This could be ascribed to the onset of irreversible termination reactions which decreases the concentration of macro-radicals $[P^\bullet]$ and possible complete consumption of the initial alkoxyamines at higher conversions.

Figure 4.3. NMP to produce poly(IBOMA-*stat*-C13MA) copolymers using Dispolreg 007 initiator in toluene (50 wt%) at 100 °C and $M_{n,target}$ = 25 kg mol^{-1}. (a) Semi-logarithmic kinetic plots of ln[(1-X)$^{-1}$] (X= monomer conversion) versus reaction time (b) The evolution of M_n and Đ with conversion (X). IBOMA100-S-100C (filled circles, ●); IBOMA80/C13MA20-S (filled triangles, ▲); IBOMA60/C13MA40-S (filled diamonds, ◆); IBOMA50/C13MA50-S (gray circles, ●); IBOMA40/C13MA60-S (gray triangles, ▲); IBOMA30/C13MA70-S (gray diamonds, ◆); IBOMA20/C13MA80-S (open circles, ○); IBOMA10/C13MA90-S (open triangles, Δ); C13MA100-S-100C (open diamonds, ◊).

4.3.1.2. Effect of Feed Composition on Poly(IBOMA-*stat*-C13MA) Solution Copolymerization by Dispolreg 007

In addition to kinetic studies, the influence of feed composition on the copolymer composition was studied in homogenous toluene solution at 100 °C. This was done to predict thermal and mechanical properties of copolymers that are subsequently made in emulsion. The composition of the copolymers was determined by ^{1}H NMR at the early stages of the copolymerization to extract the low-conversion data (X<10% for every copolymerization, Table 4.S1, Supplementary Information).

A non-linear regression fit to the Mayo-Lewis equation was used to extract the reactivity ratios of poly(IBOMA-*stat*-C13MA) and the uncertainties were provided from the standard errors of the parameters in the calculation[279]. Employing the terminal copolymerization model, it is always presumed that the reactivity of an active center depends on the nature of the terminal monomer unit of the propagating chain[280]. The commercial software MATLAB R2016a was used to solve the Mayo-Lewis equation[281]:

$$F_{IBOMA} = \frac{r_{IBOMA}f_{IBOMA,0}^2 + f_{IBOMA,0}f_{C13MA,0}}{r_{IBOMA}f_{IBOMA,0}^2 + 2f_{C13MA,0}f_{IBOMA,0} + r_{IBOMA,0}f_{TDMA,0}^2} \tag{4.3}$$

The statistical fit yielded reactivity ratios r_{IBOMA} = 0.89 ± 0.13 and r_{C13MA} = 1.80 ± 0.21, suggesting the C13MA monomer is slightly more reactive than IBOMA towards both propagating species (–IBOMA$^•$ and –C13MA$^•$). The Mayo-Lewis plot (Figure 4.4) indicates that poly(IBOMA-*stat*-C13MA) formed instantaneously by solution copolymerization was always slightly richer in C13MA without any azeotropic composition. Although IBOMA and C13MA reactivity ratios have not been reported, they can be compared to similar methacrylate copolymerizations. Lauryl methacrylate (LMA) is similar to C13MA and there are a few cases of LMA copolymerizations with other methacrylates. For instance, the reactivity ratios of lauryl methacrylate (LMA) and methyl methacrylate (MMA) in 1,1,2-trichloro-1,2,2, trifluoroethane at 60 °C were reported as r_{LMA} = 0.84 ± 0.10 and r_{MMA} = 1.22 ± 0.14[282], while using conventional free radical polymerization in toluene at 70 °C for the same monomers resulted in r_{MMA} = 1.12 ± 0.01 and r_{LMA} = 1.19 ± 0.01[283]. In another study, the reactivity ratios of IBOMA and tetrahydrofurfuryl methacrylate (THFMA)

from photo copolymerization experiments were $r_{IBOMA} = 0.47 \pm 0.10$ and $r_{THFMA} = 2.51 \pm 0.35$[284]. For the ATRP of IBOMA with 4-methoxybenzyl methacrylate (MBMA) at 100 °C in bulk, the reactivity ratios were $r_{IBOMA} = 0.89 \pm 0.01$ and $r_{MBMA} = 0.64 \pm 0.01$ [212].
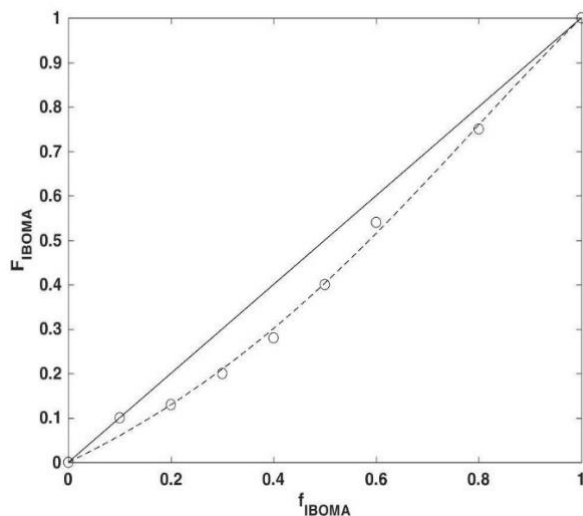
Figure 4.4. Mayo-Lewis plot of copolymer composition with respect to IBOMA molar fraction at low conversion or instantaneous composition ($F_{IBOMA,i}$) versus initial IBOMA feed composition ($f_{IBOMA} \approx f_{IBOMA,0}$). The open circles represent the experimental data and the dashed line shows the trend line. The straight line is associated with the azeotropic composition ($F_{IBOMA} = f_{IBOMA}$). The copolymerization was performed at 100 °C using Dispolreg 007 initiator in 50 wt% toluene. $F_{IBOMA,i}$ of copolymers is available in Table 4.S1 in Supplementary Information.

4.3.1.3. Chain-Extension of Poly(IBOMA) Macroinitiator with C13MA

The chain-end fidelity of polymer chains and the possibility of making block copolymers was tested by the chain-extension of poly(IBOMA) macroinitiators using a fresh batch of C13MA. The formulation and kinetic data of chain-extensions are available in Table 4.4. The poly(IBOMA) macroinitiator was prepared at 100 °C ($X = 25\%$, $M_n = 13.5$ kg mol^{-1} and $Đ = 1.47$). Then, the macroinitiator was mixed with C13MA and the chain-extension reaction continued for 180 minutes at the same temperature. The GPC chromatograms of the chain-extension are presented in Figure 4.5 Accordingly, a clear, monomodal shift of M_n toward higher molecular weight was observed, indicating nearly simultaneous growth of all chains. The increased $Đ$ is due to the appearance of the lower molecular weight tail, which suggests some dead macroinitiator was present. For the final sample chromatogram (at 180 minutes after the chain extension), multiple Gaussian peak fitting was carried out to estimate the percentage of dead polymer chains in the final sample. According to the fitting analysis presented in Figure 4.S2 (Supplementary Information) after

three hours of chain-extension, 27.5 % of the initiating polymer chains were estimated to be dead. This shows that the majority of polymer chains were active up to 55% conversion in organic solvent. This provided a basis of what to expect in emulsion conditions and we hypothesized compartmentalization effects inherent in the miniemulsion process to provide improved chain activity to higher conversions[46, 76, 250].

Table 4.4. Chain-extension of IBOMA macroinitiator with C13MA in 50 w% toluene at 100 °C for 3 hours and molecular characterization of the resulting chain-extended product.

A. Macroinitiator								
Experiment ID	X^a (%)	[Dispolreg] (M)	[IBOMA] (M)	[Toluene] (M)	$M_n{}^b$ (kg mol^{-1})	$M_{n,theo}{}^c$ (kg mol^{-1})	$Đ^b$	Time ^{d} (min)
Poly(IBOMA)-macroinitiator	25	0.020	2.212	5.409	13.6	25	1.47	90
B. Formulation and Characterization of Chain-Extension								
Experiment ID	[Macroinitiator] (M)	X^a (%)	$F_{IBOMA}{}^e$	[Toluene] (M)	$M_n{}^b$ (kg mol^{-1})	[C13MA] (mmol)	$M_{n,theo}{}^f$ (kg mol^{-1})	$Đ^b$	Time ^{d} (min)
Poly(IBOMA-*b*-C13MA)	0.009	55	0.22	5.385	37.1	1.389	40	1.93	180

^{a} Overall monomer conversion measured by ^{1}H NMR. ^{b} The final number average molecular weight (M_n) and dispersity ($Đ$) were measured by GPC relative to PMMA standards at 40 °C in THF. ^{c} The target number average molecular weight to synthesize poly(IBOMA)-macroinitiator. ^{d} The reaction time (minutes). ^{e} Molar fraction of IBOMA in the polymer chain. ^{f} The target number average molecular weight for the whole block copolymer
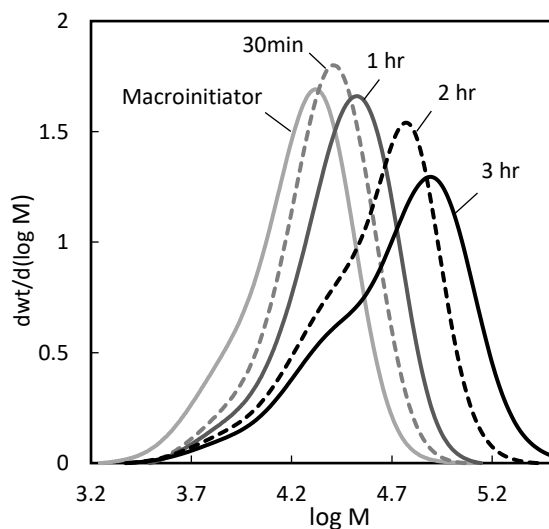
Figure 4.5. GPC traces for chain-extension of poly(IBOMA) macroinitiator (M_n = 13.6 kg mol^{-1} and $Đ$ = 1.47) with C13MA. Chain-extension was done in 50 wt% toluene at 100 °C. The gray solid line is the macro initiator while the black solid line is the chain-extended product with M_n = 40.7 kg mol^{-1} and $Đ$ = 1.93

(Dispersity is reported for the overall peak, containing the active and dead polymers). Full characterization data for the samples shown is provided in Table 4.4.

4.3.2. Copolymerization of IBOMA/C13MA by Nitroxide-Mediated Miniemulsion Polymerization Using Dispolreg 007 Initiator

The oil-soluble Dispolreg 007 initiator required balancing the amount of surfactant and costabilizer relative to other NMP miniemulsion studies [60, 66]. Accordingly, the amount of DOWFAX™ 8390 surfactant that should be added is at least 2 to 5 wbm% (weight based on the monomers) to prevent coagulation[285]. Since reduction of the amount of surfactant in the latex is desired due to environmental concerns (eg. biodegradability, toxic effects on aquatic organisms), addition of only 2 wbm% of DOWFAX™ 8390 was applied for this study [286-289]. The miniemulsion polymerization was conducted by adding 2 wt% Dowfax™ 8390 relative to monomer as the surfactant and 0.8 wt% hexadecane relative to monomer as the costabilizer. The highly hydrophobic monomers of IBOMA and specifically C13MA acted as polymerizable costabilizers inside particles, which helped retarding Ostwald ripening and compensates the need for higher concentration of n-hexadecane. The monomer content in all latexes was 24.14 wt% and $M_{n,target}$ of 45 kg mol^{-1} was considered for all the polymerizations. Figure 4.6 graphically displays the system used for this study. Table 4.5 lists all the studies for the miniemulsion polymerization of monomer feeds with different ratios of IBOMA/C13MA using Dispolreg 007 initiator.
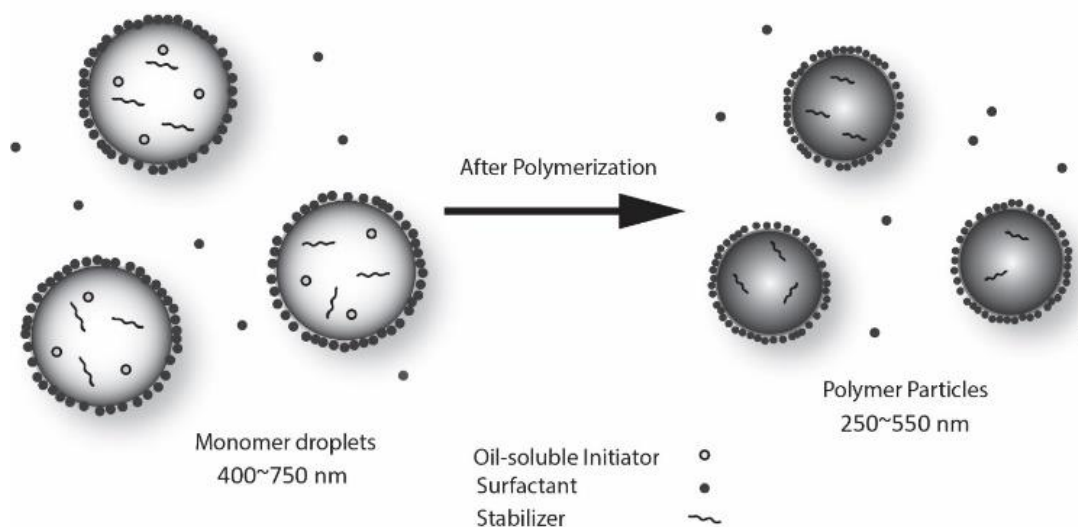
Figure 4.6. The schematic of nitroxide-mediated miniemulsion polymerization using oil-soluble Dispolreg 007 initiator.

Table 4.5. Summary of experiments for nitroxide-mediated miniemulsion polymerization of IBOMA/C13MA copolymerization.

Experiment ID	$M_{n,final}$ [b] (kg mol^{-1})	X [c] (%)	[Dispolreg 007]$_0$ (M)	[IBOMA]$_0$ (M)	[C13MA]$_0$ (M)	$Đ$ [b]	T [d] (°C)	D_z [e] (nm)
IBOMA100 [a]	42.2	82.7	0.005	1.082	0	1.50	90	548
IBOMA100-83C	39.3	67.6	0.005	1.082	0	1.58	83	441
IBOMA100-100C	33.5	64.2	0.005	1.082	0	1.54	100	526
IBOMA90/C13MA10	53.9	91.1	0.005	0.951	0.106	1.70	90	415
IBOMA80/C13MA20	57.8	83.4	0.005	0.826	0.206	1.68	90	353
IBOMA70/C13MA30	46.8	85.3	0.005	0.706	0.303	1.62	90	331
IBOMA60/C13MA40	56.2	92.4	0.005	0.592	0.395	1.63	90	291
IBOMA50/C13MA50	50.8	87.8	0.005	0.483	0.483	1.72	90	327
IBOMA40/C13MA60	64.2	88.8	0.005	0.378	0.567	1.65	90	481
IBOMA30/C13MA70	67.9	94.0	0.005	0.278	0.648	1.66	90	276
IBOMA20/C13MA80	63.8	92.7	0.005	0.181	0.726	1.68	90	270
IBOMA10/C13MA90	61.1	92.6	0.005	0.089	0.800	1.73	90	306
C13MA100	48.9	73.3	0.005	0	0.872	1.55	90	472

[a] The miniemulsion polymerization of IBOMA and C13MA monomers with the initial feed composition of 100 mol% IBOMA and 0 mol% C13MA. The monomer content for all the emulsions was 24.14 wt%. [b] The final number average molecular weight (M_n) and dispersity ($Đ$) were measured by GPC with PMMA standards in THF at 40 °C. The target number average molecular weight ($M_{n,target}$) for all the miniemulsion polymerizations was 45 kg mol^{-1}. [c] Overall monomer conversion measured gravimetrically. [d] The reaction temperature (°C). [e] Final Z-average particle size (nm).

Firstly, the miniemulsion homopolymerization of IBOMA was conducted at different temperatures using the Dispolreg 007 to confirm the optimum reaction temperature. Figure 4.S3 in the Supplementary Information displays the kinetic results at three different temperatures of 83, 90 and 100 °C for homopolymerization of IBOMA in toluene. The lowest temperature (83° C) was used to compare the results for the polymerization of methacrylates conducted by Ballard and co-workers using the Dispolreg 007 alkoxyamine[47]. Figure 4.S3(a) illustrates the linear trends for the polymerizations at 90 and 100 °C. However, the semi-logarithmic kinetic plots of $\ln[(1-X)^{-1}]$ (X= monomer conversion) versus reaction time was not linear at 83° C due to the slow initiation of Dispolreg 007 initiator. The polymerization rate of IBOMA at 83 °C was much lower than at 90 or 100 °C, as the Dispolreg 007 initiator decomposes much more readily at elevated temperatures [28, 290]. At 100 °C, the reaction was very fast and stopped at 45 minutes as particle coagulation and precipitation was observed, indicating the emulsion lost its stability (overall conversion = 64%, $Đ$ = 1.54 and $M_{n,final}$ = 33 kg mol^{-1}). This can be due to some evaporation of water at this temperature that alters the concentration of monomer/polymer in the surrounding aqueous medium and destabilizes the system. The evolution of molecular weight with overall conversion was not linear in all cases and it is higher than that predicted, especially at lower conversions. This is in agreement with previous studies of NMP using Dispolreg 007 initiator which showed slow initiation due to a strong penultimate effect [28, 43]. The molecular weight distributions were somewhat broad ($Đ$ < 1.64) but comparable with the

56

results for homogeneous polymerization in toluene. The final average particle size ranged from 441 to 548 nm. Based on these results, the optimal temperature was chosen as 90 °C, which balanced high overall conversion ($X = 82\%$) with a relatively low dispersity ($Đ < 1.57$), while still remaining colloidally stable. Therefore, ensuing binary copolymerizations in emulsion were done using these conditions.

4.3.2.1. The Copolymerization of Different Ratios of IBOMA/C13MA Using Dispolreg 007 Initiator in Emulsion

After finding an acceptable temperature from the homopolymerization kinetic studies, the copolymerization of different ratios of IBOMA and C13MA was conducted in emulsion by NMP. Figure 4.7(a) represents the semi-logarithmic kinetic plots of $\ln[(1-X)^{-1}]$ versus time for different initial ratios of IBOMA and C13MA monomers. As shown in Figure 4.7(a), the kinetic plots were linear in all cases and no significant increase in polymerization rate was observed for different ratios of $[IBOMA]_0/[C13MA]_0$ in the system for the copolymerization.

Figure 4.7. The miniemulsion polymerization of different ratios of IBOMA/C13MA using Dispolreg 007 initiator (a) Semi-logarithmic kinetic plots of $\ln[(1-X)^{-1}]$ ($X=$ monomer conversion) versus reaction time (b) Number average molecular weight M_n and dispersity $Đ$ versus conversion (X). IBOMA100 (filled circles, ●); IBOMA90/C13MA10 (filled triangles, ▲); IBOMA80/C13MA20 (filled diamonds, ♦); IBOMA70/C13MA30 (filled squares, ■); IBOMA60/C13MA40 (gray circles, ●); IBOMA50/C13MA50 (gray triangles, ▲); IBOMA40/C13MA60 (gray diamonds, ♦); IBOMA30/C13MA70 (gray squares, ■); IBOMA20/C13MA80 (open circles, ○); IBOMA10/C13MA90 (open triangles, Δ); C13MA100 (open diamonds, ◊).

57

Based on the results shown in Figure 4.7(b), it can be assumed that increasing the ratio of $[IBOMA]_0/[C13MA]_0$ slightly increases control over the polymerization. This can be due to the comparatively lower propagation rate constant k_p for IBOMA, which decreases the propagation rate for reactions with higher [IBOMA] and improves the control over the polymerization[182]. As it was shown in Figure 4.7(b), the reactions with higher initial concentrations of C13MA deviate more from the theoretical line in the M_n versus conversion (X) plot and it seems that decreasing the initial amount of IBOMA causes the control loss. It should be noted that the deviation is partly due to the calibration against PMMA standards without applying the Mark-Houwink-Sakurada coefficients for C13MA and IBOMA homopolymers as they were not available for C13MA homopolymers. This, along with the slow initiation of Dispolreg 007 alkoxyamine at lower conversions (overall conversion $< 25\%$) results in higher M_n at higher conversions, especially for the copolymers with higher [C13MA]. Interestingly, this phenomenon is only pronounced in the miniemulsion system, where the polymerization occurs inside the particles. This can be due to higher reaction temperature for polymerization in toluene (the reaction temperature in toluene and emulsion are 100 and 90 °C, respectively), the variation of particle sizes for different reactions in emulsion and also higher $M_{n,target}$ for emulsions compared to the toluene-based system ($M_{n,target,emulsion}$ = 45 kg mol^{-1} versus $M_{n,target,toluene}$ = 25 kg mol^{-1}). Final $Đ$ for miniemulsion homopolymerization of IBOMA and C13MA was $Đ_{poly(IBOMA)}$ = 1.50 and $Đ_{poly(C13MA)}$ = 1.55, respectively. For all the copolymers of IBOMA and C13MA studied in the emulsion system, the final $Đ$ was in the range of $1.62 < Đ < 1.72$ (Figure 4.7(b)). This showed that the final dispersity of emulsion samples was slightly higher than the final $Đ$ of samples prepared in toluene ($1.50 < Đ < 1.61$), considering that the $M_{n,target}$ was different in these systems. Elsewhere, compartmentalization of nitroxides and radicals has an influence on polymerization and termination rates within the monomer particles and resulted in higher dispersity of polymers made in an emulsion system [24, 76].

4.3.2.2. Study of the Particle Size in Miniemulsion NMP of IBOMA/C13MA

The Z-average particle size of latex samples was determined by DLS. All the samples were diluted in deionized water just before the test without filtration. Initially, the effect of addition of costabilizer (n-hexadecane) and surfactant on particle size was studied. As the oil-soluble Dispolreg 007 alkoxyamine was used in the system, the initiation reaction occurred inside monomer droplets and the surfactant stabilized the system[43, 103]. First, the effect of temperature on the particle size was studied by NMP of IBOMA in emulsion and the results are presented in Figure 4.S4 (a). As shown in Figure 4.S4 (a) and (b), the coagulation in the final emulsions was not significant and the final particle size in all experiments was smaller than the initial particle size [43]. Sometimes, the Z-averaged particle size fluctuated as the polymerization continued, suggesting the presence of a low concentration of micron-sized particles due to

the coagulation of monomer droplets or polymer particles[43]. Figure 4.S4 (b) illustrates the evolution of particle size during the course of each polymerization for different initial molar ratios of IBOMA:C13MA. The particle size during the copolymerization generally decreased with increasing C13MA concentration, with most particles ~ 400-500 nm for richer IBOMA compositions and decreasing to ~ 300-400 nm for lower IBOMA compositions. Interestingly, the C13MA homopolymerization in emulsion had slightly larger particle sizes compared to those with some IBOMA. The general decreases in particle size as C13MA composition increased shows the effect of the long-chain n-alkyl group in the C13MA monomers which can act as a costabilizer in the monomer particles, preventing diffusional degradation and improving the colloidal stability [74, 291, 292]. It is worth mentioning that the polymer latexes were colloidally stable at room temperature for at least three months (the duration of investigation) and no polymer precipitation nor change in particle size was observed.

4.3.2.3. Chain Extension of Poly(C13MA) with IBOMA Monomers in Emulsion Using Dispolreg 007 Initiator

Chain extension of poly(C13MA) with IBOMA monomers was conducted to check the chain-end fidelity as well as the possibility of making gradient copolymers in NMP miniemulsion [66]. First, a seed latex of poly(C13MA) with 10 wt% solid content was prepared at 90° C. After 150 minutes of the polymerization, IBOMA was added to the system to make the gradient polymer. Table 4.6 shows the kinetic data and properties of the gradient miniemulsion polymerization of C13MA and IBOMA. The shift in GPC traces toward higher molecular weights indicates the clean attainment of poly(C13MA-*grad*-IBOMA) copolymer (Figure 4.8). This is in contrast to the solution polymerization shown in Figure 4.5 which indicates some tailing. There are several differences, and it is difficult to compare the chain extensions as the macroinitiators were prepared at different conversions (the miniemulsion macrointiator was made to higher conversion) yet had no obvious tailing. It is possible that there are chain transfer effects in solvent that influence the fidelity of the macroinitiator more than any of the factors influencing the miniemulsion polymerization.

Table 4.6. Chain-extension of poly(C13MA) with IBOMA in miniemulsion system at 90 °C for 2 hours and molecular characterization of the resulting chain-extended product.

A. Macroinitiator								
Experiment ID	X^a (%)	[Dispolreg 007]$_0$ (M)	[C13MA]$_0$ (M)	$M_n{}^b$ (kg mol^{-1})	$M_{n,theo}{}^c$ (kg mol^{-1})	$Đ^b$	t^d (min)	$D_z{}^e$ (nm)
Poly(C13MA) seed latex	61	0.004	0.381	34	25	1.55	150	339

B. Formulation and Characterization of Chain-Extension							
Experiment ID	X^a (%)	$F_{IBOMA}{}^f$	$M_n{}^b$ (kg mol^{-1})	[IBOMA]$_0$ (mmol)	$Đ^b$	t^d (min)	$D_z{}^e$ (nm)
Poly(C13MA-grad-IBOMA)	87	0.51	54	0.233	1.65	120	345

C. Results for Thermal Characterization by DSC and TGA						
	$T_m{}^g$ (°C)	$T_{g,1}{}^g$ (°C)	$T_{g,2}{}^g$ (°C)	$T_{dec,1}{}^h$ (°C)	$T_{dec,max}{}^h$ (°C)	$T_{dec,2}{}^h$ (°C)
Poly(C13MA-grad-IBOMA)	-27	-32	76	220	282	470

^{a} Overall monomer conversion measured gravimetrically. ^{b} The final number average molecular weight (M_n) and dispersity ($Đ$) were measured by GPC with PMMA standards at 40 °C in THF. ^{c} The target number average molecular weight. ^{d} The reaction time (minutes). ^{e} Z-average particle size (nm). ^{f} Molar fraction of IBOMA in Poly(C13MA-grad-IBOMA) determined by ^{1}H NMR in CDCl$_3$. ^{g} T_m (melting point) and T_g (glass transition temperature) measured by DSC under nitrogen atmosphere using three scans per cycle (heat/cool/heat) at a heating rate of 15 °C min^{-1} and cooling rate of 50 °C min^{-1}. ^{h} $T_{dec,1}$ ($T_{10\%}$ or onset of decomposition), $T_{dec,max}$ (temperature at which highest weight loss occurs) and $T_{dec,2}$ (end of decomposition) measured by TGA under nitrogen atmosphere at a ramp rate of 15 °C min^{-1}.
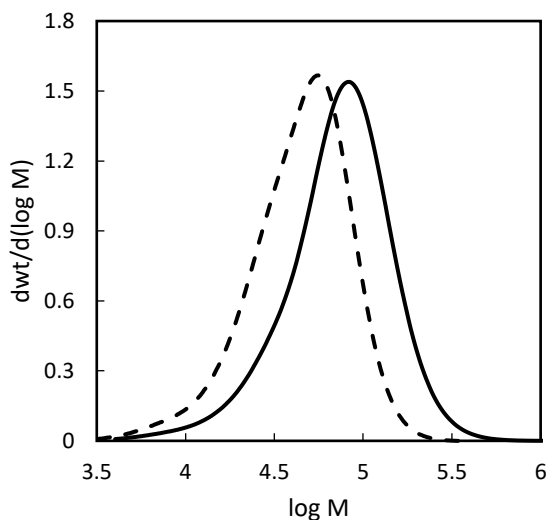
Figure 4.8. Molecular weight distribution of polymer particles in chain extension polymerization. Seed latex of poly(C13MA) (dashed black line) and poly(C13MA-*grad*-IBOMA) after the chain extension (solid black line). Characterization data for these two samples is provided in Table 4.6.

To evaluate the thermal stability and find the glass transition temperatures of poly(C13MA-*grad*-IBOMA), TGA and DSC were performed. The decomposition temperatures and glass transition temperatures are presented in Table 4.6(C). The first glass transition temperature ($T_{g,1}$) and melting temperature (T_m) corresponds to the soft C13MA block and the higher glass transition temperature ($T_{g,2}$) corresponds to the block of IBOMA-rich composition. The C13MA monomer used in this study is a mixture of methacrylic

esters with an average chain length of 13 units. This results in the presence of monomers such as dodecyl methacrylate, tetradecyl methacrylate and other long chain monomers that produce homopolymers with semi-crystalline structures and melting points (e.g. T_ms for poly(dodecyl methacrylate) and poly(tetradecyl methacrylate) are -34 °C and -2 °C respectively)[201, 293, 294]. The inclusion of these monomers in C13MA likely cause the appearance of melting for the poly(C13MA-*grad*-IBOMA). Note that the higher T_g corresponding to the IBOMA-rich segment is lower than the T_g of poly(IBOMA) homopolymer from literature ($T_g \approx 110\sim200$ °C)[201, 261-263] since there is likely some C13MA copolymerized in the former, resulting in a depression of the T_g. Still, the presence of multiple T_gs show the gradient polymerization of C13MA and IBOMA was sufficiently effective in producing compositionally distinctive blocks long enough to result in microphase separation[293]. The DSC trace for poly(C13MA-*grad*-IBOMA) is depicted in Figure 4.S5 (see Supplementary Information).

4.3.3. Thermal Studies of IBOMA/C13MA Polymers Prepared in Solution and Emulsion Systems

TGA was performed for copolymers with different ratios of IBOMA/C13MA monomers to measure the decomposition temperatures of samples. The decomposition temperatures for two different systems were given in Table 4.7. The TGA results for copolymers with a high concentration of IBOMA monomers (initial IBOMA mol% > 30 %) show a two stage decomposition. This suggests the cleavage of the O-isobornyl bond and the formation of camphene in the sample and the elimination of it at higher temperatures[211]. This result was observed in other studies for copolymers containing IBOMA [182, 212]. Therefore, it can be concluded that polymers containing high concentrations of IBOMA will decompose readily and this may limit their applications at higher temperatures, although the polymers have a high T_g. The T_g and T_m were also measured by DSC and the results are available in Table 4.7. The Fox equation was used to calculate the theoretical T_g for the resins[200]. For a polymer consisting of a mixture of different monomers, $T_{g,theo}$ can be estimated from the following equation:

$$\sum_i w_i \left(1 - \frac{T_{g,theo}}{T_{g,i}} \right) = 0 \tag{4.4}$$

where w_i is mass fraction of component i in polymer resin, $T_{g,theo}$ is the theoretical glass transition temperature of the resin and $T_{g,i}$ is the glass transition temperature of pure homopolymer of component i. $T_{g,IBOMA}$ and $T_{g,C13MA}$ were chosen from the experimental data presented in this study for each system. The resulting $T_{g,theo}$s for polymers with different ratio of IBOMA and C13MA monomers are listed in Table 4.7.

DSC indicates a single T_g for each statistical copolymerization, which is evidence of a homogeneous single-phase polymer [295]. From these measurements, the T_g of the final copolymer resins was predictably enhanced by increasing the [IBOMA]/[C13MA] ratio due to the higher T_g of IBOMA-based resins[264, 265]. The

molecular structure of IBOMA consists of a 6-membered ring, which improves the heat resistance of this monomer and the polymer resins consequently[259]. Poly(C13MA) resins have a T_m and a T_g in both systems which agrees with literature for poly(methacrylate)s with long linear aliphatic carbon chains[293, 296]. Figure 4.9 illustrates the $T_{g,theo}$s and T_gs of IBOMA/C13MA copolymers prepared in two different systems (solution and emulsion). The T_gs and T_ms for samples produced in emulsion are lower than those of samples synthesized in solution system. This likely shows the effects of the addition of n-hexadecane (costabilizer) and DOWFAX™ 8390 (surfactant) to the polymer latex, where they act as plasticizers [204, 297-299]. Some n-hexadecane molecules may present after the precipitation of polymer samples in methanol as it is insoluble in methanol at room temperature[205]. As mentioned in the previous section, the existence of melting points for samples with high concentrations of C13MA in miniemulsion polymerization can be due to the presence of long chain methacrylic esters (e.g. C12MA or C14MA). However, the copolymers obtained from emulsions with higher concentrations of IBOMA monomers are amorphous and do not have melting points (see Figure 4.S6 in Supplementary Information for lack of crystallinity in IBOMA-rich copolymers).

Table 4.7. Results for thermal characterization of IBOMA/C13MA copolymers made in homogeneous organic solvent solution and heterogeneous emulsion systems.

Solution system (polymers made in 50 wt% toluene)							
Experiment ID	$T_m{}^a$ (°C)	$T_g{}^a$ (°C)	$T_{g,theo}{}^b$ (°C)	$T_{dec,1}{}^c$ (°C)	$T_{dec,max}{}^c$(°C)	$T_{dec,2}{}^c$ (°C)	$F_{IBOMA}{}^d$	$M_n{}^e$ (kg mol^{-1})
IBOMA100-S-100C	-	169	169	278	339	478	1	16.5
C13MA100-S-110C	-18	-31	-31	221	306	463	0	20.0
IBOMA80/C13MA20-S	-	69	98	232	317	476	0.80	23.6
IBOMA60/C13MA40-S	-	33	50	215	336	472	0.58	25.0
IBOMA50/C13MA50-S	-	12	31	225	314	476	0.48	26.1
IBOMA40/C13MA60-S	-	15	15	217	308	478	0.32	24.1
IBOMA30/C13MA70-S	-	2	2	186	291	461	0.24	26.5
IBOMA20/C13MA80-S	-	-10	-11	227	308	473	0.18	27.3
IBOMA10/C13MA90-S	-	-40	-21	203	295	450	0.06	19.8
Emulsion system							
Experiment ID	T_m (°C)	T_g (°C)	$T_{g,theo}$ (°C)	$T_{dec,1}$ (°C)	$T_{dec,max}$ (°C)	$T_{dec,2}$ (°C)	F_{IBOMA}	M_n (kg mol^{-1})
IBOMA100	-	110	110	240	307	466	1	42.2
IBOMA100-83C	-	123	-	195	320	472	1	39.3
IBOMA100-100C	-	117	-	208	311	480	1	33.5
IBOMA90/C13MA10	-	81	82	235	323	470	0.9	53.9
IBOMA80/C13MA20	-	33	58	208	324	464	0.78	57.8
IBOMA70/C13MA30	-	30	39	216	335	486	0.68	46.8
IBOMA60/C13MA40	-	18	22	206	337	470	0.59	56.2
IBOMA50/C13MA50	-	-10	7	211	309	482	0.52	50.8
IBOMA40/C13MA60	-	-18	-6	224	310	501	0.38	64.2
IBOMA30/C13MA70	-	-17	-17	207	313	469	0.29	67.9
IBOMA20/C13MA80	-33	-52	-27	217	305	503	0.18	63.8

IBOMA10/C13MA90	-26	-42	-36	223	290	466	0.10	61.1
C13MA100	-19	-44	-44	174	296	468	0	48.9

[a] T_m (melting point) and T_g (glass transition temperature) measured by DSC under nitrogen atmosphere using three scans per cycle (heat/cool/heat) at a heating rate of 15 °C min^{-1} and cooling rate of 50 °C min^{-1}. [b] Theoretical glass transition temperature predicted by Fox equation. [c] $T_{dec,1}$ ($T_{10\%}$ or onset of decomposition), $T_{dec,max}$ (temperature at which highest weight loss occurs) and $T_{dec,2}$ (end of decomposition) measured by TGA under nitrogen atmosphere at a ramp rate of 15 °C min^{-1}. [d] Molar fraction of IBOMA in copolymers determined by ^{1}H NMR in CDCl$_3$. [e] The final number average molecular weight (M_n) was estimated using GPC with PMMA standards at 40 °C in THF.
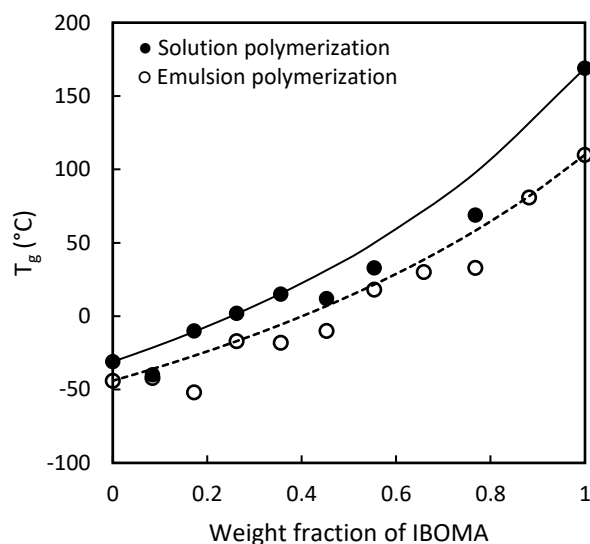
Figure 4.9. Evolution of T_g with weight fraction of IBOMA. The solid black line represents the $T_{g,theo}$ of copolymers synthesized in organic solvent as calculated by the Fox equation using the homopolymers made in solution as endpoints. The black dotted line shows the $T_{g,theo}$ for the emulsion system using homopolymers made in emulsion as endpoints. The black filled circles depict the experimental T_g for IBOMA/C13MA copolymers synthesized in 50 wt% toluene. The open circles represent the experimental T_g for IBOMA/C13MA copolymers with different weight fraction of IBOMA synthesized in emulsion.

4.3.4. Tensile Results for Poly(IBOMA-*b*-C13MA) and Poly(C13MA-*grad*-IBOMA)

To study the effect of the C13MA block on the mechanical properties of the copolymers, tensile tests were conducted on gradient and block copolymers prepared in emulsion and solution (toluene as the solvent), respectively, to illustrate the range of possible tensile properties. Figure 4.10 illustrated the stress-strain curves for poly(IBOMA-*b*-C13MA) ($F_{IBOMA} = 0.22$, $M_n = 37.1$ kg mol^{-1}, Đ = 1.93) and poly(C13MA-*grad*-IBOMA) ($F_{IBOMA} = 0.51$, $M_n = 54.0$ kg mol^{-1}, Đ = 1.65) samples at room temperature. The strain at break for poly(C13MA-*grad*-IBOMA) sample made from miniemulsion polymerization was significantly lower than the poly(IBOMA-*b*-C13MA) sample (1.5% compared to 201%) due to the higher fraction of stiff IBOMA units incorporated in the copolymer. This agrees with the thermal results where increasing IBOMA

incorporation into the copolymer increased the T_g of copolymers and subsequently made it more brittle. The linear elastic region for poly(IBOMA-*b*-C13MA) remained until 61.7% elongation and the yield strength of 0.77 MPa was achieved. The semi-plateau region (approximately 60-200% elongation) corresponds to plastic behavior of the block copolymer before finally breaking, which suggests that C13MA block can act as a plasticizer in poly(IBOMA-*b*-C13MA). These two IBOMA/C13MA copolymer examples show how mechanical properties are readily altered by simply applying different polymerization protocols and feed compositions.
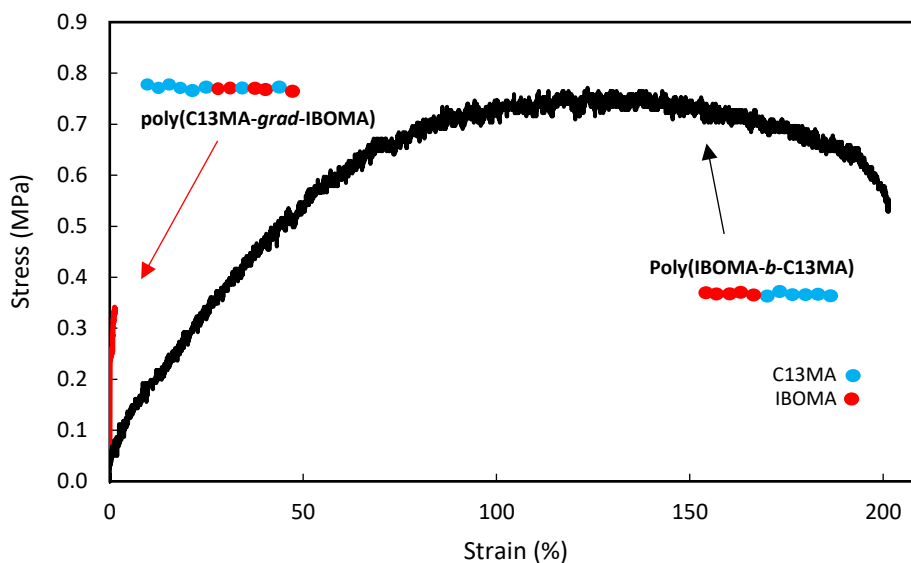
Figure 4.10. Stress-strain curves for poly(IBOMA-*b*-C13MA) (F_{IBOMA} = 0.22) and poly(C13MA-*grad*-IBOMA) (F_{IBOMA} = 0.51) samples at room temperature.

4.3.5. Rheological Measurements

The effect of monomer blocks and their compositions on rheological behavior of the resulting copolymers was done using the same copolymers in the section above (poly(IBOMA-*b*-C13MA) (F_{IBOMA} = 0.22, prepared in toluene) and poly(C13MA-*grad*-IBOMA) (F_{IBOMA} = 0.51, prepared in emulsion)) (Figure 4.11). Additionally, IBOMA20/C13MA80, IBOMA50/C13MA50 and IBOMA80/C13MA20 statistical copolymers prepared by miniemulsion NMP were also examined (Figure 4.S7, Supplementary Information). All the samples from the emulsion system were dried and precipitated in methanol and dried again before the test. Figure 4.11 shows the dependence of storage modulus (G') and loss modulus (G") on frequency for poly(IBOMA-*b*-C13MA) and poly(C13MA-*grad*-IBOMA) at 140 ºC. The frequency sweep was performed in the range of 1-1000 Hz and the temperature of 140 ºC was chosen as all the polymer samples were in the melt state and T > T_g. This temperature can be used as an initial point to process the

copolymers in the melt. The results at different temperatures were presented in Supplementary Information (Figure 4.S8). G″ for poly(C13MA-*grad*-IBOMA) was always higher than G′, suggesting a viscous liquid behavior for the resins at all considered frequencies, with no cross-over observed. Similar behaviour was reported by Larson et al[300] for poly(styrene)-block-poly(isoprene) (PS-PI) diblock copolymer below the order-disorder transition temperature (T_{ODT}). At lower frequencies ($\omega < 250$ Hz), poly(IBOMA-*b*-C13MA) shows viscoelastic solid behavior with G′ dominating. A transition region was observed at high frequencies due to relaxation and dissipation mechanisms[301-304]. During this period, the G″ increases faster than G′, which resulted in a crossover (where G′ = G″) at 250 Hz. At frequencies higher than 250 Hz, a glassy region was observed, where G″ is higher and increases more sharply in comparison to G′. Based on these results, the presence of the block of poly(C13MA) imparted more rubbery character into the final block copolymer, as expected. This also was shown in the stress-strain curves for the same samples. The viscoelastic behaviour exhibited by the block copolymer was not observed for IBOMA/C13MA copolymers prepared via statistical copolymerization. The storage modulus (G′) and loss modulus (G″) versus frequency at 140 ºC for 3 statistical copolymers with different compositions and prepared in emulsion were depicted in Figure 4.S7 (Supplementary Information). In all the samples G″ > G′ at frequencies higher than 0.5 Hz, indicating primarily viscous behaviour. Thus, only in the case for the poly(IBOMA-*b*-C13MA) was primarily elastic behavior observed. This was not the case for statistical or gradient polymers even with a high C13MA fraction (compared with the results on Figure 4.S8 in Supplementary Information) which suggests that the microstructure influenced the relaxation spectra of the material. To support the elastic behaviour of IBOMA/C13MA block copolymer, the Flory-Huggins interaction parameter χ[305] for the IBOMA/C13MA system was estimated to be 0.012 at 140 °C which suggests a partially miscible system for IBOMA/C13MA monomers (Supplementary Information Section 9). At the ODT, cN $\approx$ 10.5 and our cN < 10.5 which suggests our block copolymers are in a disordered state[306].
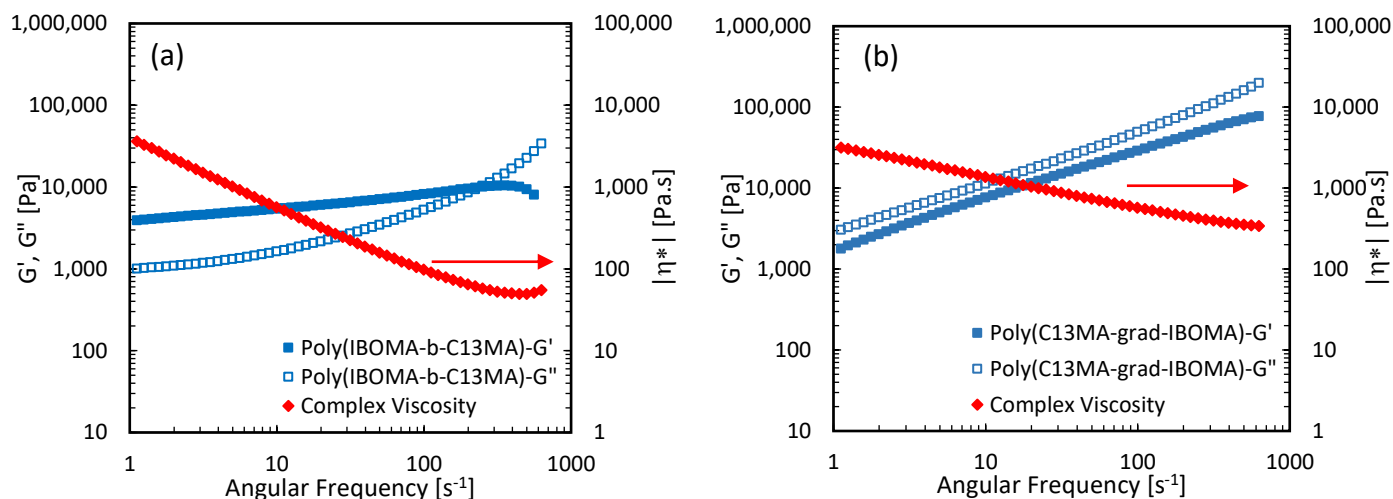
Figure 4.11. G', G" and complex viscosity plots versus shearing frequency for (a) Poly(IBOMA-*b*-C13MA) and (b) poly(C13MA-*grad*-IBOMA) polymers at 140 ℃.

4.4. CONCLUSIONS

In this study, the copolymerization of commercially available bio-based methacrylic IBOMA and C13MA monomers was conducted in homogeneous toluene solution and then in a miniemulsion system by nitroxide mediated polymerization without any controlling comonomer. The reaction temperature for having a controlled polymerization of IBOMA/C13MA in emulsion was 90°C, which was 10 °C lower than the same system in organic solvent. Copolymers with different IBOMA:C13MA composition were synthesized in toluene (50 wt%) using Dispolreg 007 initiator. The slow initiation of Dispolreg 007 alkoxyamine was observed for the methacrylates and the early termination of macro-radicals occurred at higher conversions ($X > 50\%$) for NMP in toluene. However, the dispersity was relatively low ($1.39 < Đ < 1.66$) and polymer chains were able to be re-initiated to produce block copolymers. This system has two major drawbacks: using volatile organic solvent (toluene) and relatively lower monomer conversion caused by high viscosity. To overcome these problems, a miniemulsion polymerization technique was utilized to make the overall process greener and more efficient. The oil-soluble Dispolreg 007 was used as the initiator to start the polymerization within ~300-500 nm-sized monomer droplets. The monomer conversion reached as high as 94% while the dispersity was comparable to the toluene-based system ($1.50 < Đ < 1.73$) and the average final particle size of polymer particles was 270-550 nm. The final average molecular weight of polymers in solution (50 wt% in toluene) and emulsion was higher than the $M_{n,target}$, suggesting slow initiation of the Dispolreg 007 initiator for the polymerization of methacrylates. The ability to chain-extend the polymer resins prepared in emulsion was studied to verify the chain end fidelity and show that gradient or block copolymers are possible in the emulsion system. The thermal studies showed that the addition of IBOMA

in the polymer resins increases the T_g relative to C13MA and readily allows the hardness or flexibility of the copolymers to be adjusted. Tensile tests showed that having about 80% C13MA resulted in high elongation at breaks ~ 200% and essentially elastic behavior. In the melt, the elastic modulus dominated in the block copolymer of IBOMA and C13MA always being higher than the viscous modulus in the frequency range studied, while the statistical and gradient polymers showed viscous liquid behavior.

ACKNOWLEDGMENT

Preamble to Chapter 5

To improve the thermal stability of polymers, the polymerization of methacryloisobutyl POSS (POSSMA) in miniemulsion was examined. This organic-inorganic hybrid monomer contains a silicon-oxygen cage that can improve the thermal properties of the polymers, based on various literature reports. However, the polymerization of POSSMA in solution or bulk was challenging due to the high steric hindrance of POSSMA. Here, the polymerization of POSSMA was done by nitroxide mediated miniemulsion polymerization using Dispolreg 007 alkoxyamine. We first studied the homopolymerization of POSSMA in miniemulsion. This was followed by the copolymerization of POSSMA with C13MA to increase the flexibility of polymer chains and reduce the glass transition temperature of the resulting copolymers. The kinetics of polymerization and thermal properties of polymers were studied, indicating the successful copolymerization of these monomers and the possibility of enhancing the thermal decomposition stability of the targeted polymers by increasing the POSSMA content. This chapter was published in *Journal of Polymer Science*, 58 (19), 2741-2754, 2020.

Chapter 5: Nitroxide Mediated Miniemulsion Polymerization of Methacryloisobutyl POSS: Homopolymers and Copolymers with Alkyl Methacrylates

ABSTRACT

Nitroxide mediated polymerization (NMP) of methacryloisobutyl POSS (POSSMA) was conducted in a dispersed aqueous miniemulsion at 90 °C, resulting in stable latexes with particle sizes = 225-260 nm at solids loading = 22%. POSSMA homopolymers with $\bar{M}_n$ up to 35.9 kg mol^{-1} ($Đ < 1.53$) was prepared using Dispolreg 007 alkoxyamine without any controlling comonomers, as is traditionally required for NMP of methacrylates. Copolymers with different ratios of POSSMA and bio-based C13 methacrylic esters were also synthesized (monomer conversion (X) up to 96.5% and $1.42 < Đ < 1.68$) to prepare polymer resins with a wide range of glass transition temperatures (T_g) or melting points (T_m) (-30 °C < T_g , T_m <96 °C). The resulting homopolymers and copolymers exhibited semi-crystalline properties, with crystallite size of 20.3-44.4 °A.

5.1. INTRODUCTION

Polyhedral oligomeric silsesquioxanes (POSS) have been widely incorporated into different materials as the monomer[307-310] or nano-filler[311-314] to modify the properties of organic polymers. POSS's unique properties are related to its structure (POSS's generic formula is $(RSiO_{1.5})_n$, where R is hydrogen or any organic ligands and n is often 8, 10 or 12). Thus, POSS is a hybrid of an inorganic silicon-oxygen cage and organic ligands that can be reactive or non-reactive[315]. Figure 5.1 presents some of the common cage structures of POSS. The silicon-oxygen cage in POSS-based compounds increases their heat resistance, hardness and strength[316] and also improves the oxidative resistance and mechanical properties in hybrid resins while the organic ligands improve compatibility with organic materials[317]. POSS compounds are non-toxic, cytocompatible[318, 319] and odorless and they do not release volatile organic compounds (VOCs)[317], making them desirable in coatings, paints and sealants[320-322].

Methacrylic polyhedral oligomeric silsesquioxanes contain one or more methacrylic ligands, which enables free radical polymerization. Many studies have illustrated the successful radical polymerization (conventional[323, 324], atom transfer radical polymerization (ATRP)[325-328], reversible addition-fragmentation
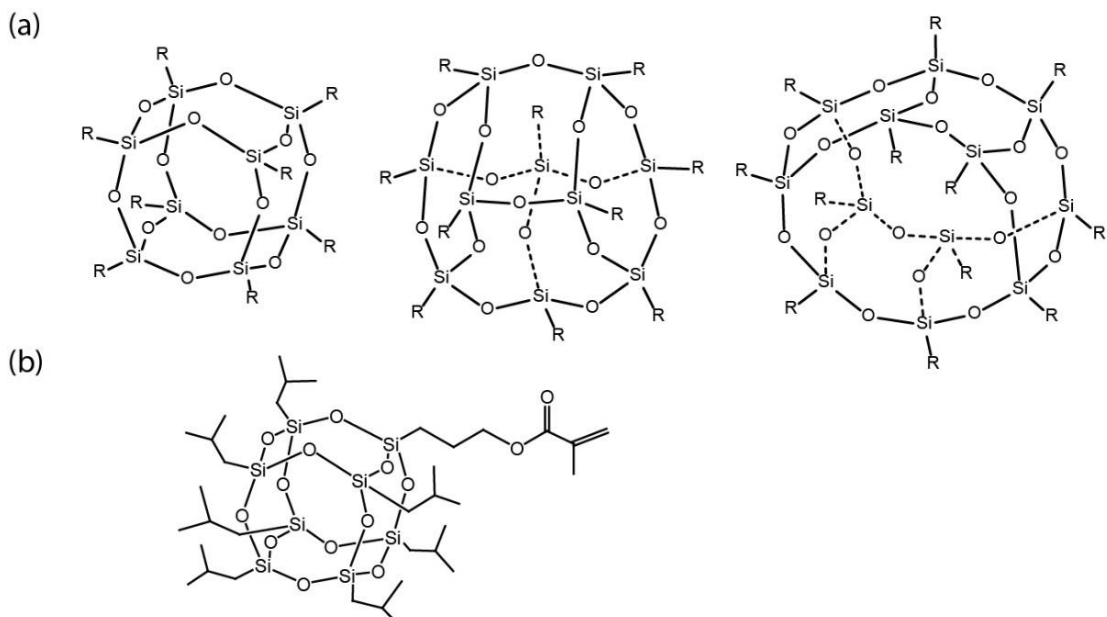
Figure 5.1. (a) Three common cage structures of POSS (b) Molecular structure of Methacryloisobutyl POSS (POSSMA).

chain transfer (RAFT)[329, 330] and nitroxide mediated polymerization (NMP)[181, 331]) of methacrylic POSS. One of the methacrylic POSS compounds is 3-(3,5,7,9,11,13,15-heptaisobutylpentacyclo[9.5.1^{3,9}.1^{5,15}.1^{7,13}] octasiloxan-1-yl)propylmethacrylate (methacryloisobutyl POSS or POSSMA), which has one methacrylic ligand and has been used to impart high hydrophobicity, toughness and thermal stability to polymers (glass transition temperature T_g of POSSMA homopolymers ≈ 85 °C)[332]. Figure 5.1 (b) illustrates the molecular structure of POSSMA used in this study.

The homopolymerization of POSSMA with high M_n using reversible-deactivation radical polymerization (RDRP) has always been challenging due to the steric hindrance of POSSMA, which inhibits the activation of radicals[325, 332]. Hirai et al[308] synthesized POSSMA homopolymers with M_n up to 29 kg mol^{-1} (DP$_n$ up to 30) by living anionic polymerization. Even though industrial processes using ionic polymerization have been done (eg. SBS or SIS triblock copolymers), routes that avoid the conditions typically employed by ionic polymerizations (such that used by Hirai et al - *sec*-BuLi initiator with LiCl/1,1-diphenylethylene at -78 °C for 6 hours) are attractive. Consequently, Mya et al[332] studied the RAFT homopolymerization of POSSMA in toluene with 2,2′-azobisisobutyronitrile (AIBN) initiator and the RAFT chain transfer agent dodecyl(α,α′-dimethylacetic acid)trithiocarbonate (DDTA)) at 70 °C, which resulted in POSSMA-based homopolymers with M_n up to 32 kg mol^{-1} and Đ = 1.6. In another study, Raus et al[333] synthesized homopolymers of POSSMA using ATRP with M_n > 100 kg mol^{-1} (Đ < 1.44). However, the nitroxide mediated homopolymerization of POSSMA has not been done due to the previous limitations of this system for methacrylates such as the need for controlling comonomers or the relatively higher reaction temperature

required of NMP. POSSMA-rich copolymers with 10 mol % acrylonitrile (AN) or styrene (S) in the initial monomer mixture was previously synthesized in our research group using N-(2-methylpropyl)-N-(1-(diethylphosphono-2,2-dimethylpropyl)-O-(2-carboxylprop-2yl)hydroxylamine) BlocBuilder-MA™ (BB, Arkema)[181, 331]. Charleux et al[174] showed that the polymerization of methacrylate-rich compositions (essentially mimicking homopolymerization) by BB alkoxyamine was feasible using a low concentration of controlling comonomer with a very low activation/deactivation equilibrium constant such as AN or S, which was thought to decrease the average equilibrium constant for activation/deactivation of the chains $\langle K \rangle$ and to also reduce cross-disproportionation side reactions[172, 173, 232].

In this study, 3-(((2-cyanopropan-2-yl) oxy) - (cyclohexyl) amino)-2, 2-dimethyl-3-phenylpropanenitrile (Dispolreg 007) alkoxyamine was used to initiate the polymerization. Dispolreg 007 was recently developed by Ballard et al[29, 243] and was used for NMP of methacrylates without the addition of controlling comonomers at temperatures < 100 °C. This allows the homo and copolymerization of methacrylates in aqueous miniemulsion or suspension systems[28, 43, 103]. As a result, NMP of POSSMA was conducted in miniemulsion without any comonomer, where the formation of nano-sized particles and compartmentalization effects allow high conversion, low dispersity and viscosity and result in latexes with high colloidal stability[46, 47, 57, 80, 122, 250]. Using water as the continuous phase helps to reduce volatile organic compounds (VOC) of the final product by decreasing the organic solvent content (which is only needed minimally to aid POSSMA suspension) and also improves the heat transfer during the polymerization[59]. To prepare polymers with lower T_gs, incorporating C13 methacrylate (C13MA from Evonik), which has a long aliphatic side-chain, was considered (T_g of poly(C13MA) = -46 °C)[201]. C13MA is a bio-based monomer derived from natural oils that acts as a plasticizing monomer and imparts flexibility and hydrophobicity into the polymer chains[179, 267, 268]. NMP of C13MA in homogeneous toluene solution and dispersed aqueous emulsion has been studied earlier and the successful homopolymerization, copolymerization and chain-extension of this monomer has been illustrated[162, 182]. Herein, the statistical copolymerization of different ratios of POSSMA/C13MA was performed in miniemulsion to synthesize copolymers with a wide range of T_gs.

5.2. EXPERIMENTAL

5.2.1. Materials

3- (3,5,7,9,11,13,15- Heptaisobutylpentacyclo [9.5.1^{3,9}.1^{5,15}.1^{7,13}] octasiloxan-1-yl) propylmethacrylate (MethacryloIsobutyl Polyhedral Oligomeric Silsesquioxane or MA0702-methacryloisobutyl POSS, termed POSSMA herewithin) was obtained from Hybrid Plastics and used as received. C13 methacrylate (termed C13MA, methacrylic esters with an average chain length of 13 units, >99%) was received from Evonik and

the monomers were passed through a column of basic alumina (Brockmann, Type 1, 150 mesh, Sigma Aldrich) and calcium hydride (5 wt% of basic alumina, 90-95% reagent, Sigma Aldrich) to remove the inhibitor. DOWFAX™ 8390 (alkyldiphenyloxide disulfonate, 35 wt% active content, Dow Chemical), n-hexadecane (99%, Sigma Aldrich) Methanol (MeOH, >99%, Fisher Scientific), tetrahydrofuran (THF, 99.9%, HPLC grade, Fisher Scientific), toluene (>99%, Fisher Scientific) and deuterated chloroform (CDCl$_3$, ≥99%, Cambridge Isotopes Laboratory) were used as received. 3-(((2-Cyanopropan-2-yl) oxy) - (cyclohexyl) amino)-2, 2-dimethyl-3-phenylpropanenitrile (Dispolreg 007) alkoxyamine was synthesized based on Ballard et al's procedure[28]. Reverse osmosis water (type 2 with the resistivity of ~ 1.10 MOhm·cm at 25 °C) was used as the aqueous phase for all miniemulsions.

5.2.2. Methods

5.2.2.1. M_n, X and $Đ$ Measurements

Number average molecular weight (M_n) and molecular weight distribution ($Đ$) were determined by gel permeation chromatography (GPC, Waters) relative to PMMA standards (from Varian Polymer Standards; M_n range of 875 to 1677000 g mol^{-1}) at 40 °C in THF. The GPC was equipped with HR1, HR2 and HR4 Styragel® GPC columns (HR1 with molecular weight measurement range of $10^2 – 5 \times 10^3$ g mol^{-1}, HR 2 with molecular weight measurement range of $5 \times 10^2 – 2 \times 10^4$ g mol^{-1} and HR 4 with molecular weight measurement range of $5 \times 10^3 – 6 \times 10^5$ g mol^{-1}, for THF solvent) and a guard column. To prepare the samples for GPC, they were diluted in HPLC grade THF at a concentration of 5 mg ml^{-1} without applying extra filtration or purification steps. The monomer conversion of the samples taken can be calculated based on the areas under the GPC peaks divided by the respective refractive index increments (dn/dc)[333]. This was permissible as the peaks were well separated and the monomers were sufficiently high in molecular weight to be distinct from solvent peaks. The dn/dc of 0.042 mL g^{-1} and 0.052 mL g^{-1} were previously reported for POSSMA monomer and POSSMA homopolymer (M_n = 171.5 kg mol^{-1}) in THF solutions, respectively[333]. The dn/dc value for C13MA or its homopolymer or copolymer is not available. However, the dn/dc of poly(octadecyl methacrylate) (C18MA) in THF was measured as 0.075 ml g^{-1} [334]. Similarly, the dn/dc for poly(n-decyl methacrylate) and poly(n-butyl acrylate) are 0.076 and 0.067 mL g^{-1}, respectively[335, 336]. As the dn/dc values were almost in the same range, we assumed an equal dn/dc value for GPC peaks to measure conversion. The calculated conversions corresponded very well with the conversions determined by gravimetry or ^{1}H NMR (not reported here).

5.2.2.2. Particle Size

Dynamic light scattering (DLS) was carried out with a Malvern Zetasizer Nano-ZS, equipped with a 4 mW He–Ne laser at 633 nm and an avalanche photodiode detector at 25 °C. Samples were diluted with water to

a concentration of 0.01-1000 mg ml^{-1} (10^{-3} – 1 % mass). The measurement angle was 173° and 5 measurements were performed for each sample to minimize the error.

5.2.2.3. Thermoanalytical Analyses

T_gs and T_ms of samples was measured by differential scanning calorimetry (DSC, Q2000 from TA Instruments, three scans per cycle, (heat/cool/heat) method) under nitrogen in the temperature range of -80 to 190 °C. The heating rate of 15 °C min^{-1} and cooling rate of 50 °C min^{-1} were considered when calculating T_gs and T_ms in re-heating cycles by inflection method. The calibration of temperature and heat flow for DSC was performed with indium and benzoic acid standards, respectively. TA Instruments TGA Q500 was used for thermogravimetric analysis (TGA) at a ramp rate of 15 °C min^{-1} from 25 to 550 °C. The samples were placed in aluminium pans and were heated under nitrogen to measure the decomposition temperatures (T_{dec}s) of samples.

To prepare the samples for thermal studies, polymer latexes were dried inside a fume hood under ambient conditions for 3-5 days to evaporate most of the water and were placed under vacuum at room temperature overnight to dry the polymers completely. Next, a small volume of toluene was added to each polymer to dissolve them, followed by addition of excess methanol to precipitate the polymer. The polymer samples were separated from the solution and dried again inside a fume hood for 6 hours and then under vacuum in ambient conditions for 12 hours.

5.2.2.4. Powder X-ray diffraction (PXRD)

The degree of crystallinity of the POSSMA homopolymers and copolymers was determined by PXRD test in a Bruker D2 PHASER diffractometer equipped with a Ni-filtered CuKα radiation tube and LynxEyr linear position sensitive detector (Bruker AXS, Madison, WI, USA). The measurements were performed on powder samples with a step of 0.02° and 0.5 seconds/step in the range of 2θ = 4-50°. The samples for PXRD were prepared based on the procedure mentioned in the thermoanalytical analyses section. The test temperature for all samples was 23 °C. Crystallinity was calculated as the ratio of the area under the crystalline peaks to total area under the PXRD curve.

5.2.3. Miniemulsion polymerization of POSSMA/C13MA mixtures

First, Dispolreg 007 alkoxyamine, n-hexadecane (co-stabilizer, 0.8 wt% based on the total weight of monomers), POSSMA and C13MA monomers were dissolved in toluene (50 wt% based on the weight of POSSMA monomers) and were stirred for 30 minutes. $M_{n,target}$ of 45 kg mol^{-1} was considered for all the polymerization of POSSMA/C13MA. As an example, for POSSMA50/C13MA50 experiment, POSSMA (6.19 g, 6.562 mmol), C13MA (1.76 g, 6.562 mmol), Dispolreg 007 (0.06 g, 0.177 mmol) and n-hexadecane

(0.06 g, 0.281 mmol) were dissolved in toluene (3.10 g, 33.602 mmol). The aqueous phase was prepared separately by the addition of 2 wt% DOWFAX 8390 surfactant (based on monomers) to the reverse osmosis water. The preparation procedure for this study was shown in Table 5.1. The two solutions were mixed together for another 30 minutes and were sonicated for 10 minutes (Hielscher sonicator UP200S, 50% duty cycle and amplitude 70%) in a cold water bath to disperse the monomer particles. The prepared latex was poured into a 50 ml three-neck round-bottom glass flask, connected to a reflux condenser filled with a mixture of ethylene glycol/distilled water (20/80 vol%)) circulating at 3 °C and a temperature controller to adjust the reaction temperature. The glass flask was heated by a heating mantle and placed on a magnetic stirrer to apply proper mixing during the polymerization. The emulsion was purged with nitrogen for 30 minutes to deoxygenate the system before starting the reaction. In the next step, the latex was heated to 90 °C at a rate of 10 °C.min^{-1} to start the polymerization, while the nitrogen flow was continued inside the reactor so that the polymerization was under inert N_2 blanket at all times. The starting point of the polymerization (t= 0 min) was considered when the temperature reached 75 °C. To study the kinetics of polymerization over time, the samples were taken periodically from the system using a syringe and were dried completely.

Table 5.1. Typical formulation for the nitroxide-mediated miniemulsion copolymerization of POSSMA and C13MA.

Component	Amount
Monomer (1) - POSSMA	Varies based on the experiment (0.075-0.275 M)
Monomer (2) – C13MA	Varies based on the experiment (0.031-0.678 M)
Alkoxyamine (Dispolreg 007)	0.006 M
DOWFAX™ 8390	2 wbm%[a]
n-Hexadecane	0.8 wbm%
Toluene	50 wt% based on the weight of POSSMA monomer
Water	3 times the total weight of all components except toluene

[a] wt% based on the monomers

5.2.4. Synthesis of POSSMA homopolymers

The homopolymerization was conducted based on the same procedure for miniemulsion copolymerization of POSSMA/C13MA. The only difference will be in the initial concentration of Dispolreg 007 that varied depending on the $M_{n,target}$ and the C13MA monomer which was removed from the miniemulsion entirely. The reaction temperature of 90 °C was chosen for all of the experiments. For example, the oily phase of the POSSMA-Mn25 experiment (homopolymerization of POSSMA with $M_{n,target} = 25$ kg mol^{-1}) was prepared by dissolving POSSMA (8.84 g, 9.365 mmol), Dispolreg 007 alkoxyamine (0.12 g, 0.353 mmol) and n-hexadecane co-stabilizer (0.07 g, 0.312 mmol) in toluene (4.42 g, 47.956 mmol). The aqueous phase was made separately by the addition of Dowfax 8390 surfactant (0.18 g, 0.275 mmol) into R.O. water (27.61 g,

1532. 848 mmol). Two solutions were stirred together for 30 minutes and sonicated (50% duty cycle and amplitude 70%) for 10 minutes to prepare the miniemulsion. The monomer latex was poured inside a three-neck reactor (same setup used as for the miniemulsion polymerization of POSSMA/C13MA) and were purged with ultra pure nitrogen for 30 minutes before heating. The polymerization was conducted under nitrogen atmosphere for 210 minutes at 90 °C ($X = 83\%$). The initial time for polymerization (t = 0 min) was considered when the reactor temperature reached 75 °C. Samples for measurement of M_n, $Đ$, X and particle size were taken periodically during the polymerization. The latex samples were dried inside a fume hood and re-dispersed into HPLC-grade THF for GPC analysis. Finally, POSSMA homopolymer with M_n = 19.2 kg mol^{-1} and $Đ = 1.36$ was produced for POSSMA-Mn25 experiment.

5.3. RESULTS AND DISCUSSION

5.3.1. Nitroxide Mediated Miniemulsion Homopolymerization of POSSMA

First, the miniemulsion homopolymerization of POSSMA was investigated. Figure 5.2 shows the schematic procedure used for preparation of POSSMA homopolymers. Three different $M_{n,target}$ of 25, 45 and 80 kg mol^{-1} (corresponding to degrees of polymerization 27, 48 and 85) were chosen to observe the effect of degree of polymerization upon the kinetics and molecular properties. Table 5.2 presents the experimental conditions for homopolymerization of POSSMA using Dispolreg 007 alkoxyamine at 90 °C.
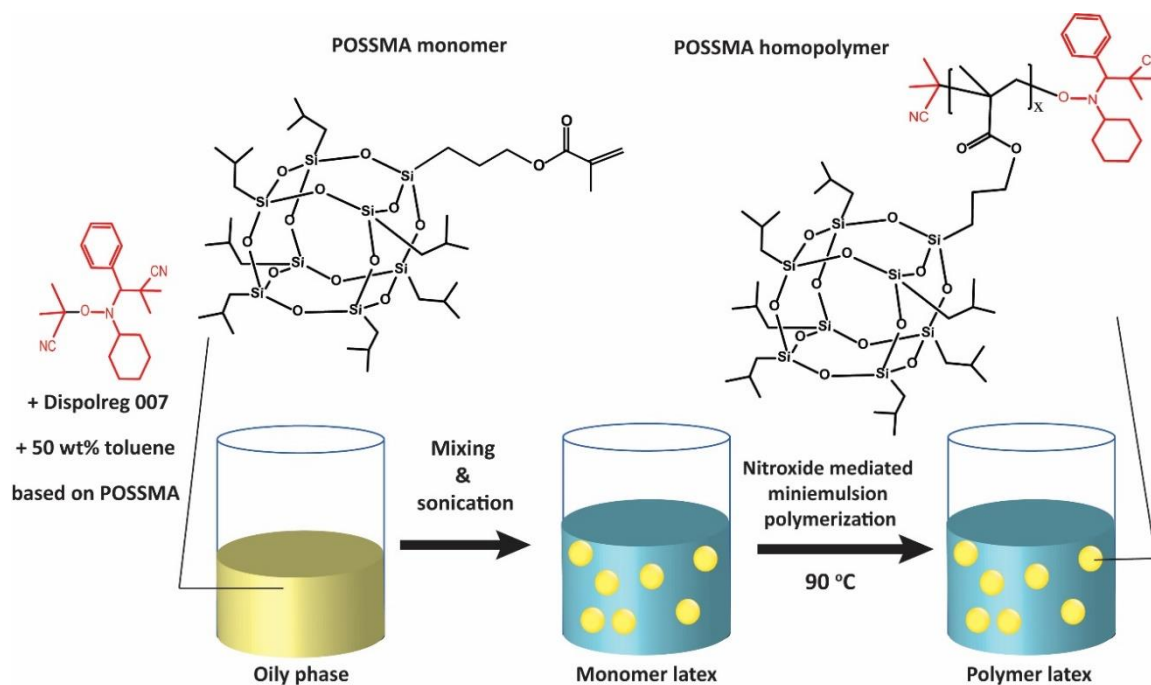
Figure 5.2. Schematic representation of nitroxide mediated miniemulsion homopolymerization of POSSMA.

Table 5.2. Experimental conditions for nitroxide-mediated miniemulsion homopolymerization of POSSMA at 90 ºC.

Experiment ID	$M_{n,target}$[b] (kg mol^{-1})	DP_n[c]	$M_{n,final}$[d] (kg mol^{-1})	X[e] (%)	[POSSMA]$_0$ (M)	[Dispolreg 007]$_0$ (M)	[Toluene]$_0$ (M)	$Đ$[d]
POSSMA-Mn25[a]	25	20	19.2	83.0	0.283	0.011	1.451	1.36
POSSMA-Mn45-No Hexadecane	45	33	31.5	96.4	0.297	0.006	1.521	1.53
POSSMA-Mn45	45	29	27.2	93.3	0.285	0.006	1.458	1.44
POSSMA-Mn80	80	38	35.9	73.7	0.286	0.003	1.465	1.50

[a] The miniemulsion homopolymerization of POSSMA monomers with the target number average molecular weight ($M_{n,target}$) of 25 kg mol^{-1}.
[b] The target number average molecular weight ($M_{n,target}$) for miniemulsion polymerization at complete conversion.
[c] Number-average degree of polymerization. $DP_{n,target} =$ 27, 48 and 85 for $M_{n,target}$ of 25, 45 and 80 kg mol^{-1}, respectively.
[d] The final number average molecular weight (M_n) and dispersity ($Đ$) were measured by GPC relative to PMMA standards in THF at 40 °C.
[e] Overall monomer conversion based on the areas under the normalized GPC peaks.

First, to check the effect of n-hexadecane as the co-stabilizer, the polymerization of POSSMA was done with and without the addition of 0.8 wt% n-hexadecane relative to monomer. The same experimental conditions and $M_{n,target}$ = 45 kg mol^{-1} was considered for both polymerizations. N-hexadecane is commonly used as a co-stabilizer to enhance the colloidal stability of the latex and reduce Ostwald ripening[57, 126, 337]. For POSSMA homopolymerization without the addition of n-hexadecane, shown in Figure 5.3 (a), a non-linear increase of conversion over time was observed and the polymerization rate was accelerated compared to the polymerization in the presence of n-hexadecane. Further, the molecular weight distribution started to broaden more for the polymerizations without the co-stabilizer (the final $Đ$ for POSSMA-Mn45-No Hexadecane = 1.53 and for POSSMA-Mn45 (with 0.8 wbm% n-hexadecane) = 1.44). The latex also lost its colloidal stability and particles started coagulating during the polymerization without co-stabilizer. This suggests the polymerization could not efficiently be controlled without the n-hexadecane in the emulsion and the stability of the latex decreases during the polymerization. In this study, only 0.8 wbm% n-hexadecane was added to the emulsion as the co-stabilizer, which is generally less than what is typically used[127]. In our study, the lower concentration of co-stabilizer still enabled latex stability, likely due to the relatively hydrophobic monomers used. Next, the miniemulsion homopolymerization of POSSMA with $M_{n,target}$ of 25 and 80 kg mol^{-1} was conducted in the presence of co-stabilizer. The polymerization rate was linear in all cases and the $Đ$ remained relatively low ($Đ_{POSSMA-Mn25}$ = 1.36 and $Đ_{POSSMA-Mn80}$ = 1.50). For the POSSMA-Mn80 experiment, $M_{n,final}$ was much lower than $M_{n,target}$ ($M_{n,final}$ = 35.9 and $M_{n,target}$ = 80 kg mol^{-1}), although the X attained was as high as 96.4%. This suggests that the polymer chains cannot grow efficiently at a certain point and reach an equilibrium with unreacted monomers at higher conversions. This

phenomenon was attributed to the low ceiling temperature (T$_c$) of POSSMA(T$_{c,POSSMA}$ = 130 °C) which is generally attributed to steric factors[333].

In Figure 5.3 (b), it is shown that the trend of the M_n increase with X is linear for all the polymerizations but does not go through zero and $M_{n,t=0}$s have values higher than expected. There are several factors that account for this observation. There is some difference due to the M_ns being reported relative to PMMA standards, in addition to the slow initiation of Dispolreg 007 that has been observed in many cases at lower conversions[43, 162, 278]. Another distinct feature of the M_n versus X plots observed for all the reactions in Figure 5.3 (b) is the flattening of M_n as the reaction proceeds (Figure 5.S1 in Supplementary Information). This is probably due to the low ceiling temperature (T$_c$) associated with POSSMA, limiting the polymerization temperature used[333, 338]. The plateau observed in the M_n versus X plots here was previously observed in our study of POSSMA NMP using BlocBuilder alkoxyamine in toluene at 90 °C and ATRP of POSSMA monomers at 60 °C for conversions higher than 75%, which was attributed to the same rate of polymerization and depolymerization at the given temperature[181, 333]. The plateauing was not observed for monomer conversions (Figure 5.3 (a)), which can be ascribed to the slow initiation of Dispolreg 007[28, 43, 162]. This can increase the possibility of initiation at higher conversions and result in improved conversions at the final stages of polymerizations.
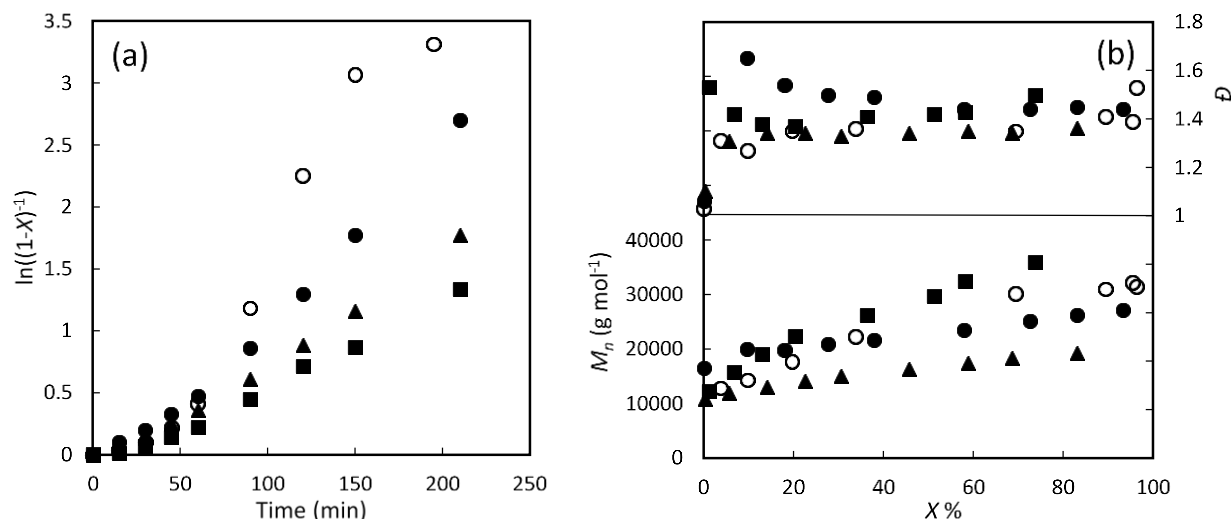
Figure 5.3. The miniemulsion homopolymerization of POSSMA using Dispolreg 007 initiator (a) Semi-logarithmic kinetic plots of ln[(1-X)$^{-1}$] (X= monomer conversion) versus reaction time (b) Number average molecular weight M_n and dispersity Đ versus conversion (X). POSSMA-Mn45-No Hexadecane (open circles, ○); POSSMA-Mn45 (filled circles, ●); POSSMA-Mn25 (filled triangles, ▲); POSSMA-Mn80 (filled squares, ■).

77

5.3.2. Miniemulsion copolymerization of POSSMA/C13MA mixtures

POSSMA/C13MA statistical copolymerization with different initial molar compositions was also conducted in miniemulsion at 90 ºC using Dispolreg 007 (Figure 5.4). The $M_{n,target}$ of 45 kg mol^{-1} and monomer content of 24.14 wt% was applied for all of the copolymerizations. 2 wbm% DOWFAX™ 8390 anionic surfactant was used to stabilize the emulsion and 0.8 wbm% n- hexadecane was added as the costabilizer to prevent Ostwald ripening. Table 5.3 lists all the results for the miniemulsion copolymerizations at 90 ºC. Monomer conversions up to 96.5% were achieved while the final dispersities remained relatively low ($1.44 < Đ < 1.68$) (GPC traces for POSSMA90/C13MA10, POSSMA50/C13MA50 and POSSMA10/C13MA90 are available in Figure 5.S2, Supplementary Information). POSSMA/C13MA NMP using BB alkoxyamine and 10 mol% acrylonitrile (AN) as the controlling comonomer was previously performed in toluene at 90 °C and the final conversion was considerably lower than in POSSMA/C13MA miniemulsion copolymerization using Dispolreg 007 alkoxyamine ($85.4 \% < X_{Miniemulsion} < 96.5 \%$ compare with $38 \% < X_{solution-based} < 81 \%$)[181]. The semi-logarithmic kinetic plots for copolymerizations were shown in Figure 5.5 (a). All the plots were first-order. Increasing the initial molar ratio of POSSMA reduced the polymerization rate in the first 50 minutes of the reaction. This was observed previously by Marcinkowska et al [339] and Hajiali et al[181] for copolymerization of POSSMA with lauryl methacrylate (C12-MA) or C13MA in homogeneous organic solvent.
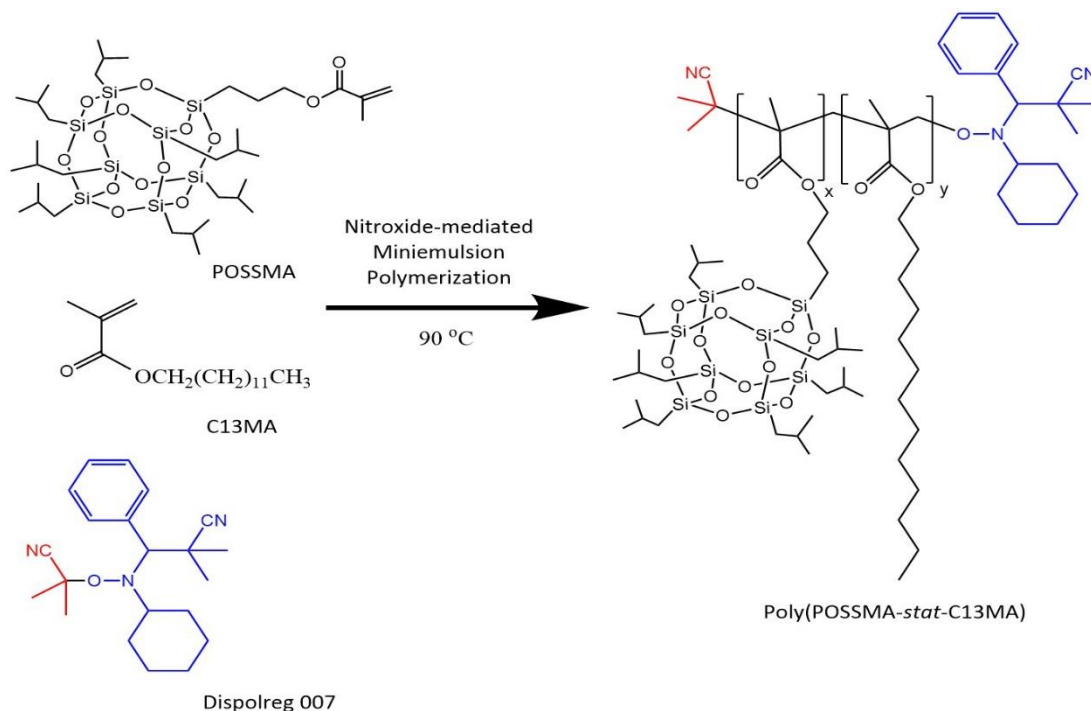
Figure 5.4. The schematic NMP of POSSMA and C13MA monomers in emulsion.

Table 5.3. Experimental conditions for nitroxide-mediated miniemulsion copolymerization of POSSMA/C13MA mixtures with $M_{n,target}$ of 45 kg mol^{-1} and solid content of 22 wt% at 90 °C.

Experiment ID	$M_{n,final}$[b] (kg mol^{-1})	X[c] (%)	[POSSMA]$_0$ (M)	[C13MA]$_0$ (M)	[Dispolreg 007] (M)	[Toluene]$_0$ (M)	$Đ$[b]
POSSMA10/C13MA90[a]	50.2	96.5	0.075	0.678	0.006	0	1.68
POSSMA20/C13MA80	40.6	92.6	0.123	0.492	0.006	0.677	1.57
POSSMA30/C13MA70	42.3	89.4	0.164	0.383	0.006	0.703	1.57
POSSMA40/C13MA60	42.2	92.9	0.197	0.296	0.006	0.725	1.59
POSSMA50/C13MA50	35.7	85.4	0.215	0.215	0.006	1.101	1.52
POSSMA60/C13MA40	35.6	91.2	0.234	0.156	0.006	1.200	1.48
POSSMA70/C13MA30	33.9	91.6	0.250	0.107	0.006	1.282	1.50
POSSMA80/C13MA20	31.2	87.2	0.264	0.066	0.006	1.351	1.44
POSSMA90/C13MA10	27.5	85.5	0.275	0.031	0.006	1.410	1.42

[a] The miniemulsion polymerization of POSSMA/C13MA mixtures are provided with the following notation to identify the initial molar feed composition: POSSMAxx/C13MAyy where xx denotes the mol% POSSMA and yy denotes the mol% C13MA.
[b] The final number average molecular weight (M_n) and dispersity ($Đ$) were estimated by GPC relative to PMMA standards at 40 °C. The target number average molecular weight ($M_{n,target}$) for all the miniemulsion polymerizations was 45 kg mol^{-1}.
[c] Overall monomer conversion was based on the areas under the normalized GPC peaks.

Based on Figure 5.5(b), the M_n increases linearly with monomer conversion. However, the trend departs noticeably from the theoretical line, especially at lower conversions. This similar departure has been observed previously for nitroxide-mediated miniemulsion copolymerization of isobornyl methacrylate (IBOMA)/C13MA mixtures using Dispolreg 007[162]. GPC calibration may be an issue as the results are reported relative to PMMA standards. However, the slow initiation of Dispolreg 007 which leads to higher M_n at low conversion has also been reported[28, 43, 162, 278]. Furthermore, the $M_{n,final}$ of copolymers decreases with increasing the initial concentration of POSSMA in the miniemulsion. This might be attributed to the low T_c of POSSMA-rich copolymerizations where chain growth can be stopped[340]. The concentration effect is another possibility as the POSSMA has a relatively high molecular weight (944 g mol^{-1}). In addition, this can correspond to a decrease in apparent polymerization rate constant ($k_p[P^•]$) with increasing POSSMA content in the initial monomer mixture. The plateau region was more apparent for copolymerizations with higher initial ratios of [POSSMA]$_0$/[C13MA]$_0$ and was less apparent for copolymerizations with higher concentrations of C13MA. The final $Đ$ of copolymers ($1.42 < Đ < 1.68$) slightly decrease by increasing the POSSMA content. This may show the effect of low T_c of POSSMA on polymerization that limits the chain growth, reduces the possibility of chain transfer reactions and acts as a controlling parameter on polymerization of POSSMA with different monomers. The particle size did not change significantly for latex resulting from different POSSMA/C13MA copolymerizations, with sizes ranging from 225-260 nm

(Figure 5.6). The DLS results with PDI are listed in Table 5.S1 (Supplementary Information). This suggests good colloidal stability likely derived from the high water insolubility of both of the constituent co-monomers, which helps to lessen Ostwald ripening[291, 292, 341].
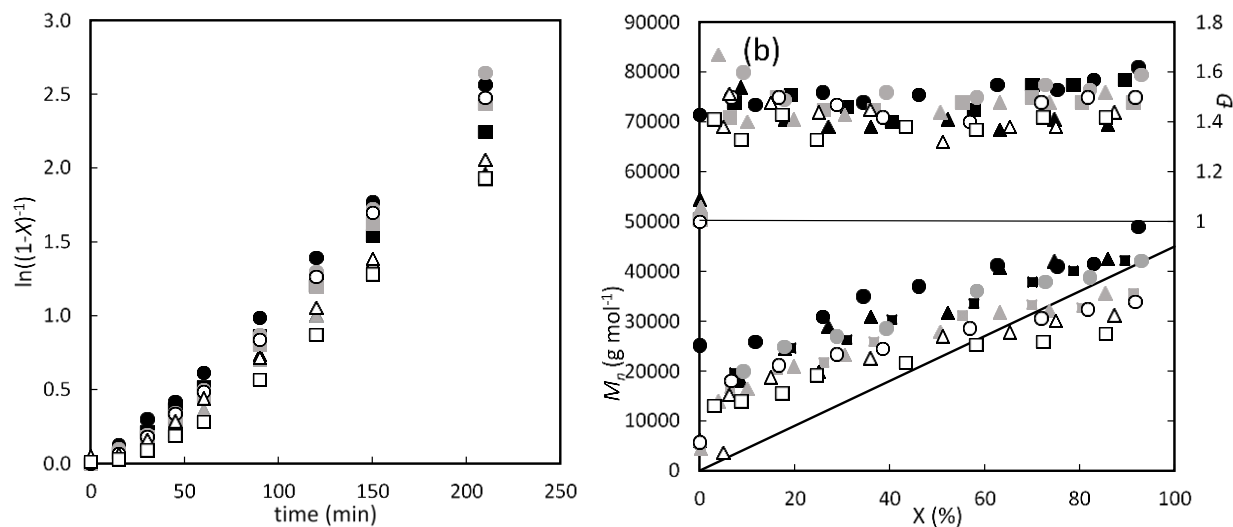
Figure 5.5. Kinetic data for miniemulsion copolymerization with different ratios of POSSMA/C13MA using Dispolreg 007 initiator at 90 °C ($M_{n,target}$ = 45 kg mol^{-1} and solid content = 22 wt%): (a) Semi-logarithmic kinetic plots of $\ln[(1-X)^{-1}]$ (X= monomer conversion) versus reaction time; (b) Number average molecular weight M_n and dispersity $Đ$ versus conversion (X). POSSMA10/C13MA90 (filled circles, ●); POSSMA20/C13MA80 (filled triangles, ▲); POSSMA30/C13MA70 (filled squares, ■); POSSMA40/C13MA60 (gray circles, ●); POSSMA50/C13MA50 (gray triangles, ▲); POSSMA60/C13MA40 (gray squares, ■); POSSMA70/C13MA30 (open circles, ○); POSSMA80/C13MA20 (open triangles, △); POSSMA90/C13MA10 (open squares, □).
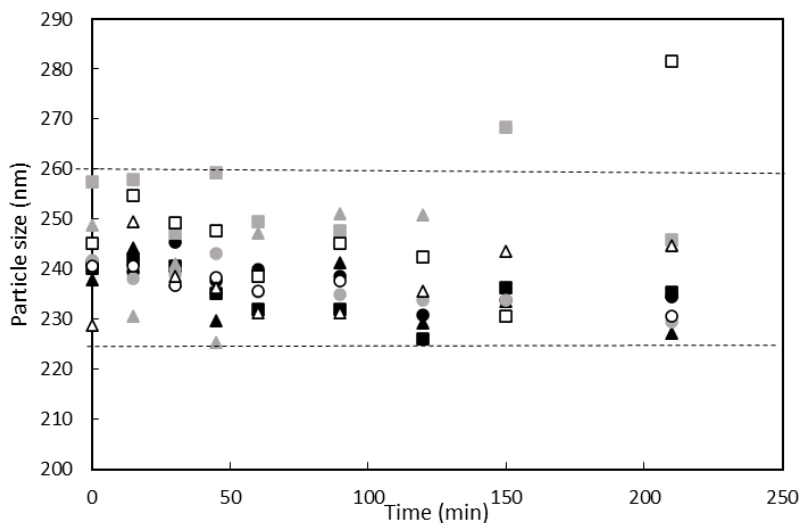
Figure 5.6. Z-average particle size for copolymerization of different ratios of POSSMA/C13MA monomers over reaction time using Dispolreg 007 alkoxyamine, 2 wbm% DOWFAX 8390 and 0.8 wbm% n-

hexadecane. POSSMA10/C13MA90 (filled circles, ●); POSSMA20/C13MA80 (filled triangles, ▲); POSSMA30/C13MA70 (filled squares, ■); POSSMA40/C13MA60 (gray circles, ●); POSSMA50/C13MA50 (gray triangles, ▲); POSSMA60/C13MA40 (gray squares, ■); POSSMA70/C13MA30 (open circles, ○); POSSMA80/C13MA20 (open triangles, Δ); POSSMA90/C13MA10 (open squares, □).

5.3.3. The Effect of POSSMA on Thermal Properties of Polymers

The thermal degradation of POSSMA/C13MA copolymers and POSSMA homopolymers was investigated by TGA. The decomposition temperatures for polymers were summarized in Table 5.4.

Table 5.4. Results for thermal characterization of POSSMA-based polymers prepared by nitroxide mediated miniemulsion polymerization.

Experiment ID	$T_m{}^a$ (°C)	$T_g{}^a$ (°C)	$T_{dec,1}{}^b$ (°C)	$T_{dec,max}{}^b$ (°C)	$T_{dec,2}{}^b$ (°C)	$F_{POSSMA}{}^c$	$M_n{}^d$ (kg mol^{-1})
POSSMA100-Mn25	106	-	277	312	487	1	19.2
POSSMA100-Mn45	98	-	278	369	455	1	27.2
POSSMA90/C13MA10	96	-	273	313	505	0.94	27.5
POSSMA80/C13MA20	92	-	256	340	459	0.88	31.2
POSSMA70/C13MA30	85	55	277	365	508	0.79	33.9
POSSMA60/C13MA40	78	55	258	316	466	0.65	35.6
POSSMA50/C13MA50	72	-29, 54	244	306	456	0.46	35.7
POSSMA40/C13MA60	-	-30, 58	255	325	491	0.40	42.2
POSSMA30/C13MA70	-29	-37, 50	236	323	467	0.20	42.3
POSSMA20/C13MA80	-28	-32, 23	232	332	472	0.07	40.6
POSSMA10/C13MA90	-25	-39	220	315	450	0.01	50.2

[a] T_m (melting point) and T_g (glass transition temperature) measured by DSC under nitrogen atmosphere using three scans per cycle (heat/cool/heat) at a heating rate of 15 °C min^{-1} and cooling rate of 50 °C min^{-1}.
[b] $T_{dec,1}$ ($T_{10\%}$ or onset of decomposition), $T_{dec,max}$ (temperature at which highest weight loss occurs) and $T_{dec,2}$ (end of decomposition) measured by TGA under nitrogen atmosphere at a ramp rate of 15 °C min^{-1}.
[c] Molar fraction of POSSMA in polymers determined by ^{1}H NMR in CDCl$_3$.
[d] The final number average molecular weight (M_n) was estimated using GPC with PMMA standards at 40 °C in THF.

The decomposition temperature for 10% weight loss ($T_{dec,1}$) for POSS homopolymers was detected at 277 and 278 °C for M_n = 19.2 and 27.2 kg mol^{-1}, respectively. For comparison, $T_{dec,1}$ for homopolymers of two similar methacrylate functionalized POSS (named herein as POSSMA$_2$ and POSSMA$_3$; organic ligands for

POSSMA$_2$ were c-C$_6$H$_{11}$ and for POSSMA$_3$ were c-C$_5$H$_9$) were 388 and 389 °C for the same M_n of 117 kg mol^{-1} [342]. The weaker interactions of the seven POSS R-groups in POSSMA can be another possible reason for comparatively lower T$_{dec,1}$[343]. Furthermore, we did not cleave the alkoxyamine; removing it would have likely enhanced thermal stability (since no radicals could be released at higher temperatures to propagate degradation reactions) as indicated by Nicolas et al[235] for chains terminated with the SG1-alkoxyamine. Others have shown the released nitroxide group's effect on increasing degradation rates via chain scission or backbiting reactions and reducing the expected T$_{dec,1}$[344, 345].

Increasing the POSSMA content generally increases the T$_{dec}$s, thereby improving the thermal stability of the copolymers. Generally, a 10% increase in molar ratio of POSSMA improves the T$_{dec,1}$ by approximately 5 °C. A similar increase in T$_{dec}$ was previously observed for polymer resins containing POSS moieties. Romo-Uribe et al[346] previously showed that the incorporation of 15 mol% POSS (n=8; n is the number of organic ligands on a generic POSS) into poly(4-methylstyrene) improved the T$_{dec,1}$ by 5.7% (from 388 to 410 °C) compared to the neat poly(4-methylstyrene). TGA traces were depicted in Figure 5.7 for all the copolymers prepared in miniemulsion and illustrate the modest shift to higher T$_{dec,1}$ with increasing POSSMA content.
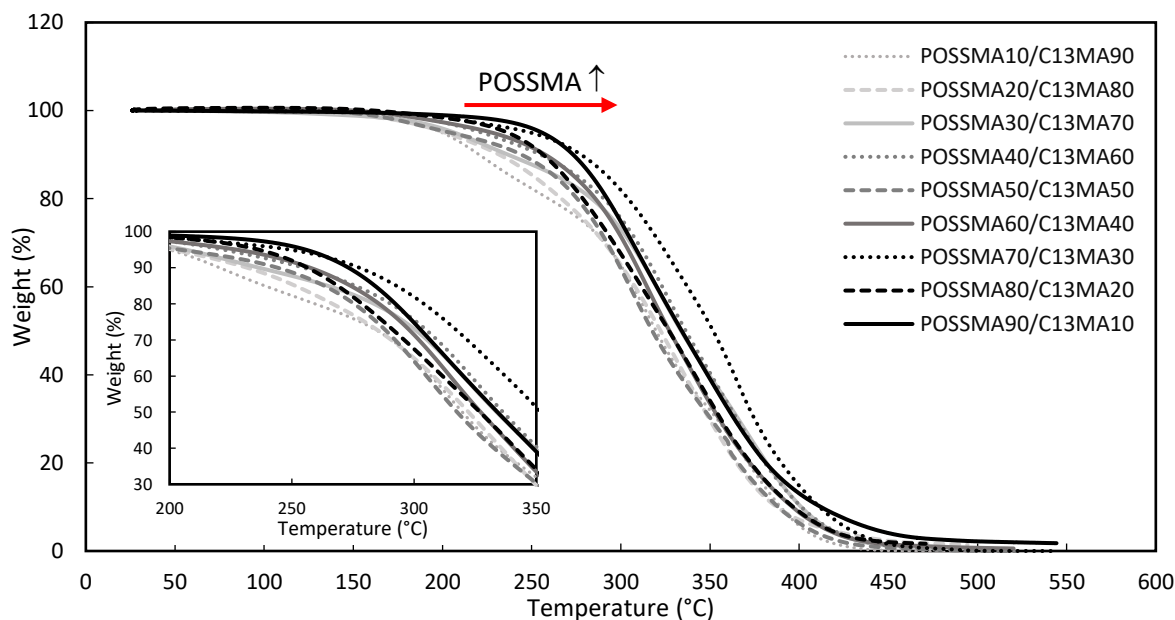
Figure 5.7. TGA traces for POSSMA/C13MA copolymers. Increasing the POSSMA content slightly increased the thermal stability of the polymers. All the tests were done under the N$_2$ atmosphere with the heating rate of 15 °C min^{-1}. The polymers were precipitated in excess methanol and completely dried under vacuum at room temperature.

The T_ms and T_gs for POSSMA/C13MA copolymers increase with increasing POSSMA content in copolymer (Figure 5.8). The melting points in the range of -25 to -30 °C corresponds to the incorporation of C13MA monomers and it becomes noticeable as the C13MA becomes the major component[162, 182, 347]. This lower bound with respect to T_m is seen quite clearly for the compositions of $F_{C13MA} > 80\%$. The melting points at higher temperatures ($T_m > 50$ °C) are indicative of incorporation of POSSMA into the copolymers, as the T_m for poly(POSSMA) approaches nearly 100 °C[181]. The absence of T_g for POSSMA homopolymers and copolymers with high molar ratios of POSSMA ($F_{POSSMA} \geq 0.88$) is probably due to the rigidity of polymer chains and the decrease in segmental mobility caused by the POSS cages[342, 348]. For intermediate POSSMA compositions = 20 to 46 mol%, two T_gs were detected. This suggests microphase separation and we speculated that the system may have formed POSSMA/C13MA gradient copolymers. Examining this, the radical reactivity ratio (r) of POSSMA and C13MA were $r_{POSSMA} = 0.91$ and $r_{C13MA} = 1.94$ (approximated using a low concentration of AN co-monomer 10 mol%)[181] and their values do not predict a strong gradient structure. For the similar copolymerization of MMA/POSSMA, $r_{POSSMA} = 0.58$ and $r_{MMA} = 1.61$ were reported[339, 349] Low reactivity ratios for other POSS containing monomers were also observed in various copolymerizations[350-353]. In some cases however, self-assembly is possible for statistical copolymers with long side branches such as mono methacrylate-terminated poly(dimethylsiloxane) (PDMS) oligomers with MMA even though the reactivity ratios are not vastly different[354]. Self-assembly properties was previously observed for statistical copolymers containing POSS-based monomers[355, 356]. A similar study by Kim et al[357] showed two distinct T_gs and self-assembly for statistical copolymers of POSSMA and poly(ethylene glycol) methyl ether methacrylate (PEGMA, $M_n = 475$ g mol^{-1}). In this particular case, with relatively low side chain length, the microphase separation was not as distinct as expected with longer PDMS or PEGMA side chains. However, the Flory-Huggins interaction parameter $\chi \gg 1$ for POSSMA/C13MA was estimated, suggesting the possibility of microphase separation[181]. In POSSMA10/C13MA90 experiment, only 1 mol% POSSMA was incorporated in the final polymer composition, resulted in the T_g and T_m close to pure C13MA homopolymer ($T_g = -44$ °C and $T_m = -19$ °C) prepared in a similar miniemulsion polymerization procedure[162].
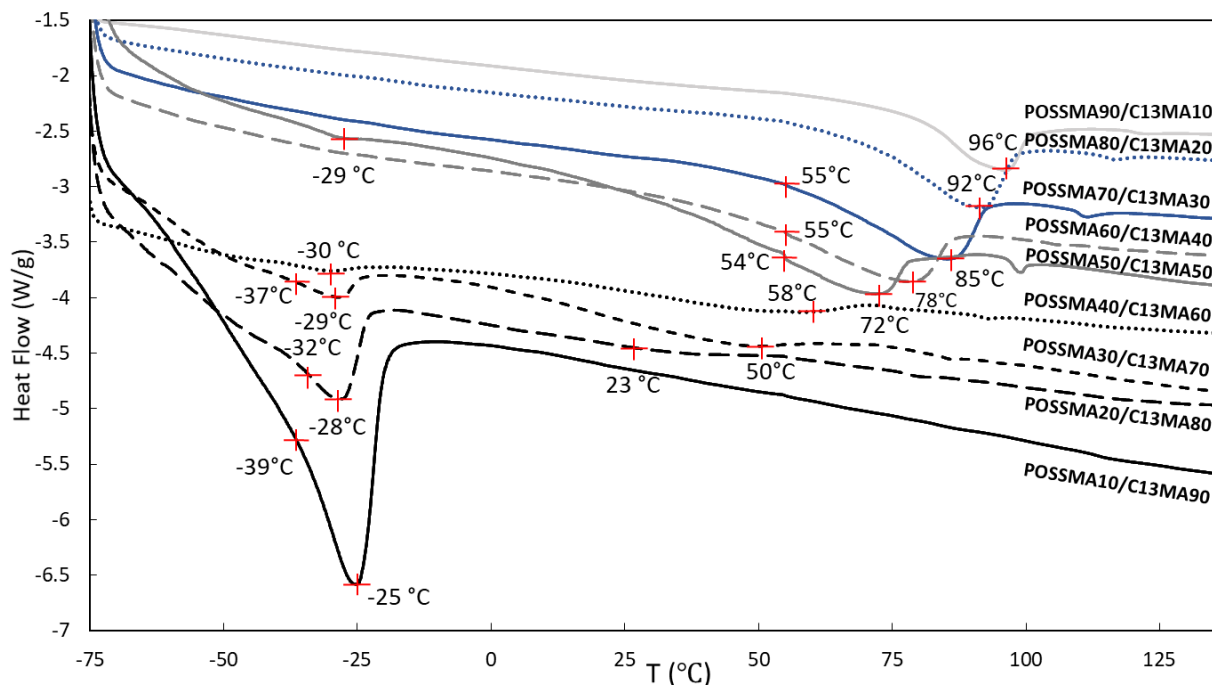
Figure 5.8. DSC traces for POSSMA/C13MA copolymers in the range of -80 to 190 °C with the heating rate of 15 °C min^{-1} and cooling rate of 50 °C min^{-1}.

5.3.5. PXRD Results

Figure 5.9 (a) presents the PXRD results for POSSMA homopolymers with different M_ns and compares the results with POSSMA monomer. The POSSMA monomer is highly crystalline (crystalline fraction = 81.7%) while the homopolymers, prepared by miniemulsion polymerization, are not as crystalline (~ 60-70%) and display a significantly smaller crystal size, almost 10 times less than the monomer (Table 5.5). Further, the POSSMA homopolymers prepared exhibited a reduction the crystal size and crystallinity with increasing M_n. For POSSMA homopolymers, a strong peak at 8.4°, two weak peaks at 11.0° and 19.2° and a wide peak at 25.4° were observed. The semi-crystalline nature was also expected for POSSMA/C13MA copolymers with the same peaks in PXRD patterns (Figure 5.9 (b)). This is in accordance with previous studies regarding POSS-based polymers[325, 346].
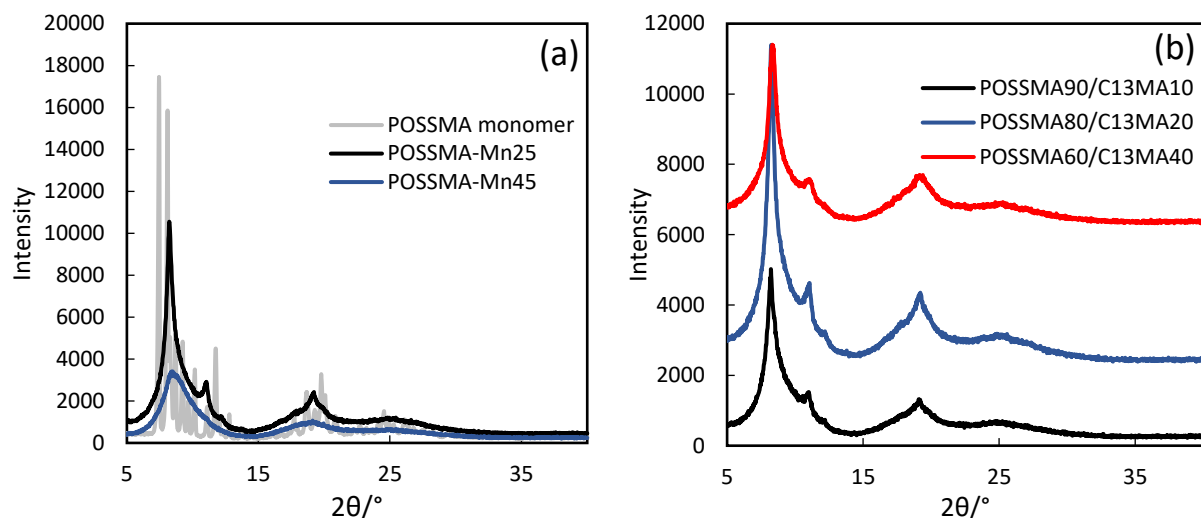
Figure 5.9. PXRD patterns for (a) POSSMA homopolymers compared to POSSMA monomer (b) Three powder POSSMA/C13MA copolymers with different monomer ratios.

Table 5.5. Crystallinity and crystallite size for POSSMA monomer, homopolymer and copolymers.

Sample name	$D_{Average}$[a] (°A)	Crystallinity (%)	M_n (kg mol^{-1})
POSSMA monomer	389.7	81.7	0.9[b]
POSSMA100-Mn25	44.3	71.4	19.2
POSSMA100-Mn45	20.3	63.8	27.2
POSSMA90/C13MA10	37.3	68.2	27.5
POSSMA80/C13MA20	44.4	70.5	31.2
POSSMA60/C13MA40	32.6	66.0	35.6

[a] Calculated by Scherrer equation. $D_{Average}$ is the average of Ds for X-ray diffraction peaks.
[b] molecular weight of POSSMA = 943.6 g mol^{-1}.

Table 5.5 summarizes the crystallite size and crystalline fraction of copolymers. Note that the crystallite size was calculated using the Scherrer equation[358, 359]:

$$D = \frac{K\lambda}{\beta \cos\theta} \tag{5.1}$$

where D is the crystallite size in the direction perpendicular to the given set of lattice planes, K is crystallite-shape factor ($K \approx 0.9$), λ is the wavelength of the radiation ($\lambda = 0.15406$ *nm*); β is the width of the X-ray diffraction peak (FWHM) in radians and θ is the Bragg angle.

Interestingly, the crystal size and the crystallinity of the copolymers did not change significantly by changing the POSS content in copolymer chains. A similar trend was observed for copolymerization of POSSMA and methacrylates with long aliphatic side-chains. In a study by Hajiali et al[181] POSSMA/AN/C13MA, the crystalline structure of POSS-based polymer chains was not sensitive to

incorporation of low fractions of C13MA. Similarly, Molina and coworkers[360] observed the almost identical crystal size, crystallinity and PXRD patterns for copolymers with different ratios of n-butyl methacrylate and POSSMA. However, this was not the case for copolymers of POSSMA and 2-ethylhexyl methacrylate, which shows that it is not a universal characteristic and it may only be valid for copolymers of POSSMA and methacrylates with long aliphatic side-chains[360].

5.4. CONCLUSIONS

We successfully synthesized POSSMA homopolymers with $\bar{M}_n$ up to 35.9 kg mol^{-1} ($Đ < 1.53$) by NMP in miniemulsion. The polymerizations were initiated by Dispolreg 007 without addition of any controlling comonomers leading to stable latex particles with polymerizations going to high conversions and relatively short polymerization times. The homopolymer was semi-crystalline with $T_m = 98\text{-}106$ °C) with high thermal stability imparted from the POSS inorganic cage ($T_{dec,1}$ ($T_{10\%}$) and $T_{dec,max}$ up to 278 and 369 °C, respectively). To adjust the T_g of the polymer and introduce flexibility, bio-based C13MA was copolymerized with POSSMA. Copolymers with different POSSMA:C13MA compositions were produced with conversions up to 96.5% and relatively low dispersity ($Đ < 1.68$) resulting in copolymers with a wide range of T_g and T_m (-39 °C < T_g and T_m < 96 °C). Adding POSSMA slightly increased the thermal stability of the copolymers (10 mol% increase in molar ratio of POSSMA in the feed, improved the $T_{dec,1}$ by 4.9 °C). All the polymerizations were conducted at 90 °C with reaction times ≤ 210 minutes and in the dispersed aqueous media with a minimum amount of toluene to dissolve POSSMA. Finally, semi-crystalline microstructures with melting points were observed for the POSSMA homopolymers and POSSMA/C13MA copolymers and it was also concluded that the copolymerization of POSSMA with long aliphatic methacrylates has a nominal impact on the crystalline size and the crystallinity of the polymeric structure.

ACKNOWLEDGMENTS

Preamble to Chapter 6

In the previous chapter, the possibility of miniemulsion polymerization of POSSMA was investigated and POSSMA/C13MA copolymers were successfully synthesized that would add flexibility and improve mechanical properties. The incorporation of POSSMA, a hybrid monomer with the silicon-containing cage, improves the thermal stability and hardness of POSSMA/C13MA copolymers. Previously, POSSMA was dissolved in toluene to be able to conduct the POSSMA homopolymerization or copolymerization with C13MA, which is a pseudo-suspension polymerization method. In this chapter, POSSMA was dissolved in a mixture of IBOMA/C13MA monomers and the miniemulsion polymerization was performed at 90 °C without the addition of organic solvents. We first studied the polymerization of POSSMA/IBOMA/C13MA in toluene to obtain the thermal stability and kinetic results and compared the results to the miniemulsion polymerization. It was shown that the addition of POSSMA successfully improved the thermal properties of the resulting polymers, which exhibited a wider range of glass transition temperatures. This study was published in the *Journal of Applied Polymer Science*,138 (13), 50095, 2021.

Chapter 6: Incorporation of Methacryloisobutyl POSS in Bio-Based Copolymers by Nitroxide Mediated Polymerization in Organic Solution and Miniemulsion

ABSTRACT

In this study, nitroxide mediated polymerization of methacryloisobutyl POSS (POSSMA) and bio-sourced monomers: isobornyl methacrylate (IBOMA) and C13 methacrylate (C13MA, an alkyl methacrylate with an average chain length of 13 units) was conducted in solution (toluene) and miniemulsion. BlocBuilder-MA (with 10 mol% acrylonitrile (AN) controlling co-monomer, for the solvent-based system) and Dispolreg 007 (for the miniemulsion) were used as the alkoxyamine for initiation and controlling the polymerization. POSSMA/IBOMA/C13MA effective terpolymerization (having 10 mol% AN controlling co-monomer) with monomer conversion (X) <72% in toluene resulted in resins with M_n up to 21.3 kg mol^{-1} and $Đ < 1.67$. Next, terpolymerizations were conducted in water to completely remove the organic solvent resulting in polymers with M_n up to 46.7 kg mol^{-1} and $Đ < 1.65$. The successful chain extension of poly(IBOMA/AN) with a mixture of POSSMA/C13MA/AN ($M_n = 74.1$ kg mol^{-1} and $Đ = 1.55$) showed high chain-end fidelity, exemplified by a clear, monomodal shift in the GPC chromatogram from the macroinitiator. Finally, it was shown that the addition of 20 mol% POSSMA improved the decomposition temperature of bio-based polymers of IBOMA/C13MA by 15%.

6.1. INTRODUCTION

The incorporation of silicon-containing compounds into polymer structures has been of great interest for the past several decades[361-363]. One example of such compounds are polyhedral oligomeric silsesquioxanes (referred as POSS), with general formula of $(RSiO_{1.5})_n$, $n \geq 6$, that usually possess one or more organic substituents[320]. This organic/inorganic hybrid can have various functional groups enabling the incorporation of the POSS into different materials[364, 365]. POSS-containing molecules are often cited as environmentally friendly, non-volatile and odorless and are frequently used as a nano-filler or modifier of material properties[366]. For example, POSS cages can improve anti-flammability, mechanical properties, thermal stability and biocompatibility and rheological properties[317, 320, 365]. Methacryloisobutyl POSS (termed herein as POSSMA) is a POSS containing molecules (n=8) with one methacrylic ligand, which can be incorporated

into polymer resins to improve the hardness (T_g of poly(POSSMA)$\approx$ 85 °C)[332] and thermal stability. The reversible-deactivation radical polymerization (RDRP) of POSSMA with different monomers was previously studied in organic solvents[331, 333, 357, 367-371] and reported in dispersed aqueous media recently[210]. Nitroxide mediated polymerization (NMP), as one of the simplest RDRP techniques, can be used to prepare POSSMA-containing polymers with active chain ends, well-defined microstructures and narrow molecular weight distributions[13, 23, 166]. These features allow lower viscosities (useful for coatings applications) and better chain—to-chain compositional homogeneity (tailoring of properties), for example.

Previously, POSSMA was incorporated into bio-based polymers and composites to enhance their mechanical and thermal properties[181, 372]. However, it was shown that only the addition of high POSSMA concentration (or similar POSS containing monomers) can efficiently increase the thermal stability of the product[369, 373, 374]. We earlier homopolymerized POSSMA and copolymerized POSSMA with C13MA, a vegetable oil-derived alkyl methacrylate with an average side chain length of 13 alkyl units. For copolymerization of POSSMA/C13MA, we observed that a 10 mol% increase in feed molar ratio of POSSMA improved the onset decomposition temperature ($T_{dec,1}$, for 10% weight loss) moderately by 4.9 to 5.8 °C[181, 210]. Here, isobornyl methacrylate (IBOMA) was incorporated into statistical terpolymers of POSSMA/IBOMA/C13MA for further improvement of thermal stability without compromising the bio-content of polymer resins. IBOMA is a bio-based monomer derived from terpenes[178]. IBOMA homopolymers have a high T_g (T_g = 110 to 200 °C, depending on the molecular weight)[201, 261-263] due to the bicyclic carbon-based group which contributes to improving hardness and thermal stability[259, 260]. As C13MA has a long alkyl group, it can effectively serve as a polymerizable plasticizer, providing flexibility to the polymer chain (T_g of poly(C13MA) homopolymer = -46 °C)[201, 375]. To understand the incorporation of these three monomers, via terpolymerization by NMP of POSSMA/IBOMA/C13MA monomers in toluene was first studied. BlocBuilder-MA alkoxyamine[27] (BB, from Arkema) was used to initiate the polymerization and 10 mol% acrylonitrile (AN) was added to the feed as the controlling co-monomer to improve the control over the polymerization[174]. Control is defined here as a linear increase of number average molecular weight M_n with monomer conversion, relatively narrow molecular weight distribution and predetermined final number-average molecular weight for polymers[166, 376, 377]. We thus target bio-based poly(methacrylate) resins by NMP with tunable T_g and excellent thermal stability due to the inclusion of POSSMA[162].

To investigate further the effect of the POSS cage on the thermal stability of polymers derived from bio-based monomers, polymerization of a low concentration of POSSMA (5, 10, 20 mol% in initial feed), with IBOMA and C13MA was performed in miniemulsion. Bypassing the use of organic solvents permitted a final product essentially free of volatile organic compounds (VOCs). To initiate the nitroxide mediated

miniemulsion polymerization of POSSMA/IBOMA/C13MA, Dispolreg 007 alkoxyamine[28, 29] was used. Dispolreg 007 has been used for NMP of methacrylates in organic solvents[28, 29, 278], miniemulsions[43, 162] and suspensions[103].This alkoxyamine enables the NMP of methacrylic monomers at moderate temperatures (T < 100 °C) without using any controlling co-monomers[43, 103, 243, 278]. In the last step, the influence of POSSMA and IBOMA on glass transition and decomposition temperatures of statistical and block copolymers was studied via thermal methods.

6.2. EXPERIMENTAL

6.2.1. Materials

Isobornyl methacrylate (IBOMA, >99%) and C13 methacrylate (Visiomer Terra C13,0-MA termed herein as C13MA, alkyl methacrylate with an average chain length of 13 units, >99%) were obtained from Evonik. To remove inhibitors before use, IBOMA and C13MA monomers were passed through a column of activated basic alumina (approximately 1 g per 50 ml monomer, Brockmann, Type 1, 150 mesh, Sigma Aldrich) and calcium hydride (5 wt% of basic alumina, 90-95% reagent, Sigma Aldrich). Methacryloisobutyl polyhedral oligomeric silsesquioxane (methacryloisobutyl POSS-MA0702 or POSSMA, from Hybrid Plastics) was used as received. Tetrahydrofuran (THF, 99.9%, HPLC grade, Fisher Scientific), n-hexadecane (~99%, Sigma Aldrich), DOWFAX™ 8390 (alkyldiphenyloxide disulfonate, Dow Chemical), Methanol (MeOH, >99%, Fisher Scientific) and toluene (>99%, Fisher Scientific) were used as received. Deuterated chloroform (CDCl$_3$, ≥99%) from Cambridge Isotopes Laboratory was used to dissolve samples for ^{1}H NMR. 3-(((2-Cyanopropan-2-yl) oxy) - (cyclohexyl) amino)-2, 2-dimethyl-3-phenylpropanenitrile (Dispolreg 007) alkoxyamine was synthesized according to Ballard et al's procedure[28]. N-(2-methylpropyl)-N-(1-diethylphosphono-2,2-dimethylpropyl)-O-(2-carboxyl prop-2-yl) hydroxylamine (BlocBuilder-MA™, termed herein as BB, 99%) was provided from Arkema. Reverse osmosis water (type 2 with the resistivity of ~ 1.1 MOhm·cm at 23 °C) was used for the miniemulsion polymerizations and DLS measurements. All the polymerizations and characterization tests (were necessary) were conducted under high purity nitrogen (99.998%, Praxair Canada).

6.2.2. Methods

6.2.2.1. M_n, X and $Đ$ Measurements

Dispersity of polymers ($Đ$) and number average molecular weight (M_n) were determined by gel permeation chromatography (GPC, Waters) relative to poly(methyl methacrylate) (PMMA) standards (from Varian Polymer Standards; M_n range of 875 to 1677000 g mol^{-1}) at an operating temperature of 40 °C. Three GPC Waters Styragel columns HR1, HR2 and HR4 (with the total molecular weight range of 10^2 to 6×10^5 g

mol^{-1}) and a guard column were used for measurements with a flow rate of 0.3 mL min^{-1}. For GPC, the samples were prepared by diluting in HPLC grade THF with a concentration of approximately 5 mg ml^{-1}. For samples from miniemulsion polymerizations, the monomer conversions were calculated from the areas under the normalized GPC peaks measured according to the method described in our recent study and the accuracy of the results was confirmed by comparing with a gravimetric method[210]. The polymer compositions and the monomer conversions for polymerization in toluene were measured by ^{1}H NMR (Bruker Avance III HD 500 MHz, 32 scans, using CDCl$_3$ deuterated solvent).

6.2.2.2. Particle Size

The Z-average particle size of miniemulsions was measured by dynamic light scattering (DLS) with a Malvern Zetasizer Nano-ZS, equipped with a 4 mW He–Ne laser at 633 nm and an avalanche photodiode detector with measurement angle of 173° at 25 °C. Latex samples were diluted with R.O. water to reach the concentration of 0.01-1000 mg ml^{-1} (10^{-3} – 1 % mass) before the DLS. 5 measurements per samples were performed to minimize the error.

6.2.2.3. Thermoanalytical Analyses

Differential scanning calorimetry (DSC, Q2000 from TA Instruments) was used to measure the T_gs of samples. Three scans per cycle (heat/cool/heat) with the heating rate of 15 °C min^{-1} and cooling rate of 50 °C min^{-1} were employed to determine T_gs during the re-heating cycle under nitrogen. The T_gs were predicted using TA universal analysis software with the inflection method. The calibration of temperature (by indium) and heat flow (by benzoic acid) was done for DSC before the tests. Thermogravimetric analysis (TGA) was performed by TGA Q500 (TA Instruments) with a ramp rate of 15 °C min^{-1} from 25 to 550 °C. The measurement of decomposition temperatures (T_{dec}s) was done in an aluminium pan under nitrogen. To provide polymer samples for DSC and TGA, latex samples were dried inside a fume hood at 23 °C for 3 days. The samples were dissolved in a minimal volume of toluene and were precipitated in excess methanol. The resulting polymer samples were then dried inside a fume hood for 6 hours and were placed under vacuum at room temperature for 12 hours. The samples from NMP in toluene were precipitated in methanol and were dried inside a fume hood and under vacuum at ambient condition for 6 and 12 hours, respectively.

6.2.3. Polymerization of POSSMA/IBOMA/C13MA/AN using BB alkoxyamine in Toluene

A mixture of monomers (IBOMA, C13MA, POSSMA and AN as the controlling co-monomer) and BB alkoxyamine were dissolved in 50 wt% toluene and were added into a 15 ml three-neck round-bottom glass reactor. The reactor was placed on a stirrer and a magnetic stir bar was added to the solution to mix the components before and during the polymerization. One of the necks was connected to a reflux condenser which was connected to a chiller (Neslab 740) that circulated a mixture of ethylene glycol/distilled water

(20/80 vol%) to provide a coolant to the condenser at a temperature of 3 °C. A temperature controller was used to maintain the reaction temperature and was connected to a heating mantle and a temperature sensor. The heating mantle was placed on the stir plate and the reactor was placed inside the mantle. A thermocouple was placed inside a temperature well in a second neck of the reactor, and the well was sufficiently deep to permit accurate estimation of the reaction temperature. The third neck was sealed with a rubber septa and a nitrogen syringe needle was inserted to provide the purge entrance (exit was via a rubber septa at the top of the condenser) and to take samples via syringe.

The solution was purged with pure nitrogen flow for 30 minutes before increasing the temperature. While still maintaining the nitrogen purge, the reactor was heated at a rate of $10\ °C \cdot min^{-1}$ and the starting point of the polymerization was taken when the reactor contents reached 75 °C ($T_{t=0}$). All the polymerizations were conducted under nitrogen atmosphere in toluene at 90 °C. Samples for kinetic analysis were taken periodically during the polymerization. As summarized in Table 6.2, polymerizations were performed using BB with 10 mol% AN and different molar fractions of POSSMA, IBOMA and C13MA. An example is given to illustrate the quadripolymerization procedure. For the experiment P10/IB44/C36/AN10, to the reactor were added BB (0.08 g, 0.21 mmol), POSSMA (1.65 g, 1.75 mmol), purified C13MA (1.71 g, 6.37 mmol), IBOMA (1.70 g, 7.65 mmol), AN (0.09 g, 1.75 mmol), and toluene (5.22 g, 56.65 mmol). The polymerization was run for 210 minutes. After precipitation into methanol and recovery, the wet product was dried under vacuum at room temperature overnight. ^{1}H NMR and GPC were used to determine the composition and molecular weight, respectively (M_n= 21.3 kg mol^{-1}, $Đ$ =1.61, F_{IBOMA} = 0.06, a sample calculation of monomer conversion and polymer composition using ^{1}H NMR peaks is available in Supplementary Information). The NMP scheme of POSSMA with C13MA and IBOMA is presented in Figure 6.1.
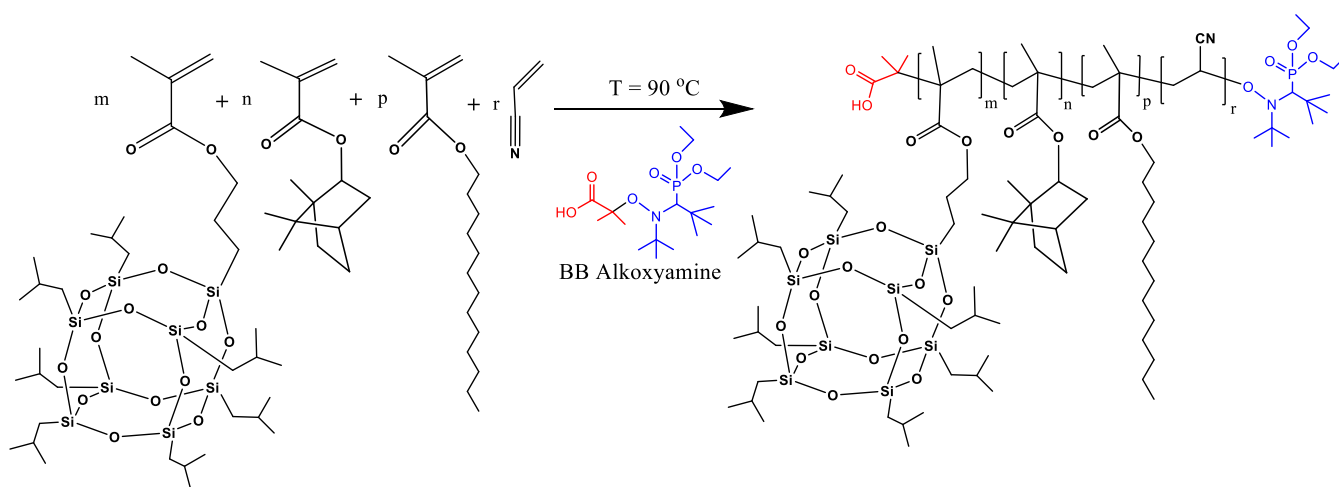
Figure 6.1. NMP scheme of p(POSSMA-*co*-C13MA-*co*-IBOMA-*co*-AN) statistical polymers using BB alkoxyamine, and AN co-monomer (10 mol% in initial feed) in 50 wt% toluene.

6.2.4. Miniemulsion Polymerization of POSSMA/IBOMA/C13MA

Terpolymerizations of POSSMA/IBOMA/C13MA was conducted in miniemulsion at 90 °C. Avoidance of organic solvent to dissolve the solid POSSMA was possible since the POSSMA monomer was completely soluble in the other liquid monomers. Unlike the polymerizations in toluene, which were initiated by BB, oil-soluble Dispolreg 007 alkoxyamine was used to initiate the NMP in miniemulsion. A favourable feature of Dispolreg 007 was the lack of necessity of a controlling co-monomer and its possible deleterious effect on the final polymer's properties. A schematic representation of the miniemulsion polymerization of POSSMA/IBOMA/C13MA is depicted in Figure 6.2. The experimental set-up for solution and miniemulsion polymerization was essentially the same. To prepare the miniemulsions, the hydrophobe and aqueous phases were made separately based on the recipe described in Table 6.1. Dispolreg 007 (alkoxyamine) and 0.8 wt% n-hexadecane (co-stabilizer) based on monomers' weight were added to a mixture of POSSMA, IBOMA and C13MA. DOWFAX 8390 surfactant (2 wt% based on monomers) was dissolved in water for the preparation of the aqueous phase. The two phases were mixed together for 30 minutes with stirring and were sonicated for 10 minutes (Hielscher sonicator UP200S, 50% duty cycle and amplitude 70%) in a cold water bath. The prepared latex was poured into the reactor and was purged with nitrogen for 30 minutes. The polymerization was conducted under ultra-pure nitrogen atmosphere at 90 °C ($T_{t=0}$ = 75 °C and heating rate of 10 °C min^{-1}). For the purpose of illustration, P5/IB47.5/C47.5 experiment ($M_{n,target}$ = 45 kg mol^{-1}) was conducted in miniemulsion under N$_2$ atmosphere at 90 °C. POSSMA (1.34 g, 1.419 mmol), IBOMA (3.62 g, 13.479 mmol) and C13MA (3.00 g, 13.479 mmol) were mixed with Dispolreg 007 (0.06 g, 0.177 mmol) and n-hexadecane (0.06 g, 0.281 mmol) to make the hydrophobic phase. The aqueous phase (Dowfax 8390 (0.16 g, 0.247 mmol) and water (24.71 g, 1371.569 mmol)) was stirred with monomer solution for 30 minutes and the final emulsion was sonicated for 10 minutes before polymerization.

Table 6.1. Polymerization formulation for the nitroxide-mediated miniemulsion terpolymerization of POSSMA/IBOMA/C13MA.

Component	Amount
Monomer (1) – POSSMA	Varies based on the experiment (0.044-0.141 M)
Monomer (2) – IBOMA	Varies based on the experiment (0.282-0.420 M)
Monomer (3) – C13MA	Varies based on the experiment (0.282-0.420 M)
Alkoxyamine (Dispolreg 007)	0.006 M

DOWFAX™ 8390	2 wbm%[a]
n-hexadecane	0.8 wbm%
Water	3 times the total weight of all components

[a] wt% based on the monomers
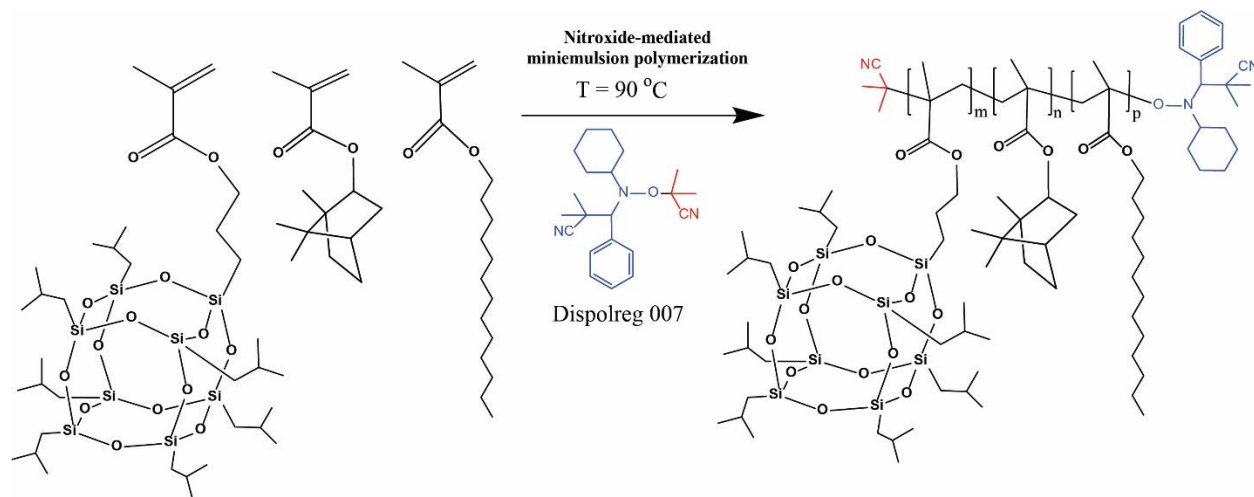
Figure 6.2. Schematic representation of nitroxide mediated emulsion polymerization of POSSMA/IBOMA/C13MA using Dispolreg 007 at 90 °C. 2 wt% DOWFAX 8390 (surfactant) and 0.8 wt% n-hexadecane (co-stabilizer) based on the weight of the monomers were added to stabilize the particles in miniemulsion.

6.3. RESULTS AND DISCUSSION

6.3.1. Polymerization of POSSMA with IBOMA/C13MA/AN in Toluene

Incorporation of POSSMA into IBOMA/C13MA co-monomers (with BB and 10 mol% AN as the controlling co-monomer) was done to obtain copolymers with improved thermal stability and hardness as IBOMA and POSSMA are known to produce polymers with relatively high T_g. First, a series of quadripolymerizations was undertaken in toluene, varying only one experimental parameter, namely the molar ratio of POSSMA in feed, ranging from 10 to 50 mol% (see Table 6.2 for experimental conditions). The weight ratio of 1:1 for IBOMA/C13MA was used for all syntheses in 50 w% toluene at 90 °C using BB with 10 mol% AN for 210 min. All kinetic plots were linear with respect to the reaction time but does not necessarily infer chain fidelity (Figure 6.3 (a)). Increasing POSSMA fraction from 0.1 to 0.5 decreased the apparent rate constant k_p [P$^\bullet$] ([P$^\bullet$] is the concentration of active polymer radicals and k_p is the rate constant of chain propagation) significantly from $(14.0 \pm 0.1) \times 10^5$ s^{-1} to $(1.8 \pm 0.1) \times 10^5$ s^{-1} (Table 6.3). Such a decrease with increasing POSSMA fraction was expected as seen earlier in POSSMA/C13MA

copolymerizations[181]. The polymer composition was listed in Table 6.3 and shows the successful incorporation of POSSMA in polymers (Figure 6.S1 in Supplementary Information shows an example ^{1}H NMR spectrum for finding the polymer composition).

M_n versus conversion plots show a relatively linear rise for all samples with subsequent plateauing at higher conversions > 60% (Figure 6.3 (b)). Such a deviation from the theoretical predicted line could be due to the irreversible termination reactions as seen in our previous studies[162, 182]. Further, in Figure 6.3 (b), Đ increases with conversion for all the experiments initiated with BB in toluene. This is probably caused by disproportionation between propagating radicals and the nitroxide at high conversions as reported elsewhere for polymerizations SG1 alkoxyamines[378]. Both Đ and M_n were also decreased from 1.61 to 1.45 and from 21.3 to 14.6 kg mol^{-1}, respectively, as POSSMA increased from $f_{POSSMA,0}$ = 0.10 to 0.50 in the initial monomer composition. The apparent decrease in final M_n values upon increasing POSSMA composition in the initial monomer mixture can be ascribed primarily due to its higher molecular weight compared to the other monomers, as the theoretical degree of polymerization was nearly halved on going from $f_{POSSMA,0}$ = 0.10 to 0.50.

The molecular weight distributions for experiments in toluene were presented in Figure 6.S2 (Supplementary Information).

Table 6.2. Experimental condition for NMP of POSSMA/IBOMA/C13MA/AN in toluene using BB at 90 °C.

Experiment ID	$f_{POSSMA,0}$[a]	$f_{IBOMA,0}$	$f_{C13MA,0}$	[BB]$_0$[b] (M)	[POSSMA]$_0$ (M)	[C13MA]$_0$ (M)	[IBOMA]$_0$ (M)	[AN]$_0$ (M)	[Toluene]$_0$ (M)
P10/ IB44/C36/AN10[c]	0.10	0.44	0.36	0.02	0.18	0.65	0.78	0.18	5.77
P20/ IB38/C32/AN10	0.20	0.38	0.32	0.02	0.32	0.51	0.62	0.16	6.50
P30/ IB33/C27/AN10	0.30	0.33	0.27	0.03	0.45	0.40	0.49	0.15	7.11
P40/ IB27/C23/AN10	0.40	0.27	0.23	0.03	0.55	0.31	0.38	0.14	7.62
P50/ IB22/C18/AN10	0.50	0.22	0.18	0.03	0.64	0.23	0.28	0.13	8.07

[a] Initial molar fraction of POSSMA in the initial feed (considering all constituent monomers). All syntheses done at 90 °C in toluene initiated by BB and targeting $M_{n,target}$ =25 kg mol^{-1}.
[b] Concentration of BB in the initial feed [mol L^{-1}].
[c] Polymerization of POSSMA, IBOMA, C13MA and AN with the initial concentrations of 10, 44, 36 and 10 mol%, respectively. AN with the initial concentration of 10 mol% was used as the controlling co-monomer for all the experiments using BB in toluene.

Table 6.3. Molecular characterization and kinetic data of poly (POSSMA/IBOMA/C13MA/AN prepared in 50 wt% toluene using BB at 90 ºC.

Experiment ID	$F_{POSSMA}{}^a$	$F_{IBOMA}{}^a$	$F_{C13MA}{}^a$	X^b (%)	$Đ^c$	$M_n{}^c$ (kg mol^{-1})^c	$k_p{}^d$ [P$^{\bullet}$] (10^5 s^{-1})^d
P10/IB44/C36/AN10^e	0.06	0.67	0.21	72.2	1.61	21.3	14.0 ± 0.1
P20/IB38/C32/AN10	0.15	0.46	0.29	59.5	1.67	19.5	12.1 ± 0.2
P30/IB33/C27/AN10	0.24	0.40	0.24	69.4	1.55	17.9	7.9 ± 0.1
P40/IB27/C23/AN10	0.30	0.38	0.20	52.4	1.45	12.8	4.0 ± 0.1
P50/IB22/C18/AN10	0.44	0.29	0.16	42.3	1.45	14.6	1.8 ± 0.1

^{a} F_{POSSMA}, F_{IBOMA} and F_{C13MA} indicate the molar fraction of POSSMA, IBOMA and C13MA (considering AN co-monomer) as determined by ^{1}H NMR in CDCl$_3$. A sample calculation to determine the composition is available in Supplementray Information,

^{b} Overall monomer conversion measured by ^{1}H NMR in CDCl$_3$.

^{c} The final product's number average molecular weight (M_n) and dispersity ($Đ$) were determined using GPC relative to PMMA standards at 40 °C.

^{d} Apparent rate constant derived from the semi-logarithmic slopes of ln[(1-X)$^{-1}$] (where X = conversion) versus time in the first 60 minutes of polymerization. Error bars were determined by finding the standard error on each slope (linear fit of semi-logarithmic plot).

^{e} Polymerization of POSSMA, IBOMA, C13MA and AN with the initial concentrations of 10, 44, 36 and 10 mol%, respectively. AN with the initial concentration of 10 mol% was used as the controlling co-monomer for all the experiments using BB in toluene.
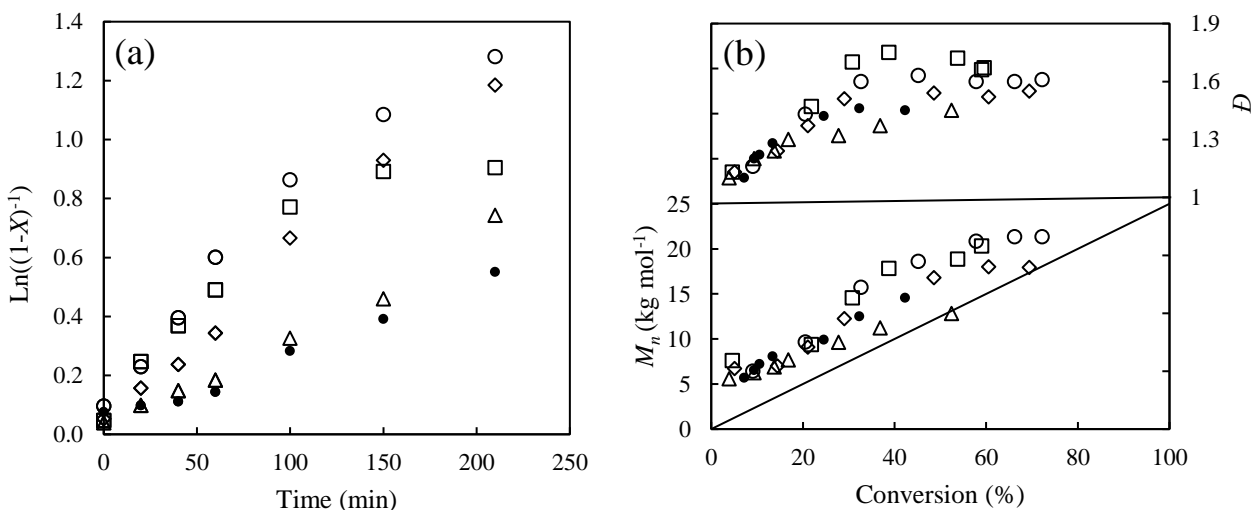
Figure 6.3. (a) Semi-logarithmic kinetic plots of ln[(1-X)$^{-1}$] (X = monomer conversion) versus polymerization time and (b) number average molecular weight M_n, and dispersity $Đ$ versus conversion (X) for NMP of IBOMA/C13MA/POSSMA using BB and $f_{AN,0}$= 0.1 at 90 °C: P10/IB44/C36/AN10 (open circles, ○), P20/IB38/C32/AN10 (open squares, □), P30/IB33/C27/AN10 (open diamonds, ◊), P40/IB27/C23/AN10 (open triangles, Δ), P50/IB22/C18/AN10 (filled circles, ●).

6.3.2. Terpolymerization of POSSMA/C13MA/IBOMA Monomers in Miniemulsion

The copolymerization of IBOMA/C13MA was previously done in organic solvent (toluene) and in aqueous miniemulsion[162, 182]. To study the effect of POSSMA on the miniemulsion polymerization of IBOMA/C13MA mixtures, terpolymerization of IBOMA/C13MA/POSSMA was conducted using similar reaction conditions at 90 °C. For miniemulsion polymerization, the feed molar ratio of 1:1 was set for IBOMA/C13MA, while the [POSSMA] varied for in each experiment. Table 6.4 illustrates the experimental conditions for terpolymerization of IBOMA/C13MA/POSSMA. The molecular weight distributions were monomodal with $Đ < 1.65$ for all samples taken during the polymerizations. The GPC peaks for NMP in miniemulsion were depicted in Figure 6.S3 (Supplementary Information). The high M_n in the beginning of the polymerization (Figure 6.4 (b)) was probably due to the strong penultimate effect associated with Dispolreg 007, which results in slow initiation[28, 43, 162, 278]. It should be noted that this curvature was not observed in the solution polymerizations as strongly, since BB was used as the alkoxyamine in the solution polymerizations. At $X > 50\%$, the slope of M_n versus X plots slightly decreases and approaches the theoretical prediction. This can be ascribed to not all chains initiating at the same rate during the early part of the polymerization but eventually at higher conversions, all chains are growing at nearly the same rate, with M_n approaching closer to the theoretical value. The k_p [P$^•$] trend for polymerizations in miniemulsion was different from the kinetic results of polymerization in toluene (Table 6.5). For P5/IB47.5/C47.5 experiment, the amount of POSSMA in polymer was negligible ($< 1\%$). Therefore, its k_p [P$^•$] does not follow the trend of other terpolymers prepared in miniemulsion. The k_p [P$^•$] for P10/IB45/C45 and P20/IB40/C40 does not increase with increasing composition of POSSMA in the terpolymers. Similarly, the k_p [P$^•$] for POSSMA/IBOMA/C13MA/AN in toluene decreased by increasing the POSSMA content in initial feed. It should be noted that the difference between alkoxyamines used in miniemulsion and organic solvent-based (Dispolreg 007 versus BB) resulted in different polymerization rates. Compartmentalization effects in miniemulsion could be also responsible for the higher polymerization rates[250, 379]. The monomer conversion for miniemulsion polymerizations were generally higher than the polymerizations in toluene at a given time ($74.4\% < X_{miniemulsion} < 96.1\%$ compared to $42.3\% < X_{toluene} < 72.2\%$; for the reaction time of 210 minutes except P5/I47.5/C47.5 experiment with reaction time of 150 minutes and X of 74.4% in miniemulsion), although the $M_{n,target}$ for polymerization in miniemulsion and toluene were 45 and 25 kg mol^{-1}, respectively. The semi-logarithmic kinetic plots with time in Figure 6.4 (a) were linear for all the experiments up to 150 minutes. Afterwards, the polymerization rate decreased, and the logarithmic kinetic plots tended to plateau, which suggested irreversible termination reactions were becoming more prevalent.

Table 6.4. Experimental formulation for nitroxide mediated miniemulsion polymerization of POSSMA/IBOMA/C13MA using Dispolreg 007 at 90 °C.

Experiment ID	$f_{POSSMA,0}$[a]	$f_{IBOMA,0}$	$[POSSMA]_0$[b] (M)	$[C13MA]_0$ (M)	$[IBOMA]_0$ (M)	[Dispolreg 007] (M)
P5/IB47.5/C47.5	0.050	0.475	0.044	0.420	0.420	0.006
P10/IB45/C45	0.100	0.450	0.081	0.366	0.366	0.006
P20/IB40/C40	0.200	0.400	0.141	0.282	0.282	0.006

[a] Initial molar fraction of POSSMA in the initial feed (considering all constituent monomers). All miniemulsion polymerizations were performed at 90 °C initiated by Dispolreg 007 with $M_{n,target}$ =45 kg mol^{-1}.
[b] Concentration of POSSMA in the initial feed [mol L^{-1}].

Table 6.5. Molecular characterization and kinetic data for miniemulsion polymerization of POSSMA/IBOMA/C13MA ($M_{n,target}$ = 45 kg mol^{-1}) using Dispolreg 007 at 90 °C.

Experiment ID	F_{POSSMA}[a]	F_{IBOMA}[a]	X^b (%)	$Đ^c$	M_n^c (kg mol^{-1})	k_p^d [P•] (10^5 s^{-1})[d]
P5/IB47.5/C47.5	0.006	0.46	74.4	1.51	46.7	14.0 ± 0.3
P10/IB45/C45	0.10	0.43	96.1	1.65	47.6	37.7 ± 0.4
P20/IB40/C40	0.21	0.39	90.3	1.58	45.0	32.7 ± 0.9

[a] F_{POSSMA} and F_{IBOMA} indicate the molar fraction of POSSMA and IBOMA in polymers determined by ^{1}H NMR in CDCl$_3$.
[b] Overall monomer conversion (%) based on the areas under the normalized GPC peaks.
[c] The final number average molecular weight (M_n) and dispersity ($Đ$) were measured by GPC relative to PMMA standards in THF at 40 °C. The target number average molecular weight ($M_{n,target}$) for all the miniemulsion polymerizations was 45 kg mol^{-1}.
[d] Apparent rate constant derived from the semi-logarithmic slopes of ln[$(1-X)^{-1}$] (where X = conversion) versus time in the first 60 minutes of polymerization. Error bars were determined by finding the standard error on each slope (linear fit of semi-logarithmic plot).
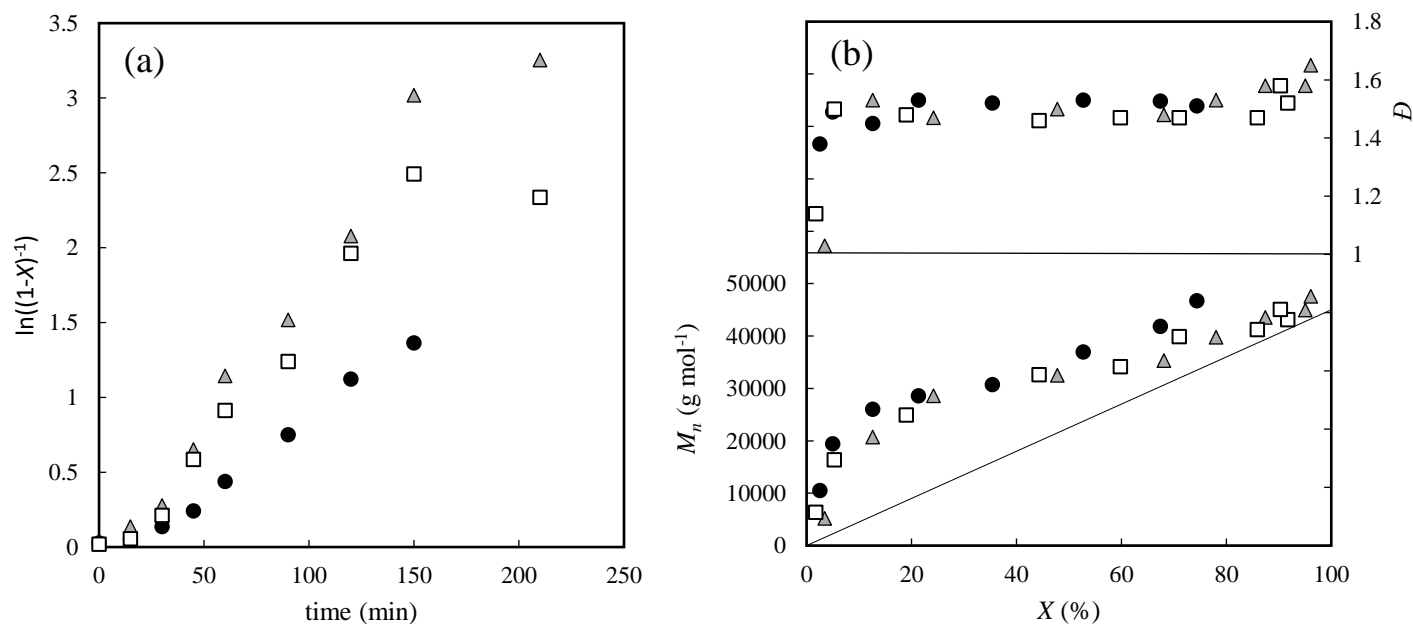
Figure 6.4. The miniemulsion terpolymerization of different ratios of POSSMA/IBOMA/C13MA using Dispolreg 007 initiator at 90 °C: (a) Semi-logarithmic kinetic plots of $\ln[(1-X)^{-1}]$ (X = monomer conversion) versus reaction time; (b) Number average molecular weight M_n and dispersity $Đ$ versus conversion (X). P5/IB47.5/C47.5 (filled circles, ●); P10/IB45/C45 (gray triangles, ▲); P20/IB40/C40 (open squares, □). Composition of terpolymers is provided in table 6.5.

6.3.3. Latex Particle Size

The average particle size for POSSMA/IBOMA/C13MA terpolymers was determined by DLS for the samples taken during the polymerization (Figure 6.5). The particle size for monomer droplets (t = 0 of polymerization) was in the size range of 286-299 nm and slightly decreased in the course of polymerization to reach final particle sizes of 243-258 nm. No precipitation or coagulation of polymer particles was observed during the miniemulsion polymerization and the particle size did not increase with reaction time, suggesting the high colloidal stability of the latexes and insignificant occurrence of Ostwald ripening events[291, 292, 341]. This is probably due to the use of highly hydrophobic monomers in the system which improves the stability of the resulting polymerization loci in dispersed aqueous media. The representative particle size distributions over time (experiment: P10/IB45/C45) were shown in Figure 6.S4 (Supplementary Information). The particle size of POSSMA/IBOMA/C13MA terpolymers was smaller than IBOMA/C13MA (50:50 molar ratio) miniemulsions studied at the same experimental conditions (particle size for POSSMA/IBOMA/C13MA latexes = 240-299 nm and for IBOMA50/C13MA50 = 321-549 nm)[162]. This illustrates that POSSMA may also act as a polymerizable co-stabilizer in miniemulsion and may reduce the required concentration of non-polymerizable co-stabilizers. However, it cannot be the sole co-stabilizer for miniemulsions and the addition of costabilizers (typically about 0.8 wbm% n-hexadecane) is required as previously observed for the miniemulsion polymerization of POSSMA/C13MA[210].
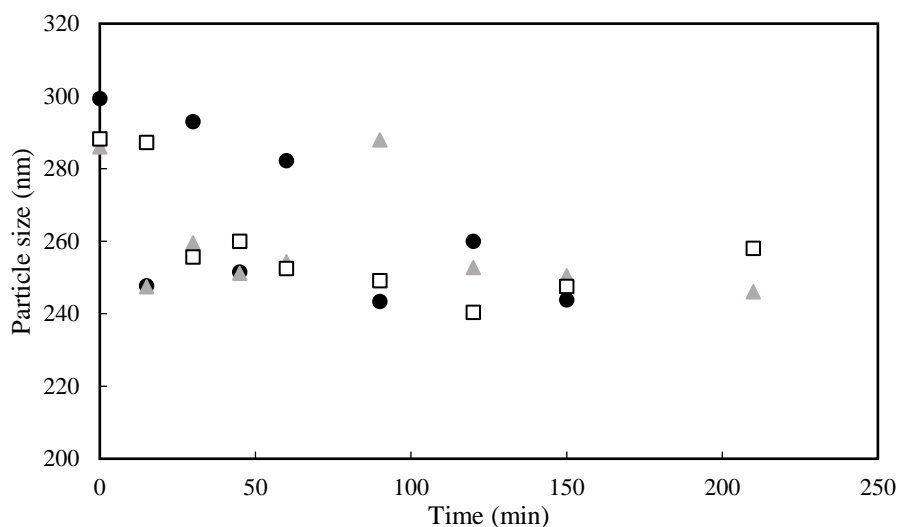
Figure 6.5. Z-average particle size for terpolymerization of POSSMA/IBOMA/C13MA versus reaction time. P5/IB47.5/C47.5 (filled circles, ●); P10/IB45/C45 (gray triangles, ▲); P20/IB40/C40 (open squares, □).

6.3.4. Preparation of block copolymer of p(IBOMA/AN)-*b*-p(POSSMA/C13MA/AN)

One observation during polymerization that suggests chain end fidelity is the steady shift of the molecular weight distribution over time, while remaining monomodal. Figure 6.S2, 6.S3 in Supplementary Information depicts the movement of the GPC peak to higher molecular weights for the experiments in toluene and miniemulsion over time. To further study the possibility of making block copolymers of POSSMA/IBOMA/C13MA and confirm the chain end fidelity, the block copolymerization of POSSMA/IBOMA/C13MA was attempted by the chain extension of IBOMA/AN copolymer (Poly(IBOMA) with 10 mol% AN in initial feed, M_n =11.0 kg mol^{-1} and $Đ$ = 1.38) with a mixture of POSSMA/C13MA/AN monomers (initial molar ratio of monomers [1:8:1], respectively). The formulation of the chain extension study and properties of macroinitiator and the final product are listed in Table 6.6. The block copolymer product had a monomodal molecular weight distribution with relatively low $Đ$ (M_n =74.1 kg mol^{-1} and $Đ$ = 1.55), indicating high activity of the chain ends, permitting the possibility of making block and gradient polymers. Figure 6.6 compares the GPC chromatogram of the poly(IBOMA)-rich macroinitiator with the chain-extended product. The $Đ$ of the copolymer was slightly elevated after the chain extension ($Đ$ = 1.55 compared to 1.38) as exemplified by the minor low molecular weight tailing, which demonstrates the presence of a low concentration of dead macroinitiator chains. The ^{1}H NMR spectra for chain extension is available in Supplementary Information (Figure 6.S5 and 6.S6).

Table 6.6. Summary of chain extension for p(IBOMA/AN) macroinitiator with POSS/C13MA/AN in 50 wt% toluene at 90 °C after 5 hours.

					A. Macroinitiator				
Experiment ID	X^a (%)	$[BB]_0$ (M)	$[IBOMA]_0$ (M)	$[AN]_0$ (M)	$[Toluene]_0$ (M)	$M_n{}^b$ (kg mol^{-1})	$M_{n,target}{}^c$ (kg mol^{-1})	$Đ^b$	Time^d (min)
p(IBOMA/AN)-macroinitiator	28	0.018	1.997	0.222	5.022	11.0	25	1.38	50

				B. Formulation and Characterization of Chain-Extension					
Experiment ID	X^a (%)	$[MI]_0{}^e$ (M)	$[POSSMA]_0$ (M)	$[C13MA]_0$ (M)	$[AN]_0$ (M)	$[Toluene]_0$ (M)	M_n (kg mol^{-1})	$M_{n,target}$ (kg mol^{-1})	$Đ$	Time^d (min)
p(IBOMA/AN) -b-p(POSSMA /C13MA/AN)	77	0.006	0.157	1.258	0.184	6.087	74.1	80	1.55	300
	$F_{POSSMA}{}^e$	F_{IBOMA}	F_{C13MA}	F_{AN}	$f_{POSSMA}{}^g$	f_{C13MA}	f_{AN}			
	0.11	0.21	0.64	0.07	0.10	0.80	0.10			

^{a} Overall monomer conversion measured by ^{1}H NMR in CDCl$_3$.

^{b} The final number average molecular weight (M_n) and dispersity ($Đ$) were measured by GPC relative to PMMA standards at 40 °C in THF.

^{c} The target number average molecular weight to synthesize poly(IBOMA/AN)-macroinitiator.

^{d} The reaction time (minutes).

^{e} The concentration of macroinitiator (MI) in initial feed (mol L^{-1}).

^{f} Molar fraction of POSSMA in the polymer chain measured by ^{1}H NMR in CDCl$_3$.

^{g} Initial molar fraction of POSSMA in the initial feed for chain-extension (considering all constituent monomers).
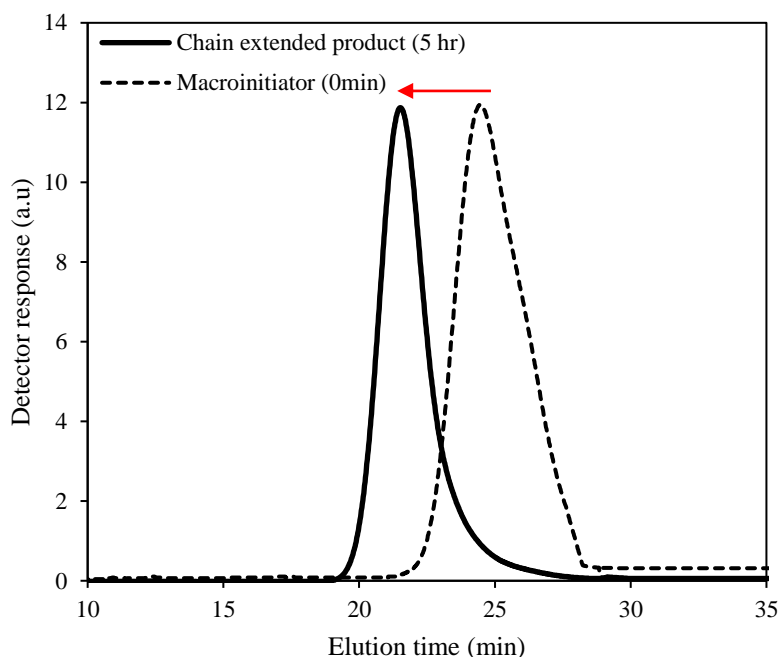
Figure 6.6. GPC peaks for the chain extension of p(IBOMA/AN) with POSSMA/C13MA/AN (the controlling co-monomer was in an initial concentration of 10 mol% AN). The dashed line depicts the GPC peak for p(IBOMA macroinitiator (M_n = 11.0 kg mol^{-1}, $Đ$ = 1.38) and the solid black line is the GPC peak of the block copolymer after 5 hours polymerization (M_n = 74.1 kg mol^{-1}, $Đ$ = 1.55). The preparation of the poly(IBOMA/AN) macroinitiator and the chain extended product were conducted under nitrogen

atmosphere in 50 wt% toluene at 90 °C. The complete characterization of macroinitiator and block copolymer is available in Table 6.6.

6.3.5. The Thermal Stability of POSSMA Containing Bio-Based Polymers

The thermal properties of the polymer resins were investigated to show the effect of incorporating POSSMA into the IBOMA/C13MA chains. The decomposition temperatures (T_{dec}s) were determined by TGA and illustrated that the addition of POSSMA slightly increases the onset of decomposition ($T_{dec,1}$ or T_{dec} for 10% weight loss). However, this was not the case for $T_{dec,max}$ (T_{dec} for the maximum rate of weight loss) and $T_{dec,2}$ (end of decomposition). $T_{dec,max}$ and $T_{dec},2$ did not show a significant change with increasing the POSSMA content in the polymers. The decomposition temperatures for all samples are summarized in Table 6.7. TGA traces were depicted in Figure 6.S7 and 6.S8 (Supplementary Information) for the POSS-containing polymers prepared in miniemulsion and the solvent-based system. For POSSMA/IBOMA/C13MA terpolymers, a two stage decomposition was observed, where the second peak was at 365-455 °C. This corresponds to the cleavage of the O-isobornyl bond in IBOMA and the formation and elimination of camphene at higher temperatures[211]. For polymers made by miniemulsion, the addition of 20 mol% POSSMA in the feed improved the $T_{dec,1}$ by 32 °C compared to the copolymer of IBOMA/C13MA ($[IBOMA]_0/[C13MA]_0 = 1:1$) in a similar system with a $T_{dec,1}$ of 211 °C[162]. As shown in Figure 6.7, this indicates that the incorporation of high concentration of inorganic POSS cages improves the thermal stability of the resin. A similar trend was previously observed for the free radical copolymerization of MMA with octavinyl-POSS[380]. Kotal et al[373] also observed a 14 to 46 °C increase in $T_{dec,1}$ by incorporating 4-17 wt% of thiol functionalized POSS compound (as initiator) in poly(MMA). However, it was not the case for using POSSMA as fillers in composites. Tanaka et al[381] showed that the addition of only 1mol% POSSMA into poly(MMA) as fillers enhanced thermal stability of composites ($T_{dec,composite}$ for 50% weight loss = 344.0 °C compared to 321.6 °C for poly(MMA)) although a slight decline in T_{dec} for 5% weight loss was observed after the addition of POSSMA filler. The presence of IBOMA also improved the $T_{dec,1}$. For instance, a study of p(POSSMA/C13MA/AN) containing 10 mol% POSSMA showed $T_{dec,1} = 220$ °C while P10/IB44/C36/AN10 with 10 mol% POSSMA and 44 mol% IBOMA in feed (prepared in toluene) had the $T_{dec,1} = 240$ °C. Previous studies on the addition of POSSMA into the bio-based polymers also indicated that $T_{dec,1}$ slightly increases by increasing the molar ratio of POSSMA in the feed, although this change was not significant. In one of the studies of the NMP of POSSMA/C13MA/AN (10 mol% AN, using BB alkoxyamine) in toluene, it was observed that increasing the molar ratio of POSSMA in feed composition by 10% improves the $T_{dec,1}$ by 5.7 °C[181]. For the miniemulsion polymerization of POSSMA/C13MA using

Dispolreg 007, this increase in $T_{dec,1}$ was about 4.9 °C for 10% increase in the initial concentration of POSSMA[210].

Interestingly, the block copolymer from p(IBOMA/AN)-*b*-p(POSSMA/C13MA/AN) experiment exhibits a comparatively higher $T_{dec,max}$. Furthermore, the $T_{dec,1}$ was slightly higher for p(IBOMA/AN)-*b*-p(POSSMA/C13MA/AN) compared to P20/IB38/C32/AN10, which had an approximately similar overall composition but higher content of POSSMA and IBOMA. This is probably due to the existence of two phase separated blocks in p(IBOMA/AN)-*b*-p(POSSMA/C13MA/AN), where one block becomes flexible during heating and delays the decomposition of the second block. A similar result was observed for block copolymers of IBOMA/C13MA compared to their counterpart statistical copolymers[182].

The glass transition temperatures (T_gs) were measured by DSC and are listed in Table 6.7. The addition of IBOMA ($T_{g,p(IBOMA)}$= 110-200 °C[201, 261-263] depending on the chain length) and POSSMA ($T_{g,p(POSSMA)}$= 85°C)[332] is expected to provide stiffness to the chains, while the long aliphatic chain in C13MA ($T_{g,p(C13MA)}$ = -46 °C) is expected to provide enhanced flexibility[179]. Accordingly, higher concentrations of POSSMA in the final polymer resulted in generally higher T_gs (for fixed ratios of the other co-monomers). The T_gs for polymers prepared in miniemulsion and toluene with similar compositions are approximately in the same range, suggesting similarity of the polymers prepared by the two different polymerization processes. This can also be validated by comparing the T_{dec} results for polymers with similar compositions prepared in organic solvent (toluene) and dispersed aquous media. Therefore, hybrid polymers of POSSMA and bio-based monomers like C13MA and IBOMA can be produced in dispersed aqueous media without compromising the thermal properties.

Table 6.7. Thermal characterization of POSSMA containing polymers prepared by NMP in solution (solvent: toluene) and miniemulsion.

Experiment ID	T_g^a (°C)	$T_{dec,1}^b$ (°C)	$T_{dec,max}^b$ (°C)	$T_{dec,2}^b$ (°C)	F_{POSSMA}^c	F_{IBOMA}	F_{C13MA}^d	M_n^e (kg mol^{-1})
Solvent-based system (prepared in 50 wt% toluene)								
P10/IB44/C36/AN10	32	240	309	467	0.06	0.21	0.67	21.3
P20/IB38/C32/AN10	41	245	307	475	0.15	0.29	0.46	19.5
P30/IB33/C27/AN10	50	250	312	473	0.24	0.24	0.40	17.9
P40/IB27/C23/AN10	73	254	315	470	0.30	0.20	0.38	12.8
P50/IB22/C18/AN10	80	257	300	480	0.44	0.16	0.29	14.6
p(IBOMA/AN)-*b*-p(POSSMA/C13MA/AN)	-33, 91	251	326	463	0.12	0.20	0.66	74.1
Water-borne system (prepared in miniemulsion)								
P5/IB47.5/C47.5	17	208	303	468	0.01	0.46	0.53	46.7
P10/IB45/C45	23	218	302	468	0.10	0.43	0.47	47.6
P20/IB40/C40	37	243	317	471	0.21	0.39	0.40	45.0

Figure 6.7. TGA thermograms for POSSMA/IBOMA/C13MA terpolymers prepared in miniemulsion. The feed molar ratio of IBOMA/C13MA remained constant for all the terpolymerizations [molar ratio 1:1]. The initial mol % of POSSMA increased from 5 to 20%.

6.4. CONCLUSIONS

Nitroxide mediated polymerization of POSSMA/IBOMA/C13MA was successfully conducted in organic solvent (toluene) and miniemulsion. The results showed the successful incorporation of POSSMA monomer into the bio-based monomer mixture of IBOMA/C13MA. Polymers with M_n up to 21.3 kg mol^{-1} ($M_{n,target}$ = 25 kg mol^{-1}, POSSMA content < 44% and 1.45 < Đ < 1.67) were synthesized in toluene. However, monomer conversion (X) decreased at 210 minutes by increasing the amount of POSSMA in the monomer feed. The X decreased from 72.2% to 42.3% as POSSMA feed content increased from 10% to 50%. The possibility of making block copolymers with IBOMA, C13MA and POSSMA monomers was investigated by the chain extension of poly(IBOMA)-rich macroinitiator (M_n = 11.0 kg mol^{-1} and Đ = 1.38) with a mixture of POSSMA and C13MA (Molar ratio of 1:8) for 5 hours in toluene at 90 °C (using BB as the unimolecular initiator and 10 mol% AN controlling co-monomer). The resulting block copolymer (M_n = 74.1 kg mol^{-1} and Đ = 1.55) had a monomodal molecular weight distribution without significant tailing, suggesting a very low concentration of dead chains. Next, the controlled radical terpolymerization of

POSSMA/IBOMA/C13MA was conducted in miniemulsion to avoid the use of organic solvents and improve the incorporation of POSSMA (i.e. higher monomer conversion in the dispersed system). The POSSMA containing polymers with IBOMA and C13MA with M_n up to 46.7 kg mol^{-1} and $Đ < 1.65$ were prepared in dispersed aqueous media using Dispolreg 007 at 90 °C. The resulting polymer latexes were colloidally stable with final average particle size = 243-258 nm. The addition of POSSMA improved the thermal stability of the resins and inhibited the pyrolysis due to the inorganic POSS cages. The most significant improvement was in the onset of decomposition ($T_{dec,1}$), in which $T_{dec,1}$ of the solvent-based polymers improved approximately by 4 °C per 10 mol% increase in POSS content while $T_{dec,1}$ of miniemulsion-based polymers improved by 23 °C per 10 mol% increment in POSS ratio.

ACKNOWLEDGMENT

Preamble to Chapter 7

This chapter is a departure from the themes established in the previous chapters. The previous chapters described the process to make a (co)polymer suitable to be applied as an aqueous-based emulsion for a coating. Besides converting the process to one with no volatile organic compounds (VOCs), the preceding chapters attempted to use bio-based monomers in place of petro-based ones as much as possible, while also adding POSS-based monomers to improve hardness and thermal stability to the resin, which is vital for the coating application. Another important property that is desirable for a coating is the use of self-healing polymers, which is the focus of this chapter. Eventually, the background established in this chapter will be used as a starting point to make self-healing polymers through a miniemulsion polymerization process and thus the self-healing polymer coating can be used as a separate polymer layer on top of the other polymer coatings to heal the scratches or various other surface damages. Most importantly, the healing has to be done at ambient temperatures and relative humidity in order to not damage the substrate. NMP was used to polymerize the monomers in the presence of BB alkoxyamine in 50 wt% 1,4-dioxane at 90 °C. Polymers were mainly synthesized from IBOMA and C13MA monomers to increase the bio-content of the coatings. A low concentration of 4-vinylphenyl boronic acid (VPBA) and glycerol monomethacrylate (GMMA) (2 to 15 mol% in the initial monomer mixture) was used for preparation of constituent polymers that are self-healing when combined. Ultimately, the use of such a system will hopefully reduce the carbon footprint and the cost of polymeric materials used for the coating, by avoiding repair steps and re-application of the coating after damage. Specifically, in this chapter, VPBA-containing polymers and GMA-containing polymers were synthesized separately and mixed together to form the dynamic boronic ester covalent bonds into the polymer microstructures. We studied how the polymerization kinetics were altered by incorporating these functional monomers and then how thermal properties were affected. The polymer blends showed excellent self-healing properties (healed scratches in 12 days and cuts in 10 days) at ambient condition and high recyclability using a simple hot press at 80 °C within 50 minutes. This chapter was published in *Reactive and Functional Polymers*,158, 104794, 2021.

Chapter 7: Highly Reprocessable, Room Temperature Self-Healable Bio-Based Materials with Boronic-Ester Dynamic Cross-Linking

ABSTRACT

Polymer blends with self-healing properties using humidity as a stimulus were prepared by mixing two polymer resins containing respectively low concentrations of 4-vinylphenylboronic acid (VPBA) and glycerol monomethacrylate (GMMA). The polymer resins were mostly made from bio-derived monomers isobornyl methacrylate (IBOMA, from terpenes) and C13 methacrylic esters (C13MA, from natural oils) to tune the thermal properties with low concentrations (2 to 15 mol% in feed) respectively of GMMA or VPBA in 1,4-dioxane at 90 °C. The VPBA and GMMA units form dynamic covalent boronic ester bonds to introduce self-healing in the presence of humidity at ambient temperature while increasing the chemical and heat resistance of the polymer blends. Polymer blend I (29 wt% VPBA-containing polymer with 2 mol% VPBA (T_g = 4.9 °C) in a terpolymer with 15 mol% GMMA (T_g = -0.4 °C)) and polymer blend II (a 29 wt% blend of a VPBA-containing polymer with 5 mol% VPBA (T_g = -13.2 °C) in a terpolymer with 15 mol% GMMA (T_g = -0.4 °C)) recovered up to 87% of the stress at break after breakage in 10 days and healed the scratches in 12 days at ambient temperature and relative humidity. The polymer blends are also recyclable and can be easily reprocessed at 80 °C within 50 minutes.

7.1. INTRODUCTION

Intrinsic self-healable materials facilitate the self-healing process using molecular interactions and bonds within the structure of the material[382, 383]. Several systems have been considered; one involves boronic ester interchange[151, 384-387]. Boronic acids (BAs) have been widely used in various biotechnological and biomedical applications for the synthesis of self-healable materials[160, 388-390], bioconjugates[391-395] and functional polymers[396-398] via bonding to diol groups of coupling molecules[399-401]. The dynamic covalent transesterification reaction of BAs with diols, as an intrinsic mechanism, has been exploited in self-healing hydrogels[402-404] and glucose sensors[405]. One way to incorporate boronic acid is through polymerization of monomers like 4-vinyl phenyl boronic acid (VPBA); there is some promise for these materials in biological applications as for example, some copolymers with VPBA showed low cytotoxicity in cells and animals[406-411]. Consequently, VPBA once incorporated into a polymer chain provides the functional group to form dynamic covalent boronate esters[150, 412, 413]. This reversible reaction can be activated and deactivated by the

presence of water or merely humidity at room temperature, making self-healing especially adaptable to many environments[414, 415]. Glycerol monomethacrylate (GMMA) is a monomer with two hydroxyl groups that is synthesized from glycerol, a by-product of microbial fermentation and biodiesel production from fats,[416, 417] and has emerged as an abundant chemical feedstock[418]. GMMA-based polymers are highly biocompatible and thus find application for example in contact lenses[419]. Consequently, incorporation of VBPA and GMMA by radical polymerization into complementary polymer chains is an attractive and relatively direct way of incorporating self-healing into commodity polymers using humidity as a trigger.

Further enhancement of properties of self-healing polymers is possible using controlled radical polymerization, more formally known as reversible deactivation radical polymerization (RDRP). Such methods rely on controlling the free radical concentration and avoiding irreversible termination reactions that are present in conventional radical polymerization. This permits RDRP processes to superficially mimic living polymerizations, resulting in predictable degree of polymerization with conversion, relatively low dispersity ($Đ \sim$ 1.2-1.5) and the ability to have an active chain end to permit formation of block copolymers[420]. VPBA has been polymerized by RDRP processes such as NMP[405, 421] and RAFT[422], while GMMA has been polymerized in a controlled fashion by atom transfer radical polymerization (ATRP)[423, 424] and reversible addition-fragmentation chain transfer (RAFT) polymerization[425-428] to produce self-assembled block copolymers. RDRP techniques have been utilized to synthesize polymeric materials with extrinsic and intrinsic self-healing properties[429-431]. We used NMP to minimize discoloration caused by residual chain transfer agents, or metallic catalysts, which is desirable particularly in biomedical applications[47, 218]. We further attempted to use bio-based monomers as the majority co-monomers to improve the sustainability features of the polymerization process[432-434]. Isobornyl methacrylate (IBOMA, 71% bio carbon content) and C13 methacrylate (methacrylic ester 13.0, C13MA, 76% bio carbon content) were chosen as the monomers to be copolymerized with GMMA and VPBA. IBOMA (made from camphene (via pine sap) and methacrylic acid) and is used in the polymer to enhance thermal stability, hardness and increase glass transition temperature (T_g)[259, 261, 435]. C13MA is derived from natural oils and in contrast to IBOMA, acts as a plasticizing monomer to improve flexibility and lower the T_g of the resin[179, 267, 268, 436]. The copolymerization of different ratios of these monomers yields a broad range of T_gs (-52 °C < T_g <169 °C)[162, 182]. This permits the study of self-healing by tuning thermal properties. We thus made complementary resins by NMP with different T_gs and compositions of the respective boronic acid and diol monomers to make blends with the objective of studying self-healing controlled by changes in humidity and the composition of the co/terpolymer. In this study, we attempted to develop polymer blends containing boronic ester dynamic bonds with self-healing properties at room temperature and high hardness (i.e. high glass transition temperature and mechanical properties), using maximum bio-content and minimum functional monomer (VPBA and GMMA) content. The hardness, self-healing properties and mechanical

properties of polymer blends are highly tunable and can be changed by changing the weight ratio of polymers in blend, or the composition of IBOMA and C13MA within the polymer chains. This enables the preparation of self-healable polymer blends for potential applications as adhesives and coatings.

7.2. MATERIALS AND METHODS

7.2.1. Materials

4-Vinylphenylboronic acid (VPBA, ≥ 97%) and glycerol monomethacrylate (GMMA, mixture of isomers, ≥ 95%) were obtained from Oakwood Chemical and Polysciences, respectively, and used as received. Isobornyl methacrylate (IBOMA, >99%, VISOMER® Terra IBOMA, Evonik) and C13 methacrylate (C13MA, methacrylic esters with an average chain length of 13 units, >99%, VISOMER® Terra C13,0-MA, Evonik) monomers were purified by passing them through a column of basic alumina (Brockmann, Type 1, 150 mesh, Sigma Aldrich) and calcium hydride (5 wt% of basic alumina, 90-95% reagent, Alfa Aesar) to remove the MEHQ inhibitor. 1,4-Dioxane (p-dioxane, ≥99%, MilliporeSigma), tetrahydrofuran (THF, 99.9%, HPLC grade, Fisher Chemical), methanol (MeOH, >99%, Fisher Chemical), methylene chloride (DCM, ≥99.5 %, Fisher Chemical), toluene (>99%, Fisher Chemical) and deuterated chloroform (CDCl$_3$, ≥99%, Cambridge Isotopes Laboratory) were used as received. N-(2-methylpropyl)-N-(1-(diethylphosphono-2,2-dimethylpropyl)-O-(2-carboxylprop-2-yl)hydroxylamine) (BlocBuilder-MA™ or BB, Arkema) was used as the alkoxyamine for all the polymerizations. Pinacol (98%, Sigma Aldrich), Molecular sieves (3 Å, pellets, 1.6 mm, Sigma Aldrich) and basic aluminum oxide (Brockmann I, Sigma Aldrich, pore size 58 Å and surface area = 155 m^2/g) were used for the esterification.

7.2.2. Methods

The number averaged molecular weight (M_n) and dispersity ($Đ$) were measured by gel permeation chromatography (GPC, Waters). The M_n of samples was determined relative to monodisperse PMMA standards (calibration was done based on 10 narrow GPC peaks of Varian polymer standards with the molecular weight ranges of 875 to 1677000 g mol^{-1}) in HPLC grade THF at 40 °C. The instrument was equipped with 1 guard column and 3 Styragel® GPC columns (Waters) termed as follows: HR1 (100 Å, M_n range of 100 to 5 × 10^3 g mol^{-1}), HR2 (500 Å, M_n range of 500 to 2 × 10^4 g mol^{-1}) and HR4 (10^4 Å, M_n range of 5 × 10^3 to 6 × 10^5 g mol^{-1}) and a differential refractive index RI 2414 detector. Polymers containing unprotected VPBA monomers had a tendency to adhere to the GPC columns and potentially interfere with the resulting measurement[437]. Thus, VPBA-containing polymers were protected by esterification with pinacol for GPC analysis. First, the molecular sieves (3 Å) (weight of molecular sieves/weight of sample = 0.25), 15 times methylene chloride and 2.5 times pinacol (based on the sample weight) were added to the

sample vials to start the esterification. The samples were stirred for 24 hours to protect the VPBA units. The final samples were purified using a 0.2 µm filter to remove the molecular sieves. Then, basic aluminum oxide (weight of aluminum oxide/weight of initial sample = 0.25) was added to the solution and stirred overnight. The samples were filtered again to remove the aluminum oxide and then dried using minimal air flow overnight to remove solvent. Afterwards, the polymer samples containing the protected VPBA units were dissolved in HPLC grade THF for subsequent GPC measurements.

The monomer conversion for polymerizations in 1,4-dioxane was calculated using the areas integrated from ^{1}H NMR (Varian 500 MHz, 32 scans) and the following equation was used to determine the overall conversion based on the conversion of different monomers in the system.

$$X = \sum_{i=1,...,n}^{n} X_i \cdot f_{i,0} \qquad (7.1)$$

In Equation (7.1), X is the overall conversion, X_i is the individual conversion of monomer ith and $f_{i,0}$ is the initial molar fractions of ith monomer in the solution and n is the number of different types of monomers in the system.

7.2.2.1. DSC and TGA

Decomposition temperatures (T_ds) and glass transition temperatures (T_gs) were obtained by thermogravimetric analysis (TGA, TGA Q500, TA Instruments) and differential scanning calorimetry (DSC, Q2000, TA Instruments), respectively. TGA was done under nitrogen at a ramp rate of 15 °C min^{-1} from 25 to 500 °C in aluminum pans. DSC was conducted under the nitrogen flow with the heating rate of 15 °C min^{-1} and cooling rate of 50 °C min^{-1} in a temperature range of -90 to 150 °C. Samples were placed into pinhole hermetic aluminum pans and three scan per cycle method (heat/cool/heat) was performed to eliminate the thermal history in the first cycle and measure the T_gs during the re-heating. DSC was calibrated using benzoic acid (for heat flow) and indium (for temperature) before the tests. The T_gs were calculated from change of slopes in DSC traces using inflection method.

7.2.2.2. Measuring the Temperature and Relative Humidity

A Fisherbrand™ Traceable™ digital humidity and temperature meter (Fisher Scientific, temperature range of -10 to 60 °C and accuracy of ±1 °C; relative humidity range of 20 to 95% with the accuracy of ±3% for mid-range and ±5% elsewhere) was used to measure the temperature and relative humidity of the room during the experiments.

7.2.2.3. Swelling Test

To perform the swelling test, a fully dried piece of sample with defined weight was placed inside an aluminum pan and excessive amount of toluene was added to completely cover the sample. The solvent

was removed, and the sample was dried using an extra-low lint Kimwipes® to measure the weight change of the samples.

7.2.2.4. Tensile Test

EZ-test-500N Shimadzu tensile tester was used to perform tensile tests on samples at room temperature and humidity (T= 19.1-23.9 °C, relative humidity of 38-58%). All dumbbell-shaped samples prepared and were tested following ASTM D638 type V[271]. The samples were extended at a rate of 15 mm min^{-1} and the reported data are the average of 5 measurements.

7.2.2.5. Rheological Measurements

Oscillatory frequency sweep, dynamic mechanical analysis (DMA) and stress relaxation experiments were performed on an Anton Paar MCR 302 rheometer connected to a CTD 450 convection oven. For oscillatory frequency sweep, the samples were placed between two parallel plates (diameter, 25 mm) and the test was conducted in the frequency range of 0.1 to 1000 Hz with a constant amplitude of 1% under a N2 atmosphere at 100 °C. A dynamic strain of 0.1% was applied for DMA experiments in the temperature range of 25-100 °C. DMA was done on original polymer blend samples and the same samples after undergoing recycling process three cycles. Stress relaxation tests were conducted at 6 different temperatures (25, 30, 35, 40 and 50 °C) with a constant strain of 0.5% to measure the stress decay over time.

7.2.3. Nitroxide-Mediated Quadripolymerization of IBOMA/C13MA/VPBA/AN

All the polymer syntheses were conducted in a three-neck round bottom glass flask connected to a temperature controller and a reflux condenser filled with the mixture of deionized water/ethylene glycol (75%/25%) with the temperature of 3 °C to prevent solvent evaporation. A thermocouple was connected to the temperature controller and was placed inside the flask to measure the temperature of the solution during the reaction. The set-up was fixed on the top of a heating mantle and placed on the magnetic stirrer. The mixture of monomers, 50 wt% 1,4-dioxane as the solvent and the BB alkoxyamine were weighed into a vial, mixed and then poured into the reactor. As an example, for the polymerization of VPBA5/IBOMA22.5/C13MA62.5/AN10, a mixture of BB (0.03 g, 0.089 mmol), IBOMA (0.98 g, 4.417 mmol), C13MA (3.29 g, 12.269 mmol), AN (0.10 g, 1.963 mmol) and VPBA (0.15 g, 0.982 mmol) was dissolved in 50 wt% 1,4-dioxane (5.07 g, 57.505 mmol) with the addition of 5 wt% water (0.51 g, 28.199 mmol) and the final solution was added to the reactor. A magnetic stir bar was added to the solution to apply proper mixing. Additionally, 5 wt% (based on the total weight of solution) reverse osmosis water was added to the solution to prevent the boroxine formation[438]. To deoxygenate the system, the solution was purged using a flow of pure nitrogen (99.99%, Praxair) for 30 minutes at 21 °C prior to the polymerizations. Then, the system was heated with the rate of 10 °C.min^{-1} and the nitrogen purging continues during the

reaction. The starting point of polymerizations ($t_{@0min}$) was considered at 75 °C and the reaction temperature for all the studies was 90 °C. The samples (~0.3 ml) were taken periodically for GPC and ^{1}H NMR measurements. Finally, after the polymerization was deemed complete, the system was cooled down and the final solution was removed when the contents were less than 40 °C. The polymers were precipitated in methanol to remove the unreacted monomers and dried under the vacuum overnight.

7.2.4. Nitroxide-Mediated Quadripolymerization of IBOMA/C13MA/GMMA/AN

The reaction set-up and polymerization method were same as the procedure for the NMP of IBOMA/C13MA/VPBA/AN. However, water was not required since no boroxine formation is possible. A typical polymerization is given as an example. For the experiment of GMMA15/IBOMA25/C13MA50/AN10, BB alkoxyamine (0.04 g, 0.105 mmol), IBOMA (1.35 g, 6.078 mmol), C13MA (3.26 g, 12.156 mmol), AN (0.13g, 2.431 mmol) and GMMA (0.58 g, 3.647 mmol) were added to 1,4-dioxane (5.37 g, 60.918 mmol) and the resulted solution was poured into a reactor. The polymerization was performed under nitrogen atmosphere at 90 °C for 120 minutes ($t_{@0min}$ = 75 °C).

7.2.5. Mixing the IBOMA/C13MA/VPBA/AN and IBOMA/C13MA/GMMA/AN Polymers

To mix the GMMA-based polymer with VPBA-based polymer, they were separately dissolved in toluene (67-90 wt% solvent for IBOMA/C13MA/VPBA/AN polymers and 50-67 wt% for IBOMA/C13MA/GMMA/AN polymers). In this point, different ratios of the two solutions of polymers were injected in a mold using two syringes. The polymers rapidly start to crosslink and form a gel. Therefore, the polymers were mixed during the injection using the syringe needles in the mold before the mixture became too viscous. The final sample was dried in the fume hood overnight, removed from the mold and dried again at room temperature to completely evaporate the solvent for one or two days. To improve the mixing process, all the polymer mixtures were pressed into dumbbell-shaped molds at 80 °C using a hot press (Carver Manual Hydraulic Press with Watlow Temperature Controllers, Carver Inc., Wabash, IN, USA). Three cycles were used to perform the hot pressing. To avoid air bubbles, the pressure released after each cycle and put to 13 metric tons for the next steps. First, the polymer mixtures were heated to 80 °C under 6-8 metric tons pressure for 12 minutes. Then, they pressed in two cycles at 13 metric tons and 80 °C for 15 minutes and 20 minutes, respectively. The prepared samples were cooled down and removed from the mold for further studies.

7.2.6. Recycling the Polymer Blends

The recycling process was started with grounding the samples to small pieces. Next, the polymer blends were pressed into molds using a hot press at 80 °C. The hot press process was as same as the hot pressing

used for preparation of polymer mixtures (three cycles, under 6-8 metric tons pressure for 12 minutes and two cycles at 13 metric tons for 15 minutes and 20 minutes, respectively).

7.2.7. De-cross-linking of polymer blends

For the chemical de-cross-linking, approximately 0.13 g of each polymer blend I and II samples were immersed in a solution of pinacol (0.5 g, 4.23 mmol) and 1,4-dioxane (7g, 79.45 mmol). A control experiment was done for each polymer blend by immersing the samples in the same amount of 1,4-dioxane (7g, 79.45 mmol) without the addition of pinacol. The vials were kept at 50 °C for 4 hours. The samples containing pinacol were precipitated in methanol for GPC and ^{1}H NMR measurements. To measure the insoluble fraction of blends I and II, the control vials containing the insoluble polymer blends remained at 50 °C for 24 hours. Next, the solvent was removed using a syringe and the samples were dried overnight at 40 °C under vacuum. The insoluble fraction of each polymer blend was determined by comparing the weight of original sample and the dried remaining polymer.

7.3. RESULTS AND DISCUSSION

The boronic ester dynamic cross-linking was investigated in resins predominantly consisting of the bio-derived IBOMA and C13MA, by incorporating VPBA and GMMA into the chains. These VPBA and GMMA monomers cannot be added to the polymerization medium at the same time (incorporating VPBA and GMMA into a single polymer chain is not applicable as they react rapidly and form an insoluble cross-linked gel). In this study, two polymers of IBOMA/C13MA/AN/GMMA and IBOMA/C13MA/AN/VPBA were prepared separately with different ratios of monomers to alter the glass transition temperature (T_g) of each polymer and prepare samples with different hardness. To observe relatively fast self-healing while maximizing the hardness of polymers, multiple polymerization studies were performed to find an optimal ratio of monomers for each polymer resin (VPBA-based and GMMA-based). All the polymerizations in 1,4-dioxane were conducted in the presence of BlocBuilder-MA™ (BB) alkoxyamine and 10 mol% AN as the controlling comonomer in the initial feed[174]. Figure 7.1 depicts the schematic representation for the synthesis of VPBA and GMMA containing polymers.
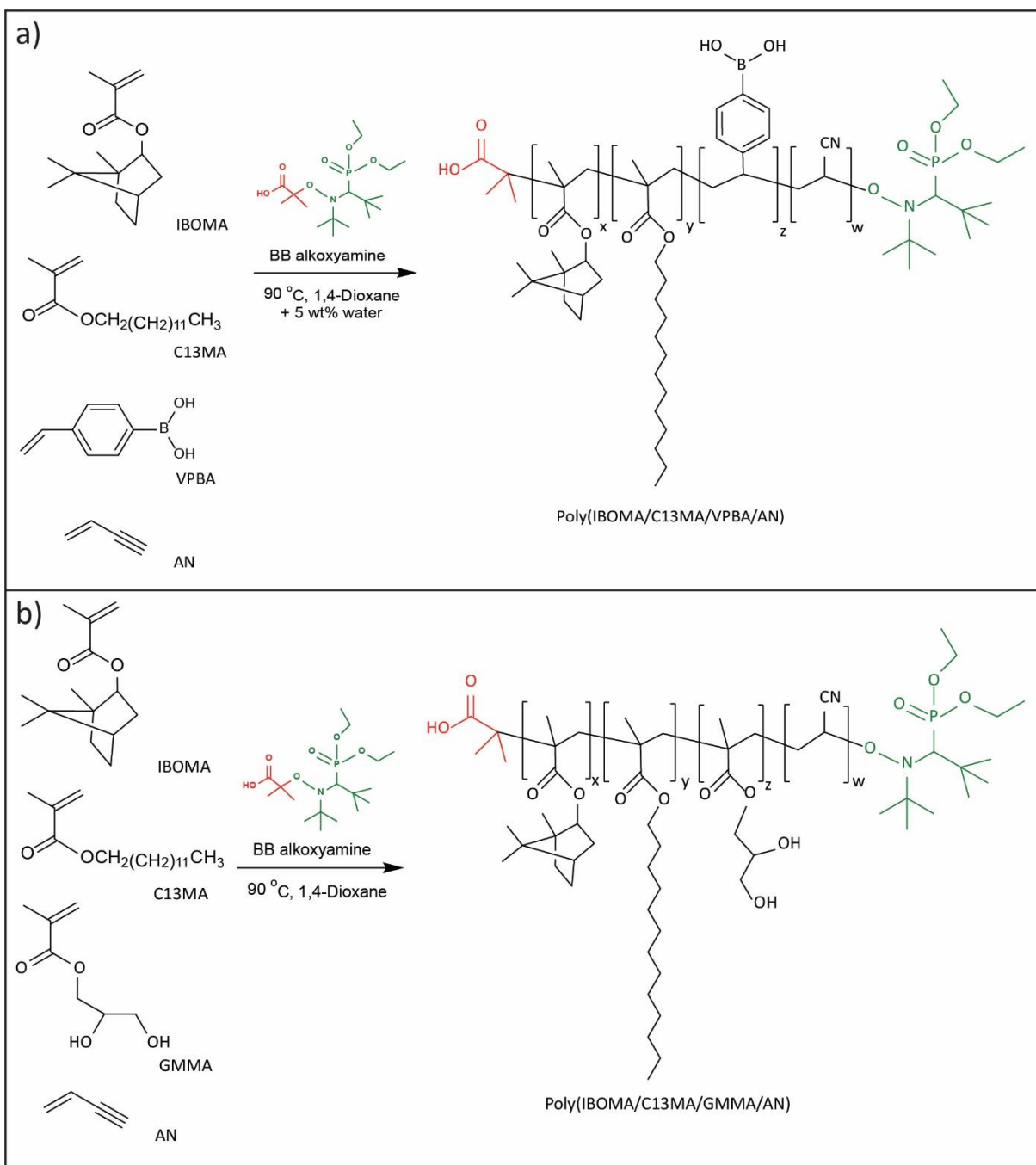
Figure 7.1. Schematic reactions for the preparation of polymer resins containing VPBA or GMMA in 1,4-dioxane at 90 °C. BlocBuilder-MA (BB) alkoxyamine was used to initiate and control the polymerization rate. 10 mol% AN was used in all the reactions in 1,4-dioxane as the controlling comonomer.

7.3.1. Polymerization of IBOMA/C13MA/AN with GMMA or VPBA Functional Monomers

The polymerization of IBOMA/C13MA/AN/GMMA with two different $M_{n,target}$ of 25 kg mol^{-1} and 50 kg mol^{-1} was conducted in 1,4-dioxane at 90 °C to prepare polymers with different chain lengths. The experimental conditions for polymerization of IBOMA/C13MA/AN/GMMA are listed in Table 7.1. Monomer conversion up to 90% were attained but the resulting polymers exhibited relatively high dispersities (1.67< $Đ$ < 2.73) (Table 7.2). The high $Đ$ was probably due to high occurrence of chain transfer reactions and high rate of termination for macroradicals as high polymerization rate and high $Đ$ was previously observed for NMP of related diol-functional glyceryl acrylates[439]. In addition, the possible interaction of carboxyl group of BB alkoxyamine with diol groups of GMMA can contribute to the higher $Đ$ as it was previously observed for the NMP of monomers containing hydroxyl groups[439, 440]. Other possible reasons for high $Đ$ are the interaction of GMMA-containing polymers with the GPC column material, which could appear as low molecular weight tails and the formation of crosslinking bonds due to ethylene glycol dimethacrylate impurities[439]. All the semi-logarithmic kinetic plots of IBOMA/C13MA/AN/GMMA polymerizations are displayed in Figure 7.2 (c), and show a deviation from linear first-order kinetics and a decrease in polymerization rate at reaction time > 60 minutes, indicating a preponderance of chain termination events at higher conversions. The M_n versus X results do not follow the theoretical line and flatter slopes were observed for GMMA-based polymers, especially with lower $M_{n,target}$. This cannot be completely explained entirely due to the GPC calibration using PMMA standards, as chain transfer side reactions would lead to a plateauing of the M_n versus X [441].

The polymerization of VPBA/IBOMA/C13MA/AN was also done with two $M_{n,target}$s of 25 kg mol^{-1} and 50 kg mol^{-1} in 50wt% 1,4-dioxane relative to monomers and 5 wt% (total weight of solution) water at 90 °C. The kinetic plots (Figure 7.2 (a) and 7.3 (a)) were linear up to 65% monomer conversion as a function of time for polymerization with different $M_{n,target}$ but they deviated from linearity at conversions > 60%. The $\ln((1-X)^{-1})$ plots for VPBA containing polymers reach a plateau after polymerizing for more than 480 minutes for $M_{n,target}$ = 25 kg mol^{-1} and 240 minutes for $M_{n,target}$ = 50 kg mol^{-1} due to termination events. As it was shown in Figure 7.2 and 7.3 (a) and (c), the polymerization rate of mixtures containing VPBA is generally lower than in polymerizations with GMMA monomers. Apparent rate constants for VPBA-containing formulations were lower than GMMA-containing formulations with similar co-monomer loadings and polymerization conditions (Table 7.S1 in Supporting Information listed all the apparent rate constants for poly(VPBA/IBOMA/C13MA/AN) and poly(GMMA/IBOMA/C13MA/AN)). This is not surprising as VPBA is a styrenic-based monomer, which have propagation rate constants about 10 times lower compared to most methacrylate-based monomers, like GMMA[437]. The M_n of polymer samples containing VPBA increased linearly with overall conversion and agreed well with predicted values,

especially at low monomer conversions. However, the M_n slightly deviates from the predicted line at higher conversions due to termination events. Finally, the molecular weight distributions were relatively broad for a typical NMP ($Đ$ up to 1.75 for $M_{n,target} = 25$ kg mol^{-1} and $Đ$ up to 2.13 for $M_{n,target} = 50$ kg mol^{-1}) but were still monomodal. Higher $Đ$s were typically observed towards the latter portion of the polymerizations, suggesting irreversible termination were becoming more prevalent, resulting in broadening of the molecular weight distribution of the samples and lowering of polymerization rate. The formation of boroxine groups (i.e. cross-linking bonds) is another reason for high values of $Đ$[153]. Increasing the $M_{n,target}$ from 25 to 50 kg mol^{-1} generally increased the $Đ$ as boroxine formation via VPBA inclusion was still possible despite the safeguards being employed to reduce this effect[438].

Table 7.1. Summary of experiments for nitroxide-mediated polymerization in 1,4-dioxane solvent using BB at 90 °C.

Experiment ID [a]	Reaction time (min)	$M_{n,target}$ (kg mol^{-1})	$M_{n,final}$ [b] (kg mol^{-1})	X [c] (%)	[IBOMA]$_0$ (M)	[C13MA]$_0$ (M)	[GMMA]$_0$ (M)	[VPBA]$_0$ (M)	[AN]$_0$ (M)	[BB] (M)
(a) poly(VPBA/IBOMA/C13MA/AN)										
VPBA5/IBOMA 42.5/C13MA42.5/AN 10	120	25	10.8	34.4	0.850	0.850	0	0.100	0.200	0.017
VPBA10/IBOMA40/ C13MA40/AN10	240	25	10.7	40.0	0.832	0.832	0	0.208	0.208	0.018
VPBA15/IBOMA37. 5/C13MA37.5/AN10	1200	25	19.9	69.6	0.812	0.812	0	0.325	0.217	0.018
VPBA2/IBOMA29/C 13MA58/AN11	480	50	29.2	77.8	0.548	1.095	0	0.038	0.208	0.009
VPBA5/IBOMA22.5/ C13MA62.5/AN10	150	50	32.5	64.3	0.429	1.191	0	0.095	0.191	0.009
VPBA10/IBOMA20/ C13MA60/AN10	300	50	23.4	60.0	0.394	1.183	0	0.197	0.197	0.009
VPBA15/IBOMA25/ C13MA50/AN10	480	50	35.1	64.0	0.525	1.050	0	0.315	0.210	0.009
(b) poly(GMMA/IBOMA/C13MA/AN)										
GMMA5/IBOMA42. 5/C13MA42.5/AN10	120	25	14.1	78.7	0.942	0.942	0.111	0	0.222	0.019
GMMA10/IBOMA40 /C13MA40/AN10	120	25	12.6	90.0	0.922	0.922	0.231	0	0.231	0.020
GMMA15/IBOMA37 .5/C13MA37.5/AN10	120	25	10.5	79.4	0.901	0.901	0.360	0	0.240	0.020
GMMA15/IBOMA25 /C13MA50/AN10	120	50	26.3	74.1	0.581	1.162	0.349	0	0.232	0.010

[a] VPBAxx/IBOMAyy/C13MAzz/ANrr or GMMAxx/IBOMAyy/C13MAzz/ANrr indicate xx mol% VPBA (or xx mol% GMMA), yy mol% IBOMA, zz mol% C13MA and rr mol% AN in the initial feed composition. Polymers were synthesized by nitroxide mediated polymerization at 90 °C.
[b] The final number-average molecular weight (M_n) was measured by GPC relative to PMMA standards in THF at 40 °C.
[c] Overall monomer conversion measured by ^{1}H NMR.
[a] VPBAxx/IBOMAyy/C13MAzz/ANrr or GMMAxx/IBOMAyy/C13MAzz/ANrr indicate xx mol% VPBA (or xx mol% GMMA), yy mol% IBOMA, zz mol% C13MA and rr mol% AN in the initial feed composition. Polymers were synthesized by nitroxide mediated polymerization at 90 °C.
[b] The final number-average molecular weight (M_n) was measured by GPC relative to PMMA standards in THF at 40 °C.
[c] Overall monomer conversion measured by ^{1}H NMR.

Table 7.2. Composition and molecular weight distribution of polymer resins.

Experiment ID	Feed composition [a] (%)			Final composition [b] (%)			$M_{n,final}$ [c] (kg mol⁻¹)	Đ [c]
(a) poly(VPBA/IBOMA/C13MA/AN)								
	f_{VPBA}	f_{IBOMA}	f_{C13MA}	F_{VPBA}	F_{IBOMA}	F_{C13MA}		
VPBA5/IBOMA 42.5/C13MA42.5/AN10 [d]	5	42.5	42.5	7.1	47.3	43.2	10.8	1.75
VPBA10/IBOMA40/C13MA40/AN10	10	40	40	10.5	44.6	40.7	10.7	1.70
VPBA15/IBOMA37.5/C13MA37.5/AN10	15	37.5	37.5	13.1	28.7	53.0	19.9	1.69
VPBA2/IBOMA29/C13MA58/AN11	2	29	62.5	1.9	29.8	67.2	29.2	1.79
VPBA5/IBOMA22.5/C13MA62.5/AN10	5	22.5	62.5	8.5	22.2	65.2	32.5	1.65
VPBA10/IBOMA20/C13MA60/AN10	10	20	60	12.1	22.8	60.4	23.4	2.13
VPBA15/IBOMA25/C13MA50/AN10	15	25	50	23.7	21.5	51.8	35.1	1.77
(b) poly(GMMA/IBOMA/C13MA/AN)								
	f_{GMMA}	f_{IBOMA}	f_{C13MA}	F_{GMMA}	F_{IBOMA}	F_{C13MA}		
GMMA5/IBOMA42.5/C13MA42.5/AN10	5	42.5	42.5	5.4	42.9	47.1	14.1	1.78
GMMA10/IBOMA40/C13MA40/AN10	10	40	40	6.9	39.0	49.7	12.6	1.82
GMMA15/IBOMA37.5/C13MA37.5/AN10	15	37.5	37.5	15.0	32.6	49.3	10.5	1.67
GMMA15/IBOMA25/C13MA50/AN10	15	25	50	10.2	18.4	64.5	26.3	2.73

[a] Feed monomer composition added into the solution (%) [b] Final composition of polymers determined by ¹H NMR in CDCL₃. [c] The final number-average molecular weight (M_n) and dispersity (Đ) were measured by GPC compared to PMMA standards in THF at 40 °C. [d] Nitroxide mediated polymerization of 5 mol% VPBA, 42.5 mol% IBOMA, 42.5 mol% C13MA and 10 mol% AN in the initial feed composition at 90 °C.
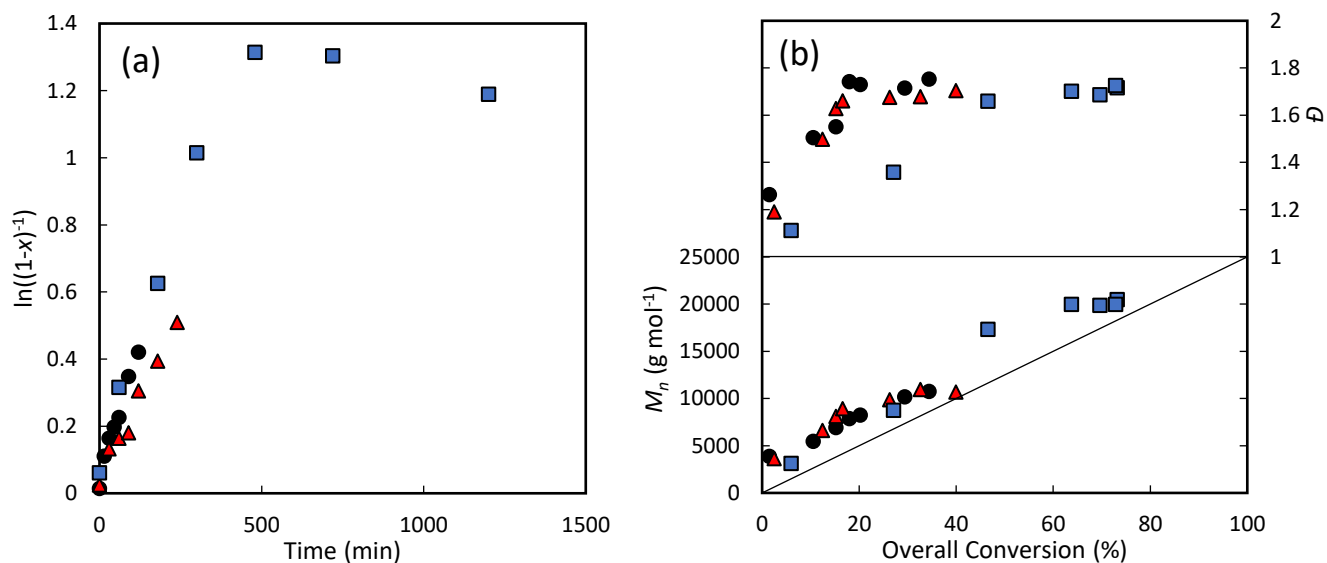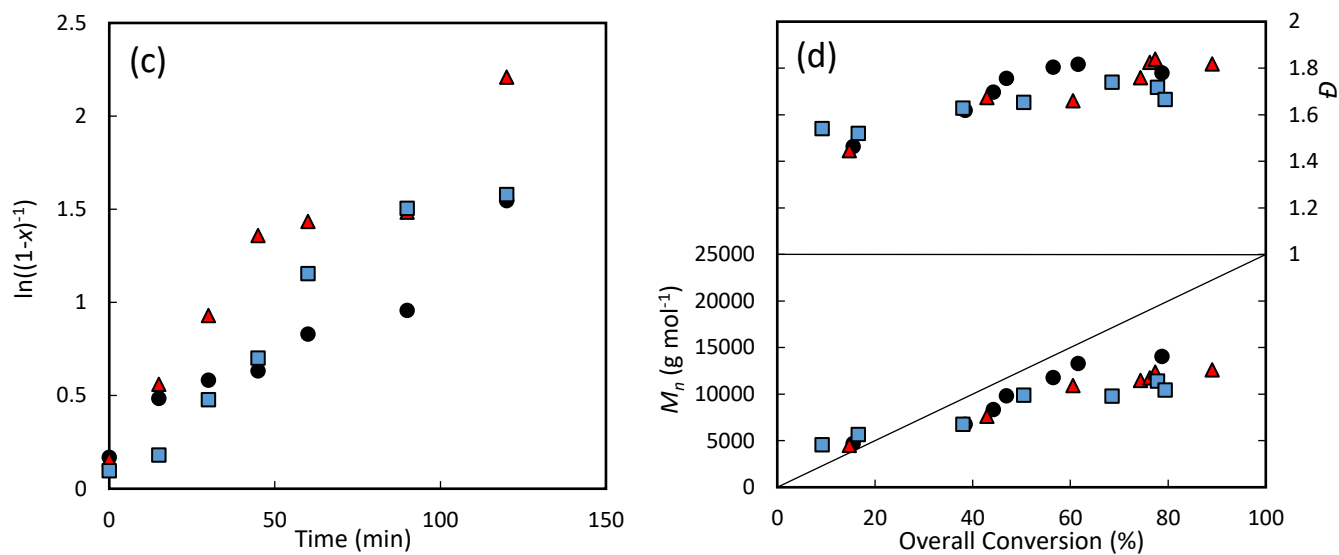
Figure 7.2. The statistical polymerization of different ratios of VPBA/IBOMA/C13MA/AN and GMMA/IBOMA/C13MA/AN with $M_{n,target} = 25$ kg mol^{-1} using BB alkoxyamine (a),(c) Semi-logarithmic kinetic plots of $\ln((1-X)^{-1})$ ($X=$ monomer conversion) versus reaction time (b),(d) Number average molecular weight M_n and dispersity $Đ$ versus conversion (X). In (a) and (b): VPBA5/IBOMA42.5/C13MA42.5/AN10 (black circles, ●); VPBA10/IBOMA40/C13MA40 /AN10 (red triangles, ▲); VPBA15/IBOMA37.5/C13MA37.5/AN10 (blue squares, ■). In (c) and (d): GMMA5/IBOMA42.5/C13MA42.5/AN10 (black circles, ●); GMMA10/IBOMA40/ C13MA40/AN10 (red triangles, ▲); GMMA15/IBOMA37.5/C13MA37.5/AN10 (blue squares, ■).
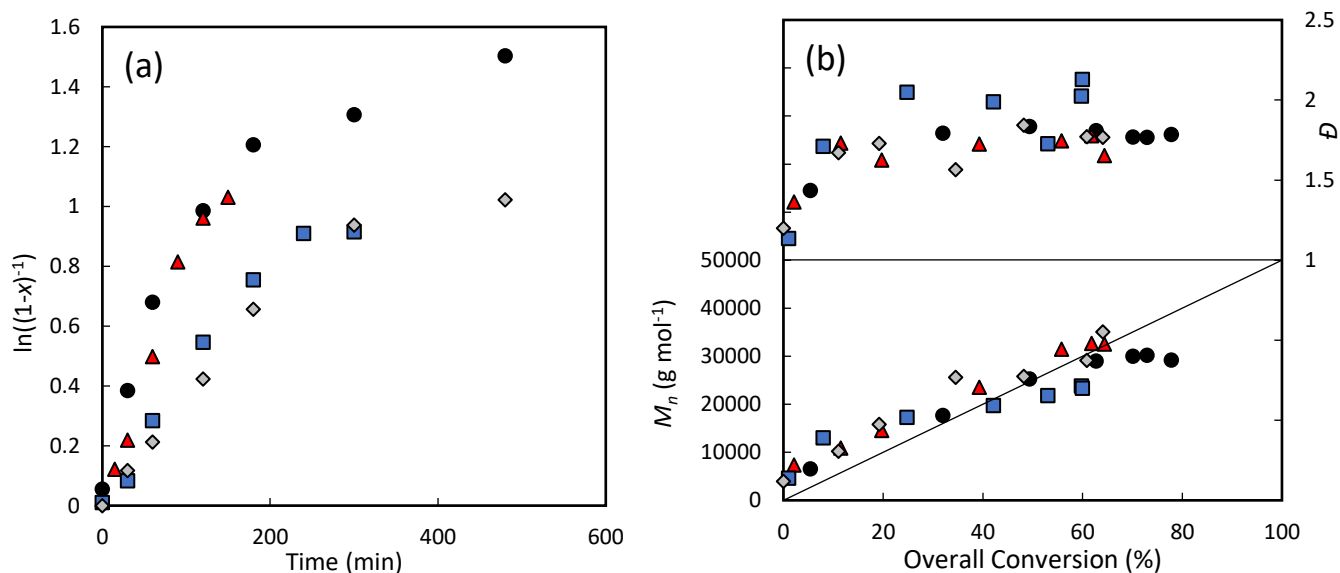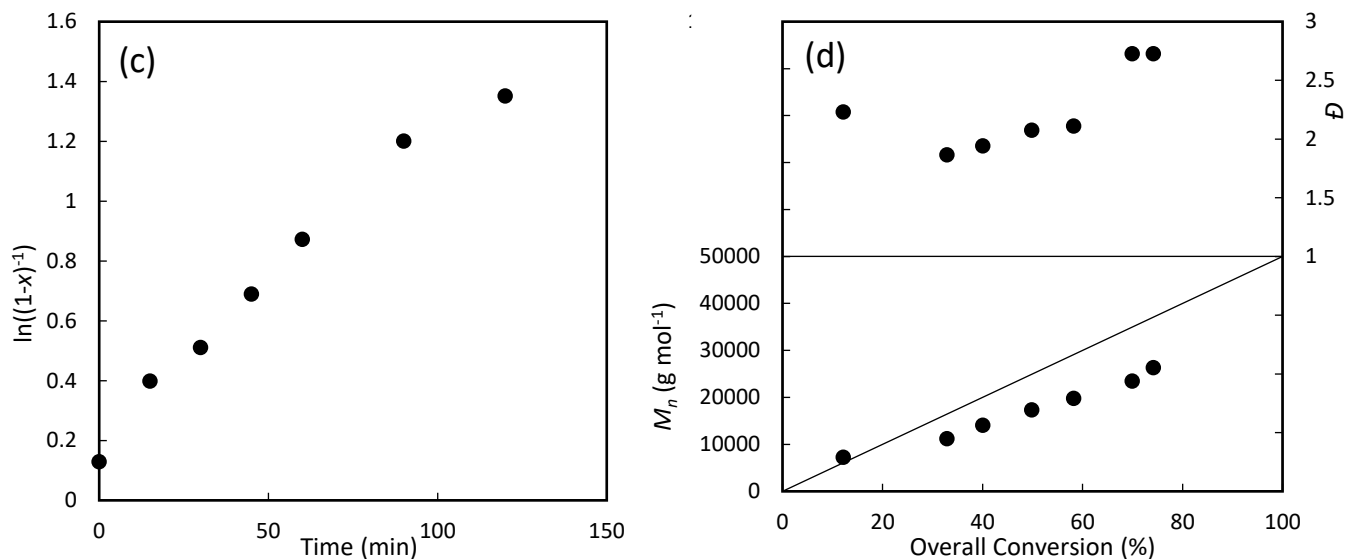
Figure 7.3. The statistical polymerization of different ratios of VPBA/IBOMA/C13MA/AN and GMMA/IBOMA/C13MA/AN with $M_{n,target}$ = 50 kg mol^{-1} using BB alkoxyamine (a),(c) Semi-logarithmic kinetic plots of ln[(1-X)$^{-1}$] (X= monomer conversion) versus reaction time (b),(d) Number average molecular weight M_n and dispersity $Đ$ versus conversion (X). In (a) and (b): VPBA2/IBOMA29/C13MA58/AN11 (black circles, ●); VPBA5/IBOMA22.5/C13MA62.5 /AN10 (red triangles, ▲); VPBA10/IBOMA20/C13MA60/AN10 (blue squares, ■); VPBA15/IBOMA25/C13MA50/AN10 (gray diamonds, ◊). In (c) and (d): GMMA15/IBOMA25/C13MA50/AN10 (filled circles, ●).

7.3.2. Determination of Glass Transition Temperature

To provide VPBA and GMMA-containing copolymers with a wide range of flexibility (T$_g$), NMP using different ratios of constitutive monomers was conducted in 1,4-dioxane using BB. The experimental T$_g$s were determined by DSC and compared with the theoretical T$_g$s (Table 7.3). The theoretical T$_g$s were calculated based on the Fox equation for all the polymer resins prepared in 1,4-dioxane[200]. The following equation was used for the estimation of T$_{g,theo}$s:

$$\sum_i w_i \left(1 - \frac{T_{g,theo}}{T_{g,i}}\right) = 0 \tag{7.2}$$

where w_i is the mass fraction of monomer i in polymer resin, T$_{g,theo}$ is the theoretical glass transition temperature of the resin and T$_{g,i}$ is the T$_g$ of pure homopolymer of monomer i. According to the literature, T$_{g,IBOMA}$ = 110~200 °C[201, 262, 263], T$_{g,C13MA}$ = -46 °C[201, 202], T$_{g,AN}$ = 95 °C[201, 203], T$_{g,GMMA}$ = 84~106 °C[442-444] and T$_{g,VPBA}$ = 198 °C[445-449]. T$_{g,IBOMA}$ = 110 °C[162, 201] and T$_{g,GMMA}$ = 84 °C[442] had the most similar

polymerization conditions with this study and were considered for the calculation of $T_{g,theo}$ for statistical polymers. As indicated in Table 7.3, the actual T_g differed from the $T_{g,theo}$ calculated for the same polymer in most cases, which can be due to the boroxine formation for VPBA-containing polymers and the formation of cross-linking bonds within the polymer structure and the existence of ethylene glycol dimethacrylate as the impurity for GMMA-containing polymers[442]. The high deviation from Fox equation was previously observed for GMMA copolymers and was attributed to strong intermolecular interactions such as hydrogen bonding[444].

Table 7.3. Glass transition temperature of polymer resins.

Experiment ID	$M_{n,final}$ (kg mol^{-1})	T_g [a] (°C)	$T_{g,theo}$ [b] (°C)
VPBA5/IBOMA 42.5/C13MA42.5/AN10	10.8	11.6	11.1
VPBA10/IBOMA40/C13MA40/AN10	10.7	22.6	15.7
VPBA15/IBOMA37.5/C13MA37.5/AN10	19.9	19.7	20.6
VPBA2/IBOMA29/C13MA58/AN11	29.2	4.9	-9.3
VPBA5/IBOMA22.5/C13MA62.5/AN10	32.5	-13.2	-16.7
VPBA10/IBOMA20/C13MA60/AN10	23.4	-1.4	-13.9
VPBA15/IBOMA25/C13MA50/AN10	35.1	6.5	0.0
GMMA5/IBOMA42.5/C13MA42.5/AN10	14.1	4.8	9.3
GMMA10/IBOMA40/C13MA40/AN10	12.6	17.1	11.7
GMMA15/IBOMA37.5/C13MA37.5/AN10	10.5	4.2	14.0
GMMA15/IBOMA25/C13MA50/AN10	26.3	-0.4	-3.2

[a] T_g (glass transition temperature) measured by DSC under nitrogen atmosphere using three scans per cycle (heat/cool/heat) at a heating rate of 15 °C min^{-1} and cooling rate of 50 °C min^{-1}.
[b] Theoretical glass transition temperature measured by Fox equation. T_g of the homopolymers were used for the calculation: $T_{g,IBOMA} = 110$ °C, $T_{g,C13MA} = -46$ °C, $T_{g,AN} = 95$ °C, $T_{g,GMMA} = 84$ °C and $T_{g,VPBA} = 198$ °C.

[a] T_g (glass transition temperature) measured by DSC under nitrogen atmosphere using three scans per cycle (heat/cool/heat) at a heating rate of 15 °C min^{-1} and cooling rate of 50 °C min^{-1}.
[b] Theoretical glass transition temperature measured by Fox equation. T_g of the homopolymers were used for the calculation: $T_{g,IBOMA} = 110$ °C, $T_{g,C13MA} = -46$ °C, $T_{g,AN} = 95$ °C, $T_{g,GMMA} = 84$ °C and $T_{g,VPBA} = 198$ °C.

Feed monomer compositions were chosen *a priori* to yield relatively soft polymers at room temperature. Measuring the T_g of polymers helped with the estimation of the hardness of polymer blends and was used for the design of polymer blends.

7.3.3. Preparation of Polymer Blends

Next, polymers containing VPBA were mixed with GMMA-containing polymers to activate the dynamic cross-linking between the boronic acid groups of the VPBA with the hydroxyl groups of GMMA and form the ester (please refer to the experimental methods section for the detailed procedure of mixing the

polymers). The cross-linking reaction was evident almost immediately upon mixing the two resin solutions with a massive increase in viscosity. Figure 7.4 depicts the preparation steps of the self-healing polymer blends. Various polymer blends were prepared to adjust the hardness or flexibility of the final polymer mixture. The prepared polymer blends are listed in Table 7.4. The weight ratio of GMMA-containing polymer was set higher in the polymer blend to have excess free hydroxyl groups for reaction with boronic acids and increase the probability of dynamic cross-links and as a consequence, improved self-healing properties[414]. Polymer blends I, II, III and IV had the highest concentration of free diol groups. In addition, due to the sufficiently low T_g of constitutive polymers, a relatively flexible polymer structure was created. Therefore, the self-healing ability was expected to be more pronounced in these blends and was investigated in more detail in the following sections.
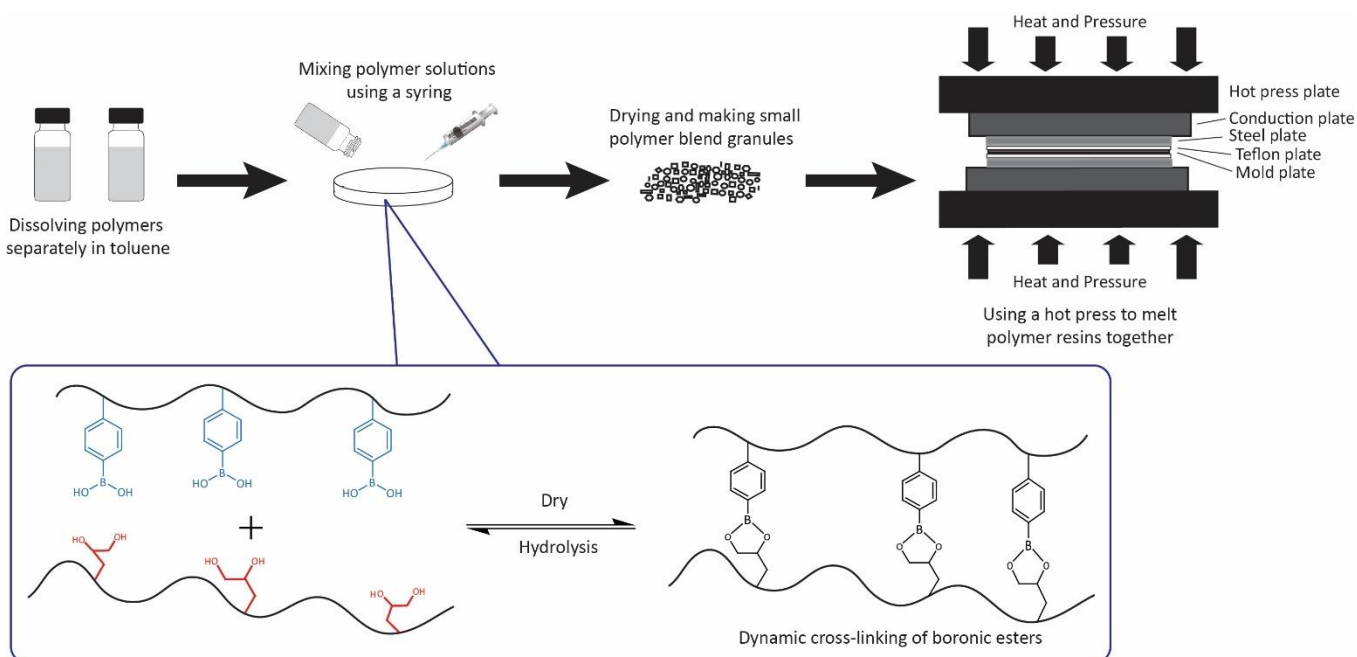
Figure 7.4. preparation of self-healing polymer blend using boronic ester dynamic cross-linking

Table 7.4. Formulations for preparation of polymer blends from their base polymers.

Polymer blend ID	A: polymer resin containing VPBA	B: polymer resin containing GMMA	Weight ratio of A:B
I	VPBA2/IBOMA29/C13MA58/AN11	GMMA15/IBOMA25/C13MA50/AN10	1:2.5
II	VPBA5/IBOMA22.5/C13MA62.5/AN10	GMMA15/IBOMA25/C13MA50/AN10	1:2.5
III	VPBA10/IBOMA20/C13MA60/AN10	GMMA15/IBOMA25/C13MA50/AN10	1:2.5
IV	VPBA15/IBOMA25/C13MA50/AN10	GMMA15/IBOMA25/C13MA50/AN10	1:2.5
V	VPBA5/IBOMA 42.5/C13MA42.5/AN10	GMMA5/IBOMA42.5/C13MA42.5/AN10	1:1
VI	VPBA5/IBOMA 42.5/C13MA42.5/AN10	GMMA5/IBOMA42.5/C13MA42.5/AN10	1:5
VII	VPBA10/IBOMA40/C13MA40/AN10	GMMA10/IBOMA40/C13MA40/AN10	1:2.5

Figure 7.5 summarizes the FTIR spectra for polymer blends I, II, III and IV. A higher intensity of O-H stretching at 3446 cm^{-1} was observed for polymer blends I and II compared to III and IV, likely due to the excess of unreacted OH (mainly hydroxyl) groups in the former two blends. This suggests lower reversible cross-linking in polymer blends I and II due to the lower VPBA content and higher availability of free hydroxyl groups for re-connection with 4-phenylboronic acid moieties. Lower VPBA content of polymer blends I and II was also confirmed by the comparison of peak intensities at 653 cm^{-1} (CB stretching, HO-B-O and O-B-CC bending), 804 cm^{-1} (CB stretching) and 1368 cm^{-1} (BO stretching) for different blends[450-452]. The peaks at 1547 and 1649 correspond to C=C and C-C stretching from the phenyl groups in VPBA and the aliphatic ring in IBOMA units.
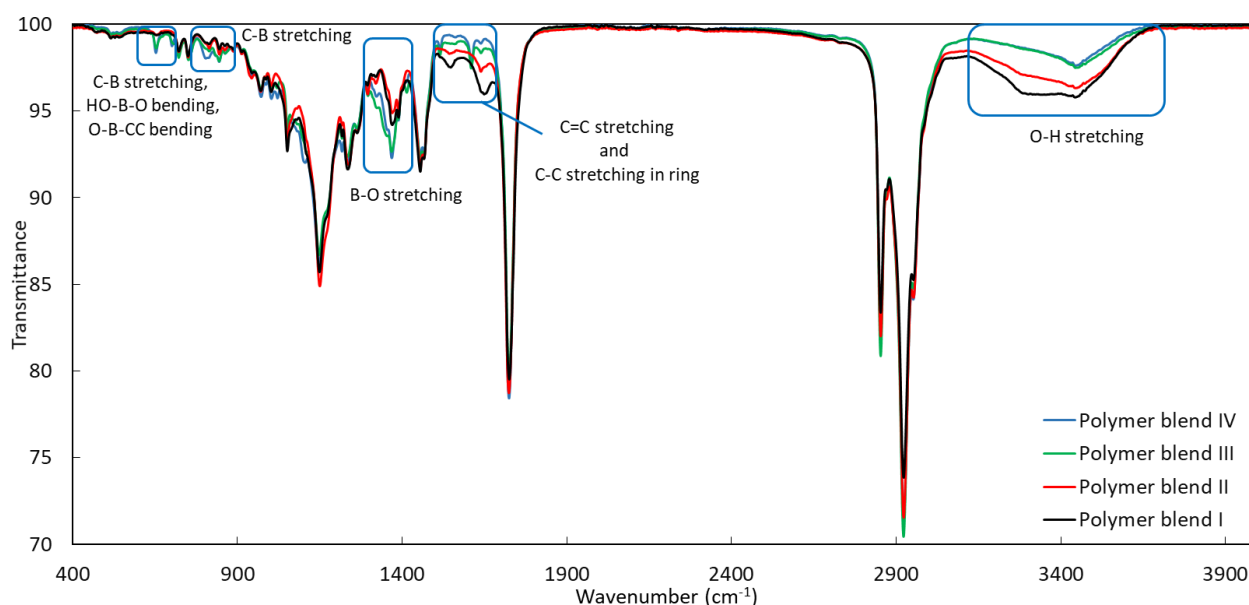
Figure 7.5. FTIR spectra for polymer blends I (—, black line), II (—, red line), III (—, green line) and IV (—, blue line) in the range of 400 to 4000 cm^{-1}.

7.3.4. Characterization of Polymer Blends Properties

7.3.4.1. Rheological Measurements

The formation of dynamic cross-linking bonds in polymer blends was investigated by oscillatory frequency sweep experiments at 100 °C. The test was conducted in frequency range of 0.1 to 1000 Hz for GMMA and VPBA-containing polymers and their blends. The storage modulus (G′) and loss modulus (G″) for polymers and blends varied with increase in frequency. It was previously observed that G′ and G″ for materials containing permanent covalent cross-linking bonds are frequency independent[142, 453]. However, G′ and G″ for prepared polymer blends (Figure 7.6 (a)) increased with increase in angular frequency,

suggesting the existence of dynamic covalent bonds within the polymeric structure[142]. At low frequencies ($\omega < 315$ Hz for blend I and $\omega < 250$ Hz for blend II), G′ > G″ indicating the rubbery behavior of blends[454]. At higher frequencies, a crossover occurs due to relaxation and dissipation of energy from the chains and a transition from the solid to a viscoelastic liquid state was observed. In addition, the higher crossover frequency (ω_c, where G′=G″) for polymer blend I compared to blend II, indicates a wider range of elastic behavior for blend I. This also was confirmed by the results from tensile tests (Figure 7.9 and Table 7.5).

G′ for VPBA2/IBOMA29/C13MA58/AN11 polymer was higher than G″ at lower frequencies ($\omega < 250$ Hz)(Figure 7.6 (b)), showing an elastic behavior at longer time scales. At $\omega_c = 250$ Hz, the relaxation of the polymer happened and the G″ dominated G′. A similar trend was observed for VPBA5/IBOMA22.5/C13MA62.5/AN10) polymer, where G′ > G″ was up to $\omega < 560$ Hz and the transition occurred at $\omega_c = 560$ Hz. According to Figure 7.6 (c), G″ was constantly higher than G′ for GMMA15/IBOMA25/C13MA50/AN10. This demonstrates the viscous liquid behavior at frequency range of 0.1 to 1000 Hz.
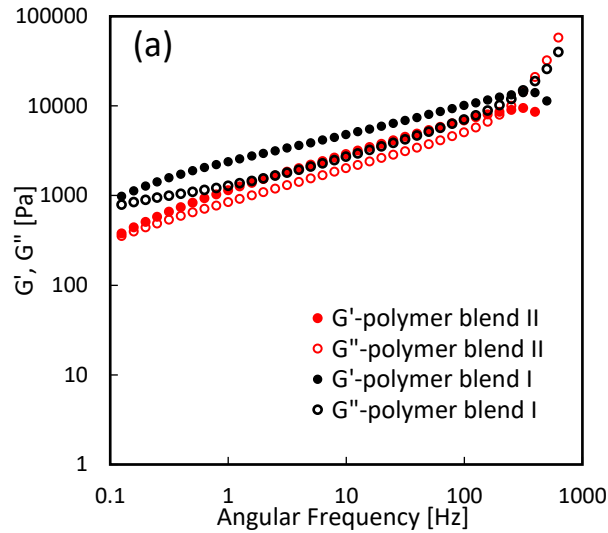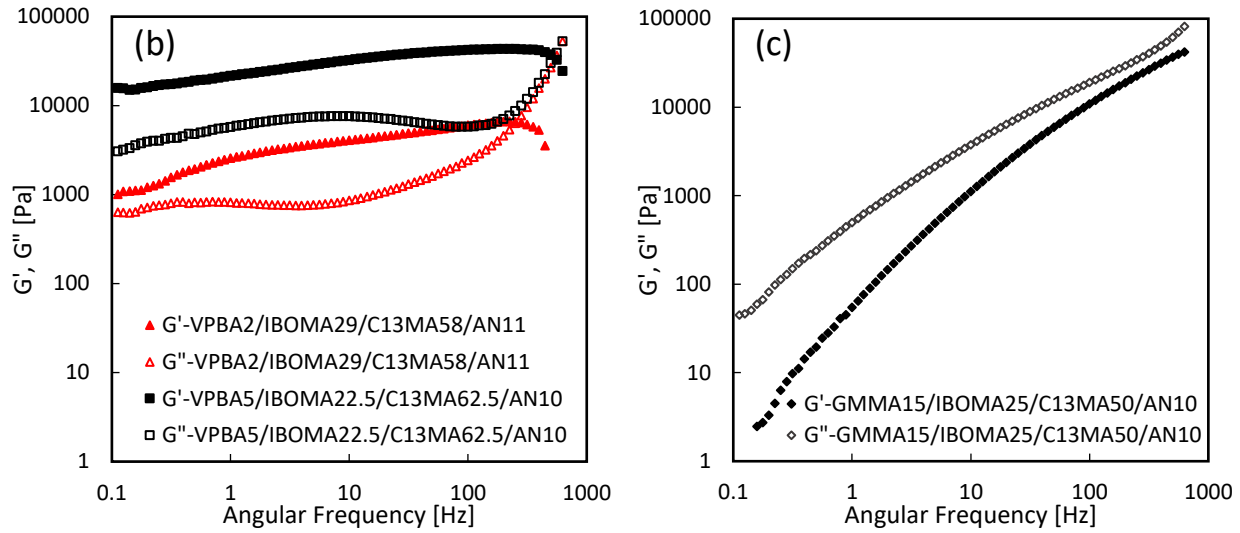
Figure 7.6. Storage (G′) and loss (G″) moduli versus angular frequency (1% strain applied) for polymers and blends at 100 °C. a) polymer blends; b) VPBA containing polymers; c) GMMA containing polymer (GMMA 15 mol%, $M_{n,target} = 50$ kg mol^{-1}).

7.3.4.2. Stress Relaxation

Stress relaxation experiments were carried out on blend I and II samples. As shown in Figure 7.7 (a) and (b), a complete stress relaxation was observed for polymer blend I and II at comparatively low temperature range of 25 to 50 °C. This is in accordance with viscoelastic fluid behavior, suggesting efficient dynamic cross-linking for blends without the formation of any nonexchangeable cross-linking bonds within the structure during stress relaxation experiments, reprocessing or curing of the samples. The relaxation time (τ^*) was almost identical for polymer blend I and II at 25 °C ($\tau^* = 9.5$ and 9.7 for blend I and II, respectively). By increasing the temperature to 50 °C, τ^* decreases to $\tau^* = 1.6$ s for blend I and $\tau^* = 2.8$ s for blend II. The decrease in τ^* escalated with the increase in temperature for blend I, resulted in a higher apparent activation energy (E_a) (Figure 7.7 (c)). E_a was estimated by Arrhenius equation[455]:

$$ln\,(\tau^*) = ln(\tau_0) + \frac{E_a}{RT} \tag{7.3}$$

where τ^* (s) represents the characteristic relaxation time at $G/G_0 = 1/e$, τ_0 (s) is τ^* at infinite temperature, E_a (J mol^{-1}) is the activation energy, R is the universal gas constant (8.314 J mol^{-1} .K^{-1}) and T is the temperature (K). The E_a for polymer blend I and II was equal to 58 and 38 kJ mol^{-1}, respectively. The calculated E_as for polymer blend I and II are comparable with the results from similar blends containing boronic ester bonds with E_a of 36 to 52 kJ mol^{-1} [151].

The lower relaxation time for blend I compared to blend II is due to the lower cross-linking density and relatively faster deformation rate. The reduced relaxation times for blend I and II were expected as it was previously shown that increasing the free diol content can lower the relaxation time for polymers under a constant shear stress[415]. This was ascribed to the higher occurrence of crosslink exchange in materials with boronic-ester bonds. In this study, the excess concentration of GMMA-containing polymers was added to the blends to increase the availability of diol groups in the blends and improve self-healing (Table 7.4).
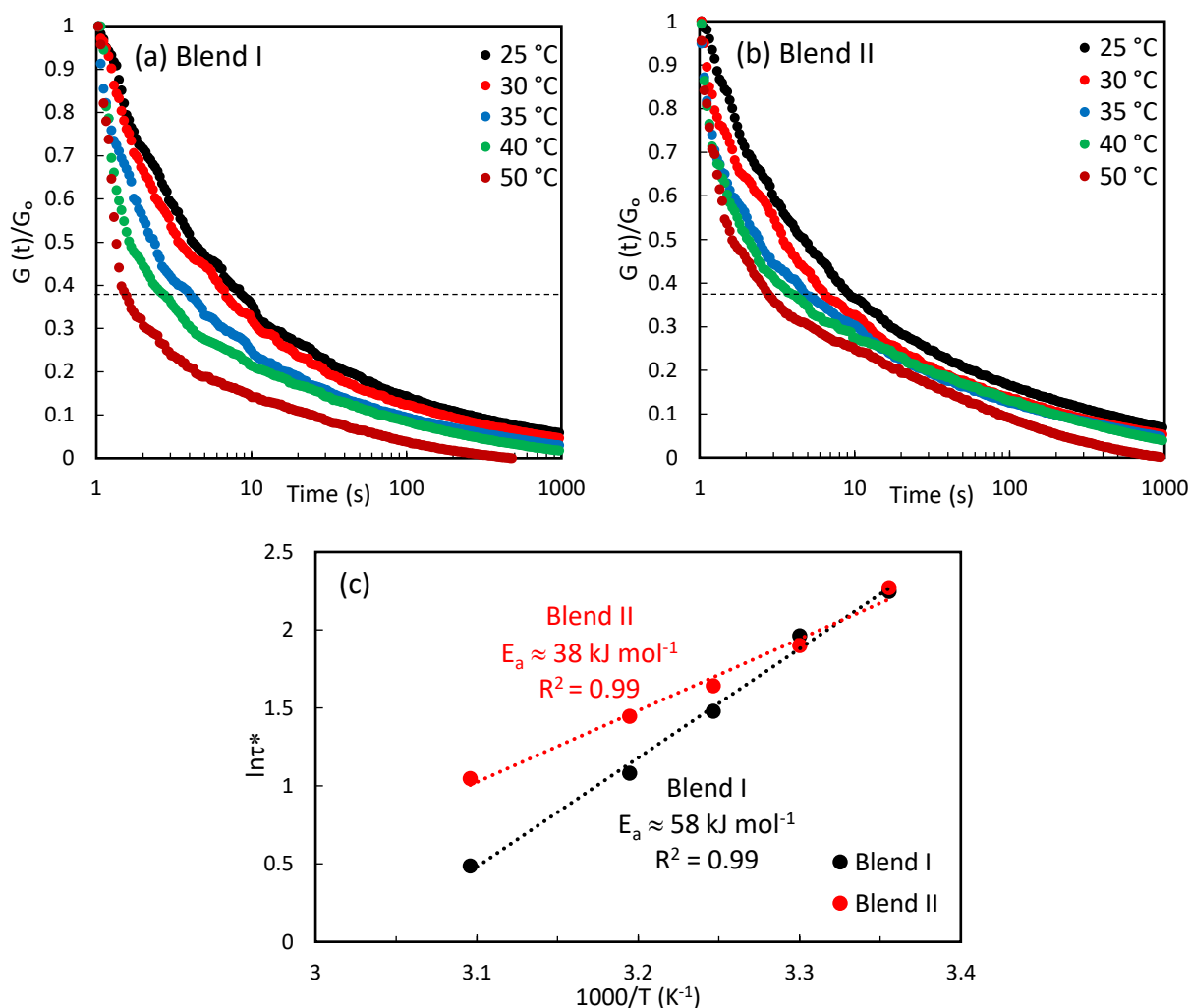
Figure 7.7. Normalized stress–relaxation curves for a) polymer blend I and b) polymer blend II at different temperatures (25-50 °C).

7.3.4.3. Swelling Test

To study the formation of cross-linking between polymer chains, the various polymer blends were immersed in toluene for 24 hours. The blends were partially soluble in toluene and a gel-like material resulted. After complete drying of the samples, the gel fractions (insoluble part of polymer blends) of

polymer blends I, II and III were 46.0, 62.7 and 66.2%, respectively. Next, a swelling test was done on blends I, II and III using toluene as the solvent. All the polymers were completely soluble in toluene before mixing together. Once the VPBA and GMMA-containing polymers were mixed, the blend with the cross-linking bonds formed, resulting in a polymer network formation. Interestingly, samples absorbed toluene up to 3.5 times of their weight and formed a gel in toluene in less than 200 minutes. The measurement was ended once the increase in the weight change stopped. A higher increase in the weight change was observed for blends with higher cross-linking density (blend II and III) compared to polymer blend I. This was due to low cross-linking density and probably the faster dissolution of the soluble part of blend I. Figure 7.8 illustrates the weight change of samples as a function of time (before dissolving in toluene).
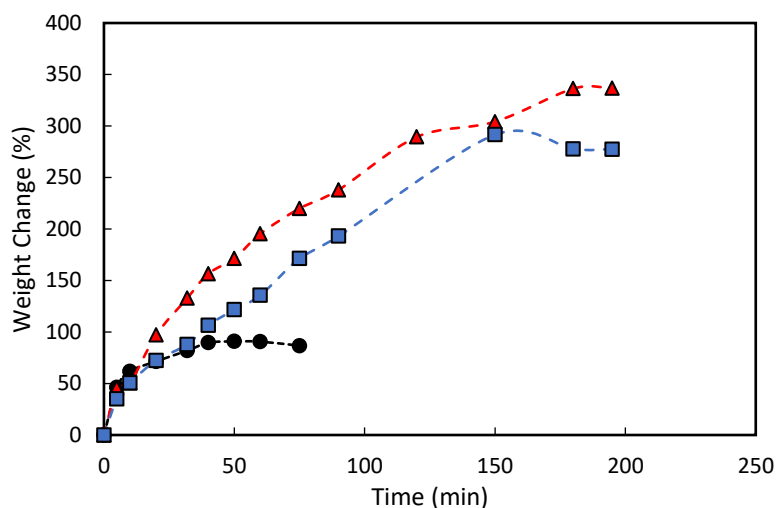
Figure 7.8. Toluene absorption of different polymer blend samples with boronic ester cross-linked network as a function of time. The samples were completely immersed in toluene. Polymer blend I (black circles, ●); polymer blend II (red triangles, ▲); polymer blend III (blue squares, ■). Polymer blend compositions are available in Table 7.4.

7.3.4.4. Tensile Results for Polymer Blends I and II Before and After Healing

Next, the self-healing of the polymer blends was characterized using tensile tests on blends I and II. First, the tensile test was conducted on uncut dumbbell shaped samples (black lines in Figure 7.9). Next, cut individual samples after the tensile test were re-connected. From these tests, the polymer blend I has a lower tensile strength compared to blend II (tensile strength at break of blend I = 0.62 MPa compared to 0.94 MPa for blend II) and the elongation at break was slightly higher for blend I (elongation at break for blend I = 112.0±19.1% and for blend II = 95.5 ±10.3 %). Note that blends I and II differ in that blend II had higher concentration of VPBA compared to blend I. The cut samples after the tensile test were attached together and healed for 3 days at 19.4-20.6 °C and relative humidity of 63.6-66.6% (Figure 7.9 (a) and (b) red

126

curves). The same test was also done by immersing the junction of two attached pieces in water for the duration of the test at the same temperature and humidity (blue curves in Figure 7.9 (a) and (b)). The results illustrated that covering the junction of two polymer pieces with water does not change the strength of the connection significantly. Figure 7.9 (c) and (d) demonstrate the results for healed samples after 10 days and 2 cycles compared to the original uncut samples. Movie S1 and S2 (Supporting Information) shows the tensile test on blend I and II samples after 10 days of healing. This test was done to check the self-healing ability of polymer blend samples after 2 cycles of damage and repair at the same place of the cut. Furthermore, it was shown that increasing the healing time from 3 days to 10 days enhances the repair only slightly. In the second cycle of healing after 10 days, the blend I and II samples lost their toughness (area under stress-strain curve) significantly. This was expected as the 2nd cycle was done on the samples, recovered 33% of their toughness in their first cycle and the cut was not fully healed. In addition, the deformation of tensile bars after 2 rounds of stretching during tensile tests and slower diffusion and connection of the chains together can cause the loss of toughness in the 2nd healing cycle and longer healing time. However, it should be noted that increasing the temperature can effectively improve the toughness of healed samples and reduce the healing time (check the Recyclability of Polymer Blends section). Table 7.5 summarizes the tensile results.
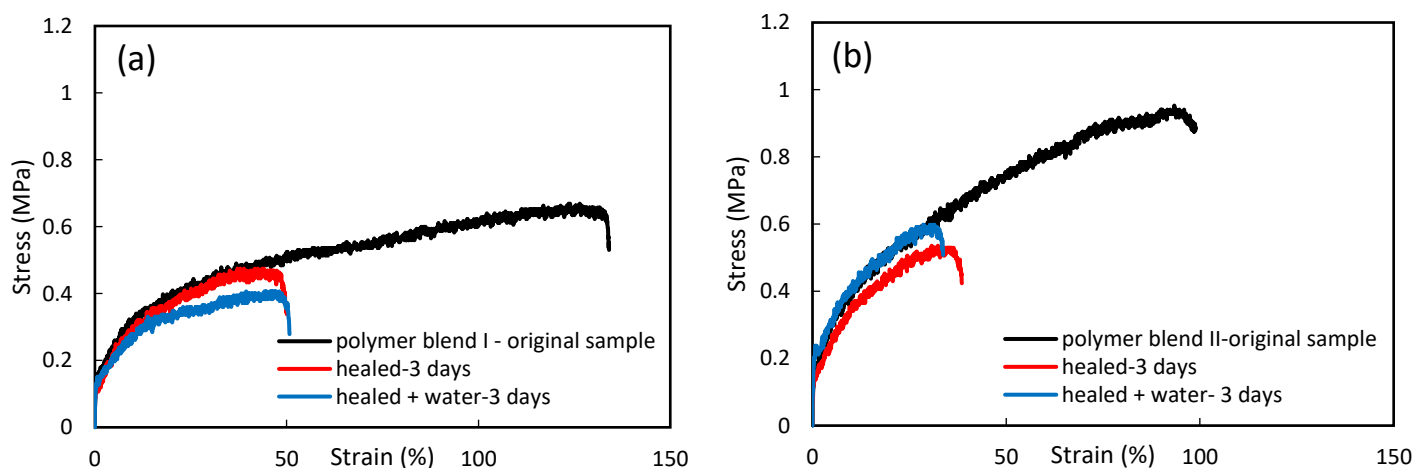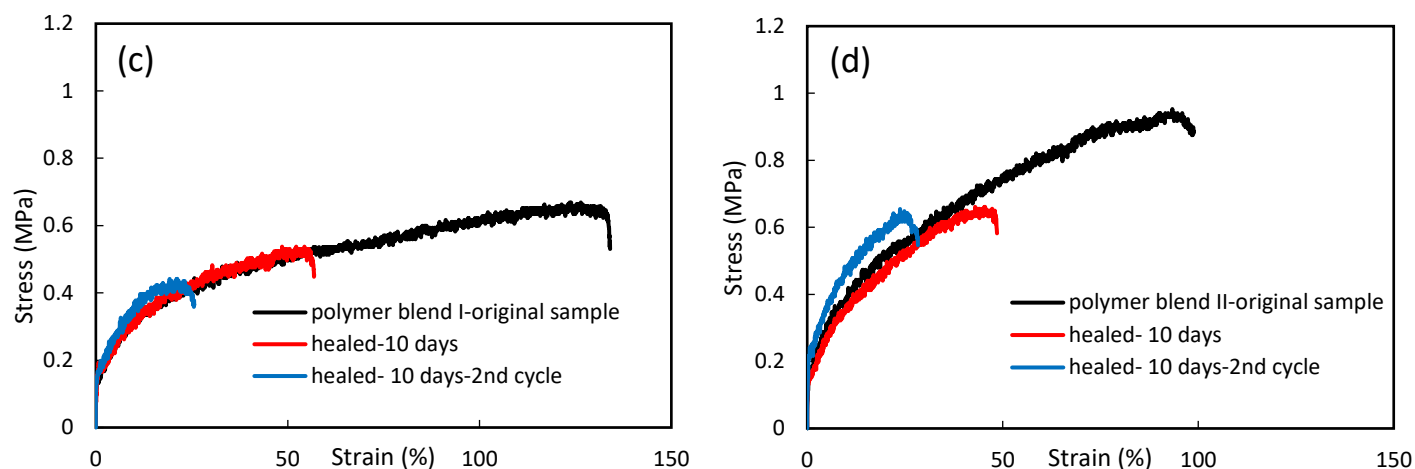
Figure 7.9. Tensile stress-strain curves for polymer blends I and II showing the effect of boronic acid/diol concentration. Tensile results for original polymer blend samples blend I and II (black lines, —). a) and b) healed after 3 days (red lines, —); healed after 3 days with presence of water (blue lines, —). c) and d) healed after 10 days (red lines, —); healed after 10 days-2nd cycle (blue lines, —). All the samples were at ambient temperature and relative humidity (19.4-20.6 °C and relative humidity of 63.6-66.6%) without applying extra heat or humidity.

Table 7.5. Summary of tensile properties of samples after each experiment.

Sample ID	Young's Modulus (MPa)	Stress at break (MPa)	Strain at break (%)	Toughness [a] (MJ m⁻³)
Polymer blend I				
Original sample	1.8±0.3	0.62±0.08	112.0±19.1	0.68
Healed-3days	1.8±0.2	0.42±0.07	48.5±6.6	0.19
Healed+Water-3days	1.6±0.2	0.41±0.08	50.2±9.3	0.17
Healed-10days	2.1±0.3	0.54±0.06	53.5±4.2	0.23
Healed-10days-2nd cycle	2.8±0.4	0.41±0.04	21.0±7.1	0.09
Polymer blend II				
Original sample	2.7±0.4	0.94±0.05	95.5±10.3	0.69
Healed-3days	2.4±0.2	0.51±0.03	31.3±10.1	0.15
Healed+Water-3days	3.1±0.86	0.66±0.08	27.9±7.9	0.15
Healed-10days	2.6±0.3	0.56±0.07	48.2±5.1	0.23
Healed-10days-2nd cycle	3.8±0.5	0.64±0.02	24.1±6.0	0.14

[a] Toughness was calculated from the area under the stress-strain curves shown in Figure 7.9.

7.3.4.5. Scratch Test

The self-healing properties of the polymer blends were investigated by applying a scratch using a blade on one head of the dumbbell shaped tensile bar samples prepared from polymer blends of I, II, III and IV. The samples were left at ambient conditions (T= 19.1-23.9 °C, relative humidity of 38-58%) without applying environmental, mechanical or chemical stresses. As shown in Figure 7.10, increasing the T_g of the resins and VPBA content (corresponding to the boronic-ester bonds) of polymer blends decreased the rate of self-healing. The polymer blend I showed the fastest scratch healing compared to the other samples and the scratch was fully removed after 12 days. The polymer blend IV showed the comparatively slowest scratch self-healing during the observation time due to its higher stiffness, although the VPBA content in the formulation was the highest. This observation regarding blend IV reflects the balance between T_g and the cross-link density when designing a self-healing system.

ID	VPBA-containing polymer		GMMA-containing polymer	
	F_{VPBA}	T_g (°C)	F_{GMMA}	T_g (°C)
Polymer blend I	1.9	4.9	10.2	-0.4
Polymer blend II	8.5	-13.2	10.2	-0.4
Polymer blend III	12.1	-1.4	10.2	-0.4
Polymer blend IV	23.7	6.5	10.2	-0.4

After applying the scratch   After 8 days   After 12 days

129
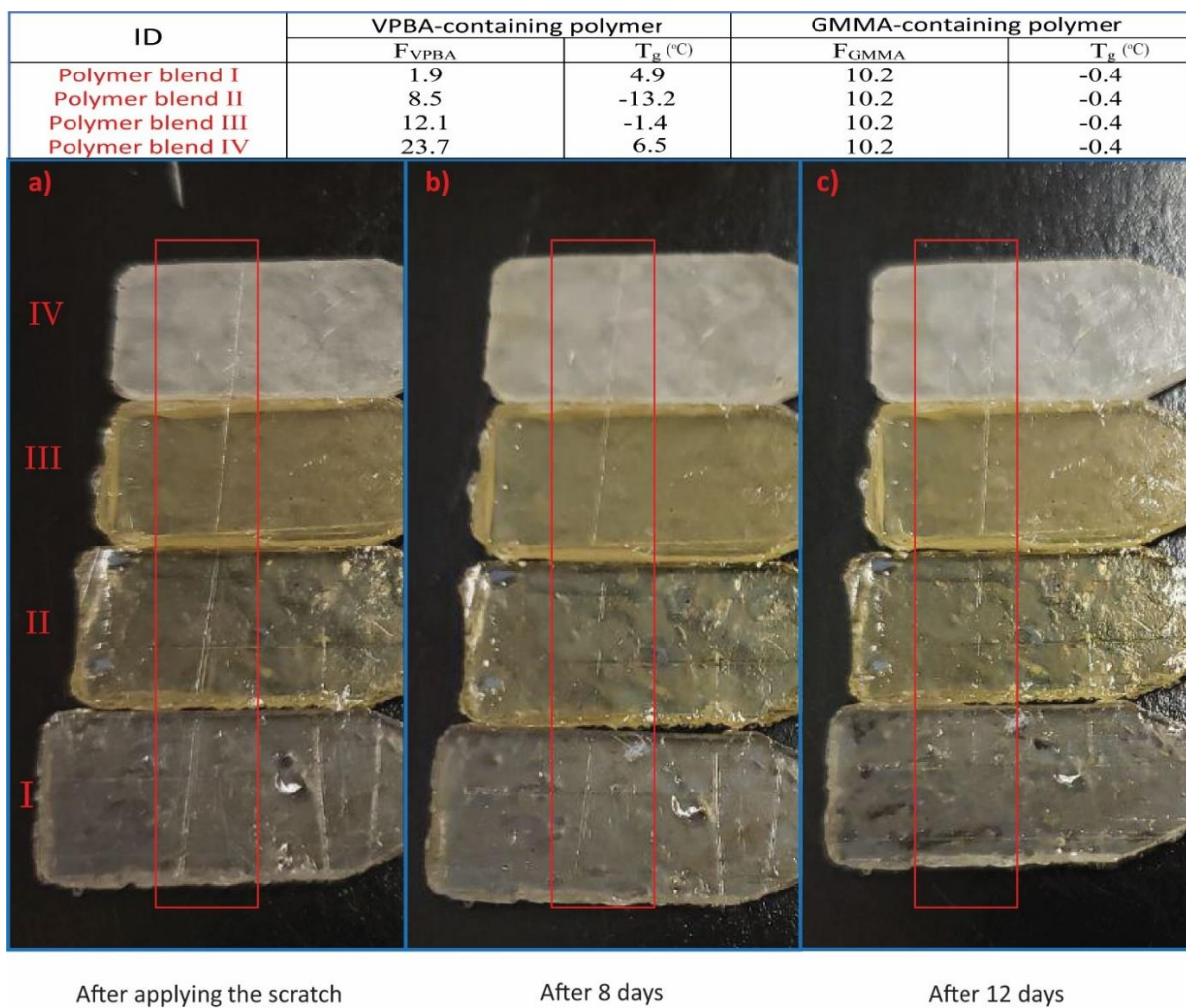
Figure 7.10. Scratch test on polymer blend I, II, III and IV samples: a) a scratch was applied on the surface of the samples; b) after 8 days c) after 12 days at room conditions (T= 19.1-23.9 °C, relative humidity of 38-58%).

7.3.4.6. Recyclability of Polymer Blends

Recyclability of polymer blends I and II was examined by applying the same hot press procedure used for the preparation of polymer blends (three cycles of hot pressing). The three-cycle hot press process prevented the formation of air bubbles in tensile bars. However, it is not necessary for reprocessing the blends for other applications. The polymer blends were ground and reprocessed in a hot press at 80 °C for 47 minutes (3 cycles: 6-8 metric tons for 12 minutes; 13 metric tons for 15 minutes and 20 minutes). For each polymer blend, three recycling processes were performed, and the tensile results presented in Figure 7.11. Based on the results presented in Figure 7.11 (a) and (b) and Table 7.6, the stress at break for samples increased after reprocessing. This suggests an improvement in blending that enhanced the possibility of boronic ester cross-linking. The toughness of polymer blend II is higher than blend I as it contains higher cross-linking density (based on the respective concentrations of boronic acid to diol in each of the respective resins), although the T_g of VPBA-based polymer resin is lower in blend II. Furthermore, the tensile stress-strain curves (Figure 7.11) illustrates that the polymer blends are highly re-processable due to the dynamic boronic-ester cross-linking and can be easily reprocessed at 80 °C in relatively short time (47 minutes).
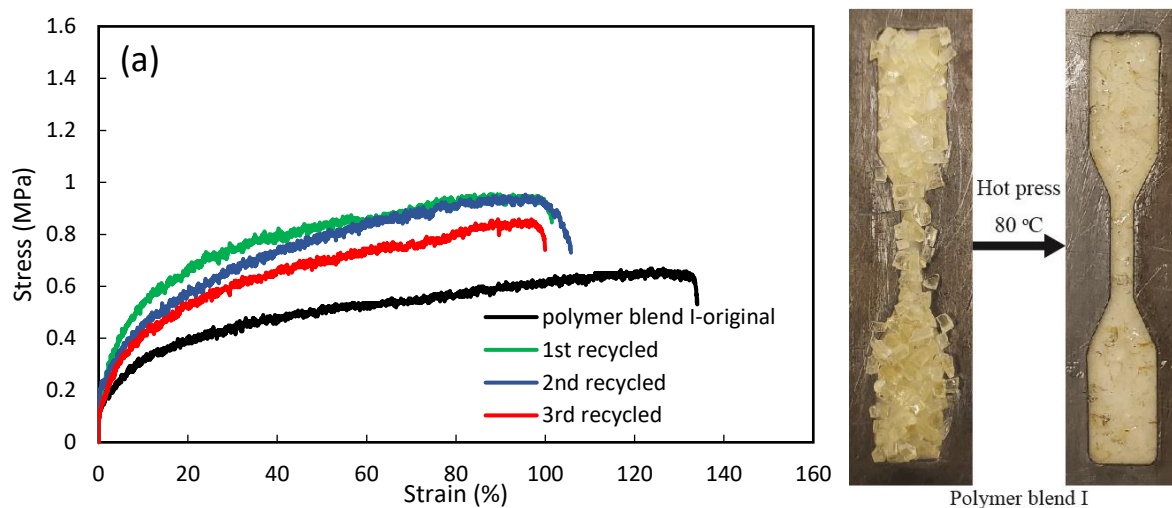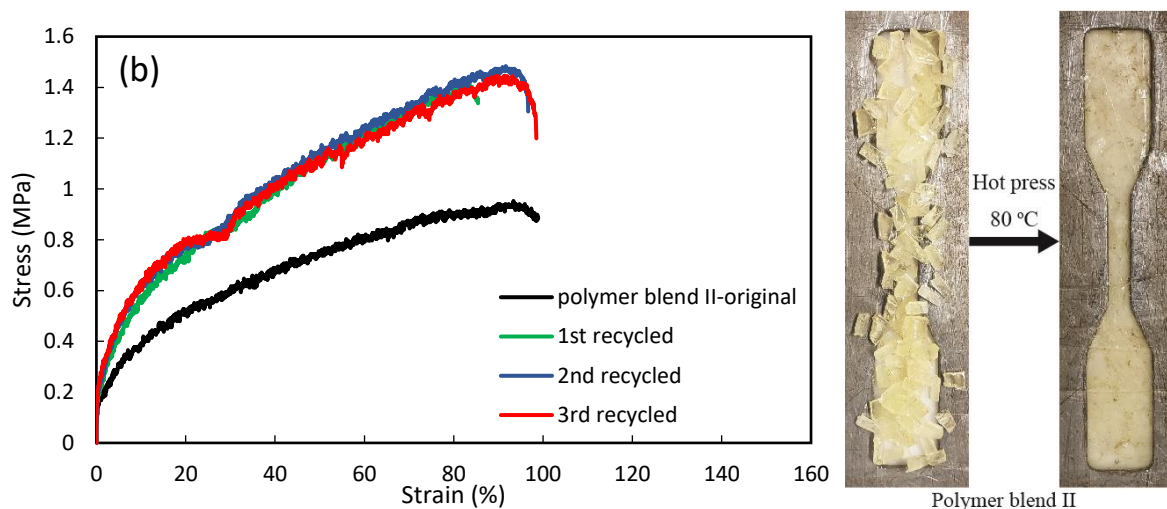
Figure 7.11. Tensile stress-strain curves for polymer blends I and II after 3 recycling cycles: a) reprocessing of polymer blend I; b) reprocessing of polymer blend II. Original samples before recycling (black lines, —); first recycle (green lines, —); second recycle (blue lines, —); third recycle (red lines, —).

Table 7.6. Tensile results for polymer blend I and II after recycling at 80 °C.

Sample ID	Young's Modulus (MPa)	Stress at break (MPa)	Strain at break (%)	Toughness [a] (MJ m^{-3})
Polymer blend I				
Original sample	1.8±0.3	0.62±0.08	112.0±19.1	0.68
After 1st recycling	3.6±0.2	1.03±0.08	98.8±26.8	0.79
After 2nd recycling	3.3±0.7	0.98±0.03	94.4±23.7	0.78
After 3rd recycling	3.0±0.2	0.89±0.09	102.6±11.9	0.65
Polymer blend II				
Original sample	2.7±0.4	0.94±0.05	95.5±10.3	0.69
After 1st recycling	3.91±0.2	1.30±0.11	79.2±5.4	0.83
After 2nd recycling	3.88±0.5	1.24±0.21	75.7±19.4	1.02
After 3rd recycling	4.03±0.4	1.25±0.19	99.6±2.3	1.03

[a] Toughness was calculated from the area under the stress-strain curves shown in Figure 7.11.

Figure 7.12 shows the DMA results for blend I and II original samples and the same blend samples after three reprocessing cycles. The storage modulus reached a plateau for all the samples at temperatures above T_g. This confirms the existence of cross-linking bonds within the polymer structure for samples before and after recycling. The similar storage moduli at the rubbery plateau confirms the full recovery of cross-linking density after reprocessing. At 85 °C, the storage modulus of samples approaches a limiting value near 0 MPa, suggesting a similar behavior before and after recycling.
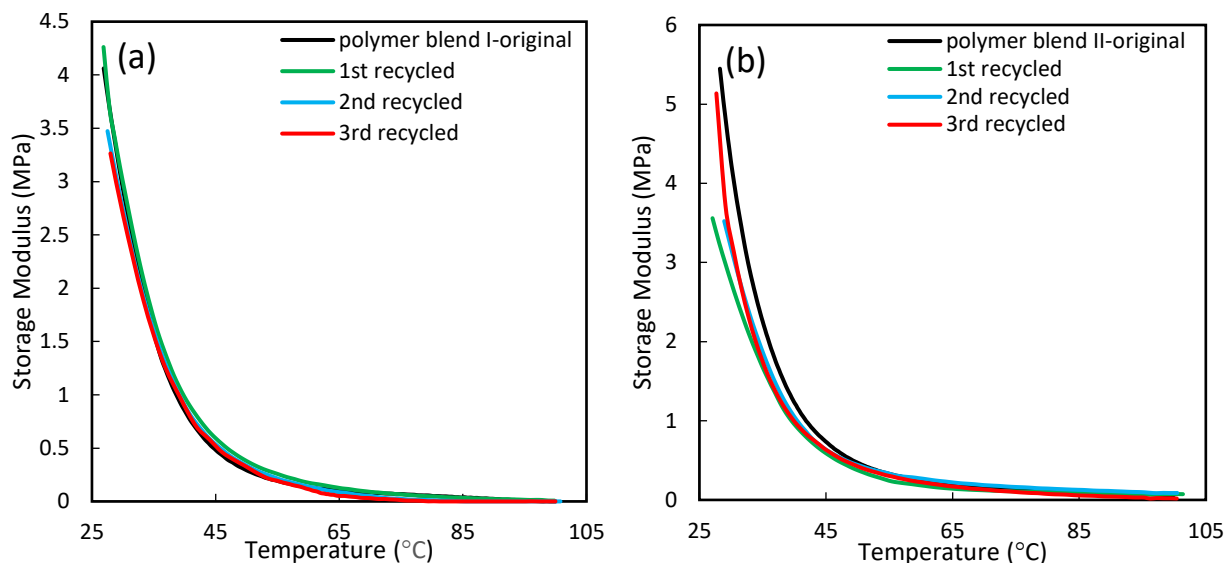
Figure 7.12. Dynamic mechanical responses for rubbery plateau moduli of the a) polymer blend I and three reprocessing cycles b) polymer blend II and three reprocessing cycles. Original samples before recycling (black lines, —); first recycle (green lines, —); second recycle (blue lines, —); third recycle (red lines, —).

7.3.4.7. De-cross-linking of Polymer Blends

To study the possibility of de-cross-linking, two samples for each polymer blend (I and II) were immersed in 1,4-dioxane. For one of the samples pinacol was added and the second sample was dissolved in 1,4-dioxane without the addition of pinacol to compare the results and observe the effect of pinacol on the solubility of polymer blends. The samples were kept at 50 °C for 4 hours. The detailed procedure of de-cross-linking of samples is available in the Methods section. As indicated in Figure 7.13, the samples were completely dissolved in the presence of pinacol, while the samples in dioxane could not. This is due to the esterification reaction between VPBA monomers and pinacol, which de-cross-links the dynamic cross-linking bonds between VPBA and GMA monomers.

For comparison, the vials containing the polymer blends I and II in 1,4-dioxane (without pinacol) were kept at 50 °C for 24 hours to measure the ultimate soluble fraction of polymer blends. Respectively, 47.77 wt% and 50.81 wt% of the polymer blends I and II were remained insoluble. This demonstrates the necessity of the addition of pinacol for the complete removal of the cross-linking bonds. To confirm the de-cross-linking of blends, samples were precipitated in methanol and GPC traces and ^{1}H NMR spectra were provided (Figure 7.S1 and 7.S2, Supporting Information).
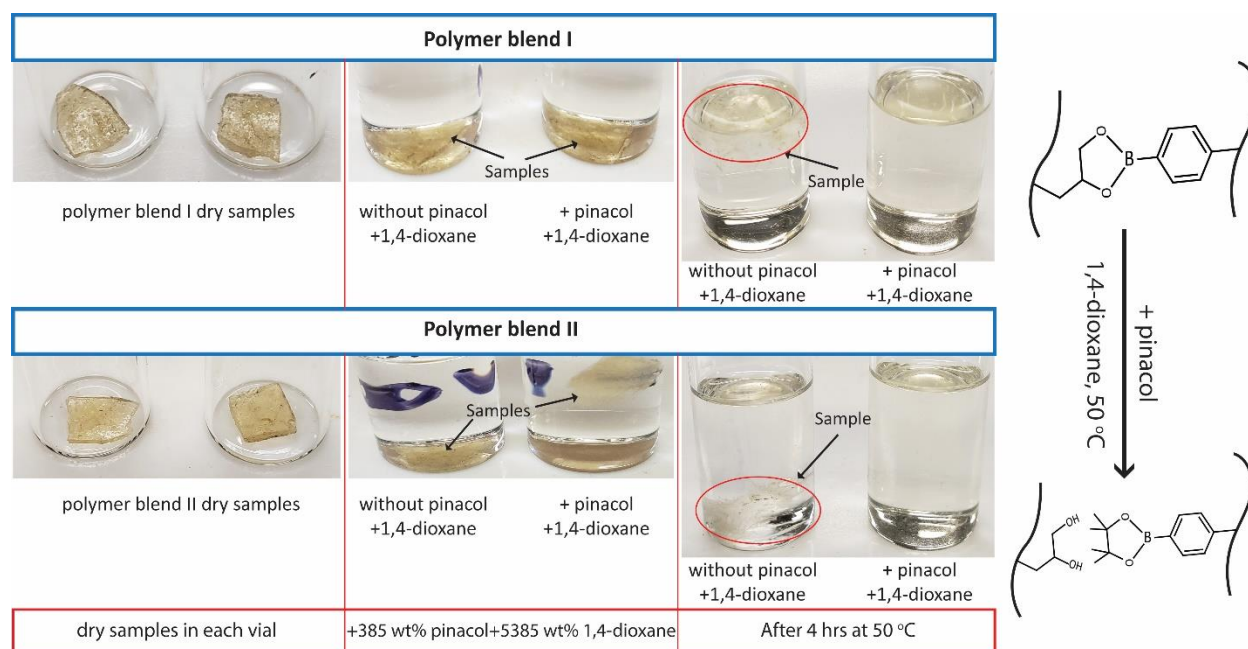
Figure 7.13. Chemical recycling of polymer blends I and II using pinacol at 50 °C in 1,4-dioxane. The whole process takes place within 4 hours. The solubilities were compared with the samples in 1,4-dioxane without adding pinacol.

7.3.4.8. Thermal Stability of Polymers and Blends

Thermal stability of the polymers and blends was investigated by TGA to determine T_{dec}s of samples (Table 7.7) and thus provide an estimate of the highest temperature range that the polymers and blends can be used or reprocessed. The decomposition temperature for 10% weight loss ($T_{dec,1}$) of polymer blends was higher for polymer blends I, II, III, IV and VII compared to each polymeric component before mixing, although this was not the case for polymer blends V and VI. This is probably due to low GMMA content in blends V and VI, which limits the chance of formation of dynamic boronic ester bonds within the structure. This confirms the effect of dynamic cross-linking on enhancing the $T_{dec,1}$ and determines the importance of higher GMMA:VPBA ratio in polymer blends for having effective cross-linking formation between the chains. For polymer blends, no significant change in $T_{dec,max}$ or $T_{dec,2}$ was detected, suggesting the almost complete dissociation of boronate ester bonds at higher temperatures (T ≈ 400 °C).

By comparing the results from our previous studies on T_{dec} of IBOMA/C13MA polymers prepared in emulsion and solution, it can be concluded that the addition of VPBA and GMMA to all the polymer formulations improved the $T_{dec,max}$ of polymer resins significantly (by up to 158 °C)[162, 182]. However, the $T_{dec,1}$ and $T_{dec,2}$ of polymers remained approximately constant. The higher degradation temperature at around 400 °C was previously observed for GMMA copolymers and polymers containing OH groups[444, 445,

[456, 457]. This was ascribed as the dehydration and cyclization side reactions and the formation of anhydrates and carboxylic groups, which occurs at the same time with depolymerization[444, 445].

Table 7.7. Thermal characterization of polymers and polymer blends.

Experiment ID	$T_{dec,1}$ [a] (°C)	$T_{dec,max}$ [a] (°C)	$T_{dec,2}$ [a] (°C)
VPBA5/IBOMA 42.5/C13MA42.5/AN10	219	426	478
VPBA10/IBOMA40/C13MA40/AN10	179	436	483
VPBA15/IBOMA37.5/C13MA37.5/AN10	229	436	486
VPBA2/IBOMA29/C13MA58/AN11	222	415	479
VPBA5/IBOMA22.5/C13MA62.5/AN10	238	413	480
VPBA10/IBOMA20/C13MA60/AN10	192	399	461
VPBA15/IBOMA25/C13MA50/AN10	198	421	486
GMMA5/IBOMA42.5/C13MA42.5/AN10	234	303	486
GMMA10/IBOMA40/C13MA40/AN10	221	425	477
GMMA15/IBOMA37.5/C13MA37.5/AN10	233	424	485
GMMA15/IBOMA25/C13MA50/AN10	239	306	472
Polymer blend ID			
I	255	419	475
II	259	421	495
III	258	407	476
IV	280	427	500
V	220	316	489
VI	217	301	490
VII	243	430	482

[a] $T_{dec,1}$ ($T_{10\%}$ or onset of decomposition), $T_{dec,max}$ (temperature at which highest weight loss occurs) and $T_{dec,2}$ (end of decomposition) measured by TGA under nitrogen atmosphere at a ramp rate of 15 °C min^{-1}. The blend compositions are available in Table 7.4.

7.4. CONCLUSIONS

The nitroxide mediated polymerization of a base mixture consisting of IBOMA/C13MA/AN with a low concentration of VPBA or GMMA (2 to 15 mol% in the initial monomer mixture) was conducted in 1,4-dioxane (50 wt%) using NMP at 90 °C. VPBA-containing polymers with M_n up to 35.1 kg mol^{-1} and monomer conversion up to 78% ($1.65 < Đ < 2.13$) and GMMA-containing polymers with maximum M_n of 26.3 kg mol^{-1} and relatively higher conversions (X up to 90% with $1.67 < Đ < 2.73$) were synthesized. By mixing polymer resins with respective concentrations of VPBA and GMMA in each copolymer, various polymer blends with self-healing properties at ambient temperature and humidity were produced. Successful formation of dynamic covalent bonds of boronate ester within the polymer structure was proven

by FTIR and confirmed by tensile, swelling and scratch tests on the polymer blends. Polymer blends I and II (VPBA2/IBOMA29/C13MA58/AN11 or VPBA5/IBOMA22.5/C13MA62.5/AN10 with GMMA15/IBOMA25/C13MA50/AN10 [1:2.5] weight ratio) exhibited the fastest self-healing and recovered scratches after 12 days at ambient temperature and humidity. Tensile results for polymer blends I and II before and after cutting show high self-healing after 10 days (87% tensile strength and 48% strain recovery for polymer blend I and 60% tensile strength and 50% strain recovery for polymer blend II). The polymer blend samples also demonstrated the ability to absorb solvent (toluene) up to 337% of their original weight in a relatively short time (200 min). As the blend hardness increases, the self-healing properties of material decreases as the effective bonds between VPBA and GMMA cannot be formed and may require a longer time for complete self-healing. The polymer blends demonstrated a high recyclability with a comparatively easy reprocessing procedure (47 minutes in hot press at 80 °C), which improves the applicability of these partially bio-based polymer blends with self-healing properties.

ACKNOWLEDGMENTS

Preamble to Chapter 8

In chapter 7, self-healing polymer blends with high bio-content were synthesized in 1,4-dioxane. This chapter investigates the possibility of making self-healing polymers in miniemulsion by complete removal of organic solvents. To reduce the solubility of GMMA and VPBA in water, a dimer of these two monomers was produced before the polymerization. The (VPBA+GMMA) dimer was dissolved in the mixture of IBOMA/C13MA monomers and the monomer phase was dispersed in water. The miniemulsion polymerization of monomers with different ratios of (VPBA+GMMA) dimer was performed in presence of Dispolreg 007 alkoxyamine at 90 °C. The final polymer latexes were dried at room temperature to form a polymer film with self-healing properties. The polymerization kinetics, thermal, rheological and mechanical properties of polymers were studied. Based on the results, the polymers had high recyclability (3 reprocessing cycles at 80 °C for 45 minutes) and showed swelling ratio up to 153% in presence of toluene.

Chapter 8: Recyclable Polymers with Boronic-Ester Dynamic Bonds Prepared by Miniemulsion Polymerization

ABSTRACT

Polymers with boronic ester dynamic covalent bonds were synthesized by nitroxide-mediated miniemulsion polymerization of isobornyl methacrylate (IBOMA, 71% bio-content), alkyl methacrylates (average aliphatic size of 13.0, C13MA, 76% bio-content), glycerol monomethacrylate (GMMA) and 4-vinylphenylboronic acid (VPBA). The miniemulsion polymerization of all monomers was enabled by the esterification reaction between GMMA and VPBA and the synthesis of (VPBA+GMMA) dimer prior to the polymerization. The formation of boronic ester dynamic covalent bonds was confirmed by rheological and mechanical measurements, indicating a higher stiffness by increasing the dimer content from 5 to 15% in the initial feed. Cross-linked polymers showed high reprocessing capability with comparatively simple recycling process (at 80 °C for 45 minutes) and the high organic solvent absorbance of polymers (swelling ratio up to 153%). Furthermore, it was shown that the addition of VPBA and GMMA significantly improved the heat resistance of polymers up to 121 °C, compared to the IBOMA/C13MA copolymers (without GMMA and VPBA functional monomers).

8.1. INTRODUCTION

Preparation of polymers containing boronic ester dynamic covalent bonds has been of interest due to their exceptional recyclability and self-healing properties[150, 384, 458]. These materials have been widely used for the preparation of hydrogels and related polymer resins for applications such as tissue engineering and drug delivery[152, 458-462], optical devices[463], solid polymer electrolytes (SPEs)[464] and coatings[465]. Different methods were utilized to produce polymers with boronic ester cross-linking bonds[150, 151, 403]. One of the most common methods is the synthesis of diol-functionalized polymer and boronic acid-containing polymers separately and mixing them together[160, 404]. The synthesis of each polymer resin or the mixing process generally involves using organic solvents, which intensifies the environmental and health concerns associated with the process[46, 251, 466]. Although using water as the dispersant phase in the system seems beneficial, the synthesis of materials containing boronic ester bonds in a water-based system has always been problematic due to relatively high water-solubility of monomers containing the boronic acid or diol functional groups[398, 467, 468]. Furthermore, the copolymerization of these monomers with water-insoluble monomers in water-based or emulsion systems usually results in uncontrolled formation of hydrogels with broad molecular

137

weight distribution and low monomer conversion[469, 470]. We prepared polymers containing boronic ester dynamic cross-linking bonds in an organic solvent (toluene) previously where we attempted to use commercially available monomers with high bio-content[471]. This was done presumably to decrease the carbon footprint of the process while still getting the desirable properties incorporated into the polymer. We attempted to take our process one step farther and eliminate the use of organic solvent in the synthesis of the recyclable polymers with boronic ester dynamic cross-links by adopting controlled radical polymerization in miniemulsion. To enhance the environmental sustainability of the polymers, 85-95 molar% of polymer resins were made of partially bio-based methacrylic monomers. Isobornyl methacrylate (IBOMA, 71% bio carbon content) derived from pine sap (camphene) has a high glass transition temperature (T_g) ($T_{g,P(IBOMA)} = 110{\sim}200$ °C)[201, 262, 263] and used to improve the T_g of polymers[472]. Alkyl methacrylates with average side-chain aliphatic size of 13.0 (termed here as C13MA, 76% bio carbon content, derived from natural oils) was incorporated into resins to decrease the T_g ($T_{g,P(C13MA)} = -46$ °C)[201, 202] and improve the flexibility of polymer chains[162, 181]. Using IBOMA and C13MA, polymers with tunable T_g can be produced to meet the criteria for a specific application[162, 180, 182, 473]. Nitroxide mediated polymerization (NMP) as one of the simplest reversible deactivation radical polymerization (RDRP) techniques was utilized to improve control over the polymerization (linear increase of average molecular weight (M_n) versus monomer conversion (X)), to reduce discoloration, to obtain tighter molecular weight distribution ($Đ$) leading to lower viscosities for application in coatings and to enhance chain-to-chain compositional homogeneity and the formation of well-defined microstructures[23, 47, 166, 218]. For the nitroxide, we used 3-(((2-cyanopropan-2-yl)oxy)-(cyclohexyl)amino)-2,2-dimethyl-3-phenylpropanenitrile (Dispolreg 007) alkoxyamine to initiate the miniemulsion polymerization of methacrylates, without any controlling co-monomer as was typically required for NMP, at temperatures below 100 °C[28, 43, 243, 278]. For miniemulsion, all that was needed besides the monomers and nitroxide was surfactant and long chain alkyl-containing co-stabilizers[57, 80, 250].

The incorporation of boronic ester bonds was more challenging; it required the esterification of glycerol monomethacrylate (GMMA, 2,3-dihydroxypropyl methacrylate) and 4-vinylphenylboronic acid (VPBA) as monomers incorporated into the respective polymer chains. Different methods have been applied for the RDRP of GMMA or VPBA (separately)[405, 423, 467, 474, 475]. Chen et al[468] prepared homopolymers of unprotected VPBA (PVPBA) (M_n up to 16.2 kg mol^{-1} and $Đ$ <1.21) by RAFT polymerization in DMF solvent. Jesson et al[419] synthesized homopolymers of GMMA (PGMMA) with relatively high M_n (M_n up to 159.5 kg mol^{-1} and $Đ$ <1.32) by RAFT emulsion polymerization of isopropylideneglycerol methacrylate with PGMMA-based macroinitiator followed by the subsequent removal of acetal protecting groups in acidic solution. However, we are unaware of reports concerning the successful controlled polymerization

for the preparation of boronic ester containing materials in miniemulsion. The VPBA-containing or GMMA-containing polymer latexes cannot be produced separately as the VPBA and GMMA are water-soluble and cannot be effectively available inside the monomer droplets during the miniemulsion polymerization[398, 467]. We report an approach using a pre-prepared dimer with the boronic acid/diol ester, which was subsequently added to the hydrophobic monomer mixture. After polymerization, the boronic ester can be de-activated, resulting in the respectively functionalized chains. Addition of water further allowed the esterification to be repeated, thus providing a moisture-controlled dynamic cross-linking process.

8.2. MATERIALS AND METHODS

8.2.1. Materials

Isobornyl methacrylate (IBOMA, >99%, VISOMER® Terra IBOMA) and C13 methacrylate (C13MA, C13,0 alkyl methacrylate, >99%, VISOMER® Terra C13,0-MA) were provided from Evonik. IBOMA and C13MA were purified by passing them through a column containing basic alumina (Brockmann, Sigma Aldrich) and calcium hydride (5 wt% of basic alumina, Alfa Aesar) to remove the MEHQ inhibitor. 4-Vinylphenylboronic acid (VPBA, ≥ 97%) was purchased from Oakwood Chemical. Glycerol monomethacrylate (GMMA, mixture of isomers, ≥ 95%) was purchased from Polysciences. DOWFAX™ 8390 (contains Disodium hexadecyldiphenyloxide disulfonate, disodium dihexadecyldiphenyloxide disulfonate, sodium sulfate, sodium chloride and water) was received from the Dow Chemical Company and used as the surfactant for emulsion polymerization. N-hexadecane (99%, Sigma Aldrich) was used as the co-stabilizer for emulsion system. 1,4-Dioxane (p-dioxane, ≥99%) was received from MilliporeSigma. HPLC grade Tetrahydrofuran (THF, 99.9%), methanol (MeOH, >99%), methylene chloride (DCM, ≥99.5 %) and toluene (>99%) were purchased from Fisher chemical. 3-(((2-Cyanopropan-2-yl) oxy) - (cyclohexyl) amino)-2, 2-dimethyl-3-phenylpropanenitrile (Dispolreg 007) alkoxyamine was synthesized in our lab based on the Ballard et al procedure[28]. Pinacol (98%) and molecular sieves (3 Å, pellets, 1.6 mm) were obtained from Sigma Aldrich. All the reactions, thermogravimetric analyses and rheological measurements were conducted under the high purity nitrogen (99.99%, Praxair).

8.2.2. Methods

The number average molecular weight (M_n) and dispersity ($Đ$) were measured by gel permeation chromatography (GPC, Waters Breeze). The instrument was equipped with 1 guard column and 3 Styragel® GPC columns (Waters) of HR1 (100 Å, M_n range of 100 to 5×10^3 g mol^{-1}), HR2 (500 Å, M_n range of 500 to 2×10^4 g mol^{-1}) and HR4 (10-4 Å, M_n range of 5×10^3 to 6×10^5 g mol^{-1}) and a differential

refractive index RI 2414 detector. The M_n of samples was determined relative to PMMA standards (calibration was done based on Varian polymer standards with the molecular weight ranges of 875 to 1677000 g mol^{-1}) in HPLC grade THF at 40 °C.

The monomer conversions (X) was estimated using the area under the GPC peaks for monomers and polymer chains divided by the respective refractive index increments (dn/dc)[333]. This was permissible as the peaks were well separated and the monomers were sufficiently high in molecular weight to be distinct from solvent peaks. The dn/dc value for poly(IBOMA) in THF is 0.108 ml g^{-1} [476]. The dn/dc value for C13MA (monomer and homopolymer) is not available in literature. However, the dn/dc of C13MA and its polymer can be reasonably estimated from the dn/dc of similar alkyl methacrylates. The dn/dc for poly(octadecyl methacrylate) (C18MA) and poly(n-decyl methacrylate) (C10MA) in THF were 0.075 and 0.076 ml g^{-1}, respectively[334, 336]. The dn/dc for heptadecanyl methacrylate (C17MA) in THF at 35 °C is 0.078 ml g^{-1} [296]. Previously, it was shown that the dn/dc of copolymers can be expressed from the following equation[477, 478]:

$$\left(\frac{\mathrm{d}n}{\mathrm{d}c}\right) = w_i \left(\frac{\mathrm{d}n}{\mathrm{d}c}\right)_i + w_j \left(\frac{\mathrm{d}n}{\mathrm{d}c}\right)_j \tag{8.1}$$

where w_i and w_j are the wight fractions of monomers (i and j) in polymer resins and $\left(\frac{\mathrm{d}n}{\mathrm{d}c}\right)_i$ and $\left(\frac{\mathrm{d}n}{\mathrm{d}c}\right)_j$ are the refractive index increments for i and j homopolymers, respectively. Here, we assumed that the synthesized polymer resins are essentially the copolymers of IBOMA and C13MA (i is IBOMA and j is C13MA) and $\left(\frac{\mathrm{d}n}{\mathrm{d}c}\right)_{C13MA} \approx \left(\frac{\mathrm{d}n}{\mathrm{d}c}\right)_{C10MA} = 0.076$ ml g^{-1}. Based on equation (8.1), the $\left(\frac{\mathrm{d}n}{\mathrm{d}c}\right)$ for Dimer 5% to 15% was calculated as 0.084-0.085 ml g^{-1}. Due to the similar dn/dc values for these systems, we assumed an equal dn/dc value for GPC peaks to estimate the monomer conversion.

8.2.2.1. FT-IR Spectrometry

The FTIR spectra were recorded in the range of 400-4000 cm^{-1} by a PerkinElmer Spectrum 2 with a single-bounce diamond and attenuated total reflectance (ATR) accessory.

8.2.2.2. Solid-State NMR

Solid-state ^{11}B and ^{13}C NMR spectra were obtained with a VNMRS 400 widebore NMR spectrometer operating at 100.5 MHz in a 4 mm Varian Chemagnetics double-resonance probe. The spectrums were acquired using multiple cross polarization (multiCP)[479] in 2048 scans and a 4 s recycle delay with 10 CP periods each of 1 ms, with 0.5 s between them, during spinning at 8 kHz. The multiCP spectrum of Dimer 15% was compared with a pulse-acquire spectrum using a recycle delay of 60 s and 2048 scans to verify

that the spectra were quantitative. The ^{13}C spectra are referencing using glycine at 176.4 ppm wrt TMS and borax was used as the standard for the solid-state ^{11}B NMR setup.

8.2.2.3. Differential Scanning Calorimetry

DSC was carried out on the samples using a TA Instruments DSC Q2000. The (heat/cool/heat) method with heating rate of 20 °C min^{-1} was performed on samples in the temperature range of -90 to 120 °C under nitrogen. The T_ms were measured in the second heating cycle by inflection method.

8.2.2.4. Thermogravimetric Analysis

Decomposition temperatures (T_{dec}s) of polymer samples were measured by thermogravimetric analysis (TGA, TGA Q500TM, TA Instruments) under the nitrogen (99.99%) at ramp rate of 15 °C min^{-1} from 25 to 550 °C in aluminum pans.

8.2.2.5. Tensile Tests

Tensile tests were performed on an EZ-test-500N Shimadzu tensile tester at room temperature and ambient relative humidity (T= 19.1-23.9 °C, relative humidity of 38-58%). To check the temperature and relative humidity during the test, Fisherbrand™ Traceable™ digital humidity and temperature meter (Fisher Scientific, temperature range of -10 to 60 °C and accuracy of ±1 °C; relative humidity range of 20 to 95% with the accuracy of ±3% for mid-range and ±5% elsewhere) was used. All dog-bone shaped samples were prepared in a hot press (Carver Manual Hydraulic Press with Watlow Temperature Controllers, Carver Inc., Wabash, IN, USA) at 80 °C. Three cycles of hot pressing were performed to avoid the formation of air bubbles in samples. In the first cycle, the polymer mixtures were heated to 80 °C under 6-8 metric tons pressure for 10 minutes. Next, two cycles of hot pressing were carried out at 20 psi and 80 °C for 15 minutes and 20 minutes, respectively. The samples were cooled down and were tested for tensile properties following the ASTM D638 type V standard[271]. The samples were extended at a rate of 5 mm min^{-1} and the reported data are the average of 5 measurements. To check the tensile results for recycled samples, dog-bone shaped samples were ground to small pieces and the same hot pressing procedure was applied to them for each recycling cycle.

8.2.2.6. Rheological Measurements

Oscillatory frequency sweep and dynamic mechanical analysis (DMA) were performed on an Anton Paar MCR 302 rheometer connected to a CTD 450 convection oven. For frequency sweep, the test was conducted on the samples between two parallel plates (diameter, 25 mm) in the frequency range of 1 to 1000 rad s^{-1} with a constant amplitude of 1% under the pure nitrogen atmosphere (purity = 99.99%) at 80 °C. DMA was carried out on samples under the pure nitrogen atmosphere (purity = 99.99%) in the temperature range of 25-80 °C. A dynamic shear strain of 0.1% was applied for DMA experiments. For DMA, rectangular bars

(60mm×10mm×2mm) prepared using the same hot pressing procedure (three cycles, 80° C) mentioned earlier in Tensile Test section.

8.2.2.7. Swelling Tests

The cross-linking density of polymer samples were examined by immersing approximately 0.13 g of polymer samples (Dimer 5-15%) in toluene (7.0 g, 5385 wt% based on samples) for 24 hours. The drying procedure started with the slow removal of the excessive solvent (toluene) using a syringe. Then, the samples were dried inside a fume hood for 24 hours at room temperature. The samples were placed under vacuum at room temperature for another 24 hours to ensure complete removal of the toluene. It was previously observed that similar polymers without cross-linking (IBOMA/C13MA, IBOMA/C13MA/GMMA and IBOMA/C13MA/VPBA) are completely soluble in toluene[162, 182, 471]. However, 53.45%, 56.28% and 63.63% of Dimer 5, 10 and 15% samples, respectively, were insoluble after one day. To further study the swelling properties of samples, a fully dried piece of each sample with defined weight was placed inside an aluminum pan and was immersed with excessive amount of toluene. Next, the solvent was carefully removed, and the sample was dried using an extra-low lint Kimwipes® to measure the weight change of the samples.

8.2.3. Preparation of (VPBA+GMMA) Dimer for a Minimulsion System

To prepare the (VPBA+GMMA) dimer (i.e. BG dimer) for miniemulsion polymerization of monomers, the mixture of 1:1 molar ratio of VPBA:GMMA were dissolved in 5 times the weight of monomers (500 wt% based on the monomers) of DCM solvent and 50 wt% of 3 Å molecular sieves based on the monomers to remove the water from the system. The mixture was stirred for 48 hours at room temperature to complete the reaction. Finally, the mixture was filtered using a 0.2 µm filter and dried for 7 days. The schematic for the reaction is shown in Figure 8.1. The FTIR spectrum of (VPBA+GMMA) dimer (Figure 8.2) shows the successful boronic ester formation.
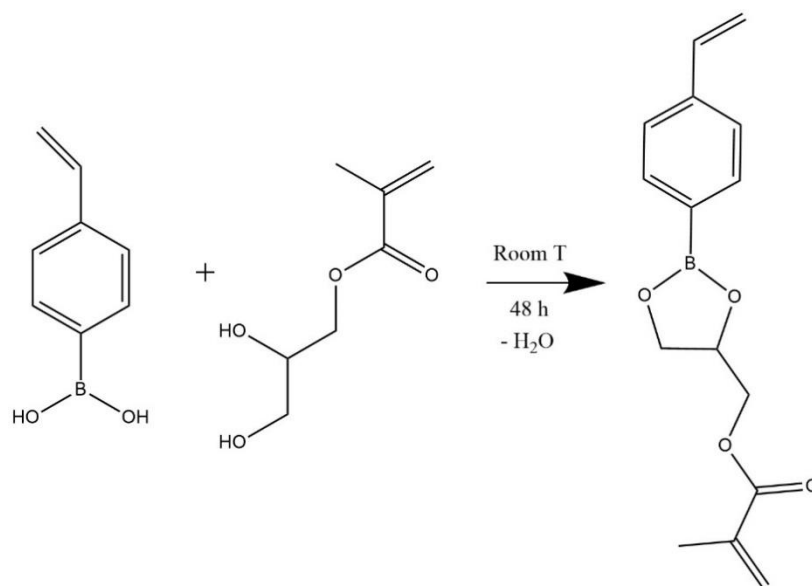
Figure 8.2. The schematic reaction for preparation of (VPBA+GMMA) dimer.

8.2.4. Miniemulsion Polymerization of IBOMA/C13MA/VPBA/GMMA

The monomers, Dispolreg 007 alkoxyamine and 0.8 wbm% n-hexadecane were mixed for 30 minutes with a stirring from a magnetic stir bar. The hexadecane was added as the co-stabilizer to improve the stability of the latex and prevent the Ostwald ripening effect[275]. The aqueous phase was prepared by dissolving 2 wbm% DOWFAX 8390™ anionic surfactant in water and stirring the resulting solution for 30 minutes. Then, two solutions were mixed together and stirred for 30 minutes to prepare the initial latex. The initial latex was sonicated for 10 minutes (cycle = 0.5 and amplitude = 70%) in an ice water bath to prepare a latex containing nano-meter sized particles. As an example, for Dimer 5% miniemulsion polymerization, the hydrophobic phase was prepared by mixing Dispolreg 007 (0.07 g, 0.2 mmol), IBOMA (2.57 g, 11.5 mmol), C13MA (6.71 g, 25.0 mmol), Dimer of VPBA and GMMA (0.52 g, 1.9 mmol) and n-hexadecane (0.08 g, 0.3 mmol) without the addition of any organic solvents. The aqueous phase was a solution of Dowfax 8390 (0.20 g, 2wbm%) in water (30.44 g, 1691.2 mmol). All the miniemulsion polymerizations were conducted in a three-necked round-bottom glass flask connected to a reflux condenser. The reflux condenser circulates a solution of 25/75 w/w glycerol/water through the condenser at 3 °C. The flask was equipped with a thermal well and a magnetic stirrer bar. The temperature sensor was placed inside the thermal well and connected to the temperature controller to keep the reaction temperature at 90 °C. The glass flask was placed in a heating mantle and on a stirrer. The latex was added to the flask and sealed with rubber septa. The system was purged using an ultrapure nitrogen flow for 30 minutes before increasing the temperature to deoxygenate the system and prevent any side reactions. To start the polymerization, the latex was heated with the rate of 10 °C min^{-1} to reach 90 °C, while the nitrogen purging continues during the polymerization.

The starting time of polymerizations (t = 0) was considered at the point at which the reaction temperature reached 75 °C. The samples were taken periodically to study the kinetics of polymerization for each experiment. At the end of the polymerization, the system was cooled down to temperatures below 40 °C and the latex was subsequently removed from the flask.

8.2.5. De-crosslinking of Polymers with Pinacol

The de-crosslinking of polymers was performed by immersing samples (approximately 0.13 g) in a solution of pinacol (0.3 g, 2.54 mmol) and 1,4-dioxane (7.0 g, 79.45 mmol). A control experiment was done at the same time for each polymer samples (~ 0.13 g). The samples were immersed in 1,4-dioxane (7.0 g, 79.45 mmol) without the addition of pinacol. The samples containing pinacol were completely dissolved in dioxane, suggesting the complete opening of boronic ester cross-linking bonds. The GPC and ^{1}H NMR measurements were conducted on samples after precipitation in methanol and complete drying. The control samples remained at room temperature for 24 hours. Then, the 1,4-dioxane was removed with a syringe. The control samples were dried in a fume hood for 24 hours and under vacuum for another 24 hours at room temperature. The insoluble fraction of samples in the control vials was measured by comparing the initial weight of samples with the weight of remaining polymer.

8.3. RESULTS AND DISCUSSION

8.3.1 Preparation of VPBA + GMMA dimer

For a successful miniemulsion polymerization, the monomers should be stabilized within the nano-meter-sized micelles. Typically, a combination of surfactant and co-stabilizer is required to afford the proper colloidal stability[47]. However, the monomers should exhibit sufficient hydrophobicity to exclusively have polymerization occur inside the stabilized particles (the requisite for miniemulsion polymerization). IBOMA and C13MA monomers are highly hydrophobic, which makes them readily available inside the monomer latex droplets[162]. However, the GMMA and VPBA are water-soluble and thus limits their availability for polymerization inside the monomer droplets[444, 480]. We attempted to adopt miniemulsion polymerization containing these monomers by synthesizing a dimer of GMMA and VPBA monomers (termed simply as BG dimer going forward) beforehand to increase their hydrophobicity and use them in miniemulsion NMP. The BG dimer has the boronic ester bond within its structure and is theoretically able to break and form the GMMA and VPBA in the presence of water. The FTIR spectrum of VPBA and GMMA monomers and the synthesized BG dimer are depicted in Figure 8.2. The successful formation of BG dimer has been previously proven in the literature[150, 151]. The peaks at a wavenumber of 3350-3500 cm⁻¹ correspond to O-H stretching in molecules. A considerable decrease in O-H stretch was observed after the

successful formation of BG dimer monomer. This confirms the formation of boronic ester bonds between VPBA and GMMA monomers[150].
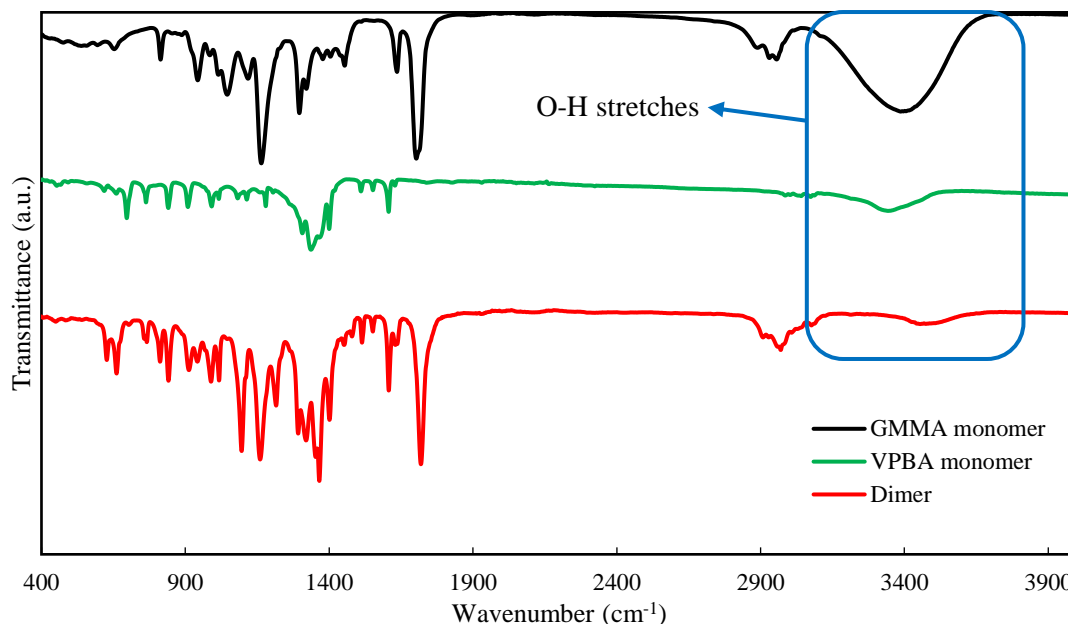
Figure 8.2. FTIR spectra for (VPBA+GMMA) dimer (red line, —), VPBA (green line, —) and GMMA monomers (black line, —). The decrease in the size of broad peak of O-H stretching at wavenumber of 3350-3500 cm^{-1} for BG dimer illustrates the successful formation of BG dimer from VPBA and GMMA.

Next, the miniemulsion NMP of IBOMA/C13MA/BG dimer was conducted at 90 °C in the presence of Dispolreg 007 alkoxyamine. Using Dispolreg 007 alkoxyamine, no controlling comonomer is required for nitroxide mediated polymerization of methacrylates[28, 29]. A target number average molecular weight ($M_{n,target}$) of 45 kg mol^{-1} was considered for all the miniemulsion NMPs. This $M_{n,target}$ was chosen to show the possibility of making relatively long polymer chains in miniemulsion using this method, to incorporate multiple BG dimers into the chains and to produce IBOMA/C13MA/BG dimer polymers with similar chain length to our previous studies concerning IBOMA/C13MA statistical copolymers prepared in miniemulsion[162]. A schematic miniemulsion polymerization of the monomers is presented in Figure 8.3. Three different initial molar concentrations of BG dimer were used in the miniemulsion polymerizations (Table 8.1) to study the effect of dimer concentration on the polymerization kinetics, cross-linking density and eventually mechanical and chemical properties of final polymers. As shown in Figure 8.4 (b) and Table 8.1, a high final dispersity (*Đ*) for polymer chains was observed for all the experiments in miniemulsion, although a linear increase of ln $((1-X)^{-1})$ plots (X = monomer conversion) and M_ns with X was generally witnessed. The relatively high *Đ* was expected as the dimer creates cross-linking bonds between the

145

polymer chains and prevents the polymerization from proceeding to higher conversions. For Dimer 15%, $Đ = 5.0$ was observed, indicating the possible droplet coalescence and the formation of boronic ester bonds between polymer chains at higher conversions. However, relatively fast polymerization ($t_{reaction} < 210$ min), polymers with high M_ns and stable latexes resulted for all polymerizations. The M_n versus conversion (X) plot was linear for all miniemulsion polymerizations with higher M_ns than the predicted linear relationship (Figure 8.4 (b)). The deviation from the theoretical line is partly due to the slow initiation of Dispolreg 007 alkoxyamine at the beginning of the polymerization, which results in higher M_n at different conversions[278]. Furthermore, the calibration against PMMA standards without applying the Mark-Houwink-Sakurada coefficients for IBOMA/C13MA/GMMA/VPBA homopolymers can cause a slight over-prediction[481]. Figure 8.4 (c) displays the particle size during the course of polymerizations. The final particle size and the final particle size distribution are presented in Table 8.1 and Figure 8.4, respectively. The particle size distributions (Figure 8.4 (d)) show a small population of micrometer-sized particles, suggesting some coagulation and formation of cross-linked latex particles.
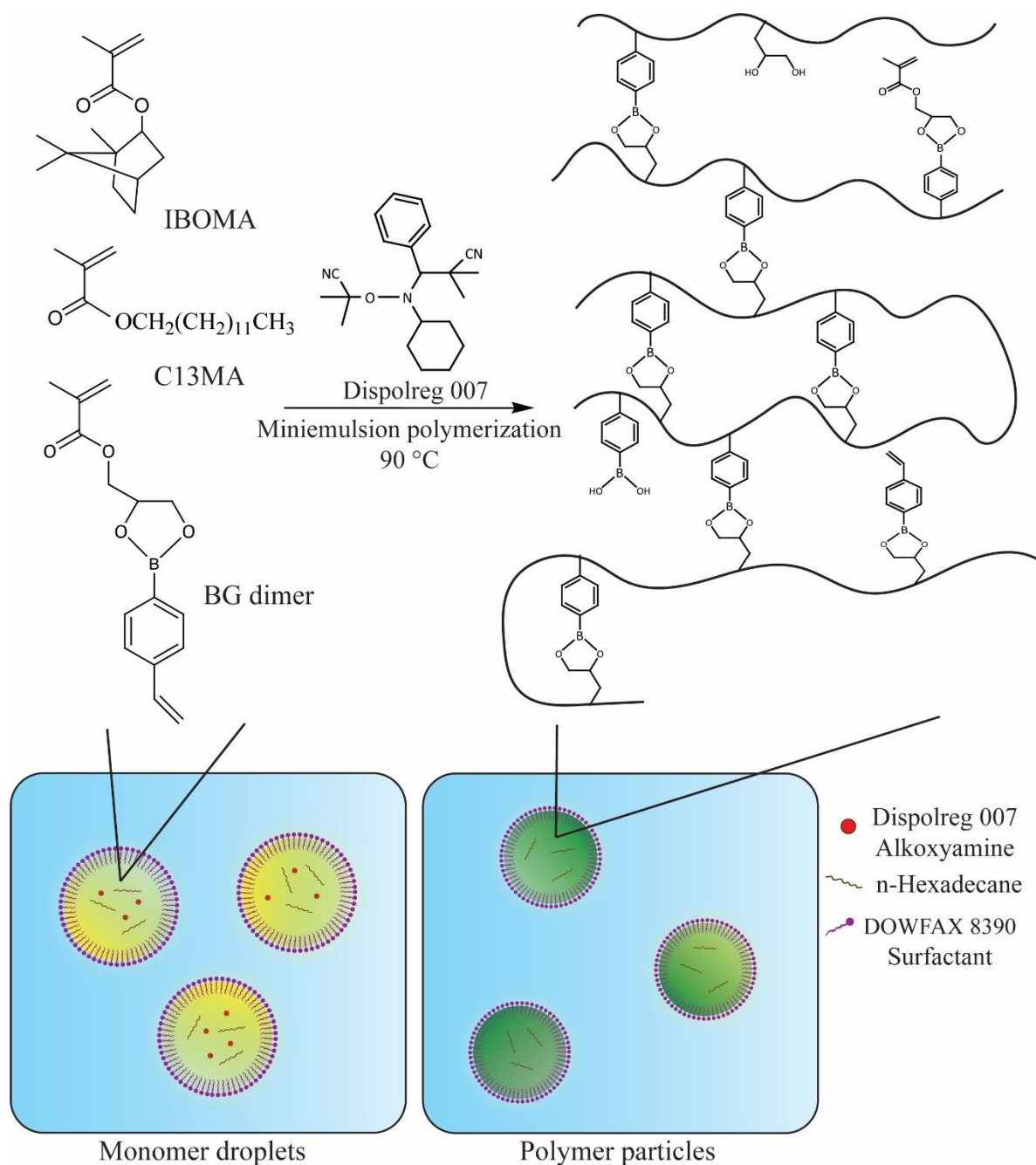
Figure 8.3. Scheme of procedure for preparation of water-borne polymers with intrinsic dynamic crosslinking bonds.

Table 8.1. Summary of experiments for nitroxide-mediated miniemulsion polymerization of IBOMA/C13MA monomers and BG dimer using Dispolreg 007 initiator.

Experiment ID	Initial monomer %[b] (Dimer/IBOMA/C13MA)	Reaction time (min)	$M_{n,final}$[c] (kg mol^{-1})	X[c] (%)	$Đ$[c]	[IBOMA]$_0$[d] (M)	[C13MA]$_0$ (M)	[BG Dimer]$_0$ (M)	[Dispolreg 007] (M)	Particle size (nm)[e]

147

Dimer 5% [a]	5/30/65	210	40.6	78.1	1.9	0.282	0.610	0.047	0.005	297
Dimer 10%	10/30/60	150	37.8	47.5	1.8	0.285	0.570	0.095	0.005	294
Dimer 15%	15/25/60	210	48.8	64.6	5.0	0.239	0.573	0.143	0.005	280

[a] Nitroxide mediated miniemulsion polymerization of monomers with 5 mol% BG dimer in the initial feed composition at 90 °C. The monomer content for all the miniemulsions was 24 wt%. The latexes were stabilized by adding 2 wt% Dowfax™ 8390 and 0.8 wt% n-hexadecane relative to monomers.

[b] The mol % of each monomer in initial monomer mixture.

[c] The final number-average molecular weight (M_n), overall monomer conversion (X) and dispersity ($Đ$) were measured by GPC with PMMA standards in THF at 40 °C. The target number-average molecular weight $M_{n,target}$ for all the miniemulsion polymerizations was 45 kg mol^{-1}.

[d] The initial concentration of IBOMA monomer in the miniemulsion.

[e] The final Z-average particle size reported from DLS.
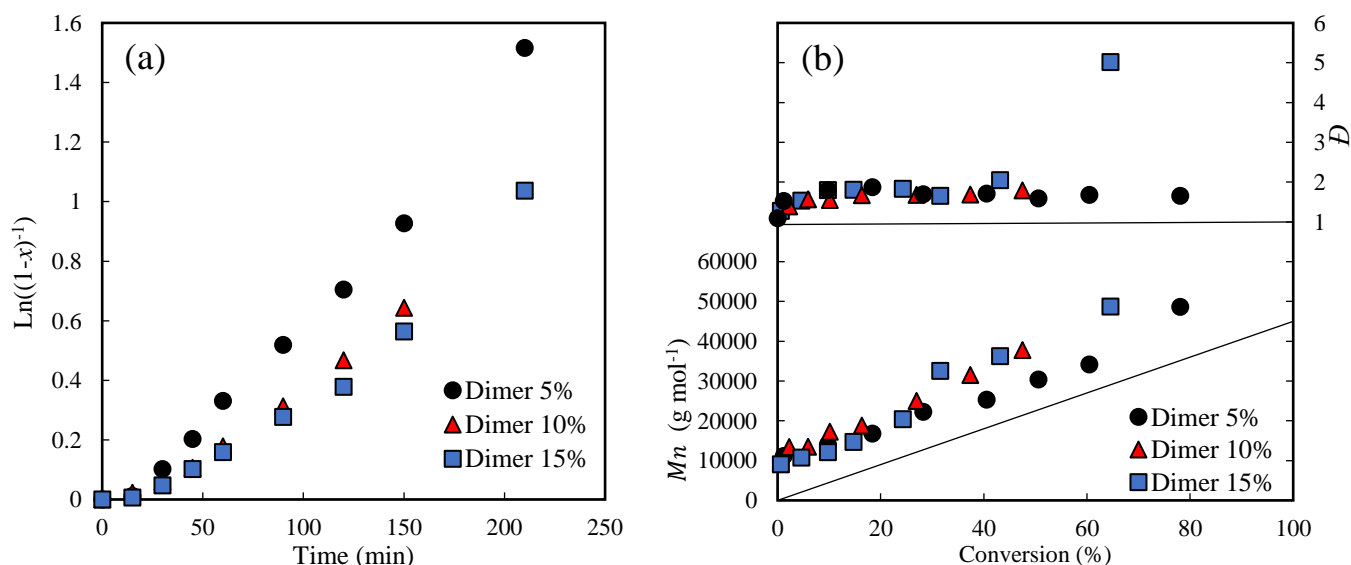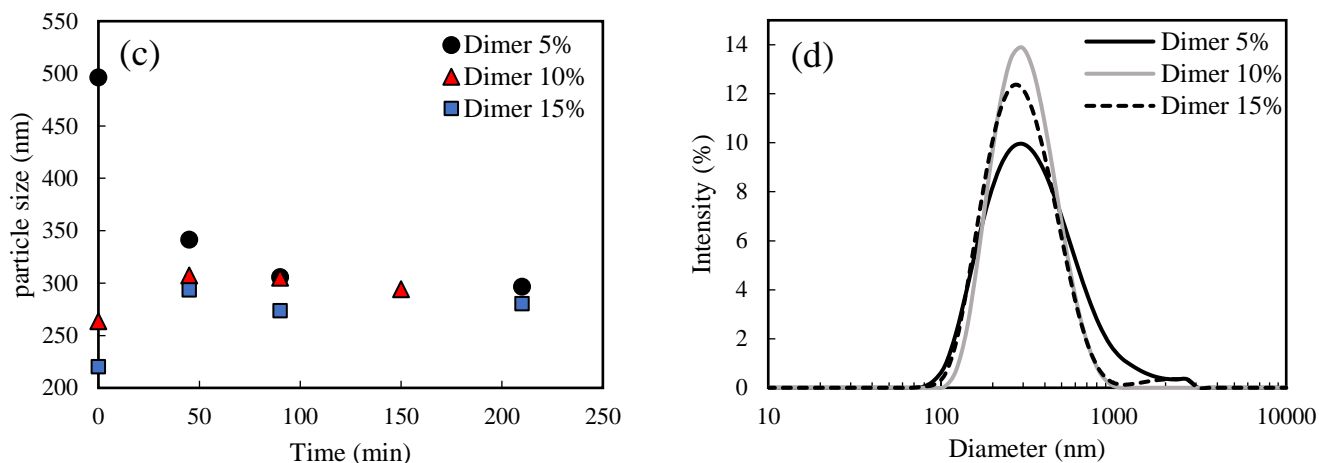
Figure 8.4. The miniemulsion polymerization of different ratios of BG dimer/IBOMA/C13MA using Dispolreg 007 initiator at 90 ºC: (a) semi-logarithmic kinetic plots of $\ln[(1-X)^{-1}]$ ($X=$ monomer conversion) versus reaction time (b) number average molecular weight M_n and dispersity $Đ$ versus conversion (X) (c) Z-average particle size over reaction time; (d) the final particle size distribution for each experiment. Dimer 5% (black circles, ●); Dimer 10% (red triangles, ▲); Dimer 15% (blue squares, ◼).

After the preparation step, the latexes were dried inside a fume hood at ambient temperature. The drying and formation of the polymer film took 24 hours to complete. The final polymer coating was transparent and exhibited a good adhesion to glass (Pyrex™ petri dish). Figure 8.5 demonstrates the polymer latex and film formation for Dimer 15% sample.

Dimer 15% polymer latex   Polymer latex was dried under the fume hood   Dried transparent polymer coating after 1 day
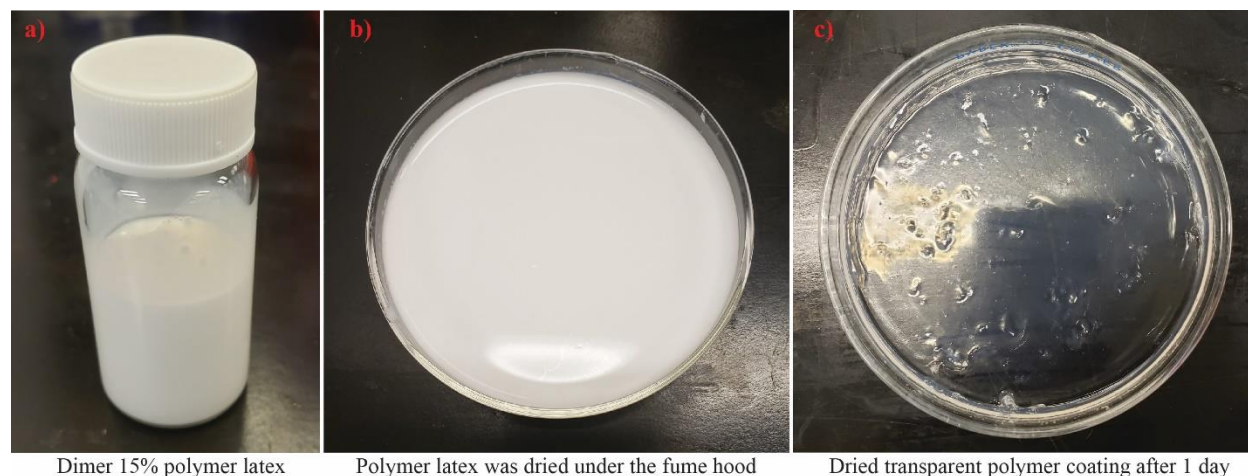
Figure 8.5. a) Dimer 15% polymer latex with 24% solid content b) The polymer latex was poured inside a Pyrex petri dish and placed inside a fume hood at room conditions (T= 21 °C and relative humidity of 22%). c) sample dried completely overnight, and a clear polymer coating was formed.

To check the availability of BG dimer monomers inside the polymer structure, FTIR results of Dimer 5-15% samples were analyzed and compared together (Figure 8.6 and Figure 8.S1 (Supporting Information)). Peaks at 653 cm^{-1} (CB stretching, HO-B-O and O-B-CC bending) and 1368 cm^{-1} (BO stretching) showed an increase in intensities with increasing the initial BG dimer content from 5 to 15%, exhibiting the availability of BG dimer monomers within the polymer[450-452]. The peaks at 1611 and 1640 cm^{-1} indicated the C-C stretching for the aliphatic ring in IBOMA and C=C and C-C stretching from the phenyl groups in the dimers. The broad intensity peak at 3446 cm^{-1} corresponded to O-H stretching, which increased with increasing the BG dimer content. Although the samples were dried under vacuum at room temperature before the test, this peak could also be due to the water trapped inside the polymer structure or the existence of un-cross-linked BG dimers (i.e. VPBA and GMMA monomers) within the polymer.
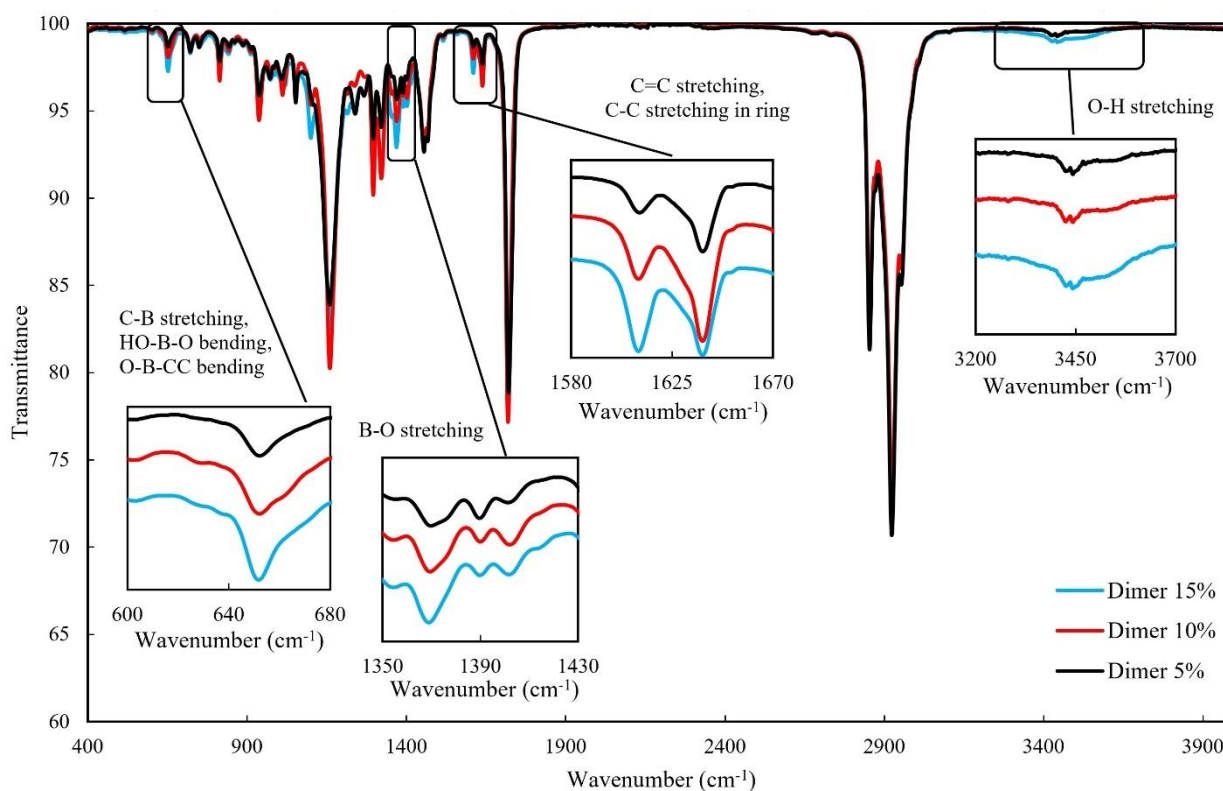
Figure 8.6. FTIR spectra for Dimer 5% (—, black line), Dimer 10% (—, red line) and Dimer 15% (—, blue line). Peaks corresponding to B-O and B-C became increasingly more intense with increasing the initial BG dimer content from 5 to 15%.

The solid-state ^{11}B NMR spectrum in Figure 8.S2 (Supporting Information) displays [11]B chemical shifts at $\delta = 19\text{-}21$ ppm, indicating the boronic esters and boronic acid groups[482, 483]. Furthermore, the solid-state ^{13}C NMR on Dimer 5%, 10% and 15% (Figure 8.S3, Supporting Information) showed a wide peak at around δ

= 111 ppm, displaying the presence of unreacted dimers, free boronic acid groups (without esterification) and open rings of boronic ester groups in the polymer structure, which enables the self-healing properties.

To further investigate the formation of dynamic cross-linking bonds within the polymer structure, an oscillatory frequency sweep experiment was conducted on the dried samples from frequencies (ω) 1-1000 rad s^{-1} at 80 °C. As depicted in Figure 8.7, storage modulus (G′) was higher than loss modulus (G″) for all samples at lower frequencies, indicating the dominance of rubbery behavior[454]. By increasing the BG dimer content, the G′ increased, while preserving the linear trend and constant value up to $\omega \cong 100$ rad s^{-1}. For Dimer 5% and 10%, a minimum was observed for G″, which shows the quasi-solid like properties for these polymers[484]. However, the great difference between G′ and G″ for Dimer 5% and Dimer 10%, intensified the rubbery behavior. This trend was not indicated for Dimer 15% as the cross-linking density is high enough to maintain elastic solid behavior for a wide range of frequencies (from 1 to 500 rad s^{-1}). At approximately $\omega \cong 100$ rad s^{-1}, G″ increased sharply to reach a transition and the G′ started to decrease slowly. A sharp increase in G″ was observed for Dimer 5% and 10%, indicating fast relaxation and energy dissipation from the chains. The crossover (G′ = G″) occurred at crossover frequencies (ω_c) of 315, 450 and 500 rad s^{-1} for Dimer 5%, 10% and 15%, respectively. At $\omega > \omega_c$, the polymers start behaving like viscous liquids and the G″ > G′. The crossover and the transition to the liquid state occurred at lower frequencies for Dimer 5% due to the lower cross-linking density compared to Dimer 10% and Dimer 15%.
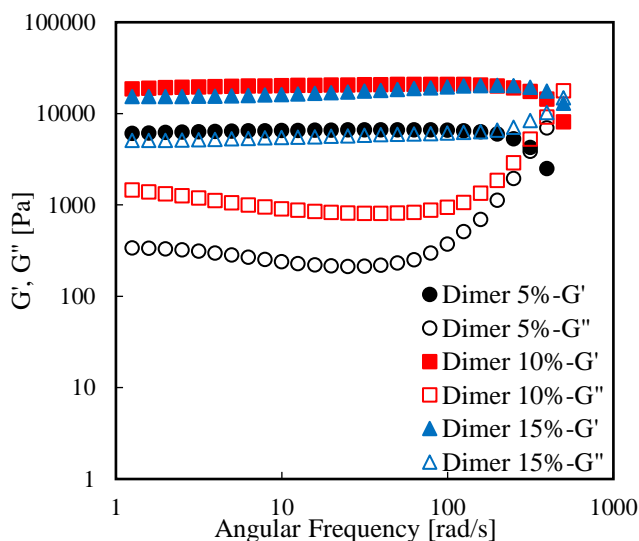
Figure 8.7. Storage (G′) and loss (G″) moduli versus angular frequency under N$_2$ at 80 °C (1% strain applied). Dimer 5% (black circles); Dimer 10% (red squares); Dimer 15% (blue triangles).

8.3.2. Recyclability of polymers

To check the recyclability of the polymer samples, tensile tests were conducted on samples before and after reprocessing. First, the tensile test was done on the original samples to check the mechanical properties initially (Figure 8.8 (a)). The Dimer 15% had the highest stress at break, while the elongation was the lowest among the samples (stress and strain at break for Dimer 15% were 0.46±0.06 MPa and 3.6±0.1 %, respectively). Based on the results, increasing the BG dimer concentration in the polymerization feed improved the stress at break and reduced elongation of the samples. This confirms the formation of the dynamic covalent bonds within the polymer structure due to the successful statistical terpolymerization of BG dimer monomers with IBOMA and C13MA. This also indicates the possibility of changing the mechanical properties of the polymer resins by a simple modification of the BG dimer concentration in the initial feed. Next, the reprocessability of the polymers was tested for up to three recycling cycles. The stress and strain at break for all the recycled samples remained in the same range as the original samples, which suggests a minimal change during the reprocessing. However, the slight change in values was observed due to the presence of unreacted monomers within the polymer structure that may change the mechanical properties during the recycling. The tensile results for Dimer 5-15% and the recycled samples were listed in Table 8.2.
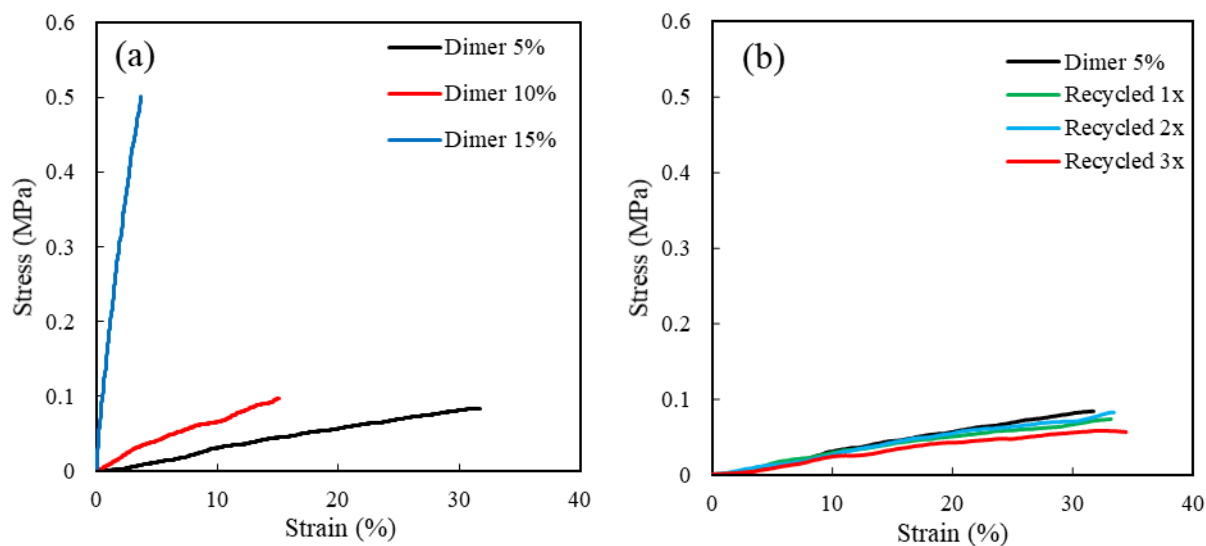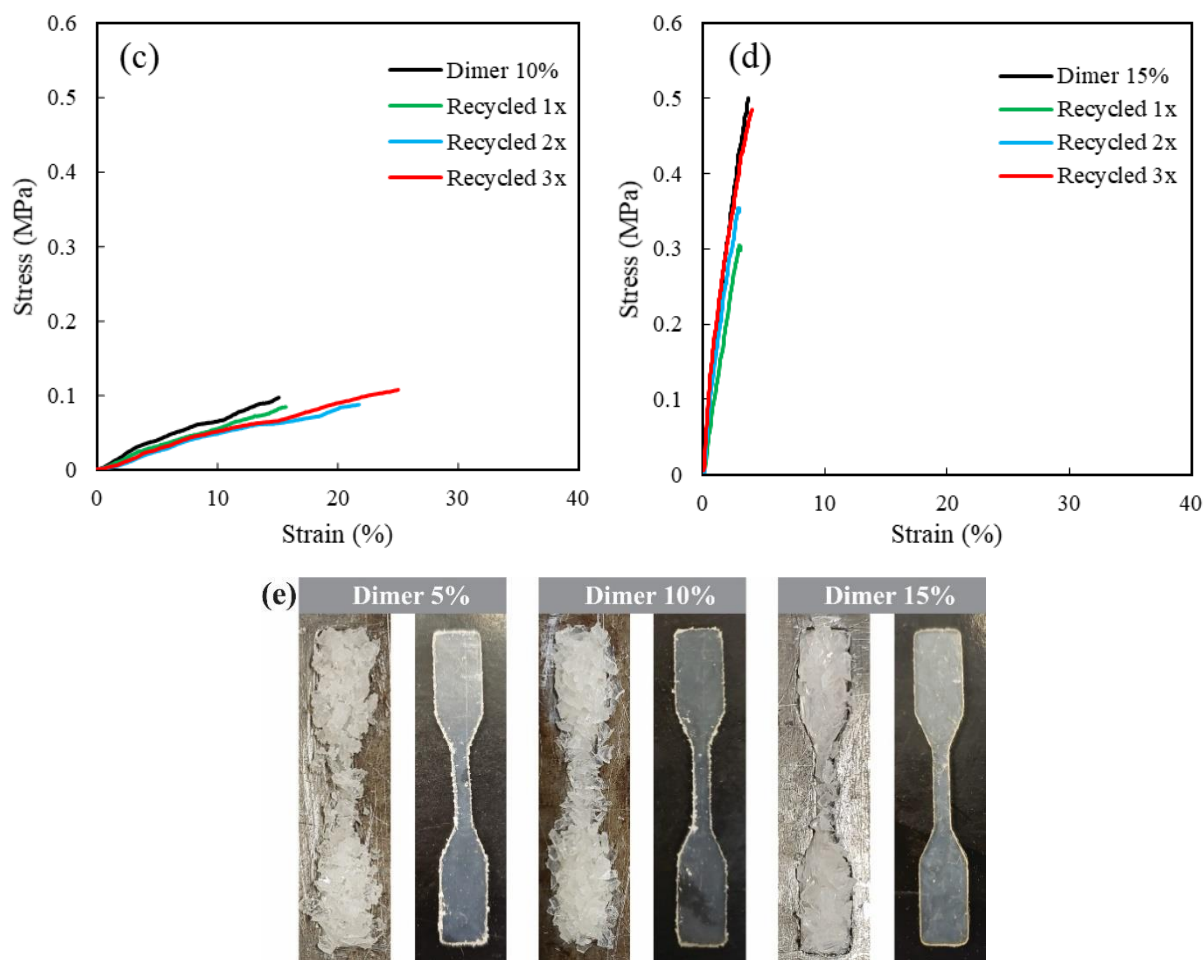
Figure 8.8. Tensile stress-strain curves for Dimer 5-15% samples before and after recycling. a) tensile results for original samples b) recycling of Dimer 5% sample c) recycling of Dimer 10% sample d) recycling of Dimer 15% sample e) photos of Dimer 5, 10 and 15% samples after recycling process. Grounded samples were hot-pressed at 80 °C for 45 minutes.

Table 8.2. Tensile results for Dimer 5-15% polymers before and after recycling at 80 °C.

Sample ID	Young's Modulus (MPa)	Stress at break (MPa)	Strain at break (%)
Dimer 5%			
Original sample	0.34±0.05	0.07±0.02	25.0±9.5
After 1st recycling	0.27±0.03	0.06±0.01	27.6±7.9
After 2nd recycling	0.27±0.01	0.08±0.01	31.7±2.4
After 3rd recycling	0.23±0.05	0.06±0.01	33.8±4.4
Dimer 10%			
Original sample	0.67±0.15	0.10±0.01	16.4±3.3
After 1st recycling	0.57±0.04	0.08±0.01	16.5±1.3

After 2nd recycling	0.48±0.04	0.09±0.01	22.4±1.0
After 3rd recycling	0.48±0.05	0.11±0.01	27.1±2.6
Dimer 15%			
Original sample	22.85±6.56	0.46±0.06	3.6±0.1
After 1st recycling	12.39±0.03	0.31±0.01	2.8±0.4
After 2nd recycling	13.50±1.48	0.35±0.07	2.9±0.8
After 3rd recycling	19.04±0.24	0.42±0.06	3.9±0.8

[a] Toughness was calculated from the area under the stress-strain curves shown in Figure 8.8.

To examine the effect of BG dimer concentration on rheological behavior of original and recycled polymers, dynamic mechanical analysis (DMA) (Figure 8.9) of samples was conducted in the temperature range of 25 to 80 °C. All the samples were in the rubbery state with nearly constant storage modulus during the test. This demonstrates the structural integrity of polymers at higher temperatures and the availability of dynamic cross-linking within the polymer structure[151]. In addition, the detachment and attachment of boronic ester dynamic bonds obey the associative exchange mechanism, preventing an increase or decrease of storage modulus[385]. The similarity of storage modulus for original and recycled samples at the rubbery state, suggests a negligible change in cross-linking density and polymer structure during the recycling[144, 485]. The higher concentration of boronic ester bonds improved the cross-linking density and resulted in the reduced mobility of polymer chains. Therefore, Dimer 15% samples exhibited the highest G′ in comparison with Dimer 5% and 10% samples (G′$_{Dimer 15\%}$ = 5-7 MPa, G′$_{Dimer 10\%}$ = 0.5-0.8 MPa and G′$_{Dimer 5\%}$ = 0.1-0.3 MPa). According to the results, enhancing the boronic ester content of polymers can significantly improve the storage modulus. As an example, increasing the BG dimer concentration from 10 to 15 mol% in initial feed, improved the G′ by up to 1400%. This indicates the importance of BG dimer content for modifying the rheological properties of polymers.
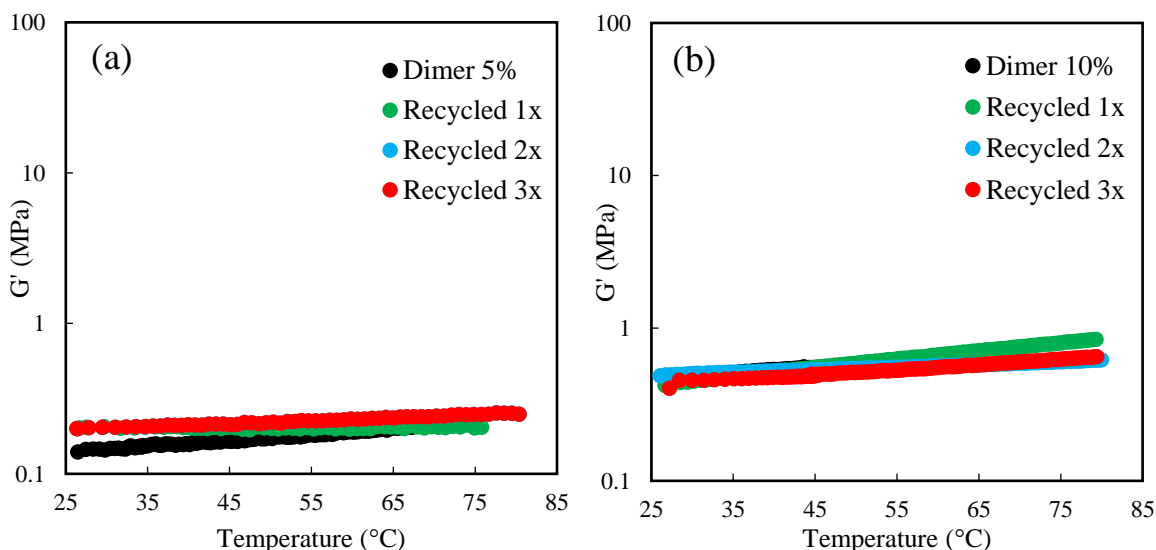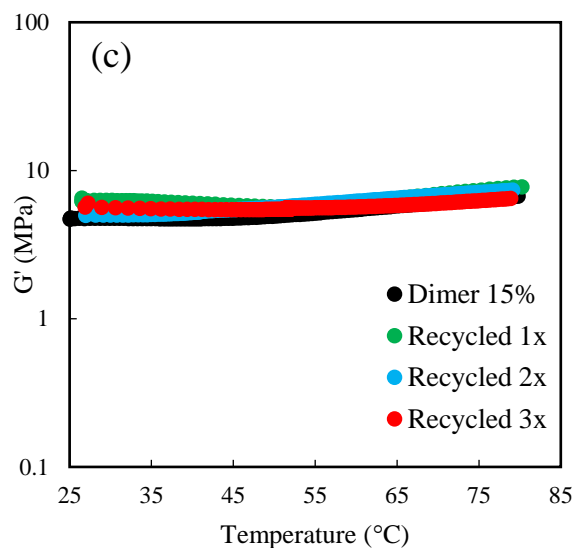
Figure 8.9. Dynamic mechanical responses for rubbery plateau moduli of samples before and after three recycling stages in the temperature range of 25 to 80 °C. a) Dimer 5% b) Dimer 10% c) Dimer 15%. Original samples before recycling (black circles, ●); first recycle (green circles, ●); second recycle (blue circles, ●); third recycle (red circles, ●).

8.3.3. Swelling test for water-borne samples

The absorption of organic solvents in the water-borne polymer structure was also investigated by measuring the weight change of samples placed in excess toluene. First, the polymers (dried samples) were immersed in toluene for 24 hours. Next, toluene was removed, and samples were completely dried. As a consequence, 53.5 wt%, 56.3 wt% and 63.6 wt% of Dimer 5%, 10% and 15%, respectively, remained insoluble. This shows a high degree of cross-linking bonds within the polymer microstructure. The samples can absorb toluene up to 250% of their original weight in a relatively short time (t < 300 minutes). The final swelling ratio (after 24 hours) of samples in toluene were listed in Table 8.S1 (Supporting Information). The results of solvent absorption (for t < 300 minutes) were presented in Figure 8.10 for three water-borne samples. As indicated, Dimer 15% polymer blend had the lowest swelling in toluene due to the comparatively highest cross-linking density. To examine the possibility of dimer breakage in the presence of toluene, FTIR was conducted on the Dimer 5% sample, submerged in toluene for 24 hours and dried using extra-low lint Kimwipes®. The absence of the broad O-H stretching peak at 3500 cm^{-1} suggested that no dissociation occurred between the VPBA/GMMA boronate ester contained with each dimer (Figure 8.11). In addition, the FTIR peaks confirms the existence of a high concentration of toluene in the gel-like structure.
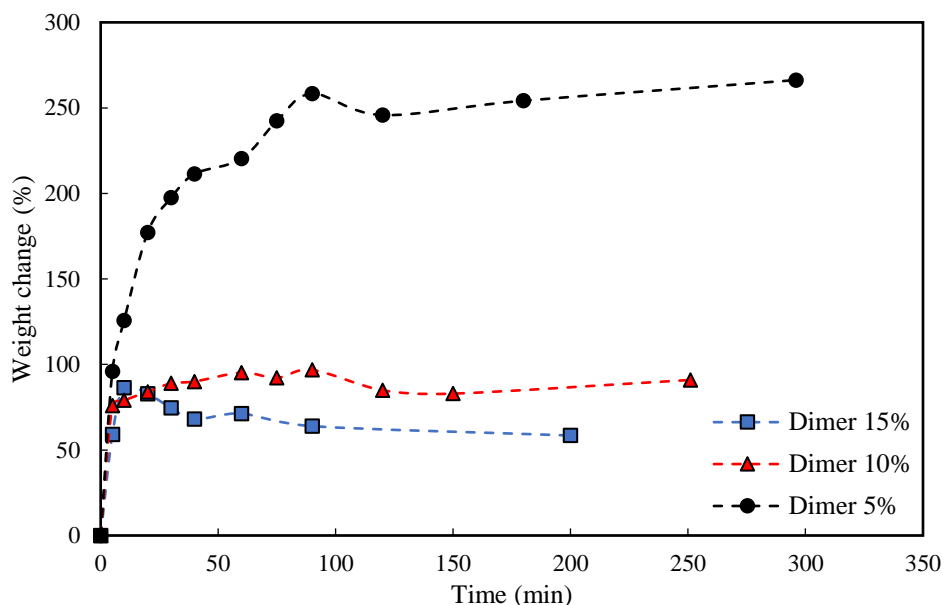
Figure 8.10. Swelling results for Dimer 5%, 10% and 15% samples in toluene. All the samples absorbed relatively high amount of toluene. Dimer 5% (black circles, ●); Dimer 10% (red triangles, ▲); Dimer 15% (blue squares, ■).
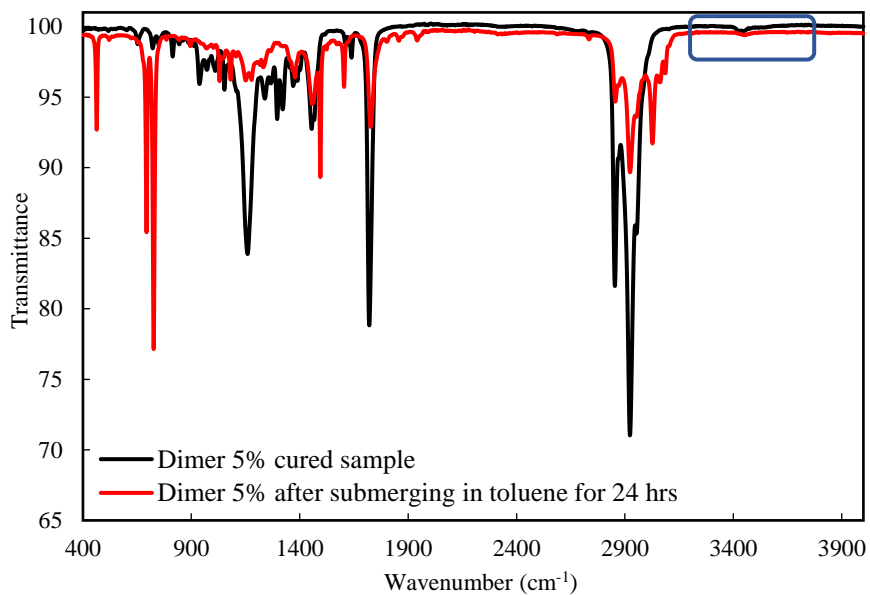
Figure 8.11. FTIR spectra for Dimer 5% cured sample (black line, —) and Dimer 5% sample after submerging in toluene for 24 hours and drying by an extra-low lint Kimwipes® (Red line, —). No significant increase in O-H stretching peak (~ 3500 cm^{-1}) after the addition of toluene indicates the durability of boronic ester bonds within BG dimers.

To further study the network stability and possible interactions, water-borne samples were thoroughly submerged in RO water using the same procedure used for the swelling test. No significant weight change was observed in these samples, suggesting the insolubility of samples in water. However, the color of samples slightly changed, and they become cloudy due to the absorbance of water into the polymer chains (Figure 8.12). The FTIR spectrum of samples after submerging them in water for 24 hours (Figure 8.12) illustrates the presence of water in the polymer.
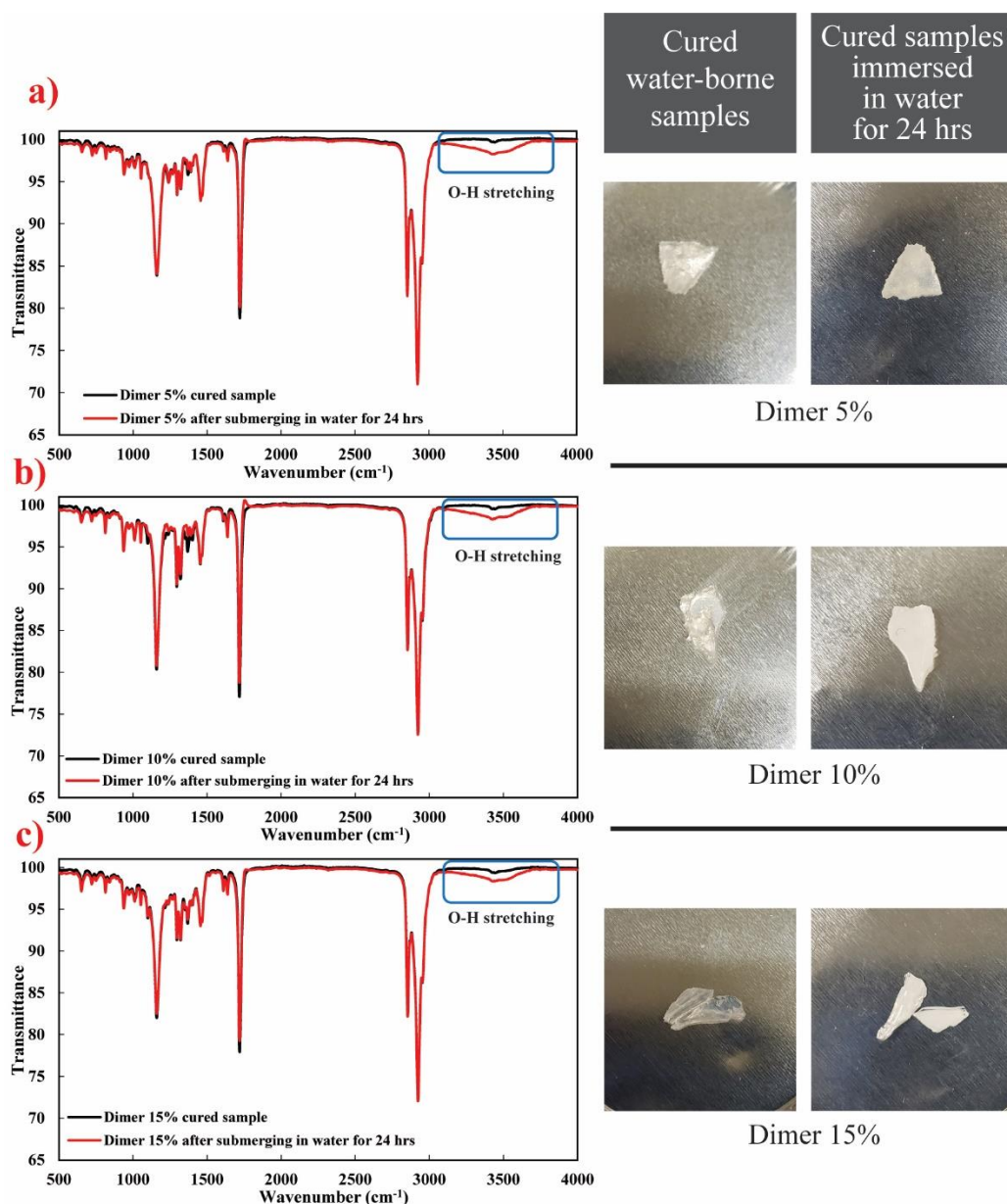
Figure 8.12. Cured polymers prepared by miniemulsion polymerization before and after submerging in water for 24 hours. FTIR spectra shows the completely cured samples (black line, —) and the same sample after submerging in water for 24 hours (Red line, —). (a) Dimer 5% (b) Dimer 10% (c) Dimer 15%.

It was observed that the samples containing higher molar ratios of BG dimer groups had a higher swelling ratio in the presence of water (Table 8.S1, Supporting Information; the swelling ratios of Dimer 15% and 5% are 7.9 and 2.2%, respectively, after 24 hours at room temperature). This indicates an increase in water absorption for polymers with higher VPBA and GMMA content in the respective components. Boronic acids are highly hygroscopic[398]. However, in this study, the water absorption was limited through esterification with diol groups of GMMA prior to the miniemulsion polymerization, along with the use of highly hydrophobic monomers of IBOMA and C13MA.

8.3.4. Thermal properties of polymers and blends

Thermal properties of water-borne polymer resins were investigated by DSC and TGA and the results were listed in Table 8.3. Figure 8.13 exhibits the DSC traces for three samples containing (VPBA+GMMA) dimers. A melting point (T_m) was observed for the samples at -25 to -29 °C due to the presence of crystallizable C13MA in the polymer chains[162, 210]. T_ms were previously observed for polymers with different dynamic cross-linking bonds (e.g. vitrimers)[486-488]. Considering the literature values of $T_{g,poly(IBOMA)}$ ≈ 110-200 °C[201, 262, 263] and $T_{g,poly(C13MA)}$ = -46 °C[201, 202], the low T_ms were expected as similar IBOMA/C13MA copolymers with 20-40 mol% IBOMA in the initial feed prepared in miniemulsions had T_gs in the range of -17 to -52 °C[162]. T_ms were previously detected for statistical copolymers containing C13MA prepared in miniemulsion[162, 210]. For IBOMA/C13MA copolymer with 18% IBOMA in polymer composition, a T_m at -33 °C was indicated[162]. It should be noted that the existence of DOWFAX 8390, n-hexadecane and unreacted C13MA monomers in the dried samples caused some plasticizing effect and further depressed the T_ms[162, 297, 298]. For this study, it can be assumed that increasing the amount of GMMA ($T_{g,poly(GMMA)}$ = 84~106 °C)[442-444] and VPBA ($T_{g,poly(VPBA)}$ = 198 °C)[445-449] (herein dimer of GMMA and VPBA) in the initial monomer mixture can result in slightly higher T_g or T_m of polymers. However, it was not the case for Dimer 5 to 15% samples due to the different $\frac{[C13MA]_0}{[IBOMA]_0}$, different $M_{n,final}$ and $Đ$ of polymer chains and non-identical concentration of residual unreacted monomers, especially C13MA, trapped within the polymer cross-linked network (see X values reported in Table 8.1).

TGA was carried out on samples to examine the thermal stability of polymers containing (GMMA+VPBA) dimers. The TGA traces in Figure 8.14 demonstrated a multi-stage decomposition of polymers versus temperature. The decomposition of unreacted monomers occurs at temperatures below 200 °C, causing an increase in decomposition rate (i.e. formation of a peak in derivative weights (%/°C) versus temperature graphs, Figure 8.14). The first decomposition temperature ($T_{dec,1}$, 10% weight loss) might correspond to the breakage of dynamic covalent bonds within the BG dimers and the last stage suggests the cleavage of the O-isobornyl bond in IBOMA and the formation and elimination of camphene at higher temperatures[180, 211].

According to the results, $T_{dec,1}$s for Dimer 5, 10 and 15% are slightly lower than the $T_{dec,1}$s for IBOMA/C13MA copolymers with the same monomer ratios prepared in miniemulsion[162]. This decrease in $T_{dec,1}$s is even higher if it is compared to our previous results on boronic ester cross-linked polymer blends with similar monomer compositions ($\Delta T_{dec,1}$ up to 104 °C)[471]. The difference in $T_{dec,1}$s is due to the presence of unreacted monomers, surfactant and co-stabilizer within the polymer chains. The decomposition temperatures at highest weight loss ($T_{dec,max}$) for the prepared samples were significantly higher than the IBOMA/C13MA copolymers with similar compositions ($\Delta T_{dec,max}$ up to 121 °C). This suggests that the addition of VPBA and GMMA to the polymer resins can improve the $T_{dec,max}$ of polymer resins [162, 182].

Increasing the initial BG dimer content (probably the cross-linking density) enhanced thermal stability of the polymers. This can be observed from the overall shift of the TGA curve to higher temperatures with increasing the BG dimer content (Figure 8.14 (d)) and comparatively higher ash content (ash content of Dimer 15% = 1.65 wt%; Dimer 10% = 0.72 wt% and Dimer 5% = 0.93 wt%). Furthermore, comparison of the decomposition temperatures for 50% weight loss ($T_{dec,50\%}$) of the polymer samples confirms the improvement of heat resistance with increasing the ratio of BG dimer in the initial hydrophobic mixture ($T_{dec,50\%}$ for Dimer 5, 10 and 15% were listed in Table 8.3).

Table 8.3. Thermal characterization of polymers and polymer blends.

Experiment ID	$M_{n,final}$ (kg mol^{-1})	T_m [a] (°C)	$T_{dec,1}$ [b] (°C)	$T_{dec,50\%}$ [b] (°C)	$T_{dec,max}$ [b] (°C)	$T_{dec,2}$ [b] (°C)
Dimer 5%	40.6	-25	197	338	417	487
Dimer 10%	37.8	-28	176	357	426	486
Dimer 15%	48.8	-29	196	369	403	471

[a] T_m (melting point) measured by DSC under nitrogen atmosphere using three scans per cycle (heat/cool/heat) at a heating rate of 20 °C min^{-1} and cooling rate of 50 °C min^{-1} in the range of -90 to 120 °C.
[c] $T_{dec,1}$ ($T_{10\%}$ or onset of decomposition), $T_{dec,50\%}$ (temperatures for 50% weight loss), $T_{dec,max}$ (temperature at which highest weight loss occurs) and $T_{dec,2}$ (end of decomposition) measured by TGA under nitrogen atmosphere at a ramp rate of 15 °C min^{-1}.
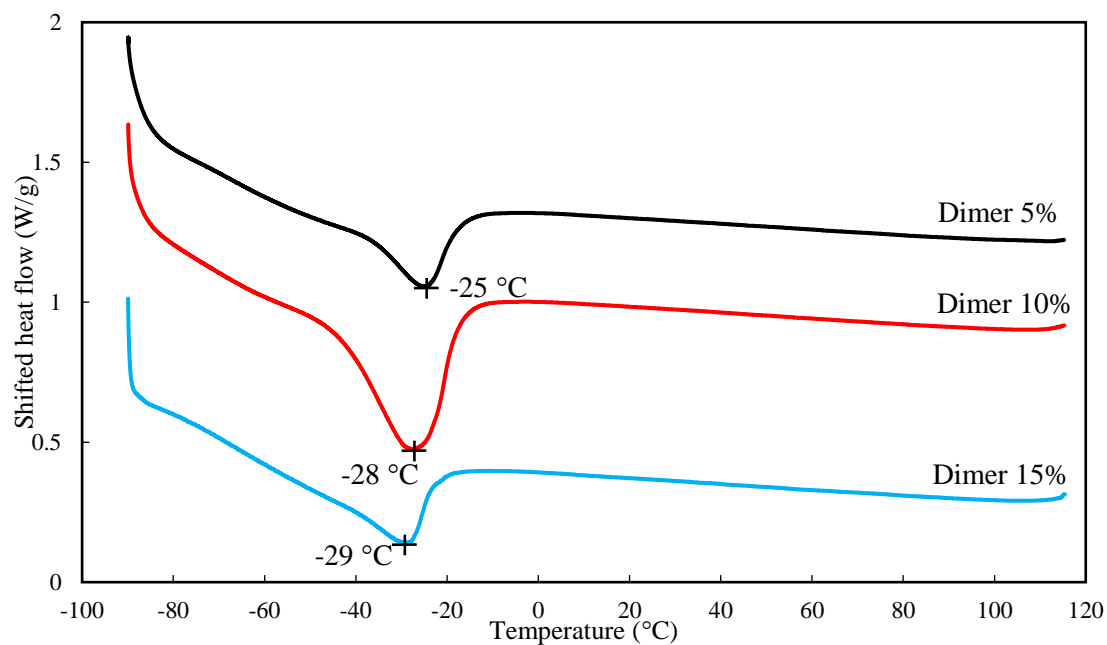
Figure 8.13. DSC traces for Dimer 5-15% samples in the temperature range of -90 to 120 °C. 2nd heating cycle in heat/cool/heat method with heating rate = 20 °C min^{-1} and cooling rate = 50 °C min^{-1}.
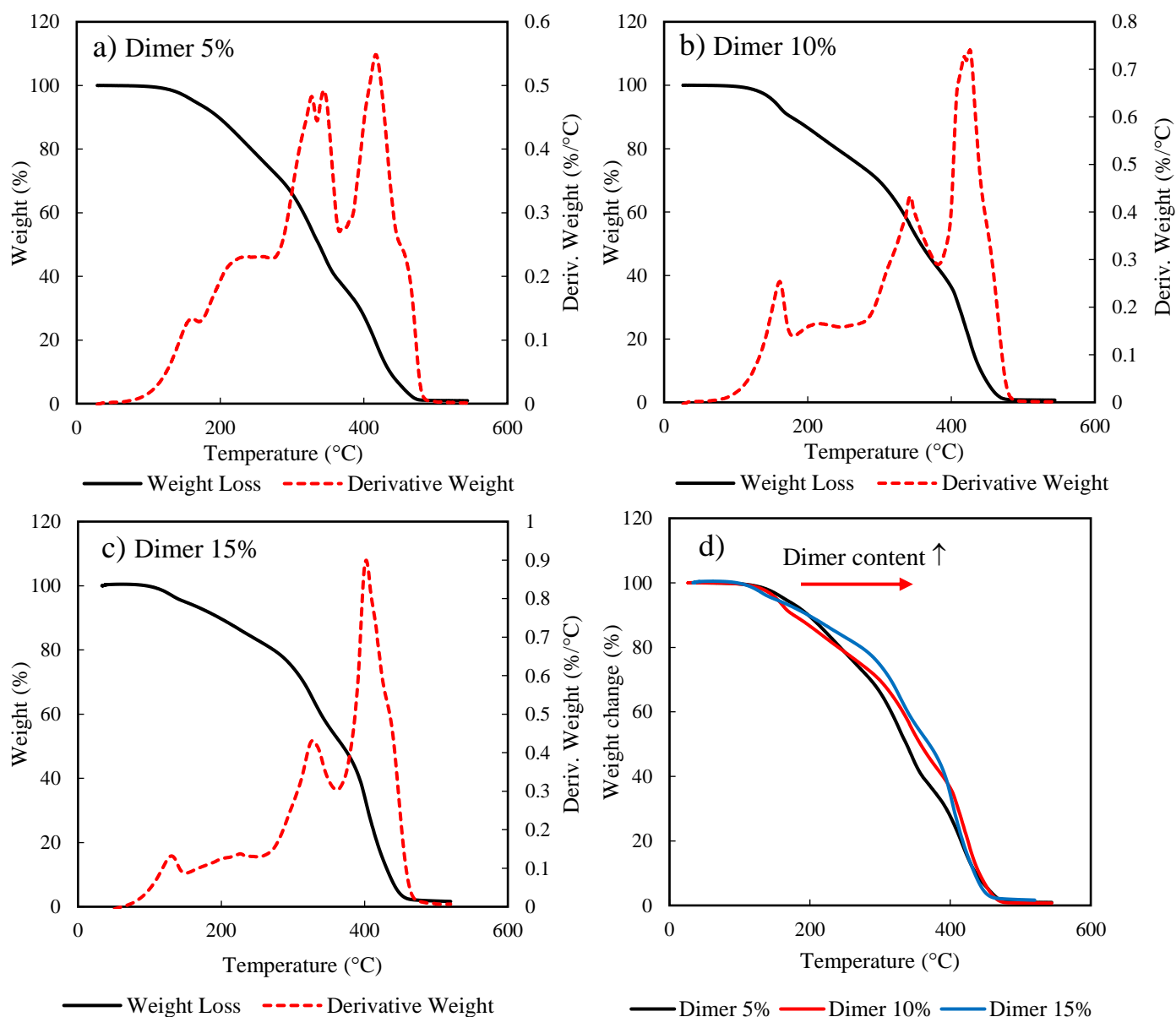
Figure 8.14. TGA traces for a) Dimer 5% b) Dimer 10% c) Dimer 15% d) comparison of decomposition properties for Dimer 5% (black line, —); Dimer 10% (Red line, —); Dimer 15% (blue line, —) samples. Increasing the BG dimer content slightly increased the thermal stability of the polymers. The samples were heated under the N_2 atmosphere with the heating rate of 15 °C min^{-1}. The polymers were completely dried under a fume hood at room temperature for 5 days before TGA.

8.3.5. De-crosslinking of polymers with pinacol

The dynamic covalent bonds of boronic esters can be easily cleaved in the presence of a diol-functionalized molecule. Herein, the de-crosslinking of samples was conducted using pinacol in 1,4-dioxane. It was previously shown that the IBOMA/C13MA/VPBA and IBOMA/C13MA/GMA copolymers are completely

soluble in 1,4-dioxane[471]. To better examine the effect of pinacol on solubility of samples, control samples were used in a similar test condition without the addition of pinacol. As seen in Figure 8.15, the samples were dissolved completely within 4 hours at 50 °C using pinacol (above the T_g of the samples). Without the addition of pinacol (control samples), 70.7 wt%, 66.0 wt% and 65.8 wt% of the total weight of the respective Dimer 5%, 10% and 15% samples remained insoluble. In addition, the swelling ratio of the control samples submerged in 1,4-dioxane for 24 hours revealed a high swelling ratio of polymers (up to 111.6%) (Table 8.S1, Supporting Information). The swelling ratio decreased by increasing the initial BG dimer content from 5% to 15% (i.e. cross-linking density).
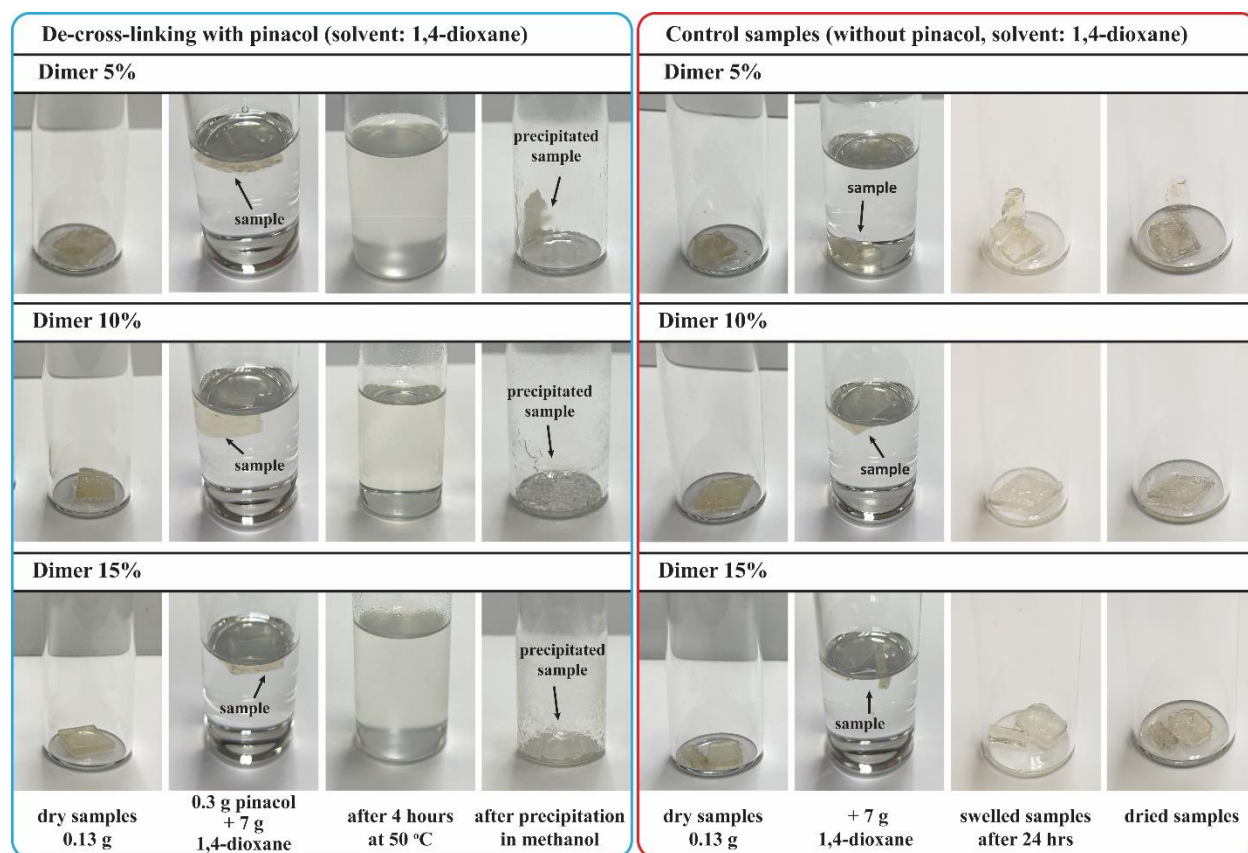
Figure 8.15. De-crosslinking of polymer samples using pinacol in 1,4-dioxane after 4 hours at 50 °C.

8.4. CONCLUSIONS

To prepare polymer resins with recyclability, the nitroxide-mediated polymerization of IBOMA and C13MA with 5-15 mol% VPBA and GMMA in initial feed (for the formation of boronic ester dynamic cross-linking) was conducted in a dispersed aqueous medium. To introduce moisture-activated dynamic cross-linking, a VPBA+GMMA dimer was formed and then added to increase the hydrophobicity of these monomers and thus incorporate them more easily into the monomer droplets. The nitroxide-mediated

miniemulsion polymerization of IBOMA, C13MA with three different ratios of BG dimer (5%, 10% and 15%) was conducted using Dispolreg 007 alkoxyamine at 90 °C. Later, after the latex dried, the boronic ester dynamic cross-linking bonds formed. The formation of cross-linking bonds was confirmed by FTIR and rheological measurements. The recyclability of samples was investigated by performing three recycling stages and comparing the mechanical properties of recycled samples with the original ones. The results suggested a higher stiffness (i.e. Young's modulus) for original and recycled samples containing higher BG dimer contents (Young's modulus for Dimer 5%, 10% and 15% is 0.23-0.34 MPa, 0.48-0.67 MPa and 12.39-22.85 MPa). The dried polymers, prepared in miniemulsion, can absorb toluene up to 266% of their initial weight in less than 300 minutes (ultimate swelling ratio up to 153%). However, a negligible water absorbance was observed for samples (less than 7.9 wt%). The T_ms of polymers were in the range of -29 to -25 °C and T_{dec}s showed the negligible effect of boronic ester cross-linking density on thermal stability of polymers. However, the heat resistance of polymers improved significantly compared to IBOMA/C13MA copolymers due to the presence of VPBA and GMMA monomers in the chains. Lastly, the chemical de-crosslinking of boronic ester bonds in polymers were examined by the addition of pinacol at 50 °C. It was shown that the samples can be completely dissolved in 1,4-dioxane within 4 hours due to the esterification of VPBA with pinacol.

ACKNOWLEDGMENT

Preamble to Chapter 9

In previous chapters, the preparation of polymers in miniemulsion for coating applications was investigated. Then, self-healing polymers with high bio-content were synthesized in organic solvents and miniemulsion. This chapter focused on an alternative approach for the preparation of polymer coatings using glycidyl methacrylate (GMA) and alkyl methacrylates (C13MA). The GMA improves the adhesion of the polymer chains to the wood surface and can react with amine-functionalized cross-linkers to form crosslinking bonds at room temperature. As the epoxy functionalized GMA has a high hydrophilicity, the NMP of the GMA/C13MA monomers was conducted in 50 wt% 1,4-dioxane. By changing the ratio of GMA/C13MA in copolymers, glass transition temperature of polymers can be modified. In this study, statistical, gradient, diblock and triblock copolymers with different GMA/C13MA content were synthesized and polymerization kinetics, thermal and rheological properties of the resulting polymers were examined. This study developed a new approach for preparation of the polymer coatings that can be used for future industrial projects.

Chapter 9: Epoxy-based Triblock, Diblock, Gradient and Statistical Copolymers of Glycidyl Methacrylate and Alkyl Methacrylates by Nitroxide Mediated Polymerization

ABSTRACT

A series of triblock, diblock, gradient and statistical copolymers of glycidyl methacrylate (GMA) and C13 methacrylates (C13MA, alkyl methacrylates with the average side-chain length of 13.0) were synthesized by nitroxide mediated polymerization (NMP) using Dispolreg 007 in 50 wt% dioxane at 90 °C. The polymers had the number average molecular weights (M_n) in the range of 23-46 kg mol^{-1} and dispersities (Đ) of 1.5-1.9. For the GMA/C13MA statistical copolymerization, reactivity ratios $r_{GMA} = 1.17 \pm 0.09$ and $r_{C13MA} = 0.65 \pm 0.09$ were determined. For statistical copolymers with GMA ratio (F_{GMA}) of 0.5-0.8, the appearance of a melting point (T_m) at -43 to -19 °C and two glass transition temperatures (T_g) in the range of -53 to 11 °C indicated the possibility of micro-phase separation and a weak gradient polymerization. TGA showed ash content up to 13 wt% for GMA/C13MA copolymers at 600 °C, suggesting the possibility of high flame retardancy. Furthermore, a transition from elastic solid to viscous liquid behavior was detected by an oscillatory frequency sweep at 30 °C for triblock copolymers of GMA/C13MA ($F_{GMA} = 0.6$-0.7, crossovers at 100-200 rad s^{-1}) and gradient polymers with high GMA content ($F_{GMA} = 0.88$, crossover at 10 rad s^{-1}).

9.1. INTRODUCTION

Epoxy-functional polymers via incorporation of glycidyl methacrylate (GMA) have been widely used for applications such as coatings[489-491], adhesives[492-494], enzyme immobilisation[495, 496], surface functionalization[497-499] and dental composites[500, 501] due to their strong adhesion properties[502, 503], multiple epoxy ring-opening reactions[504-506] and chemical and corrosion resistance[507]. GMA's oxirane group readily react with amines and form cross-linking bonds required for coatings, adhesives and gel and matrix structures[505, 508, 509]. However, the existence of hydrophilic epoxy groups in the polymer structure introduces the possibility of water absorption that can limit their application[510]. Bonora et al[511] reported water-absorption of up to 11% v/v after 20 h for a cross-linked epoxy coating. Another issue with epoxy-based resins is their brittleness[512]. One method to reduce the wettability of the epoxy polymers, improve their hydrophobicity and increase the flexibility of resins, is to copolymerize the epoxy monomers with

165

monomers containing long alkyl groups[513]. This improves the water resistance along with the toughness of polymers, providing a wider application range as coatings and adhesives. To impart flexibility into polymer chains, C13 alkyl methacrylates (C13MA, C12-C16 methacrylates with average chain length of 13.0, 76% bio-carbon content) is one such example. C13MA with a long alkyl chain lowers the glass transition temperature (T_g) of copolymers (T_g for tridecyl methacrylate homopolymers = -46 °C)[201] and effectively acts as an internal plasticizer within the polymer structure. Recently, the atom transfer radical polymerization of GMA with C18 alkyl methacrylate (stearyl methacrylate) was reported as an additive to diesel fuel[514]. Our study mainly focuses on the nitroxide mediated polymerization (NMP) of GMA with C13MA for preparation of statistical, gradient, block and triblock copolymers with different ratios of GMA/C13MA. NMP is one of the simplest reversible deactivation radical polymerization (RDRP) techniques, which only relies on alkoxyamines and heat to start the polymerization[23, 166, 169]. NMP of methacrylates, with some modification, was enabled by the advent of 2,2,5-tri-methyl-4-phenyl-3-azahexane-3-nitroxide (TIPNO)[26, 169] and SG1-based alkoxyamines such as N-(2-methylpropyl)-N-(1-(diethylphosphono-2,2-dimethylpropyl)-O-(2-carboxylprop-2 yl)hydroxylamine) BlocBuilder-MA™[23, 230, 231]. The modification to make NMP possible for methacrylates involved the addition of a low concentration of controlling comonomers with a very low activation/deactivation equilibrium constant (K) such as styrene and acrylonitrile to reduce the cross-disproportionation effect and high K of methacrylates[172, 173, 232]. Here, we used 3-(((2-cyanopropan-2-yl) oxy) - (cyclohexyl) amino)-2, 2-dimethyl-3-phenylpropanenitrile (Dispolreg 007 alkoxyamine with D7 nitroxide) that was recently developed by Ballard *et al.*[28, 29] and enabled the homopolymerization and copolymerization of methacrylates in organic solvents[435, 515] and dispersed aqueous systems[43, 103, 162, 210, 436] without the addition of any controlling comonomers at temperatures below 100 ºC[243]. This has the added advantage as any possible negative effect of the controlling co-monomer is eliminated (eg. solubility changes, glass transition) and we attempt to show how these two monomers can produce epoxy-functional copolymers with various microstructures by NMP.

9.2. EXPERIMENTAL SECTION

9.2.1. Materials

Glycidyl methacrylate (GMA, 97 %), C13 alkyl methacrylate (C13MA, n-alkylic average chain length of 13.0 units,>99%, Visiomer Terra C13-MA) were obtained from Sigma and Evonik, respectively. The monomers were passed through a column of aluminum oxide (Brockmann I grade, Sigma-Aldrich), mixed with 5 wt% calcium hydride (90-95% reagent, Sigma-Aldrich) based on aluminum oxide, to remove the inhibitors. 3-(((2-Cyanopropan-2-yl) oxy) - (cyclohexyl) amino)-2, 2-dimethyl-3-phenylpropanenitrile (Dispolreg 007) alkoxyamine was prepared according to the Ballard et al's method to initiate the NMP of

methacrylates[28]. Dispolreg 007-based difunctional alkoxyamine was synthesized following Nicolas et al's procedure, except using Dispolreg 007 instead of BlocBuilder alkoxyamine[60]. 1,4-dioxane ($\geq$99.9%, Sigma), methanol (>99%, Fisher Scientific), tetrahydrofuran (THF, 99.9%, HPLC grade, Fisher Scientific), toluene (>99%, Fisher Scientific), hexane ($\geq$98.5%, Fisher Scientific) and deuterated chloroform ($CDCl_3$, $\geq$99%, Cambridge Isotopes Laboratory) were used as received. All the polymerizations were conducted under ultra pure nitrogen (99.99%, Praxair).

9.2.2. Methods

Monomer conversions (X) and polymer compositions were determined from ^1H NMR results on a Bruker Avance III HD (500 MHz, 32 scans). Polymer samples were dissolved in $CDCl_3$ before the measurements (a sample ^1H NMR spectrum is available in Figure 9.S1 (Supplementary Information)). Number average molecular weight (M_n) and dispersity of polymer samples ($\DJ$) were obtained from gel permeation chromatography with a differential refractive index detector (RI 2414) (GPC, Waters Breeze), relative to PMMA standards (M_n = 875 - 1,677,000 g mol^{-1}, Varian Polymer) at 40 °C. The GPC was equipped with a guard column and three GPC columns (HR1, HR 2 and HR 4 with the total M_n range of 10^2-6×10^5 g mol^{-1}, THF solvent, Styragel Waters). GPC samples with an approximate concentration of 5 mg ml^{-1} were prepared by the addition of HPLC grade THF to the samples without any filtration.

Glass transition temperature (T_g) and melting point (T_m) were measured using a differential scanning calorimetry (DSC, Q2000 from TA Instruments) in the temperature range of -80 to 130 °C under pure nitrogen gas flow. Three cycles of heating (to 130 °C), cooling (to -80 °C) and reheating (-80 to 130 °C) were performed on the samples to find the T_gs and T_ms on the third cycle (reheating) using the inflection method. Hermetic aluminium pans were used to prepare samples for DSC. Thermogravimetric analysis (TGA) of 5-10 mg of each polymer sample was conducted on a TGAQ500 (TA instruments) in a platinum pan with heating rate of 15 °C min^{-1} up to 600 °C under N_2. Oscillatory frequency sweep was performed on an Anton Paar MCR 302 rheometer equipped with a CTD 450 convection oven under nitrogen atmosphere at 30 °C. The test was done between two parallel plates (D = 25 mm) with 1% amplitude. For DSC, TGA and oscillatory frequency sweep, samples were precipitated in methanol or hexane to remove unreacted monomers and residual solvents. Then, the polymers were dried inside a fume hood for 2 days and under vacuum for 1 day.

9.2.3. Nitroxide mediated statistical copolymerization of GMA/C13MA

Figure 9.1 shows a schematic presentation of nitroxide mediated polymerization of GMA/C13MA mixtures. For statistical copolymerization, different ratios of GMA and C13MA monomers were dissolved

in 50 wt% 1,4-dioxane. Dispolreg 007 alkoxyamine was used to initiate the NMP of the binary methacrylate mixture. A target number average molecular weight ($M_{n,target}$) of 45 kg mol^{-1} was considered for all the statistical copolymerizations (this target is defined as the molecular weight for 100% conversion of the monomers). The solution was stirred for 10 minutes and transferred to a PYREX round-bottom angled three-neck reactor connected to a reflux condenser, a temperature sensor and nitrogen gas inlet. The condenser (Neslab 740) circulates a mixture of ethylene glycol/RO water [20:80 vol%] at a temperature of 2 °C. The reactor was placed inside a heating mantle, connected to a temperature controller, on top of a stirrer. A magnetic stir bar was added for mixing and a purge of pure nitrogen gas deoxygenated the solution for 30 minutes before the polymerizations. The N_2 purging continued during the polymerization. The temperature was set at 90 °C and the polymerization start point (t=0 min) was considered at 75 °C. The samples were taken during the polymerization for kinetic studies. After the polymerization, the polymers were precipitated in methanol or hexane (based on GMA/C13MA ratios; polymers with high GMA content were precipitated in hexane). Next, the polymers were dried inside a fume hood for 2 days and under vacuum for 1 day. In this study, a similar setup and procedure was used for preparation of gradient, block or triblock copolymers of GMA/C13MA.
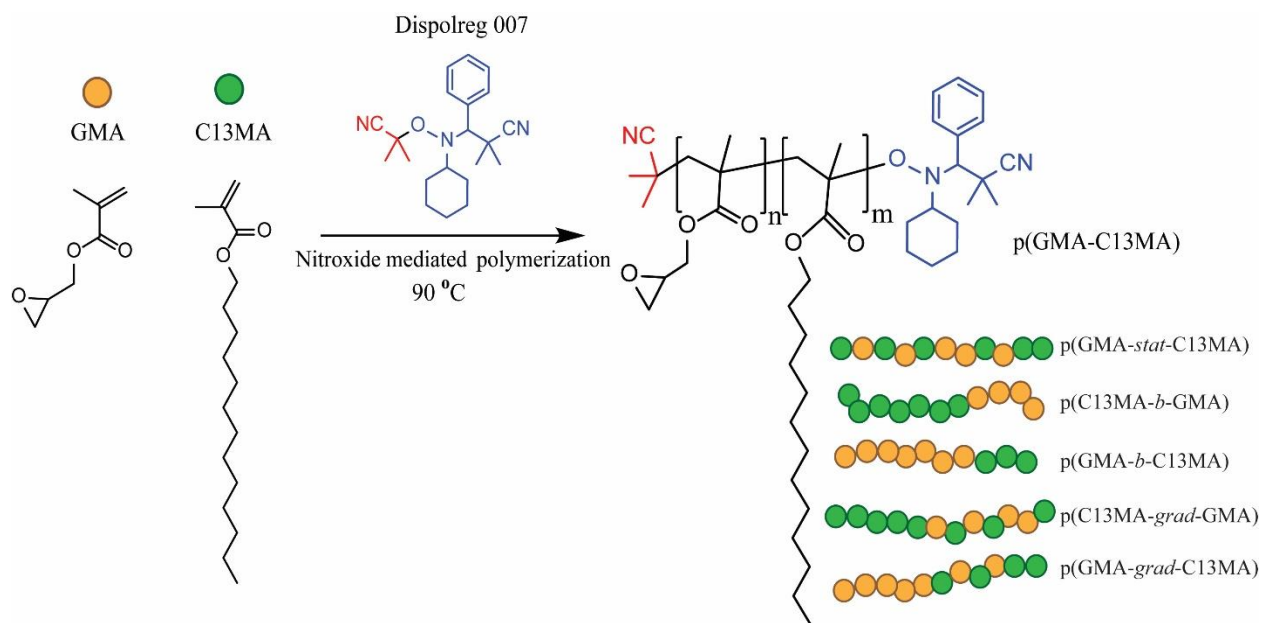
Figure 9.1. The schematic presentation of GMA/C13MA polymerization for preparation of statistical, block and gradient copolymers using Dispolreg 007 in dioxane at 90 °C.

9.2.4. Block copolymerization of GMA/C13MA

First, NMP of GMA or C13MA was done in the presence of Dispolreg 007 for 90 minutes to prepare homo-GMA or C13MA macroinitiators in dioxane. The macroinitiators in both cases were precipitated in excess

hexane and were dried inside a fume hood for 2 days and under vacuum for 1 day at room temperature. Then, the dried macroinitiator and second monomer (0.25 times initial moles of the monomer used for synthesis of macroinitiator) were dissolved in 50 wt% 1,4-dioxane to prepare the solution for block copolymerization of GMA/C13MA at 90 °C. As an example for block copolymerization of GMA/C13MA starting from GMA macroinitiators (GMA-b-C13MA experiment), Dispolreg 007 (0.1 g, 0.295 mmol) and GMA (13.26 g, 93.253 mmol) were dissolved in 1,4-dioxane (13.36 g, 151.583 mmol). The polymerization was continued for 90 minutes at 90 °C. The GMA macroinitiator (GMA-MI, M_n = 32.9 kg mol^{-1} and Đ = 1.52) was precipitated in hexane and dried completely to remove unreacted monomers and solvent. Next, the dried MI (5.33 g, 0.162 mmol) and C13MA (6.26 g, 23.320 mmol, 0.25 times the initial mol of GMA monomer) were dissolved in 1,4-dioxane (23.19 g, 263.194 mmol) and the polymer chain extension was conducted for 4 h at 90 °C. The resulting polymer was precipitated using the same procedure as for precipitation of GMA-MI.

9.2.5. Gradient copolymerization of GMA/C13MA

To prepare gradient copolymers, first, nitroxide mediated homopolymerization of GMA or C13MA was conducted at 90 °C using Dispolreg 007 alkoxyamine. The second monomer was dissolved in 50 wt% dioxane and was purged with pure nitrogen gas for 40 minutes in a separate vial with septum cap. After 90 minutes of homopolymerization, the solution of 50 wt% second monomer in dioxane was injected in one shot to the reaction medium. The amount of second monomer was 0.25 times the initial moles of the monomer used for the synthesis of macroinitiator. The reaction stopped after 240 minutes and the gradient copolymers were dried inside a fume hood for 2 days and under vacuum for 1 day.

9.2.6. Synthesis of triblock copolymers of GMA/C13MA

Figure 9.2 displays the steps required for preparation of triblock copolymers of GMA/C13MA. The synthesis of triblock copolymers of GMA/C13MA started with the preparation of bifunctional alkoxyamine using Dispolreg 007 (D7 nitroxide group) according to modification from Nicolas et al's procedure[60]. The ^{1}H NMR and ^{13}C NMR spectra in Figure 9.S2 (Supplementary Information) confirms the synthesis of D7-based difunctional alkoxyamine. The bifunctional D7 alkoxyamine initiated the nitroxide mediated homopolymerization of GMA or C13MA in 50 wt% dioxane at 90 °C. The polymerization was stopped after 75 minutes by cooling, resulting in macroinitiators with two active chain ends. The macroinitiators with two active chain ends were precipitated in hexane and were dried inside a fume hood for 2 days and under vacuum for 1 day at room temperature. The macroinitiator and the second monomer were dissolved in 50 wt% dioxane and the NMP was conducted at 90 °C for 120 minutes. Finally, the triblock copolymers

were precipitated in hexane and were dried inside a fume hood for 2 days and under vacuum for 1 day at room temperature.
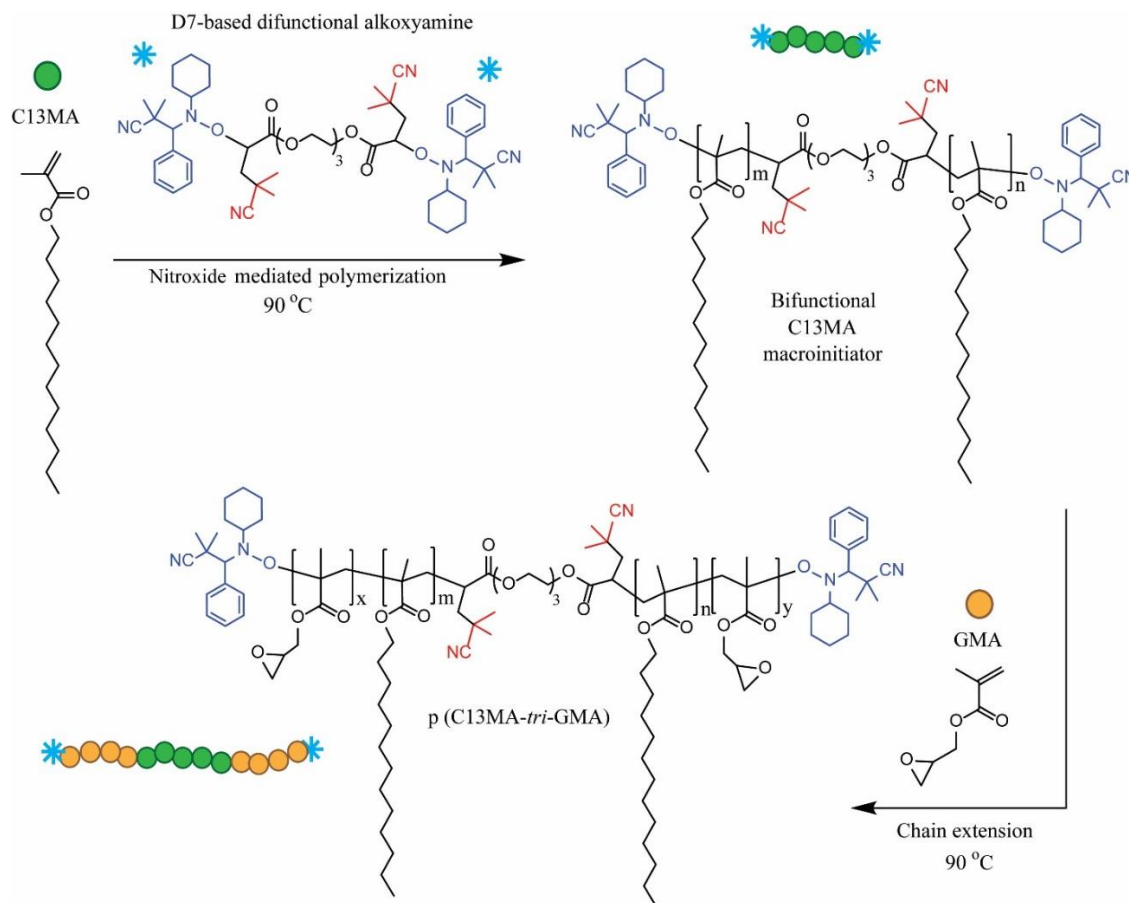
Figure 9.2. Schematic triblock copolymerization of C13MA/GMA using D7-based difunctional alkoxyamine at 90 °C. First, a macroinitiator was synthesized by the homopolymerization of C13MA. Next, the chain extension of bifunctional p(C13MA) macroinitiator was done at 90 °C by the addition of GMA monomer.

9.3. RESULTS AND DISCUSSION

9.3.1. Nitroxide mediated polymerization of GMA/C13MA

We started our investigations with NMP using different ratios of GMA/C13MA in the presence of Dispolreg 007 alkoxyamine. Different statistical, block, gradient and triblock copolymers were synthesized, and the polymerization kinetics were studied thoroughly. The following sections describe the experimental conditions and kinetic results for each polymer microstructure (statistical, gradient, di and triblock).

9.3.2. Statistical copolymerization of GMA/C13MA

The copolymerization of different ratios of GMA/C13MA was conducted in dioxane using Dispolreg 007 at 90 °C. The homopolymerization of GMA was also performed in the same conditions for comparison. The experimental conditions and polymerization characteristics are listed in Table 9.1. The copolymerization of GMA/C13MA resulted in copolymers with M_ns = 23-32 kg mol^{-1} and $Đ$ = 1.56-1.77 (relative to PMMA standards). Figure 9.3 displays the kinetic results for all the polymerizations. The semi-logarithmic plot of conversion versus time is linear for all of the statistical polymerizations up to 210 minutes (Figure 9.3a). Figure 9.3b presents the M_n trends with X for all the statistical polymerizations and compares them with the theoretical linear prediction if the polymerization was truly living. Accordingly, higher values of M_ns were observed at X near zero, showing the slow initiation and penultimate effect of Dispolreg 007[28, 43, 103, 515]. Furthermore, the measurement of M_ns relative to PMMA standards could also deviate the results from the theoretical line. A linear trend of M_n with X can be seen for X >10% with plateauing or termination at higher conversions. Generally, an increase in the values of $Đ$ with X can be observed in Figure 9.3c. However, the increase in $Đ$s was higher for copolymerization of GMA/C13MA with higher ratio of $\frac{[GMA]_0}{[C13MA]_0}$. The reactivity ratios (r_{GMA} and r_{C13MA}) were first estimated by a non-linear regression fit to the Mayo-Lewis equation (Equation 9.1)[279, 281].

$$F_{GMA} = \frac{r_{GMA}f_{GMA,0}^2 + f_{GMA,0}f_{C13MA,0}}{r_{GMA}f_{GMA,0}^2 + 2f_{C13MA,0}f_{GMA,0} + r_{GMA}f_{C13MA,0}^2} \qquad (9.1)$$

Based on the fit to the Mayo-Lewis equation, r_{GMA} = 1.52 ± 0.20 and r_{C13MA} = 0.56 ± 0.08 were estimated. The Mayo-Lewis plot for statistical copolymers of GMA/C13MA (Figure 9.4a) displayed higher fractions of GMA monomer in the copolymer compared to the initial concentration of GMA in feed. For high initial GMA feed composition ($f_{GMA,0}$ > 0.8), an azeotropic behavior was indicated. The azeotropic points at high $f_{GMA,0}$ was previously observed for GMA and maleic anhydride (MAn) copolymers with r_{GMA} = 0.83 and r_{MAn} = 0.26 (prepared by conventional free radical polymerization in THF)[516]. The reactivity ratios of r_{GMA} = 1.17 ± 0.09 and r_{C13MA} = 0.65 ± 0.09 were also measured by Equation 9.2 using an analytical solution of Skeist's equation for binary copolymerization, developed by Meyer and Lowry[435, 517, 518]. This method considered the monomer feed changes in the course of polymerization[519].

$$1 - \frac{M}{M_0} = 1 - \left[\frac{f_1}{f_{1,0}}\right]^\alpha \left[\frac{f_2}{f_{2,0}}\right]^\beta \left[\frac{f_{1,0}-\delta}{f_1-\delta}\right]^\gamma \qquad (9.2)$$

Here, $\frac{M}{M_0}$ is mole conversion, f_1 and f_2 are the molar compositions of monomer 1 and 2 in mixture and $f_{1,0}$ and $f_{2,0}$ are the initial values. α, β, γ and δ were calculated from $\alpha = \frac{r_2}{1-r_2}, \beta = \frac{r_1}{1-r_1}, \gamma = \frac{1-r_1r_2}{(1-r_1)(1-r_2)}$ and

171

$\delta = \frac{1-r_2}{2-r_1-r_2}$. This equation takes into account the compositional drift in the molar feed of GMA with X as depicted in Figure 9.4b. The slightly higher value of r_{GMA} compared to r_{C13MA} indicates the higher reactivity of macroradicals towards the GMA monomers and the possibility of the formation of GMA or C13MA blocky sequences during the statistical copolymerization. For comparison, reactivity ratios of $r_{GMA} = 1.29$ and $r_{ODA} = 0.68$ were calculated for conventional free radical copolymerization of GMA and octadecyl acrylate (ODA)[520]. Multiple studies regarding the copolymerization of GMA and styrene (S) indicated the $r_{GMA} = 0.55 \pm 0.08$ and $r_S = 0.40 \pm 0.10$[521-524]. For NMP of methacryloisobutyl POSS (POSSMA) and C13MA, $r_{POSSMA} = 0.91 \pm 0.07$ and $r_{C13MA} = 1.94 \pm 0.13$ was observed[181]. NMP of isobornyl methacrylate (IBOMA) and C13MA using a similar alkoxyamine (Dispolreg 007) resulted in $r_{IBOMA} = 0.89 \pm 0.13$ and $r_{C13MA} = 1.80 \pm 0.21$[162].

Table 9.1. Experimental conditions and polymer characteristics for statistical copolymerization of GMA/C13MA in 50 wt% dioxane using Dispolreg 007 at 90 °C.

Experiment ID	$f_{GMA,0}$[a]	F_{GMA}[b]	X[c] (%)	M_n[d] (kg mol^{-1})	$Ð$[d]	[Dispolreg]$_0$[e] (M)	[GMA]$_0$ (M)	[C13MA]$_0$ (M)	[Dioxane]$_0$ (M)
GMA100 [f]	1	1	71.9	24.1	1.76	0.017	3.671	0	5.989
GMA90/C13MA10	0.9	0.92	54.6	23.0	1.72	0.017	2.980	0.331	5.882
GMA80/C13MA20	0.8	0.81	63.3	28.8	1.69	0.017	2.412	0.603	5.794
GMA70/C13MA30	0.7	0.75	54.9	29.0	1.77	0.017	1.938	0.830	5.720
GMA60/C13MA40	0.6	0.65	69.3	26.5	1.68	0.016	1.535	1.023	5.657
GMA50/C13MA50	0.5	0.53	73.9	32.2	1.76	0.016	1.189	1.189	5.603
GMA40/C13MA60	0.4	0.45	54.1	29.8	1.60	0.016	0.889	1.333	5.557
GMA30/C13MA70	0.3	0.35	71.5	27.7	1.61	0.016	0.625	1.459	5.516
GMA20/C13MA80	0.2	0.24	54.9	25.1	1.61	0.016	0.393	1.571	5.480
GMA10/C13MA90	0.1	0.09	46.9	27.2	1.56	0.016	0.186	1.670	5.447

[a] Initial molar fraction of GMA in the initial feed, considering only GMA and C13MA monomers.
[b] Molar fraction of GMA in polymer composition as determined by ^{1}H NMR in CDCl$_3$. A sample ^{1}H NMR spectrum for GMA40/C13MA60 after 210 minutes of polymerization is provided in Figure 9.S1 (Supplementary Information).
[c] Final monomer conversion (%).
[d] The final number average molecular weight (M_n) and dispersity ($Ð$) were determined using GPC relative to PMMA standards in THF at 40 °C. $M_{n,target} = 30$ kg mol^{-1} was considered for all statistical copolymerizations.
[e] Initial concentration of components in polymerization medium.
[f] NMP of GMA/C13MA in 50 wt% dioxane using Dispolreg 007 at 90 °C. GMAxx/C13MAyy shows the initial molar feed composition, where xx is the mol% GMA and yy is the mol% C13MA.
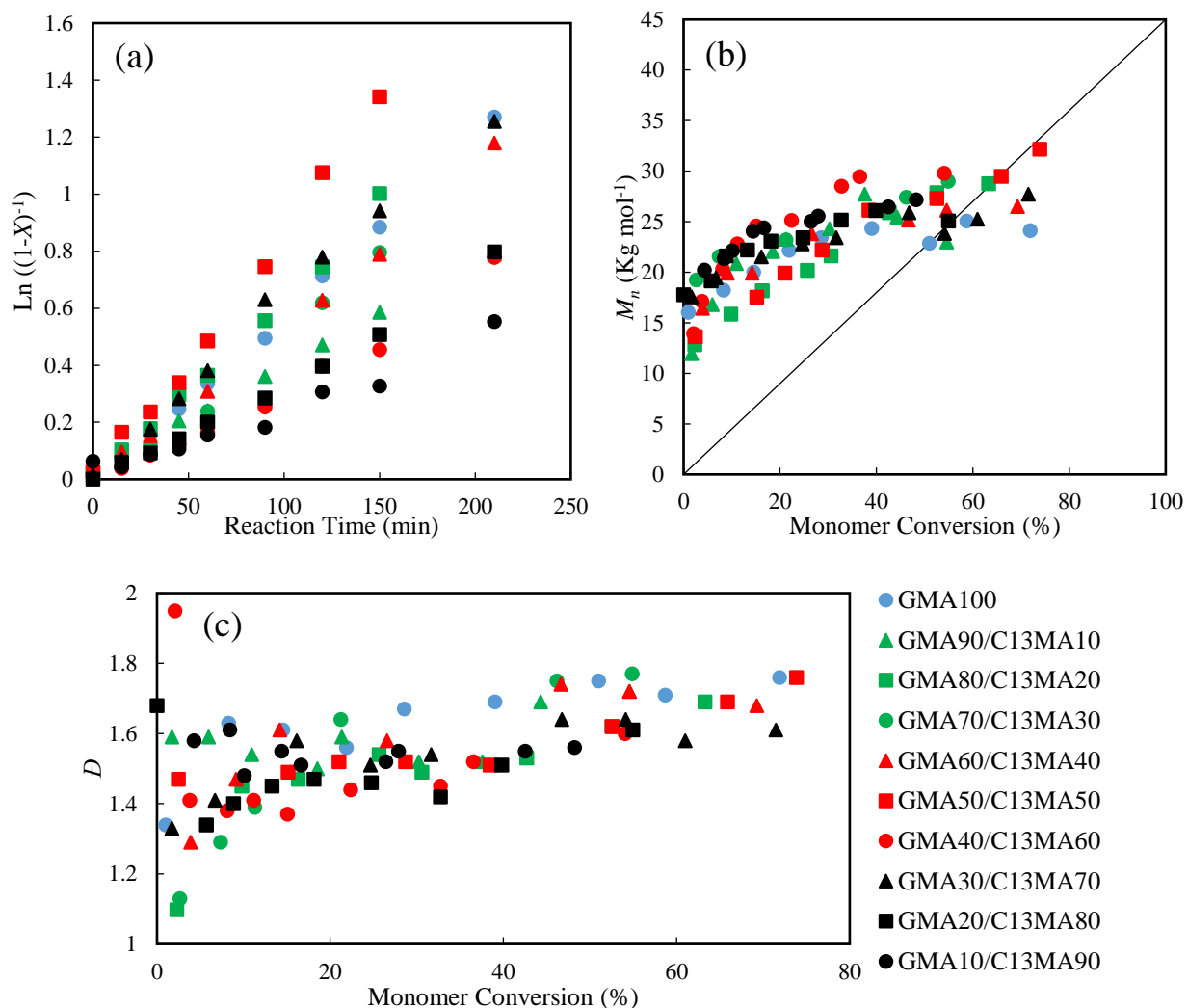
Figure 9.3. Nitroxide mediated statistical copolymerization of GMA/C13MA using Dispolreg 007 in dioxane at 90 °C. The complete kinetic results and polymerization conditions are provided in Table 9.1. a) semi-logarithmic kinetic plots of $\ln[(1-X)^{-1}]$ ($X=$ monomer conversion) versus reaction time b) the evolution of number average molecular weight (M_n) with conversion (X) c) dispersity ($Đ$) versus conversion (X).
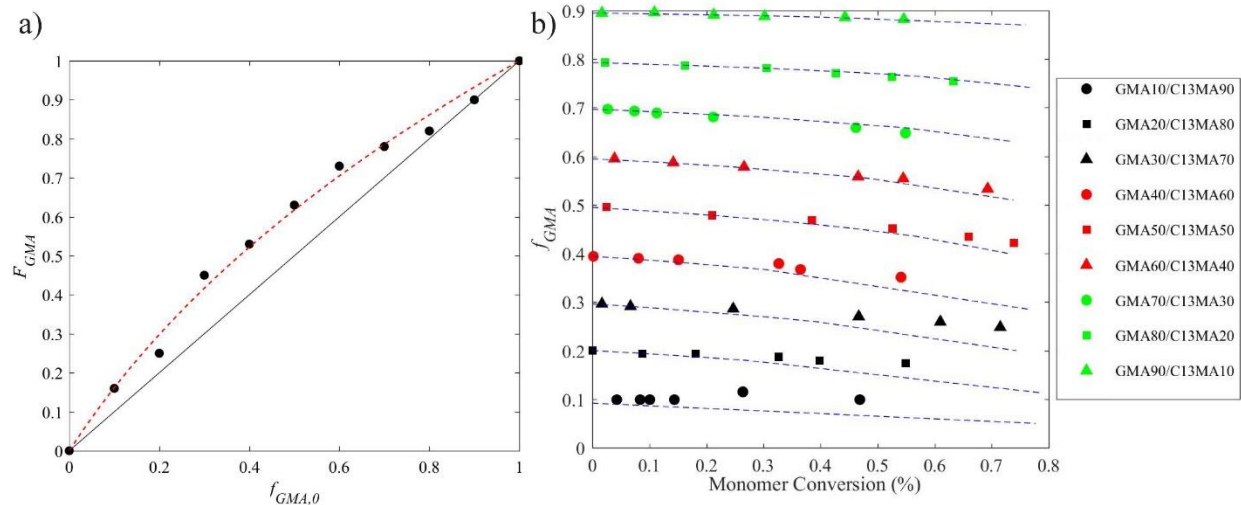
Figure 9.4. a) Mayo-Lewis plot of GMA in copolymer composition (F_{GMA}) with respect to initial GMA molar feed composition ($f_{GMA,0}$) (The dashed red line is the fitted curve with $R^2 = 0.99$). The black line shows the theoretical azeotropic composition ($F_{GMA} = f_{GMA,0}$) for statistical copolymerization of GMA/C13MA. b) The drift in GMA molar feed (f_{GMA}) with monomer conversion for copolymerization with different ratios of GMA/C13MA. The fitted curves were determined with $r_{GMA} = 1.17 \pm 0.09$ and $r_{C13MA} = 0.65 \pm 0.09$ from the Meyer Lowry method.

9.3.3. Gradient copolymerization of GMA/C13MA

Two gradient copolymers were prepared starting from GMA-based or C13MA-based macroinitiators. Table 9.2 describes the polymerization conditions and polymer properties for gradient copolymers starting from GMA-based macroinitiator (GMA-*grad*-C13MA) and C13MA-based macroinitiator (C13MA-*grad*-GMA). The conversion trends in Figure 9.5a were linear for the synthesis of macroinitiators and for the chain extensions, although a delay in polymerization can be observed due to the addition of second monomer to the polymerization medium. A similar trend was also determined for M_n versus X plots (Figure 9.5b). However, the strong penultimate effect and the slow decomposition of initiator and nitroxide in Dispolreg 007 alkoxyamine resulted in M_ns higher than theoretically predicted in the beginning of polymerization[28, 43, 290]. Once the second monomer was added to the system, the reaction temperature decreased, and the polymerization rate was reduced. The chain extension continued after reaching the reaction temperature of 90 °C. In addition, change in the slope of $\ln((1-X)^{-1})$ versus time was observed for gradient copolymerizations after the addition of the second monomer. This shows two different apparent rate constant $k_P[P^•]$ (k_P = propagation rate constant and $[P^•]$ is the concentration of active macroradicals) for the synthesis of GMA or C13MA macroinitiators (poly(GMA) and poly(C13MA)) compared to gradient copolymerization with the second monomer. In addition, the conversion plots over time displayed a higher

slope (i.e. $k_P[P^•]$) for GMA homopolymerization (poly(GMA)) compared to C13MA (poly(C13MA)) before the addition of second monomer, suggesting a faster polymerization rate, probably due to the concentration effects. Based on the results on gradient copolymerization of GMA/C13MA, listed in Table 9.2, the change in $Đ$ was not significant after the addition of second monomer and chain extension. The $Đ$ values during the polymerizations are shown in Figure 9.5c.

Table 9.2. Experimental conditions and polymer characteristics for preparation of block copolymers of GMA/C13MA in 50 wt% dioxane using Dispolreg 007 at 90 °C.

GMA-*grad*-C13MA								
Experiment ID	$f_{GMA,0}{}^a$	X^c (%)	$M_n{}^d$ $(kg\ mol^{-1})$	$Đ^d$	$[Dispolreg]_0$ (M)	$[GMA]_0$ (M)	time (min)	$V_{0,\ Dioxane}{}^e$ (mL)
Poly(GMA)	1	24.8	26.5	1.75	0.012	3.678	90	
	$F_{GMA}{}^b$	X^c (%)	$M_n{}^d$ $(kg\ mol^{-1})$	$Đ^d$	$[C13MA]_0$ (M)	time (min)		13
GMA-*grad*-C13MA	0.88	37.8	35.7	1.79	0.718	240		
C13MA-*grad*-GMA								
Experiment ID	$F_{C13MA,0}{}^a$	X^c (%)	$M_n{}^d$ $(kg\ mol^{-1})$	$Đ^d$	$[Dispolreg]_0$ (M)	$[C13MA]_0$ (M)	time (min)	$V_{0,\ Dioxane}{}^e$ (mL)
Poly(C13MA)	1	12.3	21.3	1.57	0.011	1.762	90	
	$F_{GMA}{}^b$	X^c(%)	$M_n{}^d$ $(kg\ mol^{-1})$	$Đ^d$	$[GMA]_0$ (M)	time (min)		13
C13MA-*grad*-GMA	0.22	25.8	27.6	1.60	0.416	240		

[a] Initial molar fraction of GMA in the initial feed, considering only GMA and C13MA monomers.
[b] Molar fraction of GMA in polymer composition as determined by ^{1}H NMR in CDCl$_3$.
[c] Final monomer conversion (%).
[d] The final number average molecular weight (M_n) and dispersity ($Đ$) were determined using GPC relative to PMMA standards in THF at 40 °C.
[e] Volume of dioxane added at the beginning and was constant during the polymerization[mL] (assuming no evaporation).

Figure 9.5. Nitroxide mediated gradient copolymerization of GMA/C13MA for preparation of GMA-*grad*-C13MA (black circles ●, M_n = 35.7 kg mol^{-1}, Đ = 1.79) and C13MA-*grad*-GMA (red triangles ▲, M_n = 27.6 kg mol^{-1}, Đ = 1.60) in 1,4-dioxane at 90 °C. Full characterization results for gradient copolymerization of GMA/C13MA are available in Table 9.2. The results were shown before and after addition of the second monomer to reaction. a) semi-logarithmic kinetic plots of ln[(1-*X*)$^{-1}$] (*X*= total monomer conversion) versus reaction time b) the evolution of M_n with total monomer conversion (*X*) c) the evolution of Đ with conversion (*X*). d and e) The shift in GPC peaks for gradient copolymerization of GMA/C13MA.

9.3.4. Block copolymers of GMA/C13MA

The experimental conditions for block copolymerization of GMA/C13MA and final polymer characteristics are shown in Table 9.3. To prepare block copolymers of GMA/C13MA, first, a GMA-based and C13MA-based macroinitiator (GMA-MI (M_n = 32.9 kg mol^{-1}, Đ = 1.52) and C13MA-MI (M_n = 33.1 kg mol^{-1}, Đ = 1.68), respectively) were synthesized. Figure 9.6 (black circles) presents the kinetic results for the

preparation of macroinitiators. As it was shown in Figure 9.6a and 6c, the $k_P[P^\bullet]$ value (slope in conversion plots) for the preparation of GMA-MI ($k_P[P^\bullet]_{GMA-MI} = 6.8\times10^{-5} \pm 10^{-6}$ s^{-1}) was higher than that of C13MA-MI ($k_P[P^\bullet]_{C13MA-MI} = 2.8\times10^{-5} \pm 10^{-6}$ s^{-1}) under similar experimental conditions. This showed a faster polymerization rate for GMA-MI, which can be simply due to concentration effects. The chain extension of macroinitiators with the second monomer is shown in kinetic plots with red triangles (Figure 9.6). The GMA-b-C13MA and C13MA-b-GMA block copolymers were designed to be GMA-rich ($F_{GMA} = 0.81$) and C13MA-rich ($F_{GMA} = 0.36$) polymers, respectively. The trend of scaled conversion over time was linear for both the synthesis of macroinitiators and the subsequent chain extensions to the block copolymers. However, the $k_P[P^\bullet]$ changed after the chain extension with the second monomer, displaying different polymerization rates for the two monomers in question. The semi-logarithmic kinetic plots for chain extension of GMA-MI and C13MA-MI showed monomer conversion at $t = 0$, indicating the polymerization before starting point (t=0 min) at temperatures lower than 75 °C. The linear trend was also observed for M_ns versus conversions, which showed the predictable control of the polymerizations. The higher initial values for M_ns were detected in the synthesis of macroinitiators. This was due to measuring M_ns relative to PMMA standards in addition to the strong penultimate effect of Dispolreg 007 alkoxyamine[28, 436]. For GMA-b-C13MA and C13MA-b-GMA experiments, Đ of macroinitiators slightly increased after chain extension (Đ increased from 1.52 to 1.78 for GMA-b-C13MA experiment and from 1.68 to 1.89 for C13MA-b-GMA experiment). However, the linear increase of M_n with X (Figure 9.6 b and d) and the shift in monomodal GPC peak of polymers with chain extension (Figure 9.6 e and f) suggested a high chain end fidelity for macroinitiators and successful controlled block copolymerization of GMA/C13MA.

Table 9.3. Experimental conditions and kinetic results for preparation of block copolymers of GMA/C13MA.

GMA-b-C13MA								
Macroinitiator	$f_{GMA,0}$[a]	X [c] (%)	M_n [d] (kg mol^{-1})	Đ[d]	[Dispolreg]$_0$[e] (M)	[GMA]$_0$ (M)	[Dioxane]$_0$ (M)	time (min)
GMA-MI	1	32.4	32.9	1.52	0.012	3.678	5.978	90
Chain extension	F_{GMA}[b]	X [c] (%)	M_n [d] (kg mol^{-1})	Đ[d]	[MI]$_0$ [f] (M)	[C13MA]$_0$ (M)	[Dioxane]$_0$ (M)	time (min)
GMA-b-C13MA	0.81	28.1	43.1	1.78	0.005	0.787	8.883	240
C13MA-b-GMA								
Macroinitiator	$F_{C13MA,0}$[a]	X [c] (%)	M_n [d] (kg mol^{-1})	Đ[d]	[Dispolreg]$_0$[e] (M)	[C13MA]$_0$ (M)	[Dioxane]$_0$ (M)	time (min)
C13MA-MI	1	14.9	33.1	1.68	0.011	1.762	5.408	90

Chain extension	$F_{GMA}{}^b$	X^c (%)	$M_n{}^d$ (kg mol^{-1})	$Đ^d$	$[MI]_0{}^f$ (M)	$[GMA]_0$ (M)	$[Dioxane]_0$ (M)	time (min)
C13MA-*b*-GMA	0.36	39.9	43.0	1.89	0.007	1.309	9.656	180

[a] Initial molar fraction of GMA in the initial feed, considering only GMA and C13MA monomers.

[b] Molar fraction of GMA in polymer composition as determined by ^{1}H NMR in CDCl$_3$.

[c] Final monomer conversion (%).

[d] The final number average molecular weight (M_n) and dispersity ($Đ$) were determined using GPC relative to PMMA standards in THF at 40 °C.

[e] Initial concentration of components in polymerization medium.

[f] Initial concentration of macroinitiator for chain extension.
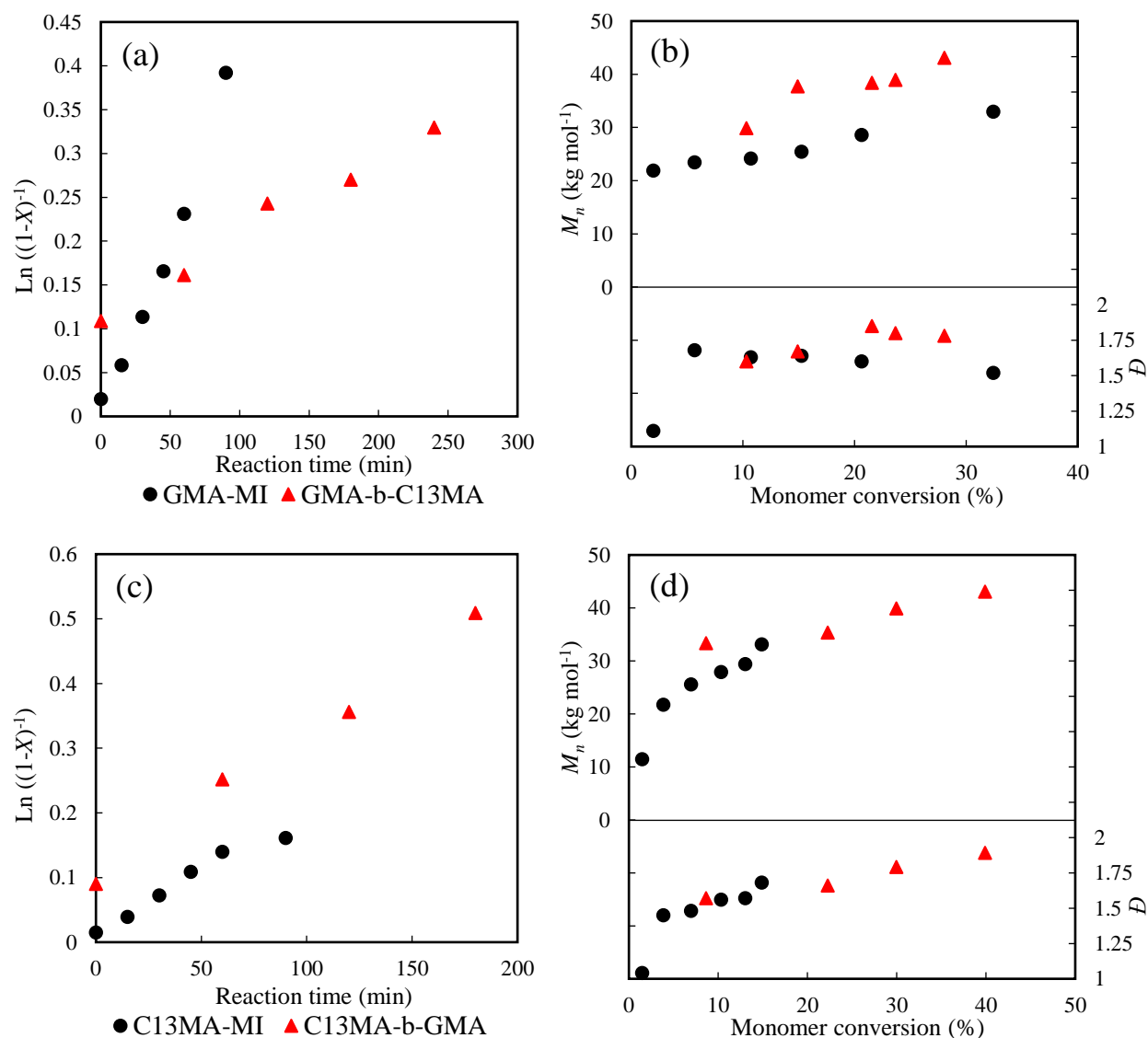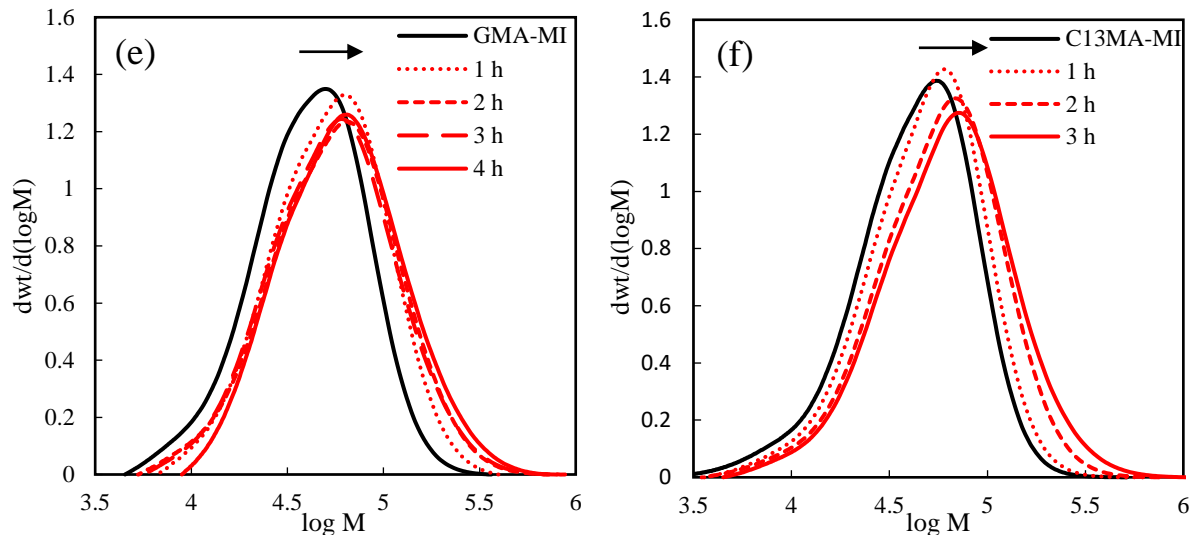
Figure 9.6. Kinetic results for preparation of GMA-*b*-C13MA (a, b and e) and C13MA-*b*-GMA (c, d and f) block copolymers (red triangles ▲) by chain extension of GMA-MI and C13MA-MI macroinitiators (black circles ●) in dioxane at 90 °C. The experimental conditions and polymers' characteristics were listed on Table 9.3. a) and c) semi-logarithmic kinetic plots of $\ln[(1-X)^{-1}]$ ($X=$ monomer conversion) versus reaction time b) and d) the evolution of M_n and $Đ$ with monomer conversion (X) e) and f) The shift in GPC peaks after the chain extension of macroinitiators.

9.3.5. Triblock copolymerization of GMA/C13MA

Preparation of triblock polymers of GMA/C13MA started with the synthesis of macroinitiators with two active chain ends. A bifunctional alkoxyamine based on Dispolreg 007 was used to produce GMA-based bifunctional macroinitiator (Bi-GMA-MI, M_n = 19.9 kg mol^{-1}, $Đ$ = 1.58) and C13MA-based bifunctional macroinitiator (Bi-C13MA-MI, M_n = 24.1 kg mol^{-1}, $Đ$ = 1.46). The chain extension of these two macroinitiators with the second monomer (GMA or C13MA; different from the monomers in bifunctional macroinitiator) resulted in GMA/C13MA triblock copolymers with M_n = 43.0-45.5 kg mol^{-1}, $Đ$ = 1.70-1.85 and 58-71 mol% GMA in copolymer composition. The results for triblock copolymerization of GMA/C13MA are listed in Table 9.4. Figures 9.7 and 9.8 present the kinetic data for Bi-GMA-*tri*-C13MA (C13MA-GMA-C13MA triblock) and Bi-C13MA-*tri*-GMA (GMA-C13MA-GMA triblock) experiments, respectively. A change in polymerization rate can be observed for synthesis of macroinitiators and chain extension due to the chain growth with different monomers (GMA or C13MA). Interestingly, no noticeable sign of slow initiation or pronounced penultimate effect associated with Dispolreg 007 (i.e. high M_n values at low conversions) can be observed for NMP with D7-based bifunctional macroinitiators. Figure 9.7c and 8c display the complete shift in polymer GPC peaks by chain extension of macroinitiators for 120 minutes. For Bi-GMA-*tri*-C13MA, a semi-bimodal GPC peak can be observed in Figure 9.7c. To estimate the

percentage of dead chains, multiple Gaussian peak fitting was performed for GPC peak after 2 hours (Figure 9.S3, Supplementary Information). It was shown that 37% of the polymers are dead chains. The semi-bimodal molecular weight distribution was not observed for chain extension of Bi-C13MA-MI, suggesting a comparatively higher chain-end fidelity for macroradicals in Bi-C13MA-*tri*-GMA experiment.

Table 9.4. Experimental conditions and kinetic results for preparation of triblock copolymers of GMA/C13MA.

Bi-GMA-*tri*-C13MA								
Macroinitiator	$f_{GMA,0}{}^a$	X^c (%)	$M_n{}^d$ (kg mol^{-1})	$Đ^d$	$[Bi\text{-}D7]_0{}^e$ (M)	$[GMA]_0$ (M)	$[Dioxane]_0$ (M)	time (min)
Bi-GMA-MI	1	45.7	19.9	1.58	0.006	3.673	5.986	75
Chain extension	$F_{GMA}{}^b$	X^c (%)	$M_n{}^d$ (kg mol^{-1})	$Đ^d$	$[MI]_0{}^f$ (M)	$[C13MA]_0$ (M)	$[Dioxane]_0$ (M)	time (min)
Bi-GMA-*tri*-C13MA	0.58	31.0	43.0	1.85	0.006	1.578	6.065	120
Bi-C13MA-*tri*-GMA								
Macroinitiator	$f_{C13MA,0}{}^a$	X^c (%)	$M_n{}^d$ (kg mol^{-1})	$Đ^d$	$[Bi\text{-}D7]_0{}^e$ (M)	$[C13MA]_0$ (M)	$[Dioxane]_0$ (M)	time (min)
Bi-C13MA-MI	1	41.7	24.1	1.46	0.005	1.759	5.416	75
Chain extension	$F_{GMA}{}^b$	X^c (%)	$M_n{}^d$ (kg mol^{-1})	$Đ^d$	$[MI]_0{}^f$ (M)	$[GMA]_0$ (M)	$[Dioxane]_0$ (M)	time (min)
Bi-C13MA-*tri*-GMA	0.71	49.2	45.5	1.70	0.006	2.823	7.306	120

[a] Initial molar fraction of GMA in the initial feed, considering only GMA and C13MA monomers.

[b] Molar fraction of GMA in polymer composition as determined by ^{1}H NMR in CDCl$_3$.

[c] Final monomer conversion (%).

[d] The final number average molecular weight (M_n) and dispersity ($Đ$) were determined using GPC relative to PMMA standards in THF at 40 °C. $M_{n,target}$ = 45 kg mol^{-1} was considered for preparation of macroinitiators

[e] Initial concentration of bifunctional Dispolreg 007-based alkoxyamine for preparation of macroinitiators in 50 wt% dioxane.

[f] Initial concentration of macroinitiator for chain extension.

Figure 9.7. Preparation of triblock copolymer of GMA/C13MA (Bi-GMA-*tri*-C13MA, red triangles ▲, $M_n = 43.0$ kg mol^{-1}, $Đ = 1.85$) by chain extension of bifunctional GMA-based macroinitiator (Bi-GMA-MI, black circles ●, $M_n = 19.9$ kg mol^{-1}, $Đ = 1.58$) for 2h in dioxane at 90 °C. a) semi-logarithmic kinetic plots of ln[(1-X)$^{-1}$] (X= monomer conversion) versus reaction time b) the evolution of M_n with conversion (X) c) GPC peaks for macroinitiator and triblock copolymers d) the evolution of $Đ$ with conversion (X).

Figure 9.8. Preparation of triblock copolymer of GMA/C13MA (Bi-C13MA-*tri*-GMA, red triangles ▲, $M_n = 45.5$ kg mol⁻¹, Đ = 1.70) by chain extension of C13MA-based bifunctional macroinitiator (Bi-C13MA-MI, black circles ●, $M_n = 24.1$ kg mol⁻¹, Đ = 1.46) for 2h in dioxane at 90 °C. a) semi-logarithmic kinetic plots of ln[(1-X)⁻¹] (X= monomer conversion) versus reaction time b) the evolution of M_n with conversion (X) c) GPC peaks for macroinitiator and triblock copolymers d) the evolution of Đ with conversion (X).

9.3.6. Thermal properties of GMA/C13MA copolymers

The thermal properties of statistical, gradient, diblock and triblock copolymers of GMA/C13MA were investigated by DSC and TGA. Table 9.5 reports the T_gs, T_ms and decomposition temperatures (T_{dec}s) and Figure 9.9a shows the DSC curves for GMA/C13MA statistical copolymers. The $-53 \leq T_g \leq 21$ and $T_g = 68$ °C were measured for the statistical copolymers and GMA homopolymer, respectively. To compare, $T_g = 44$-76 °C for GMA homopolymers and $T_g = -46$ °C for homopolymers of tridecyl methacrylate have been

reported[201, 525-529]. For statistical copolymers, T_ms were observed for copolymers, when $F_{C13MA} \geq 0.20$ in polymer compositions. The appearance of T_ms at low temperatures and two different T_gs correspond to the formation of C13MA blocks[162, 181, 347]. The difference in reactivity ratios ($r_{GMA} = 1.17 \pm 0.09$ and $r_{C13MA} = 0.65 \pm 0.09$) is not significant enough to suggest blockiness in the microstructure. The solubility parameters of GMA/C13MA (C13MA ($\delta = 15.43$ MPa$^{1/2}$) and GMA ($\delta = 19.25$ MPa$^{1/2}$))[530] are sufficiently different to consider micro-phase separation. This was also shown in our previous studies on nitroxide mediated copolymerization of monomers (IBOMA or POSSMA) with C13MA with different reactivity ratios and solubility parameters initiated by Dispolreg 007[162, 210]. Similar DSC curves were also detected for polymers prepared from methyl methacrylate, GMA and butyl acrylate[531]. Another reason for the appearance of two different T_gs or T_m for statistical GMA/C13MA copolymers is the formation of side-chain alkyl crystallites for the comb-like polymers containing alkyl methacrylates[532-534]. The T_g at higher temperature associated with the polymer backbone segmental motion and the T_g or T_m at lower temperatures (T < -19 °C) is due to the side alkyl chains away from the backbone[532, 535, 536].

Furthermore, self-assembly could be another reason for detection of two distinct T_gs in statistical copolymers containing monomers with long side branches[354, 357]. Many studies showed the self-assembly for GMA-containing copolymers[537, 538]. Zhu et al[539] reported the self-assembly for poly(ethylene oxide)-block-poly(GMA) (M_n of methoxy poly(ethylene oxide) = 1900 g mol^{-1}). Self-assembly was also reported for RAFT-mediated emulsion polymerization of GMA and poly(ethylene glycol) methyl ether methacrylate ($M_n = 500$ g mol^{-1})[526]. A low T_g of -46 °C was reported for poly(tridecyl methacrylate) in the literature[201, 269]. In addition, C13MA monomer might contain alkyl methacrylates with longer or shorter aliphatic side-chains. For instance, T_ms of -34 °C and -2 °C were determined for poly(dodecyl methacrylate) and poly(tetradecyl methacrylate), respectively[201, 293, 294]. For C13MA homopolymer ($M_n = 20.0$ kg mol^{-1} and Đ = 1.59) synthesized by NMP (in toluene using Dispolreg 007 at 110 °C), the T_m = -18 °C and T_g = -31 °C were indicated. For gradient copolymerization of GMA and C13MA, the C13MA-*grad*-GMA polymer with F_{C13MA} = 0.78 showed a T_m = -19 °C due to the high concentration of C13MA in the copolymer. However, no T_m was observed for GMA-*grad*-C13MA (F_{C13MA} = 0.12) and T_g of 50 °C was obtained for the polymer sample. For block copolymers of GMA and C13MA, T_ms and T_gs were observed for the C13MA and GMA blocks, suggesting micro-phase separation for GMA/C13MA block copolymers. This was also confirmed in our previous study on a block copolymer of GMA/C13MA ($M_n = 25.3$ kg mol^{-1} and Đ = 1.87, F_{GMA} = 0.83) by estimation of the solubility parameters for C13MA and GMA from Hansen solubility parameters[540]. The micro phase separation and two different T_gs were detected for triblock copolymers of GMA/C13MA when the macroinitiator was C13MA-based (Figure 9.9d). However, only one T_m at -20 °C was indicated for Bi-GMA-*tri*-C13MA polymers (prepared from GMA-based macroinitiator).

The decomposition temperatures are listed in Table 9.5 and the TGA curves are presented in Figure 9.10. For all the GMA/C13MA copolymers, three peaks were observed in the derivative weight (%/°C) versus temperature (°C) graphs, showing the temperature regions with highest decomposition rates (Figure 9.S4-S7, Supplementary Information). The first decomposition temperature peak ($T_{dec,1}$) was between 191 and 249 °C for GMA/C13MA statistical copolymers. For the statistical copolymers, the second peak ($T_{dec,2}$) was in the temperature range of 292-335 °C and the third decomposition peak ($T_{dec,3}$) was at the higher temperature range of 332-415 °C. The existence of different thermal degradation regions for GMA-based polymers can be due to the formation of volatile intermediate products, including carbon dioxide, acrolein, allyl alcohol and glycidyl methacrylate, during thermal degradation analysis[541]. Hasanzadeh et al[516] also suggested that the appearance of the thermal degradation peaks for GMA homopolymers in the temperature range of 250-370 °C can be due to the degradation of pendent ester groups and loss of CO_2. The T_{dec} for 10% weight loss ($T_{dec,10\%}$) (Table 9.5) was slightly higher for polymers with more than 80 mol% GMA in polymer composition. This was also the case for final decomposition temperature ($T_{dec,final}$). However, no significant improvement of maximum decomposition temperature ($T_{dec,max}$) with increasing the GMA content was found. Interestingly, $T_{dec,max}$ emerged at $T_{dec,2}$ for statistical copolymers with compositions above 75 mol% GMA. As the C13MA in polymer composition increased, the $T_{dec,max}$ shifted to higher temperatures and $T_{dec,3}$ was more dominant. The $T_{dec,max}$s were equal to $T_{dec,3}$s for gradient, triblock and diblock copolymers of GMA/C13MA, except GMA-*b*-C13MA. In the case of GMA-*b*-C13MA, the semi-bimodal peak at 253- 408 °C was considered as $T_{dec,2}$ and the peak at 408-469 °C was corresponded to $T_{dec,3}$. However, the value of $T_{dec,max}$ for GMA-*b*-C13MA was in the $T_{dec,max}$ range of gradient, deblock and triblock copolymers prepared in this study. The appearance of $T_{dec,3}$ for GMA-*b*-C13MA at 408-469 °C is probably due to the formation of GMA monomers by cleavage in the GMA-blocks and elimination of them at higher temperatures[541]. For GMA/C13MA statistical copolymers, ash content up to 13.1 wt% was obtained by increasing the temperature up to 600 °C under N_2. For GMA homopolymer and GMA/C13MA block copolymers the ash content was approximately 6.6 and 6 wt%, respectively. This is consistent with Zulfiqar et al's[541] study that reported high ash content (8 wt%) during TGA of GMA homopolymer (M_n = 7250 g mol^{-1}) at 450 °C (heating rate = 10 °C min^{-1}; N_2 atmosphere). Ash content up to 12 wt% was also observed for TGA of GMA/acrylonitrile (AN) statistical copolymers at 500 °C (under N_2; heating rate = 10 °C min^{-1}) prepared by conventional radical polymerization[542]. In another study, Kaya et al[543] reported the thermal stability of copolymers of GMA with methyl, ethyl and butyl methacrylate (M_n = 440-555 kg mol^{-1}, Đ = 1.28-1.59 and polymer composition of GMA/MMA [62:38], GMA/EMA [56:44], GMA/BMA [59:41] (mol%/mol%)). Comparing the thermal properties of GMA/MMA, GMA/EMA and GMA/BMA copolymers with GMA/C13MA copolymers with approximately similar compositions suggest no

significant change in thermal stability or ash content of the copolymers for copolymers with longer alkyl groups, although the polymerization process and TGA procedure were different. Thus, GMA can be copolymerized with the bio-based C13MA instead of synthetic monomers to improve the physical properties of polymers without compromising the thermal stability of copolymers.

Table 9.5. Thermal characterization of POSSMA containing polymers prepared by NMP in solution (solvent: toluene) and miniemulsion.

Experiment ID	T_g^a (°C)	T_m^a (°C)	$T_{dec,10\%}^b$ (°C)	$T_{dec,max}^b$ (°C)	$T_{dec,1}^b$ (°C)	$T_{dec,2}^b$ (°C)	$T_{dec,3}^b$ (°C)	$T_{dec,final}^b$ (°C)	F_{GMA}^c	M_n^d (kg mol^{-1})	Ash content (%)
Statistical copolymers											
GMA100	68.0	-	234	342	219	342	421	485	1	24.1	6.6
GMA90/C13MA10	21	-	254.5	335	191	335	415	464	0.92	23.0	7.0
GMA80/C13MA20	-53, 11	-43	237	292	249	292	363	453	0.81	28.8	12.6
GMA70/C13MA30	-50, 8	-36	221.25	296	225	296	335	446	0.75	29.0	13.1
GMA60/C13MA40	-49, 3	-40	228	332	225	304	332	445	0.65	26.5	6.2
GMA50/C13MA50	-47, -1	-38	214	295	248	295	363	454	0.53	32.2	0.5
GMA40/C13MA60	-34	-25	219.25	338	225	303	338	440	0.45	29.8	7.8
GMA30/C13MA70	-33	-26	227.75	342	226	304	342	444	0.35	27.7	6.7
GMA20/C13MA80	-26	-20	225.25	338	248	299	338	441	0.24	25.1	2.2
GMA10/C13MA90	-23	-19	211.5	299	238	299	342	439	0.09	27.2	2.1
Gradient copolymers											
GMA-*grad*-C13MA	50	-	232	372	235	309	372	486	0.88	35.7	0.5
C13MA-*grad*-GMA	-	-19	147	348	169	297	348	431	0.22	27.6	0
Diblock copolymers											
GMA-*b*-C13MA	-31, 49	-24	247	351	190	351	424	486	0.81	43.1	6.2
C13MA-*b*-GMA	18	-20	231	350	226	299	350	437	0.36	43.0	6.1
Triblock copolymers											
Bi-GMA-*tri*-C13MA	-	-20	186	347	199	273	347	472	0.58	43.0	0
Bi-C13MA-*tri*-GMA	-28,34	-20	212	387	264	320	387	486	0.71	45.5	0

[a] Glass transition temperature (T_g) and melting point (T_m) determined by DSC under N_2 atmosphere using three scans per cycle (heat/cool/heat) at a heating rate of 15 °C min^{-1} and cooling rate of 50 °C min^{-1}.

[b] $T_{dec,10\%}$ (decomposition temperature for 10% weight loss), $T_{dec,max}$ (maximum decomposition temperature), $T_{dec,1}$, $T_{dec,2}$, $T_{dec,3}$ (The first, second and third peak in derivative weight (%/°C) versus temperature (°C) graphs) and $T_{dec,final}$ (end of decomposition) measured by TGA under N_2 atmosphere at a ramp rate of 15 °C min^{-1}. Graphs of derivative weight (%/°C) versus temperature (°C) for all polymers are available in Figure 9.S4 to 9.S7, Supplementary Information. The blue cells in Table 9.5 show the TGA peaks where $T_{dec,max}$ occurred.

[c] Molar fraction of GMA in polymer composition indicated by ^{1}H NMR in CDCl$_3$.

[d] The final number average molecular weight (M_n) was estimated using GPC with PMMA standards at 40 °C in THF.

Figure 9.9. DSC curves a) statistical copolymers b) gradient polymers c) block copolymers and d) triblock copolymers of GMA/C13MA in temperature range of -80 to 130 °C. T_gs and T_ms of polymers are presented in Table 9.5.
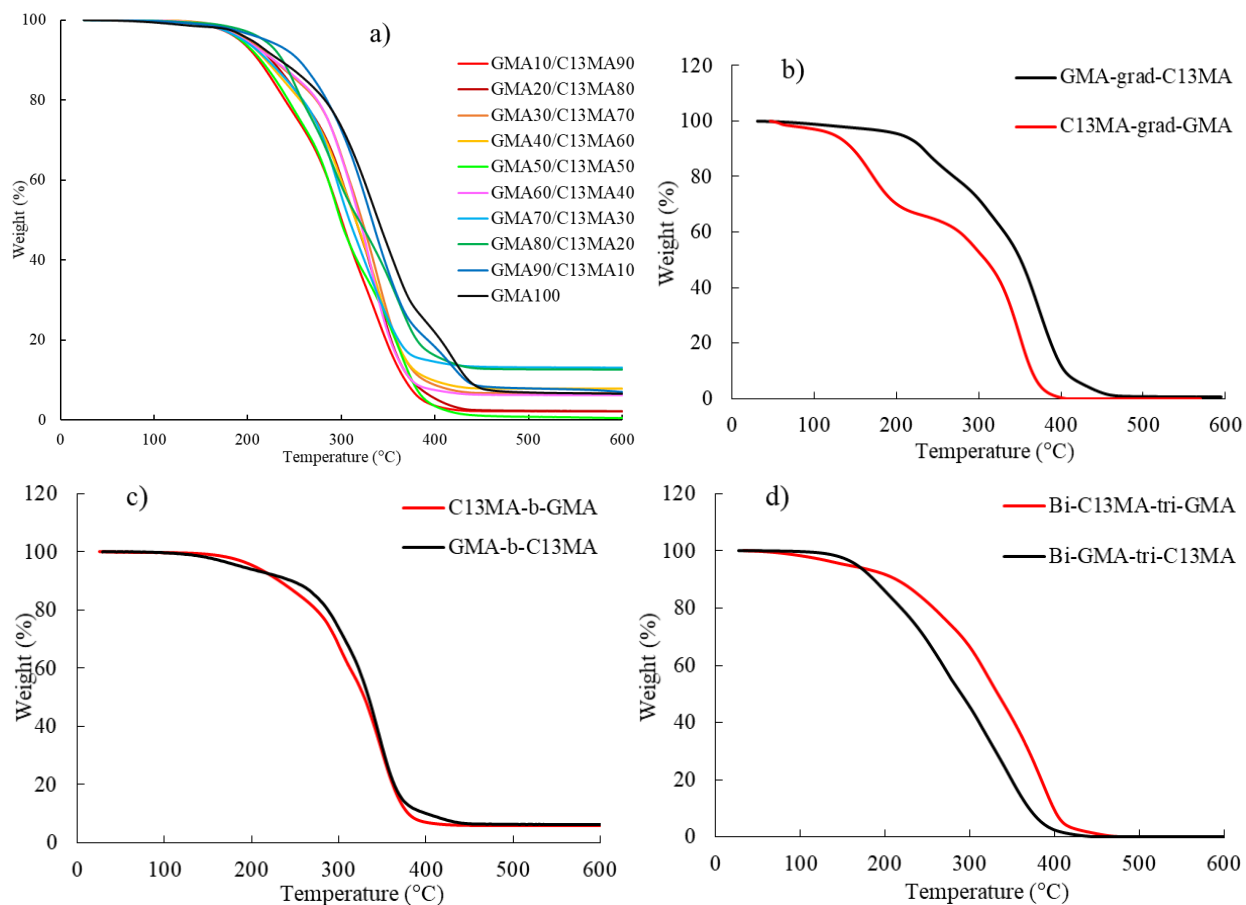
Figure 9.10. TGA curves a) statistical copolymers b) gradient polymers c) block copolymers and d) triblock copolymers of GMA/C13MA with heating rate of 15 °C min^{-1} in temperature range of 25-600 °C. The decomposition temperatures (T_{dec}s) are listed in Table 9.5.

9.3.7. Rheological Measurements

The effect of GMA and C13MA blocks on the rheological properties of copolymers was investigated using oscillatory frequency sweep experiments at 30 °C. The low temperature of 30 °C was chosen for rheological measurements as the diblock, triblock and gradient copolymers were soft at room temperature. Figure 9.11 shows the results of rheological measurements performed with gradient, block and triblock copolymers. From the oscillatory experiments, G′ and G″ increased with increase in angular frequency, although the rate of increase in G″ was higher than G′. At lower frequencies, G′> G″ and a rubbery behavior can be observed for GMA-*grad*-C13MA. At 10 rad s^{-1}, a crossover occurred (relaxation time = 0.63 s) and a viscoelastic liquid region with G″> G′ was observed. This is due to dissipation of energy and consequential relaxation of polymer structure at higher frequencies[301, 303, 304]. A similar rheological behavior was also determined for

GMA/C13MA triblock copolymers. However, the crossovers for Bi-GMA-*tri*-C13MA and Bi-C13MA-*tri*-GMA occurred at 200 and 100 rad s[-1], respectively. The difference between the values of G′ and G″ at a given frequency in the solid region was higher for Bi-GMA-*tri*-C13MA compared to Bi-C13MA-*tri*-GMA or GMA-*grad*-C13MA. This suggests the comparatively stiffer polymer structure for Bi-GMA-*tri*-C13MA due to higher Van der Waals interactions between polymer chains. Furthermore, G′ for Bi-GMA-*tri*-C13MA remained constant at frequencies < 200 rad s[-1]. For C13MA-*grad*-GMA polymer, G″ dominated G′ in all frequencies, suggesting a viscous liquid behavior. A similar trend was also obtained for GMA-*b*-C13MA with comparatively higher values of G′ and G″. The domination of G″ over G′ (viscoelastic liquid state) was observed for C13MA-*b*-GMA at the wide frequency range of 1 to 628 rad s[-1]. The crossover frequency was at 1 rad s[-1] and G′> G″ for frequencies lower than 1 rad s[-1]. Finally, the complex viscosity was higher for the gradient, block and triblock polymers with higher GMA content, showing stronger interactions between polymer chains with higher GMA ratios[544].
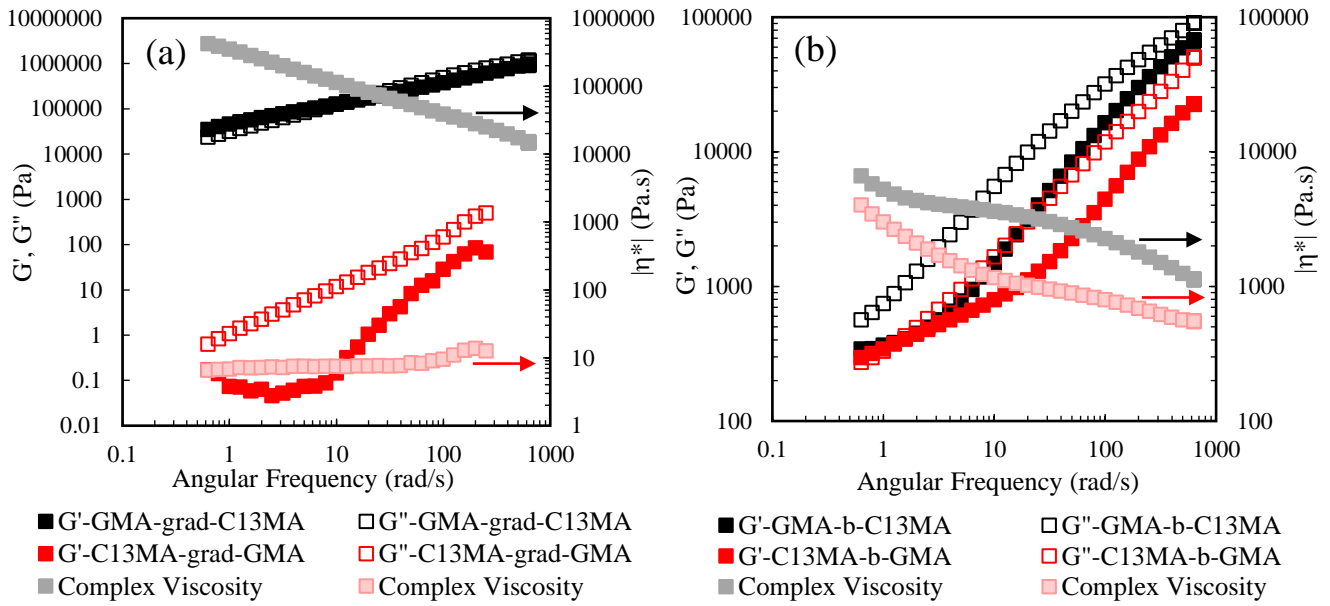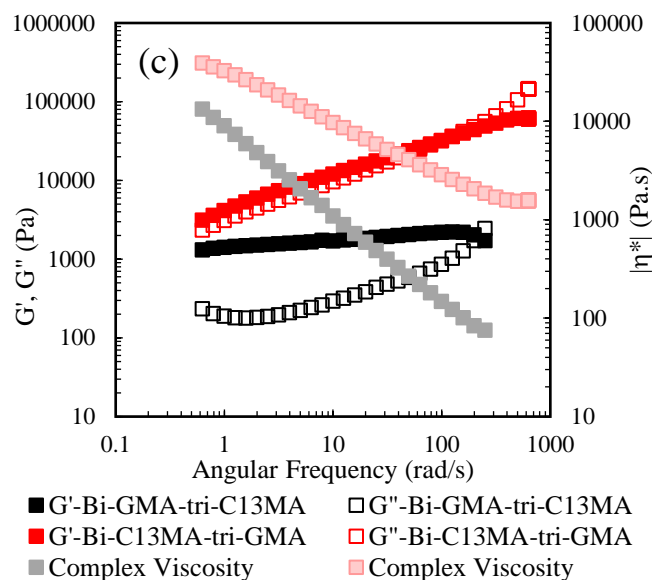
188

Figure 9.11. Storage modulus (G′), loss modulus (G″) and complex viscosity versus angular frequency (1% strain) for a) GMA/C13MA gradient, b) block and c) triblock copolymers at 30 °C.

9.4. CONCLUSIONS

Nitroxide mediated copolymerization of GMA/C13MA was conducted in 50 wt% dioxane using Dispolreg 007 alkoxyamine at 90 °C. Statistical copolymers of GMA/C13MA (M_n = 23-32 kg mol^{-1} and Đ = 1.56-1.77) with different compositions and -53 °C ≤ T_g ≤ 21 °C were synthesized. The slow initiation and penultimate effect of Dispolreg 007 resulted in higher M_ns at low monomer conversions (X < 50 %) compared to the theoretical prediction. Two distinct T_gs and a T_m were observed for GMA/C13MA copolymers with F_{GMA} = 0.5-0.8 due to the incorporation of C13MA and possible micro-phase separation (reactivity ratios = r_{GMA} = 1.17 ± 0.09 and r_{C13MA} = 0.65 ± 0.09; solubility parameters = δ_{C13MA} = 15.43 MPa$^{1/2}$ and δ_{GMA} = 19.25 MPa$^{1/2}$). GMA-*grad*-C13MA (M_n = 35.7 kg mol^{-1} and Đ = 1.79) and C13MA-*grad*-GMA (M_n = 27.6 kg mol^{-1} and Đ = 1.60) gradient copolymers showed different thermal and rheological behaviors. T_g = 50 °C and T_m = -19 °C were measured for GMA-*grad*-C13MA and C13MA-*grad*-GMA, respectively. GMA-*grad*-C13MA had a crossover at 10 rad s^{-1}, indicating the transition from solid rubbery state to a viscous liquid at higher frequencies. However, a viscous liquid behavior was observed for C13MA-*grad*-GMA at all frequencies. Block copolymers of GMA-*b*-C13MA (F_{GMA}= 0.81, M_n = 43.1 kg mol^{-1} and Đ =1.78) and C13MA-*b*-GMA (F_{GMA}= 0.36, M_n = 43.0 kg mol^{-1} and Đ =1.89) showed T_ms, corresponded to C13MA blocks, at -20 °C and -24 °C and T_gs at 49 °C and 18 °C probably due to GMA blocks. The similar DSC trends were also presented for triblock copolymers of GMA/C13MA

(Bi-GMA-*tri*-C13MA (M_n = 43.0 kg mol^{-1} and Đ = 1.85); Bi-C13MA-*tri*-GMA (M_n = 45.5 kg mol^{-1} and Đ = 1.70)). For diblock copolymers, a viscous liquid behavior was observed at frequencies higher than 1 rad s^{-1}. The Bi-GMA-*tri*-C13MA and Bi-C13MA-*tri*-GMAwere in solid state at low frequencies with respective crossover frequencies at 200 and 100 rad s^{-1} to reach liquid viscous region at higher frequencies up to 1000 rad s^{-1}. A higher thermal stability (i.e. higher $T_{dec,10\%}$; $T_{dec,max}$ and $T_{dec,final}$) were determined for gradient, diblock and triblock copolymers with higher GMA content during TGA. This suggests the importance of GMA blocks on improving the thermal degradation stability of polymer resins. However, no significant and meaningful improvement in thermal stability was observed for statistical copolymers of GMA/C13MA, although polymers with $F_{GMA} \geq 0.9$ had the highest $T_{dec,max}$ and $T_{dec,final}$ (Table 9.5). During the TGA under N_2, three thermal degradation regions with peaks at $T_{dec,1}$, $T_{dec,2}$ and $T_{dec,3}$ were detected. This shows the formation of intermediate species during the thermal degradation study and their further breakdown at higher temperatures. For statistical copolymers of GMA/C13MA, the ash content up to 13 wt% was achieved at 600 °C under N_2, suggesting the possibility of high flame retardancy. In addition, the remaining ash of block copolymers at 600 °C was 6 wt %. However, no significant ash content (less than 0.5 wt%) was collected for gradient or triblock copolymers of GMA/C13MA.

ACKNOWLEDGMENTS

Chapter 10: Conclusions and future work

10.1. Conclusions

The main objective of this thesis was to develop various functional polymers that can be used in different wood coating formulations. We divided our study into several steps to prepare the polymer coatings. The synthesized polymers with different properties such as anti-flammability, self-healing and good adhesion can eventually be coated on a wood surface as separate layers. Each polymer layer can introduce a new functionality to the final polymer coating and enhance the applicability of the coating formulation. Three following steps were considered for preparation of polymers in this thesis:

- Preparation of water-borne polymers using monomers with high bio-content.
- Development of self-healing polymers with high bio-carbon content.
- Alternative approach to synthesize epoxy-based polymer resins for wood coatings.

To synthesize the polymers in all three steps, nitroxide mediated polymerization (termed as NMP) was carried out in organic solvents and miniemulsion. Using controlled radical polymerization (herein termed as reversible deactivation radical polymerization (RDRP), of which NMP is one variant), control over the polymerization increased (compared to the conventional radical polymerization) and polymers with lower dispersities and viscosities were produced. Furthermore, NMP was easy to apply and no post-polymerization treatment was required to remove catalysts, ligands or chain transfer agents. Chapters 3, 4, 5 and 6 investigated the preparation of polymers with high bio-content in miniemulsion. For the first time, IBOMA/C13MA copolymers were synthesized using two different approaches by miniemulsion polymerization. The first approach was to initiate the nitroxide mediated miniemulsion polymerization of IBOMA/C13MA (10 mol% AN controlling monomer) by SG1-based amphiphilic macroinitiators. The effect of additives (i.e. surfactant and co-stabilizer) and different reaction temperatures on NMP of IBOMA in miniemulsion was studied, indicating the best control over the polymerization (linear increase of M_n with X and $Đ$ = 1.71) in the presence of 2 wt% DOWFAX 8390 and 0.8 wt% n-hexadecane at 90 °C. However, the two-step polymerization (preparation of macroinitiator in toluene and the miniemulsion polymerization of monomers) and high $Đ$ values ($Đ$ = 1.7-2.2) for NMP of IBOMA/C13MA in miniemulsion limited the industrial application of this method. Next, the NMP of IBOMA/C13MA was done in miniemulsion using Dispolreg 007 alkoxyamine. Using this oil-soluble alkoxyamine, the complexity of the polymerization procedure (e.g. one step polymerization without the addition of controlling comonomers) decreased and polymers with lower $Đ$ ($Đ$ = 1.5-1.7) were produced. The glass transition temperature (T_g) of polymers was

modified by changing the ratio of IBOMA ($T_{g,IBOMA}$ =110~200 °C) and C13MA ($T_{g,C13MA}$ =-46 °C) in polymer chains. As a result, IBOMA/C13MA copolymers with -52 °C < T_g <123 °C were synthesized.

Subsequently, the incorporation of POSSMA for enhancing the thermal stability of polymers was investigated. First, the possibility of nitroxide mediated miniemulsion polymerization of POSSMA using Dispolreg 007 alkoxyamine was examined and POSSMA homopolymers (M_n up to 35.9 kg mol^{-1} and $Đ <$ 1.53) and POSSMA/C13MA copolymers (M_n up to 50.2 kg mol^{-1} and 1.42 < $Đ$ < 1.68) were successfully produced. The POSSMA/C13MA copolymers had -39 °C < T_g and T_m < 96 °C. Then, the polymerization of POSSMA/IBOMA/C13MA was conducted in miniemulsion using Dispolreg 007 alkoxyamine at 90 °C (M_n up to 46.7 kg mol^{-1} and $Đ$ < 1.65). It was shown that the decomposition temperature for 10% weight loss ($T_{dec,1}$) of polymers improved by 23 °C by 10 mol% increase in POSS ratio in initial monomer feed. This is a modest improvement despite the literature stating the dramatic effect POSS-containing species have on thermal stability in polymers.

Further studies were focused on preparation of self-healing polymers with high bio-carbon content (high IBOMA and C13MA content) in organic solvents and miniemulsion. Two polymers of IBOMA/C13MA/AN/VPBA (M_n up to 35.1 kg mol^{-1} and 1.65 < $Đ$ < 2.13) and IBOMA/C13MA/AN/ GMMA (M_n of 26.3 kg mol^{-1} and 1.67 < $Đ$ < 2.73) were synthesized by NMP in 1,4-dioxane at 90 °C. The polymers were mixed together to prepare polymer blends with boronic ester dynamic cross-linking bonds. The hardness, mechanical properties and T_g of polymers were modified by changing the molar ratios of monomers in the initial monomer feed. The polymer blends healed scratches after 12 days at ambient temperature and humidity and recovered 87% tensile strength and 48% strain after cutting and healing for 10 days at ambient condition. To prepare polymers containing boronic ester dynamic covalent bonds in miniemulsion, a dimer of VPBA and GMMA was synthesized before the miniemulsion polymerization to improve the hydrophobicity of VPBA and GMMA and enhance their availability inside the monomer droplets for polymerization. After the polymerization, the polymer latexes were cast and dried to form a polymer coating containing boronic ester cross-linking bonds. The polymers showed high recyclability at 80 °C for 45 minutes and could absorb a high amount of toluene (ultimate swelling ratio up to 153%) in a relatively short time (t= 300 min). In this study, for the first time, boronic ester bonds were successfully incorporated into polymer chains by miniemulsion polymerization.

Finally, the NMP of GMA/C13MA was studied as an alternative for the proposed wood coating formulation. The epoxy-based monomer of GMA had excellent adhesion to the wood surfaces and can easily react with bifunctional amines to form permanent covalent bonds for cross-linking. In contrast to the polymer coatings containing dynamic amine-ketone crosslinking, the coatings with permanent epoxy-

amine crosslinking can provide the good adhesion to the wood surface and prevent the polymer coating from melting at elevated temperatures or in the presence of flame. Statistical GMA/C13MA copolymers with different molar ratios of monomers were synthesized by NMP using Dispolreg 007 in 50 wt% 1,4-dioxane at 90 °C. The GMA/C13MA statistical copolymers (M_n = 23-32 kg mol^{-1} and $Đ$ = 1.56-1.77) had -53 °C ≤ T_g ≤ 21 °C. Ash content up to 13 wt% was observed for GMA/C13MA statistical copolymers at 600 °C under N_2, indicating the possibility of high flame retardancy. Furthermore, gradient, diblock and triblock copolymers of GMA/C13MA were produced to study the effect of GMA or C13MA blocks on the thermal, mechanical and rheological properties of the polymers. Accordingly, GMA blocks improved the thermal degradation stability of polymer and resulted in ash content of 6 wt% for diblock copolymers. However, no significant ash content was detected for gradient or triblock copolymers of GMA/C13MA. Based on the results, the statistical copolymers of GMA/C13MA can be used as an alternative polymer coating formulation for wood surfaces due to their high thermal stability and ash content and good adhesion to veneers.

10.2. Suggestions for future direction of research

In this thesis, polymers with high bio-carbon content were prepared in miniemulsion. We also developed self-healing polymers containing boronic ester covalent bonds in organic solvents and miniemulsion. The author suggests further investigations in the following topics:

- Improving the bio-content of polymers by using alternative monomers with higher bio-carbon content. As an example, the NMP or photoinduced metal free ATRP of limonene (T_g~ 10 °C) or vanillin methacrylate (T_g~ 180 °C) can be considered.
- The suspension polymerization of the monomers for the similar formulations to reduce the surfactant concentration and avoid intensive agitation.
- Rheological measurements for polymer latexes with different solid contents. This can help with finding the optimum viscosity and highest solid content required for spray coating.
- Enhancing the flame-retardancy properties of polymers by incorporating phosphate-based monomers (e.g. ethylene glycol methacrylate phosphate) into the polymer chains using emulsion polymerization. Sulfur-free RAFT polymerization can be employed to avoid the cross-linking side reactions.
- Study the effect of environmental conditions (i.e. temperature, humidity) on the film formation of the synthesized polymer latexes.
- Development of self-healing polymers containing POSSMA or phosphate-based monomers for higher thermal stability and anti-flammability properties. This can be done by preparation of the

block copolymers or the addition of the POSSMA-based or phosphate-based polymers as additives to the self-healing coating.

- Incorporation of IBOMA into GMA/C13MA copolymers to improve the hardness and bio-content of polymer resins.
- Addition of multi-functionalized amines for the formation of amine-epoxy cross-linking bond in GMA/C13MA polymers for preparation of polymer coatings.

Supporting Information
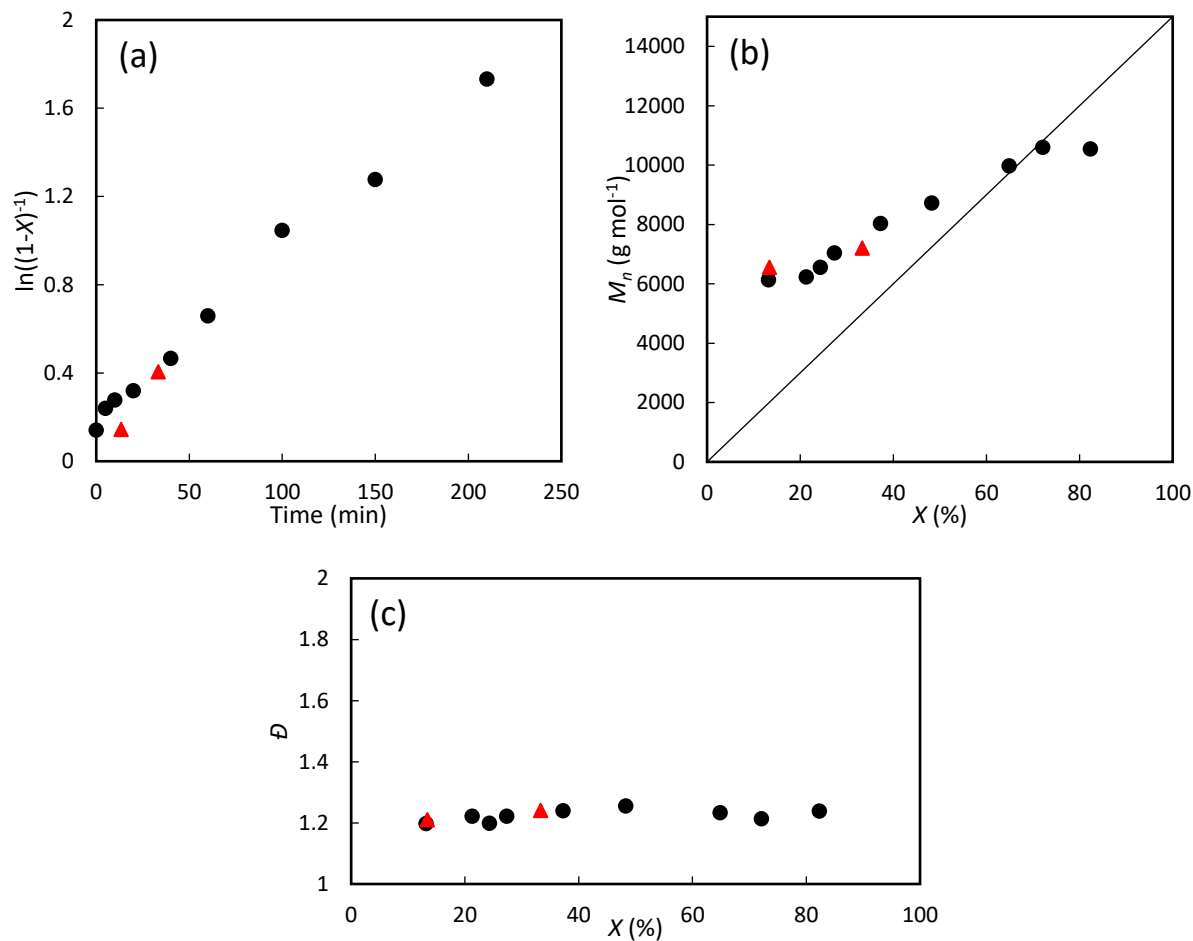
Figure 3.S1 Kinetic results for nitroxide mediated emulsion polymerization of PEGMA monomers with 10 mol% AN as the controlling comonomer (filled circles, ●); and for the synthesis of p(PEGMA-*co*-AN) macroinitiator (red triangles, ▲). (a) Semi-logarithmic kinetic plots of $\ln[(1-X)^{-1}]$ (X= monomer conversion) versus reaction time (b) Number average molecular weight M_n versus conversion (X). (c) dispersity $Đ$ versus conversion (X).
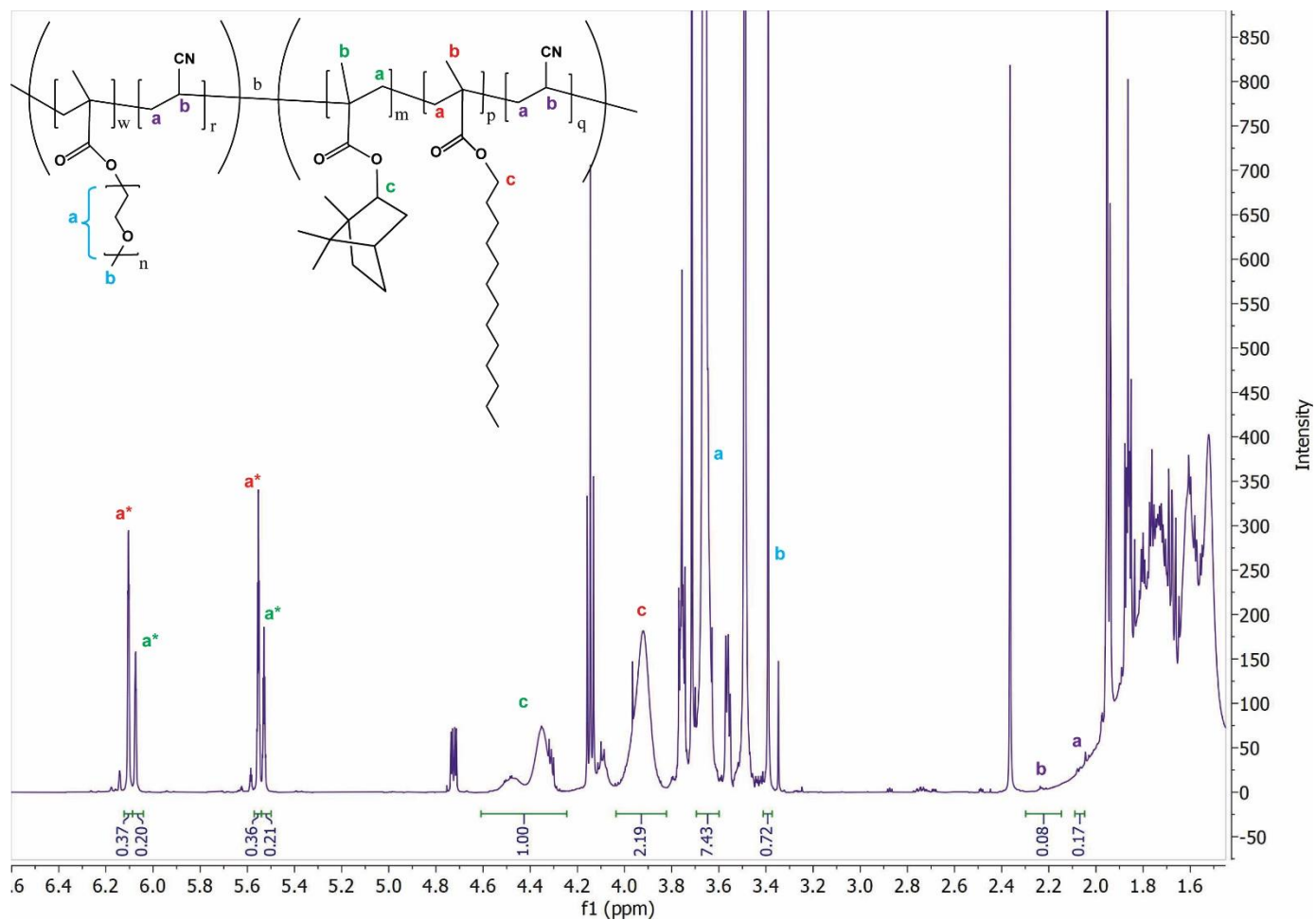
Figure 3.S2. ^{1}H NMR spectra for IBOMA45/C13MA45/AN10 after 150 minutes of polymerization using p(OEGMA-*stat*-AN) macroinitiator. * corresponds to unreacted monomers. ^{1}H NMR (CDCl$_3$, 500 MHz, ppm): 6.09-6.12 (m, 1 H^{C13MA}), 6.04-6.09 (m, 1 H^{IBOMA}), 5.54-5.57 (m, 1 H^{C13MA}), 5.50-5.54 (m, 1 H^{IBOMA}), 4.25-4.61 (d, 1 H$^{p(IBOMA)}$), 3.82-4.04 (s, 2 H$^{p(C13MA)}$), 3.60-3.69 (m, 10 H$^{p(OEGMA)}$), 3.37-3.41 (s, 3 H$^{p(OEGMA)}$), 2.14-2.30 (m, 1 H$^{p(AN)}$), 2.05-2.09 (m, 2 H$^{p(AN)}$).

SUPPORTING INFORMATION: CHAPTER 4

S4.1. The Composition of Copolymers at the Early Stages of Polymerization

Table 4.S1. The composition of copolymers at the early stages of polymerization determined by ^{1}H NMR.

Experiment ID	$f_{IBOMA,0}$ [a]	$F_{IBOMA,15min}$ [b]	X_{15min} [c] (%)
IBOMA80/C13MA20-S	0.8	0.75	13.6
IBOMA60/C13MA40-S	0.6	0.54	16.7
IBOMA50/C13MA50-S	0.5	0.41	7.5
IBOMA40/C13MA60-S	0.4	0.27	11.6
IBOMA30/C13MA70-S	0.3	0.19	14.8
IBOMA20/C13MA80-S	0.2	0.12	11.4
IBOMA10/C13MA90-S	0.1	0.10	12.1

[a] Initial molar fraction of IBOMA in the initial feed.
[b] Molar fraction of IBOMA in copolymers after 15 minutes of polymerization determined by ^{1}H NMR in CDCl₃.

[c] monomer conversion after 15 minutes of polymerization measured by ^{1}H NMR.

S4.2. Temperature Studies in Solution Polymerization

The homopolymerization of IBOMA (Experiment ID = IBOMA100-S-90C, IBOMA100-S-100C and IBOMA100-S-110C) and C13MA (Experiment ID = C13MA100-S-90C, C13MA100-S-100C and C13MA100-S-110C) were carried out at various temperatures of 90, 100 and 110 °C to find the optimal reaction temperature required to keep a proper control over the polymerization while having high polymerization rate in toluene. Figure 4.S1(a) and (b) (Supplementary Information) present the kinetic plots for IBOMA and C13MA homopolymers at different temperatures and shows an increase in polymerization rate by increasing the reaction temperature. As Figure 4.S1(c) and (d) in the Supplementary Information indicate, the number average molecular weight $\overline{M}_n$ of samples was higher than the theoretical linear prediction at low monomer conversions. This can be due to the slow decomposition rate of the Dispolreg 007 alkoxyamine which decreases the number of initial active polymer chains and increases the average molecular weight of samples [28, 515]. However, $\overline{M}_n$ increases linearly with conversion at 90 and 100 °C, suggesting control of the polymerization was adequate. At 110 °C, $\overline{M}_n$ of samples deviates more from the predicted linear relationship, especially at higher conversion, suggesting a difficult control over the polymerization of methacrylates at higher temperatures. The curvature at higher conversions indicates a decrease in concentration of propagating macro-radicals [P•], a higher concentration of dead chains and an increase in irreversible termination reactions[345]. This phenomenon was also observed in our previous study regarding the polymerization of IBOMA and C13MA using BlocBuilder-MA™ (BB, Arkema) as the

initiator[182]. The higher dispersity at higher conversions is a result of slow initiation of alkoxyamines which causes the polymer chains with different lengths and also the chain transfer reactions within the system at longer reaction time due to decrease in propagating events[103, 515, 545]. Finally, the optimal temperature for solution polymerization was considered to be 100 °C due to linear evolution of $\bar{M}_n$ with conversion up to relatively high conversions, relatively low dispersity (For poly(IBOMA) : Đ < 1.54 and poly(C13MA): Đ < 1.39) and relative high polymerization rate in solution (43% conversion within 45 min for poly(IBOMA) and 34% conversion within 45 min for poly(C13MA).

199
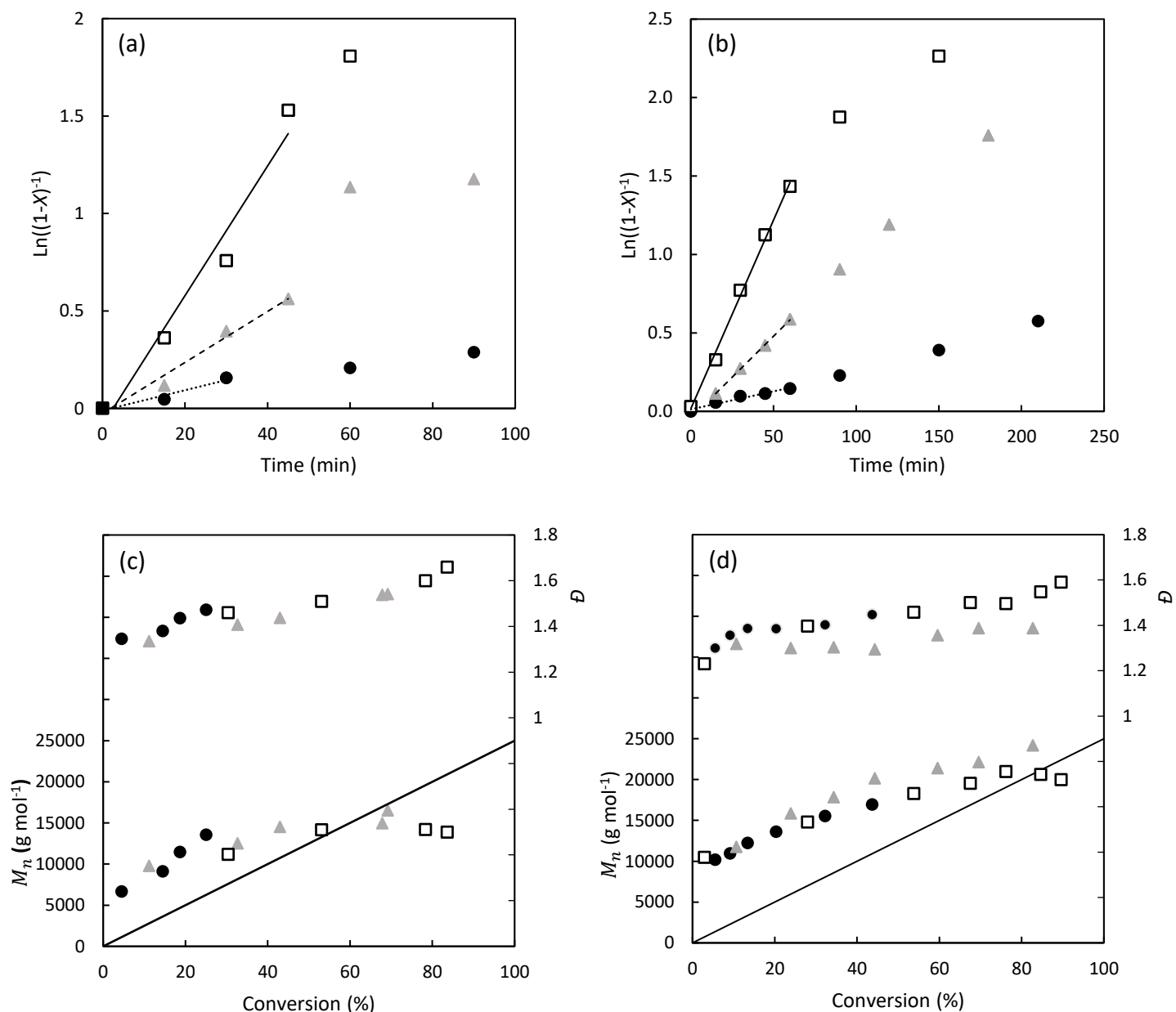
Figure 4.S1. The effect of various reaction temperatures on the homopolymerization of IBOMA and C13MA using Dispolreg 007 initiator in toluene. Semi-logarithmic kinetic plots of $\ln[(1-X)^{-1}]$ (X= monomer conversion) versus reaction time for (a) IBOMA (b) C13MA at different temperatures. Number average molecular weight M_n and dispersity Đ versus conversion (X) for (c) IBOMA and (d) C13MA at different temperatures. (a) and (b): IBOMA100-S-90C (filled circles, ●); IBOMA100-S-100C (gray triangles, ▲); IBOMA100-S-110C (open squares, □). (c) and (d): C13MA100-S-90C (filled circles, ●); C13MA100-S-100C (gray triangles, ▲); C13MA100-S-110C (open squares, □).

S4.3. Multiple Gaussian Peak Fitting for Estimation of Dead Polymer Chains in Poly(IBOMA-*b*-C13MA)
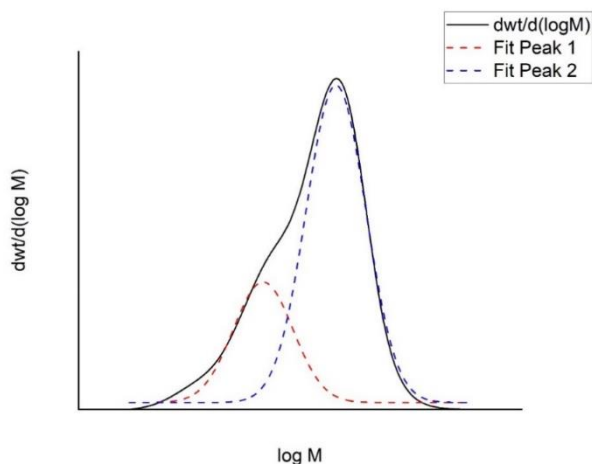
Figure 4.S2. Multiple Gaussian peak fitting for estimation of the percentage of dead polymer chains for Poly(IBOMA-*b*-C13MA) at 180 minutes after chain extension. Solid black line represents the GPC chromatogram and dashed lines Isolated Gaussian peaks for dead chains and living and active polymer chain.

S4.4. Temperature Studies in Miniemulsion Polymerization
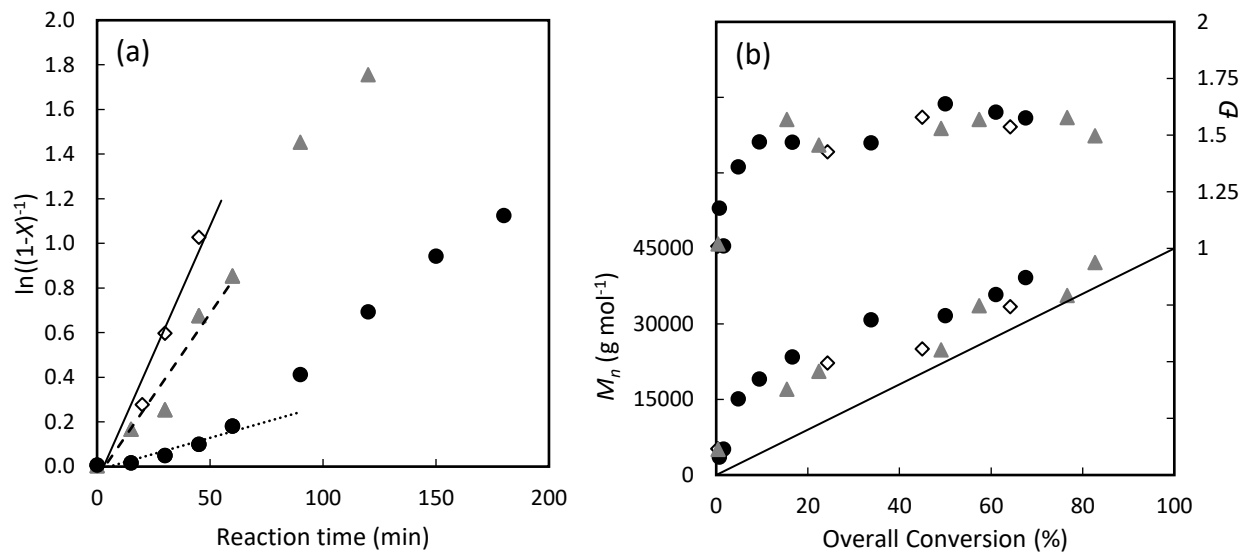
Figure 4.S3. The effect of temperature on nitroxide mediated miniemulsion polymerization of IBOMA using Dispolreg 007 initiator (a) Semi-logarithmic kinetic plots of $\ln[(1-X)^{-1}]$ (X= monomer conversion) versus polymerization time (b) Number average molecular weight M_n and $Đ$ versus conversion (X). IBOMA100-83C (filled circles, ●); IBOMA100-90C (gray triangles, ▲); IBOMA100-100C (open diamonds, ◊).

S4.5. Particle Size in Miniemulsion Polymerization
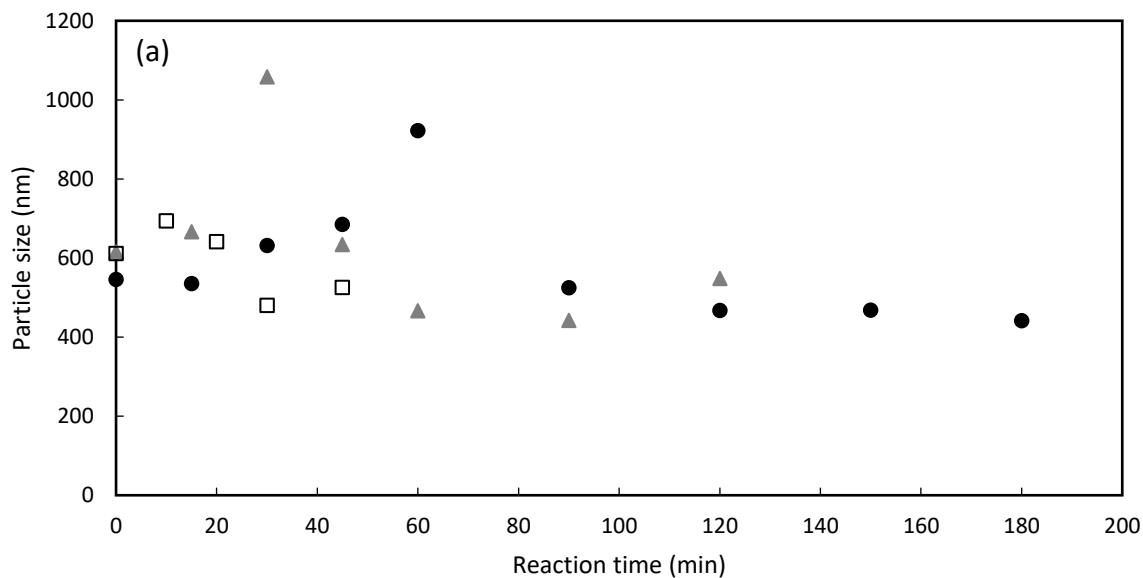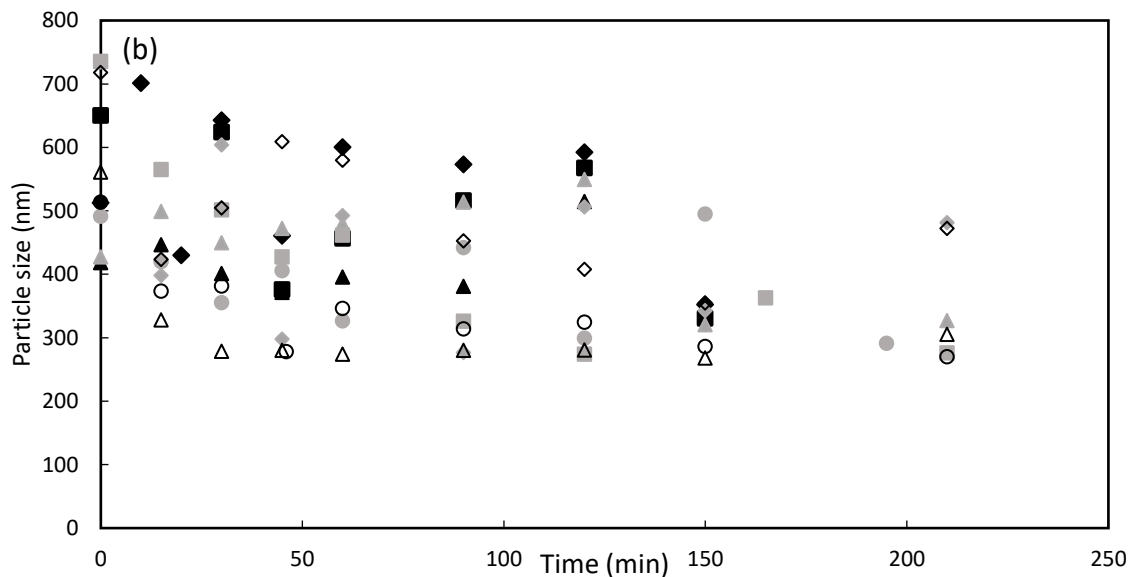
Figure 4.S4. (a) The effect of reaction temperature on particle size during the homopolymerization of IBOMA monomers using Dispolreg 007 alkoxyamine, 2 wbm% DOWFAX 8390 and 0.8 wbm% n-hexadecane. IBOMA100-83C (filled circles, ●); IBOMA100 (gray triangles, ▲); IBOMA100-100C (open diamonds, ◊); (b) Z-average particle size for copolymerization of different ratios of IBOMA/C13MA monomers over reaction time using Dispolreg 007 alkoxyamine, 2 wbm% DOWFAX 8390 and 0.8 wbm% n-hexadecane. IBOMA100 (filled circles, ●); IBOMA90/C13MA10 (filled triangles, ▲); IBOMA80/C13MA20 (filled diamonds, ♦); IBOMA70/C13MA30 (filled squares, ■); IBOMA60/C13MA40 (gray circles, ●); IBOMA50/C13MA50 (gray triangles, ▲); IBOMA40/C13MA60 (gray diamonds, ♦); IBOMA30/C13MA70 (gray squares, ■); IBOMA20/C13MA80 (open circles, ○); IBOMA10/C13MA90 (open triangles, Δ); C13MA100 (open diamonds, ◊).

S4.6. DSC Trace for p(C13MA-*grad*-IBOMA) Gradient Copolymer
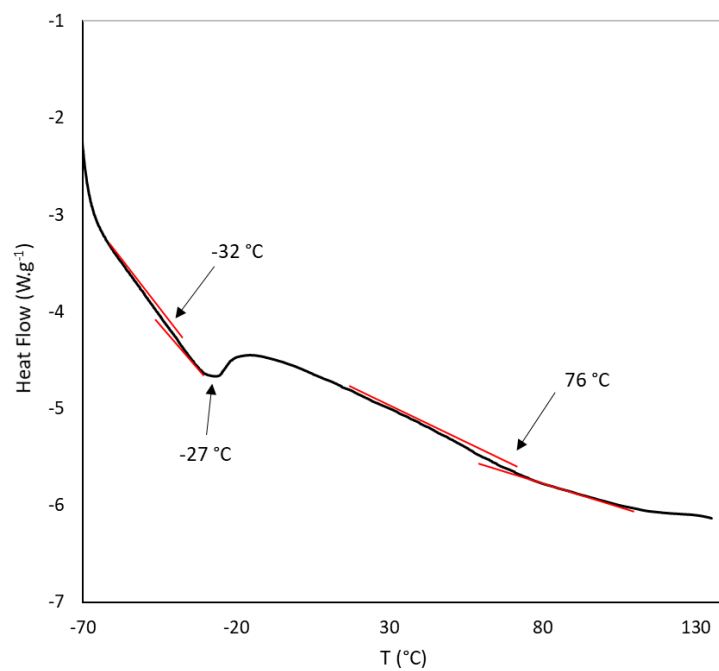
Figure 4.S5. DSC trace for p(C13MA-*grad*-IBOMA) gradient copolymer.

S4.7. PXRD Results
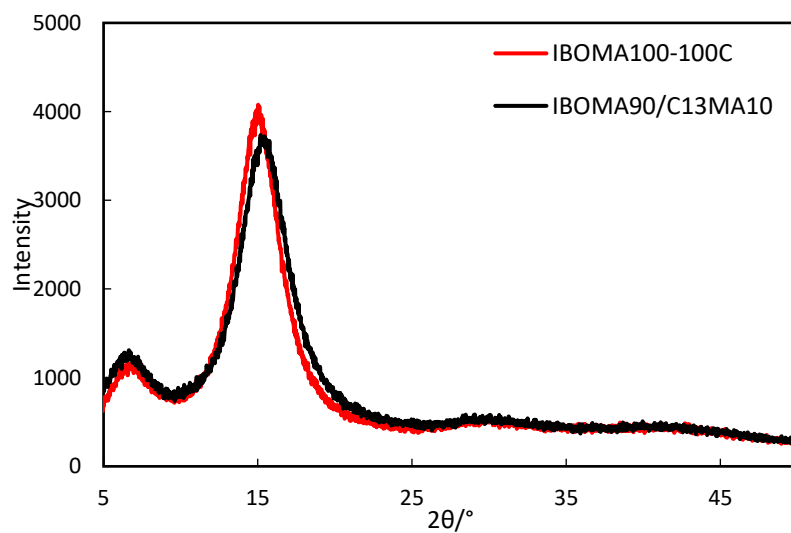
Figure 4.S6. PXRD patterns of IBOMA100-100C and IBOMA90/C13MA10 in miniemulsion system.

S4.8. Rheological Measurements
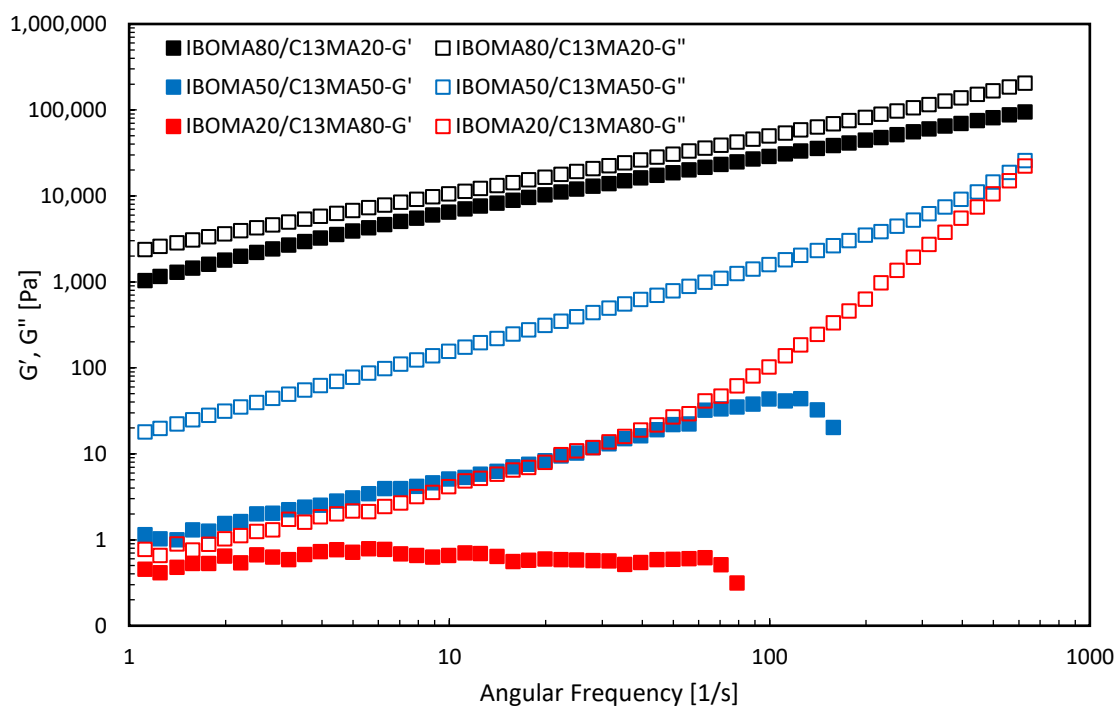
Figure 4.S7. G′ and G″ plots versus shearing frequency for IBOMA80/C13MA20 (black squares, □ and ■); IBOMA50/C13MA50 (blue squares, □ and ■) and IBOMA20/C13MA80 (red squares, □ and ■) statistical copolymers at 140 °C.
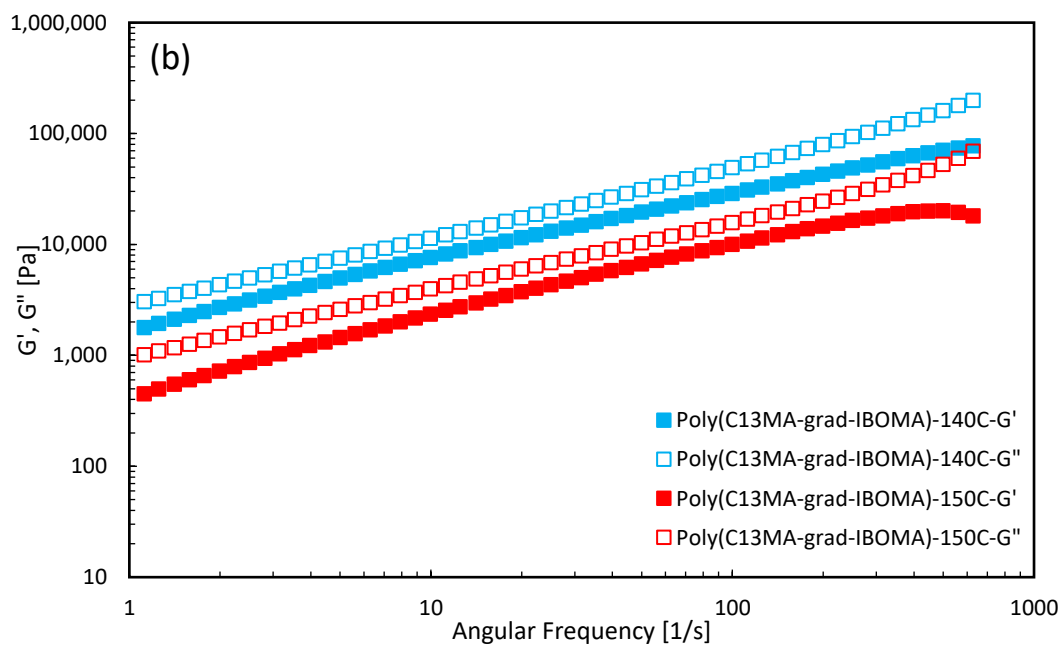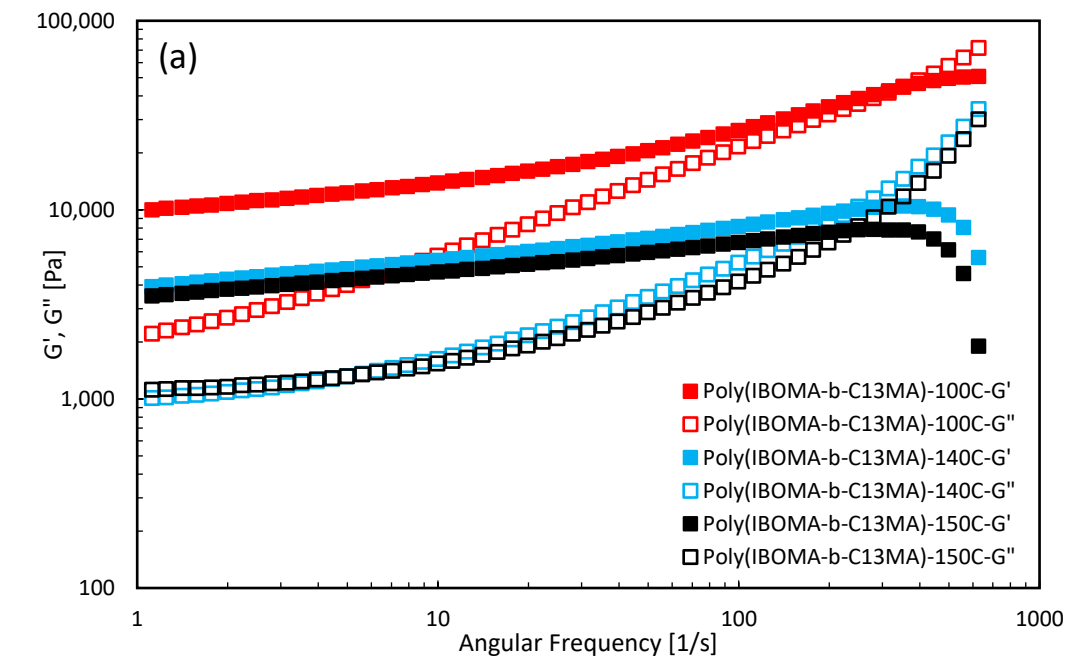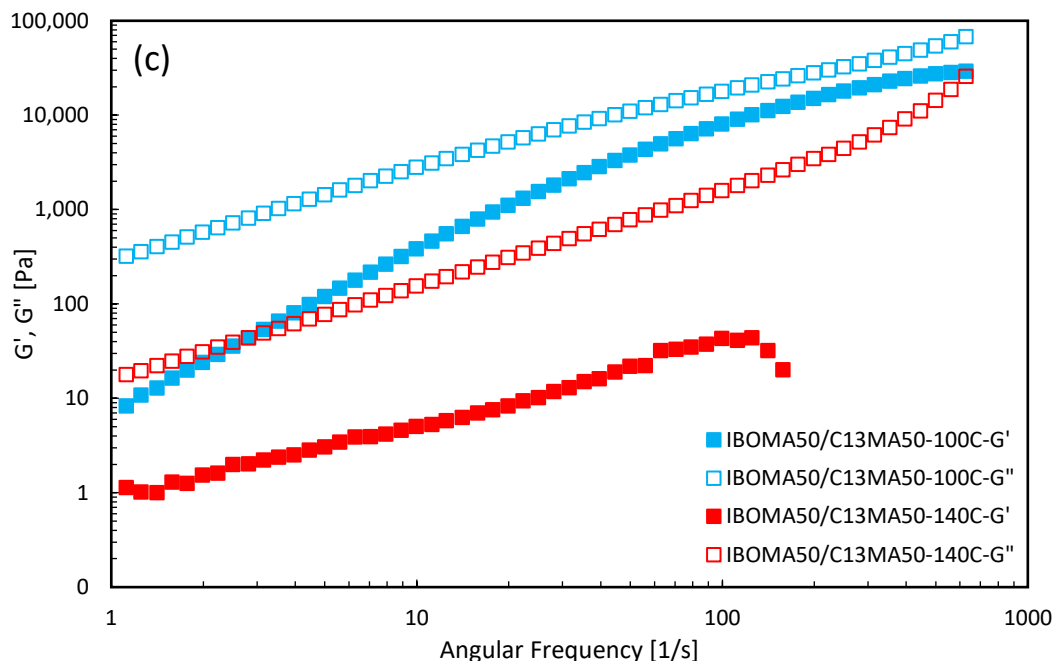
Figure 4.S8. G′ and G″ plots versus shearing frequency for (a) Poly(IBOMA-*b*-C13MA) at 100 °C (red squares, □ and ■); at 140 °C (blue squares, □ and ■) and 150 °C. (b) Poly(C13MA-*grad*-IBOMA) at 140 °C (blue squares, □ and ■) and 150 °C (red squares, □ and ■). (c) IBOMA50/C13MA50 at 100 °C (blue squares, □ and ■) and 140 °C (red squares, □ and ■).

S4.9. Flory-Huggins Interaction Parameter for Poly(IBOMA-*b*-C13MA)

To calculate the Flory-Huggins enthalpic interaction parameter χ for IBOMA/C13MA system, Equation (S1) can be used.

$$\chi_{IBOMA-C13MA} = \frac{V_m(\delta_{IBOMA} - \delta_{C13MA})^2}{RT} \tag{4.S1}$$

Here, $\chi_{IBOMA-C13MA}$ corresponds to the difference between the interaction energies of two species and is used to predict the miscibility of two components (the IBOMA and C13MA blocks) in the chains. V_m is the reference molar volume calculated based on molar volume of monomers ($M_{w,\,IBOMA}$ = 222.328 g mol^{-1}, $V_{m,IBOMA}$ = 226.9 cm^3 mol^{-1} [546]; $M_{w,\,C13MA}$ = 268.441 g mol^{-1}, $V_{m,C13MA}$ = 305.0 cm^3 mol^{-1} [547]) and solubility parameter for IBOMA monomers δ_{IBOMA} = 17.0 (J cm^{-3})$^{1/2}$ [182, 262, 548]. The solubility parameter for C13MA is not available in the literature. However, it can be reasonably estimated by the solubility parameter of

lauryl methacrylate. Hence, it was assumed that $\delta_{C13MA} \approx \delta_{C12MA}$ is the average in a range of 15.4-17.8 (J cm^{-3})$^{1/2}$ [182, 549-552].

At T = 140 °C (The temperature for rheological measurements in this study) and 20 °C (Room temperature), the interaction parameters for IBOMA/C13MA were estimated to be 0.012 and 0.017. This shows that the system is not strongly segregated at these temperatures for Poly(IBOMA-b-C13MA) ($F_{IBOMA} = 0.22$, $M_n = 37.1$ kg mol^{-1}, $Đ = 1.93$).

S4.10. ^{1}H NMR spectra for IBOMA30/C13MA70-S at 60 minutes
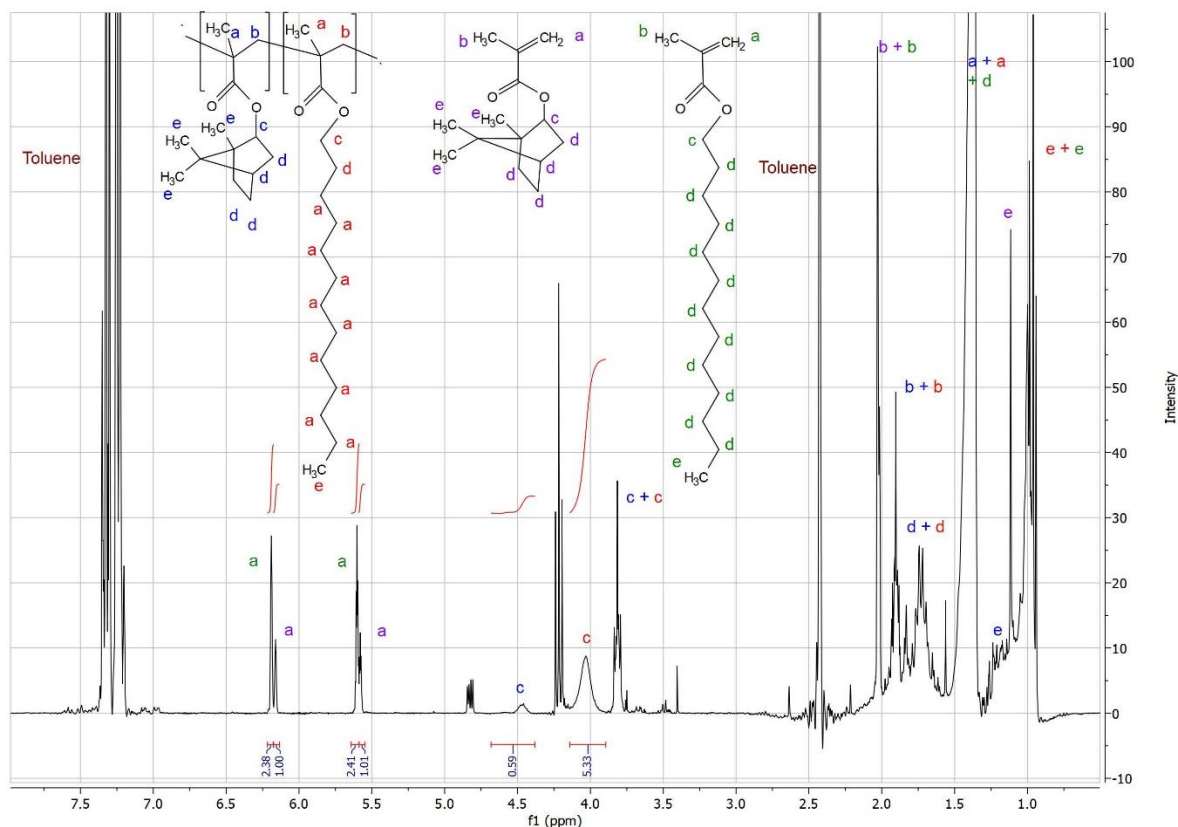
Figure 4.S9. ^{1}H NMR spectra for IBOMA30/C13MA70-S after 60 minutes of starting the reaction. ^{1}H NMR (CDCl$_3$, ppm): 6.17-6.22 (m, 1 H^{C13MA}), 6.14-6.17 (m, 1 H^{IBOMA}), 5.59-5.63 (m, 1 H^{C13MA}), 5.56-5.59 (m, 1 H^{IBOMA}), 4.41-4.65 (d, 1 H$^{p(IBOMA)}$), 3.93-4.13 (s, 2 H$^{p(C13MA)}$), 3.77-3.86 (m, 2 H$^{p(C13MA)}$ + 1 H$^{p(IBOMA)}$), 2.00-2.04 (m, 3 H^{IBOMA} + 3 H^{C13MA}), 1.87-1.94 (m, 2 H$^{p(IBOMA)}$ + 2 H$^{p(C13MA)}$), 1.67-1.80 (m, 7 H$^{p(IBOMA)}$ + 2 H$^{p(C13MA)}$), 1.34-1.51 (m, 3 H$^{p(IBOMA)}$ + 23 H$^{p(C13MA)}$ + 22 H^{C13MA}), 1.13-1.31 (m, 9 H$^{p(IBOMA)}$), 1.10-1.13 (s, 9 H^{IBOMA}), 0.92-1.07 (m, 3 H^{C13MA} + 3 H$^{p(C13MA)}$).
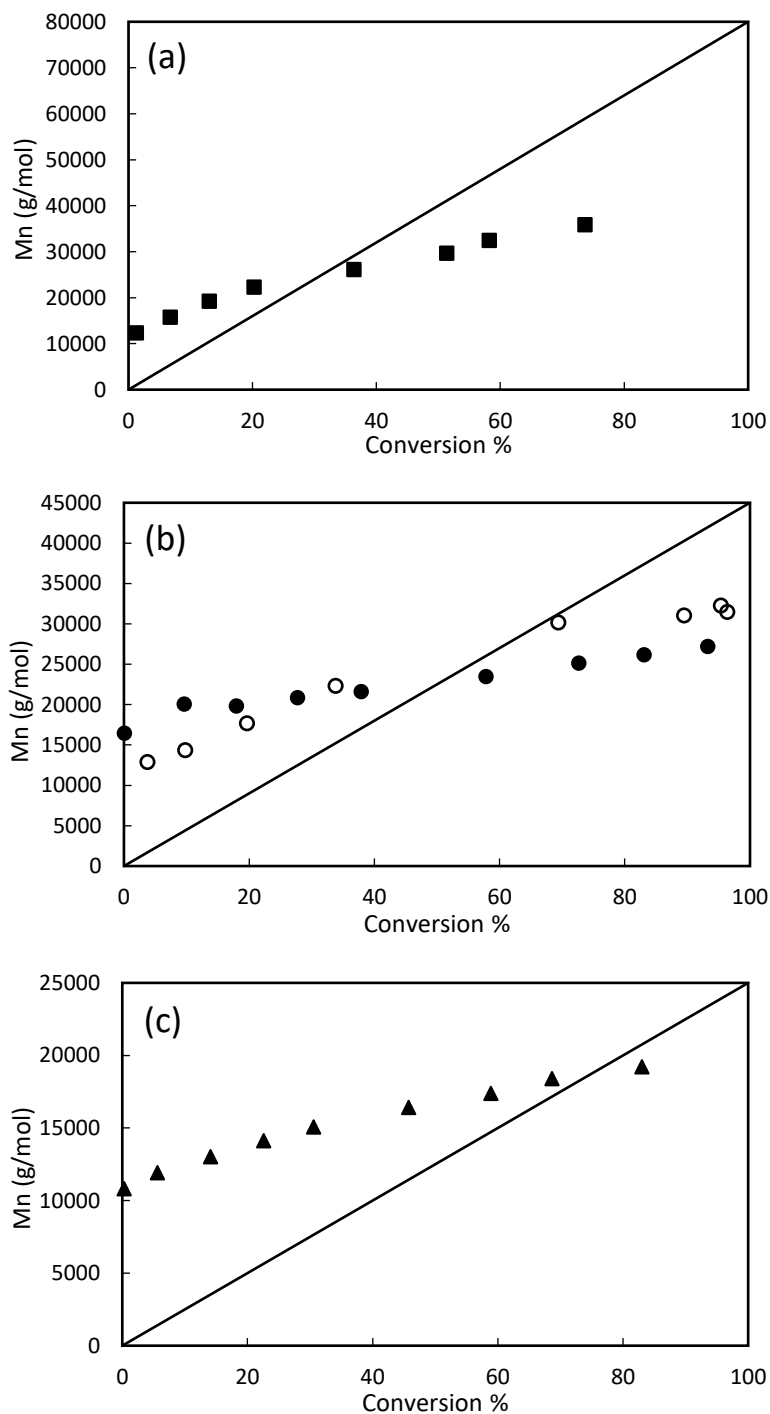
Figure 5.S1. Number average molecular weight M_n versus conversion (X) for homopolymerization of POSSMA. The results were compared with the corresponded theoretical line. POSSMA-Mn80 (filled

squares, ■); POSSMA-Mn45-No Hexadecane (open circles, ○); POSSMA-Mn45 (filled circles, ●); POSSMA-Mn25 (filled triangles, ▲).
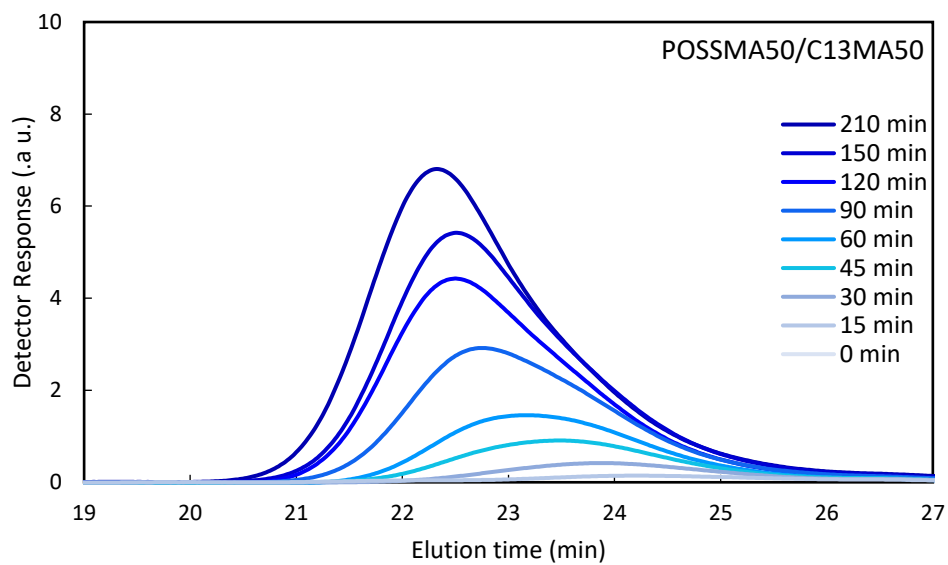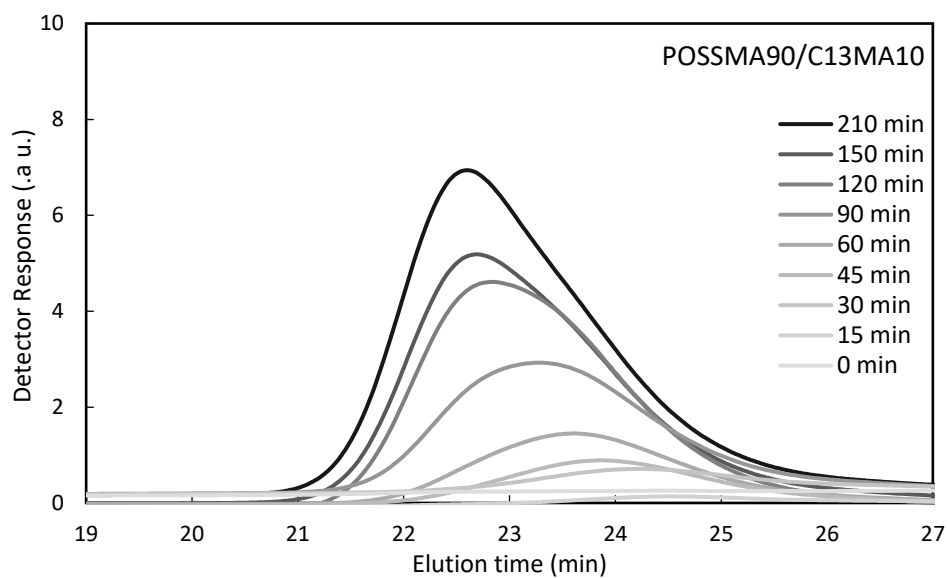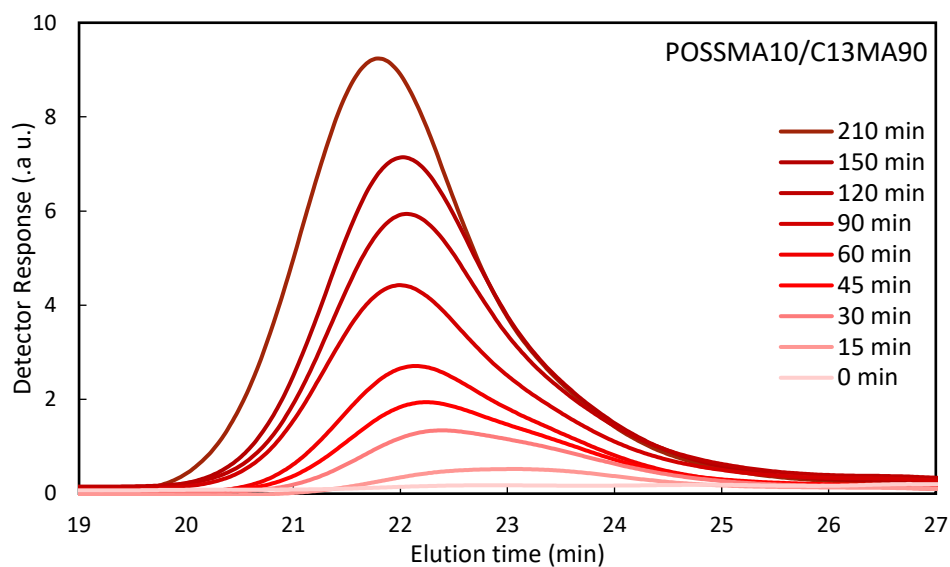
Figure 5.S2. GPC traces for POSSMA90/C13MA10, POSSMA50/C13MA50 and POSSMA10/C13MA90 during the polymerization at 90 °C.

Table 5.S1 Z-average particle size and dispersity of the particles for miniemulsion copolymerization of POSSMA/C13MA.

Reaction time (min)	Particle size (nm)	PDI
POSSMA10/C13MA90 [a]		
0	241.6	0.209
15	239.5	0.232
30	245.4	0.244
45	237.7	0.195
60	239.9	0.159
90	238.6	0.240
120	230.9	0.224
150	233.9	0.193
210	234.4	0.249
POSSMA20/C13MA80		
0	237.9	0.225
15	244.3	0.22
30	237.6	0.177
45	229.8	0.215
60	232.1	0.170
90	241.4	0.243
120	229.2	0.234
150	233.7	0.234
210	227.2	0.243
POSSMA30/C13MA70		
0	240.2	0.234

15	241.9	0.268
30	240.7	0.242
45	235.2	0.178
60	232	0.223
90	232.1	0.191
120	226.1	0.211
150	236.4	0.235
210	235.5	0.222
POSSMA40/C13MA60		
0	241.7	0.211
15	238.2	0.192
30	239.1	0.229
45	243.2	0.236
60	235.3	0.220
90	234.9	0.226
120	233.9	0.163
150	233.8	0.241
210	229.5	0.200
POSSMA50/C13MA50		
0	248.8	0.223
15	230.7	0.226
30	241.1	0.232
45	225.5	0.180
60	247.2	0.261
90	251.1	0.250
120	250.8	0.293
150	230.7	0.235
210	245	0.216
POSSMA60/C13MA40		
0	257.4	0.234
15	258	0.287
30	247.2	0.187
45	259.4	0.268
60	249.5	0.243
90	247.7	0.227
150	268.5	0.347
210	245.8	0.171
POSSMA70/C13MA30		
0	240.7	0.222
15	240.7	0.196
30	236.8	0.194
45	238.3	0.191
60	235.7	0.202
90	237.7	0.169
210	230.6	0.225
POSSMA80/C13MA20		
0	228.8	0.183

15	249.5	0.229
30	238.7	0.181
45	236.4	0.148
60	231.3	0.171
90	231.4	0.174
120	235.6	0.169
150	243.6	0.163
210	244.7	0.163
POSSMA90/C13MA10		
0	245.2	0.160
15	254.7	0.220
30	249.3	0.176
45	247.7	0.199
60	238.6	0.193
90	245.1	0.166
120	242.4	0.249
150	230.7	0.204
210	281.5	0.281

[a] The miniemulsion polymerization of POSSMA/C13MA mixtures with the initial molar feed composition: POSSMAxx/C13MAyy where xx denotes the mol% POSSMA and yy denotes the mol% C13MA. $M_{n,target}$ = 45 kg mol^{-1}, solid content = 22 wt% and reaction temperature = 90 °C. 2 wbm% DOWFAX 8390 and 0.8 wbm% n-hexadecane stabilized all the miniemulsions.
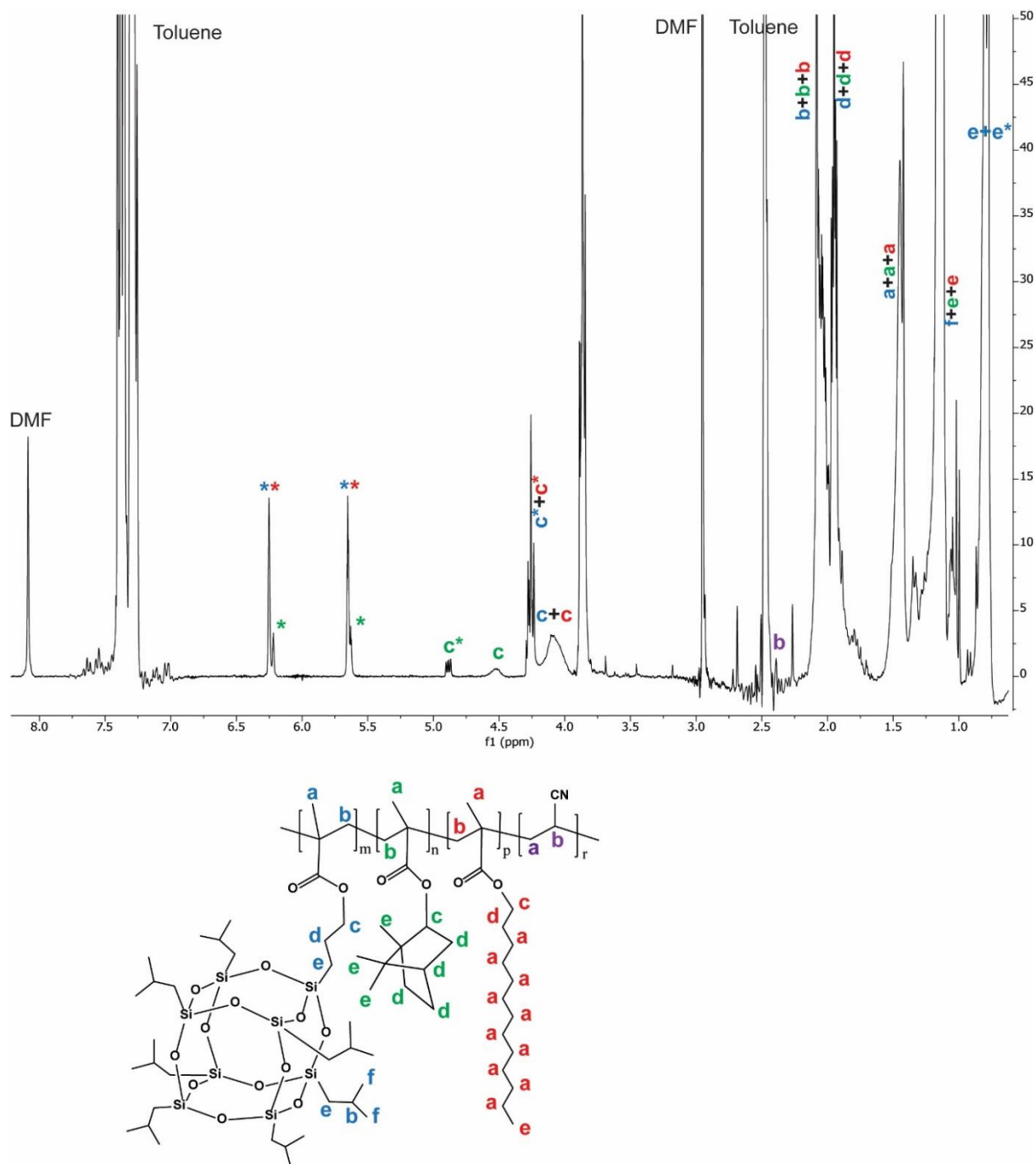
Figure 6.S1. ^{1}H NMR spectrum for P50/IB22/C18/AN10 polymer (prepared in toluene using BB alkoxyamine and 10 mol% AN in initial feed) after 210 minutes of starting the reaction. * corresponds to unreacted monomers. ^{1}H NMR (500 MHz) at room temperature (CDCl$_3$, ppm): 4.85-4.92 (m, 1 H^{IBOMA}),

4.40-4.81 (d, 1 $H^{p(IBOMA)}$), 4.20-4.31 (m, 2 H^{POSSMA} + 2 H^{C13MA}), 3.94-4.20 (s, 2 $H^{p(POSSMA)}$ + 2 $H^{p(C13MA)}$), 2.34-2.42 (s, 1 $H^{p(AN)}$), 1.99-2.16 (m, 9 $H^{p(POSSMA)}$ + 2 $H^{p(IBOMA)}$ + 2 $H^{p(C13MA)}$), 1.83-1.99 (m, 2 $H^{p(POSSMA)}$ + 7 $H^{p(IBOMA)}$ + 2 $H^{p(C13MA)}$), 1.39-1.57 (m, 3 $H^{p(POSSMA)}$ + 3 $H^{p(IBOMA)}$ + 23 $H^{p(C13MA)}$), 1.09-1.24 (m, 42 $H^{p(POSSMA)}$ + 9 $H^{p(IBOMA)}$ + 3 H^{C13MA}), 0.73-0.90 (m, 16 $H^{p(POSSMA)}$ + 16 H^{POSSMA}). vinylic protons of monomers: 6.19-6.23 (s, 1 H^{IBOMA}), 5.59-5.64 (s, 1 H^{IBOMA}), 6.23-6.27 (s, 1 H^{POSSMA} + 1 H^{C13MA}), 5.64-5.68 (s, 1 H^{POSSMA} + 1 H^{C13MA}).

To determine the monomer conversion (X) via ^{1}H NMR results, the following equation was used:

$$X\,(\%) = X_{POSSMA}f_{POSSMA,0} + X_{C13MA}f_{C13MA,0} + X_{IBOMA}f_{IBOMA,0} + X_{AN}f_{AN,0} \tag{6.S1}$$

where X_{POSSMA}, X_{C13MA}, X_{IBOMA} X_{AN} are the individual conversions of POSSMA, C13MA, IBOMA and AN monomers, respectively. $X_{Individual\,monomer}$ can be calculated based on the following equation:

$$X_{Individual\,monomer} = \cfrac{\cfrac{\text{polymer peak}}{\text{\# of protons corresponding to the peak}}}{\cfrac{\text{polymer peak}}{\text{\# of protons corresponding to the peak}} + \cfrac{\text{monomer peak}}{\text{\# of protons corresponding to the peak}}} \tag{6.S2}$$

$f_{POSSMA,0}$, $f_{C13MA,0}$, $f_{IBOMA,0}$ and $f_{AN,0}$ are the initial molar fractions of POSSMA, C13MA, IBOMA and AN in the solution.

The molar fraction of monomers can be determined by using the following equation:

$$F_i = \cfrac{\cfrac{\text{polymer peak for monomer } i}{\text{\# of protons corresponding to the peak}}}{\sum_{j=1}^{n}\left(\cfrac{\text{polymer peak for monomer } j}{\text{\# of protons corresponding to the peak}}\right)} \tag{6.S3}$$

Where F_i is the molar fraction of monomer i in polymer (i = POSSMA, C13MA, IBOMA or AN) and n is the number of different types of monomers, presented in the polymer (herein $n = 4$). ^{1}H NMR polymer and monomer peaks for an experiment (P50/IB22/C18/AN10) are shown in Figure 6.S1. ^{1}H NMR peaks for the block copolymerization are shown in Figure 6.S2 and 6.S3.
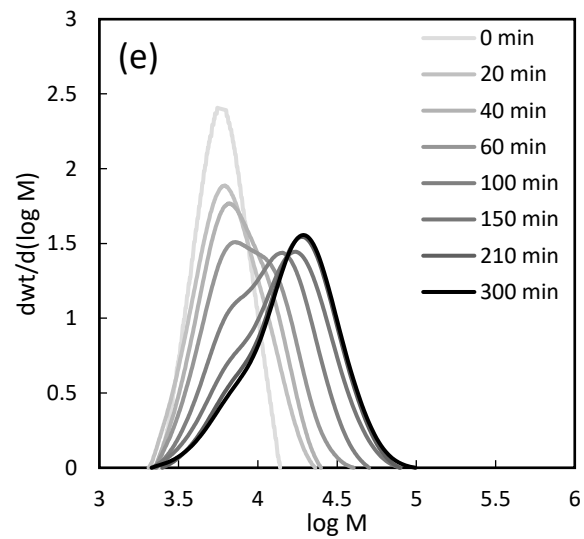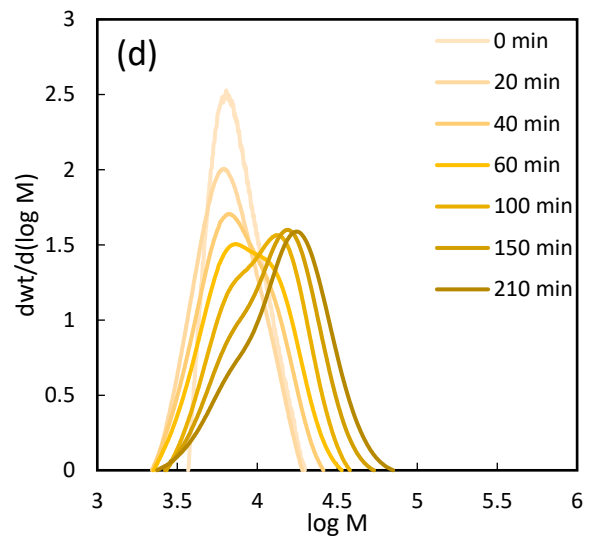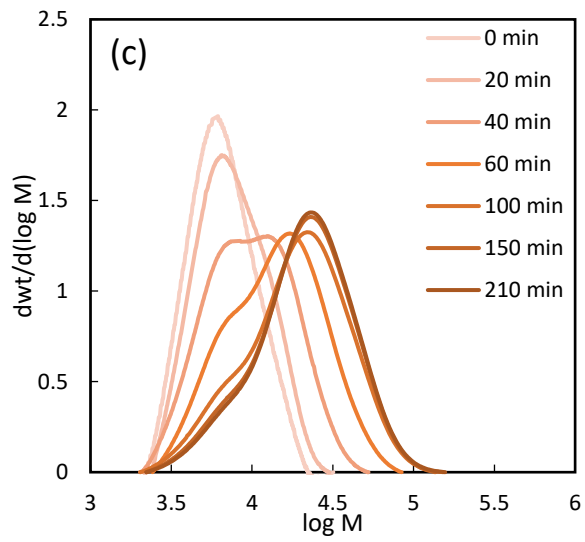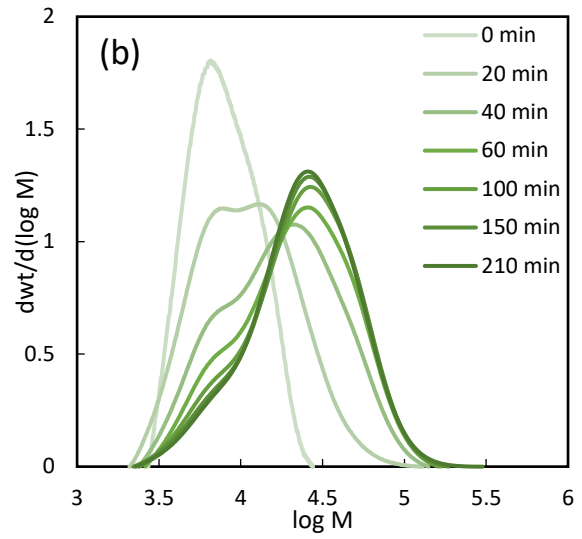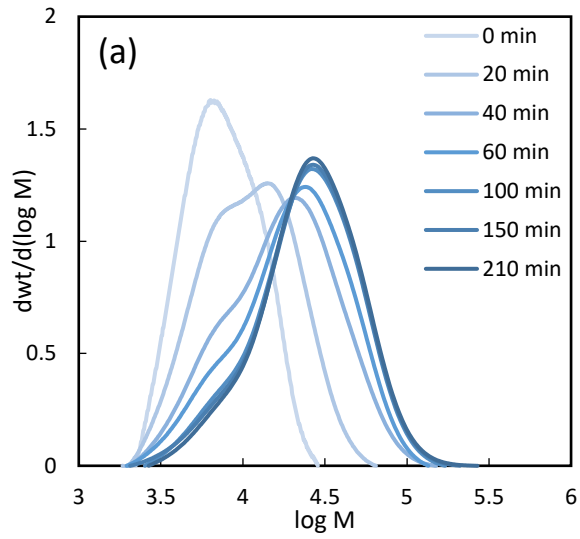
Figure 6.S2. GPC peaks for a) P10/IB44/C36/AN10, b) P20/IB38/C32/AN10, c) P30/IB33/C27/AN10, d) P40/IB27/C23/AN10 and e) P50/IB22/C18/AN10 experiments during the polymerization in toluene (the controlling co-monomer (AN) was in an initial concentration of 10 mol%). The NMP was conducted in toluene using BB at 90 °C and the reaction time was 210 minutes.
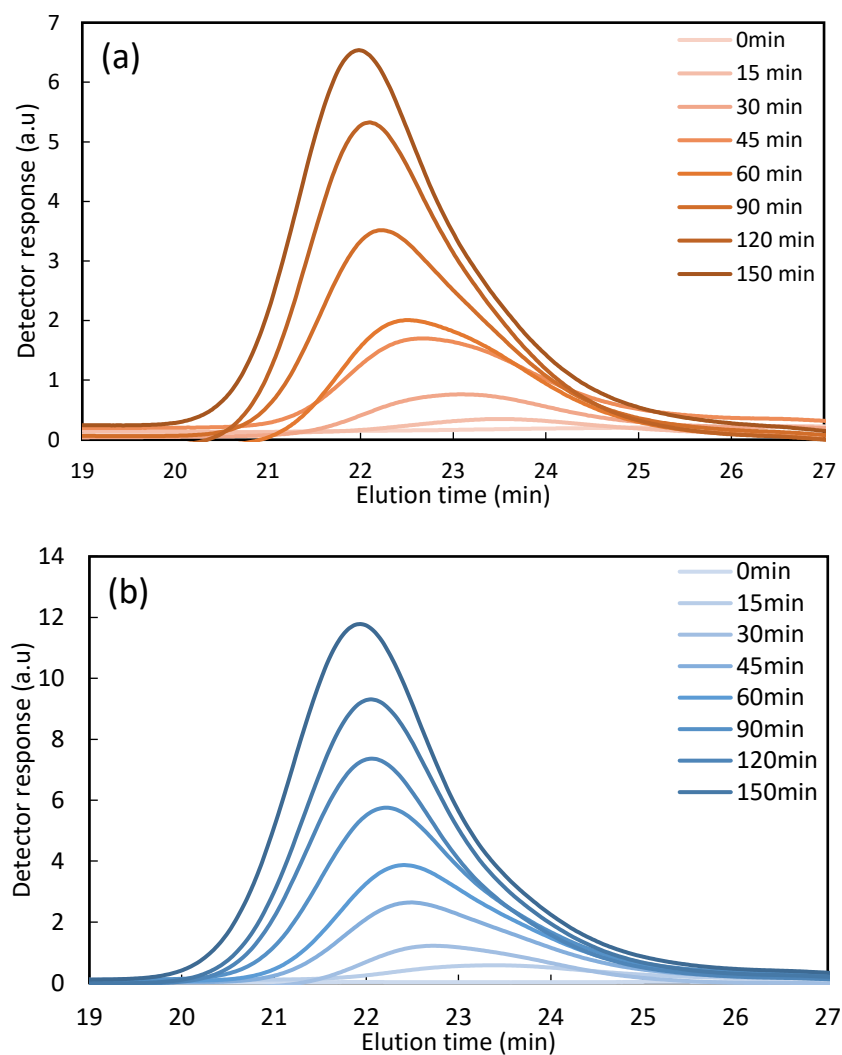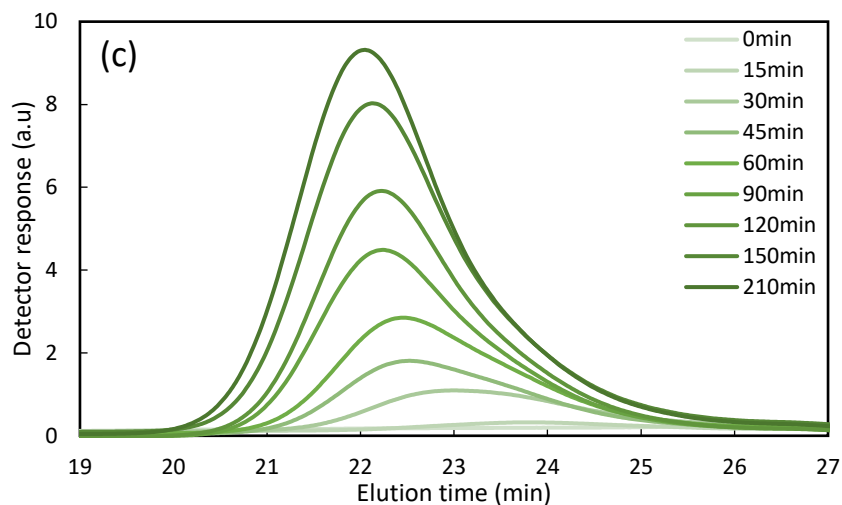
Figure 6.S3. GPC peaks for P5/IB47.5/C47.5, P10/IB45/C45 and P20/IB40/C40 experiments during the miniemulsion polymerization. The NMP was initiated by Dispolreg 007 alkoxyamine and the reaction temperature was 90 °C.
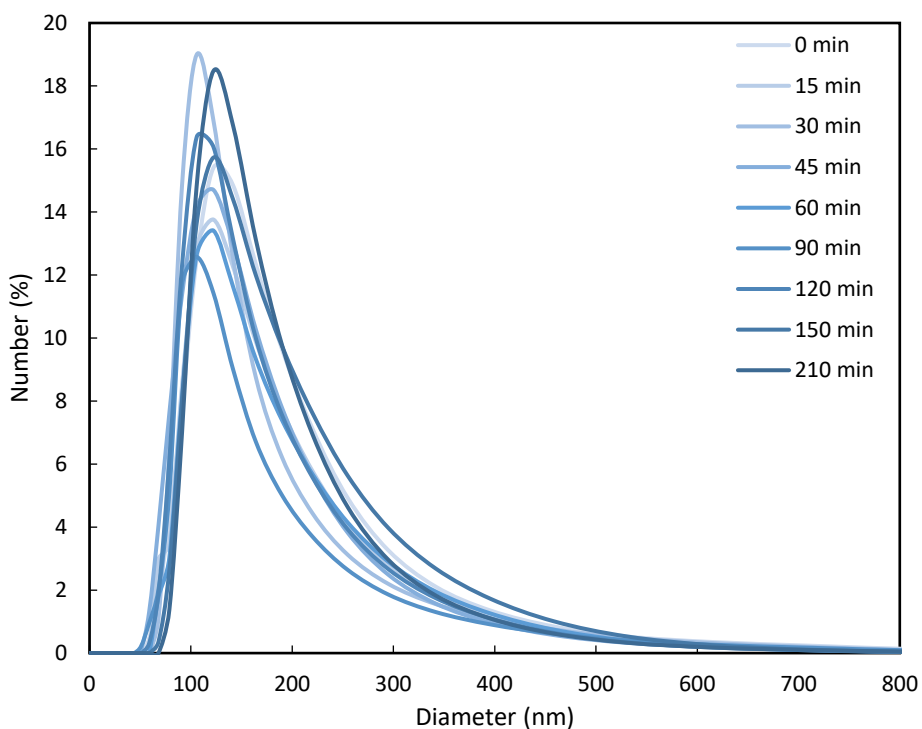
Figure 6.S4. Number-average particle size distributions for P10/IB45/C45 experiment over time.

H[1] NMR for Chain Extension of Poly(IBOMA) with POSSMA/C13MA in Toluene
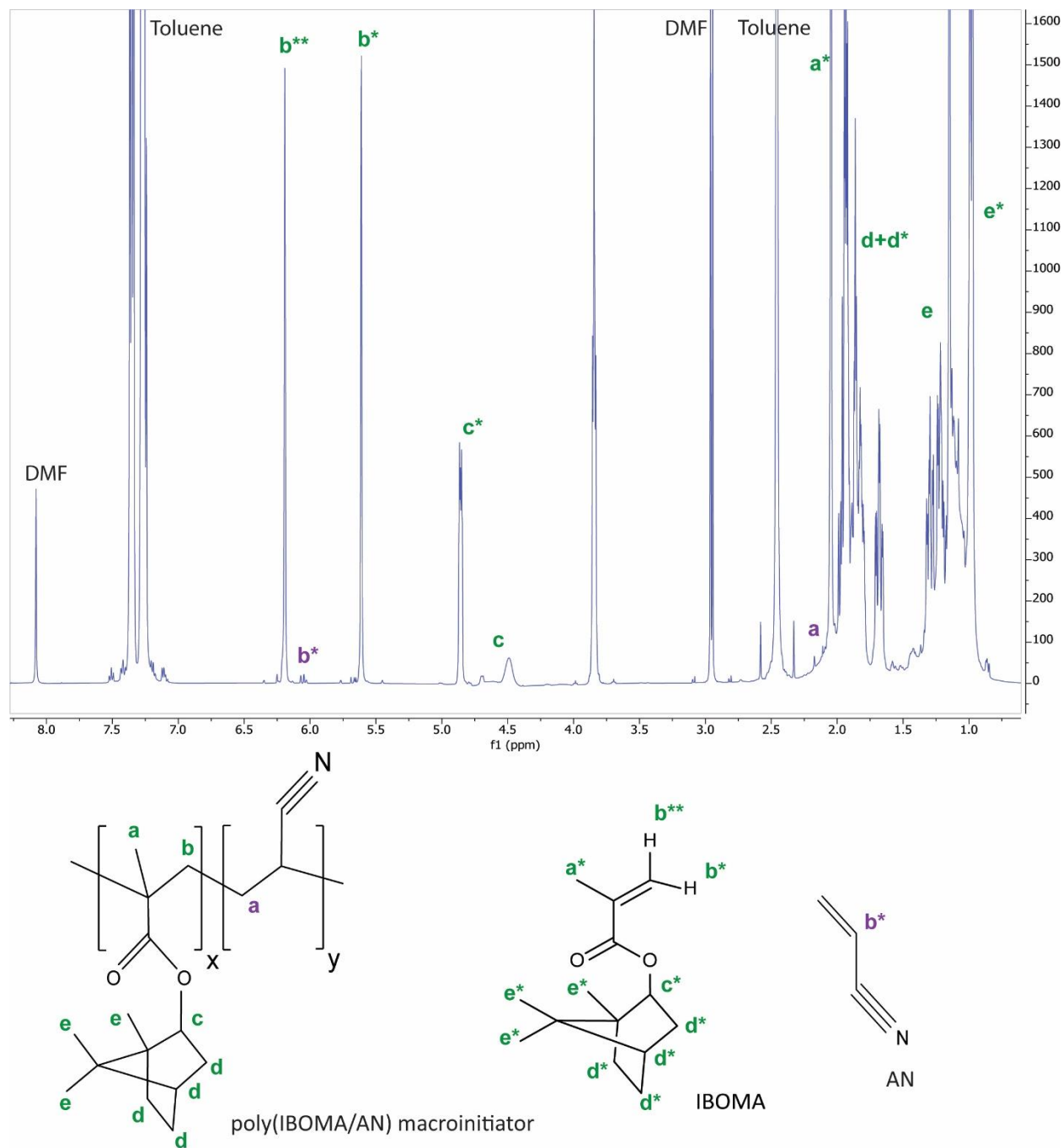
Figure 6.S5. ^{1}H NMR spectrum of poly(IBOMA/AN) macroinitiator after 50 minutes from starting the reaction (before precipitation; containing unreacted monomers). Note that the poly(IBOMA/AN) macroinitiator was prepared in toluene using BB alkoxyamine and 10 mol% AN in initial feed (* corresponds to unreacted monomers). ^{1}H NMR (500 MHz) at room temperature (CDCl$_3$, ppm): 4.81-4.90

(m, 1 H^{IBOMA}), 4.40-4.77 (d, 1 H$^{p(IBOMA)}$), 2.07-2.13 (s, 2 H$^{p(AN)}$), 2.01-2.09 (s, 3 H^{IBOMA}), 1.75-2.01 (m, 7 H^{IBOMA} + 7 H$^{p(IBOMA)}$), 1.18-1.35 (m, 9 H$^{p(IBOMA)}$), 0.93-1.03 (m, 9 H^{IBOMA}). Vinylic protons of monomers: 6.16-6.22 (s, 1 H^{IBOMA}), 5.58-5.64 (s, 1 H^{IBOMA}).
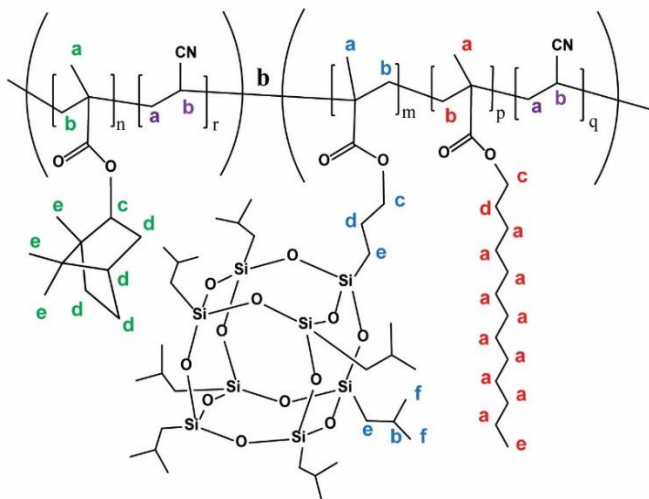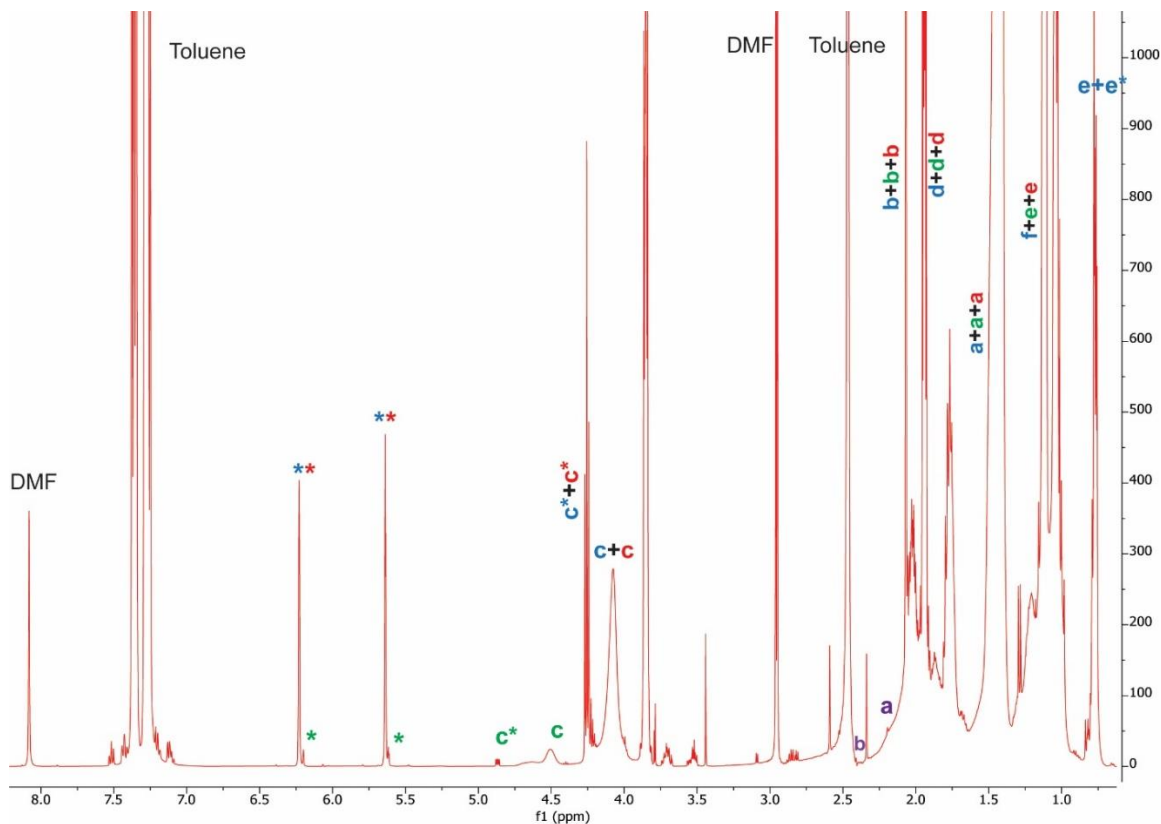
Figure 6.S6. ^{1}H NMR spectrum for p(IBOMA/AN)-b-p(POSSMA /C13MA/AN) block copolymer (prepared in toluene starting from poly(IBOMA/AN) macroinitiator and 10 mol% AN in the feed) after 5 hours of chain extension at 90 °C. * corresponds to unreacted monomers. ^{1}H NMR (500 MHz) at room

temperature (CDCl$_3$, ppm): 4.85-4.89 (m, 1 H^{IBOMA}), 4.42-4.79 (d, 1 H$^{p(IBOMA)}$), 4.19-4.28 (m, 2 H^{POSSMA} + 2 H^{C13MA}), 3.95-4.18 (s, 2 H$^{p(POSSMA)}$ + 2 H$^{p(C13MA)}$), 2.37-2.43 (s, 1 H$^{p(AN)}$), 2.12-2.26 (s, 2 H$^{p(AN)}$), 2.06-2.09 (s, 9 H$^{p(POSSMA)}$ + 2 H$^{p(IBOMA)}$ + 2 H$^{p(C13MA)}$), 1.90-1.98 (m, 2 H$^{p(POSSMA)}$ + 7 H$^{p(IBOMA)}$ + 2 H$^{p(C13MA)}$), 1.35-1.55 (m, 3 H$^{p(POSSMA)}$ + 3 H$^{p(IBOMA)}$ + 23 H$^{p(C13MA)}$), 0.95-1.17 (m, 42 H$^{p(POSSMA)}$ + 9 H$^{p(IBOMA)}$ + 3 H^{C13MA}), 0.71-0.81 (m, 16 H$^{p(POSSMA)}$ + 16 H^{POSSMA}). vinylic protons of monomers: 6.19-6.21 (s, 1 H^{IBOMA}), 5.60-5.62 (s, 1 H^{IBOMA}), 6.21-6.25 (s, 1 H^{POSSMA} + 1 H^{C13MA}), 5.62-5.66 (s, 1 H^{POSSMA} + 1 H^{C13MA}).
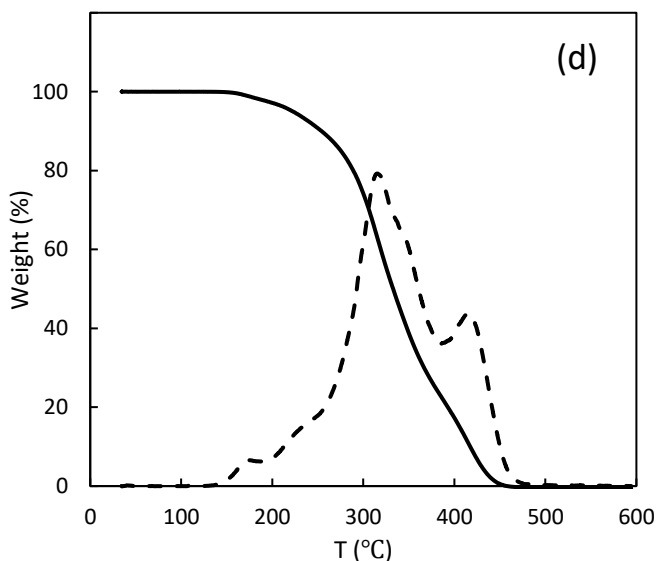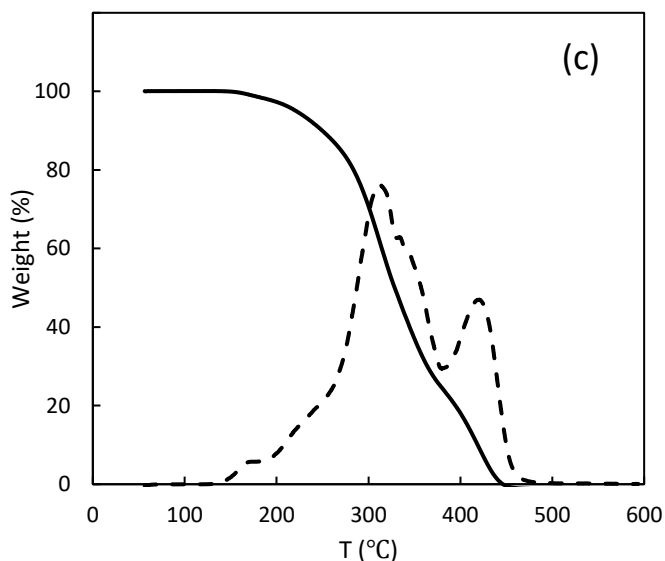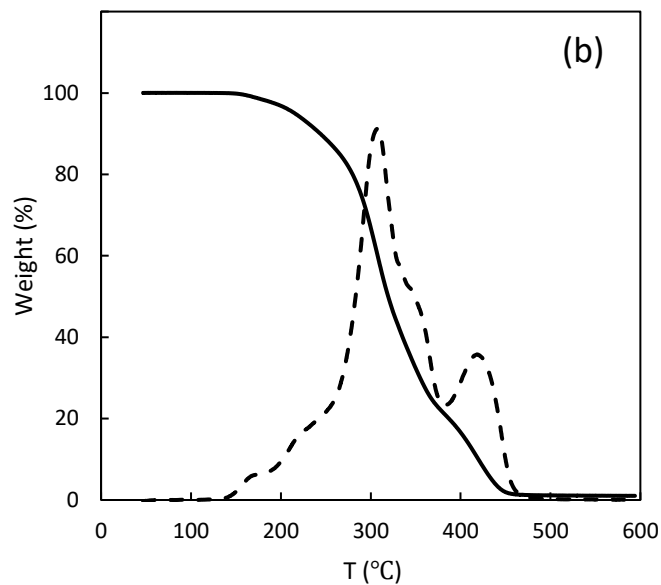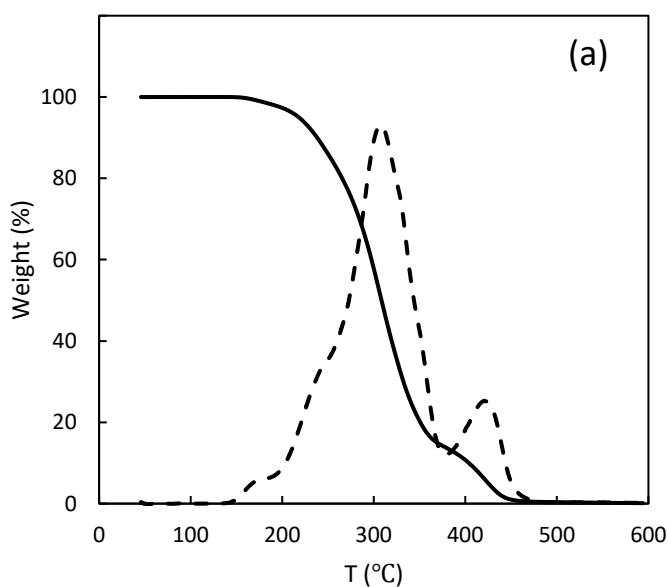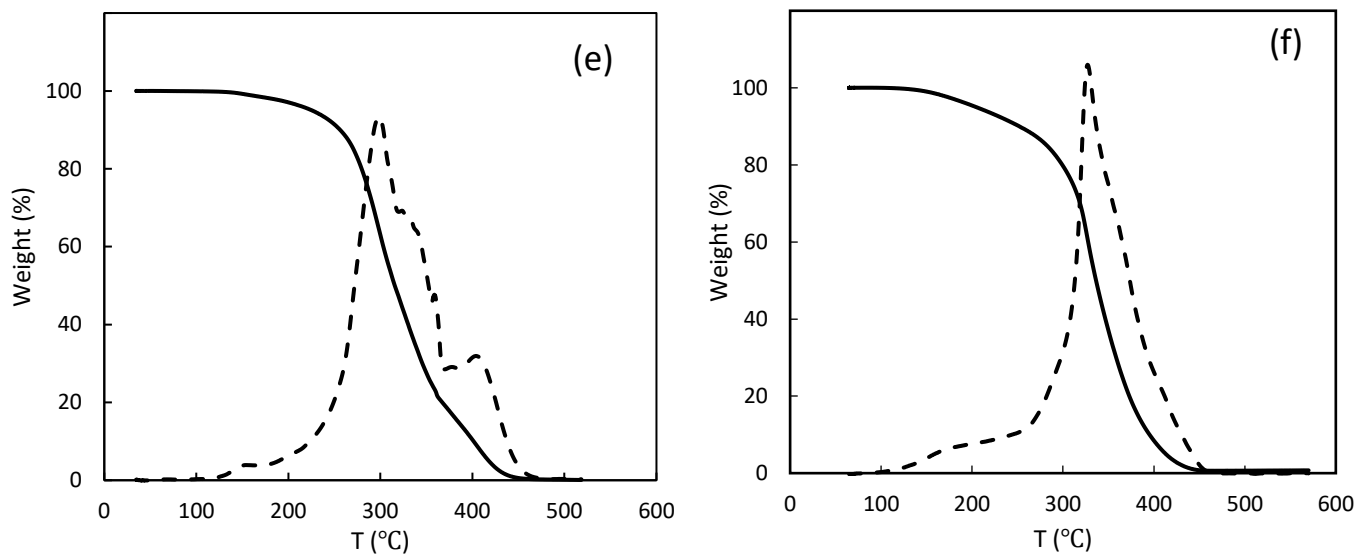
Figure 6.S7. Thermal degradation of polymer resins prepared in toluene. a) P10/IB44/C36/AN10, b) P20/IB38/C32/AN10, c) P30/IB33/C27/AN10, d) P40/IB27/C23/AN10, e) P50/IB22/C18/AN10 and f) p(IBOMA/AN)-*b*-p(POSSMA/C13MA/AN). Measurements performed under nitrogen flow at a ramp rate of 15 °C.min^{-1}. Sample weight versus temperature is represented by the solid line whereas the dotted line represents the derivative of weight relative to the temperature versus temperature in order to determine precisely the temperature at which weight loss is most apparent ($T_{dec,max}$).
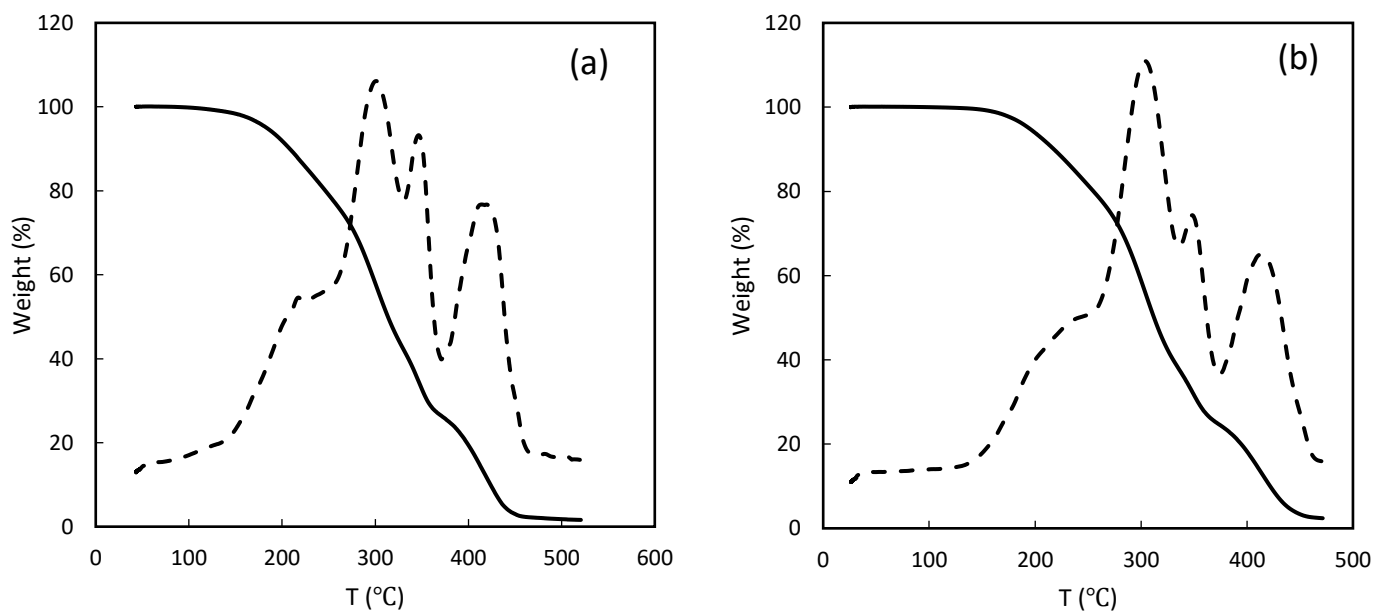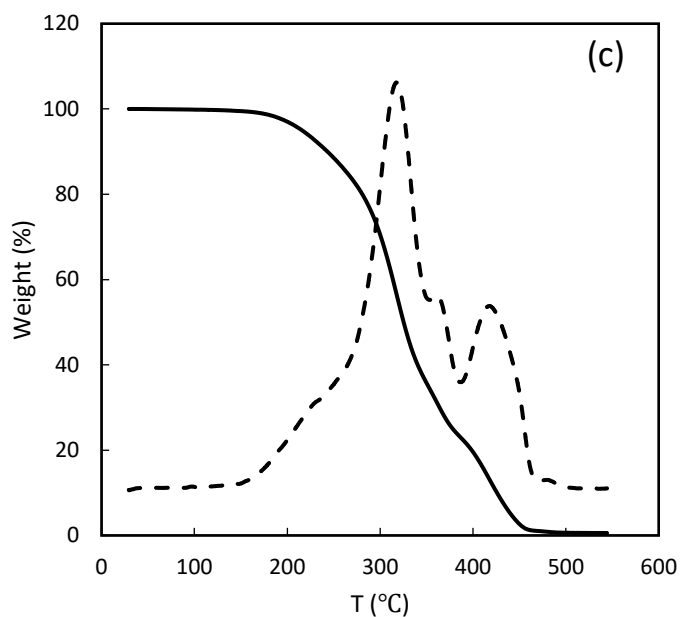
Figure 6.S8. TGA traces for POSS/IBOMA/C13MA polymers prepared by miniemulsion polymerization. a) P5/IB47.5/C47.5 b) P10/IB45/C45 c) P20/IB40/C40 Measurements performed under nitrogen flow at a ramp rate of 15 °C.min^{-1}. Sample weight versus temperature is represented by the solid line whereas the dotted line represents the derivative of weight relative to the temperature versus temperature in order to determine precisely the temperature at which weight loss is most apparent ($T_{dec,max}$).

Table 7.S1. Apparent rate constants for poly(VPBA/IBOMA/C13MA/AN) and poly(GMMA/IBOMA/C13MA/AN) prepared in 50 wt% 1,4-dioxane (and 5 wt% water for VPBA-containing polymers) using BB at 90 $^{\circ}$C.

poly(VPBA/IBOMA/C13MA/AN)				
Experiment ID	F_{VPBA}^{a} (%)	$M_{n,target}$ (kg mol^{-1})	$M_{n,final}$ (kg mol^{-1})	Apparent rate constant^{b} $k_P[P^{\bullet}]$ (10^5 s^{-1})
VPBA5/IBOMA 42.5/C13MA42.5/AN10	7.1	25	10.8	5.7 ± 0.2
VPBA10/IBOMA40/C13MA40/AN10	10.5	25	10.7	3.8 ± 0.1
VPBA15/IBOMA37.5/C13MA37.5/AN10	13.1	25	19.9	7.0 ± 0.1
VPBA2/IBOMA29/C13MA58/AN11	1.9	50	29.2	17.3 ± 0.1
VPBA5/IBOMA22.5/C13MA62.5/AN10	8.5	50	32.5	13.3 ± 0.1
VPBA10/IBOMA20/C13MA60/AN10	12.1	50	23.4	7.7 ± 0.1
VPBA15/IBOMA25/C13MA50/AN10	23.7	50	35.1	5.8 ± 0.1
poly(GMMA/IBOMA/C13MA/AN)				
Experiment ID	F_{GMMA}^{a} (%)	$M_{n,target}$ (kg mol^{-1})	$M_{n,final}$ (kg mol^{-1})	Apparent rate constant^{b} $k_P[P^{\bullet}]$ (10^5 s^{-1})
GMMA5/IBOMA42.5/C13MA42.5/AN10	5.4	25	14.1	16.3 ± 2.1
GMMA10/IBOMA40/C13MA40/AN10	6.9	25	12.6	37.2 ± 1.7
GMMA15/IBOMA37.5/C13MA37.5/AN10	15.0	25	10.5	29.3 ± 0.1
GMMA15/IBOMA25/C13MA50/AN10	10.2	50	26.3	19.7 ± 1.0

^{a}Concentration of VPBA or GMMA in final composition of polymers determined by ^{1}H NMR in CDCl$_3$.
^{b}Apparent rate constant derived from the slopes of $\ln[(1\text{-}X)^{-1}]$ (where X = conversion) versus reaction time for the first 60 minutes of polymerizations. k_P is propagation rate constant and $[P^{\bullet}]$ is the concentration of macroradicals.
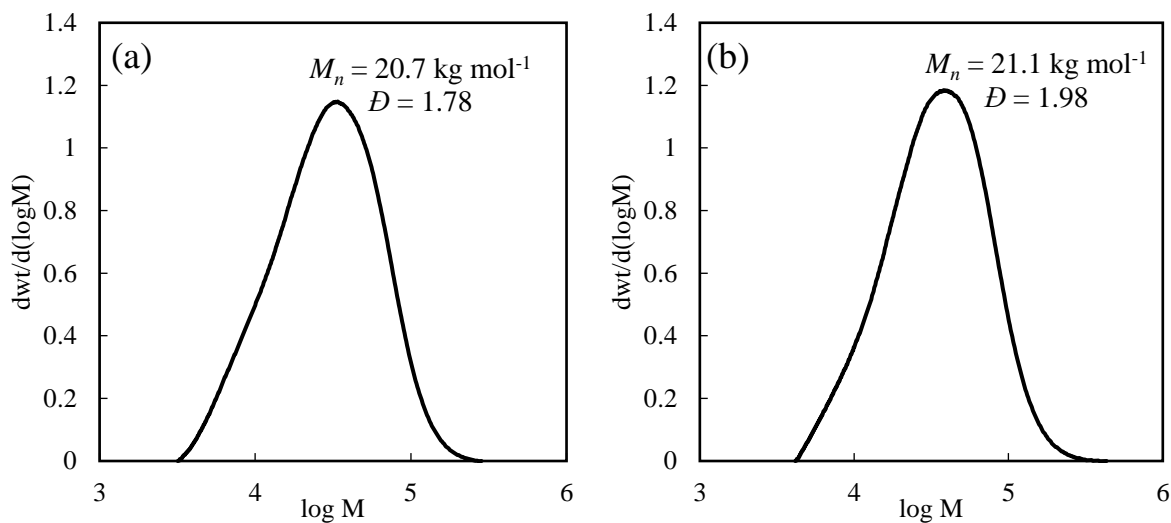
Figure 7.S1. GPC peaks of polymer blend I and II after decrosslinking with pinacol. M_n and $Đ$ were measured by GPC relative to PMMA standards in THF at 40 °C.
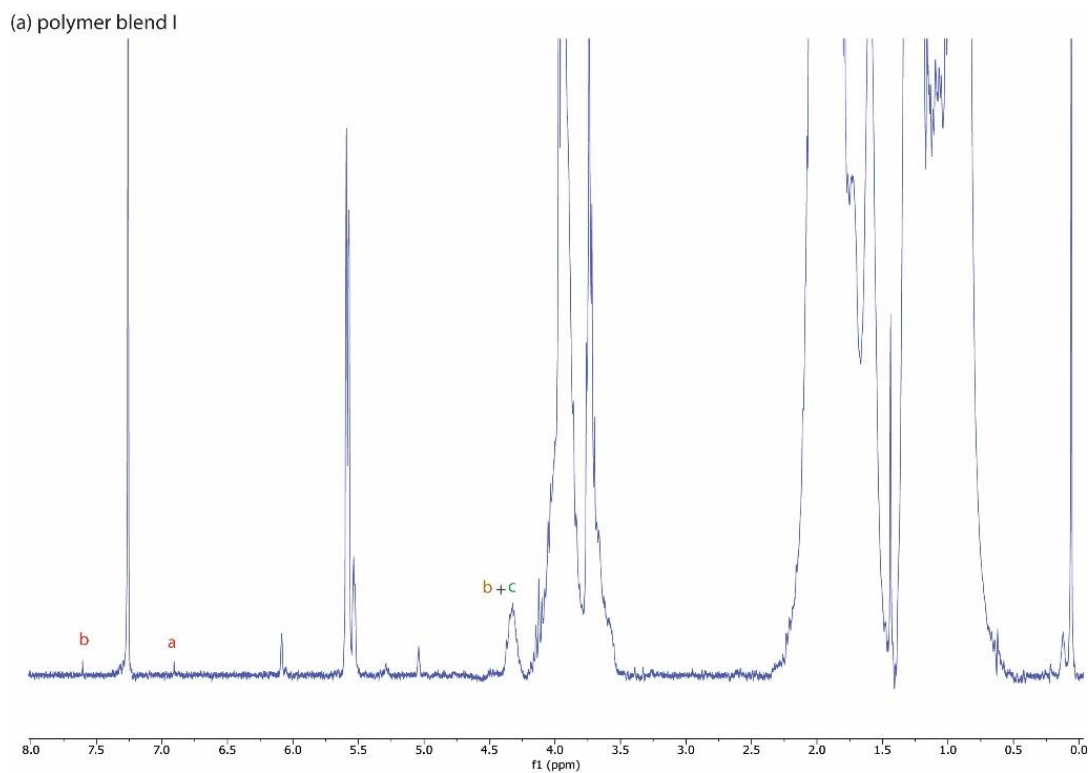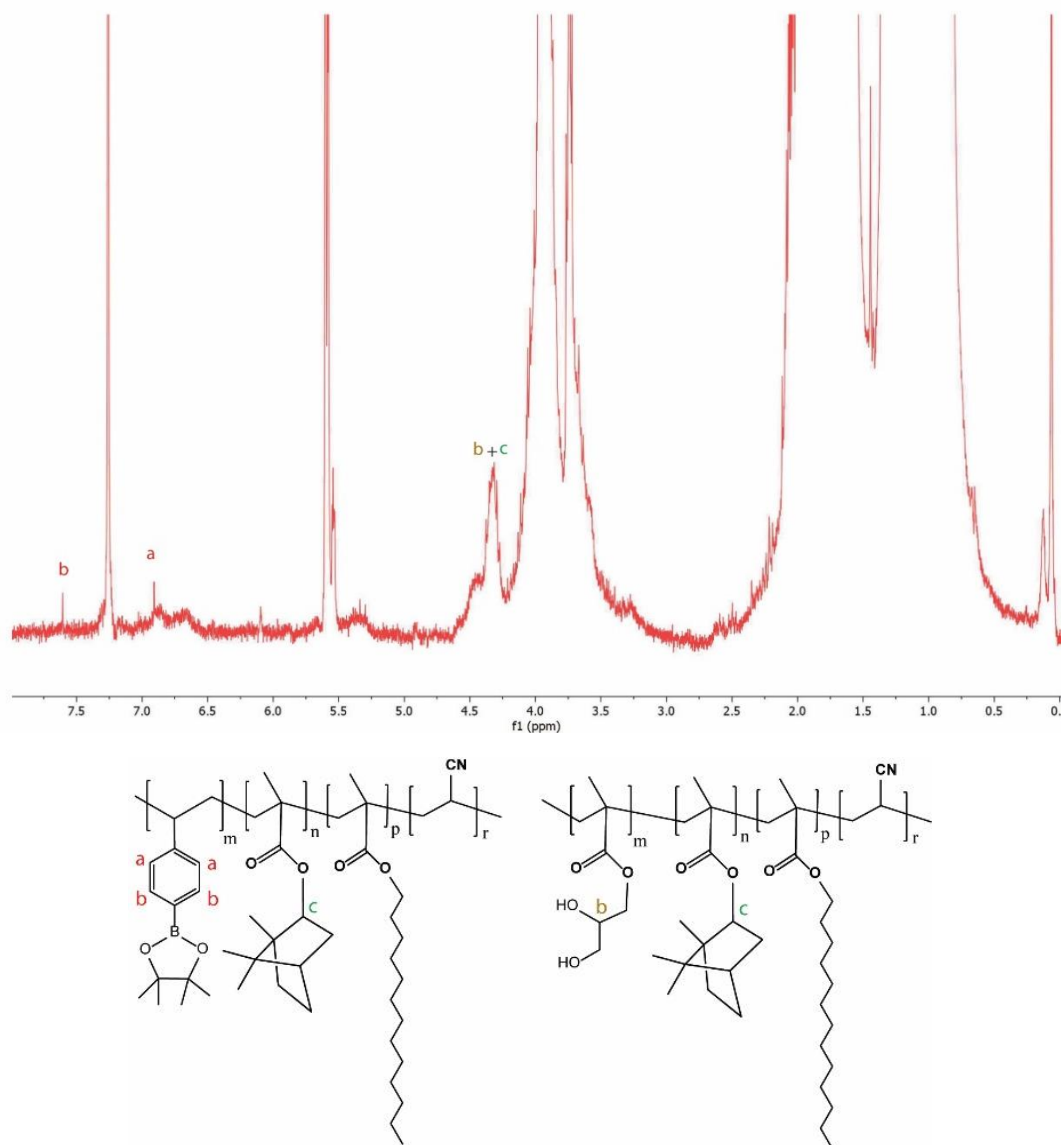
(a) polymer blend I

Figure 7.S2. ^{1}H NMR spectra for polymer blend I and II after decrosslinking with pinacol in dioxane. The polymers were precipitated in methanol and dried under vacuum for 24 hours. ^{1}H NMR (CDCl$_3$, ppm): 4.22-4.55 (d, 1 H$_{p(IBOMA)}$ + 1 H$_{p(GMMA)}$), 6.90-6.91 (s, 2 H$_{p(VPBA)}$), 7.60-7.61 (s, 2 H$_{p(VPBA)}$).

SUPPORTING INFORMATION: CHAPTER 8

Table 8.S1. Swelling ratios for polymer samples in Toluene and 1,4-dioxane after 24 hours.

Sample ID	Swelling ratio in Toluene (%)	Swelling ratio in 1,4-dioxane (%)	Swelling ratio in water (%)
Dimer 5%	- *	111.6	2.2
Dimer 10%	153.0	89.8	5.8
Dimer 15%	135.5	78.8	7.9

* The measurement of swelling ratio for Dimer 5% in toluene for 24 hours was not possible due to difficult process of separating dispersed gel-like polymer from toluene.
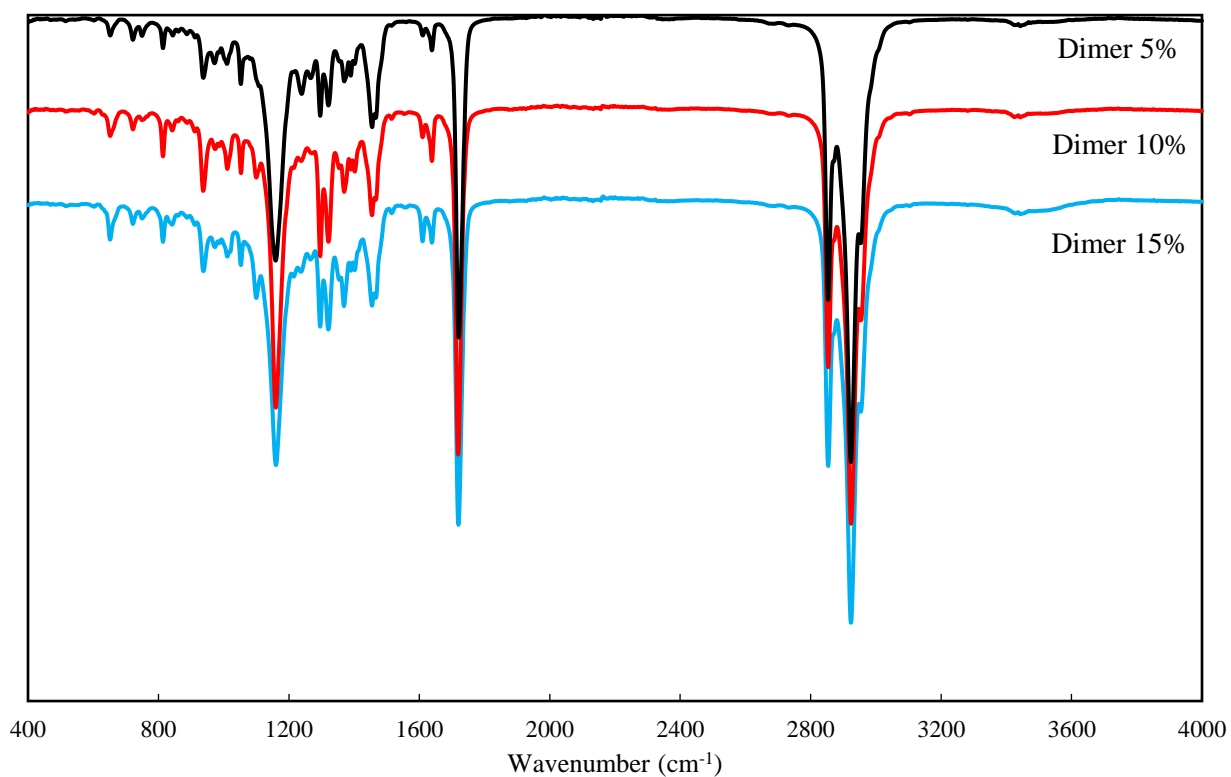
Figure 8.S1. FTIR spectra for Dimer 5-15% samples.
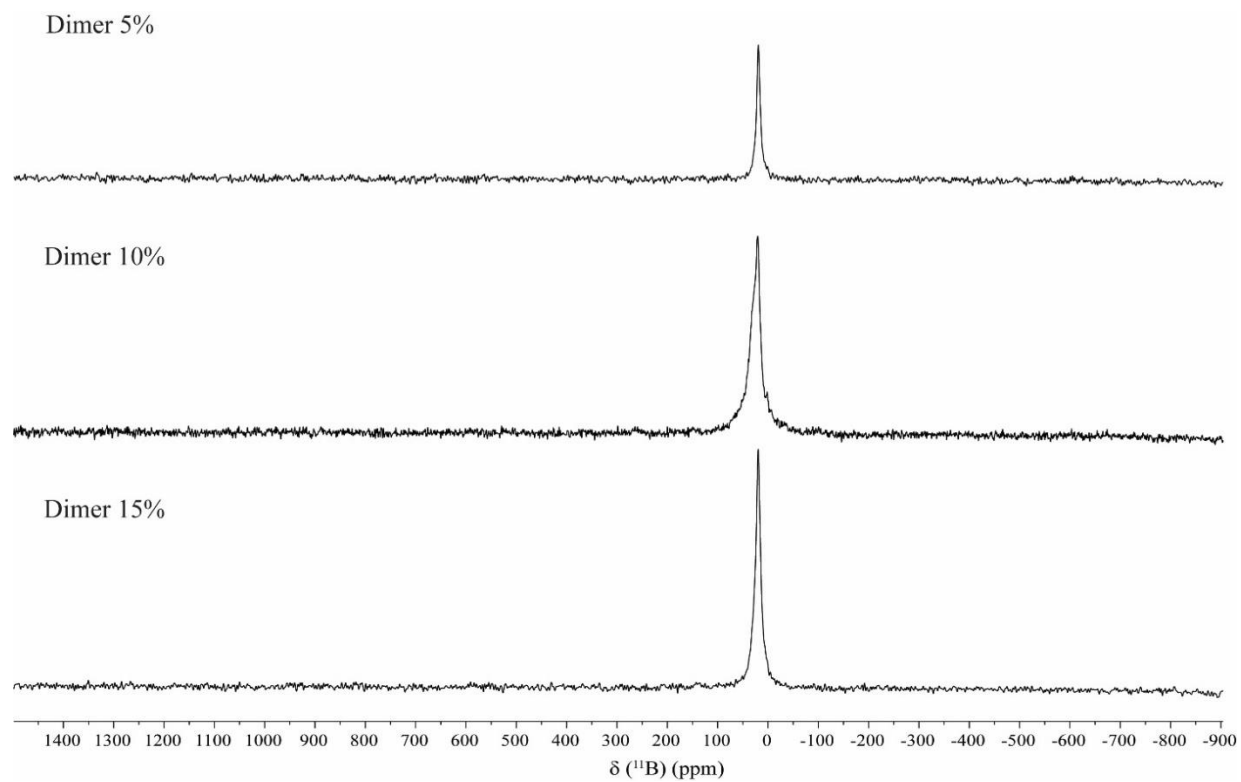
Figure 8.S2. ^{11}B solid-state NMR for Dimer 5%-15% samples. The peaks at 19-21 ppm indicate the boronic esters and boronic acids in the polymer.
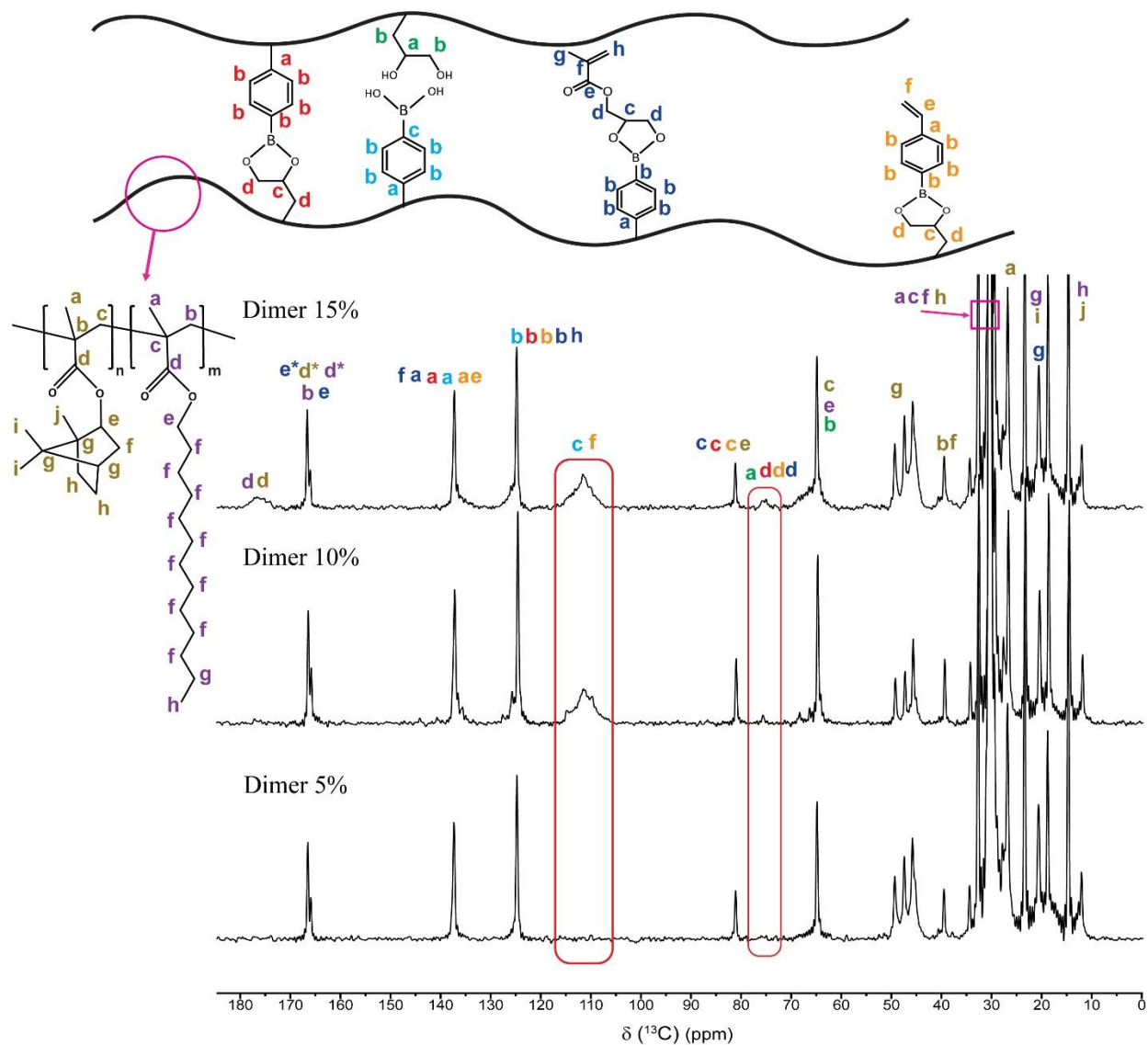
Figure 8.S3. ^{13}C solid-state NMR for Dimer 5%-15% samples. The peak at 111 ppm suggests the existence of open ring boronic esters (boronic acid groups) and unreacted vinyl groups of VPBA. By increasing the BG dimer concentration in Dimer 15% compared to Dimer 5 and 10%, an increase in the intensity of the peak at 75 ppm was also detected.
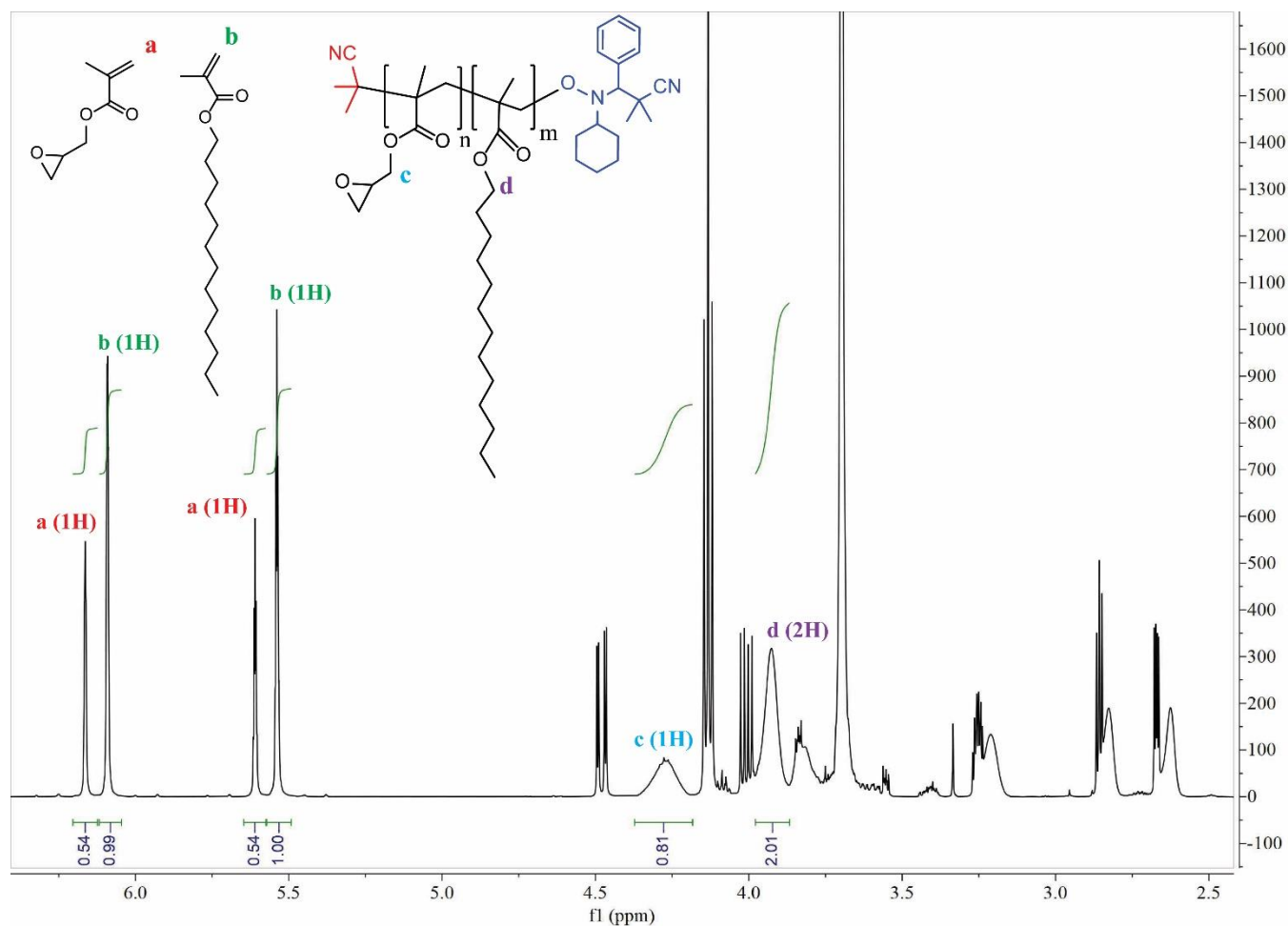
Figure 9.S1. ^{1}H NMR spectrum for GMA40/C13MA60 after 210 minutes. ^{1}H NMR (CDCl$_3$, ppm): 6.13-6.20 (m, 1 H^{GMA}), 6.04-6.12 (m, 1 H^{C13MA}), 5.57-5.65 (m, 1 H^{GMA}), 5.48-5.57 (m, 1 H^{C13MA}), 4.18-4.38 (m, 1 H$^{p(GMA)}$), 3.87-3.98 (s, 2 H$^{p(C13MA)}$).
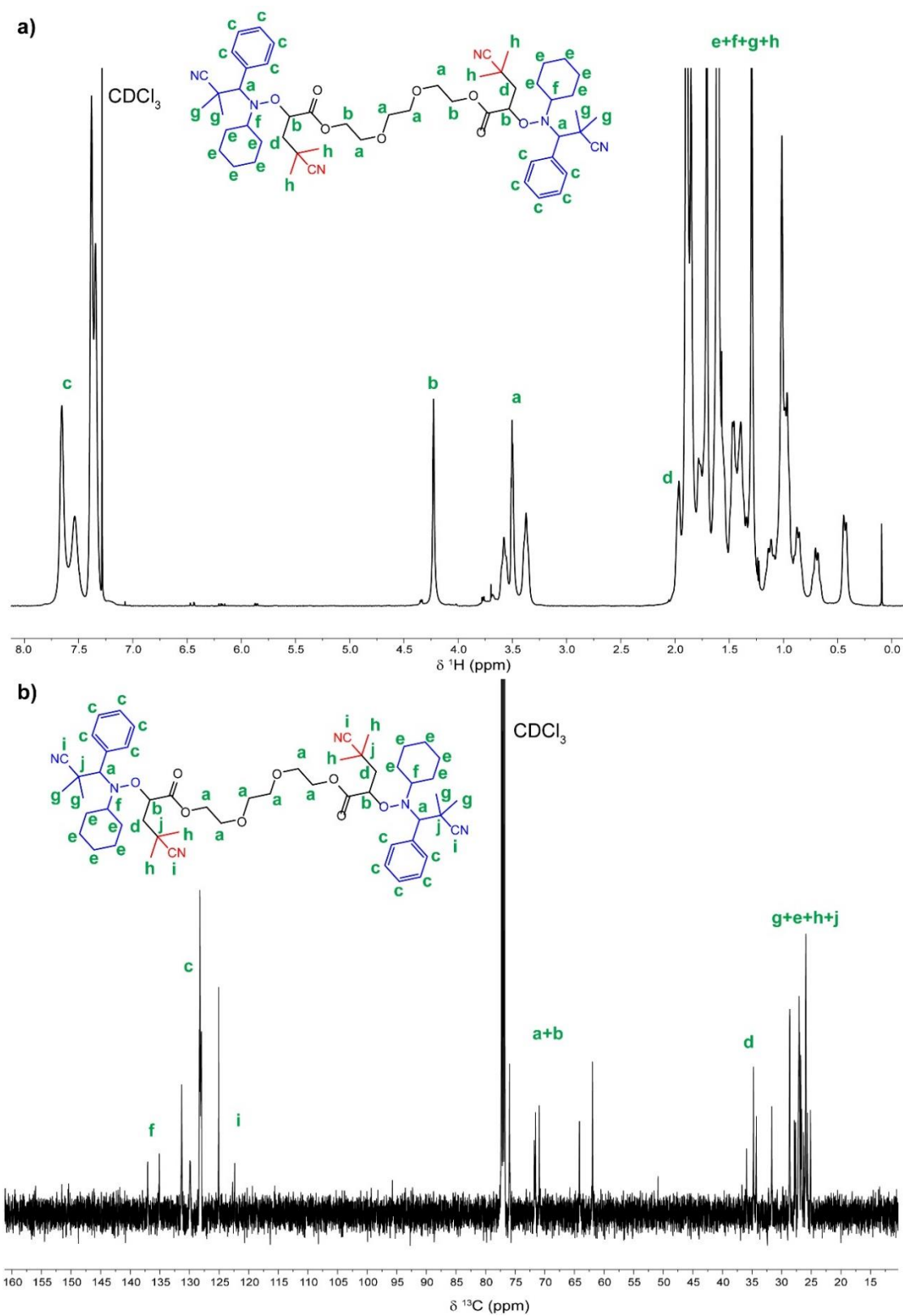
Figure 9.S2. a) ^{1}H NMR spectrum and b) ^{13}C NMR spectrum for D7-based difunctional alkoxyamine in CDCl$_3$.
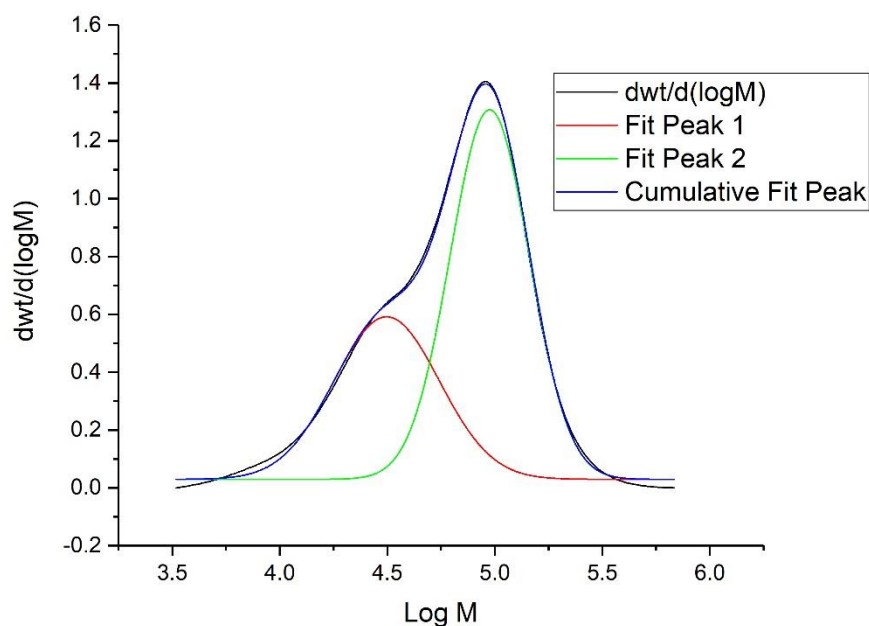
Figure 9.S3. 37% of the total Bi-GMA-*tri*-C13MA triblock copolymers were dead chains after 2 hours of chain extension of Bi-GMA-MI with C13MA. The percentage of dead polymers was estimated by Multiple Gaussian peak fitting.
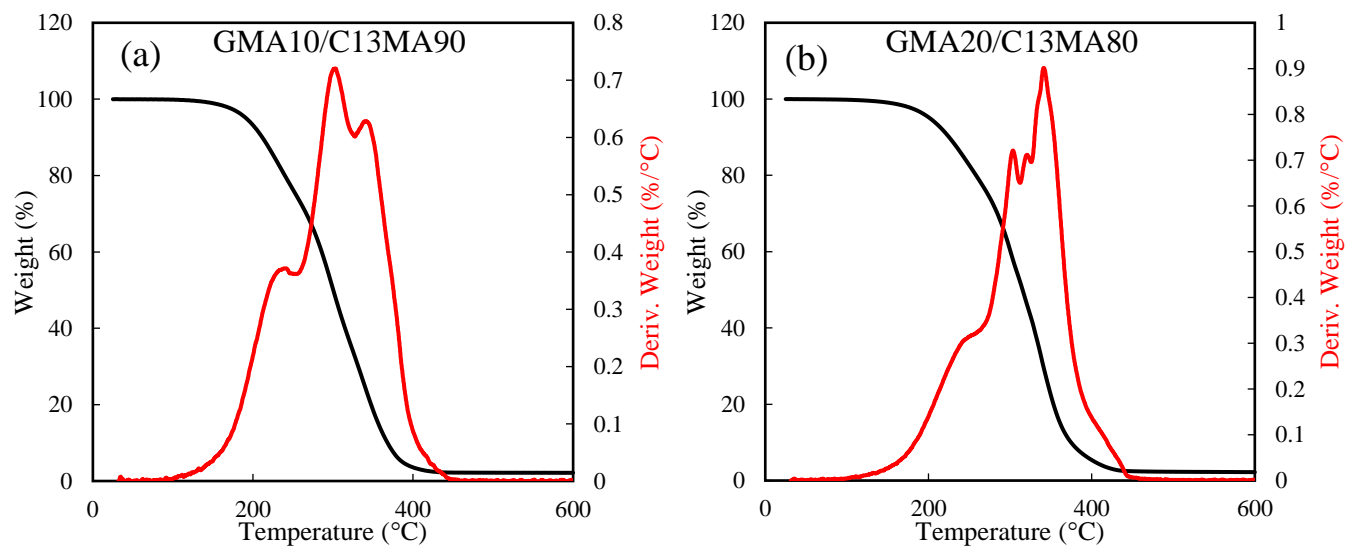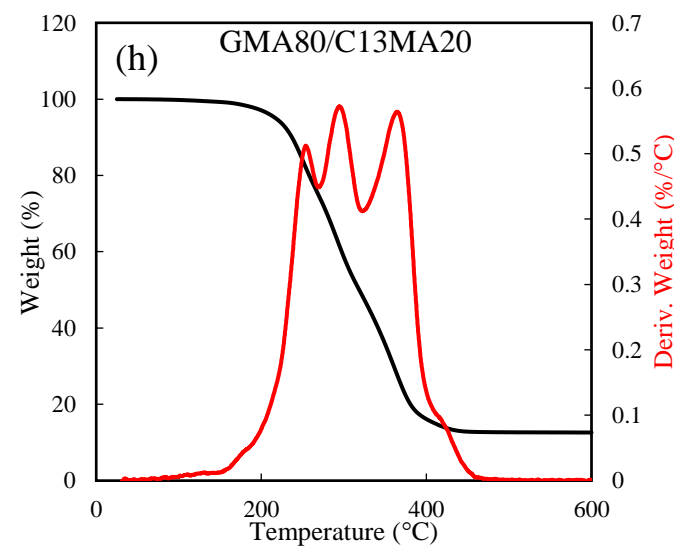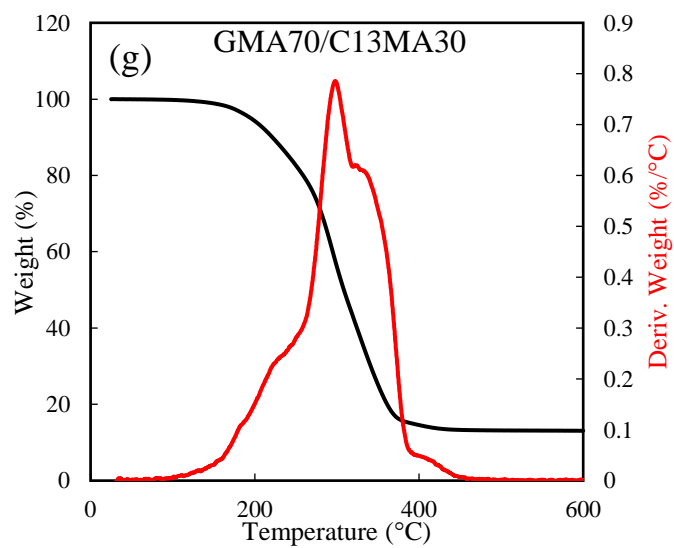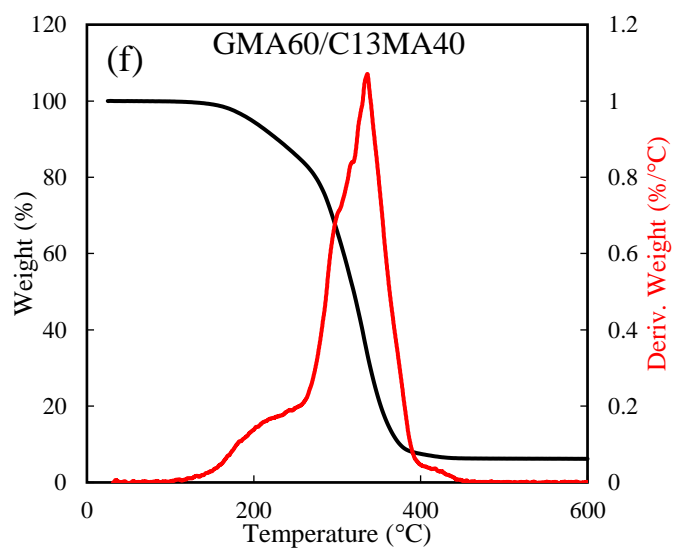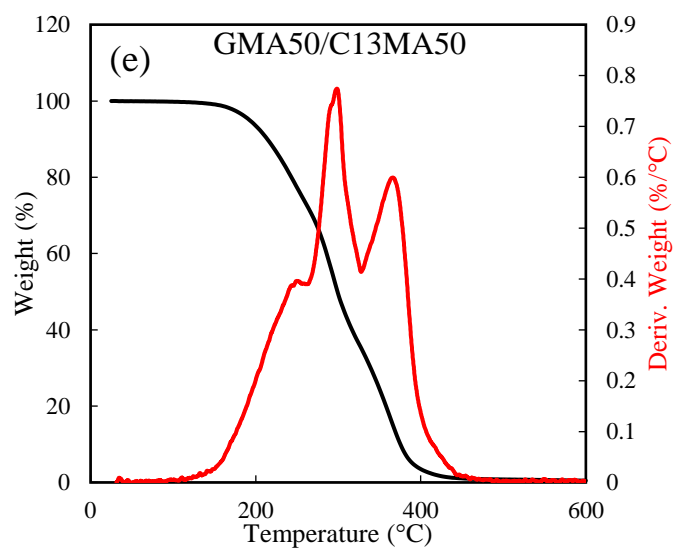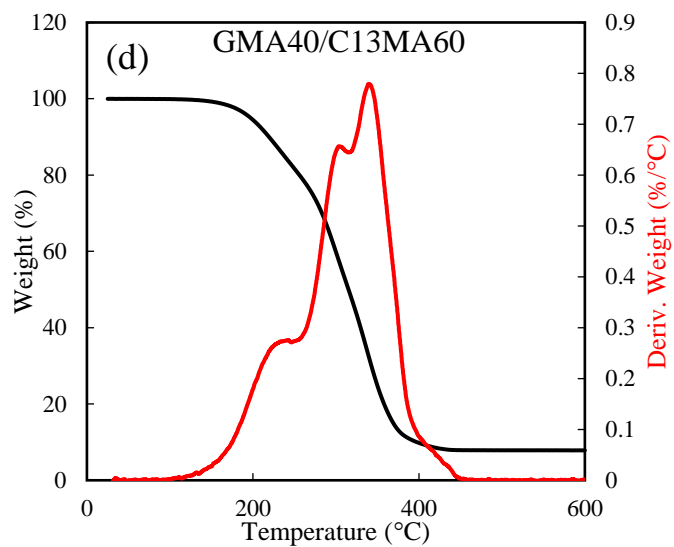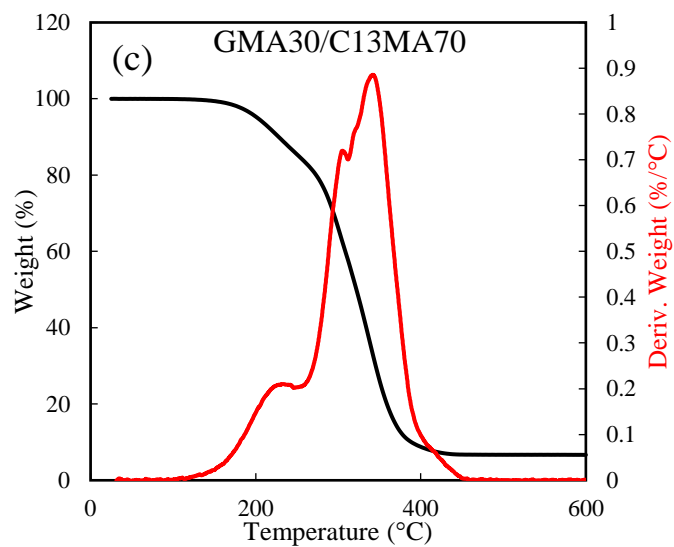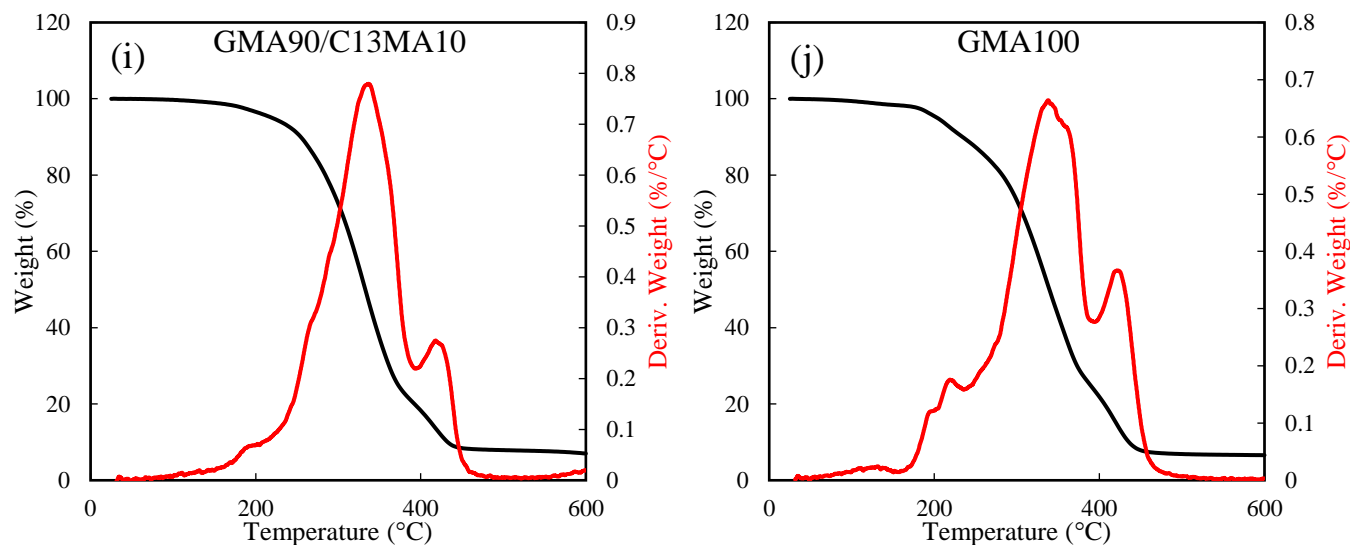
Figure 9.S4. TGA traces for a) to i) statistical copolymers of GMA/C13MA (M_n = 23.0-32.2 kg mol⁻¹, Đ = 1.56-1.77) and j) GMA homopolymer (M_n = 24.1 kg mol⁻¹, Đ = 1.76) in the range of 25 to 600 °C.
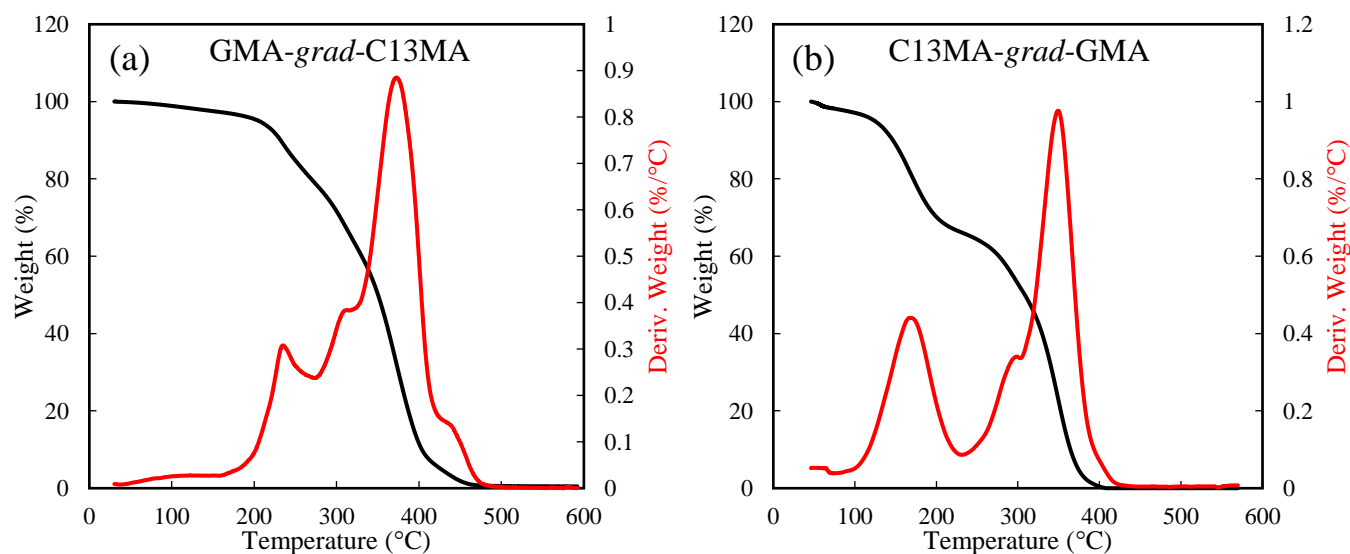
Figure 9.S5. TGA traces for a) GMA-*grad*-C13MA (M_n = 35.7 kg mol⁻¹, Đ = 1.79) and b) C13MA-*grad*-GMA (M_n = 27.6 kg mol⁻¹, Đ = 1.60) block copolymers in the range of 25 to 600 °C.
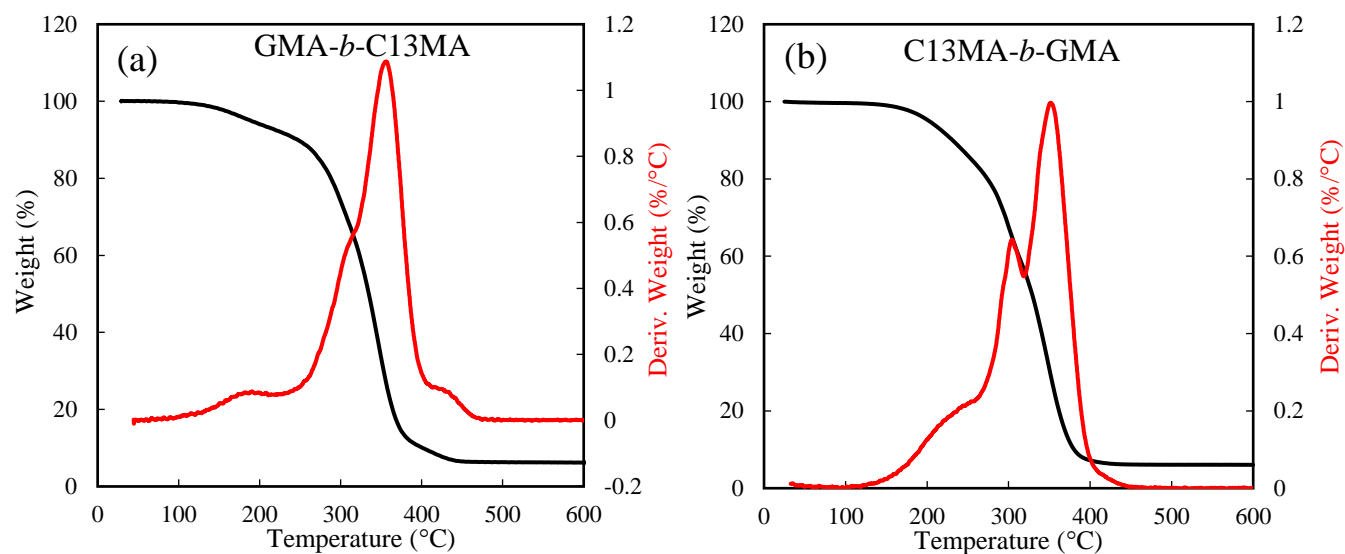
Figure 9.S6. TGA traces for a) GMA-*b*-C13MA (M_n = 43.1 kg mol^{-1}, Đ = 1.78) and b) C13MA-*b*-GMA (M_n = 43.0 kg mol^{-1}, Đ = 1.89) block copolymers in the range of 25 to 600 °C.
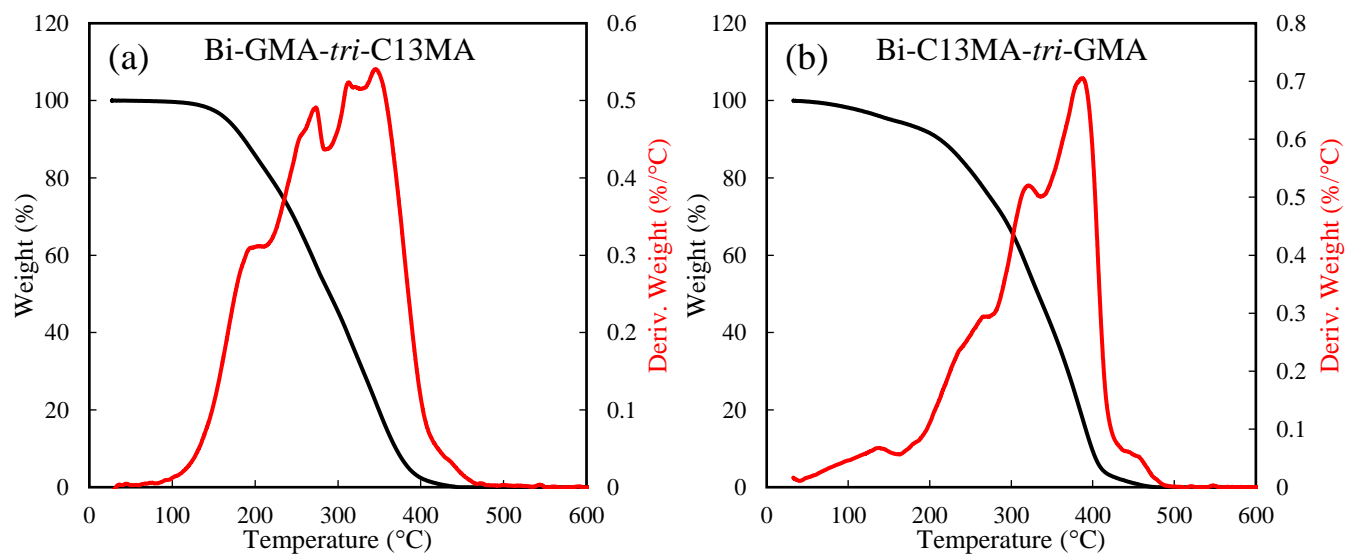
Figure 9.S7. TGA traces for a) Bi-GMA-*tri*-C13MA (M_n = 43.0 kg mol^{-1}, Đ = 1.85) and b) Bi-C13MA-*tri*-GMA (M_n = 45.5 kg mol^{-1}, Đ = 1.70) triblock copolymers in the range of 25 to 600 °C.

SUPPORTING INFORMATION: Development of water-borne coating formulation

S.1. Cross-linking of coatings

Cross-linking of polymer chains is an important process in coating formation for many applications such as production of latex paints [553-555]. This process enhances thermal, chemical, physical and dimensional stability of the coatings and as a consequence, it directly improves the resistance of coatings against cracks, scratches and stress factors[556]. Two main methods of cross-linking are generally used. The first method is two-component cross-linking where one of the cross-linking components is added just before application. The second method is self-cross-linking systems where all cross-linking monomers and crosslinkers are present in the dispersion. This method is more desirable for industrial applications because latexes with self-cross-linking properties can be stored or transferred easily and they are not required to be mixed before the coating process[557].

The properties of coatings change by variation in cross-linking density. The cross-linking density determines the number of free functional groups in polymer chains and thus the amount of free volume between the chains, which can be related to the modulus of the material [558, 559]. To make cross-linked polymers, one or more types of cross-linking monomer should be added to the formulation. These monomers with functional groups react with cross-linkers. Acetoacetoxyethyl methacrylate (AAEMA) can be used as a precursor in the polymers of interest in this thesis (Figure S.1)[519]. This monomer increases the adhesion of the coating and in conjunction with polyfunctional amines, provides the cross-linking of water-borne coatings[560].
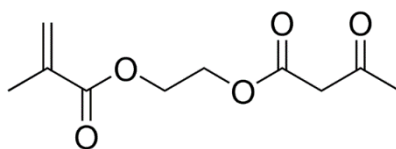
Figure S.1. Molecular structure of AAEMA[519].

In this study, adipic acid dihydrazide (AAD) was used as the cross-linker. AAD is water-soluble and it can be added to the final polymer latex before coating. By the evaporation of water and the formation of polymer film, acylhydrazone bonds will form between polymer chains. Figure S.2 shows a schematic reaction of AAD and AAEMA monomers in polymer chains. An alternative to this method is the addition of

acrylamido-based monomers (e.g. diacetone acrylamide) as the cross-linking monomer and adipic acid dihydrazide as the cross-linker [561, 562].
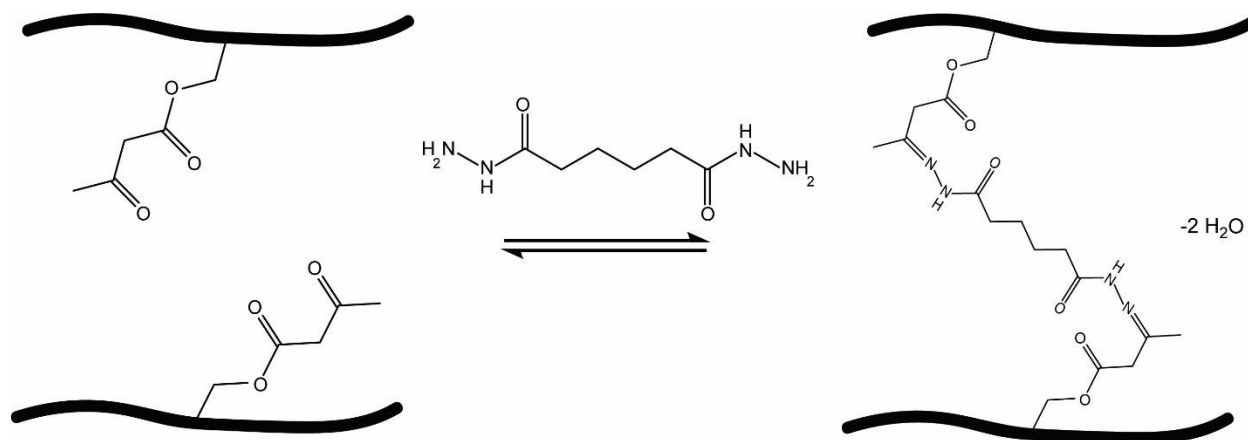
Figure S.2. The schematic reaction of AAEMA monomers in polymer chains with AAD and the formation of acylhydrazone bonds.

S.2. Film formation of water-borne coatings

The film formation of the latexes can be generally broken down into three steps [563-565]. A schematic of film formation is shown in Figure S.3.
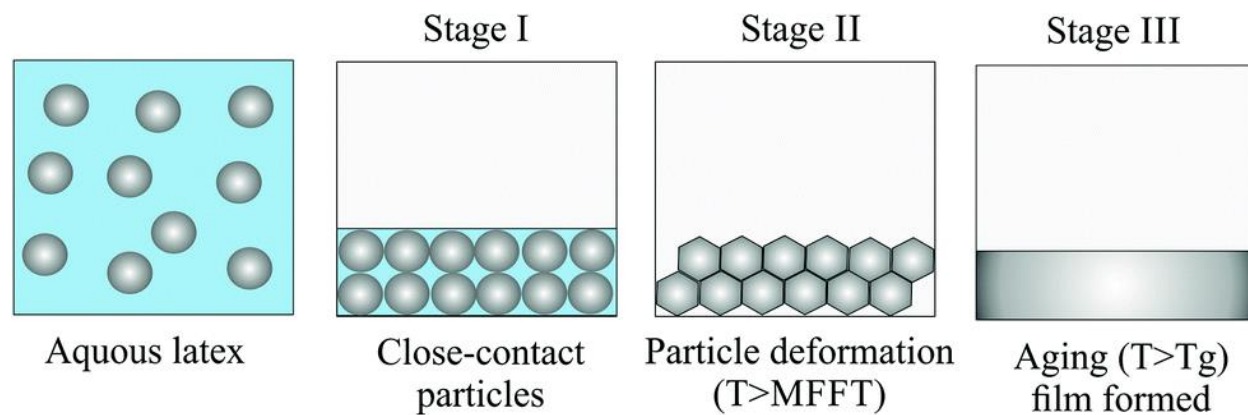
Figure S.3. Stages of the film formation for waterborne coatings. Adapted with permission from Royal Society of Chemistry[566].

In the first stage, polymer particles become more and more concentrated as water evaporates. The evaporation of water continues, and the particles get very close to each other. In the second stage, the polymer particles come into irreversible contact and the deformation of particles begins to bind particles

together and form a compact coating. Finally, in the third stage the water completely evaporates via remaining interparticle channels and capillary forces and cross-linking bonds push the particles together to form a completely dry film [557, 565, 567, 568]. During this stage the soft latex becomes a continuous film with the mechanical properties of the polymer resins[568]. The minimum temperature that the coalescence of polymer particles occurs and when film formation is possible is called the minimum film formation temperature (MFFT). The measurement of MFFT for polymer latexes is based on the optical method and the T_g of polymers in particles can directly change the value of MFFT[109].

In the following sections, the effect of different polymer compositions, cross-linking density, co-stabilizer, temperature and relative humidity and the addition of coalescing agents on the film formation were discussed.

S.3. Preparation of polymer latexes

First, polymer coatings with different IBOMA/POSSMA/C13MA/AAEMA monomer compositions were synthesized by nitroxide mediated miniemulsion polymerization at 90 °C. Dispolreg 007 alkoxyamine was used to initiate the polymerization and $M_{n,target} = 45$ kg mol^{-1} was considered for the polymerizations. The reaction time for all the polymerizations was 210 minutes. Table S.1 presents the experimental conditions and polymer characteristics for each experiment.

Table S.1. water-borne coating formulations prepared by nitroxide mediated miniemulsion polymerization using Dispolreg 007 at 90 °C.

Sample name	Initial Composition				M_n (kg mol^{-1})	Đ	T_g (°C)
	f_{IBOMA}	f_{POSSMA}	f_{C13MA}	f_{AAEMA}			
F1[a]	0.50	0.20	0.20	0.10	46.5	1.61	30
F2	0.60	0.10	0.10	0.20	-	-	-
F3	0.50	0.10	0.20	0.20	54.6	1.60	33
F4	0.50	0.10	0.30	0.10	55	1.65	27
F5	0.60	0.10	0.20	0.10	50.0	1.74	50
F6	0.55	0.10	0.25	0.10	60.2	1.56	33
F7	0.50	0.05	0.25	0.20	49.7	1.88	-
F8	0.49	0.05	0.26	0.20	52.8	1.89	-

[a] 12.5 wbm% toluene was added for F1 formulation to dissolve POSSMA.

S.4. The effect of the cross-linker ratio on the curing time and film formation

Next, we studied the effect of the AAD content on the film formation. Figure S.4 displays the coating formation with different cross-linker content. F1 formulation was used as the base polymer latex and AAD with the ratio of [0:1, 0.5:1 and 2:1 mol/mol AAEMA] were added to the polymer latex before coating on the wood surface. Based on the results, increasing the AAD content reduced the curing time, while causing some surface defects for the sample with $\frac{2 \text{ mol AAD}}{1 \text{ mol AAEMA}}$. This was due to the fast cross-linking inside the coating while water was evaporating and the formation of cracks on the film surface.
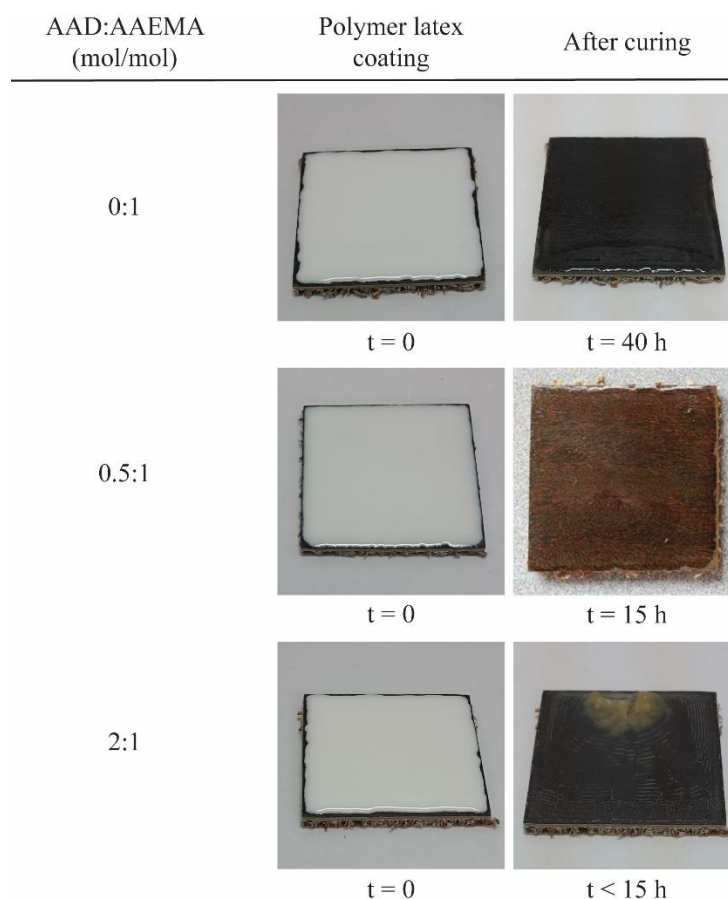
Figure S.4. The effect of the cross-linker (AAD) ratio on the film formation for F1 formulation at room temperature inside a fume hood. Increasing the AAD content reduced the curing time. However, it caused some surface defects due to the fast drying.

S.5. The effect of different co-stabilizers

In this experiment, the effect of reactive and unreactive costabilizer on polymer film formation was investigated. A similar coating formulation (F1) was used for this study and coatings were dried under the same environmental conditions inside a fume hood at 21 °C. 0.8 wbm% (weight based on monomers) of co-stabilizers were added to the monomer mixture before the miniemulsion polymerization. C17-MA is a mixture of alkyl methacrylates with average C17 aliphatic side chains. This monomer can act as a co-stabilizer in the monomer droplets and react with other monomers during the miniemulsion polymerization. Therefore, there would not be a residue in the polymer coating after drying and its effect on the mechanical, thermal and chemical properties of the final coating would be minimized. N-hexadecane is one of the most common nonreactive costabilizers that can improve the stability of the latex. The T_g and T_{dec}s for coating samples were presented in Table S.2. Based on the results, T_g and T_{dec}s of coating increases by removing hexadecane from the system and replacing it with C17-MA. This shows improved hardness and anti-flammability of the coating containing C17-MA stabilizer. However, the final coating was brittle and white. It seems that the addition of n-hexadecane helps with the flexibility of resins and formation of a solid and clear coating. The C17-MA monomers were polymerized with other monomers and they cannot act as the stabilizer significantly. Figure S.5 shows the difference between the coatings with different costabilizers.

Coating Formulation	Co-stabilizer	
F1	n-hexadecane	
F1	C17-MA	
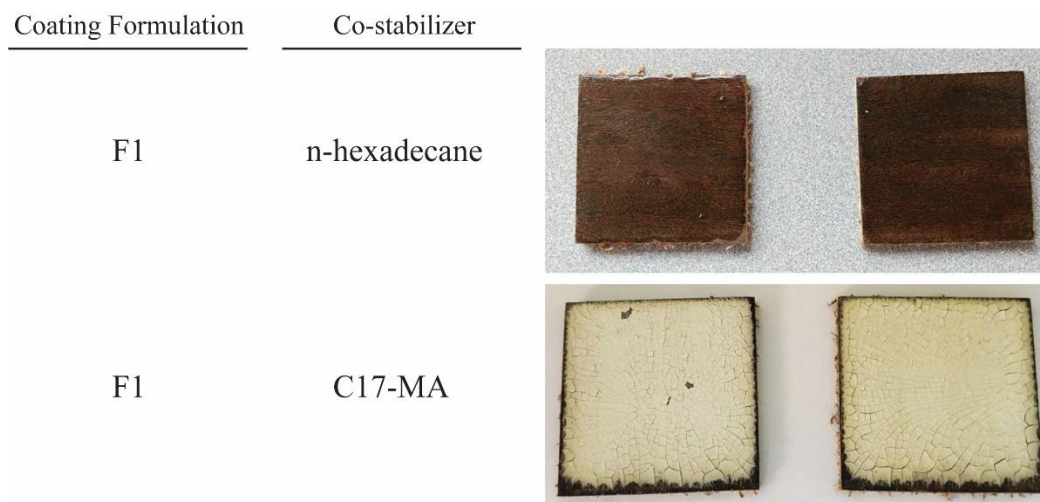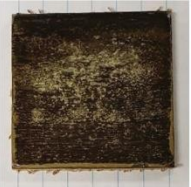
Figure S.5. The effect of different costabilizers on the film formation at ambient condition inside a fume hood. The clear coating was developed using n-hexadecane and the white and brittle coating was developed using C17-MA as the co-stabilizer. In both cases 0.8 wt% costabilizer based on monomers' weight was added.

S.6. Polymer film formation

The main problem with the first coating formulation (F1 and F1*) was that the coating was not hard enough and a small amount of toluene was added to dissolve POSS-MA monomers and mix them with other monomers. Therefore, a low concentration of toluene was present in the final polymer latex and consequently, in the final coating film. To address this problem, we developed three new formulations (F2, F3 and F4) by decreasing the amount of POSS-MA monomer and eliminating the toluene as the co-solvent. Among F2, F3 and F4 formulations, F3 had the best results in term of a clear coating formation. Therefore, F3 Latex was coated on veneer samples at different relative humidities and temperatures to find the minimum film formation temperature (MFFT) and humidity required for the coating process. We also studied the addition of different ratios of cross-linker to the coating to improve its hardness and resistance. To apply a layer of coating latex on veneer, a blade coating technique was used. The final samples were placed inside an oven with a temperature controller. First, a sample was prepared at room temperature (19-21 ºC) under the fume hood. Next, we tried different temperature ranges in the oven. At first, by increasing the temperature, the rate of water evaporation increases and resulted in a higher humidity inside the oven. It was also shown that, the addition of a small amount of cross-linker improves the coalescence of polymer particles, which is desired in this study. Figure S.6 shows the coating samples at different temperatures and relative humidity after curing for 24 h in oven. Based on the results, the temperature of 45-50 ºC and the cross-linker with the ratio of $\frac{0.1 \ mol_{cross-linker}}{1 \ mol_{AAEMA \ monomer}}$ will show the best results in terms of lowest surface defects for this coating process inside an oven. Furthermore, the F3 coating formulation had a MFFT $\cong$ 40 °C.

AAD:AAEMA [mol/mol]	T = 20 ± 1 °C H = 56 ± 8 %	T = 30 ± 5 °C H = 58 ± 25 %	T = 43 ± 5 °C H = 56 ± 20 %	T = 54 ± 4 °C H = 58 ± 27 %
0:1				
0.1:1				
0.2:1				
0.3:1				

Figure S.6. The effect of the different cross-linking densities and oven temperatures on the film formation of F3 water-borne coating formulation. The oven temperature was controlled and no control on humidity was applied.

To improve the hardness of polymer coatings, the F5 formulation with higher IBOMA concentration in the copolymer was prepared (Table S.1). F5 coating had a high glass transition temperature of 50 °C. Therefore, the final coating had a high MFFT and a higher booth temperature was required for the coalescence of polymer particles and the film formation. To decrease the MFFT and T_g, F6 coating was prepared by using a lower IBOMA content compared to F5. The problem with coalescence and the appearance of the cracks on the samples, prepared at room temperature, was due to the high MFFT of the coating latex. As we improve the hardness of the coating, the MFFT increases accordingly. Therefore, the samples require higher booth temperature and a controlled environment to form a hard, glassy and transparent coating. A MFFT below 40 °C was targeted in this study as it can facilitate the application of the water-borne coatings in an industrial setting. The coalescence of polymer particles and the appearance of polymer coating formulations were tested in an oven at 40 °C. The humidity inside the oven was also higher than the fume hood (our previous studies). The effect of the co-solvent (toluene) on the MFFT and the appearance of the coatings

was studied by comparing F6 formulation containing toluene (10 wbm%) and without toluene in monomer mixture. F1* (or F1 (+ 0.8 wbm% C17-MA co-stabilizer)), F1 (+ 0.8 wbm% n-hexadecane co-stabilizer), F3, F4, F5, F6 (+ 10 wbm% toluene cosolvent) and F6 (without toluene) polymer latexes were used for this study. Figure S.7 shows the polymer coatings prepared at 40 °C inside an oven.
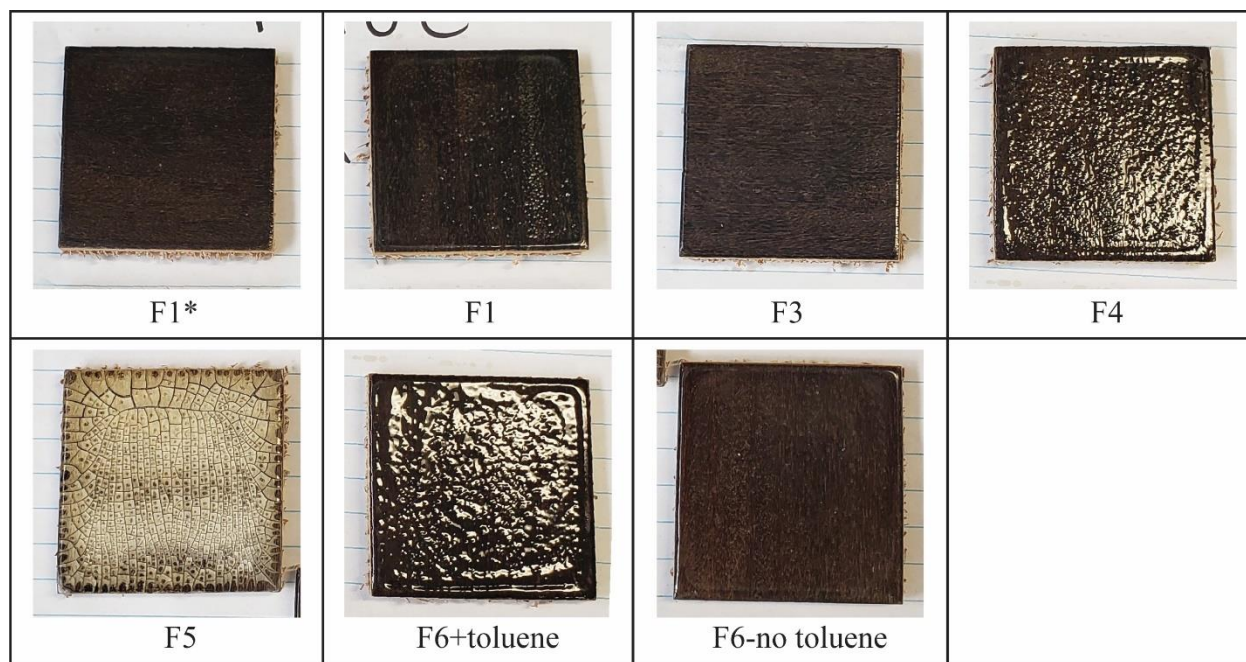
Figure S.7. coating samples prepared at 40 °C in the oven.

The drying time was 3 to 4 days (depends on the coating samples). The high humidity inside the oven slowed down the water evaporation. For this study, no crosslinker was added to the coating latexes. Based on the results, F1*, F3 and F6 (without toluene) were hard, transparent and showed a good adhesion to the wood surface. F3 and F6 (without toluene) did not have any organic solvents. F5 had multiple cracks, indicating the high glass transition temperature (T_g = 50 °C) and MFFT of the coating. F1, F4 and F6(+Toluene) had solvent bubbles at 40 °C although F1 and F4 can make a clear coating at room temperature.

S.7. Thermal properties of polymers

We also studied the thermal properties of the coating formulations and compared them with the previous results in emulsion and solvent systems. Based on the results, the decomposition temperature of the water-borne coatings containing POSS monomer are high which shows the successful incorporation of POSS monomers in coating formulation. This results in the coatings with higher resistant against the elevated temperatures and may improve the anti-flammability properties of the final coatings (the flame resistance

of the water-borne coatings should be tested at the industrial partner site). It was also shown that the addition of POSS nanoparticles may not be necessary for improving the anti-flammability of the water-based coatings and we can only use 10% POSS-MA monomers to improve the flame resistance. This can be tested in the next studies. Table S.2 compares the thermal properties of the water-based and solvent-based coatings.

Table S.2. Thermal properties of some of the coatings prepared in aqueous and solvent based systems.

Experiment ID	Solid content %	Reaction time (Min)	T_g (°C)	$T_{dec,1}$ (°C)	$T_{dec,max}$ (°C)	$T_{dec,2}$ (°C)	Coating appearance
Solvent-based coatings							
The solvent-based formulation without POSS nanoparticles	-	-	60	230	-	-	Clear/cracks
The solvent-based formulation with 20 wt% POSS nanoparticles	-	-	60	250	-	-	Clear/cracks
Water-based coatings							
F1 (+ Hexadecane)	24	210	30	222	291	467	Clear/transparent
F1 (+ C17-MA)	24	210	35	236	312	478	White/brittle
F4	24	210	27	233	306	487	Clear/transparent
F5	24	210	50	224	291	475	White/ brittle
F6	24	210	33	231	304	484	Clear/transparent

The film formation of the water-borne coating depends on temperature and relative humidity of the environment. The change in temperature and humidity can result in changes in the appearance of final coatings and the formation of cracks or bubbles in the polymer film. This is mainly due to the high MFFT of the coating formulations and corresponds to high hardness (T_g) of the coating. To preserve the required hardness and decrease the MFFT, coalescing agents were added to the formulations. However, the hardness of the final coating decreased, and the surface defects were observed on the final coating layer. To solve this problem, we will slightly increase the T_g of coatings by changing the formulation and add more coalescence agents (8-10 wt%) to enhance the film formation process.

S.8. Addition of coalescing agents

Previously, we prepared 2 coating formulations (F7 & F8) with 32% solid content and we applied them on the wood samples using spray coating method at Safran company. However, these two coating formulations require high booth temperature (>35 °C) to be above the MFFT (Minimum film formation temperature) for a clear and hard coating. To decrease the MFFT, coalescing agents such as Texanol or Elevance Unify® 270 (herein termed as Unify) were used. Figure S.8 displays the chemical structures of Texanol and Unify.

Coalescing agents reduce the T_g during the polymer film formation and they slowly vaporize after the coating is applied. However, it can adversely affect the initial hardness of coatings.

a)   b)
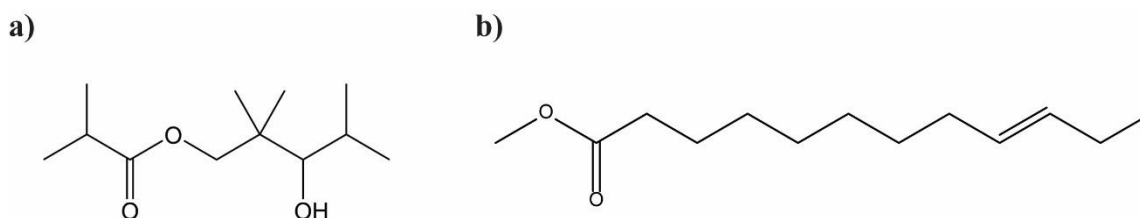
Figure S.8. chemical structures of a) Texanol b) Elevance Unify 270

Texanol is a conventional coalescence agent, which has been used in many water-borne coatings. Elevance Unify® 270 is bio-based (75% Bio-renewable carbon content) and biodegradable and it has a boiling point of 267 °C which makes it a great choice for our formulation. These agents were added during the polymerization to help with the film formation during the water evaporation and to decrease the MFFT of the final polymer latexes. Table S.3 presents the F8 and F9 formulations with different amounts of coalescing agents (weight % based on the monomers). The T_g of F8 and F9 coating formulations was around 33 °C (without coalescing agents).

Table S.3. Experimental conditions and polymer characteristics for F8 and F9 with coalescing agents.

Sample name	Initial Composition				[Unify] mol L^{-1}	[Texanol] mol L^{-1}	M_n (Kg mol^{-1})	X (%)	Đ	Solid content %
	f_{IBOMA}	f_{POSSMA}	f_{C13MA}	f_{AAEMA}						
F8 + 2% Texanol*	0.49	0.05	0.26	0.20		0.03	51.9	100	1.66	32
F8 + 3% Unify	0.49	0.05	0.26	0.20	0.047		48.2	100	1.70	32
F8 + 5% Unify	0.49	0.05	0.26	0.20	0.077		49.1	49	1.53	32
F8+8% Unify	0.49	0.05	0.26	0.20	0.092		51.2	77	1.59	32
F9 + 3% Unify	0.40	0.10	0.30	0.20	0.037		46.0	100	1.63	24

* F8 formulation containing 2 wt% Texanol coalescing agent based on monomers' weight.
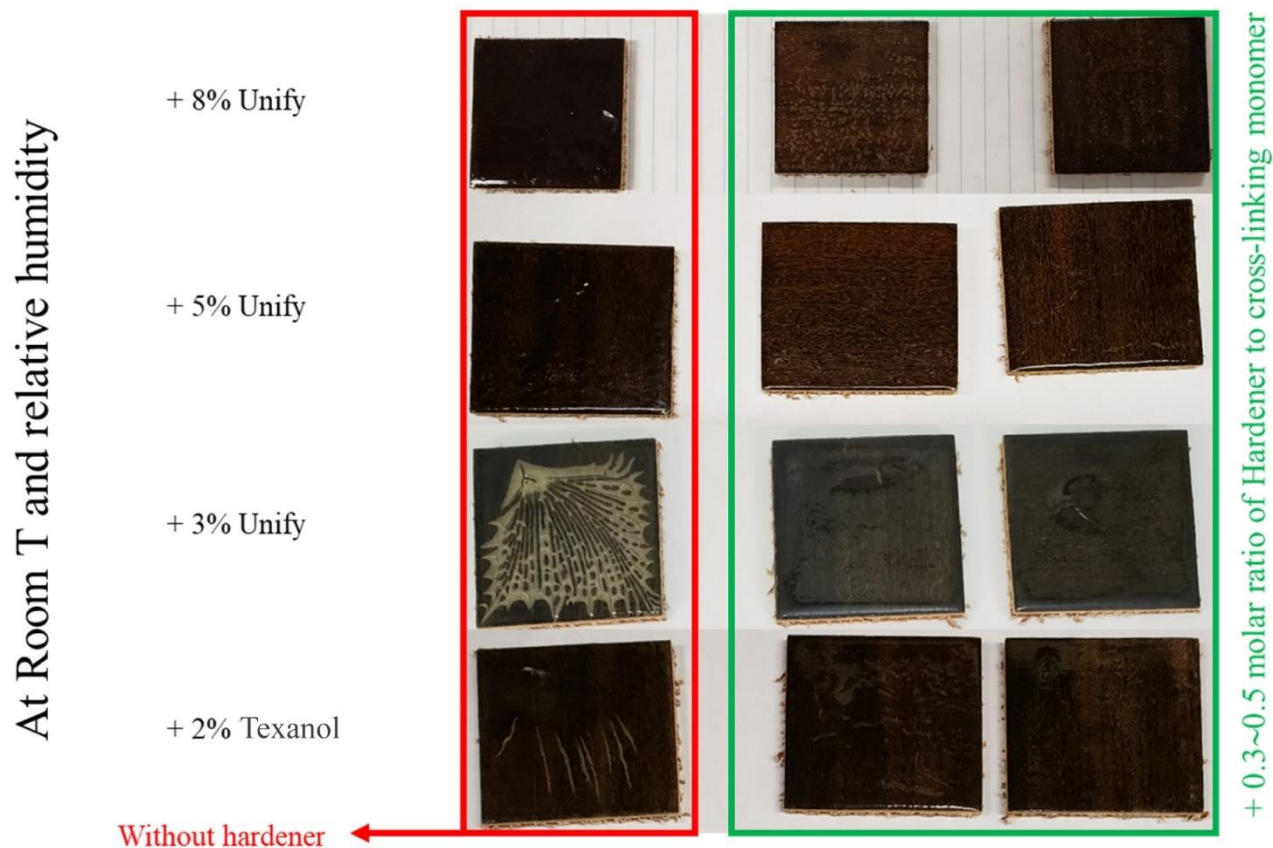
Figure S.9. The effect of coalescing agent and hardener (AAD) on the F8 film formation at room temperature.

Figure S.9 illustrates the effect of coalescing agent on the F8 film formation. Based on the results, the samples become clear after the water evaporation, which shows a successful film formation at room temperature. Also, samples with cross-linker showed a better coagulation and fewer number of cracks. However, some water pathways and cracks can be observed on the samples. This is due to the water evaporation in the coatings. As the coating becomes harder and the cross-linking bonds are formed, the water traps inside the coating and to evaporate and to escape from the film, they will move toward the softer parts where the coating is not fully developed, and the water evaporates from the formed cracks. To solve the cracking problem, we developed another formulation (F9) with higher percentage of POSS-MA monomers (10 mol% compared to 5% in F8 & F7). We previously observed that the addition of POSS-MA monomers helps with the hardness and the film formation. In addition, the solid content decreased to 24% to increase the time of film formation. Also, the addition of different amounts of cross-linker was investigated to see the effect of cross-linker concentration on the crack formation. Figure S.10 presents the results for F9 polymer latex (All the coating samples were prepared in a fume hood at room temperature

(21 °C). Based on the results, it can be concluded that increasing the amount of POSS-MA improved the film formation. Furthermore, increasing the concentration of cross-linker improves the coalescence of particles.

$$+ \frac{0 \text{ mol AAD}}{1 \text{ mol AAEMA}} \qquad + \frac{0.1 \text{ mol AAD}}{1 \text{ mol AAEMA}} \qquad + \frac{0.3 \text{ mol AAD}}{1 \text{ mol AAEMA}} \qquad + \frac{0.5 \text{ mol AAD}}{1 \text{ mol AAEMA}}$$
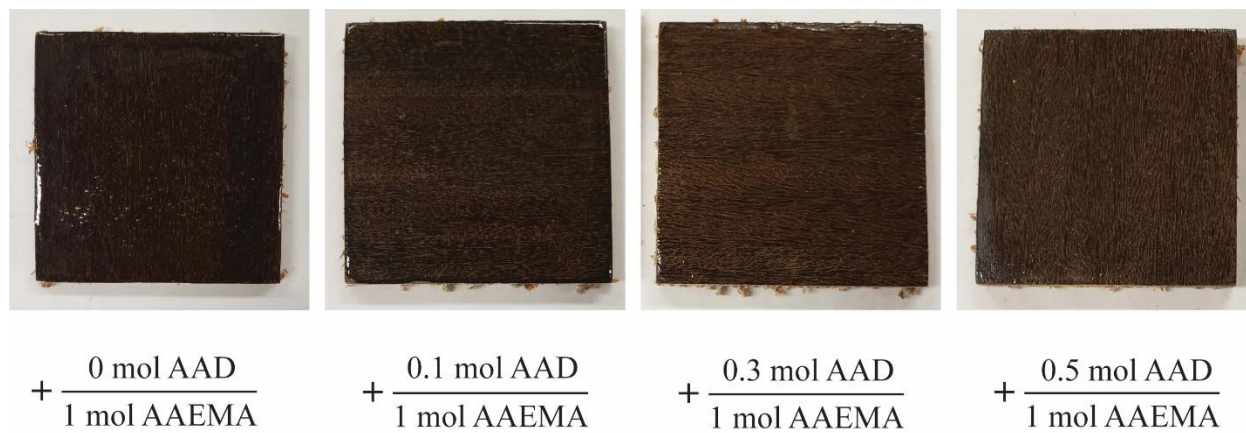
Figure S.10. F9 coating samples with different ratios of AAD based on initial AAEMA content. The samples had 3 % Unify coalescing agent and were coated at room temperature in a fume hood.

S.9. Impact test results

To test the hardness and impact resistance of coating formulations, the polymer coatings were subjected to a falling weight (total mass = 2 lb) using an Elcometer 1615 hardness tester. The impact results (Table S.4) were approximately the same for water-borne formulations and impact results were lower than samples prepared in toluene.

Table S.4. Impact results for polymer coatings (water-borne coatings and epoxy-based coating) compared to the previous formulations.

Sample Name	Height (cm)	Impact energy (mJ)	Reference
F1*	3	270	This study
F1	3	270	This study
F3	4	360	This study
F4	4	360	This study
F6+toluene	3	270	This study
F6-No toluene	3	270	This study
Organic solvent-based formulation	6	530	569
Safran's varnish (Hentzen product)	16	1420	569

246

* The final thickness of coatings after drying was 0.3 to 0.6 mm. The weight of the falling weight for impact test was 2 lb (0.907 kg).

S.10. Adhesion test

The pull-off adhesion tests were performed on coating samples using a dolly, attached to the polymer coating on the wood surface. The results for the adhesion test are listed in Table S.5. It was shown that increasing the solid content from 24 wt% to 35 wt% (increasing the surfactant concentration from 2 wt% to 5 wt% based on monomers' weight) reduced the pull-off strength by 31 psi. In general, the pull of strength was in the range of 182-264 psi, which is lower than Hentzen product (pull-off strength = 890 psi). To improve the adhesion, one method is to use insulators (silane coupling agents) on the wood surface before applying the water-borne coatings. Using insulators, the penetration of polymer coatings to wood surface increases.

Table S.5. Adhesion of the F3 and F6 water-borne coatings to the wood surface.

Formulation	M_n (kg mol^{-1})	$Đ$	Amount of cross-linker ($\frac{\text{mol AAD}}{\text{1 mol AAEMA}}$)	Pull-Off Strength (psi)**
F3-35%S*	50.8	1.67	0.5	200
F3-35%S	50.8	1.67	0.3	182
F3	54.6	1.60	0.5	231
F3	54.6	1.60	0	264
F6	60.2	1.56	0	231

* F3 formulation with 35% solid content (5 wbm% surfactant + 0.8 wbm% co-stabilizer)
**Without applying insulator

247

REFERENCES

1.   Walker, J. C. F., Basic wood chemistry and cell wall ultrastructure. In *Primary Wood Processing: Principles and practice*, Springer Netherlands: Dordrecht, 1993; pp 23-67.

2.   Feist, W. C.; Hon, D. N.-S., Chemistry of weathering and protection. In *The chemistry of solid wood*, Rowell, R., Ed. American Chemical Society, Washington: 1984; Vol. 207, pp 401-451.

3.   Schaller, C.; Rogez, D., New approaches in wood coating stabilization. *J. Coat. Technol. Res.* **2007,** *4* (4), 401-409.

4.   Procopio, L. J.; Larson, G. R.; Rosano, W. J., Low-VOC waterborne coatings for use in industrial maintenance painting. *JCT Coatings Tech* **2007,** *4* (3), 50-59.

5.   Philipp, C.; Eschig, S., Waterborne polyurethane wood coatings based on rapeseed fatty acid methyl esters. *Prog. Org. Coat.* **2012,** *74* (4), 705-711.

6.   Król, P.; Chmielarz, P., Recent advances in ATRP methods in relation to the synthesis of copolymer coating materials. *Prog. Org. Coat.* **2014,** *77* (5), 913-948.

7.   Bulian, F.; Graystone, J. A., Chapter 3 - Raw Materials for Wood Coatings (1) – Film Formers (Binders, Resins and Polymers). In *Wood Coatings*, Bulian, F.; Graystone, J. A., Eds. Elsevier: Amsterdam, 2009; pp 53-94.

8.   Hatton, F. L., Recent advances in RAFT polymerization of monomers derived from renewable resources. *Polym. Chem.* **2020,** *11* (2), 220-229.

9.   Barner-Kowollik, C., *Handbook of RAFT polymerization*. John Wiley & Sons: Weinheim, 2008.

10.   Matyjaszewski, K., Atom Transfer Radical Polymerization (ATRP): Current Status and Future Perspectives. *Macromolecules* **2012,** *45*, 4015.

11.   Matyjaszewski, K.; Xia, J., Atom transfer radical polymerization. *Chem. Rev.* **2001,** *101* (9), 2921-2990.

12.   Matyjaszewski, K., Advanced Materials by Atom Transfer Radical Polymerization. *Adv. Mater.* **2018,** *30* (23), 1706441.

13.   Destarac, M., Controlled radical polymerization: industrial stakes, obstacles and achievements. *Macromol. React. Eng.* **2010,** *4* (3-4), 165-179.

14.   Chiefari, J.; Chong, Y.; Ercole, F.; Krstina, J.; Jeffery, J.; Le, T. P.; Mayadunne, R. T.; Meijs, G. F.; Moad, C. L.; Moad, G., Living free-radical polymerization by reversible addition− fragmentation chain transfer: the RAFT process. *Macromolecules* **1998,** *31* (16), 5559-5562.

15.   Moad, G.; Solomon, D. H., 9 - Living Radical Polymerization. In *The Chemistry of Radical Polymerization (Second Edition)*, Moad, G.; Solomon, D. H., Eds. Elsevier Science Ltd: Amsterdam, 2005; pp 451-585.

16.   Corrigan, N.; Jung, K.; Moad, G.; Hawker, C. J.; Matyjaszewski, K.; Boyer, C., Reversible-deactivation radical polymerization (Controlled/living radical polymerization): From discovery to materials design and applications. *Prog. Polym. Sci.* **2020,** *111*, 101311.

17.   Moad, G.; Rizzardo, E.; Thang, S. H., Living radical polymerization by the RAFT process–a second update. *Aust. J. Chem.* **2009,** *62* (11), 1402-1472.

18.   di Lena, F.; Matyjaszewski, K., Transition metal catalysts for controlled radical polymerization. *Prog. Polym. Sci.* **2010,** *35* (8), 959-1021.

19.   Min, K.; Matyjaszewski, K., Atom transfer radical polymerization in aqueous dispersed media. *Cent. Eur. J. Chem.* **2009,** *7* (4), 657-674.

20.   Mei, W.; Maric, M., Nitroxide-Mediated Polymerization of 2-Hydroxyethyl Methacrylate (HEMA) Controlled with Low Concentrations of Acrylonitrile and Styrene. *Macromol. React. Eng.* **2017,** *11* (3), 1600067.

21.   Grubbs, R. B., Nitroxide-mediated radical polymerization: limitations and versatility. *Polym. Rev.* **2011,** *51* (2), 104-137.

22.   Beaudoin, E.; Bertin, D.; Gigmes, D.; Marque, S. R. A.; Siri, D.; Tordo, P., Alkoxyamine C–ON Bond Homolysis: Stereoelectronic Effects. *Eur. J. Org. Chem.* **2006,** *2006* (7), 1755-1768.

23.   Nicolas, J.; Guillaneuf, Y.; Lefay, C.; Bertin, D.; Gigmes, D.; Charleux, B., Nitroxide-mediated polymerization. *Prog. Polym. Sci.* **2013,** *38* (1), 63-235.

24.   Gigmes, D., *Nitroxide Mediated Polymerization : From Fundamentals to Applications in Materials Science*. Royal Society of Chemistry: Croydon, 2015; pp 1-493.

25.   Moad, G.; Rizzardo, E., Chapter 1 The History of Nitroxide-mediated Polymerization. In *Nitroxide Mediated Polymerization: From Fundamentals to Applications in Materials Science*, The Royal Society of Chemistry: Croydon, 2016; pp 1-44.

26.   Benoit, D.; Chaplinski, V.; Braslau, R.; Hawker, C. J., Development of a universal alkoxyamine for "living" free radical polymerizations. *J. Am. Chem. Soc.* **1999,** *121* (16), 3904-3920.

27.   Couturier, J.-L.; Gigmes, D.; Guerret, O.; Guillaneuf, Y. Process for the Preparation of the Alkoxyamine 2-Methyl-2-[N-(Diethoxyphosphoryl-2, 2-Dimethylpropyl)-Aminoxy] Propionic Acid. U.S. Patent 11,596,306, Sep. 11, 2008.

28.   Ballard, N.; Aguirre, M.; Simula, A.; Agirre, A.; Leiza, J. R.; Asua, J. M.; van Es, S., New Class of Alkoxyamines for Efficient Controlled Homopolymerization of Methacrylates. *ACS Macro Lett.* **2016,** *5* (9), 1019-1022.

29.   Simula, A.; Aguirre, M.; Ballard, N.; Veloso, A.; Leiza, J. R.; van Es, S.; Asua, J. M., Novel alkoxyamines for the successful controlled polymerization of styrene and methacrylates. *Polym. Chem.* **2017,** *8* (10), 1728-1736.

30.   Nicolas, J., Drug-Initiated Synthesis of Polymer Prodrugs: Combining Simplicity and Efficacy in Drug Delivery. *Chem. Mater.* **2016,** *28* (6), 1591-1606.

31.   Vinciguerra, D.; Denis, S.; Mougin, J.; Jacobs, M.; Guillaneuf, Y.; Mura, S.; Couvreur, P.; Nicolas, J., A facile route to heterotelechelic polymer prodrug nanoparticles for imaging, drug delivery and combination therapy. *J. Controlled Release* **2018,** *286*, 425-438.

32.   Kavand, A.; Anton, N.; Vandamme, T.; Serra, C. A.; Chan-Seng, D., Synthesis and functionalization of hyperbranched polymers for targeted drug delivery. *J. Controlled Release* **2020,** *321*, 285-311.

33.   Bouchet, R.; Maria, S.; Meziane, R.; Aboulaich, A.; Lienafa, L.; Bonnet, J.-P.; Phan, T. N. T.; Bertin, D.; Gigmes, D.; Devaux, D.; Denoyel, R.; Armand, M., Single-ion BAB triblock copolymers as highly efficient electrolytes for lithium-metal batteries. *Nat. Mater.* **2013,** *12* (5), 452-457.

34.   Bouchet, R.; Phan, T. N. T.; Beaudoin, E.; Devaux, D.; Davidson, P.; Bertin, D.; Denoyel, R., Charge Transport in Nanostructured PS–PEO–PS Triblock Copolymer Electrolytes. *Macromolecules* **2014,** *47* (8), 2659-2665.

35.   Yuan, K.; Li, F.; Chen, L.; Chen, Y., Approach to a block polymer precursor from poly(3-hexylthiophene) nitroxide-mediated in situ polymerization for stabilization of poly(3-hexylthiophene)/ZnO hybrid solar cells. *Thin Solid Films* **2012,** *520* (19), 6299-6306.

36.   Van De Wetering, K.; Brochon, C.; Ngov, C.; Hadziioannou, G., Design and Synthesis of a Low Band Gap Conjugated Macroinitiator: Toward Rod−Coil Donor−Acceptor Block Copolymers. *Macromolecules* **2006,** *39* (13), 4289-4297.

37.   Richard, F.; Brochon, C.; Leclerc, N.; Eckhardt, D.; Heiser, T.; Hadziioannou, G., Design of a Linear Poly(3-hexylthiophene)/Fullerene-Based Donor-Acceptor Rod-Coil Block Copolymer. *Macromol. Rapid Commun.* **2008,** *29* (11), 885-891.

38.   Shum, R. L.; Liu, S. R.; Caschera, A.; Foucher, D. A., UV-Curable Surface-Attached Antimicrobial Polymeric Onium Coatings: Designing Effective, Solvent-Resistant Coatings for Plastic Surfaces. *ACS Appl. Bio Mater.* **2020,** *3* (7), 4302-4315.

39.   Lamontagne, H. R.; Lessard, B. H., Nitroxide-Mediated Polymerization: A Versatile Tool for the Engineering of Next Generation Materials. *ACS Appl. Polym. Mater.* **2020,** *2* (12), 5327-5344.

40.   Ignatova, M.; Voccia, S.; Gilbert, B.; Markova, N.; Mercuri, P. S.; Galleni, M.; Sciannamea, V.; Lenoir, S.; Cossement, D.; Gouttebaron, R.; Jérôme, R.; Jérôme, C., Synthesis of Copolymer Brushes Endowed with Adhesion to Stainless Steel Surfaces and Antibacterial Properties by Controlled Nitroxide-Mediated Radical Polymerization. *Langmuir* **2004,** *20* (24), 10718-10726.

41.   Delaittre, G.; Nicolas, J.; Lefay, C.; Save, M.; Charleux, B., Surfactant-free synthesis of amphiphilic diblock copolymer nanoparticles via nitroxide-mediated emulsion polymerization. *Chem. Commun.* **2005,** *2005* (5), 614-616.

42.   Cresidio, S. P.; Aldabbagh, F.; Busfield, W. K.; Jenkins, I. D.; Thang, S. H.; Zayas-Holdsworth, C.; Zetterlund, P. B., Alkoxyamine-mediated "living" radical polymerization: MS investigation of the early stages of styrene polymerization initiated by cumyl-TEISO. *J. Polym. Sci., Part A: Polym. Chem.* **2001,** *39* (8), 1232-1241.

43.   Ballard, N.; Aguirre, M.; Simula, A.; Leiza, J. R.; van Es, S.; Asua, J. M., High solids content nitroxide mediated miniemulsion polymerization of n-butyl methacrylate. *Polym. Chem.* **2017,** *8* (10), 1628-1635.

44.   Jašo, V.; Stoiljković, D.; Radičević, R.; Bera, O., Kinetic modeling of bulk free-radical polymerization of methyl methacrylate. *Polym. J.* **2013,** *45* (6), 631-636.

45.   Dvornić, P. R.; Jaćović, M. S., The viscosity effect on autoacceleration of the rate of free radical polymerization. *Polym. Eng. Sci.* **1981,** *21* (12), 792-796.

46.   Zetterlund, P. B.; Thickett, S. C.; Perrier, S.; Bourgeat-Lami, E.; Lansalot, M., Controlled/Living Radical Polymerization in Dispersed Systems: An Update. *Chem. Rev.* **2015,** *115* (18), 9745-9800.

47.   Cunningham, M. F., Controlled/living radical polymerization in aqueous dispersed systems. *Prog. Polym. Sci.* **2008,** *33* (4), 365-398.

48.   Agarwal, S., *Engineering Chemistry: Fundamentals and Applications*. 2nd ed.; Cambridge University Press: New York, 2019.

49.   Asua, J. M., Emulsion polymerization: From fundamental mechanisms to process developments. *J. Polym. Sci., Part A: Polym. Chem.* **2004,** *42* (5), 1025-1041.

50.   Lovell, P. A.; El-Aasser, M. S.; Lovell, P., *Emulsion polymerization and emulsion polymers*. John Wiley & Sons, New York: 1997.

51.   Warson, H.; Finch, C. A., *Applications of Synthetic Resin Latices, Latices in Diverse Applications*. John Wiley & Sons: Chichester, England, 2001; Vol. 3.

52.   Chern, C., Emulsion polymerization mechanisms and kinetics. *Prog. Polym. Sci.* **2006,** *31* (5), 443-486.

53.   El-Aasser, M. S.; Sudol, E. D., Miniemulsions: overview of research and applications. *JCT Res.* **2004,** *1* (1), 21-32.

54.   Roe, C. P., Surface chemistry aspects of emulsion polymerization. *Ind. Eng. Chem.* **1968,** *60* (9), 20-33.

55.   Fitch, R. M.; Tsai, C., Particle formation in polymer colloids, III: Prediction of the number of particles by a homogeneous nucleation theory. In *Polymer colloids*, Springer: Boston, MA, 1971; pp 73-102.

56.   Harkins, W. D., A general theory of the mechanism of emulsion polymerization1. *J. Am. Chem. Soc.* **1947,** *69* (6), 1428-1444.

57.   Asua, J. M., Miniemulsion polymerization. *Prog. Polym. Sci.* **2002,** *27* (7), 1283-1346.

58.   Lovell, P. A.; Schork, F. J., Fundamentals of Emulsion Polymerization. *Biomacromolecules* **2020,** *21* (11), 4396-4441.

59.   Marestin, C.; Noël, C.; Guyot, A.; Claverie, J., Nitroxide mediated living radical polymerization of styrene in emulsion. *Macromolecules* **1998,** *31* (12), 4041-4044.

60.   Nicolas, J.; Charleux, B.; Guerret, O.; Magnet, S., Nitroxide-Mediated Controlled Free-Radical Emulsion Polymerization Using a Difunctional Water-Soluble Alkoxyamine Initiator. Toward the Control of Particle Size, Particle Size Distribution, and the Synthesis of Triblock Copolymers. *Macromolecules* **2005,** *38* (24), 9963-9973.

61.   Groison, E.; Brusseau, S.; D'Agosto, F.; Magnet, S.; Inoubli, R.; Couvreur, L.; Charleux, B., Well-Defined Amphiphilic Block Copolymer Nanoobjects via Nitroxide-Mediated Emulsion Polymerization. *ACS Macro Lett.* **2012,** *1* (1), 47-51.

62.   Cao, J.; He, J.; Li, C.; Yang, Y., Nitroxide-mediated radical polymerization of styrene in emulsion. *Polym. J.* **2001,** *33* (1), 75-80.

63.   Simms, R. W.; Hoidas, M. D.; Cunningham, M. F., Nitroxide-Mediated Styrene Surfactant-Free Emulsion Polymerization. *Macromolecules* **2008,** *41* (4), 1076-1079.

64.   Cunningham, M. F., Living/controlled radical polymerizations in dispersed phase systems. *Prog. Polym. Sci.* **2002,** *27* (6), 1039-1067.

65.   Cunningham, M. F.; Tortosa, K.; Lin, M.; Keoshkerian, B.; Georges, M. K., Influence of camphorsulfonic acid in nitroxide-mediated styrene miniemulsion polymerization. *J. Polym. Sci., Part A: Polym. Chem.* **2002,** *40* (16), 2828-2841.

66.   Farcet, C.; Charleux, B.; Pirri, R., Nitroxide-mediated miniemulsion polymerization of n-butyl acrylate: synthesis of controlled homopolymers and gradient copolymers with styrene. *Macromol. Symp.* **2002,** *182* (1), 249-260.

67.   Lin, M.; Cunningham, M. F.; Keoshkerian, B., Achieving high conversions in nitroxide-mediated living styrene miniemulsion polymerization. *Macromol. Symp.* **2004,** *206* (1), 263-274.

68.   Farcet, C.; Lansalot, M.; Charleux, B.; Pirri, R.; Vairon, J., Mechanistic aspects of nitroxide-mediated controlled radical polymerization of styrene in miniemulsion, using a water-soluble radical initiator. *Macromolecules* **2000,** *33* (23), 8559-8570.

69.   Keoshkerian, B.; MacLeod, P. J.; Georges, M. K., Block copolymer synthesis by a miniemulsion stable free radical polymerization process. *Macromolecules* **2001,** *34* (11), 3594-3599.

70.   Charleux, B.; Nicolas, J., Water-soluble SG1-based alkoxyamines: A breakthrough in controlled/living free-radical polymerization in aqueous dispersed media. *Polymer* **2007,** *48* (20), 5813-5833.

71.   Prodpran, T.; Dimonie, V. L.; Sudol, E. D.; El-Aasser, M. S., Nitroxide-mediated living free radical miniemulsion polymerization of styrene. *Macromol. Symp.* **2000,** *155* (1), 1-14.

72.   Landfester, K.; Schork, F. J.; Kusuma, V. A., Particle size distribution in mini-emulsion polymerization. *C. R. Chim.* **2003,** *6* (11), 1337-1342.

73.   Meliana, Y.; Suprianti, L.; Huang, Y. C.; Lin, C. T.; Chern, C.-S., Effect of mixed costabilizers on Ostwald ripening of monomer miniemulsions. *Colloids Surf., A* **2011,** *389* (1), 76-81.

74.   Chern, C.-S.; Liou, Y.-C., Effects of mixed surfactants on the styrene miniemulsion polymerization in the presence of an alkyl methacrylate. *Macromol. Chem. Phys.* **1998,** *199* (9), 2051-2061.

75.   Bigon, J. P.; Montoro, F. E.; Lona, L. M. F., Vegetable Oils Acting as Encapsulated Bioactives and Costabilizers in Miniemulsion Polymerization Reactions. *European Journal of Lipid Science and Technology* **2018,** *120* (1), 1700130.

76.   Zetterlund, P. B., Controlled/living radical polymerization in nanoreactors: compartmentalization effects. *Polym. Chem.* **2011,** *2* (3), 534-549.

77.   Sugihara, Y.; Zetterlund, P. B., Synergistic Effects of Compartmentalization and Nitroxide Exit/Entry in Nitroxide-Mediated Radical Polymerization in Dispersed Systems. *ACS Macro Lett.* **2012,** *1* (6), 692-696.

78.   Wang, S.; Schork, F., Miniemulsion polymerization of vinyl acetate with nonionic surfactant. *J. Appl. Polym. Sci.* **1994,** *54* (13), 2157-2164.

79.   Schork, F. J.; Guo, J., Continuous miniemulsion polymerization. *Macromol. React. Eng.* **2008,** *2* (4), 287-303.

80.   Alduncin, J. A.; Forcada, J.; Asua, J. M., Miniemulsion polymerization using oil-soluble initiators. *Macromolecules* **1994,** *27* (8), 2256-2261.

81.   Benoit, D.; Grimaldi, S.; Robin, S.; Finet, J.; Tordo, P.; Gnanou, Y., Kinetics and Mechanism of Controlled Free-Radical Polymerization of Styrene and n -Butyl Acrylate in the Presence of an Acyclic. *J. Am. Chem. Soc.* **2000,** *122*, 5929.

82.   Georges, M. K.; Veregin, R. P.; Kazmaier, P. M.; Hamer, G. K.; Saban, M., Narrow polydispersity polystyrene by a free-radical polymerization process-rate enhancement. *Macromolecules* **1994,** *27* (24), 7228-7229.

83.   Karine, T.; Jodi-Anne, S.; F., C. M., Synthesis of Polystyrene-block-poly(butyl acrylate) Copolymers Using Nitroxide-Mediated Living Radical Polymerization in Miniemulsion. *Macromol. Rapid Commun.* **2001,** *22* (12), 957-961.

84.   Guo, Y.; Zetterlund, P. B., Synthesis of nanosized (< 20 nm) polymer particles by radical polymerization in miniemulsion employing in situ surfactant formation. *Macromol. Rapid Commun.* **2011,** *32* (20), 1669-1675.

85.   Lansalot, M.; Farcet, C.; Charleux, B.; Vairon, J.-P.; Pirri, R., Controlled free-radical miniemulsion polymerization of styrene using degenerative transfer. *Macromolecules* **1999,** *32* (22), 7354-7360.

86.   Groison, E.; Brusseau, S. g. n.; D'Agosto, F.; Magnet, S. p.; Inoubli, R.; Couvreur, L.; Charleux, B., Well-defined amphiphilic block copolymer nanoobjects via nitroxide-mediated emulsion polymerization. *ACS Macro Lett.* **2011,** *1* (1), 47-51.

87.   Delplace, V.; Harrisson, S.; Ho, H. T.; Tardy, A.; Guillaneuf, Y.; Pascual, S.; Fontaine, L.; Nicolas, J., One-step synthesis of azlactone-functionalized SG1-based alkoxyamine for nitroxide-mediated polymerization and bioconjugation. *Macromolecules* **2015,** *48* (7), 2087-2097.

88.   Cunningham, M. F.; Xie, M.; McAuley, K. B.; Keoshkerian, B.; Georges, M. K., Nitroxide-mediated styrene miniemulsion polymerization. *Macromolecules* **2002,** *35* (1), 59-66.

89.   Nakamura, T.; Zetterlund, P. B.; Okubo, M., Particle Size Effects in TEMPO-Mediated Radical Polymerization of Styrene in Aqueous Miniemulsion: Part CCLXXXII of the series "Studies on Suspension and Emulsion". *Macromol. Rapid Commun.* **2006,** *27* (23), 2014-2018.

90.   Pan, G.; Sudol, E. D.; Dimonie, V. L.; El-Aasser, M. S., Nitroxide-mediated living free radical miniemulsion polymerization of styrene. *Macromolecules* **2001,** *34* (3), 481-488.

91.   Zetterlund, P. B.; Okubo, M., Compartmentalization in NMP in dispersed systems: relative contributions of confined space effect and segregation effect depending on nitroxide type. *Macromol. Theory Simul.* **2009,** *18* (4-5), 277-286.

92.   Zetterlund, P. B., Nitroxide-mediated radical polymerization in nanoreactors: can dilution or increased nitroxide concentration provide benefits similar to compartmentalization? *Aust. J. Chem.* **2010,** *63* (8), 1195-1200.

93.   Lansalot, M.; Farcet, C.; Charleux, B.; Vairon, J. P.; Pirri, R.; Tordo, P., Nitroxide-Mediated Controlled Free-Radical Emulsion and Miniemulsion Polymerizations of Styrene. In *Controlled/Living Radical Polymerization*, Matyjaszewski, K., Ed. American Chemical Society: Washington, 2000; Vol. 768, pp 138-151.

94.   Qiu, J.; Charleux, B.; Matyjaszewski, K., Controlled/living radical polymerization in aqueous media: homogeneous and heterogeneous systems. *Prog. Polym. Sci.* **2001,** *26* (10), 2083-2134.

95.   MacLeod, P. J.; Barber, R.; Odell, P. G.; Keoshkerian, B.; Georges, M. K., Stable free radical miniemulsion polymerization. *Macromol. Symp.* **2000,** *155* (1), 31-38.

96.   Rempel, G. L.; Wang, H., Microemulsion Polymerization. In *Encyclopedia of Polymeric Nanomaterials*, Kobayashi, S.; Müllen, K., Eds. Springer: Berlin, Heidelberg, 2015; pp 1241-1250.

97.   Yong, C. P.; Gan, L. M., Microemulsion Polymerizations and Reactions. In *Polymer Particles*, Okubo, M., Ed. Springer: Berlin, Heidelberg, 2005; pp 257-298.

98.   Monteiro, M. J., Nanoreactors for polymerizations and organic reactions. *Macromolecules* **2010,** *43* (3), 1159-1168.

99.   Li, W. J.; Cunningham, M. F., Nitroxide-mediated microemulsion polymerization of n-butyl acrylate: decoupling of target molecular weight and particle size. *Polym. Chem.* **2014,** *5* (12), 3804-3816.

100.   Zetterlund, P. B.; Wakamatsu, J.; Okubo, M., Nitroxide-mediated radical polymerization of styrene in aqueous microemulsion: Initiator efficiency, compartmentalization, and nitroxide phase transfer. *Macromolecules* **2009,** *42* (18), 6944-6952.

101.   Brooks, B., Suspension polymerization processes. *Chem. Eng. Technol.* **2010,** *33* (11), 1737-1744.

102.   Vivaldo-Lima, E.; Wood, P. E.; Hamielec, A. E.; Penlidis, A., An updated review on suspension polymerization. *Ind. Eng. Chem. Res.* **1997,** *36* (4), 939-965.

103.   Ballard, N.; Aguirre, M.; Simula, A.; Leiza, J. R.; van Es, S.; Asua, J. M., Nitroxide mediated suspension polymerization of methacrylic monomers. *Chem. Eng. J.* **2017,** *316* ((Supplement C)), 655-662.

104.   Gonçalves, O. H.; Machado, R. A.; de Araújo, P. H. H.; Asua, J. M., Secondary particle formation in seeded suspension polymerization. *Polymer* **2009,** *50* (2), 375-381.

105.   Biensan, M. Process for the preparation of polymer powders by suspension polymerization. U.S. Patent 5,840,819, Nov. 24, 1998.

106.   Georges, M. K.; Veregin, R. P.; Kazmaier, P. M.; Hamer, G. K., Narrow molecular weight resins by a free-radical polymerization process. *Macromolecules* **1993,** *26* (11), 2987-2988.

107. Tanaka, T.; Suzuki, T.; Saka, Y.; Zetterlund, P. B.; Okubo, M., Mechanical properties of cross-linked polymer particles prepared by nitroxide-mediated radical polymerization in aqueous micro-suspension. *Polymer* **2007,** *48* (13), 3836-3843.

108. Aramendia, E.; Barandiaran, M. J.; Grade, J.; Blease, T.; Asua, J. M., Improving water sensitivity in acrylic films using surfmers. *Langmuir* **2005,** *21* (4), 1428-1435.

109. Keddie, J. L., Film formation of latex. *Mater. Sci. Eng. R Rep.* **1997,** *21* (3), 101-170.

110. Keddie, J. L.; Routh, A. F., An Introduction to Latex and the Principles of Colloidal Stability. In *Fundamentals of Latex Film Formation: Processes and Properties*, Springer Netherlands: Dordrecht, 2010; pp 1-26.

111. Unzué, M. J.; Schoonbrood, H. A.; Asua, J. M.; Goñi, A. M.; Sherrington, D. C.; Stähler, K.; Goebel, K. H.; Tauer, K.; Sjöberg, M.; Holmberg, K., Reactive surfactants in heterophase polymerization. VI. Synthesis and screening of polymerizable surfactants (surfmers) with varying reactivity in high solids styrene—butyl acrylate—acrylic acid emulsion polymerization. *J. Appl. Polym. Sci.* **1997,** *66* (9), 1803-1820.

112. Yokota, K.; Ichihara, A.; Shinike, H. Surfactant. U.S. Patent 5,332,854, Jul. 26, 1994.

113. Pan, G.; Sudol, E. D.; Dimonie, V. L.; El-Aasser, M. S., Surfactant concentration effects on nitroxide-mediated living free radical miniemulsion polymerization of styrene. *Macromolecules* **2002,** *35* (18), 6915-6919.

114. Asua, J. M., Challenges for industrialization of miniemulsion polymerization. *Prog. Polym. Sci.* **2014,** *39* (10), 1797-1826.

115. Campbell, S. B.; Larson, T.; Smeets, N. M.; El-Jaby, U.; McKenna, T. F., Miniemulsification by catastrophic phase inversion. *Chem. Eng. J.* **2012,** *183*, 534-541.

116. Cunningham, M. F.; Lin, M.; Keoshkerian, B., Optimizing nitroxide-mediated miniemulsion polymerization processes. *JCT Res.* **2004,** *1* (1), 33-39.

117. Ouzineb, K.; Lord, C.; Lesauze, N.; Graillat, C.; Tanguy, P. A.; McKenna, T., Homogenisation devices for the production of miniemulsions. *Chem. Eng. Sci.* **2006,** *61* (9), 2994-3000.

118. Manea, M.; Chemtob, A.; Paulis, M.; de la Cal, J. C.; Barandiaran, M. J.; Asua, J. M., Miniemulsification in high-pressure homogenizers. *AIChE J.* **2008,** *54* (1), 289-297.

119. Thakur, R.; Vial, C.; Nigam, K.; Nauman, E.; Djelveh, G., Static mixers in the process industries—a review. *Chem. Eng. Res. Des.* **2003,** *81* (7), 787-826.

120. Prokopov, N. I.; Gritskova, I. A., Characteristic features of heterophase polymerisation of styrene with simultaneous formation of surfactants at the interface. *Russ. Chem. Rev.* **2001,** *70* (9), 791-800.

121. Parker, D. K.; Feher, F. J.; Mahadevan, V. Controlled polymerization. U.S. Patent 6,992,156, Jan. 31, 2006.

122. Guo, Y.; Liu, J.; Zetterlund, P. B., Nitroxide-mediated radical polymerization in miniemulsion on the basis of in situ surfactant formation without use of homogenization device. *Macromolecules* **2010,** *43* (14), 5914-5916.

123. Guo, Y.; Teo, V. L.; Ting, S. S.; Zetterlund, P. B., Miniemulsion polymerization based on in situ surfactant formation without high-energy homogenization: effects of organic acid and counter ion. *Polym. J.* **2012,** *44* (5), 375.

124. Okubo, M.; Minami, H.; Zhou, J., Preparation of block copolymer by atom transfer radical seeded emulsion polymerization. *Colloid Polym. Sci.* **2004,** *282* (7), 747-752.

125.   Min, K.; Gao, H.; Matyjaszewski, K., Development of an ab Initio Emulsion Atom Transfer Radical Polymerization: From Microemulsin to Emulsion. *J. Am. Chem. Soc.* **2006,** *128* (32), 10521-10526.

126.   Lim, M. S.; Chen, H., Miniemulsion polymerization of styrene with a block copolymer surfactant. *J. Polym. Sci., Part A: Polym. Chem.* **2000,** *38* (10), 1818-1827.

127.   Asua, J. M., Ostwald ripening of reactive costabilizers in miniemulsion polymerization. *Eur. Polym. J.* **2018,** *106*, 30-41.

128.   Delaittre, G.; Nicolas, J.; Lefay, C.; Save, M.; Charleux, B., Aqueous suspension of amphiphilic diblock copolymer nanoparticles prepared in situ from a water-soluble poly(sodium acrylate) alkoxyamine macroinitiator. *Soft Matter* **2006,** *2* (3), 223-231.

129.   Dire, C.; Magnet, S.; Couvreur, L.; Charleux, B., Nitroxide-mediated controlled/living free-radical surfactant-free emulsion polymerization of methyl methacrylate using a poly (methacrylic acid)-based macroalkoxyamine initiator. *Macromolecules* **2008,** *42* (1), 95-103.

130.   Brusseau, S.; Belleney, J.; Magnet, S.; Couvreur, L.; Charleux, B., Nitroxide-mediated copolymerization of methacrylic acid with sodium 4-styrene sulfonate: Towards new water-soluble macroalkoxyamines for the synthesis of amphiphilic block copolymers and nanoparticles. *Polym. Chem.* **2010,** *1* (5), 720-729.

131.   Stoffelbach, F.; Belardi, B.; Santos, J. M. R. C. A.; Tessier, L.; Matyjaszewski, K.; Charleux, B., Use of an Amphiphilic Block Copolymer as a Stabilizer and a Macroinitiator in Miniemulsion Polymerization under AGET ATRP Conditions. *Macromolecules* **2007,** *40* (25), 8813-8816.

132.   Manguian, M.; Save, M.; Charleux, B., Batch Emulsion Polymerization of Styrene Stabilized by a Hydrophilic Macro-RAFT Agent. *Macromol. Rapid Commun.* **2006,** *27* (6), 399-404.

133.   Božović-Vukić, J.; Mañon, H. T.; Meuldijk, J.; Koning, C.; Klumperman, B., SAN-b-P4VP Block Copolymer Synthesis by Chain Extension from RAFT-Functional Poly(4-vinylpyridine) in Solution and in Emulsion. *Macromolecules* **2007,** *40* (20), 7132-7139.

134.   Ying, H.; Zhang, Y.; Cheng, J., Dynamic urea bond for the design of reversible and self-healing polymers. *Nat. Commun.* **2014,** *5* (1), 3218.

135.   Toohey, K. S.; Sottos, N. R.; Lewis, J. A.; Moore, J. S.; White, S. R., Self-healing materials with microvascular networks. *Nat. Mater.* **2007,** *6* (8), 581-585.

136.   Cho, S. H.; White, S. R.; Braun, P. V., Self-Healing Polymer Coatings. *Adv. Mater.* **2009,** *21* (6), 645-649.

137.   Rowan, S. J.; Cantrill, S. J.; Cousins, G. R. L.; Sanders, J. K. M.; Stoddart, J. F., Dynamic Covalent Chemistry. *Angew. Chem., Int. Ed.* **2002,** *41* (6), 898-952.

138.   Maeda, T.; Otsuka, H.; Takahara, A., Dynamic covalent polymers: Reorganizable polymers with dynamic covalent bonds. *Prog. Polym. Sci.* **2009,** *34* (7), 581-604.

139.   Montarnal, D.; Capelot, M.; Tournilhac, F.; Leibler, L., Silica-Like Malleable Materials from Permanent Organic Networks. *Science* **2011,** *334* (6058), 965-968.

140.   Capelot, M.; Montarnal, D.; Tournilhac, F.; Leibler, L., Metal-Catalyzed Transesterification for Healing and Assembling of Thermosets. *J. Am. Chem. Soc.* **2012,** *134* (18), 7664-7667.

141.   Zhang, Z. P.; Rong, M. Z.; Zhang, M. Q., Polymer engineering based on reversible covalent chemistry: A promising innovative pathway towards new materials and new functionalities. *Prog. Polym. Sci.* **2018,** *80*, 39-93.

142.   Kloxin, C. J.; Bowman, C. N., Covalent adaptable networks: smart, reconfigurable and responsive network systems. *Chem. Soc. Rev.* **2013,** *42* (17), 7161-7173.

143.   Denissen, W.; Winne, J. M.; Du Prez, F. E., Vitrimers: permanent organic networks with glass-like fluidity. *Chem. Sci.* **2016,** *7* (1), 30-38.

144.   Denissen, W.; Rivero, G.; Nicolaÿ, R.; Leibler, L.; Winne, J. M.; Du Prez, F. E., Vinylogous Urethane Vitrimers. *Adv. Funct. Mater.* **2015,** *25* (16), 2451-2457.

145.   Altuna, F. I.; Hoppe, C. E.; Williams, R. J. J., Epoxy Vitrimers: The Effect of Transesterification Reactions on the Network Structure. *Polymers* **2018,** *10* (1), 43.

146.   Chen, M.; Zhou, L.; Wu, Y.; Zhao, X.; Zhang, Y., Rapid Stress Relaxation and Moderate Temperature of Malleability Enabled by the Synergy of Disulfide Metathesis and Carboxylate Transesterification in Epoxy Vitrimers. *ACS Macro Lett.* **2019,** *8* (3), 255-260.

147.   Ruiz de Luzuriaga, A.; Matxain, J. M.; Ruipérez, F.; Martin, R.; Asua, J. M.; Cabañero, G.; Odriozola, I., Transient mechanochromism in epoxy vitrimer composites containing aromatic disulfide crosslinks. *J. Mater. Chem. C* **2016,** *4* (26), 6220-6223.

148.   Azcune, I.; Odriozola, I., Aromatic disulfide crosslinks in polymer systems: Self-healing, reprocessability, recyclability and more. *Eur. Polym. J.* **2016,** *84*, 147-160.

149.   Krishnakumar, B.; Sanka, R. V. S. P.; Binder, W. H.; Parthasarthy, V.; Rana, S.; Karak, N., Vitrimers: Associative dynamic covalent adaptive networks in thermoset polymers. *Chem. Eng. J.* **2020,** *385*, 123820.

150.   Cash, J. J.; Kubo, T.; Bapat, A. P.; Sumerlin, B. S., Room-Temperature Self-Healing Polymers Based on Dynamic-Covalent Boronic Esters. *Macromolecules* **2015,** *48* (7), 2098-2106.

151.   Wang, Z.; Gu, Y.; Ma, M.; Chen, M., Strong, Reconfigurable, and Recyclable Thermosets Cross-Linked by Polymer–Polymer Dynamic Interaction Based on Commodity Thermoplastics. *Macromolecules* **2020,** *53* (3), 956-964.

152.   Liu, Y.; Liu, Y.; Wang, Q.; Han, Y.; Tan, Y., Boronic ester-based self-healing hydrogels formed by using intermolecular B-N coordination. *Polymer* **2020,** *202*, 122624.

153.   Ogden, W. A.; Guan, Z., Recyclable, Strong, and Highly Malleable Thermosets Based on Boroxine Networks. *J. Am. Chem. Soc.* **2018,** *140* (20), 6217-6220.

154.   Lai, J.-C.; Mei, J.-F.; Jia, X.-Y.; Li, C.-H.; You, X.-Z.; Bao, Z., A Stiff and Healable Polymer Based on Dynamic-Covalent Boroxine Bonds. *Adv. Mater.* **2016,** *28* (37), 8277-8282.

155.   Wu, Y.; Wang, J.; Li, L.; Fei, X.; Xu, L.; Wang, Y.; Tian, J.; Li, Y., A novel hydrogel with self-healing property and bactericidal activity. *J. Colloid Interface Sci.* **2021,** *584*, 484-494.

156.   Saed, M. O.; Gablier, A.; Terentejv, E. M., Liquid Crystalline Vitrimers with Full or Partial Boronic-Ester Bond Exchange. *Adv. Funct. Mater.* **2020,** *30* (3), 1906458.

157.   García, F.; Smulders, M. M. J., Dynamic covalent polymers. *J. Polym. Sci., Part A: Polym. Chem.* **2016,** *54* (22), 3551-3577.

158.   Tarus, D.; Hachet, E.; Messager, L.; Catargi, B.; Ravaine, V.; Auzély-Velty, R., Readily Prepared Dynamic Hydrogels by Combining Phenyl Boronic Acid- and Maltose-Modified Anionic Polysaccharides at Neutral pH. *Macromol. Rapid Commun.* **2014,** *35* (24), 2089-2095.

159.   Kotsuchibashi, Y.; Agustin, R. V. C.; Lu, J.-Y.; Hall, D. G.; Narain, R., Temperature, pH, and Glucose Responsive Gels via Simple Mixing of Boroxole- and Glyco-Based Polymers. *ACS Macro Lett.* **2013,** *2* (3), 260-264.

160.   Deng, C. C.; Brooks, W. L. A.; Abboud, K. A.; Sumerlin, B. S., Boronic Acid-Based Hydrogels Undergo Self-Healing at Neutral and Acidic pH. *ACS Macro Lett.* **2015,** *4* (2), 220-224.

161.	Scholten, P. B. V.; Detrembleur, C.; Meier, M. A. R., Plant-Based Nonactivated Olefins: A New Class of Renewable Monomers for Controlled Radical Polymerization. *ACS Sustainable Chem. Eng.* **2019,** *7* (2), 2751-2762.

162.	Tajbakhsh, S.; Hajiali, F.; Marić, M., Nitroxide Mediated Miniemulsion Polymerization of Bio-based Methacrylates. *Ind. Eng. Chem. Res.* **2020,** *59* (19), 8921-8936.

163.	Noppalit, S.; Simula, A.; Billon, L.; Asua, J. M., On the nitroxide mediated polymerization of methacrylates derived from bio-sourced terpenes in miniemulsion, a step towards sustainable products. *Polym. Chem.* **2020,** *11* (6), 1151-1160.

164.	Qu, W.; Huang, Y.; Luo, Y.; Kalluru, S.; Cochran, E.; Forrester, M.; Bai, X., Controlled Radical Polymerization of Crude Lignin Bio-oil Containing Multihydroxyl Molecules for Methacrylate Polymers and the Potential Applications. *ACS Sustainable Chem. Eng.* **2019,** *7* (9), 9050-9060.

165.	Scholten, P. B. V.; Moatsou, D.; Detrembleur, C.; Meier, M. A. R., Progress Toward Sustainable Reversible Deactivation Radical Polymerization. *Macromol. Rapid Commun.* **2020,** *41* (16), 2000266.

166.	Braunecker, W. A.; Matyjaszewski, K., Controlled/living radical polymerization: Features, developments, and perspectives. *Prog. Polym. Sci.* **2007,** *32* (1), 93-146.

167.	Heinrich, L. A., Future opportunities for bio-based adhesives – advantages beyond renewability. *Green Chem.* **2019,** *21* (8), 1866-1888.

168.	Papageorgiou, G. Z.; Papageorgiou, D. G.; Tsanaktsis, V.; Bikiaris, D. N., Synthesis of the bio-based polyester poly(propylene 2,5-furan dicarboxylate). Comparison of thermal behavior and solid state structure with its terephthalate and naphthalate homologues. *Polymer* **2015,** *62*, 28-38.

169.	Hawker, C. J.; Bosman, A. W.; Harth, E., New polymer synthesis by nitroxide mediated living radical polymerizations. *Chem. Rev.* **2001,** *101* (12), 3661-3688.

170.	Benoit, D.; Grimaldi, S.; Robin, S.; Finet, J.-P.; Tordo, P.; Gnanou, Y., Kinetics and mechanism of controlled free-radical polymerization of styrene and n-butyl acrylate in the presence of an acyclic β-phosphonylated nitroxide. *J. Am. Chem. Soc.* **2000,** *122* (25), 5929-5939.

171.	Maric, M., Application of Nitroxide Mediated Polymerization in Different Monomer Systems. *Curr. Org. Chem.* **2018,** *22* (13), 1264-1284.

172.	Dire, C.; Belleney, J.; Nicolas, J.; Bertin, D.; Magnet, S.; Charleux, B., β-Hydrogen transfer from poly (methyl methacrylate) propagating radicals to the nitroxide SG1: Analysis of the chain-end and determination of the rate constant. *J. Polym. Sci., Part A: Polym. Chem.* **2008,** *46* (18), 6333-6345.

173.	Greene, A. C.; Grubbs, R. B., Nitroxide-Mediated Polymerization of Methyl Methacrylate and Styrene with New Alkoxyamines from 4-Nitrophenyl 2-Methylpropionat-2-yl Radicals. *Macromolecules* **2010,** *43* (24), 10320-10325.

174.	Charleux, B.; Nicolas, J.; Guerret, O., Theoretical Expression of the Average Activation−Deactivation Equilibrium Constant in Controlled/Living Free-Radical Copolymerization Operating via Reversible Termination. Application to a Strongly Improved Control in Nitroxide-Mediated Polymerization of Methyl Methacrylate. *Macromolecules* **2005,** *38* (13), 5485-5492.

175.	Dire, C.; Magnet, S.; Couvreur, L.; Charleux, B., Nitroxide-Mediated Controlled/Living Free-Radical Surfactant-Free Emulsion Polymerization of Methyl Methacrylate Using a Poly(methacrylic acid)-Based Macroalkoxyamine Initiator. *Macromolecules* **2009,** *42* (1), 95-103.

176.	Tortosa, K.; Smith, J.-A.; Cunningham, M. F., Synthesis of Polystyrene-block-poly(butyl acrylate) Copolymers Using Nitroxide-Mediated Living Radical Polymerization in Miniemulsion. *Macromol. Rapid Commun.* **2001,** *22* (12), 957-961.

177.   Nicolas, J.; Charleux, B.; Guerret, O.; Magnet, S., Nitroxide-Mediated Controlled Free-Radical Emulsion Polymerization of Styrene and n-Butyl Acrylate with a Water-Soluble Alkoxyamine as Initiator. *Angew. Chem., Int. Ed.* **2004,** *43* (45), 6186-6189.

178.   Knebel, J.; Saal, D. Process for synthesis of isobornyl (Meth) acrylate. U.S. Patent 6,329,543, Dec. 11, 2001.

179.   Meier, M. A. R.; Metzger, J. O.; Schubert, U. S., Plant oil renewable resources as green alternatives in polymer science. *Chem. Soc. Rev.* **2007,** *36* (11), 1788-1802.

180.   Tajbakhsh, S.; Hajiali, F.; Marić, M., Incorporation of Methacryloisobutyl POSS in Bio-Based Copolymers by Nitroxide Mediated Polymerization in Organic Solution and Miniemulsion. *J. Appl. Polym. Sci.* **2020**.

181.   Hajiali, F.; Marić, M., Incorporation of POSS to improve thermal stability of bio-based polymethacrylates by nitroxide-mediated polymerization: polymerization kinetics and characterization. *J Polym Sci.* **2020,** *58* (11), 1503-1520.

182.   Hajiali, F.; Métafiot, A.; Benitez-Ek, L.; Alloune, L.; Marić, M., Nitroxide mediated polymerization of sustainably sourced isobornyl methacrylate and tridecyl methacrylate with acrylonitrile co-monomer. *J. Polym. Sci., Part A: Polym. Chem.* **2018,** *56* (21), 2422-2436.

183.   Lesage de la Haye, J.; Martin-Fabiani, I.; Schulz, M.; Keddie, J. L.; D'Agosto, F.; Lansalot, M., Hydrophilic MacroRAFT-Mediated Emulsion Polymerization: Synthesis of Latexes for Cross-Linked and Surfactant-Free Films. *Macromolecules* **2017,** *50* (23), 9315-9328.

184.   Shamsuri, A. A.; Md. Jamil, S. N. A., A Short Review on the Effect of Surfactants on the Mechanico-Thermal Properties of Polymer Nanocomposites. *Appl. Sci.* **2020,** *10* (14), 4867.

185.   Nunes, J. d. S.; Asua, J. M., Synthesis of High Solids Content Low Surfactant/Polymer Ratio Nanolatexes. *Langmuir* **2013,** *29* (12), 3895-3902.

186.   Muñoz-Bonilla, A.; van Herk, A. M.; Heuts, J. P. A., Preparation of Hairy Particles and Antifouling Films Using Brush-Type Amphiphilic Block Copolymer Surfactants in Emulsion Polymerization. *Macromolecules* **2010,** *43* (6), 2721-2731.

187.   Holder, S. J.; Durand, G. G.; Yeoh, C.-T.; Illi, E.; Hardy, N. J.; Richardson, T. H., The synthesis and self-assembly of ABA amphiphilic block copolymers containing styrene and oligo(ethylene glycol) methyl ether methacrylate in dilute aqueous solutions: Elevated cloud point temperatures for thermoresponsive micelles. *J. Polym. Sci., Part A: Polym. Chem.* **2008,** *46* (23), 7739-7756.

188.   Wang, W.; Liu, R.; Li, Z.; Meng, C.; Wu, Q.; Zhu, F., Synthesis and Self-Assembly of New Double-Crystalline Amphiphilic Polyethylene-block-Poly[oligo(ethylene glycol) Methyl Ether Methacrylate] Coil-Brush Diblock Copolymer. *Macromol. Chem. Phys.* **2010,** *211* (13), 1452-1459.

189.   Coumes, F.; Beauté, L.; Domurado, D.; Li, S.; Lecommandoux, S.; Coudane, J.; Darcos, V., Self-assembly of well-defined triblock copolymers based on poly(lactic acid) and poly(oligo(ethylene glycol) methyl ether methacrylate) prepared by ATRP. *RSC Adv.* **2016,** *6* (58), 53370-53377.

190.   Xu, F. J.; Neoh, K. G.; Kang, E. T., Bioactive surfaces and biomaterials via atom transfer radical polymerization. *Prog. Polym. Sci.* **2009,** *34* (8), 719-761.

191.   Yu, Q.; Zhang, Y.; Wang, H.; Brash, J.; Chen, H., Anti-fouling bioactive surfaces. *Acta Biomater.* **2011,** *7* (4), 1550-1557.

192.   Qiao, X. G.; Lansalot, M.; Bourgeat-Lami, E.; Charleux, B., Nitroxide-Mediated Polymerization-Induced Self-Assembly of Poly(poly(ethylene oxide) methyl ether methacrylate-co-styrene)-b-poly(n-butyl methacrylate-co-styrene) Amphiphilic Block Copolymers. *Macromolecules* **2013,** *46* (11), 4285-4295.

193.   Dong, H.; Matyjaszewski, K., Thermally Responsive P(M(EO)2MA-co-OEOMA) Copolymers via AGET ATRP in Miniemulsion. *Macromolecules* **2010,** *43* (10), 4623-4628.

194.   Mertoglu, M.; Garnier, S.; Laschewsky, A.; Skrabania, K.; Storsberg, J., Stimuli responsive amphiphilic block copolymers for aqueous media synthesised via reversible addition fragmentation chain transfer polymerisation (RAFT). *Polymer* **2005,** *46* (18), 7726-7740.

195.   Lutz, J.-F.; Hoth, A., Preparation of Ideal PEG Analogues with a Tunable Thermosensitivity by Controlled Radical Copolymerization of 2-(2-Methoxyethoxy)ethyl Methacrylate and Oligo(ethylene glycol) Methacrylate. *Macromolecules* **2006,** *39* (2), 893-896.

196.   Lu, Q.; Weng, Z.-X.; Shan, G.-R.; Lai, G.-Q.; Pan, Z.-R., Effect of acrylonitrile water solubility on the suspension copolymerization of acrylonitrile and styrene. *J. Appl. Polym. Sci.* **2006,** *101* (6), 4270-4274.

197.   Farcet, C.; Nicolas, J.; Charleux, B., Kinetic study of the nitroxide-mediated controlled free-radical polymerization of n-butyl acrylate in aqueous miniemulsions. *J. Polym. Sci., Part A: Polym. Chem.* **2002,** *40* (24), 4410-4420.

198.   Brown, W.; Zhao, J. J. M., Adsorption of sodium dodecyl sulfate on polystyrene latex particles using dynamic light scattering and zeta potential measurements. **1993,** *26* (11), 2711-2715.

199.   Shnoudeh, A. J.; Hamad, I.; Abdo, R. W.; Qadumii, L.; Jaber, A. Y.; Surchi, H. S.; Alkelany, S. Z., Chapter 15 - Synthesis, Characterization, and Applications of Metal Nanoparticles. In *Biomater. Bionanotechnol.*, Tekade, R. K., Ed. Academic Press: 2019; pp 527-612.

200.   Fox, T. G., Influence of Diluent and Copolymer Composition on the Glass Temperature of a Polymer System. *Bull. Am. Phys. Soc* **1956,** *1*, 123.

201.   Ellis, B.; Smith, R., *Polymers: a property database*. 2nd ed.; CRC Press: Boca Raton, 2008; pp 241-691.

202.   Brandrup, J.; Immergut, E. H.; Grulke, E. A.; Abe, A.; Bloch, D. R., *Polymer Handbook*. Wiley New York: 1999; Vol. 89.

203.   Minagawa, M.; Kanoh, H.; Tanno, S.; Satoh, M., Glass-Transition Temperature (Tg) of Free-Radically Prepared Polyacrylonitrile by Inverse Gas Chromatography, 2. Molecular-Weight Dependence of Tg of Two Different Types of Aqueous Polymers. *Macromol. Chem. Phys.* **2002,** *203* (17), 2481-2487.

204.   Gruber, B. A.; Vratsanos, M. S.; Smith, C. D., Effects of colloidal stabilizer on vinyl acetate-ethylene copolymer emulsions and films. *Macromol. Symp.* **2000,** *155* (1), 163-170.

205.   Rogalski, M.; Stryjek, R., Mutual solubility of binary n-hexadecane and polar compound systems. *Bull. Acad. Pol. Sci., Ser. Sci. Chim.* **1980,** *28* (2), 139-147.

206.   Bergman, M.; Bergfelt, A.; Sun, B.; Bowden, T.; Brandell, D.; Johansson, P., Graft copolymer electrolytes for high temperature Li-battery applications, using poly(methyl methacrylate) grafted poly(ethylene glycol)methyl ether methacrylate and lithium bis(trifluoromethanesulfonimide). *Electrochim. Acta* **2015,** *175*, 96-103.

207.   Munch Elmér, A.; Jannasch, P., Solid electrolyte membranes from semi-interpenetrating polymer networks of PEG-grafted polymethacrylates and poly(methyl methacrylate). *Solid State Ionics* **2006,** *177* (5), 573-579.

208.   Bergfelt, A.; Rubatat, L.; Mogensen, R.; Brandell, D.; Bowden, T., d8-poly(methyl methacrylate)-poly[(oligo ethylene glycol) methyl ether methacrylate] tri-block-copolymer electrolytes: Morphology, conductivity and battery performance. *Polymer* **2017,** *131*, 234-242.

209.   Iborra, A.; Salvatierra, L.; Giussi, J. M.; Azzaroni, O., Synthesis of lauryl methacrylate and poly(ethylene glycol) methyl ether methacrylate copolymers with tunable microstructure and emulsifying properties. *Eur. Polym. J.* **2019,** *116*, 117-125.

210.   Tajbakhsh, S.; Marić, M., Nitroxide mediated miniemulsion polymerization of methacryloisobutyl POSS: Homopolymers and copolymers with alkyl methacrylates. *J Polym Sci.* **2020,** *58* (19), 2741-2754.

211.   Matsumoto, A.; Mizuta, K.; Otsu, T., Synthesis and thermal properties of poly(cycloalkyl methacrylate)s bearing bridged- and fused-ring structures. *J. Polym. Sci., Part A: Polym. Chem.* **1993,** *31* (10), 2531-2539.

212.   Kaya, E., Copolymers of 4-methoxybenzyl methacrylate and isobornyl methacrylate: synthesis, characterization and determination of monomer reactivity ratios. *J. Chem. Soc. Pak.* **2011,** *33*, 555-561.

213.   Grishin, D.; Grishin, I., Controlled radical polymerization: Prospects for application for industrial synthesis of polymers. *Russ. J. Appl. Chem.* **2011,** *84* (12), 2021-2028.

214.   Destarac, M., Industrial development of reversible-deactivation radical polymerization: is the induction period over? *Polym. Chem.* **2018,** *9* (40), 4947-4967.

215.   Matyjaszewski, K.; Spanswick, J., Controlled/living radical polymerization. *Mater. Today* **2005,** *8* (3), 26-33.

216.   Moad, G.; Barner-Kowollik, C., The Mechanism and Kinetics of the RAFT Process: Overview, Rates, Stabilities, Side Reactions, Product Spectrum and Outstanding Challenges. In *Handbook of RAFT Polymerization*, Barner-Kowollik, C., Ed. Wiley-VCH: Weinheim, 2008; pp 51-104.

217.   Monteiro, M. J.; Cunningham, M. F., Polymer Nanoparticles via Living Radical Polymerization in Aqueous Dispersions: Design and Applications. *Macromolecules* **2012,** *45* (12), 4939-4957.

218.   Kobatake, S.; Harwood, H. J.; Quirk, R. P.; Priddy, D. B., Synthesis of Nitroxide-Functionalized Polybutadiene Using Halogen-Containing Benzyloxyamine as Terminators for Anionic Polymerization. *Macromolecules* **1999,** *32* (1), 10-13.

219.   Percec, V.; Guliashvili, T.; Ladislaw, J. S.; Wistrand, A.; Stjerndahl, A.; Sienkowska, M. J.; Monteiro, M. J.; Sahoo, S., Ultrafast synthesis of ultrahigh molar mass polymers by metal-catalyzed living radical polymerization of acrylates, methacrylates, and vinyl chloride mediated by SET at 25 C. *J. Am. Chem. Soc.* **2006,** *128* (43), 14156-14165.

220.   Fleischmann, S.; Rosen, B. M.; Percec, V., SET-LRP of acrylates in air. *J. Polym. Sci., Part A: Polym. Chem.* **2010,** *48* (5), 1190-1196.

221.   Jakubowski, W.; Matyjaszewski, K., Activators Regenerated by Electron Transfer for Atom-Transfer Radical Polymerization of (Meth)acrylates and Related Block Copolymers. *Angew. Chem., Int. Ed.* **2006,** *45* (27), 4482-4486.

222.   Jakubowski, W.; Min, K.; Matyjaszewski, K., Activators Regenerated by Electron Transfer for Atom Transfer Radical Polymerization of Styrene. *Macromolecules* **2006,** *39* (1), 39-45.

223.   Engelis, N. G.; Anastasaki, A.; Nurumbetov, G.; Truong, N. P.; Nikolaou, V.; Shegiwal, A.; Whittaker, M. R.; Davis, T. P.; Haddleton, D. M., Sequence-controlled methacrylic multiblock copolymers via sulfur-free RAFT emulsion polymerization. *Nat. Chem.* **2017,** *9* (2), 171.

224.   Zetterlund, P. B.; Yamazoe, H.; Yamada, B., Addition-Fragmentation Chain Transfer Involving Dimers of α-Methylvinyl Monomers Studied by ESR Spectroscopy: Competition between Fragmentation and Bimolecular Termination. *Macromol. Rapid Commun.* **2003,** *24* (2), 197-201.

225.   Tian, X.; Ding, J.; Zhang, B.; Qiu, F.; Zhuang, X.; Chen, Y., Recent advances in RAFT polymerization: Novel initiation mechanisms and optoelectronic applications. *Polymers* **2018,** *10* (3), 318.

226.   Treat, N. J.; Sprafke, H.; Kramer, J. W.; Clark, P. G.; Barton, B. E.; Read de Alaniz, J.; Fors, B. P.; Hawker, C. J., Metal-free atom transfer radical polymerization. *J. Am. Chem. Soc.* **2014,** *136* (45), 16096-16101.

227.   Pearson, R. M.; Lim, C.-H.; McCarthy, B. G.; Musgrave, C. B.; Miyake, G. M., Organocatalyzed Atom Transfer Radical Polymerization Using N-Aryl Phenoxazines as Photoredox Catalysts. *J. Am. Chem. Soc.* **2016,** *138* (35), 11399-11407.

228.   Wang, J.; Yuan, L.; Wang, Z.; Rahman, M. A.; Huang, Y.; Zhu, T.; Wang, R.; Cheng, J.; Wang, C.; Chu, F.; Tang, C., Photoinduced Metal-Free Atom Transfer Radical Polymerization of Biomass-Based Monomers. *Macromolecules* **2016,** *49* (20), 7709-7717.

229.   Discekici, E. H.; Anastasaki, A.; Read de Alaniz, J.; Hawker, C. J., Evolution and Future Directions of Metal-Free Atom Transfer Radical Polymerization. *Macromolecules* **2018,** *51* (19), 7421-7434.

230.   Lessard, B.; Ling, E. J. Y.; Morin, M. S. T.; Marić, M., Nitroxide-mediated radical copolymerization of methyl methacrylate controlled with a minimal amount of 9-(4-vinylbenzyl)-9H-carbazole. *J. Polym. Sci., Part A: Polym. Chem.* **2011,** *49* (4), 1033-1045.

231.   Marić, M.; Lessard, B. H.; Consolante, V.; Ling, E. J. Y., Incorporating primary amine pendant groups into copolymers via nitroxide mediated polymerization. *React. Funct. Polym.* **2011,** *71* (12), 1137-1147.

232.   Ananchenko, G. S.; Souaille, M.; Fischer, H.; Le Mercier, C.; Tordo, P., Decomposition of model alkoxyamines in simple and polymerizing systems. II. Diastereomeric N-(2-methylpropyl)-N-(1-diethyl-phosphono-2, 2-dimethyl-propyl)-aminoxyl-based compounds. *J. Polym. Sci., Part A: Polym. Chem.* **2002,** *40* (19), 3264-3283.

233.   Darabi, A.; Cunningham, M. F., Preparation of Poly (poly (ethylene glycol) methyl ether methacrylate-co-styrene)-b-poly (2-(diethylamino) ethyl methacrylate-co-acrylonitrile) by nitroxide-mediated polymerisation in water. *Polymer* **2017,** *115*, 255-260.

234.   Darabi, A.; Shirin-Abadi, A. R.; Jessop, P. G.; Cunningham, M. F., Nitroxide-mediated polymerization of 2-(diethylamino) ethyl methacrylate (DEAEMA) in water. *Macromolecules* **2014,** *48* (1), 72-80.

235.   Nicolas, J.; Brusseau, S.; Charleux, B., A minimal amount of acrylonitrile turns the nitroxide-mediated polymerization of methyl methacrylate into an almost ideal controlled/living system. *J. Polym. Sci., Part A: Polym. Chem.* **2010,** *48* (1), 34-47.

236.   Lessard, B.; Ling, E. J. Y.; Morin, M. S. T.; Marić, M., Nitroxide-mediated radical copolymerization of methyl methacrylate controlled with a minimal amount of 9-(4-vinylbenzyl)-9H-carbazole. *J. Polym. Sci., Part A: Polym. Chem.* **2011,** *49* (4), 1033-1045.

237.   Lessard, B. H.; Guillaneuf, Y.; Mathew, M.; Liang, K.; Clement, J.-L.; Gigmes, D.; Hutchinson, R. A.; Marić, M., Understanding the controlled polymerization of Methyl Methacrylate with low concentrations of 9-(4-Vinylbenzyl)-9 H-carbazole comonomer by nitroxide-mediated polymerization: The pivotal role of reactivity ratios. *Macromolecules* **2013,** *46* (3), 805-813.

238.   Consolante, V.; Marić, M., Nitroxide-Mediated Polymerization of an Organo-Soluble Protected Styrene Sulfonate: Development of Homo-and Random Copolymers. *Macromol. React. Eng.* **2011,** *5* (11-12), 575-586.

239.   Darabi, A.; García-Valdez, O.; Champagne, P.; Cunningham, M. F., PEGylation of Chitosan Via Nitroxide-Mediated Polymerization in Aqueous Media. *Macromol. React. Eng.* **2016,** *10* (1), 82-89.

240.   Greene, A. C.; Grubbs, R. B., Nitroxide-Mediated Polymerization of Methyl Methacrylate and Styrene with New Alkoxyamines from 4-Nitrophenyl 2-Methylpropionat-2-yl Radicals. *Macromolecules* **2010,** *43*, 10320.

241.   Detrembleur, C.; Teyssié, P.; Jérôme, R., Control of the Radical Polymerization of tert-Butyl Methacrylate in Water by a Novel Combination of Sodium Nitrite and Iron(II) Sulfate. *Macromolecules* **2002,** *35* (5), 1611-1621.

242.   Guillaneuf, Y.; Gigmes, D.; Marque, S. R.; Astolfi, P.; Greci, L.; Tordo, P.; Bertin, D., First effective nitroxide-mediated polymerization of methyl methacrylate. *Macromolecules* **2007,** *40* (9), 3108-3114.

243.   Simula, A.; Ruipérez, F.; Ballard, N.; Leiza, J. R.; van Es, S.; Asua, J. M., Why can Dispolreg 007 control the nitroxide mediated polymerization of methacrylates? *Polym. Chem.* **2019,** *10* (1), 106-113.

244.   Porzio, R. S.; Zhao, C.-L.; Anchor, M. J. Low-VOC emulsion polymer coating compositions. U.S. Patent 7,705,081, Apr. 27, 2010.

245.   Batlaw, R.; Moore, P. D. Printing ink emulsion having reduced VOC. U.S. Patent 5,389,130, Feb. 14, 1995.

246.   Mehravar, E.; Agirre, A.; Ballard, N.; van Es, S.; Arbe, A.; Leiza, J. R.; Asua, J. M., Insights into the Network Structure of Cross-Linked Polymers Synthesized via Miniemulsion Nitroxide-Mediated Radical Polymerization. *Macromolecules* **2018,** *51* (23), 9740-9748.

247.   Li, W. S. J.; Cunningham, M. F., Nitroxide-mediated microemulsion polymerization of n-butyl acrylate: decoupling of target molecular weight and particle size. *Polym. Chem.* **2014,** *5* (12), 3804.

248.   Schork, F. J.; Luo, Y.; Smulders, W.; Russum, J. P.; Butté, A.; Fontenot, K., Miniemulsion Polymerization. In *Polymer Particles*, Okubo, M., Ed. Springer Berlin Heidelberg: Berlin, Heidelberg, 2005; pp 129-255.

249.   Landfester, K., Miniemulsions for Nanoparticle Synthesis. In *Colloid Chemistry II*, Antonietti, M., Ed. Springer: Berlin, Heidelberg, 2003; pp 75-123.

250.   Zetterlund, P. B.; Okubo, M., Compartmentalization in Nitroxide-Mediated Radical Polymerization in Dispersed Systems. *Macromolecules* **2006,** *39* (26), 8959-8967.

251.   Molina-Gutiérrez, S.; Ladmiral, V.; Bongiovanni, R.; Caillol, S.; Lacroix-Desmazes, P., Radical polymerization of biobased monomers in aqueous dispersed media. *Green Chem.* **2019,** *21* (1), 36-53.

252.   Zhu, Y.; Romain, C.; Williams, C. K., Sustainable polymers from renewable resources. *Nature* **2016,** *540*, 354-362.

253.   Meek, K. M.; Eaton, T. R.; Rorrer, N. A.; Brandner, D. G.; Manker, L. P.; Karp, E. M.; Biddy, M. J.; Bratis, A. D.; Beckham, G. T.; Naskar, A. K., Emulsion polymerization of acrylonitrile in aqueous methanol. *Green Chem.* **2018,** *20* (23), 5299-5310.

254.   Semsarilar, M.; Perrier, S., 'Green' reversible addition-fragmentation chain-transfer (RAFT) polymerization. *Nat. Chem.* **2010,** *2*, 811-820.

255.   Satoh, K., Controlled/living polymerization of renewable vinyl monomers into bio-based polymers. *Polym. J.* **2015,** *47*, 527-536.

256.   Okada, S.; Matyjaszewski, K., Synthesis of bio-based poly(N-phenylitaconimide) by atom transfer radical polymerization. *J. Polym. Sci., Part A: Polym. Chem.* **2015,** *53* (6), 822-827.

257.   Hatton, F. L., Recent advances in RAFT polymerization of monomers derived from renewable resources. *Polym. Chem.* **2019,** *11* (2), 220-229.

258.   Zheng, Y.; Yao, K.; Lee, J.; Chandler, D.; Wang, J.; Wang, C.; Chu, F.; Tang, C., Well-Defined Renewable Polymers Derived from Gum Rosin. *Macromolecules* **2010,** *43* (14), 5922-5924.

259.   Chen, L.; Bao, Z.; Fu, Z.; Li, W., Preparation and characterisation of novel cross-linked poly (IBOMA-BA-DFMA) latex. *Pigm. Resin Technol.* **2015,** *44* (6), 333-338.

260.   Park, S. I.; Lee, S. I.; Hong, S.-J.; Cho, K. Y., Suspension polymerization and characterization of transparent poly(methyl methacrylate-co-isobornyl methacrylate). *Macromol. Res.* **2007,** *15* (5), 418-423.

261.   Yu, J. M.; Dubois, P.; Jérôme, R., Synthesis and properties of poly [isobornyl methacrylate (IBMA)-b-butadiene (BD)-b-IBMA] copolymers: New thermoplastic elastomers of a large service temperature range. *Macromolecules* **1996,** *29* (23), 7316-7322.

262.   Kaya, İ.; Özdemir, E., Thermodynamic interactions and characterisation of poly(isobornyl methacrylate) by inverse gas chromatography at various temperatures. *Polymer* **1999,** *40* (9), 2405-2410.

263.   Kurt, A.; Kaya, E., Synthesis, characterization, and thermal degradation kinetics of the copolymer poly(4-methoxybenzyl methacrylate-co-isobornyl methacrylate). *J. Appl. Polym. Sci.* **2010,** *115* (4), 2359-2367.

264.   Yu, J. M.; Dubois, P.; Jérôme, R., Synthesis and Properties of Poly[isobornyl methacrylate (IBMA)-b-butadiene (BD)-b-IBMA] Copolymers: New Thermoplastic Elastomers of a Large Service Temperature Range. *Macromolecules* **1996,** *29* (23), 7316-7322.

265.   Zhang, B.; Ma, Y.; Chen, D.; Xu, J.; Yang, W., Preparation of poly(styrene-co-isobornyl methacrylate) beads having controlled glass transition temperature by suspension polymerization. *J. Appl. Polym. Sci.* **2013,** *129* (1), 113-120.

266.   Fenn, D. R.; Hughes, V. L. Coating compositions comprising isobornyl methacrylate and 4-hydroxybutyl acrylate. U.S. Patent 5,514,755, May 7, 1996.

267.   Kitagawa, S.; Baba, M. Thermoplastic elastomer and a process for its production. U.S. Patent 5,183,856, Feb. 2, 1993.

268.   Aoki, H.; Ito, M.; Miura, T.; Osuka, M. Thermoplastic resin composition and molded article comprising the same. U.S. Patent 7,589,151, Sep. 15, 2009.

269.   Kawaguchi, Y.; Itamura, Y.; Onimura, K.; Oishi, T., Effects of the chemical structure on the heat resistance of thermoplastic expandable microspheres. *J. Appl. Polym. Sci.* **2005,** *96* (4), 1306-1312.

270.   Qi, G.; Nolan, M.; Schork, F. J.; Jones, C. W., Emulsion and controlled miniemulsion polymerization of the renewable monomer γ-methyl-α-methylene-γ-butyrolactone. *J. Polym. Sci., Part A: Polym. Chem.* **2008,** *46* (17), 5929-5944.

271.   ASTM D638-14, Standard Test Method for Tensile Properties of Plastics. ASTM International, West Conshohocken, PA, 2014.

272.   Sabatini, D. A.; Harwell, J. H.; Hasegawa, M.; Knox, R., Membrane processes and surfactant-enhanced subsurface remediation: results of a field demonstration. *J. Membr. Sci.* **1998,** *151* (1), 87-98.

273.   Hitchens, L.; Vane, L. M.; Alvarez, F. R., VOC removal from water and surfactant solutions by pervaporation: a pilot study. *Sep. Purif. Technol.* **2001,** *24* (1-2), 67-84.

274.   Lee, D.-H.; Cody, R. D.; Kim, D.-J., Surfactant recycling by solvent extraction in surfactant-aided remediation. *Sep. Purif. Technol.* **2002,** *27* (1), 77-82.

275.   Farcet, C.; Charleux, B.; Pirri, R., Poly(n-butyl acrylate) Homopolymer and Poly[n-butyl acrylate-b-(n-butyl acrylate-co-styrene)] Block Copolymer Prepared via Nitroxide-Mediated Living/Controlled Radical Polymerization in Miniemulsion. *Macromolecules* **2001,** *34* (12), 3823-3826.

276.   Babu, K. N.; Divakaran, M.; Ravindran, P.; Peter, K., Long pepper. In *Handbook of Herbs and Spices*, Peter, K. V., Ed. Woodhead Publishing: Cambridge, 2006; pp 420-437.

277.   Callaghan, A. V.; Tierney, M.; Phelps, C. D.; Young, L. Y., Anaerobic biodegradation of n-hexadecane by a nitrate-reducing consortium. *Appl. Environ. Microbiol* **2009,** *75* (5), 1339-1344.

278.   Simula, A.; Ballard, N.; Aguirre, M.; Leiza, J. R.; Es, S. v.; Asua, J. M., Nitroxide mediated copolymerization of acrylates, methacrylates and styrene: The importance of side reactions in the polymerization of acrylates. *Eur. Polym. J.* **2019,** *110*, 319-329.

279.   Tidwell, P. W.; Mortimer, G. A., An improved method of calculating copolymerization reactivity ratios. *J. Polym. Sci., Part A: Gen. Pap.* **1965,** *3* (1), 369-387.

280.   Odian, G., *Principles of Polymerization*. 4th ed.; John Wiley & Sons: Hoboken, 2004; pp 1-812.

281.   Mayo, F. R.; Lewis, F. M., Copolymerization. I. A Basis for Comparing the Behavior of Monomers in Copolymerization; The Copolymerization of Styrene and Methyl Methacrylate. *J. Am. Chem. Soc.* **1944,** *66* (9), 1594-1601.

282.   Stahl, G. A., Copolymerization of methyl methacrylate and dodecyl methacrylate. *J. Polym. Sci., Polym. Chem. Ed.* **1979,** *17* (6), 1883-1886.

283.   Šoljić, I.; Jukić, A.; Janović, Z., Terpolymerization kinetics of N,N-dimethylaminoethyl methacrylate/alkyl methacrylate/styrene systems. *Polym. Eng. Sci.* **2010,** *50* (3), 577-584.

284.   Rajdeo, K. S.; Ponrathnam, S.; Pardeshi, S.; Chavan, N. N.; Bhongale, S. S.; Harikrishna, R., Ambient Temperature Photocopolymerization of Tetrahydrofurfuryl Methacrylate and Isobornyl Methacrylate: Reactivity Ratios and Thermal Studies. *J. Macromol. Sci., Part A* **2015,** *52* (12), 982-991.

285.   Makati, A. C.; Kan, C. S.; Iwamasa, R. T.; Lee, D. I. Polymeric adhesion promoter and latexes; and polymeric adhesion promoter, epoxy resins and latexes are used to improve adherence between various substrates. U.S. Patent 5,569,686, Oct. 29, 1996.

286.   Ivanković, T.; Hrenović, J., Surfactants in the environment. *Arch. Ind. Hyg. Toxicol.* **2010,** *61* (1), 95-110.

287.   Cserháti, T.; Forgács, E.; Oros, G., Biological activity and environmental impact of anionic surfactants. *Environment International* **2002,** *28* (5), 337-348.

288.   Önder, E.; Koparal, A. S.; Öğütveren, Ü. B., An alternative method for the removal of surfactants from water: Electrochemical coagulation. *Sep. Purif. Technol.* **2007,** *52* (3), 527-532.

289.   Yuan, C.; Xu, Z.; Fan, M.; Liu, H.; Xie, Y.; Zhu, T., Study on characteristics and harm of surfactants. *J. Chem. Pharm. Res.* **2014,** *6* (7), 2233-2237.

290.   Guillaneuf, Y.; Gigmes, D.; Marque, S. R. A.; Tordo, P.; Bertin, D., Nitroxide-Mediated Polymerization of Methyl Methacrylate Using an SG1-Based Alkoxyamine: How the Penultimate Effect Could Lead to Uncontrolled and Unliving Polymerization. *Macromol. Chem. Phys.* **2006,** *207* (14), 1278-1288.

291.   Chern, C.-S.; Liou, Y.-C., Kinetics of styrene miniemulsion polymerization stabilized by nonionic surfactant/alkyl methacrylate. *Polymer* **1999,** *40* (13), 3763-3772.

292.   Chern, C. S.; Chen, T. J., Miniemulsion polymerization of styrene using alkyl methacrylates as the reactive cosurfactant. *Colloid Polym. Sci.* **1997,** *275* (6), 546-554.

293.   Fleischhaker, F.; Haehnel, A. P.; Misske, A. M.; Blanchot, M.; Haremza, S.; Barner-Kowollik, C., Glass-Transition-, Melting-, and Decomposition Temperatures of Tailored Polyacrylates and Polymethacrylates: General Trends and Structure–Property Relationships. *Macromol. Chem. Phys.* **2014,** *215* (12), 1192-1200.

294.   Greenberg, S. A.; Alfrey, T., Side Chain Crystallization of n-Alkyl Polymethacrylates and Polyacrylates1. *J. Am. Chem. Soc.* **1954,** *76* (24), 6280-6285.

295.   Chen, L.; Jiang, W.; Wu, F., Nanometre fluorinated acrylate latex prepared with gemini surfactant. *Micro Nano Lett.* **2012,** *7* (8), 810-813.

296.   Haehnel, A. P.; Schneider-Baumann, M.; Hiltebrandt, K. U.; Misske, A. M.; Barner-Kowollik, C., Global Trends for kp? Expanding the Frontier of Ester Side Chain Topography in Acrylates and Methacrylates. *Macromolecules* **2013,** *46* (1), 15-28.

297.   Haq, Z.; Thompson, L., Significance of glass transition temperature to polymer latex stabilisation by nonionic surfactants. *Colloid Polym. Sci.* **1982,** *260* (2), 212-217.

298.   Bouissou, C.; Rouse, J. J.; Price, R.; van der Walle, C. F., The Influence of Surfactant on PLGA Microsphere Glass Transition and Water Sorption: Remodeling the Surface Morphology to Attenuate the Burst Release. *Pharm. Res.* **2006,** *23* (6), 1295-1305.

299.   McKinney, P. V., Processing of poly(vinyl chloride) polymers correlated with composition, glass transition, and viscosity. *J. Appl. Polym. Sci.* **1965,** *9* (10), 3359-3382.

300.   Larson, R. G.; Winey, K. I.; Patel, S. S.; Watanabe, H.; Bruinsma, R., The rheology of layered liquids: lamellar block copolymers and smectic liquid crystals. *Rheol. Acta* **1993,** *32* (3), 245-253.

301.   Barnes, H. A., *A Handbook of Elementary Rheology*. University of Wales, Institute of Non-Newtonian Fluid Mechanics: Aberystwyth, 2000; pp 81-106.

302.   Vinogradov, G. V., Limiting regimes of deformation of polymers. *Polym. Eng. Sci.* **1981,** *21* (6), 339-351.

303.   Borisenkova, E. K.; Dreval, V. E.; Vinogradov, G. V.; Kurbanaliev, M. K.; Moiseyev, V. V.; Shalganova, V. G., Transition of polymers from the fluid to the forced high-elastic and leathery states at temperatures above the glass transition temperature. *Polymer* **1982,** *23* (1), 91-99.

304.   Vinogradov, G. V.; Dreval, V. Y.; Borisenkova, Y. K.; Kurbanaliyev, M. K.; Shalganova, V. G., Longitudinal deformation and rupture of linear flexible-chain polymers. *Polym. Sci. U.S.S.R.* **1981,** *23* (12), 2847-2860.

305.   Flory, P. J., *Principles of Polymer Chemistry*. Cornell University Press: New York, 1953; pp 29-657.

306.   Matsen, M. W.; Bates, F. S., Unifying Weak- and Strong-Segregation Block Copolymer Theories. *Macromolecules* **1996,** *29* (4), 1091-1098.

307.   Li, L.; Lu, B.; Wu, J.; Fan, Q.; Guo, X.; Liu, Z., Synthesis and self-assembly behavior of thermo-responsive star-shaped POSS–(PCL–P(MEO2MA-co-PEGMA))16 inorganic/organic hybrid block copolymers with tunable lower critical solution temperature. *New J. Chem.* **2016,** *40* (5), 4761-4768.

308.   Hirai, T.; Leolukman, M.; Jin, S.; Goseki, R.; Ishida, Y.; Kakimoto, M.-a.; Hayakawa, T.; Ree, M.; Gopalan, P., Hierarchical Self-Assembled Structures from POSS-Containing Block Copolymers Synthesized by Living Anionic Polymerization. *Macromolecules* **2009,** *42* (22), 8835-8843.

309.   Haddad, T. S.; Lichtenhan, J. D., Hybrid Organic−Inorganic Thermoplastics: Styryl-Based Polyhedral Oligomeric Silsesquioxane Polymers. *Macromolecules* **1996,** *29* (22), 7302-7304.

310.   Zhang, W.; Fang, B.; Walther, A.; Müller, A. H., Synthesis via RAFT polymerization of tadpole-shaped organic/inorganic hybrid poly (acrylic acid) containing polyhedral oligomeric silsesquioxane (POSS) and their self-assembly in water. *Macromolecules* **2009,** *42* (7), 2563-2569.

311.   Tan, B. H.; Hussain, H.; He, C. B., Tailoring Micelle Formation and Gelation in (PEG−P(MA-POSS)) Amphiphilic Hybrid Block Copolymers. *Macromolecules* **2011,** *44* (3), 622-631.

312.   Zhao, Y.; Schiraldi, D. A., Thermal and mechanical properties of polyhedral oligomeric silsesquioxane (POSS)/polycarbonate composites. *Polymer* **2005,** *46* (25), 11640-11647.

313.   Ayandele, E.; Sarkar, B.; Alexandridis, P., Polyhedral oligomeric silsesquioxane (POSS)-containing polymer nanocomposites. *Nanomaterials* **2012,** *2* (4), 445-475.

314.   Liu, Y.; Sun, Y.; Zeng, F.; Chen, Y., Influence of POSS as a Nanofiller on the Structure, Dielectric, Piezoelectric and Ferroelectric Properties of PVDF. *Int. J. Electrochem. Sci* **2013,** *8* (4), 5688-5697.

315.   Provatas, A.; Matisons, J., Silsesquioxanes: synthesis and applications. *Trends Polym. Sci.* **1997,** *10* (5), 327-332.

316.   Wang, F.; Lu, X.; He, C., Some recent developments of polyhedral oligomeric silsesquioxane (POSS)-based polymeric materials. *J. Mater. Chem.* **2011,** *21* (9), 2775-2782.

317.   Li, G.; Wang, L.; Ni, H.; Pittman, C. U., Polyhedral Oligomeric Silsesquioxane (POSS) Polymers and Copolymers: A Review. *J. Inorg. Organomet. Polym.* **2001,** *11* (3), 123-154.

318.   Kim, S. K.; Heo, S. J.; Koak, J. Y.; Lee, J. H.; Lee, Y. M.; Chung, D. J.; Lee, J. I.; Hong, S. D., A biocompatibility study of a reinforced acrylic-based hybrid denture composite resin with polyhedraloligosilsesquioxane. *J. Oral Rehabil.* **2007,** *34* (5), 389-395.

319.   Punshon, G.; Vara, D. S.; Sales, K. M.; Kidane, A. G.; Salacinski, H. J.; Seifalian, A. M., Interactions between endothelial cells and a poly(carbonate-silsesquioxane-bridge-urea)urethane. *Biomaterials* **2005,** *26* (32), 6271-6279.

320.   Wu, J.; Mather, P. T., POSS Polymers: Physical Properties and Biomaterials Applications. *Polym. Rev.* **2009,** *49* (1), 25-63.

321.   Le Bras, M.; Wilkie, C. A.; Bourbigot, S., Micro-Sized Fire Retarding Mineral Fillers. Polyhedral oligomeric silsesquioxanes–Application to Flame Retardant Textile. In *Fire retardancy of polymers: new applications of mineral fillers*, The Royal Society of Chemistry: Cambridge, 2005; pp 187-200.

322.   Ghanbari, H.; Cousins, B. G.; Seifalian, A. M., A nanocage for nanomedicine: polyhedral oligomeric silsesquioxane (POSS). *Macromol. Rapid Commun.* **2011,** *32* (14), 1032-1046.

323.   Chatterjee, S.; Ooya, T., Hydrophobic Nature of Methacrylate-POSS in Combination with 2-(Methacryloyloxy)ethyl Phosphorylcholine for Enhanced Solubility and Controlled Release of Paclitaxel. *Langmuir* **2019,** *35* (5), 1404-1412.

324.   Li, M.; Zhang, H.; Wu, W.; Li, M.; Xu, Y.; Chen, G.; Dai, L., A Novel POSS-Based Copolymer Functionalized Graphene: An Effective Flame Retardant for Reducing the Flammability of Epoxy Resin. *Polymers* **2019,** *11* (2), 241.

325.   Pyun, J.; Matyjaszewski, K.; Wu, J.; Kim, G.-M.; Chun, S. B.; Mather, P. T., ABA triblock copolymers containing polyhedral oligomeric silsesquioxane pendant groups: synthesis and unique properties. *Polymer* **2003,** *44* (9), 2739-2750.

326.   Pyun, J.; Matyjaszewski, K., The synthesis of hybrid polymers using atom transfer radical polymerization: homopolymers and block copolymers from polyhedral oligomeric silsesquioxane monomers. *Macromolecules* **2000,** *33* (1), 217-220.

327.   Hussain, H.; Tan, B. H.; Seah, G. L.; Liu, Y.; He, C. B.; Davis, T. P., Micelle Formation and Gelation of (PEG−P(MA-POSS)) Amphiphilic Block Copolymers via Associative Hydrophobic Effects. *Langmuir* **2010,** *26* (14), 11763-11773.

328.   Pyun, J.; Matyjaszewski, K., The Synthesis of Hybrid Polymers Using Atom Transfer Radical Polymerization: Homopolymers and Block Copolymers from Polyhedral Oligomeric Silsesquioxane Monomers. *Macromolecules* **2000,** *33* (1), 217-220.

329.   Xu, Y.; Chen, M.; Xie, J.; Li, C.; Yang, C.; Deng, Y.; Yuan, C.; Chang, F.-C.; Dai, L., Synthesis, characterization and self-assembly of hybrid pH-sensitive block copolymer containing polyhedral oligomeric silsesquioxane (POSS). *React. Funct. Polym.* **2013,** *73* (12), 1646-1655.

330.   Deng, Y.; Bernard, J.; Alcouffe, P.; Galy, J.; Dai, L.; Gérard, J.-F., Nanostructured hybrid polymer networks from in situ self-assembly of RAFT-synthesized POSS-based block copolymers. *J. Polym. Sci., Part A: Polym. Chem.* **2011,** *49* (20), 4343-4352.

331.   Ullah, A.; Shah, S. M.; Hassan, A.; Maric, M.; Hussain, H., Nitroxide-mediated radical polymerization of methacryloisobutyl POSS and its block copolymers with poly(n-acryloylmorpholine). *J. Polym. Sci.* **2020,** *58* (3), 428-437.

332.   Mya, K. Y.; Lin, E. M. J.; Gudipati, C. S.; Shen, L.; He, C., Time-Dependent Polymerization Kinetic Study and the Properties of Hybrid Polymers with Functional Silsesquioxanes. *J. Phys. Chem. B* **2010,** *114* (28), 9119-9127.

333.   Raus, V.; Čadová, E.; Starovoytova, L.; Janata, M., ATRP of POSS Monomers Revisited: Toward High-Molecular Weight Methacrylate–POSS (Co)Polymers. *Macromolecules* **2014,** *47* (21), 7311-7320.

334.   Jackson, C.; Chen, Y.-J.; Mays, J. W., Size exclusion chromatography with multiple detectors: Solution properties of linear chains of varying flexibility in tetrahydrofuran. *J. Appl. Polym. Sci.* **1996,** *61* (5), 865-874.

335.   Malihi, F. B.; Kuo, C.-Y.; Provder, T., Determination of the absolute molecular weight of a styrene–butyl acrylate emulsion copolymer by low-angle laser light scattering (LALLS) and GPC/LALLS. *J. Appl. Polym. Sci.* **1984,** *29* (3), 925-931.

336.   Floudas, G.; Štepánek, P., Structure and Dynamics of Poly(n-decyl methacrylate) below and above the Glass Transition. *Macromolecules* **1998,** *31* (20), 6951-6957.

337.   Tang, P.; Sudol, E.; Adams, M.; El-Aasser, M.; Asua, J., Seeded emulsion polymerization of n-butyl acrylate utilizing miniemulsions. *J. Appl. Polym. Sci.* **1991,** *42* (7), 2019-2028.

338.   Otsu, T.; Yamada, B.; Sugiyama, S.; Mori, S., Effects of ortho-substituents on reactivities, tacticities, and ceiling temperatures of radical polymerizations of phenyl methacrylates. *J. Polym. Sci., Polym. Chem. Ed.* **1980,** *18* (7), 2197-2207.

339.   Marcinkowska, A.; Przadka, D.; Dudziec, B.; Szczesniak, K.; Andrzejewska, E., Anchor Effect in Polymerization Kinetics: Case of Monofunctionalized POSS. *Polymers* **2019,** *11* (3), 515.

340.   Strąkowska, A.; Członka, S.; Strzelec, K., POSS Compounds as Modifiers for Rigid Polyurethane Foams (Composites). *Polymers* **2019,** *11* (7), 1092.

341.   Castelvetro, V.; Ciardelli, F.; De Vita, C.; Puppo, A., Hybrid Nanocomposite Films from Mono- and Multi-Functional POSS Copolyacrylates in Miniemulsion. *Macromol. Rapid Commun.* **2006,** *27* (8), 619-625.

342.   Lichtenhan, J. D.; Otonari, Y. A.; Carr, M. J., Linear Hybrid Polymer Building Blocks: Methacrylate-Functionalized Polyhedral Oligomeric Silsesquioxane Monomers and Polymers. *Macromolecules* **1995,** *28* (24), 8435-8437.

343.   Wu, J.; Haddad, T. S.; Kim, G.-M.; Mather, P. T., Rheological Behavior of Entangled Polystyrene−Polyhedral Oligosilsesquioxane (POSS) Copolymers. *Macromolecules* **2007,** *40* (3), 544-554.

344.   Petton, L.; Ciolino, A. E.; Dervaux, B.; Du Prez, F. E., From one-pot stabilisation to in situ functionalisation in nitroxide mediated polymerisation: an efficient extension towards atom transfer radical polymerisation. *Polym. Chem.* **2012,** *3* (7), 1867-1878.

345.   Métafiot, A.; Kanawati, Y.; Gérard, J.-F.; Defoort, B.; Marić, M., Synthesis of β-Myrcene-Based Polymers and Styrene Block and Statistical Copolymers by SG1 Nitroxide-Mediated Controlled Radical Polymerization. *Macromolecules* **2017,** *50* (8), 3101-3120.

346. Romo–Uribe, A.; Mather, P. T.; Haddad, T. S.; Lichtenhan, J. D., Viscoelastic and morphological behavior of hybrid styryl-based polyhedral oligomeric silsesquioxane (POSS) copolymers. *J. Polym. Sci., Part B: Polym. Phys.* **1998,** *36* (11), 1857-1872.

347. Çayli, G.; Meier, M. A. R., Polymers from renewable resources: Bulk ATRP of fatty alcohol-derived methacrylates. *Eur. J. Lipid Sci. Technol.* **2008,** *110* (9), 853-859.

348. Liu, Y. R.; Huang, Y. D.; Liu, L., Effects of TriSilanolIsobutyl-POSS on thermal stability of methylsilicone resin. *Polym. Degrad. Stab.* **2006,** *91* (11), 2731-2738.

349. Zhang, H.-x.; Lee, H.-y.; Shin, Y.-j.; Lee, D.-h.; Noh, S. K., Preparation and Properties of MMA/1-Propylmethacrylate-POSS Copolymer with Atom Transfer Radical Polymerization. *Chin. J. Polym. Sci.* **2008,** *26* (05), 533-537.

350. Zhang, H.-x.; Jung, M.-s.; Shin, Y.-j.; Yoon, K.-b.; Lee, D.-h., Preparation and properties of ethylene/POSS copolymer with rac-Et(Ind)2ZrCl2 catalyst. *J. Appl. Polym. Sci.* **2009,** *111* (6), 2697-2702.

351. Moore, B. M.; Haddad, T. S.; Gonzalez, R. I.; Schlaefer, C. *Reactivity Ratios of Isobutyl POSS-Styrene and Styrene Monomers*; Air Force Research Lab Edwards AFB CA: Defence Technical Information Center, 2003; pp 1-2.

352. Groch, P.; Dziubek, K.; Czaja, K.; Dudziec, B.; Marciniec, B., Copolymers of ethylene with monoalkenyl- and monoalkenyl(siloxy)silsesquioxane (POSS) comonomers – Synthesis and characterization. *Eur. Polym. J.* **2017,** *90*, 368-382.

353. Zhang, H.; Lee, H.; Shin, Y.; Lee, D.; Noh, S., Effect of 3rdmonomer addition on styrene/styryl-polyhedral oligomeric silsesquioxane (POSS) copolymerization. *Macromol. Res.* **2009,** *17* (5), 352-355.

354. Smith, S. D.; DeSimone, J. M.; Huang, H.; York, G.; Dwight, D. W.; Wilkes, G. L.; McGrath, J. E., Synthesis and characterization of poly(methyl methacrylate)-g-poly(dimethylsiloxane)copolymers. I. Bulk and surface characterization. *Macromolecules* **1992,** *25* (10), 2575-2581.

355. Wei, K.; Li, L.; Zheng, S.; Wang, G.; Liang, Q., Organic–inorganic random copolymers from methacrylate-terminated poly(ethylene oxide) with 3-methacryloxypropylheptaphenyl polyhedral oligomeric silsesquioxane: synthesis via RAFT polymerization and self-assembly behavior. *Soft Matter* **2014,** *10* (2), 383-394.

356. Wang, Z.; Tan, B. H.; Hussain, H.; He, C., pH-responsive amphiphilic hybrid random-type copolymers of poly(acrylic acid) and poly(acrylate-POSS): synthesis by ATRP and self-assembly in aqueous solution. *Colloid Polym. Sci.* **2013,** *291* (8), 1803-1815.

357. Kim, S., K; Kim, D., G; Lee, A.; Sohn, H., S; Wie, J., Jae; Nguyen, N., A; Mackay, M., E; Lee, J., Chan, Organic/Inorganic Hybrid Block Copolymer Electrolytes with Nanoscale Ion-Conducting Channels for Lithium Ion Batteries. *Macromolecules* **2012,** *45* (23), 9347-9356.

358. Scherrer, P., Nachr Ges wiss goettingen. *Math. Phys.* **1918,** *2*, 98-100.

359. Holzwarth, U.; Gibson, N., The Scherrer equation versus the 'Debye-Scherrer equation'. *Nat. Nanotechnol.* **2011,** *6* (9), 534-534.

360. Molina, D.; Levi, M.; Turri, S.; Penso, M., Self-Assembly of Methacrylic Nanostructured Copolymers Containing Polyhedral Oligomeric Silsesquioxanes. *e-Polym.* **2007,** *7* (1), 011.

361. Tajbakhsh, S.; Hajiali, F., A comprehensive study on the fabrication and properties of biocomposites of poly(lactic acid)/ceramics for bone tissue engineering. *Mater. Sci. Eng., C* **2017,** *70*, 897-912.

362. Zou, H.; Wu, S.; Shen, J., Polymer/Silica Nanocomposites: Preparation, Characterization, Properties, and Applications. *Chem. Rev.* **2008,** *108* (9), 3893-3957.

363.   Hajiali, F.; Tajbakhsh, S.; Shojaei, A., Fabrication and Properties of Polycaprolactone Composites Containing Calcium Phosphate-Based Ceramics and Bioactive Glasses in Bone Tissue Engineering: A Review. *Polym. Rev.* **2018,** *58* (1), 164-207.

364.   Cordes, D. B.; Lickiss, P. D.; Rataboul, F., Recent Developments in the Chemistry of Cubic Polyhedral Oligosilsesquioxanes. *Chem. Rev.* **2010,** *110* (4), 2081-2173.

365.   Phillips, S. H.; Haddad, T. S.; Tomczak, S. J., Developments in nanoscience: polyhedral oligomeric silsesquioxane (POSS)-polymers. *Curr. Opin. Solid State Mater. Sci.* **2004,** *8* (1), 21-29.

366.   Kuo, S.-W.; Chang, F.-C., POSS related polymer nanocomposites. *Prog. Polym. Sci.* **2011,** *36* (12), 1649-1696.

367.   Chen, R.; Feng, W.; Zhu, S.; Botton, G.; Ong, B.; Wu, Y., Surface-initiated atom transfer radical polymerization of polyhedral oligomeric silsesquioxane (POSS) methacrylate from flat silicon wafer. *Polymer* **2006,** *47* (4), 1119-1123.

368.   Janata, M.; Sikora, A.; Látalová, P.; Čadová, E.; Raus, V.; Matějka, L.; Vlček, P., Synthesis of defined polyhedral oligosilsesquioxane-containing diblock and triblock methacrylate copolymers by atom transfer radical polymerization. *J. Appl. Polym. Sci.* **2013,** *128* (6), 4294-4301.

369.   Dou, Q.; Abdul Karim, A.; Loh, X. J., Modification of thermal and mechanical properties of PEG-PPG-PEG copolymer (F127) with MA-POSS. *Polymers* **2016,** *8* (9), 341.

370.   Goseki, R.; Hirai, T.; Ishida, Y.; Kakimoto, M.-a.; Hayakawa, T., Rapid and reversible morphology control in thin films of poly(ethylene oxide)-block-POSS-containing poly(methacrylate). *Polym. J.* **2012,** *44* (6), 658-664.

371.   Li, X.; Zhang, K.; Zhao, Y.; Zhu, K.; Yuan, X., Formation of icephobic film from POSS-containing fluorosilicone multi-block methacrylate copolymers. *Prog. Org. Coat.* **2015,** *89*, 150-159.

372.   Balanuca, B.; Lungu, A.; Hanganu, A.-M.; Stan, L. R.; Vasile, E.; Iovu, H., Hybrid nanocomposites based on POSS and networks of methacrylated camelina oil and various PEG derivatives. *Eur. J. Lipid Sci. Technol.* **2014,** *116* (4), 458-469.

373.   Kotal, A.; Si, S.; Paira, T. K.; Mandal, T. K., Synthesis of semitelechelic POSS-polymethacrylate hybrids by thiol-mediated controlled radical polymerization with unusual thermal behaviors. *J. Polym. Sci., Part A: Polym. Chem.* **2008,** *46* (3), 1111-1123.

374.   Markovic, E.; Clarke, S.; Matisons, J.; Simon, G. P., Synthesis of POSS−Methyl Methacrylate-Based Cross-Linked Hybrid Materials. *Macromolecules* **2008,** *41* (5), 1685-1692.

375.   Hopfinger, A. J.; Koehler, M. G.; Pearlstein, R. A.; Tripathy, S. K., Molecular modeling of polymers. IV. Estimation of glass transition temperatures. *J. Polym. Sci., Part B: Polym. Phys.* **1988,** *26* (10), 2007-2028.

376.   Goto, A.; Fukuda, T., Kinetics of living radical polymerization. *Prog. Polym. Sci.* **2004,** *29* (4), 329-385.

377.   Matyjaszewski, K.; Gaynor, S.; Greszta, D.; Mardare, D.; Shigemoto, T., 'Living' and controlled radical polymerization. *J. Phys. Org. Chem.* **1995,** *8* (4), 306-315.

378.   McHale, R.; Aldabbagh, F.; Zetterlund, P. B., The Role of Excess Nitroxide in the SG1 (N-tert-Butyl-N-[1-diethylphophono-(2,2-dimethylpropyl)] Nitroxide)-Mediated Polymerization of Methyl Methacrylate. *J. Polym. Sci., Part A: Polym. Chem.* **2007,** *45*, 2194.

379.   Zetterlund, P. B.; D'hooge, D. R., The Nanoreactor Concept: Kinetic Features of Compartmentalization in Dispersed Phase Polymerization. *Macromolecules* **2019,** *52* (21), 7963-7976.

380.   Xu, H.; Yang, B.; Wang, J.; Guang, S.; Li, C., Preparation, Tg improvement, and thermal stability enhancement mechanism of soluble poly(methyl methacrylate) nanocomposites by incorporating octavinyl polyhedral oligomeric silsesquioxanes. *J. Polym. Sci., Part A: Polym. Chem.* **2007,** *45* (22), 5308-5317.

381.   Tanaka, K.; Kozuka, H.; Ueda, K.; Jeon, J.-H.; Chujo, Y., POSS-based molecular fillers for simultaneously enhancing thermal and viscoelasticity of poly(methyl methacrylate) films. *Mater. Lett.* **2017,** *203*, 62-67.

382.   Chen, Y.; Kushner, A. M.; Williams, G. A.; Guan, Z., Multiphase design of autonomic self-healing thermoplastic elastomers. *Nat. Chem.* **2012,** *4* (6), 467-472.

383.   Diba, M.; Spaans, S.; Ning, K.; Ippel, B. D.; Yang, F.; Loomans, B.; Dankers, P. Y. W.; Leeuwenburgh, S. C. G., Self-Healing Biomaterials: From Molecular Concepts to Clinical Applications. *Adv. Mater. Interfaces* **2018,** *5* (17), 1800118.

384.   Chen, Y.; Tang, Z.; Zhang, X.; Liu, Y.; Wu, S.; Guo, B., Covalently Cross-Linked Elastomers with Self-Healing and Malleable Abilities Enabled by Boronic Ester Bonds. *ACS Appl. Mater. Interfaces* **2018,** *10* (28), 24224-24231.

385.   Röttger, M.; Domenech, T.; van der Weegen, R.; Breuillac, A.; Nicolaÿ, R.; Leibler, L., High-performance vitrimers from commodity thermoplastics through dioxaborolane metathesis. *Science* **2017,** *356* (6333), 62-65.

386.   Ricarte, R. G.; Tournilhac, F.; Leibler, L., Phase Separation and Self-Assembly in Vitrimers: Hierarchical Morphology of Molten and Semicrystalline Polyethylene/Dioxaborolane Maleimide Systems. *Macromolecules* **2019,** *52* (2), 432-443.

387.   Ricarte, R. G.; Tournilhac, F.; Cloître, M.; Leibler, L., Linear Viscoelasticity and Flow of Self-Assembled Vitrimers: The Case of a Polyethylene/Dioxaborolane System. *Macromolecules* **2020,** *53* (5), 1852-1866.

388.   Fujita, N.; Shinkai, S.; James, T. D., Boronic acids in molecular self-assembly. *Chem. - Asian J.* **2008,** *3* (7), 1076-1091.

389.   Cromwell, O. R.; Chung, J.; Guan, Z., Malleable and Self-Healing Covalent Polymer Networks through Tunable Dynamic Boronic Ester Bonds. *J. Am. Chem. Soc.* **2015,** *137* (20), 6492-6495.

390.   Bapat, A. P.; Sumerlin, B. S.; Sutti, A., Bulk network polymers with dynamic B–O bonds: healable and reprocessable materials. *Mater. Horiz.* **2020,** *7* (3), 694-714.

391.   António, J. P. M.; Russo, R.; Carvalho, C. P.; Cal, P. M. S. D.; Gois, P. M. P., Boronic acids as building blocks for the construction of therapeutically useful bioconjugates. *Chem. Soc. Rev.* **2019,** *48* (13), 3513-3536.

392.   Zhang, X.; Alves, D. S.; Lou, J.; Hill, S. D.; Barrera, F. N.; Best, M. D., Boronic acid liposomes for cellular delivery and content release driven by carbohydrate binding. *Chem. Commun.* **2018,** *54* (48), 6169-6172.

393.   Wang, W.; Gao, X.; Wang, B., Boronic Acid-Based Sensors. *Curr. Org. Chem.* **2002,** *6* (14), 1285-1317.

394.   Gray, C. W.; Houston, T. A., Boronic Acid Receptors for α-Hydroxycarboxylates: High Affinity of Shinkai's Glucose Receptor for Tartrate. *J. Org. Chem.* **2002,** *67* (15), 5426-5428.

395.   Sun, X.; Chapin, B. M.; Metola, P.; Collins, B.; Wang, B.; James, T. D.; Anslyn, E. V., The mechanisms of boronate ester formation and fluorescent turn-on in ortho-aminomethylphenylboronic acids. *Nat. Chem.* **2019,** *11* (9), 768-778.

396.   Yang, Q.; Pan, X., Bifunctional Porous Polymers Bearing Boronic and Sulfonic Acids for Hydrolysis of Cellulose. *ACS Sustainable Chem. Eng.* **2016,** *4* (9), 4824-4830.

397.   Simocko, C.; Young, T. C.; Wagener, K. B., ADMET Polymers Containing Precisely Spaced Pendant Boronic Acids and Esters. *Macromolecules* **2015,** *48* (16), 5470-5473.

398.   Cambre, J. N.; Roy, D.; Gondi, S. R.; Sumerlin, B. S., Facile Strategy to Well-Defined Water-Soluble Boronic Acid (Co)polymers. *J. Am. Chem. Soc.* **2007,** *129* (34), 10348-10349.

399.   Cambre, J. N.; Sumerlin, B. S., Biomedical applications of boronic acid polymers. *Polymer* **2011,** *52* (21), 4631-4643.

400.   Bull, S. D.; Davidson, M. G.; van den Elsen, J. M. H.; Fossey, J. S.; Jenkins, A. T. A.; Jiang, Y.-B.; Kubo, Y.; Marken, F.; Sakurai, K.; Zhao, J.; James, T. D., Exploiting the Reversible Covalent Bonding of Boronic Acids: Recognition, Sensing, and Assembly. *Acc. Chem. Res.* **2013,** *46* (2), 312-326.

401.   Hall, D. G., *Boronic Acids: Preparation, Applications in Organic Synthesis and Medicine*. John Wiley & Sons: 2006.

402.   Taylor, D. L.; in het Panhuis, M., Self-Healing Hydrogels. *Adv. Mater.* **2016,** *28* (41), 9060-9093.

403.   Collins, J.; Nadgorny, M.; Xiao, Z.; Connal, L. A., Doubly Dynamic Self-Healing Materials Based on Oxime Click Chemistry and Boronic Acids. *Macromol. Rapid Commun.* **2017,** *38* (6), 1600760.

404.   Smithmyer, M. E.; Deng, C. C.; Cassel, S. E.; LeValley, P. J.; Sumerlin, B. S.; Kloxin, A. M., Self-Healing Boronic Acid-Based Hydrogels for 3D Co-cultures. *ACS Macro Lett.* **2018,** *7* (9), 1105-1110.

405.   Vancoillie, G.;   Pelz, S.;   Holder, E.; Hoogenboom, R., Direct nitroxide mediated (co)polymerization of 4-vinylphenylboronic acid as route towards sugar sensors. *Polym. Chem.* **2012,** *3* (7), 1726-1729.

406.   Ishiyama, N.; Moro, T.; Ohe, T.; Miura, T.; Ishihara, K.; Konno, T.; Ohyama, T.; Kimura, M.; Kyomoto, M.; Saito, T.; Nakamura, K.; Kawaguchi, H., Reduction of Peritendinous Adhesions by Hydrogel Containing Biocompatible Phospholipid Polymer MPC for Tendon Repair. *J Bone Joint Surg Am* **2011,** *93* (2), 142-149.

407.   Saito, A.; Konno, T.; Ikake, H.; Kurita, K.; Ishihara, K., Control of cell function on a phospholipid polymer having phenylboronic acid moiety. *Biomed Mater* **2010,** *5* (5), 054101.

408.   Ryu, J. H.; Lee, G. J.; Shih, Y.-R. V.; Kim, T.-i.; Varghese, S., Phenylboronic acid-polymers for biomedical applications. *Curr. Med. Chem.* **2019,** *26* (37), 6797-6816.

409.   Choi, J.;   Konno, T.;   Matsuno, R.;   Takai, M.; Ishihara, K., Surface immobilization of biocompatible phospholipid polymer multilayered hydrogel on titanium alloy. *Colloids Surf., B* **2008,** *67* (2), 216-223.

410.   Wu, J.-z.; Bremner, D. H.; Li, H.-y.; Sun, X.-z.; Zhu, L.-M., Synthesis and evaluation of temperature- and glucose-sensitive nanoparticles based on phenylboronic acid and N-vinylcaprolactam for insulin delivery. *Mater. Sci. Eng. C* **2016,** *69*, 1026-1035.

411.   Kim, J.; Lee, Y. M.; Kim, H.; Park, D.; Kim, J.; Kim, W. J., Phenylboronic acid-sugar grafted polymer architecture as a dual stimuli-responsive gene carrier for targeted anti-angiogenic tumor therapy. *Biomaterials* **2016,** *75*, 102-111.

412.   Brooks, W. L. A.; Sumerlin, B. S., Synthesis and Applications of Boronic Acid-Containing Polymers: From Materials to Medicine. *Chem. Rev.* **2016,** *116* (3), 1375-1397.

413.   Amado, E.; Kressler, J., Reversible Complexation of Iminophenylboronates with Mono- and Dihydroxy Methacrylate Monomers and Their Polymerization at Low Temperature by Photoinduced ATRP in One Pot. *Macromolecules* **2016,** *49* (5), 1532-1544.

414.   Kim, C.; Ejima, H.; Yoshie, N., Polymers with autonomous self-healing ability and remarkable reprocessability under ambient humidity conditions. *J. Mater. Chem. A* **2018,** *6* (40), 19643-19652.

415.   Cash, J. J.; Kubo, T.; Dobbins, D. J.; Sumerlin, B. S., Maximizing the symbiosis of static and dynamic bonds in self-healing boronic ester networks. *Polym. Chem.* **2018,** *9* (15), 2011-2020.

416.   Wang, Z.; Zhuge, J.; Fang, H.; Prior, B. A., Glycerol production by microbial fermentation: a review. *Biotechnol. Adv.* **2001,** *19* (3), 201-223.

417.   Pham, P. D.; Monge, S.; Lapinte, V.; Raoul, Y.; Robin, J. J., Various radical polymerizations of glycerol-based monomers. *Eur. J. Lipid Sci. Technol.* **2013,** *115* (1), 28-40.

418.   Zheng, Y.; Chen, X.; Shen, Y., Commodity chemicals derived from glycerol, an important biorefinery feedstock. *Chem. Rev.* **2008**.

419.   Jesson, C. P.; Cunningham, V. J.; Smallridge, M. J.; Armes, S. P., Synthesis of High Molecular Weight Poly(glycerol monomethacrylate) via RAFT Emulsion Polymerization of Isopropylideneglycerol Methacrylate. *Macromolecules* **2018,** *51* (9), 3221-3232.

420.   Shipp, D. A., Reversible-Deactivation Radical Polymerizations. *Polym. Rev.* **2011,** *51* (2), 99-103.

421.   Guselnikova, O.; Marque, S. R. A.; Tretyakov, E. V.; Mares, D.; Jerabek, V.; Audran, G.; Joly, J.-P.; Trusova, M.; Svorcik, V.; Lyutakov, O.; Postnikov, P., Unprecedented plasmon-induced nitroxide-mediated polymerization (PI-NMP): a method for preparation of functional surfaces. *J. Mater. Chem. A* **2019,** *7* (20), 12414-12419.

422.   Maji, S.; Vancoillie, G.; Voorhaar, L.; Zhang, Q.; Hoogenboom, R., RAFT Polymerization of 4-Vinylphenylboronic Acid as the Basis for Micellar Sugar Sensors. *Macromol. Rapid Commun.* **2014,** *35* (2), 214-220.

423.   Save, M.; Weaver, J. V. M.; Armes, S. P.; McKenna, P., Atom Transfer Radical Polymerization of Hydroxy-Functional Methacrylates at Ambient Temperature: Comparison of Glycerol Monomethacrylate with 2-Hydroxypropyl Methacrylate. *Macromolecules* **2002,** *35* (4), 1152-1159.

424.   Giacomelli, C.; Borsali, R., ATRP of Silylated Glycerol Monomethacrylate in Organic Medium for Convenient Synthesis of Amphiphilic Copolymers. *Macromol. Rapid Commun.* **2008,** *29* (7), 573-579.

425.   Cunningham, V. J.; Alswieleh, A. M.; Thompson, K. L.; Williams, M.; Leggett, G. J.; Armes, S. P.; Musa, O. M., Poly(glycerol monomethacrylate)–Poly(benzyl methacrylate) Diblock Copolymer Nanoparticles via RAFT Emulsion Polymerization: Synthesis, Characterization, and Interfacial Activity. *Macromolecules* **2014,** *47* (16), 5613-5623.

426.   Blanazs, A.; Madsen, J.; Battaglia, G.; Ryan, A. J.; Armes, S. P., Mechanistic Insights for Block Copolymer Morphologies: How Do Worms Form Vesicles? *J. Am. Chem. Soc.* **2011,** *133* (41), 16581-16587.

427.   Blanazs, A.; Ryan, A. J.; Armes, S. P., Predictive Phase Diagrams for RAFT Aqueous Dispersion Polymerization: Effect of Block Copolymer Composition, Molecular Weight, and Copolymer Concentration. *Macromolecules* **2012,** *45* (12), 5099-5107.

428.   Li, Y.; Armes, S. P., RAFT Synthesis of Sterically Stabilized Methacrylic Nanolatexes and Vesicles by Aqueous Dispersion Polymerization. *Angew. Chem., Int. Ed.* **2010,** *49* (24), 4042-4046.

429.   Syrett, J. A.; Mantovani, G.; Barton, W. R. S.; Price, D.; Haddleton, D. M., Self-healing polymers prepared via living radical polymerisation. *Polym. Chem.* **2010,** *1* (1), 102-106.

430.   Wang, H. P.; Yuan, Y. C.; Rong, M. Z.; Zhang, M. Q., Self-Healing of Thermoplastics via Living Polymerization. *Macromolecules* **2010,** *43* (2), 595-598.

431.   Yao, L.; Yuan, Y. C.; Rong, M. Z.; Zhang, M. Q., Self-healing linear polymers based on RAFT polymerization. *Polymer* **2011,** *52* (14), 3137-3145.

432.   Kristufek, S. L.; Wacker, K. T.; Tsao, Y.-Y. T.; Su, L.; Wooley, K. L., Monomer design strategies to create natural product-based polymer materials. *Nat. Prod. Rep.* **2017,** *34* (4), 433-459.

433. Wilbon, P. A.; Chu, F.; Tang, C., Progress in Renewable Polymers from Natural Terpenes, Terpenoids, and Rosin. *Macromol. Rapid Commun.* **2013,** *34* (1), 8-37.

434. Vendamme, R.; Schüwer, N.; Eevers, W., Recent synthetic approaches and emerging bio-inspired strategies for the development of sustainable pressure-sensitive adhesives derived from renewable building blocks. *J. Appl. Polym. Sci.* **2014,** *131* (17).

435. Hajiali, F.; Tajbakhsh, S.; Marić, M., Thermally reprocessable bio-based polymethacrylate vitrimers and nanocomposites. *Polymer* **2021,** *212*, 123126.

436. Tajbakhsh, S.; Hajiali, F.; Marić, M., Incorporation of methacryloisobutyl POSS in bio-based copolymers by nitroxide mediated polymerization in organic solution and miniemulsion. *J. Appl. Polym. Sci.* **2021,** *138* (13).

437. Savelyeva, X.; Chondon, D.; Marić, M., Vinyl phenylboronic acid controlling co-monomer for nitroxide mediated synthesis of thermoresponsive poly(2-N morpholinoethyl methacrylate). *J. Polym. Sci., Part A: Polym. Chem.* **2016,** *54* (11), 1560-1572.

438. Tokunaga, Y.; Ueno, H.; Shimomura, Y., Formation of boroxine: its stability and thermodynamic parameters in solution. *Heterocycles* **2002,** *57* (5), 787-790.

439. Popescu, D.; Hoogenboom, R.; Keul, H.; Möller, M., Free radical and nitroxide mediated polymerization of hydroxy–functional acrylates prepared via lipase–catalyzed transacylation reactions. *J. Polym. Sci., Part A: Polym. Chem.* **2010,** *48* (12), 2610-2621.

440. Eggenhuisen, T. M.; Becer, C. R.; Fijten, M. W. M.; Eckardt, R.; Hoogenboom, R.; Schubert, U. S., Libraries of Statistical Hydroxypropyl Acrylate Containing Copolymers with LCST Properties Prepared by NMP. *Macromolecules* **2008,** *41* (14), 5132-5140.

441. Gryn'ova, G.; Lin, C. Y.; Coote, M. L., Which side-reactions compromise nitroxide mediated polymerization? *Polym. Chem.* **2013,** *4* (13), 3744-3754.

442. Mohomed, K.; Moussy, F.; Harmon, J. P., Dielectric analyses of a series of poly(2-hydroxyethyl methacrylate-co-2,3-dihydroxypropyl methacylate) copolymers. *Polymer* **2006,** *47* (11), 3856-3865.

443. Gates, G.; Harmon, J. P.; Ors, J.; Benz, P., Intra and intermolecular relaxations 2,3-dihydroxypropyl methacrylate and 2-hydroxyethyl methacrylate hydrogels. *Polymer* **2003,** *44* (1), 207-214.

444. Kyeremateng, S. O.; Amado, E.; Kressler, J., Synthesis and characterization of random copolymers of (2,2-dimethyl-1,3-dioxolan-4-yl)methyl methacrylate and 2,3-dihydroxypropyl methacrylate. *Eur. Polym. J.* **2007,** *43* (8), 3380-3391.

445. Kahraman, G.; Beşkardeş, O.; Rzaev, Z. M. O.; Pişkin, E., Bioengineering polyfunctional copolymers. VII. Synthesis and characterization of copolymers of p-vinylphenyl boronic acid with maleic and citraconic anhydrides and their self-assembled macrobranched supramolecular architectures. *Polymer* **2004,** *45* (17), 5813-5828.

446. Çimen, E. K.; Rzaev, Z. M. O.; Pişkin, E., Bioengineering functional copolymers: V. Synthesis, LCST, and thermal behavior of poly(N-isopropyl acrylamide-co-p-vinylphenylboronic acid). *J. Appl. Polym. Sci.* **2005,** *95* (3), 573-582.

447. Qin, Y.; Cheng, G.; Achara, O.; Parab, K.; Jäkle, F., A New Route to Organoboron Polymers via Highly Selective Polymer Modification Reactions. *Macromolecules* **2004,** *37* (19), 7123-7131.

448. Qin, Y.; Sukul, V.; Pagakos, D.; Cui, C.; Jäkle, F., Preparation of Organoboron Block Copolymers via ATRP of Silicon and Boron-Functionalized Monomers. *Macromolecules* **2005,** *38* (22), 8987-8990.

449. Brunet, J.; Collas, F.; Humbert, M.; Perrin, L.; Brunel, F.; Lacôte, E.; Montarnal, D.; Raynaud, J., High Glass-Transition Temperature Polymer Networks Harnessing the Dynamic Ring Opening of Pinacol Boronates. *Angew. Chem., Int. Ed.* **2019,** *58* (35), 12216-12222.

450.	Piergies, N.; Proniewicz, E.; Ozaki, Y.; Kim, Y.; Proniewicz, L. M., Influence of Substituent Type and Position on the Adsorption Mechanism of Phenylboronic Acids: Infrared, Raman, and Surface-Enhanced Raman Spectroscopy Studies. *J. Phys. Chem. A* **2013,** *117* (27), 5693-5705.

451.	Piergies, N.; Proniewicz, E., - Structure Characterization of [N-Phenylamino(2-boronphenyl)-R-methyl]phosphonic Acid by Vibrational Spectroscopy and Density Functional Theory Calculations. *J. Spectrosc.* **2014,** *2014.*

452.	Chen, H.; Lee, M.; Lee, J.; Kim, J.-H.; Gal, Y.-S.; Hwang, Y.-H.; An, W. G.; Koh, K., Formation and Characterization of Self-Assembled Phenylboronic Acid Derivative Monolayers toward Developing Monosaccaride Sensing-Interface. *Sensors* **2007,** *7*, 1480-1495.

453.	Zhou, Y.; Goossens, J. G. P.; Sijbesma, R. P.; Heuts, J. P. A., Poly(butylene terephthalate)/Glycerol-based Vitrimers via Solid-State Polymerization. *Macromolecules* **2017,** *50* (17), 6742-6751.

454.	Appel, E. A.; Biedermann, F.; Rauwald, U.; Jones, S. T.; Zayed, J. M.; Scherman, O. A., Supramolecular Cross-Linked Networks via Host−Guest Complexation with Cucurbit[8]uril. *J. Am. Chem. Soc.* **2010,** *132* (40), 14251-14260.

455.	Obadia, M. M.; Mudraboyina, B. P.; Serghei, A.; Montarnal, D.; Drockenmuller, E., Reprocessing and Recycling of Highly Cross-Linked Ion-Conducting Networks through Transalkylation Exchanges of C–N Bonds. *J. Am. Chem. Soc.* **2015,** *137* (18), 6078-6083.

456.	Demirelli, K.; Coşkun, M. F.; Kaya, E.; Coşkun, M., Investigation of the thermal decomposition of poly(2-hydroxypropyl methacrylate). *Polym. Degrad. Stab.* **2002,** *78* (2), 333-339.

457.	Demirelli, K.; Coşkun, M.; Kaya, E., A detailed study of thermal degradation of poly(2-hydroxyethyl methacrylate). *Polym. Degrad. Stab.* **2001,** *72* (1), 75-80.

458.	Marco-Dufort, B.; Tibbitt, M. W., Design of moldable hydrogels for biomedical applications using dynamic covalent boronic esters. *Mater. Today Chem.* **2019,** *12*, 16-33.

459.	Amaral, A. J. R.; Gaspar, V. M.; Mano, J. F., Responsive laminarin-boronic acid self-healing hydrogels for biomedical applications. *Polym. J.* **2020,** *52* (8), 997-1006.

460.	Chen, W.; Zhen, X.; Wu, W.; Jiang, X., Responsive boron biomaterials and their biomedical applications. *Sci. China: Chem.* **2020,** *63* (5), 648-664.

461.	Zhang, Y.; Qi, Y.; Ulrich, S.; Barboiu, M.; Ramström, O., Dynamic covalent polymers for biomedical applications. *Mater. Chem. Front.* **2020,** *4* (2), 489-506.

462.	Gaballa, H.; Theato, P., Glucose-Responsive Polymeric Micelles via Boronic Acid–Diol Complexation for Insulin Delivery at Neutral pH. *Biomacromolecules* **2019,** *20* (2), 871-881.

463.	Tang, J.; Yang, J.; Yang, H.; Miao, R.; Wen, R.; Liu, K.; Peng, J.; Fang, Y., Boronic ester-based dynamic covalent ionic liquid gels for self-healable, recyclable and malleable optical devices. *J. Mater. Chem. C* **2018,** *6* (46), 12493-12497.

464.	Li, S.; Zuo, C.; Zhang, Y.; Wang, J.; Gan, H.; Li, S.; Yu, L.; Zhou, B.; Xue, Z., Covalently cross-linked polymer stabilized electrolytes with self-healing performance via boronic ester bonds. *Polym. Chem.* **2020**.

465.	de Souza, M.; Dubois, C.; Zhang, J.; Varley, R. J., Water activated healing of thiolene boronic ester coatings. *Prog. Org. Coat.* **2020,** *139*, 105424.

466.	Zhang, Y.; Dubé, M. A., Green Emulsion Polymerization Technology. In *Polymer Reaction Engineering of Dispersed Systems: Volume I*, Pauer, W., Ed. Springer International Publishing: Cham, 2018; pp 65-100.

467.   Amado, E.; Augsten, C.; Mäder, K.; Blume, A.; Kressler, J., Amphiphilic Water Soluble Triblock Copolymers Based on Poly(2,3-dihydroxypropyl methacrylate) and Poly(propylene oxide): Synthesis by Atom Transfer Radical Polymerization and Micellization in Aqueous Solutions. *Macromolecules* **2006,** *39* (26), 9486-9496.

468.   Chen, Q.; Hill, M. R.; Brooks, W. L. A.; Zhu, A.; Sumerlin, B. S.; An, Z., Boronic Acid Linear Homopolymers as Effective Emulsifiers and Gelators. *ACS Appl. Mater. Interfaces* **2015,** *7* (39), 21668-21672.

469.   Pettignano, A.; Grijalvo, S.; Häring, M.; Eritja, R.; Tanchoux, N.; Quignard, F.; Díaz Díaz, D., Boronic acid-modified alginate enables direct formation of injectable, self-healing and multistimuli-responsive hydrogels. *Chem. Commun.* **2017,** *53* (23), 3350-3353.

470.   Marco-Dufort, B.; Tibbitt, M. W., Design of moldable hydrogels for biomedical applications using dynamic covalent boronic esters. *Materials Today Chemistry* **2019,** *12*, 16-33.

471.   Tajbakhsh, S.; Hajiali, F.; Guinan, K.; Marić, M., Highly reprocessable, room temperature self-healable bio-based materials with boronic-ester dynamic cross-linking. *React. Funct. Polym.* **2021,** *158*.

472.   Hajiali, F.; Tajbakhsh, S.; Marić, M., Thermally Reprocessable Bio-Based Polymethacrylate Vitrimers and Nanocomposites. *Polymer* **2020**.

473.   Tajbakhsh, S.; Marić, M., Synthesis of bio-based poly(methacrylates) using SG1-containing amphiphilic macroinitiators by nitroxide mediated miniemulsion polymerization. *J. Polym. Sci.* **2021**.

474.   Liu, S.; Weaver, J. V. M.; Save, M.; Armes, S. P., Synthesis of pH-Responsive Shell Cross-Linked Micelles and Their Use as Nanoreactors for the Preparation of Gold Nanoparticles. *Langmuir* **2002,** *18* (22), 8350-8357.

475.   Maji, S.; Vancoillie, G.; Voorhaar, L.; Zhang, Q.; Hoogenboom, R., RAFT Polymerization of 4-Vinylphenylboronic Acid as the Basis for Micellar Sugar Sensors. *Macromol. Rapid Commun.* **2014,** *35* (2), 214-220.

476.   Zhang, X. Q.; Wang, C. H., Solution characterization of poly(isobornyl methacrylate) in tetrahydrofuran. *J. Polym. Sci., Part B: Polym. Phys.* **1994,** *32* (11), 1951-1956.

477.   Huglin M. B., *Light Scattering from Polymer Solutions*. Academic Press Inc. London, 1972.

478.   Medrano, R.; Laguna, M. T. R.; Saiz, E.; Tarazona, M. P., Analysis of copolymers of styrene and methyl methacrylate using size exclusion chromatography with multiple detection. *Phys. Chem. Chem. Phys.* **2003,** *5* (1), 151-157.

479.   Johnson, R. L.; Schmidt-Rohr, K., Quantitative solid-state 13C NMR with signal enhancement by multiple cross polarization. *J. Magn. Reson.* **2014,** *239*, 44-49.

480.   Shaw, S. E.; Russo, T.; Solomon, D. H.; Qiao, G. G., An alternative pathway for the hydrolysis of epoxy ester compounds. *Polymer* **2006,** *47* (25), 8247-8252.

481.   Pasch, H.; Trathnigg, B., *Multidimensional HPLC of polymers*. Springer: Berlin, 2013; pp 37-90.

482.   Weiss, J. W. E.; Bryce, D. L., A Solid-State 11B NMR and Computational Study of Boron Electric Field Gradient and Chemical Shift Tensors in Boronic Acids and Boronic Esters. *The Journal of Physical Chemistry A* **2010,** *114* (15), 5119-5131.

483.   Nöth, H.; Wrackmeyer, B. In *11B Chemical Shifts of Three Coordinate Boron*, Nuclear Magnetic Resonance Spectroscopy of Boron Compounds, Berlin, Heidelberg, 1978//; Nöth, H.; Wrackmeyer, B., Eds. Springer Berlin Heidelberg: Berlin, Heidelberg, 1978; pp 16-65.

484.   Wang, L.; Cheng, L.; Li, G.; Liu, K.; Zhang, Z.; Li, P.; Dong, S.; Yu, W.; Huang, F.; Yan, X., A Self-Cross-Linking Supramolecular Polymer Network Enabled by Crown-Ether-Based Molecular Recognition. *J. Am. Chem. Soc.* **2020,** *142* (4), 2051-2058.

485.   Chen, X.; Li, L.; Wei, T.; Venerus, D. C.; Torkelson, J. M., Reprocessable Polyhydroxyurethane Network Composites: Effect of Filler Surface Functionality on Cross-link Density Recovery and Stress Relaxation. *ACS Appl. Mater. Interfaces* **2019,** *11* (2), 2398-2407.

486.   Caffy, F.; Nicolaÿ, R., Transformation of polyethylene into a vitrimer by nitroxide radical coupling of a bis-dioxaborolane. *Polym. Chem.* **2019,** *10* (23), 3107-3115.

487.   Zych, A.; Pinalli, R.; Soliman, M.; Vachon, J.; Dalcanale, E., Polyethylene vitrimers via silyl ether exchange reaction. *Polymer* **2020,** *199*, 122567.

488.   Shi, J.; Zheng, T.; Guo, B.; Xu, J., Solvent-free thermo-reversible and self-healable crosslinked polyurethane with dynamic covalent networks based on phenol-carbamate bonds. *Polymer* **2019,** *181*, 121788.

489.   Cvek, M.; Mrlik, M.; Ilcikova, M.; Plachy, T.; Sedlacik, M.; Mosnacek, J.; Pavlinek, V., A facile controllable coating of carbonyl iron particles with poly(glycidyl methacrylate): a tool for adjusting MR response and stability properties. *J. Mater. Chem. C* **2015,** *3* (18), 4646-4656.

490.   Tang, Q.; Wang, B.; Shi, Y.; Song, L.; Hu, Y., Microencapsulated Ammonium Polyphosphate with Glycidyl Methacrylate Shell: Application to Flame Retardant Epoxy Resin. *Ind. Eng. Chem. Res.* **2013,** *52* (16), 5640-5647.

491.   Li, M.; Li, Y.; Zhang, J.; Zhang, D.; Li, J.; He, K.; Xu, Y.; Zeng, B.; Dai, L., Fabrication of graphene-coated poly(glycidyl methacrylate) microspheres by electrostatic interaction and their application in epoxy anticorrosion coatings. *J. Coat. Technol. Res.* **2020**.

492.   Selvamalar, C. S. J.; Krithiga, T.; Penlidis, A.; Nanjundan, S., Copolymerization of 4-benzyloxycarbonylphenyl methacrylate with glycidyl methacrylate: synthesis, characterization, reactivity ratios and application as adhesives. *React. Funct. Polym.* **2003,** *56* (2), 89-101.

493.   Buhl, K. B.; Agergaard, A. H.; Møller, R. K.; Kongsfelt, M.; Heide-Jørgensen, S.; Budzik, M. K.; Hinge, M.; Pedersen, S. U.; Daasbjerg, K., Facile Access to Disulfide/Thiol Containing Poly(glycidyl methacrylate) Brushes as Potential Rubber Adhesive Layers. *ACS Appl. Polym. Mater.* **2020,** *2* (6), 2380-2388.

494.   Yamada, K.; Takeda, S.; Hirata, M., Improvement of autohesive and adhesive properties of polyethylene plates by photografting with glycidyl methacrylate. *J. Appl. Polym. Sci.* **2007,** *103* (1), 493-500.

495.   Bayramoğlu, G.; Akgöl, S.; Bulut, A.; Denizli, A.; Yakup Arıca, M., Covalent immobilisation of invertase onto a reactive film composed of 2-hydroxyethyl methacrylate and glycidyl methacrylate: properties and application in a continuous flow system. *Biochem. Eng. J.* **2003,** *14* (2), 117-126.

496.   Xu, F. J.; Cai, Q. J.; Li, Y. L.; Kang, E. T.; Neoh, K. G., Covalent Immobilization of Glucose Oxidase on Well-Defined Poly(glycidyl methacrylate)−Si(111) Hybrids from Surface-Initiated Atom-Transfer Radical Polymerization. *Biomacromolecules* **2005,** *6* (2), 1012-1020.

497.   Lillethorup, M.; Shimizu, K.; Plumeré, N.; Pedersen, S. U.; Daasbjerg, K., Surface-Attached Poly(glycidyl methacrylate) as a Versatile Platform for Creating Dual-Functional Polymer Brushes. *Macromolecules* **2014,** *47* (15), 5081-5088.

498.   Undin, J.; Finne-Wistrand, A.; Albertsson, A.-C., Copolymerization of 2-Methylene-1,3-dioxepane and Glycidyl Methacrylate, a Well-Defined and Efficient Process for Achieving Functionalized Polyesters for Covalent Binding of Bioactive Molecules. *Biomacromolecules* **2013,** *14* (6), 2095-2102.

499.   Edmondson, S.; Huck, W. T. S., Controlled growth and subsequent chemical modification of poly(glycidyl methacrylate) brushes on silicon wafers. *J. Mater. Chem.* **2004,** *14* (4), 730-734.

500. Labella, R.; Braden, M.; Davy, K. W. M., Novel acrylic resins for dental applications. *Biomaterials* **1992,** *13* (13), 937-943.

501. Elizalde-Peña, E. A.; Flores-Ramirez, N.; Luna-Barcenas, G.; Vásquez-García, S. R.; Arámbula-Villa, G.; García-Gaitán, B.; Rutiaga-Quiñones, J. G.; González-Hernández, J., Synthesis and characterization of chitosan-g-glycidyl methacrylate with methyl methacrylate. *Eur. Polym. J.* **2007,** *43* (9), 3963-3969.

502. Zhang, Y.; Hasegawa, K.; Kamo, S.; Takagi, K.; Takahara, A., Adhesion enhancement of Poly(etheretherketone) via surface-initiated photopolymerization of glycidyl methacrylate. *Polymer* **2020,** *209*, 122971.

503. Zhang, Y.; Hasegawa, K.; Kamo, S.; Takagi, K.; Ma, W.; Takahara, A., Enhanced Adhesion Effect of Epoxy Resin on Metal Surfaces Using Polymer with Catechol and Epoxy Groups. *ACS Appl. Polym. Mater.* **2020,** *2* (4), 1500-1507.

504. Kocak, G.; Solmaz, G.; Tuncer, C.; Bütün, V., Modification of glycidyl methacrylate based block copolymers and their aqueous solution behaviours. *Eur. Polym. J.* **2019,** *110*, 364-377.

505. Muzammil, Ezzah M.; Khan, A.; Stuparu, M. C., Post-polymerization modification reactions of poly(glycidyl methacrylate)s. *RSC Adv.* **2017,** *7* (88), 55874-55884.

506. Benaglia, M.; Alberti, A.; Giorgini, L.; Magnoni, F.; Tozzi, S., Poly(glycidyl methacrylate): a highly versatile polymeric building block for post-polymerization modifications. *Polym. Chem.* **2013,** *4* (1), 124-132.

507. Frigione, M. E.; Mascia, L.; Acierno, D., Oligomeric and polymeric modifiers for toughening of epoxy resins. *Eur. Polym. J.* **1995,** *31* (11), 1021-1029.

508. Ghosh, S.; Krishnamurti, N., Use of glycidyl methacrylate monomers for developing cross-linkable pressure sensitive adhesives. *Eur. Polym. J.* **2000,** *36* (10), 2125-2131.

509. París, R.; Mosquera, B.; de la Fuente, J. L., Atom transfer radical copolymerization of glycidyl methacrylate and allyl methacrylate, two functional monomers. *Eur. Polym. J.* **2008,** *44* (9), 2920-2926.

510. Ji, W.-G.; Hu, J.-M.; Zhang, J.-Q.; Cao, C.-N., Reducing the water absorption in epoxy coatings by silane monomer incorporation. *Corros. Sci.* **2006,** *48* (11), 3731-3739.

511. Bonora, P. L.; Deflorian, F.; Fedrizzi, L., Electrochemical impedance spectroscopy as a tool for investigating underpaint corrosion. *Electrochim. Acta* **1996,** *41* (7), 1073-1082.

512. Grubbs, R. B.; Dean, J. M.; Broz, M. E.; Bates, F. S., Reactive Block Copolymers for Modification of Thermosetting Epoxy. *Macromolecules* **2000,** *33* (26), 9522-9534.

513. Bryuzgin, E.; Klimov, V.; Le, M. D.; Navrotskiy, A.; Novakov, I., The Superhydrophobic State Stability of Coatings Based on Copolymers of Glycidyl Methacrylate and Alkyl Methacrylates on Cotton Fabric Surface. *Fibers Polym.* **2020,** *21* (5), 1032-1038.

514. Pavlovskaya, M. V.; Kriulichev, I. P.; Grishin, D. F., Synthesis of Stearyl Methacrylate–Glycidyl Methacrylate Copolymers and Their Use as Multifunctional Additives to Diesel Fuel. *Russ. J. Appl. Chem.* **2020,** *93* (9), 1332-1339.

515. Ballard, N.; Simula, A.; Aguirre, M.; Leiza, J. R.; van Es, S.; Asua, J. M., Synthesis of poly(methyl methacrylate) and block copolymers by semi-batch nitroxide mediated polymerization. *Polym. Chem.* **2016,** *7* (45), 6964-6972.

516. Hasanzadeh, R.; Moghadam, P. N.; Bahri-Laleh, N.; Ziaee, F., A reactive copolymer based on Glycidylmethacrylate and Maleic Anhydride: 1-synthesis, characterization and monomer reactivity ratios. *J. Polym. Res.* **2016,** *23* (8), 150.

517.	Skeist, I., Copolymerization: the Composition Distribution Curve. *J. Am. Chem. Soc.* **1946,** *68* (9), 1781-1784.

518.	Meyer, V. E.; Lowry, G. G., Integral and differential binary copolymerization equations. *J. Polym. Sci., Part A: Gen. Pap.* **1965,** *3* (8), 2843-2851.

519.	Zoller, A.; Kockler, K. B.; Rollet, M.; Lefay, C.; Gigmes, D.; Barner-Kowollik, C.; Guillaneuf, Y., A complete kinetic study of a versatile functional monomer: acetoacetoxyethyl methacrylate (AAEMA). *Polym. Chem.* **2016,** *7* (35), 5518-5525.

520.	Darvishi, A.; Zohuriaan Mehr, M. J.; Marandi, G. B.; Kabiri, K.; Bouhendi, H.; Bakhshi, H., Copolymers of glycidyl methacrylate and octadecyl acrylate: synthesis, characterization, swelling properties, and reactivity ratios. *Des. Monomers Polym.* **2013,** *16* (1), 79-88.

521.	Benvenuta-Tapia, J. J.; Tenorio-López, J. A.; Vivaldo-Lima, E., Estimation of Reactivity Ratios in the RAFT Copolymerization of Styrene and Glycidyl Methacrylate. *Macromol. React. Eng.* **2018,** *12* (5), 1800003.

522.	Soundararajan, S.; Reddy, B. S. R.; Rajadurai, S., Synthesis and characterization of glycidyl methacrylate-styrene copolymers and determination of monomer reactivity ratios. *Polymer* **1990,** *31* (2), 366-370.

523.	Wang, W.; Hutchinson, R. A., PLP/SEC/NMR Study of Free Radical Copolymerization of Styrene and Glycidyl Methacrylate. *Macromolecules* **2008,** *41* (23), 9011-9018.

524.	Brar, A. S.; Yadav, A.; Hooda, S., Characterization of glycidyl methacrylate/styrene copolymers by one- and two-dimensional NMR spectroscopy. *Eur. Polym. J.* **2002,** *38* (8), 1683-1690.

525.	Brandrup, J.; Immergut, E. H.; Grulke, E. A., Polymer handbook. 4th ed.; Wiley: New York, 1999.

526.	Dai, X.; Yu, L.; Zhang, Y.; Zhang, L.; Tan, J., Polymerization-Induced Self-Assembly via RAFT-Mediated Emulsion Polymerization of Methacrylic Monomers. *Macromolecules* **2019,** *52* (19), 7468-7476.

527.	Radzir, N. N. M.; Hanifah, S. A.; Ahmad, A.; Hassan, N. H.; Bella, F., Effect of lithium bis(trifluoromethylsulfonyl)imide salt-doped UV-cured glycidyl methacrylate. *J. Solid State Electrochem.* **2015,** *19* (10), 3079-3085.

528.	Kim, K.; Yu, S.; Kim, S.-W.; Kim, T.; Kim, S.-M.; Kang, S.-Y.; Han, S. M.; Jang, J.-H., Highly transparent poly(glycidyl methacrylate-co-acryloisobutyl POSS) for 100 μm-thick submicron patterns with an aspect ratio over 100. *Chem. Commun.* **2017,** *53* (58), 8172-8175.

529.	Nanjundan, S.; Unnithan, C. S.; Selvamalar, C. S. J.; Penlidis, A., Homopolymer of 4-benzoylphenyl methacrylate and its copolymers with glycidyl methacrylate: synthesis, characterization, monomer reactivity ratios and application as adhesives. *React. Funct. Polym.* **2005,** *62* (1), 11-24.

530.	Hajiali, F.; Tajbakhsh, S.; Maric, M., Epoxidized block and statistical copolymers reinforced by organophosphorous-titanium-silicon hybrid nanoparticles: morphology and thermal and mechanical properties. *ACS Omega* **2021,** *6* (17), 11679-11692.

531.	Mishra, S.; Singh, J.; Choudhary, V., Synthesis and characterization of butyl acrylate/methyl methacrylate/glycidyl methacrylate latexes. *J. Appl. Polym. Sci.* **2010,** *115* (1), 549-557.

532.	Mao, H.; Wang, H.; Li, J.; Zhang, L.; Shi, J.; Shi, H., Side-chain crystallization and segment packing of poly(isobutylene-alt-maleic anhydride)-g-alkyl alcohol comb-like polymers. *Polymer* **2020,** *202*, 122721.

533.	Hempel, E.; Huth, H.; Beiner, M., Interrelation between side chain crystallization and dynamic glass transitions in higher poly(n-alkyl methacrylates). *Thermochim. Acta* **2003,** *403* (1), 105-114.

534.	Gupta, G.; Danke, V.; Babur, T.; Beiner, M., Interrelations Between Side Chain and Main Chain Packing in Different Crystal Modifications of Alkoxylated Polyesters. *J. Phys. Chem. B* **2017,** *121* (17), 4583-4591.

535.	Beiner, M.; Schröter, K.; Hempel, E.; Reissig, S.; Donth, E., Multiple Glass Transition and Nanophase Separation in Poly(n-alkyl methacrylate) Homopolymers. *Macromolecules* **1999,** *32* (19), 6278-6282.

536.	Reimschuessel, H. K., On the glass transition temperature of comblike polymers: Effects of side chain length and backbone chain structure. *J. Polym. Sci., Polym. Chem. Ed.* **1979,** *17* (8), 2447-2457.

537.	Li, Q.-L.; Gu, W.-X.; Gao, H.; Yang, Y.-W., Self-assembly and applications of poly(glycidyl methacrylate)s and their derivatives. *Chem. Commun.* **2014,** *50* (87), 13201-13215.

538.	Hatton, F. L.; Lovett, J. R.; Armes, S. P., Synthesis of well-defined epoxy-functional spherical nanoparticles by RAFT aqueous emulsion polymerization. *Polym. Chem.* **2017,** *8* (33), 4856-4868.

539.	Zhu, H.; Liu, Q.; Chen, Y., Reactive Block Copolymer Vesicles with an Epoxy Wall. *Langmuir* **2007,** *23* (2), 790-794.

540.	Hansen, C. M., *Hansen solubility parameters: a user's handbook*. CRC press: 2007.

541.	Zulfiqar, S.; Zulfiqar, M.; Nawaz, M.; McNeill, I. C.; Gorman, J. G., Thermal degradation of poly(glycidyl methacrylate). *Polym. Degrad. Stab.* **1990,** *30* (2), 195-203.

542.	Soykan, C.; Obuz, H., Spectroscopic characterization of glycidyl methacrylate with acrylonitrile copolymers and monomer reactivity ratios. *Microsc. Res. Tech.* **2020,** *83* (1), 22-34.

543.	Kaya, İ.; İlter, Z.; Şenol, D., Thermodynamic interactions and characterisation of poly[(glycidyl methacrylate-co-methyl, ethyl, butyl) methacrylate] by inverse gas chromatography. *Polymer* **2002,** *43* (24), 6455-6463.

544.	Yang, W.; Wang, X.-L.; Li, J.; Yan, X.; Ge, S.; Tadakamalla, S.; Guo, Z., Polyoxymethylene/ethylene butylacrylate copolymer/ethylene-methyl acrylate-glycidyl methacrylate ternary blends. *Polym. Eng. Sci.* **2018,** *58* (7), 1127-1134.

545.	Zetterlund, P. B.; Saka, Y.; McHale, R.; Nakamura, T.; Aldabbagh, F.; Okubo, M., Nitroxide-mediated radical polymerization of styrene: Experimental evidence of chain transfer to monomer. *Polymer* **2006,** *47* (23), 7900-7908.

546.	Yaws, C. L., Chapter 1 - Physical Properties – Organic Compounds. In *The Yaws Handbook of Physical Properties for Hydrocarbons and Chemicals (Second Edition)*, Yaws, C. L., Ed. Gulf Professional Publishing: Boston, 2015; pp 1-683.

547.	Rumble, J. R.; Lide, D. R.; Bruno, T. J., *CRC Handbook of Chemistry and Physics [2019-2020] : a ready-reference book of chemical and physical data*. 100th ed.; CRC Press: Boca Raton, 2019.

548.	Wohlfarth, C., Solubility parameter of poly(isobornyl methacrylate): Datasheet from Landolt-Börnstein - Group VIII Advanced Materials and Technologies. In *Polymer Solutions*, Lechner, M. D.; Arndt, K. F., Eds. SpringerMaterials: Berlin Heidelberg, 2010; Vol. 6D2.

549.	Ruzette, A. V. G.; Banerjee, P.; Mayes, A. M.; Pollard, M.; Russell, T. P.; Jerome, R.; Slawecki, T.; Hjelm, R.; Thiyagarajan, P., Phase Behavior of Diblock Copolymers between Styrene and n-Alkyl Methacrylates. *Macromolecules* **1998,** *31* (24), 8509-8516.

550.	Ueda, T.; Oshida, H.; Kurita, K.; Ishihara, K.; Nakabayashi, N., Preparation of 2-Methacryloyloxyethyl Phosphorylcholine Copolymers with Alkyl Methacrylates and Their Blood Compatibility. *Polym. J.* **1992,** *24* (11), 1259-1269.

551.   Yaws, C. L.; Li, K. Y., Chapter 13 - Solubility parameter and liquid volume—Organic compounds. In *Thermophysical Properties of Chemicals and Hydrocarbons*, Yaws, C. L., Ed. William Andrew Publishing: Norwich, NY, 2009; pp 597-643.

552.   Gee, G., VI. Swelling and solubility in mixed liquids. *Trans. Faraday Soc.* **1944,** *40*, 468-480.

553.   Nakayama, Y., Polymer blend systems for water-borne paints. *Prog. Org. Coat.* **1998,** *33* (2), 108-116.

554.   Zweigle, M. L.; Lamphere, J. C. Cross-linked water-swellable polymer particles. U.S. Patent 4,059,552, Nov. 22, 1977.

555.   Wen, M.; Dušek, K., *Protective Coatings: Film Formation and Properties*. Springer: Cham, 2017.

556.   Dušek, K.; Dušková-Smrčková, M., Network structure formation during crosslinking of organic coating systems. *Prog. Polym. Sci.* **2000,** *25* (9), 1215-1260.

557.   Buckmann, A.; Nabuurs, T.; Overbeek, G., Self crosslinking. Polymeric Dispersants Used in Emulsion Polymerization. *Paint & Coatings Industry* **2002,** *18* (10), 96-98.

558.   Ogata, M.; Kinjo, N.; Kawata, T., Effects of crosslinking on physical properties of phenol–formaldehyde novolac cured epoxy resins. *J. Appl. Polym. Sci.* **1993,** *48* (4), 583-601.

559.   Urbaczewski-Espuche, E.; Galy, J.; Gerard, J. F.; Pascault, J. P.; Sautereau, H., Influence of chain flexibility and crosslink density on mechanical properties of epoxy/amine networks. *Polymer engineering & science* **1991,** *31* (22), 1572-1580.

560.   Esser, R. J.; Devona, J. E.; Setzke, D. E.; Wagemans, L., Waterbased crosslinkable surface coatings. *Prog. Org. Coat.* **1999,** *36* (1-2), 45-52.

561.   Schellekens, M. A. J.; Nabuurs, T.; Geurts, J.; Overbeek, G. C. Water-borne crosslinkable block copolymers obtained using raft. U.S. Patent 9,567,476, Feb. 14, 2017.

562.   Foster, A. B.; Lovell, P. A.; Rabjohns, M. A., Control of adhesive properties through structured particle design of water-borne pressure-sensitive adhesives. *Polymer* **2009,** *50* (7), 1654-1670.

563.   Winnik, M. A., Latex film formation. *Curr. Opin. Colloid Interface Sci.* **1997,** *2* (2), 192-199.

564.   Winnik, M. A., The formation and properties of latex films. *Emulsion polymerization and emulsion polymers* **1997**, 467-518.

565.   Routh, A. F.; Russel, W. B., Deformation mechanisms during latex film formation: Experimental evidence. *Ind. Eng. Chem. Res.* **2001,** *40* (20), 4302-4308.

566.   Sonzogni, A. S.; Passeggi, M. C. G.; Wedepohl, S.; Calderón, M.; Gugliotta, L. M.; Gonzalez, V. D. G.; Minari, R. J., Thermoresponsive nanogels with film-forming ability. *Polym. Chem.* **2018,** *9* (8), 1004-1011.

567.   Jiang, S.; Van Dyk, A.; Maurice, A.; Bohling, J.; Fasano, D.; Brownell, S., Design colloidal particle morphology and self-assembly for coating applications. *Chem. Soc. Rev.* **2017,** *46* (12), 3792-3807.

568.   Steward, P.; Hearn, J.; Wilkinson, M., An overview of polymer latex film formation and properties. *Adv. Colloid Interface Sci.* **2000,** *86* (3), 195-267.

569.   Hajiali, F. Designing Polymer Coatings for Aerospace Industry. Ph.D. Thesis, McGill University, 2021.